Contemporary Cardiology
Series Editor: Christopher P. Cannon

Saif Anwaruddin
Joseph M. Martin
John C. Stephens
Arman T. Askari *Editors*

Cardiovascular Hemodynamics

An Introductory Guide

Humana Press

Contemporary Cardiology

Christopher P. Cannon, MD
Series Editor

For further volumes:
http://www.springer.com/series/7677

Saif Anwaruddin • Joseph M. Martin
John C. Stephens • Arman T. Askari
Editors

Cardiovascular Hemodynamics

An Introductory Guide

Humana Press

Editors
Saif Anwaruddin
Cardiovascular Medicine
The University of Pennsylvania
School of Medicine
Philadelphia, PA, USA

John C. Stephens
Cardiovascular Medicine
The Cleveland Clinic
Cleveland, OH, USA

Joseph M. Martin
Cardiovascular Medicine
The Cleveland Clinic
Cleveland, OH, USA

Arman T. Askari
Western Reserve Heart Care
Hudson,OH, USA

ISBN 978-1-60761-194-3 ISBN 978-1-60761-195-0 (eBook)
DOI 10.1007/978-1-60761-195-0
Springer New York Heidelberg Dordrecht London

Library of Congress Control Number: 2012951845

Printed on acid-free paper

Humana Press is a brand of Springer
Springer is part of Springer Science+Business Media (www.springer.com)

Preface

Our goal with putting together *Cardiovascular Hemodynamics: An Introductory Guide*, was to provide the reader with a broad and fundamental overview of basic cardiovascular hemodynamic principles. The importance of an excellent understanding of these principles cannot be overstated, particularly in the management of a patient with complex cardiovascular issues. As our patient population ages, we will be expected to diagnose and manage patients with more advanced coronary artery disease, ventricular dysfunction and more advanced valvular disease. As such, knowing what to measure, how to measure it, and how best to interpret that information becomes crucial.

In order to help accomplish our goal, we intentionally divided this book up into three different sections. The first four chapters fall under the section entitled "Components of Myocardial Performance." In this section we introduce the reader to the very basic concepts of cardiovascular hemodynamics, including preload, afterload, myocardial contractility and cardiac output. At first glance, this may seem very basic to the experienced cardiovascular physician or allied health professional. Beyond the basic definitions, however, we attempt to delve into the subtleties of each of these concepts to provide the reader with an in depth understanding.

The second section is entitled "Methods of Hemodynamic Evaluation." In these 4 chapters, there is an emphasis on the tools used for hemodynamic evaluation. Equally as important as understanding the hemodynamic principles is familiarity with the tools used to obtain hemodynamic information from the patient. Whether it's as basic as the physical examination or so advanced such as MR derived hemodynamics, the importance of knowing what to look for and how to look for it cannot be overemphasized.

The third and final section entitled "Specific Disease States" is comprised of 8 chapters each examining a specific disease state in which the proper diagnosis, evaluation and management of patients is dependent on a solid grasp of the underlying hemodynamic data. Our hope with this last section, is that it is able to bring together many of the principles explored in the previous two sections.

In order to reinforce the principles of cardiovascular hemodynamics emphasized in this book we have included board-style questions at the end of every chapter. In addition, the use of clinical cases and vignettes where appropriate throughout the book will further emphasize the key concepts of cardiovascular hemodynamics.

We would be remiss if we did not recognize the hard work and efforts of all the contributors. For each chapter we paired a recognized expert in the field with a cardiovascular medicine fellow from the Cleveland Clinic. Having already worked alongside and trained with many of these fellows, it has been a great privilege having worked with them on this endeavor. They are a group of dedicated, highly accomplished, and hard working individuals whose passion for this subject matter is evidenced by the quality of the work at hand.

We sincerely hope that this book can be used as a valuable tool in not only understanding and applying the basic principles of cardiovascular hemodynamics but also to gain an appreciation of the importance of this topic in proper care of the patient with cardiovascular disease.

Philadelphia, PA, USA — Saif Anwaruddin, MD
Cleveland, OH, USA — Joseph M. Martin, MD
Cleveland, OH, USA — John C. Stephens, MD
Hudson, OH, USA — Arman T. Askari, MD

Contents

Contributors

Olcay Aksoy MD Heart and Vascular Inst. Cleveland Clinic, Cleveland, OH, USA

Michael P. Brunner The Cleveland Clinic, Cleveland, OH, USA

George M. Cater The Cleveland Clinic, Cleveland, OH, USA

Milind Desai The Cleveland Clinic, Cleveland, OH, USA

Justin M. Dunn The Cleveland Clinic, Cleveland, OH, USA

Stephen G. Ellis The Cleveland Clinic, Cleveland, OH, USA

Sachin S. Goel The Cleveland Clinic, Cleveland, OH, USA

Michael D. Faulx The Cleveland Clinic, Cleveland, OH, USA

Andrew D.M. Grant UTMB Department of Microbiology and Immunology, Galveston, TX, USA

Brian P. Griffin Department of Cardiovascular Medicine, Cleveland Clinic, Cleveland, OH, USA

Richard A. Grimm The Cleveland Clinic, Cleveland, OH, USA

Mazen A. Hanna The Cleveland Clinic, Cleveland, OH, USA

Michael A. Hanna Chief of Medicine Huron Hospital, Chief of Cardiology Hillcrest Hospital, Medical Director of Heart Failure Center, OH, USA

James E. Harvey The Cleveland Clinic, Cleveland, OH, USA

Frederick Heupler Jr. The Cleveland Clinic, Cleveland, OH, USA

Allan Klein The Cleveland Clinic, Cleveland, OH, USA

Richard A. Krasuski The Cleveland Clinic, Cleveland, OH, USA

Amar Krishnaswamy Department of Cardiovascular Medicine, Cleveland Clinic, Cleveland, OH, USA

Praneet Kumar The Cleveland Clinic, Cleveland, OH, USA

Venugopal Menon The Cleveland Clinic, Cleveland, OH, USA

Alper Ozkan Heart and Vascular Inst. Cleveland Clinic, Cleveland, OH, USA

Parag Patel Cleveland Clinic, Heart and Vascular Institute, Cleveland, OH, USA

Leonardo Rodriguez The Cleveland Clinic, Cleveland, OH, USA

Marwa Sabe The Cleveland Clinic, Cleveland, OH, USA

William J. Stewart The Cleveland Clinic, Cleveland, OH, USA

E. Murat Tuzcu Heart and Vascular Inst. Cleveland Clinic, Cleveland, OH, USA

Amanda R. Vest Cardiovascular Medicine Fellow, Heart and Vascular Institute, Cleveland Clinic, Ohio, USA

Omeed Zardkoohi The Cleveland Clinic, Cleveland, OH, USA

Andrew O. Zurick III Medical Director Cardiovascular Imaging, St Thomas Heart, Nashville, TN, USA

Part I
Components of Myocardial Performance

Chapter 1
Preload

Amanda R. Vest and Frederick Heupler Jr.

Understanding the Concept

The four major determinants of cardiac output are cardiac preload, myocardial contractility, heart rate, and afterload. Of these four elements, preload is the primary determinant. Cardiac preload is a semi-quantitative composite assessment that is variously described in different cardiovascular physiology texts and articles as end-diastolic myocardial fiber tension, end-diastolic myocardial fiber length, ventricular end-diastolic volume, and ventricular end-diastolic filling pressure [1]. There is a general recognition that preload is not synonymous with any one of these measurable parameters, but is rather a physiological concept that encompasses all of the factors that contribute to passive ventricular wall stress at the end of diastole.

Cardiac preload may be expressed as a mathematical concept based upon the Law of LaPlace. This law states that, for a thin-walled spherical structure, $T = PR/2$, where T is wall tension, P is chamber pressure, and R is chamber radius. In the case of a thick-walled structure such as the left ventricle, the relationship is better described by $\sigma = PR/2w$, where σ is wall stress, and w is wall thickness, and where $T = \sigma w$. From the structure of the LaPlace's equation, the preload for the ventricle can be described as the left ventricular σ, whereby $\sigma\mathrm{LV} = (\mathrm{EDPLV})(\mathrm{EDRLV})/2w\mathrm{LV}$, with EDPLV representing the left ventricular end-diastolic pressure and EDR as the left ventricular end-diastolic radius. Thus the parameters of pressure, radius (a surrogate for volume), and wall thickness are all demonstrated to contribute to this mathematical definition.

Clinically, a more tangible and measurable definition of preload has been sought by some. Given the host of experience with invasive hemodynamic monitoring from

A.R. Vest (✉)
Cardiovascular Medicine Fellow, Heart and Vascular Institute, Cleveland Clinic, Ohio, USA
e-mail: vesta@ccf.org

F. Heupler Jr., MD
The Cleveland Clinic, Cleveland, OH, USA
e-mail: heuplef@ccf.org

A.T. Askari et al. (eds.), *Cardiovascular Hemodynamics: An Introductory Guide*,
Contemporary Cardiology, DOI 10.1007/978-1-60761-195-0_1,

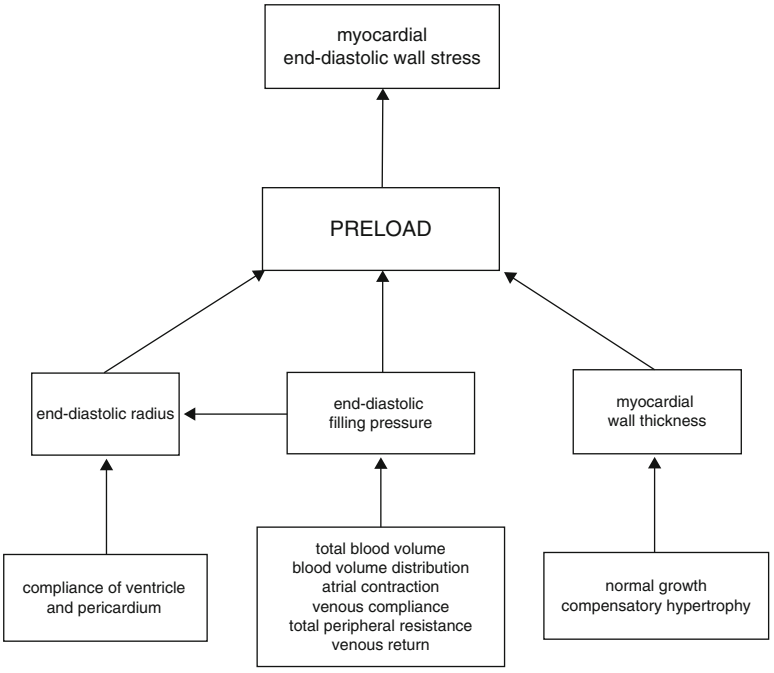

Fig. 1.1 Factors determining preload

the pre-Starling era to the modern catheterization lab or intensive care unit, it is an assessment of end-diastolic pressure—the ventricular pressure measured after atrial contraction just before the onset of systole—that is the most relevant parameter to many clinicians. Noninvasive assessments of end-diastolic chamber volume are possible, but volume assessments rely on geometric assumptions that can be undermined by arrhythmias, changes in heart rate, localized wall motion abnormalities, and the chronic ventricular dilatation that occurs in many forms of heart failure. The passive pressure-volume relationship within a chamber, which is a reflection of the passive length-tension curve in isolated myocardium, is exponential rather than linear. This fact poses one of the greatest limitations to the use of pressure as a surrogate for preload, with the ratio of change in chamber pressure to volume being greater at higher volumes compared to lower volumes. In addition, the relationship between pressure and volume will also be distorted by various cardiac pathologies, such as the presence of pericardial constriction. Overall, it should be remembered that preload as a physiological concept encompasses more than just a single value on a pressure tracing (Fig. 1.1).

The concept of preload can be applied to either the atria or the ventricles. In the structurally normal heart, the preload experienced by the right atrium will determine the subsequent preloads in the right ventricle and ultimately the left side of the heart. The other determinants of cardiac output will be addressed in later chapters of this section.

Preload Physiology and Theory

Chamber Anatomy and Function

Cardiac preload will increase with a rise in total circulating volume or greater venous return, which increases myocardial wall stress and the pressure within a chamber at the end of its diastolic phase. Conversely, hypovolemia or decreased venous return will result in decreased chamber filling and wall stress and hence a decreased end-diastolic pressure. The chamber most easily and frequently accessed for invasive monitoring of cardiac preload is the right atrium. A central venous catheter, commonly employed in intensive care settings, can contribute useful information for the clinician when assessing the patient's preload status.

The cardiac cycle comprises diastolic ventricular filling, augmentation by atrial systole to achieve the end-diastolic volume, isovolumic contraction, and then aortic (and pulmonary) valve opening, and stroke volume ejection. Meanwhile, atrial pressure progressively increases during ventricular systole as blood continues to enter the atrium while the atrioventricular valves are closed. Once the ventricle reaches its end-systolic volume, there is a period of isovolumic relaxation, which brings about mitral and tricuspid opening and diastolic filling from the atrium into the ventricle to begin the next cycle. Throughout the diastolic ventricular filling period, the pressure gradient between the atrium and ventricle is minimal. This is because a normal open mitral or tricuspid valve offers little resistance to flow; there is also significant passive filling of both the atrium and ventricle as blood returns from the systemic or pulmonary venous system. At a normal resting heart rate, diastole occupies approximately two-thirds of the cardiac cycle. With increased heart rate, both systolic and diastolic intervals will shorten (Fig. 1.2) [2].

The main difference between the left and right pumping systems is the pressure magnitude. In the normal heart, the pressures developed in the right heart are significantly lower than those on the left side, because resistance across the pulmonary vasculature is far less than the resistance to flow offered by the systemic vascular system. Normal pulmonary artery systolic and diastolic pressures typically do not exceed 30 and 15 mmHg respectively; maximal right atrial pressure is generally 8 mmHg (Fig. 1.3).

The Right Atrial Pressure Waveform

A central venous catheter is correctly placed when its tip is situated in the distal superior vena cava [3]; at this position it approximates pressures within the right atrium. As illustrated above, right atrial pressure also approximates the right ventricular end-diastolic pressure, because minimal pressure gradient exists across the normal tricuspid valve. In turn, the right ventricular end-diastolic pressure is proportional to the right ventricular end-diastolic volume and, due to the conservation of volume passing through the right and left ventricles, it will also mirror left ventricular end-diastolic

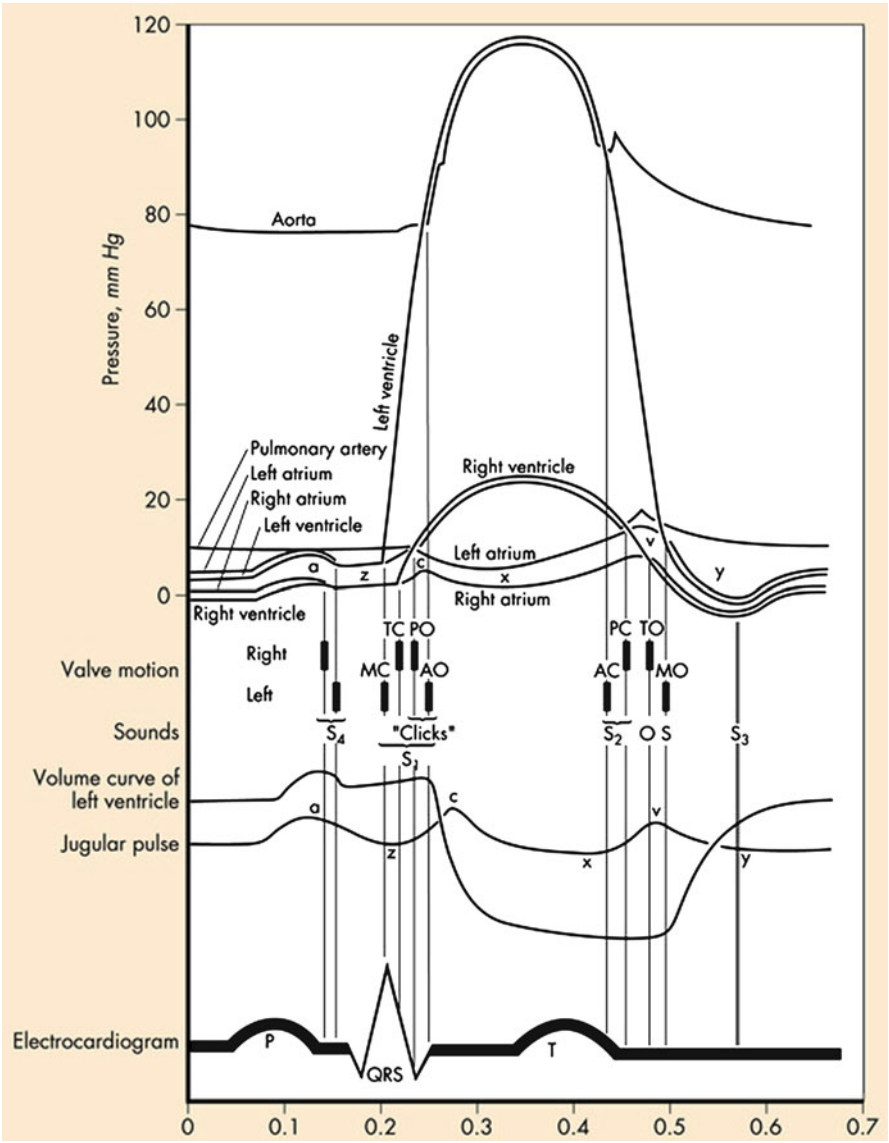

Fig. 1.2 The cardiac cycle

pressure (LVEDP) and volume. Hence the right atrial pressure alone can serve as a useful surrogate for cardiac preload while requiring slightly less invasive catheter insertion than pulmonary artery catheterization. However, it is also evident that abnormalities of cardiac structure and function will interfere with the assumptions by which

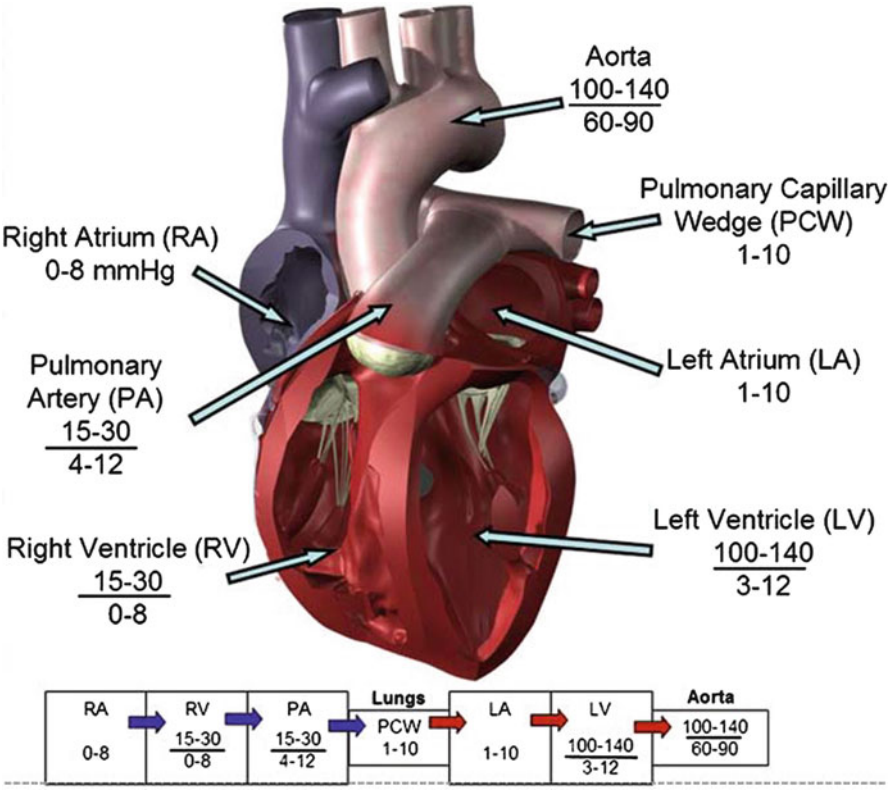

Fig. 1.3 Average pressures within the chambers and great vessels of the heart

central venous pressure monitoring can approximate left ventricular preload. Therefore, the central venous pressure has a greater role in preload assessment in the medical and surgical intensive care units than in critically ill cardiac patients. The right atrial pressure waveform demonstrates pressure elevations concurrent with atrial contraction (the *a* wave), reflection of ventricular systole as transmitted by the tricuspid valve (the *c* wave), and venous filling of the right atrium against a closed tricuspid valve (the *v* wave). The *x* descent probably arises from right ventricular contraction pulling the tricuspid annulus downward, whereas the *y* descent corresponds to blood emptying from the right atrium into the ventricle [4] (Fig. 1.4).

As illustrated, there is generally an electromechanical delay of approximately 80 ms between the atrial depolarization of the p wave and the pressure deflection of atrial systole represented by the *a* wave. The degree of delay is dependent upon the length of tubing used for pressure transduction.

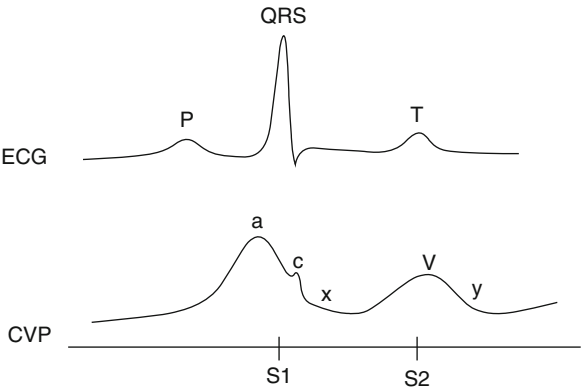

Fig. 1.4 Example of a typical central venous pressure waveform

Table 1.1 Variations of the right atrial waveform and their implications

Finding	Implication
Absence of the *a* wave	Atrial fibrillation
Cannon waves	Atrioventricular dissociation—atrial contraction against a closed tricuspid valve
Elevation of all chamber pressures, with prominent *x* descent	Cardiac tamponade
Elevation of all chamber pressures, with steep *y* descent	Constrictive pericarditis
Large systolic wave	Tricuspid regurgitation

The normal right atrial pressure, or central venous pressure, ranges from 0 to 8 mmHg (approximately 0–10 cmH_2O if measured with a water manometer). The atrial pressure is usually taken to be the mean peak of the *a* waves on the pressure tracing. Because the central veins lie within the thorax, the waveform obtained will be influenced by intrathoracic pressure changes during inspiration and expiration. Inspiration is achieved by creating a negative intrathoracic pressure (by expansion of the thoracic cavity) which will be reflected by a downward shift of the central venous tracing. Exaggerated spontaneous inspirations or mechanical ventilation may magnify this deviation. Therefore it is customary to read the mean pressure at end-expiration, just before the inspiratory drop.

Other variations of the waveform that should be taken into account are listed in Table 1.1. Of particular relevance is the large systolic wave seen in tricuspid regurgitation. In the setting of significant tricuspid regurgitation, the *c* wave and *x* descent will be replaced by a prominent upward deflection (the "systolic wave") occurring just before the *v* wave would be expected. This wave represents the regurgitant flow of blood back into the atrium with ventricular contraction.

Assessing Preload from the Right Atrial Pressure

The mean right atrial pressure, or central venous pressure, is primarily a reflection of venous return to the heart and thus the volume status of the patient. Lower pressures will be seen in the hypovolemic patient, as well as those in vasodilatory shock, e.g., due to sepsis or anaphylaxis. Elevated right atrial pressures are seen in cases of right ventricular failure (such as right ventricular infarction, pulmonary embolus), pulmonary hypertension (which is currently defined as mean pulmonary artery pressure at rest ≥25 mmHg [5]), tricuspid stenosis or regurgitation, cardiac tamponade, pericardial constriction, and hypervolemia (during anuric renal failure for example). The right atrial pressure may also be elevated in chronic or acutely decompensated left ventricular failure with either systolic or diastolic failure mechanisms.

Preload Reserve and the Venous System

In one of the early studies of preload dependence on human subjects, individuals with both normal hearts and diseased hearts were observed to sustain a reduction in LVEDP and a reduction in cardiac index upon inflation of an occlusive balloon in the inferior vena cava, just caudal to the liver [6]. Conversely, it has been demonstrated in various settings that passive leg raising (PLR) from the horizontal plane in the supine subject increases the volume of blood returning to the right heart and, for a heart that is under filled and demonstrates "preload reserve", this additional volume will boost left ventricular stroke volume. The venous system contains the major portion of circulating volume—up to 75% in some situations—because of the greater capacitance of veins than arteries. Therefore, venoconstriction has the potential to displace significant quantities of blood from the peripheral vasculature to the central circulation.

Venous return is the rate of blood flow from the periphery to the right atrium and depends upon the pressure gradient and the resistance to venous return. If blood were removed from a subject's circulating volume until there was no pressure within the venous system (i.e., no outward luminal force distending blood vessel walls) the volume of blood still contained within the system would be called the "unstressed volume." The unstressed volume can be modulated by altering the contractile state of the venous smooth muscle. Venoconstriction decreases unstressed volume and, all other parameters being equal, will increase venous return and right atrial pressure. Venodilation increases unstressed volume and decreases right atrial pressure. In experiments using hexamethonium chloride, the unstressed volume has been seen to increase by almost 18 ml/kg, demonstrating the range of reflex compensation available [7]. During exercise, such as running, reflex venoconstriction of vascular beds in the spleen and skin, in combination with the action of the skeletal muscle pump, all help to increase venous return to the higher output heart and hence maintain sufficient pressure in the right atrium to support ventricular filling. In response to a sudden reduction in cardiac output, passive recoil of the veins will redistribute blood to the heart and act to restore adequate stroke volume.

Conversely, sequential reductions in cardiac pump output lead to consequent decreases in arterial pressure and increases in venous pressure [8].

Movement of a volume of blood from the arterial system to the venous system will lower arterial pressure and raise venous pressure. However, due to the differing capacitances in these two systems, the arterial pressure change will be 19 times greater than that in the veins [9]. If cardiac output were to fall suddenly, the drop in pressure in the arterial system would far exceed the small rise in pressure in the venous system. Likewise, a large rise in arterial pressure will cause only a small reciprocal fall in venous pressure. All other factors being equal, the relationship venous pressure and cardiac output is reciprocal. Therefore a constant interplay occurs between the heart and venous system to accommodate changes in posture and volume status. An equilibrium state can be reached at a right atrial pressure where venous return equals cardiac output. The reflex control of venous tone, and the signals governing this primary reservoir for cardiovascular homeostasis, are still incompletely understood.

Preload and the Respiratory Cycle

During inspiration, the negative intrathoracic cavity pressure is transmitted to the thoracic structures resulting in a decrease in the observed intravascular and intracardiac pressures. As previously described, right atrial and pulmonary wedge pressure tracings will be seen to fall. However, calculation of the transmural pressure, by subtraction of the pleural pressure from the measured hemodynamic pressure, would show a more complex sequence of changes during the respiratory cycle. Intra-pleural pressures can be measured with esophageal catheters, or roughly estimated based on the pressure settings of a patient's mechanical ventilation mode. Inspiration will be followed by an increase in right atrial filling as an increased venous blood volume moves down the pressure gradient toward the heart. This leads to increased right ventricular volume and end-diastolic pressure in relation to the pleural pressure, although overall the expansion of the thoracic cavity causes the absolute right ventricular end-diastolic pressure to fall. Increased right-sided flow results in a slight increase in transmural pulmonary pressure during spontaneous inspiration. Events on the left side of the heart are inconsistent, as they are influenced by potentially contradictory changes in several parameters. However, the augmented blood volume moving through the right ventricle has been shown in closed-chest animal models to transiently decrease left ventricular stroke volume, likely due to deviation of the intraventricular septum into the left ventricular cavity which decreases its end-diastolic volume [10].

The Pulmonary Capillary Wedge Pressure Waveform

A key tenet of using the central venous pressure to assess cardiac preload is the relationship of right ventricular end-diastolic pressure to the left ventricular end-

diastolic pressure. Experience has shown that there are many situations in which this pressure relationship does not hold true [11]. Pulmonary artery catheterization was previously a procedure limited to the research laboratory, but it made the transition to the bedside in the 1970s following the advent of the Swan-Ganz catheter. This is a multiple lumen catheter that permits pulmonary artery pressure measurement at the distal injection port and right atrial pressure at the proximal injection port. The balloon inflation port is used to inflate and deflate a small air-filled balloon at the distal catheter tip, which is introduced into a pulmonary artery branch. When the balloon is inflated and advanced within a pulmonary arterial branch, a column of blood will exist between the left atrium and the catheter tip, enabling measurement of the downstream pressure in the left atrium (Figs. 1.5 and 1.6).

The waveform obtained at balloon inflation is a backward reflection of the left atrial pressure and therefore it will show a similar contour as the right atrial tracing with *a*, *c,* and *v* waves produced by the corresponding left-sided physiologic events, although the wedge pressure is normally higher than the right atrial pressure. The pulmonary capillary wedge pressure (PCWP) is read from the tracing as the average amplitude of the *a* waves. Note should also be made if a large systolic wave, suggesting mitral regurgitation, is present. The PCWP should be calculated at end-expiration if the waveform has respiratory variation.

The total electromechanical time delay is greater for the wedge waveform than for the right atrium as the changes in left atrial pressure have to be transmitted back through the pulmonary vasculature to the catheter tip. A balloon-tipped pulmonary artery catheter typically shows a mechanical time delay of 150–160 ms. A pressure gradient should exist between the mean pulmonary artery and the PCWP, with a gradual drop in PCWP occurring as the balloon is inflated. Indeed, there is usually a gradient of approximately 1–4 mmHg between the pulmonary artery diastolic (PAD) pressure and the mean PCWP to ensure forward movement of blood through the pulmonary vasculature, although rarely the PAD and PCWP can be measured as almost equal [12]. However, a wedge pressure that exceeds PAD suggests an error in measurement, such as balloon inflation in a very small branch vessel ("overwedging"). The difference between PAD and PCWP will be greater in the setting of pulmonary hypertension, where elevated pulmonary artery pressures are seen without a concurrent PCWP elevation. Any elevation in PCWP is indicative of elevated left atrial pressures.

Assessing Preload from the Pulmonary Capillary Wedge Pressure

The value in the PCWP lies in its ability to represent (a) the volume status of the patient and (b) the adequacy of left ventricular function. If correctly obtained, the PCWP measures the capillary hydrostatic pressure that will tend to force movement of fluid out of the capillaries and into the pulmonary interstitium. This force is normally 6–12 mmHg and is opposed by the capillary plasma colloid oncotic pressure at approximately 20–25 mmHg and acts to retain fluid in the vessel [13]. An imbal-

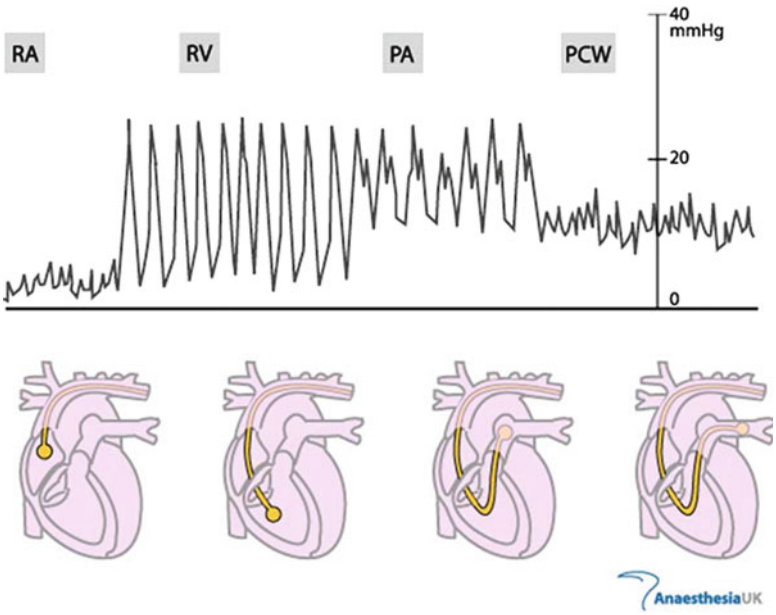

Fig. 1.5 Characteristic intra-cardiac pressure waveforms derived from the pulmonary artery catheter

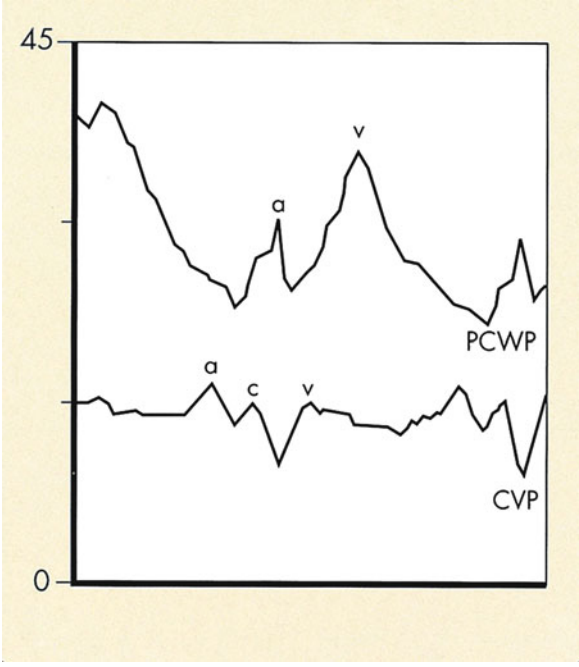

Fig. 1.6 Example of a typical pulmonary capillary wedge pressure waveform, compared to a central venous pressure waveform

Table 1.2 Situations where pulmonary capillary wedge pressure may inaccurately represent left ventricular end-diastolic pressure

May falsely elevate PCWP
Positive pressure ventilation
Mitral stenosis
Mitral regurgitation
Pulmonary venous obstruction between pulmonary capillary and left atrium
Left atrial myxoma

Table 1.3 Techniques for clinical assessment of cardiac preload

Technique	Pros	Cons
Pulmonary capillary wedge pressure (PCWP) [15]	Multiple right heart and pulmonary pressures, cardiac output and indexall measurable	Invasive, inaccurate with some structural diseases, requires interpretation
Left ventricular end-dia stolic pressure (LVEDP) [15]	Gold standard for preload measurement	Requires arterial cannulation, traversing the aortic valve
Vena caval ultrasound assessment	Noninvasive and simple to perform	Sensitivity may be poor
Passive leg raising (PLR) [7]	Noninvasive and simple to perform	Requires bed that performs appropriate movements
Right ventricular end-dia stolic volume index (RVEDVI) [30]	Predicts change in stroke volume in response to fluids	Requires a rapid response thermistor and PA catheterization
Left ventricular end-dia stolic area (EDA) [33]	No vascular access required	Requires a transesopha-geal echocardiogram study
Intrathoracic blood volume assessment (ITBV) [35]	Stronger predictor of preload than PCWP or CVP	Requires femoral artery cannulation
Esophageal Doppler [38]	Esophageal probe is minimally invasive	Role in medical intensive care is still to be defined

ance of these opposing forces, or a change in the filtration coefficient, can promote the movement of fluid into the interstitium resulting in pulmonary edema. When the only altered parameter is hydrostatic pressure, there is a useful correlation between PCWP and the chest X-ray. From 18 mmHg features of pulmonary edema may be seen; once hydrostatic pressure exceeds oncotic pressure around 25 mmHg frank pulmonary edema would be expected. Therefore a PCWP cut-off of 18 mmHg is often used as the hemodynamic numeric correlate of pulmonary edema [14]. A normal PCWP is usually quoted as 8–12 mmHg [12].

The gold standard invasive clinical assessment of cardiac preload is the left ventricular end-diastolic pressure (LVEDP), which is measured with a catheter retrogradely via the arterial system by crossing the aortic valve into the left ventricle. The correlation of PCWP with the left ventricular end-diastolic pressure, but not pulmonary artery pressures, has previously been demonstrated in settings such as acute myocardial infarction [15]. It is important to understand situations in which the PCWP will not accurately assess preload. As previously mentioned, there is an exponential relationship between left ventricular end-diastolic pressure and volume. Therefore the same volume change will cause a small pressure change at a low ventricular volume and a large pressure change in a more distended ventricle. The relationship between left ventricular volume and pressure may also be skewed in pericardial tamponade or constriction.

The PCWP can potentially misrepresent the LVEDP in several settings, as outlined in Table 1.2. Mitral regurgitation causes a systolic regurgitant wave with onset just before the *v* wave, with similar morphology to that seen in tricuspid regurgitation in the central venous waveform. In pure mitral stenosis, the *a* wave will be prominent and elevated due to the resistance to blood flow through the narrowed valve orifice during atrial systole. The *y* descent is usually prolonged, indicative of the increased resistance to passive left ventricular filling.

In the absence of any of these complicating factors, the wedge pressure should reflect the end-diastolic filling pressure in the left ventricle. The LVEDP is considered the gold standard single parameter in quantifying cardiac preload with the caveat that, as defined above, preload is a composite of several elements that contribute to passive ventricular wall stress at the end of diastole. The downside is that the LVEDP requires arterial cannulation and retrograde passage of the catheter across the aortic valve into the left ventricle. This procedure is associated with risks and is usually performed only as a component of a more extensive left heart catheterization procedure. In addition, as the catheter enters the left ventricle for only a matter of minutes, usually only a single measurement of LVEDP is obtained during a patient's hospitalization. This is in contrast to the Swan-Ganz catheter which may remain in place for many days, with many critically ill patients having serial PCWP measurements throughout their intensive care admission (Fig. 1.7).

A "normal" LVEDP is often quoted as 8–12 mmHg, with 16 or 18 mmHg usually being used as the cut-off for significant elevation in clinical trials [16]. As illustrated in Fig. 1.3, chamber pressures on the left side of the heart are normally higher than those in the low-pressure system on the right.

Preload Dependency and Pressure–Volume Loops

Having successfully obtained an accurate hemodynamic estimate of preload, the next challenge is to interpret the impact of that parameter on overall cardiac function. The first concept is the "preload dependency" of ventricular performance. Carl Ludwig is reported as being the first to describe the dependence of cardiac work on diastolic filling, when he wrote in 1856 "… a strong heart that is filled with blood

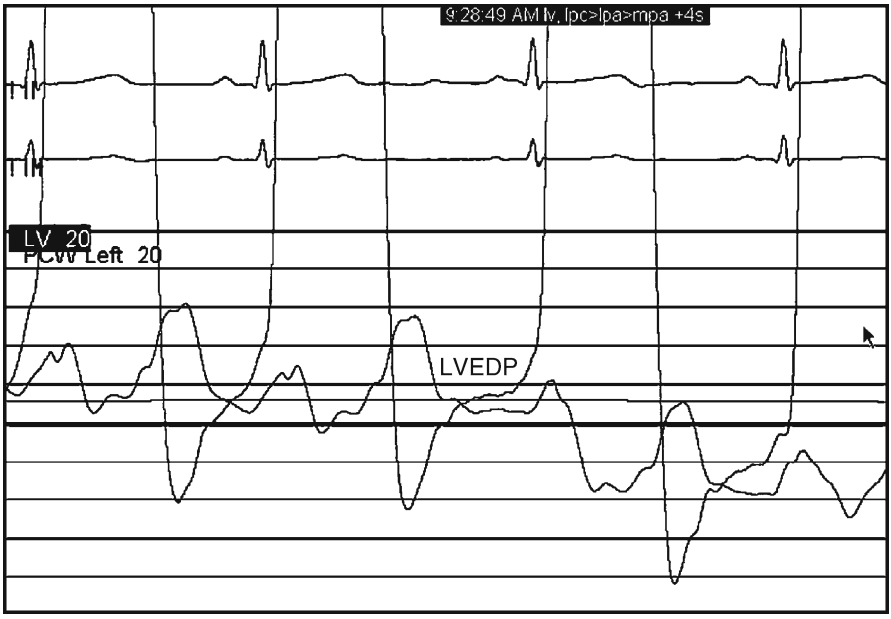

Fig. 1.7 Example of a typical left ventricular pressure waveform, compared to a pulmonary capillary wedge pressure

empties itself more or less completely, in other words, [filling of the heart with blood] changes the extent of contractile power" [17]. This relationship of preload to performance was described in detail by Ernest Henry Starling, who published this relationship in a series of papers between 1912 and 1914 and in his 1915 Linacre Lecture at Cambridge University [18]. The relationship between ventricular pressure and volume during the cardiac cycle can be illustrated by pressure–volume loops, as depicted in Fig. 1.8. End-diastole is located at the lower right corner of the loop. The subsequent upstroke (the vertical line on the right of the graph) is isovolumic contraction. This is followed by ejection, with end-systole located in the upper left corner, and then the downstroke of isovolumic relaxation. As illustrated, increases in preload will result in a greater volume of blood ejection during systole—at least up until a point. Controversy exists as to whether the non-diseased human heart reaches a point of preload at which further end-diastolic stretch will result in decreasing blood ejection [19]. This "descending limb of the Frank-Starling curve" is better described in the failing heart and will be discussed elsewhere in this book (Fig. 1.8).

At this point it is valuable to reflect on the myocardial cellular mechanics that underlie the preload concept. The term "preload" originally arose from the isolated myofiber studies where myocytes were physically loaded with defined forces in the form of a weight applied to one end of a quiescent muscle sample, such as papillary muscle. The other end remains tethered and the force applied prior to contraction is the preload. By varying preload, the relationship between initial length and shortening (isotonic contraction), or developed force (isometric contraction), can be recorded. The maximal force

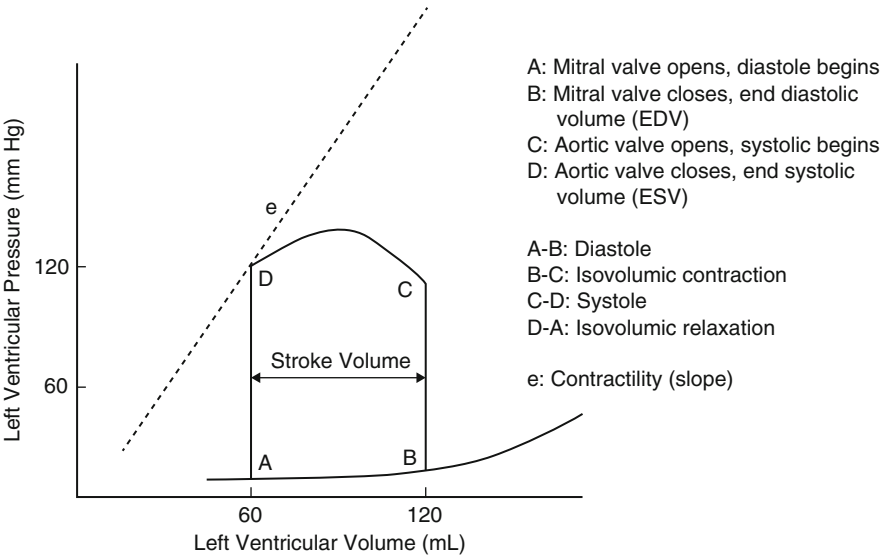

Fig. 1.8 Pressure-volume loop for a single cardiac cycle

developed at any sarcomere length is determined by the degree of overlap of thick and thin filaments and therefore the number of available actin-myosin crossbridges. Forces increase linearly until a sarcomere length with maximal overload (approx 2.2 μm) is achieved [20]. Structural proteins constitute a strong parallel elastic component within the myocardium and prevent an increase in developed force beyond this maximal degree of preload. The ascending limb of the myofiber length-tension relationship, which is analogous to the increase in stroke volume with increasing preload in the whole heart, is also modulated by length-dependent increases in myofilament calcium sensitivity [21]. Proposed mechanisms include enhanced calcium binding to troponin C, narrower interfilament gaps at longer sarcomere length, and increased sarcoplasmic reticulum calcium release and uptake at longer sarcomere lengths.

Returning to the whole heart, the major determinants of the left ventricular pressure-volume relationship are the initial ventricular volume, chamber geometry, wall thickness, and myocardial stiffness. Pressure-volume loops highlight the nonlinear pressure and volume relationship during diastolic filling. The instantaneous slope of the curve in the filling phase (i.e., change in pressure/change in volume) represents diastolic stiffness. This parameter is correctly termed as “elastance” and can be conceptualized by the ventricle behaving as a spring with a stiffness (elastance) that increases during contraction and decreases during relaxation. Elastance can be calculated at any point during the ventricle’s diastole by calculating the gradient of the curve. Beyond a volume of approximately 140 mL (the exact volume will depend on individual heart dimensions) the chamber becomes progressively more difficult to fill, requiring a greater pressure increase to effect volume changes than

earlier in diastole. A thicker, stiffer ventricle, for example in an individual with left ventricular hypertrophy, will show a steeper gradient to the diastolic curve, and hence a greater elastance. The mathematical inverse of elastance (i.e., change in volume/change in pressure) is compliance. The thicker, stiffer ventricle would be described as having reduced compliance. It should be remembered that diastole is an active process that consumes energy; ATP is hydrolyzed to break the actin-myosin crosslink and permit sarcomere lengthening. Therefore ventricular compliance also often falls during ischemia. In the setting of low compliance, a high LVEDP may actually reflect a relatively small LVEDV. Conversely in the normal left ventricle, compliance is high within the typical physiological range, because the chamber operates on the flatter region of the curve where reasonably small pressure rises give significant volume increases, promoting optimal stroke volume.

The importance of the physiological pressure-volume relationship is its role in modulating ventricular performance by the changes in preload. This "heterometric regulation" occurs on a beat-by-beat basis and ensures matching of the right and left ventricular output with changes in respiration and body posture [22]. In response to myocardial pathology, rises in end-diastolic pressure and volume can also provide a longer-term compensatory increase in stroke volume due to increased myocardial fiber length in the remaining functional myocardium. However, the scope of this compensation is limited, as the dilated failing heart will also develop fibrosis, adverse remodeling, and unfavorable metabolic status. This explains the disparity between acute increases in end-diastolic volume resulting in augmented stroke volume, vs. the chronically dilated heart generating a poorer stroke volume.

These considerations illuminate the inherent difficulties in judging preload adequacy. The level of preload at which the heart will show its optimal stroke volume will be dependent on not only the intravascular volume status but also the ventricular compliance and geometry unique to the individual heart. Clinical experience has shown that some dilated, failing ventricles perform optimally at a higher wedge and LVEDP than would be judged normal. However, this cannot be assumed to be the case, as many heart failure patients show improved symptom status and cardiac output following aggressive diuresis and return of their wedge pressure to a value that would be considered to lie in the normal range (Fig. 1.9).

Preload in Clinical Practice

Invasive Hemodynamics

Assessment of "preload reserve" and "preload adequacy" is of particular relevance to the management of hypovolemic or septic shock patients. The use of invasive hemodynamic monitoring, with either a central venous catheter or pulmonary artery catheter, is generally the standard technique in the intensive care unit or operating room. Fluid resuscitation is titrated to right atrial or pulmonary wedge pressure, or to the central or mixed venous saturation which serves as a reflection of tissue

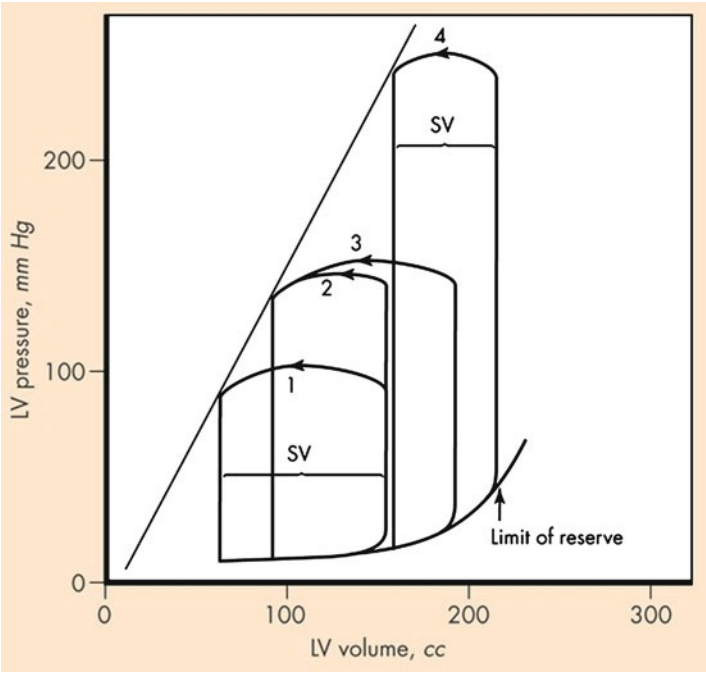

Fig. 1.9 Effects of acutely increasingly preload on the pressure-volume loop, to the point of maximal preload reserve

oxygenation adequacy. Various goal-directed algorithms have been developed in the research setting and have demonstrated the value of early effective volume resuscitation in trauma, surgical, or sepsis patients [23]. However, since its introduction to clinical care almost 40 years ago, the limitations of the pulmonary artery catheter in actual clinical practice have been well documented. As described earlier, for the pulmonary wedge pressure to accurately reflect LVEDP, the following criteria must be met: (a) the catheter is correctly positioned with a valid and accurate wedge tracing obtained, (b) the wedge pressure is correctly interpreted, (c) the wedge pressure is an accurate reflection of LVEDP, and (d) there is a linear and predictable relationship between left ventricular end-diastolic pressure and volume. In an assessment of the technical adequacy of 2,711 pulmonary wedge recordings, the authors reported that 31% of these recordings were technically inadequate [24]. Even if a valid waveform is obtained, it is estimated that in approximately a third of cases data will be incorrectly interpreted by the physician making management decisions [25]. These issues, and the added difficulties brought by positive pressure ventilation, changes in myocardial compliance, and ventricular interdependence, can severely impact on the utility of the pulmonary capillary wedge pressure in accurately reflecting cardiac preload. Such factors may partially explain why randomized controlled trials have, to date, not shown improved outcomes with pulmonary artery catheterization in critically ill patients.

Noninvasive Preload Assessment Techniques

Alternative techniques for assessment of preload adequacy, and responsiveness of the stroke volume to further preload delivery, have also been trialed over recent years. Various transthoracic and transesophageal echocardiographic measurements have been experimented with. One simple strategy is assessment of venal caval collapse during positive pressure ventilation, with the goal being to identify those patients with a RA pressure less than 10 mmHg who would benefit from further intravenous volume before being subjected to positive pressure ventilation [26]. Another related technique is passive leg raising (PLR) which has gained interest as a maneuver for assessing functional hemodynamic status and assessing potential fluid responsiveness. As described above, passive leg raising from the horizontal position effects a transient increase in preload and acts as an endogenous "fluid challenge." Radiolabeled erythrocyte studies to determine venous blood volume in the lower extremities have demonstrated a reduction of approximately 150 mL in each leg when this maneuver is performed [27]. If the right ventricle is preload responsive, the 300 mL increase in venous return will augment right ventricular output and hence left ventricular filling. A small number of studies have proven increases in pulmonary wedge pressure and LVED dimensions with PLR, supporting the theory that the transfer of this volume of blood into the right atrium does significantly contribute to cardiac preload. However, in situations where the "preload reserve" of the heart is limited, meaning that further diastolic filling will not raise left ventricular stroke volume, the increased venous return will not result in greater cardiac output. The transient increase in cardiac output seen in the preload responsive heart has been observed to be greater after withdrawal of 500 mL blood [28], suggesting that the effect of this maneuver is dependent upon the volume status of the individual. The clinical utility of this observation was highlighted in a study of mechanically ventilated patients judged to be requiring volume expansion, with recording of aortic blood flow after PLR and then a 500 mL intravenous fluid challenge. The PLR was achieved by taking the patient from a semi-recumbent position with 45° head elevation, through a negative 45° tilt of the bed, so that the upper body lay parallel to the horizontal with the lower extremities elevated at a 45° angle. An increase in aortic blood flow of at least 10% by PLR predicted a volume expansion-induced increase in aortic blood flow of at least 15% with a sensitivity of 97% and specificity of 94% [29]. Thus, an initial trial of PLR appears to offer a potentially useful noninvasive clinical tool for assessing which critically ill patients will be preload responsive and should receive further volume expansion.

Additional Invasive Preload Assessment Techniques

The use of a pulmonary artery catheter with a rapid response thermistor and an ECG electrode allows computation of the right ventricular ejection fraction, from which right ventricular end-diastolic and end-systolic volumes can be calculated. Right

ventricular end-diastolic volume index (RVEDVI) is calculated by dividing right ventricular end-diastolic volume by body surface area, and has been evaluated in surgical critical care settings in mechanically ventilated patients. One such study aimed to determine preload status in acute respiratory failure patients. The degree of positive end-expiratory pressure (PEEP) was titrated and corresponding serial measurement of RVEDVI, wedge pressure, and cardiac index were recorded. They found that, at all levels of PEEP, cardiac index correlated significantly better with RVEDVI than with wedge pressure—at high levels of PEEP, cardiac index inversely correlated with wedge pressure, but remained positively correlated with the RVEDVI [30]. The value of RVEDVI is its ability to predict the change in stroke volume in response to a fluid challenge, and has been demonstrated to be a superior predictor of recruitable cardiac output than wedge pressure [31]. Of note though, some authors suggest that the RVEDVI overestimates the preload in comparison to echocardiographic techniques [32].

Left ventricular dimensions have also been employed in the assessment of preload adequacy. Transesophageal echocardiography is also increasingly used to assess left ventricular filling, with the LV end-diastolic area (EDA) in the transgastric midpapillary short axis view proving to be a useful parameter that correlated with cardiac preload. In a cohort of heterogeneous medical intensive care unit patients, the left ventricular EDA was significantly lower in those patients who showed a good response to volume challenge [33]. However, the utility of EDA assessment was felt to be lower in this study than in several others evaluating EDA and preload in cardiac surgery patients. Nonetheless, at least one intensive care center has had such success with left ventricular echocardiographic assessment of preload reserve that it has become the primary method for hemodynamic assessment [34].

Another technique that features in the anesthesiology and surgical literature is transpulmonary thermal-dye indicator dilution, which enables bedside measurement of intrathoracic blood volume (ITBV). ITBV has been shown to be a stronger predictor of preload than PCWP and CVP [35]. Transpulmonary double indicator dilution measurements of cardiac output and ITBV can be performed using a catheter positioned in the descending aorta (via the femoral artery) that simultaneously measures thermodilution and dye-dilution. The two indicators are the freely diffusible cold saline and a plasma bound indicator such as indocyanine green (ICG). When injected simultaneously, the cold indicator will equilibrate with the interstitium whereas the ICG will remain in the intravascular space. Based upon the conservation of mass, intrathoracic blood volume (ITBV) can then be calculated from cardiac output and the mean transit time of the dye tracer between the site of injection—the right atrium—and the site of detection. A study in 10 anesthetized patients observed significant decreases in ITBV after a standardized change from supine to sitting body position, which correlated with changes in the stroke volume index. This study found ITBV and EDV to be equivalent indices of cardiac preload in their small sample of anesthetized patients [36]. Another group that compared preload variables in the early phase of hemodynamic stabilization of 57 critical care patients found ITBV to be a more reliable indicator of preload than CVP or PCWP [37]. However, femoral artery catheterization is required for this technique.

A final technique for assessing preload adequacy that is gaining acceptance in high-risk surgical patients is esophageal Doppler. This is a minimally-invasive method of measuring real-time descending aortic blood flow that employs the Doppler shift phenomenon as a marker for blood cell velocity. A probe situated in the esophagus is in close proximity to the descending aorta and provides an excellent window for obtaining Doppler flow signal from which cardiac output can be calculated. The left ventricular ejection time (or flow time) corrected for heart rate correlates well with left ventricular preload. In general, a corrected flow time of less than 0.35 s suggests a potential to respond to volume expansion, whereas reading above 0.45 s suggests that volume expansion will not stimulate further increases in cardiac output [38]. Esophageal Doppler has been demonstrated to be effective in guiding nurse-led, protocolized resuscitation in the early post-operative hours, resulting in reduced complications and shorter hospital stays for cardiac surgery patients [39]. Its promise has also been recognized in the medical intensive care setting, where the continuous real-time monitoring could be of use in gaining instantaneous feedback on interventions. Probe insertion takes only minutes, requires minimal technical skill, and is not associated with any major complications [40]. However, the calculations that generate measurements of aortic blood flow do depend upon aortic geometric assumptions.

Bullet Point Summary

- Preload is a composite assessment of cardiac filling that represents the primary determinant of cardiac output.
- End-diastolic left ventricular pressure and volume are common surrogates for preload.
- The passive myocardial length-tension relationship is exponential rather than linear.
- Preload increases with greater circulating volume, venoconstriction, exercise, arterioventricular fistulae, increased ventricular compliance, increased ventricular filling time, left ventricular systolic failure.
- Preload decreases with volume depletion, decreased venous return, impaired atrial contraction, tricuspid or mitral stenosis, less compliant ventricles.
- The right atrial pressure waveform comprises *a*, *c,* and *v* waves, with *x* and *y* descents.
- The mean right atrial pressure is usually taken as the peak of the *a* wave.
- Inspiration normally decreases all intracardiac pressures.
- Inflation of the Swan-Ganz catheter balloon within a pulmonary artery branch enables measurement of downstream pressure in the left atrium.
- Pressure-volume loops are orientated with end-diastole located at the lower right corner of the loop.
- The instantaneous slope of the pressure-volume curve in the filling phase represents elastance.

- Invasive methods of assessing left ventricular preload adequacy include: central venous pressure, pulmonary artery diastolic pressure, and pulmonary capillary wedge pressure. Left ventricular end-diastolic pressure is considered the gold standard.
- Noninvasive methods of assessing left ventricular preload adequacy include vena caval collapse, right ventricular end-diastolic volume index, left ventricular end-diastolic area, esophageal Doppler evaluation of left ventricular inflow, and intrathoracic blood volume.

Review Questions

1. Which of the following has *not* been used as surrogate parameter for cardiac preload?

   a. Left ventricular end-systolic pressure
   b. Pulmonary capillary wedge pressure
   c. Intrathoracic blood volume
   d. End-diastolic myocardial fiber tension
   e. Degree of venal caval collapse

   Answer is a). However, left ventricular end-*diastolic* pressure is a commonly used clinical surrogate for cardiac preload.

2. Which one of the following statements is true regarding central venous pressure monitoring?

   a. The normal central venous pressure in a healthy adult ranges from 5 to 12 mmHg
   b. The central venous pressure should be taken to be the lowest point between the *a* and v waves as measured during inspiration
   c. Central venous pressure rises during deep inspiration
   d. The *x* descent is absent in cardiac tamponade
   e. Significant tricuspid regurgitation will cause a prominent upward deflection just before the *v* wave would be expected

   Answer is e). The normal central venous pressure is 0–8 mmHg, although a higher rage may well be an appropriate target for a critically ill individual in whom maintenance of preload is important. The pressure is usually read as the mean peak of the *a* waves, ideally at the end of expiration, just before the inspiratory fall in central venous pressure. Cardiac tamponade causes absence of the *y d*escent, and often results in a prominent *x d*escent.

3. Which of the following does *not* generally cause the pulmonary capillary wedge pressure to be unrepresentative of the left atrial pressure?

   a. Pulmonary venous hypertension
   b. Balloon inflation in a very small branch vessel
   c. Aortic stenosis
   d. Mitral regurgitation

Answer is c). Pulmonary venous hypertension, "overwedging" of the Swan-Ganz balloon and an atrial myxoma can all cause the pulmonary capillary wedge pressure to read higher than the actual left atrial pressure. Severe mitral regurgitation causes a large systolic regurgitant wave with onset just before the *v* wave, and so care must be taken to correctly interpret the pressure waveform and estimate the pressure as the peak of the a waves, because inclusion of the regurgitant upward deflection will cause overestimation of the true pressure. The presence of mitral stenosis and aortic regurgitation can cause the pulmonary capillary wedge pressure to misrepresent the left ventricular end-diastolic pressure.

4. Which one of the following statements is true regarding ventricular 'elastance'?

   a. This is an expression of the ease of diastolic stretching of the myocardium
   b. Can be a calculated as the change in pressure divided by change in volume, which is the instantaneous slope of the pressure-volume curve in the filling phase
   c. Beyond a volume of 40 mL in the adult heart, the left ventricle becomes more difficult to fill, and shows lower elastance.
   d. A heart with left ventricular hypertrophy shows lower elastance than normal.
   e. In the setting of low elastance, a high LVEDP ay actually reflect a relatively small LVEDV

   Answer is b). Elastance is a measure of the diastolic stiffness of the myocardium, and is the inverse of compliance. Elastance is decreased above approximately 140 mL in the adult left ventricle. Left ventricular hypertrophy results in higher elastance and lower compliance than normal. It is a higher elastance ventricle in which a high LVEDP may actually reflect a relatively small LVEDV.

5. A 74-year-old female with long-standing hypertension and diabetes presents with confusion, fever and hypotension, with a blood pressure of 88/48. She is diagnosed with urosepsis and admitted to an intensive care unit. A prior outpatient echocardiogram showed severe left ventricular hypertrophy, most marked in the upper septal region, with a left ventricular ejection fraction of 65%. Are the following statements true or false?

   a. The concentric hypertrophy confers greater elastance, compared to a normal left ventricle.
   b. Preload is increased in a stiffer left ventricle.
   c. This individual may be particularly sensitive to volume depletion.
   d. After recovery from sepsis, beta-blockers and nitrates should be included in this individual's outpatient medication regimen.

      a. True. A stiffer ventricle has greater elastance, and lesser compliance—these two parameters are inversely related.
      b. False. As a ventricle becomes less compliant, the preload will decrease as the end-diastolic volume achieved with the same degree of venous return and filling time will be less.

c. True. Due to the decreasing end-diastolic volume with worsening left ventricular hypertrophy, this heart becomes more 'preload dependent', meaning that the same reduction in preload will cause a greater fall in stroke volume compared to a structurally normal heart. An individual such as the one described can show significantly reduced stroke volumes in the setting of volume depletion or distributive shock, due to the development left ventricular outflow tract obstruction, with or without systolic anterior motion of the mitral valve. This patient's blood pressure will likely improve markedly when the preload is augmented, for example, by intravenous volume resuscitation.
d. False. Beta-blockers are often indicated in patients with significant left ventricular hypertrophy, or hypertrophic cardiomyopathy. By reducing heart rate, the diastolic ventricular filling period is increased, so improving the preload. Conversely, nitrates cause venodilatation and a reduction in preload, and hence may decrease this patient's preload and induce a left ventricular outflow tract gradient.

6. A 60-year-old male with coronary artery disease, hypertension, and active tobacco use presents with chest pain and inferior ST elevations. He was also noted to be in complete heart block with a heart rate of 48 bpm. At emergent cardiac catheterization there was an acute right coronary occlusion, which was successfully intervened upon. However, the peak troponin T was 28 ng/mL, signifying a significant inferior myocardial infarction. On arrival in the coronary intensive care unit the blood pressure was 90/72, with a right atrial pressure of 21, PA pressure 27/17, pulmonary capillary wedge pressure 14, cardiac index 1.8 l/min/m^2. Are the following statements true or false?

a. Passive leg raising could be used as a measure of preload dependence.
b. Positive end-expiratory pressure will not affect the cardiac index as the pulmonary capillary wedge pressure is normal.
c. Atrioventricular pacing would be expected to improve the cardiac index.
d. Use of dobutamine in this setting will increase the preload.

a. True. Passive leg raising provides an 'endogenous fluid challenge' and temporarily enhanced venous return and therefore preload. If the blood pressure and/or cardiac index improves immediately after this maneuver, it suggests that the patient will be responsive to volume resuscitation. The scenario described is consistent with a right ventricular infarction. In this setting, the blood pressure and cardiac index often improve with judicious use of small fluid boluses, as the patient is highly preload dependent.
b. False. Mechanical ventilation with positive end-expiratory pressure will hinder venous return to the thorax during inspiration and hence may decrease stroke volume, especially in the heart with inadequate preload.
c. True. The loss of atrial contraction, which usually supplies approximately 20% of ventricular filling, may be particularly detrimental for the preload-dependent right ventricle in this individual. Restoration

of atrioventricular coordination with temporary pacing wires can significantly augment ventricular performance.

d. False. Use of dobutamine in this setting would be expected to enhance contractility and decrease the right ventricular afterload by inducing some vasodilatation in the pulmonary vasculature. The preload may be slightly decreased by systemic peripheral vasculature dilatation.

References

1. Norton JM. Towards consistent definitions for preload and afterload. Adv Physiol Educ. 2001;25:53–61.
2. Mohrman DE, Lois JH. Cardiovascular physiology, Lange physiology series. 5th ed. London: McGraw Hill; 2003.
3. Schuster M, Nave H, Piepenbrock S, Pabst R, Panning B. The carina as a landmark in central venous catheter placement. Br J Anaesth. 2000;85:192–4.
4. Daily EK, Schoroeder JS. Techniques in bedside hemodynamic monitoring. 2nd ed. St. Louis: Mosby; 1994.
5. Badesch DB, Champion HC, Sanchez MA, Hoeper MM, Loyd JE, Manes A, McGoon M, Naeije R, Olschewski H, Oudiz RJ, Torbicki A. Diagnosis and assessment of pulmonary arterial hypertension. J Am Coll Cardiol. 2009;54(1 Suppl):S55–66.
6. Ross Jr J, Braunwald E. Studies on Starling's Law of the Heart: IX. The effect of impeding venous return on performance of the normal and failing human left ventricle. Circulation. 1964;30:719–27.
7. Rothe CF. Physiology of venous return. An unappreciated boost to the heart. Arch Intern Med. 1986;146(5):977–82.
8. Tyberg JV. Venous modulation of ventricular preload. Am Heart J. 1992;123(4 Pt 1): 1098–104.
9. Johnson LR. Essential medical physiology. 3rd ed. San Diego: Academic; 2003.
10. Peters J, Fraser C, Stuart RS, Baumgartner W, Robotham JL. Negative intrathoracic pressure decreases independently left ventricular filling and emptying. Am J Physiol. 1989;257(1 Pt 2): H120–31.
11. Forrester JS, Diamond G, McHugh TJ, Swan HJ. Filling pressures in the right and left sides of the heart in acute myocardial infarction. A reappraisal of central-venous-pressure monitoring. N Engl J Med. 1971;285(4):190–3.
12. Ahrens TS, Taylor LA. Hemodynamic waveform analysis. Philadelphia: WB Saunders; 1992.
13. Warren SE, Dennish G. Vasodilator treatment for acute and chronic heart failure. Br Heart J. 1978;40:1059–60.
14. Yamamuro A, Yoshida K, Hozumi T, Akasaka T, Takagi T, Kaji S, Kawamoto T, Yoshikawa J. Noninvasive evaluation of pulmonary capillary wedge pressure in patients with acute myocardial infarction by deceleration time of pulmonary venous flow velocity in diastole. J Am Coll Cardiol. 1999;34:90–4.
15. Rahimtoola SH, Loeb HS, Ehsani A, Sinno MZ, Chuquimia R, Lal R, Rosen KM, Gunnar RM. Relationship of pulmonary artery to left ventricular diastolic pressures in acute myocardial infarction. Circulation. 1972;46:283–90.
16. Zile MR, Gaasch WH, Carroll JD, Feldman MD, Aurigemma GP, Schaer GL, Ghali JK, Liebson PR. Heart failure with a normal ejection fraction: is measurement of diastolic function necessary to make the diagnosis of diastolic heart failure? Circulation. 2001;104:779–82.
17. Katz AM. Ernest Henry Starling, his predecessors, and the "law of the heart." Circulation. 2002;106:2986–92.

18. Starling EH. The Linacre lecture on the law of the heart. In: Chapman CB, Mitchell JH, editors. Starling on the heart. London: Dawsons of Pall Mall; 1965. p. 119–47.
19. Ross J Jr, Franklin D, Sasayama S. Preload, afterload, and the role of afterload mismatch in the descending limb of cardiac function. Eur J Cardiol. 1976;4 Suppl:77–86.
20. Julian FJ, Morgan DL. The effect on tension of non-uniform distribution of length changes applied to frog muscle fibres. J Physiol. 1979;293:379–92.
21. Fuchs F, Smith SH. Calcium, cross-bridges, and the Frank-Starling relationship. News Physiol Sci. 2001;16:5–10.
22. Fuster V, Walsh R. Hurst's the heart, vol. 1. 13th ed. McGraw Hill: Harrington; 2011.
23. Plnsky PR. Hemodynamic evaluation and monitoring in the ICU. Chest. 2007;132:2020–9.
24. Morris AH, Chapman RH, Gardner RM. Frequency of technical problems encountered in the measurement of pulmonary artery wedge pressure. Crit Care Med. 1984;12:164–70.
25. Iberti TJ, Fischer EP, Leibowitz AB, Panacek EA, Silverstein JH, Albertson TE. A multicenter study of physicians' knowledge of the pulmonary artery catheter. Pulmonary Artery Catheter Study Group. JAMA. 1990;264:2928–32.
26. Jellinek H, Krafft P, Fitzgerald RD, Schwarz S, Pinsky MR. Right atrial pressure predicts hemodynamic response to apneic positive airway pressure. Crit Care Med. 2000;28(3): 672–8.
27. Pinsky MR, Brochard L, Mancebo J. Applied physiology in intensive care medicine. Berlin: Springer; 2006.
28. Wong DH, O'Connor D, Tremper KK, Zaccari J, Thompson P, Hill D. Changes in cardiac output after acute blood loss and position change in man. Crit Care Med. 1989;17:979–83.
29. Monnet X, Rienzo M, Osman D, Anguel N, Richard C, Pinsky MR, Teboul JL. Passive leg raising predicts fluid responsiveness in the critically ill. Crit Care Med. 2006;34(5):1402–7.
30. Cheatham ML, Nelson LD, Chang MC, Safcsak K. Right ventricular end-diastolic volume index as a predictor of preload status in patients on positive end-expiratory pressure. Crit Care Med. 1998;26(11):1801–6.
31. Diebel L, Wilson RF, Heins J, Larky H, Warsow K, Wilson S. End-diastolic volume versus pulmonary artery wedge pressure in evaluating cardiac preload in trauma patients. J Trauma. 1994;37(6):950–5.
32. Kraut EJ, Owings JT, Anderson JT, Hanowell L, Moore P. Right ventricular volumes overestimate left ventricular preload in critically ill patients. J Trauma. 1997;42(5):839–46.
33. Tousignant CP, Walsh F, Mazer CD. TEE and preload assessment in critically ill patients. Anesthesiol Analg. 2000;90:351–5.
34. Loubieres Y, Vieillard-Baron A, Beauchet A, Fourme T, Page B, Jardin F. Echocardiographic evaluation of left ventricular function in critically ill patients: dynamic loading challenge using medical antishock trousers. Chest. 2000;118:1718–23.
35. Hoeft A, Schorn B, Weyland A, Scholz M, Buhre W, Stepanek E, Allen SJ, Sonntag H. Bedside assessment of intravascular volume status in patients undergoing coronary bypass surgery. Anesthesiology. 1994;81:76–86.
36. Buhre W, Buhre K, Kazmaier S, Sonntag H, Weylandà A. Assessment of cardiac preload by indicator dilution and transoesophageal echocardiography. Eur J Anaesthesiol. 2001;18: 662–7.
37. Sakka SG, Meier-Hellmann A. Evaluation of cardiac output and cardiac preload. In: Vincent JL, editor. Yearbook of intensive care and emergency medicine. Berlin: Springer; 2000. p. 671–9.
38. Barash PG, Cullen BF, Stoelting RK, editors. Clinical anesthesia. Philadelphia: Lippincott Williams & Wilkins; 2009.
39. McKendry M, McGloin H, Saberi D, Caudwell L, Brady AR, Singer M. Randomised controlled trial assessing the impact of a nurse delivered, flow monitored protocol for optimisation of circulatory status after cardiac surgery. BMJ. 2004;329:258–61.
40. Marik ME. Pulmonary artery catheterization and esophageal Doppler monitoring in the ICU. Chest. 1999;116:1085–91.

Suggested Reading

Daily EK, Schoroeder JS. Techniques in bedside hemodynamic monitoring. 5th ed. St. Louis: Mosby; 1994.
Ahrens TS, Taylor LA. Hemodynamic waveform analysis. Philadelphia: WB Saunders; 1992. Chapters 2 and 3.
Fuster V, Walsh R. Hurst's the heart, vol. 1. 13th ed. McGraw Hill: Harrington; 2011. Part 2, Chapter 5.

Chapter 2
Afterload

Amanda R. Vest and Frederick Heupler Jr.

Understanding the Concept

As discussed in Chap. 1 regarding preload, cardiac afterload is also a semi-quantitative composite assessment of a determinant of cardiac output. The four major determinants of cardiac output are cardiac preload, myocardial contractility, heart rate, and afterload. Afterload is the force against which the heart has to pump to expel blood into the vasculature. In isolated myofiber experiments, myocytes are physically loaded with defined forces in the form of a weight, to the lower end of a vertically mounted quiescent muscle sample. The opposing end of the myofiber remains tethered. The muscle is then electrically stimulated to contract and lift the additional weight. Once stimulated, the muscle develops tension, or force, until it meets and then overcomes the opposing force of the applied load, which is termed the afterload. Once the afterload is exceeded, the weight will be physically lifted and fiber shortening occurs. The degree and velocity of myofiber shortening is inversely related to the afterload applied. If both ends of the muscle sample are tethered and immobilized, or if the afterload applied is in excess of the myofiber's maximal force generation, the resulting contraction will remain isometric, meaning that the fiber length will be unchanged when tension is generated during contraction [1].

An alternate expression of the afterload is as a "stress" (defined as unit force per crosssectional area) enabling comparison of differently sized samples of myofiber. It also permits transfer of the concept to the intact ventricle. Afterload in the whole heart can be understood as the stress encountered by left ventricular myofibers as they contract against the end-diastolic volume. Ventricular wall

A.R. Vest (✉)
Cardiovascular Medicine Fellow, Heart and Vascular Institute,
Cleveland Clinic, Ohio, USA
e-mail: vesta@ccf.org

F. Heupler Jr., MD
The Cleveland Clinic, Cleveland, OH, USA
e-mail: heuplef@ccf.org

S. Anwaruddin et al. (eds.), *Cardiovascular Hemodynamics: An Introductory Guide*,
Contemporary Cardiology, DOI 10.1007/978-1-60761-195-0_2,

forces are difficult to directly measure, but the wall tension can be described by LaPlace's equation through $\sigma = PR/2w$, where σ is wall stress, P is pressure, R is ventricular radius and w is wall thickness. More complex mathematical calculations that take into account chamber geometry can also be used to quantify end-systolic wall stress. It can be seen from the law of LaPlace that a dilated heart, with a greater radius, will have to develop a greater inward force than a smaller heart to generate the same systolic pressure.

Another concept for defining afterload is in terms of the impedance to blood flow entering the aorta, known as arterial input impedance. This parameter quantifies the ratio of change in pressure to change in flow. It can be calculated using values for arterial pressure, elasticity, vessel dimension, and blood viscosity, and requires invasive instantaneous aortic pressure and flow measurements which render it a research tool only. With the two principal determinants of ventricular afterload being systolic pressure and ventricular radius, and because the ventricular dimensions are assumed to remain relatively consistent, the systolic arterial pressure is the parameter most commonly used as a surrogate for afterload in clinical practice. In the absence of aortic or pulmonic stenosis, the maximum systolic pressure beyond the valve reflects the maximum pressure generated by the corresponding ventricle. Hence the peak aortic pressure and peak pulmonary pressure can be measured to reflect the left and right ventricular afterloads, respectively.

An inverse relationship exists between stroke volume and the afterload [2]. As above, this is a consequence of the fact that muscle cannot shorten in excess of the length determined by the total load acting upon it. When this load is increased, sarcomere shortening will stop at a greater length, and so the extent of thick-thin filament overlap and cross-bridge formation will be diminished compared to a lower afterload (Fig. 2.1).

Afterload Physiology and Theory

Afterload and Arterial Vasculature

The forces that oppose ventricular shortening are a summation of factors encountered throughout the arterial tree and can be referred to as arterial impedance. The total systolic load includes not only the impedance to flow from the large arteries, but also the impedance provided by the medium peripheral arteries and smaller arterioles. Hales suggested a simplistic model for the function of the arterial system, with the functions of cushion, conduit, and resistance being fulfilled by the proximal elastic arteries, medium-sized muscular arteries, and peripheral arterioles, respectively [3]. This classic model is useful in defining the differing properties of vessels along the arterial tree and in highlighting the peripheral arterioles as the site of the majority of peripheral resistance.

The three major determinants of arterial impedance are resistance, inertia, and compliance. Resistance in a vessel is described by the Poiseuille equation $R = 8 \times \eta \times l/\pi r^4$, where R is resistance, η represents the viscosity of blood, l is vessel

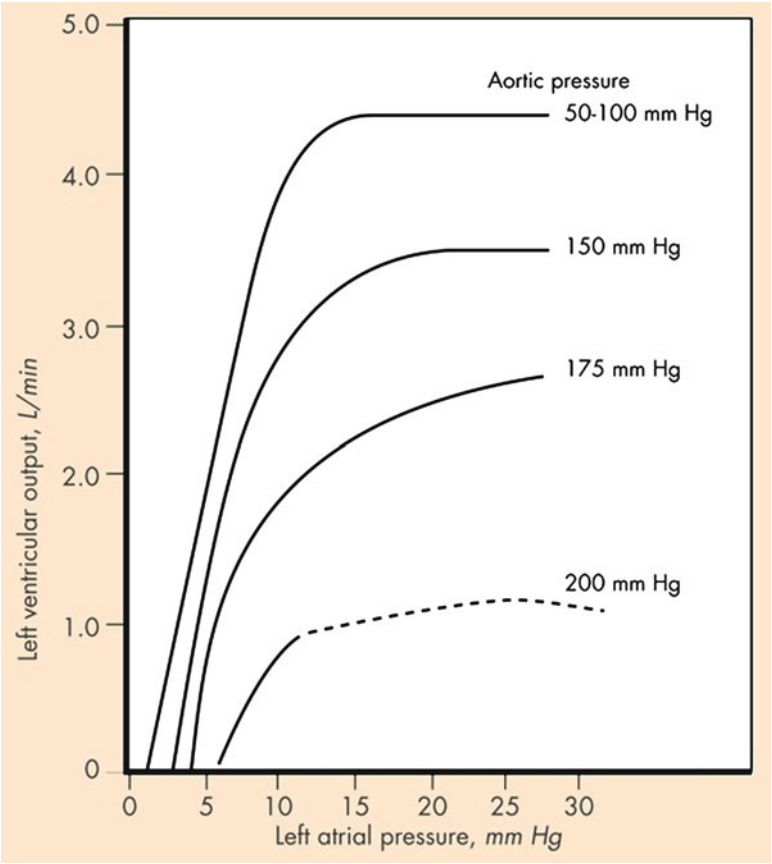

Fig. 2.1 The inverse relationship between afterload and cardiac performance. Sagawa K. Analysis of the ventricular pumping capacity as function of input and output pressure loads (Adapted from Sagawa K. Analysis of the ventricular pumping capacity as function of input and output pressure loads. In: Reeve EB, Guyton AC, editors. Physical Bases of Circulatory Transport: Regulation and Exchange. Philadelphia: WB Saunders; 1967; 141–149)

length, and r is vessel radius. Thus it can be seen that elevated viscosity, such as in polycythemia, will increase resistance to flow. Importantly, resistance is inversely proportional to the fourth power of the radius, enabling small changes in arteriolar diameter to have profound changes on total peripheral resistance [4]. Total peripheral resistance can be expressed with regard to the ascending aorta as $R = P_o/\mathrm{CO}$ where P_o represents the mean arterial pressure, CO is the cardiac output, and R is the total peripheral vascular resistance. This can be re-arranged to $P_o = (\mathrm{CO})R = (\mathrm{SV})(\mathrm{HR})R$ by inputting the equation for cardiac output. This expression allows appreciation that the mean aortic pressure is directly related to both the cardiac output and the peripheral resistance. Inertia, which is related to the mass of the blood column, opposes acceleration of blood flow and is dependent upon the heart rate. Compliance is a property of the vascular walls, with highly compliant vessels being more distensible.

Elastance is the reciprocal of compliance. Compliance is also heart rate dependent; the rate dependence of both inertia and compliance leads to phase shifts between instantaneous pressure and flow within the pulsatile arterial system [1]. The arterial pulse waveform begins with the upstroke imposed by ventricular systole, with a rapid increase in aortic pressure in early systole. The peak proximal aortic flow velocity slightly precedes the peak pressure. The aorta and large arteries expand during systole to accommodate some of the pressure fluctuation. This intermittent input into the proximal system is translated to an almost constant flow into the distal capillary bed, fulfilling the "cushion" function of the Hales model. This is achieved by absorption of stroke volume by the large elastic vessels, with conversion of the energy of systole into stretch of the arterial walls. The walls recoil as pressure within the vessel falls, and the stored energy is returned during diastole to maintain the blood pressure and distal blood flow during this period of the cardiac cycle. This is termed the "Windkessel effect" and is dependent both upon the capacitance of the aorta and large arteries, and the resistance to flow in the smaller vessels that do not show systolic expansion.

Reflected Pressure Waves

An additional potential contributor to the afterload, not accounted for in the Hales model, is the phenomenon of retrogradely reflected pressure waves traveling from the periphery back toward the ventricle. The speed of propagation, known as the pulse wave velocity, is high enough for the reflected wave to arrive in the proximal aorta within the same cardiac cycle and so the reflection overlays the incident wave with both contributing to the arterial waveform. A reflected wave occurring during systole will increase the afterload; a reflected wave arriving in the proximal aorta during diastole is more advantageous as it will augment coronary blood flow. Major sites of reflection are arterial branch points, particularly the renal artery branches off the abdominal aorta, and the iliac bifurcation. The degree of wave reflection can change the pressure and flow waveforms seen in older subjects and in hypertensive individuals. Aging is accompanied by rises in systolic pressure and decreased arterial compliance; diastolic pressures tend to fall slightly. Medial degeneration occurs, which causes progressive stiffening of the aging larger elastic arteries, resulting in elevation of aortic systolic and pulse pressures due to a combination of a rise in the forward incident wave and early return of the reflected wave [5] (Fig. 2.2).

A Framingham sub-study documented the increases in arterial stiffness ("elastance") with advancing age [6]. The result is increased velocity of both the incident and retrograde reflection waves, with an increase in systolic and pulse pressures. The enhanced incident wave raises myocardial oxygen demand, which can induce ventricular hypertrophy over time. In addition, the early return of reflected pressure waves adds to the afterload by augmenting late systolic pressure and removes the diastolic support of coronary blood flow; hence the favorable ventriculo-arterial coupling is progressively lost [7]. Studies have confirmed

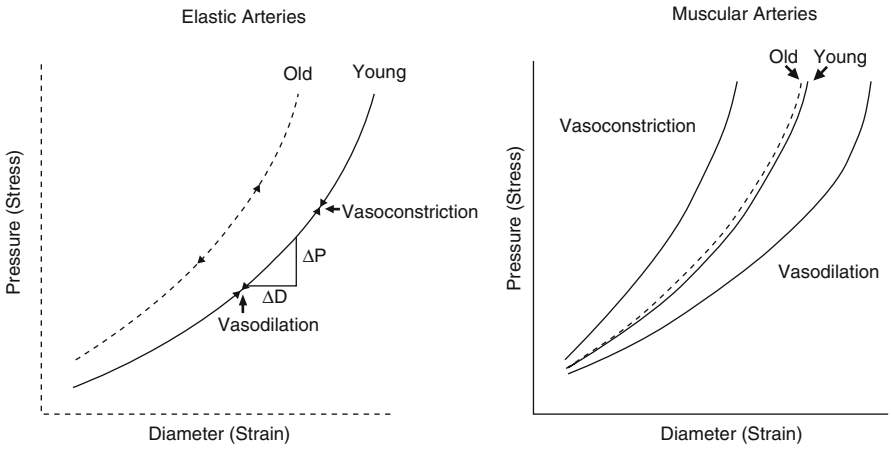

Fig. 2.2 Pressure-diameter relations for elastic and muscular arteries (From Nichols WW, Edwards DG. Arterial elastance and wave reflection augmentation of systolic blood pressure: deleterious effects and implications for therapy. J Cardiovasc Pharmacol Ther. 2001;6:5)

that it is the large central arteries, rather than the peripheral vasculature, that undergo the greatest capacitance changes with age. Decreased compliance in the large arteries may also induce macrovascular damage in organs such as the kidneys and the brain once the "cushion" effect that absorbs systolic pulsations is lost, causing the microvasculature to be subjected to pulsatile flow. The microvasculature is generally considered to include the small arteries of less than 400 μm diameter, arterioles of less than 100 μm diameter and the capillaries with their single layer of endothelial cells. These distal vessels usually receive an almost constant, rather than pulsatile, blood flow. It is hypothesized that a more pulsatile microvasculature flow induced by age-related decline in the Windkessel effect, is a contributor to end-organ damage [8].

Input Impedance and Characteristic Impedance

Parallels have been suggested between the flow of blood in the arterial system and the flow of current within an AC electrical circuit [9]. An analogous electrical circuit would contain capacitors and resistors, with the alternating storage and discharge of the capacitor separating peak pressure and flow. The complex ratio that results from these values has two parts: the magnitude or "modulus" of the impedance and the "phase angle" that represents the number of degrees by which the sinusoidal pressure is separated from the sinusoidal flow. This combined single vector of "impendence" is often translated into arterial impendence. Impedance is defined as the relationship between the pressure difference and flow of sinusoidal signals in a linear system. However, it should be remembered that blood does not

behave sinusoidally, and so biological pressure and flow values must be converted into a fundamental sine wave and a series of harmonic waves using Fourier analysis prior to calculation of arterial input impedance (Z_{in}). A value for impedance is derived from each pair of sine waves of pressure and flow (i.e., harmonics) at their specific phase angle. To validly apply Ohm's law in this setting, the system should be in the steady state (vasomotor tone should be constant), time-invariant (free of beat-to-beat changes in resistance) and linear. The non-linearity of the ventricle during contraction does somewhat limit this technique, with the variations in elastance of the chamber during contraction being unaccounted for. Therefore, it would not be accurate to derive input impedance from invasive values for the left ventricular pressure and aortic flow, because the intervening aortic valve adds significant non-linearity. However, when considering the arterial tree, the variations in pressure and flow are minor enough to enable systemic and pulmonary arterial input impendence to be considered valid mathematical descriptions of the systemic and pulmonary arterial trees, respectively.

When using the impedance concept in a compliant vascular system, the flow will be advanced with respect to the pressure sine wave. This is depicted as −90° in the phase angle. With inertance the flow is delayed, giving a +90° phase angle. The modulus of impedance will decrease with increasing frequency. In a large elastic artery, the compliance and inertia effects interact to keep pressure and flow sine waves in phase. This gives a pulsatile or "characteristic" impedance with a phase angle of 0. In this setting the modulus will be constant and independent of changes in frequency. If the system were without reflection waves, the input impendence would equal the characteristic impedance. However the reflected waves moving retrogradely toward the proximal aorta result in a significant difference between arterial input impedance and the characteristic impedance, which incorporates the reflected waves. This difference is more apparent at lower frequencies, where reflected waves return out of phase. Conversely, at high frequencies the wavelengths are less than the arterial system length and so reflected waves are out of phase and cancel each other out. Therefore, at high frequencies, input impedance is almost equal to characteristic impendence [10]. The aortic input impedance spectrum gives information in the frequency domain about the arterial elastance, pulse wave reflectance, and the peripheral resistance. The clinical relevance is that increases in the pulsatile components—the elastance and reflectance—will lead to ventriculo-arterial mismatch and are therefore detrimental to cardiac efficiency (Fig. 2.3).

Assessing Afterload from Invasive Hemodynamics

Efforts to apply the impedance concept as a clinically measurable tool have been hampered by the complexity of the many advanced analytic functions required to derive values, and hence the much simpler mean aortic pressure or mean systolic pressure remains the more commonly used surrogate of afterload. It is customary to use the mean pressure value because this somewhat accounts for the fluctuations in aortic pressure that occur during the cardiac cycle. Clinically, the invasive measurement of cardiac afterload is usually achieved with a pressure tracing from a fluid-filled catheter with its tip lying just above the aortic valve in the ascending aorta.

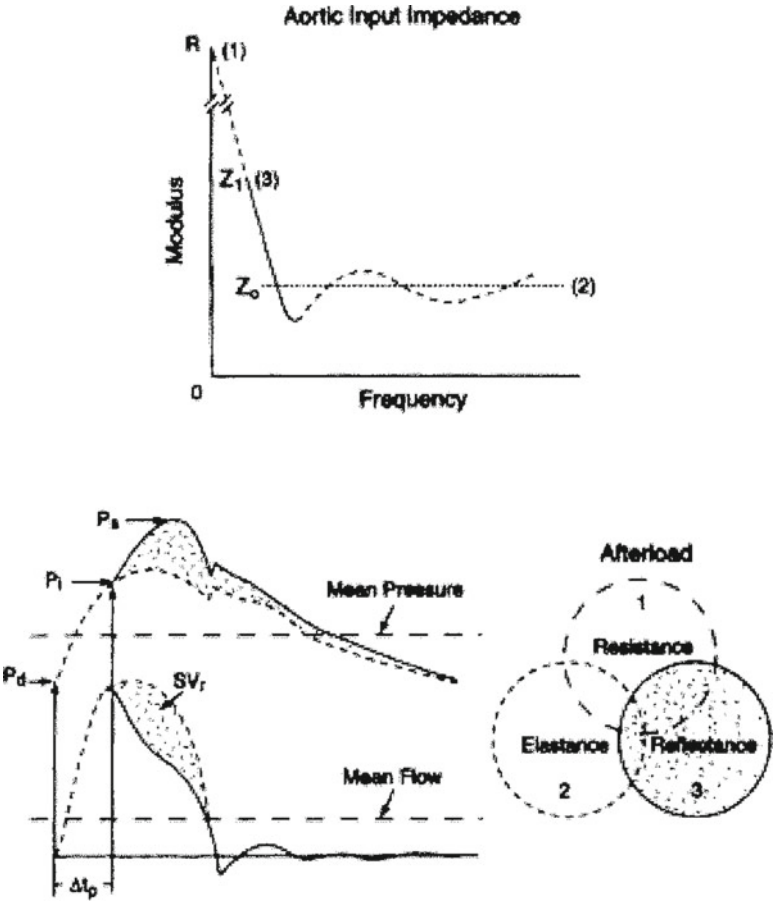

Fig. 2.3 The components of aortic input impedance (From Nichols WW, Edwards DG. Arterial elastance and wave reflection augmentation of systolic blood pressure: deleterious effects and implications for therapy. J Cardiovasc Pharmacol Ther. 2001;6:5)

One phenomenon that the clinician must bear in mind in this setting is the possibility of "pressure recovery." This describes the increase of pressure downstream from a stenosis caused by reconversion of kinetic energy to potential energy, and can be a source of discrepancy between catheter and Doppler valvular pressure gradients. Bernoulli's theorem, from which Doppler evaluations of flow across a stenosis can be derived, requires that the sum of the pressure head, potential energy, and kinetic energy must be equivalent throughout all parts of the flow system. Therefore, in the setting of aortic stenosis, the lowest pressure is found where the velocity is highest and hence where the valve orifice is the smallest. Beyond the stenosis, velocity decreases and so pressure will increase, with the total amount of pressure increase (pressure recovery) being dependent upon the dissipation of kinetic energy due to flow separation and vortex formation across the valve. The consequence is that when Doppler gradients are measured at the point of minimal diameter of the stream

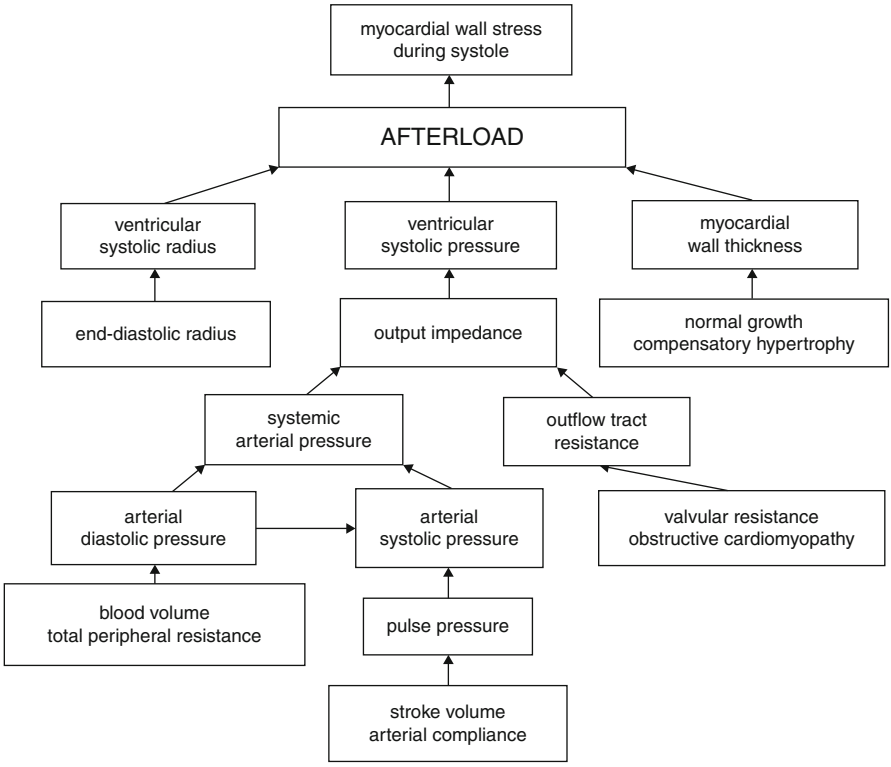

Fig. 2.4 Factors determining afterload (From Norton JM. Toward consistent definitions for preload and afterload. Adv Physiol Educ. 2001;25(1–4):53–61)

of blood flow (the "vena contracta"), they will be higher than the invasive catheter measurements obtained in the proximal aorta, where pressure has been recovered. It has been noted that in milder aortic stenosis the cusps of the valve form a funnel-shaped orifice and cause greater pressure recovery than in a more severely stenosed valve [11]. The extent of the phenomena is also dependent upon the relationship between the dimensions of the valve orifice and the ascending aorta. A smaller aorta will lead to a lesser pressure loss and hence increased pressure recovery, compared to a larger aorta with the same degree of aortic stenosis.

The complexity of the relationship between the contracting ventricle, the arterial system, and its blood flow is such that finding a single parameter to fully encompass the cardiac afterload is probably impossible (Fig. 2.4).

Ventricular Wall Stress Versus Arterial Input Impedance

As previously introduced, aortic input impedance is only one of two biophysical concepts available to define afterload; the other is ventricular wall stress, defined

by LaPlace as $PR/2w$. Wall stress also carries with it some clinical limitations, as the values for pressures and dimensions are instantaneous and cannot account for rapidly changing loads encountered during the cardiac cycle. The calculations are also highly dependent upon ventricular geometric assumptions. The two differing afterload approaches of input impedance and wall stress have been compared in their validity as indicators of ventricular performance. Ross et al constructed an animal model protocol to elucidate the relative importance of wall stress and impedance in negatively impacting ventricular stroke volume. These early experiments concluded that the dominant factor in regulating ventricular performance, as demonstrated by reduced fractional shortening, was the level of wall stress, rather than input resistance or pulsatile impendence [12].

Afterload Mismatch

Allied to this observation is the recognition that when pulsatile impedance is greater, changes in mean resistance produce greater changes in wall stress. This is presumably the result of the large increase in ventricular volume when pulsatile resistance rises, again emphasizing the impact of ventricular geometry on the outcome of these maneuvers. This appreciation led to the concept of "afterload mismatch" in 1976, as a framework for assessing the matching between the afterload and the inotropic state in the whole heart. Under normal physiologic circumstances, an increase in afterload is usually accompanied by increased venous return (due to movement of blood from the arterial to venous systems) and hence increased end-diastolic volume. This helps to maintain stroke volume in the face of an increased afterload. A mismatch can be induced acutely in a normal heart if end-diastolic volume is not allowed to compensate for the increase in afterload [13]. The result will be a fall in stroke volume, ejection fraction and ventricular circumference. An example of mismatch creation could be a scenario with sudden infusion of vasopressor into a volume depleted vascular system, or in the setting of partial inferior vena cava occlusion. An afterload mismatch can also be induced in a normal left ventricle in the opposite hemodynamic situation when the limit of preload reserve has already been reached and the average sarcomere length exceeds 2.2 μm. Additional afterload applied to the ventricle already working at a maximal end-diastolic volume will cause a sharp drop in stroke volume, unless contractility is also enhanced by an inotrope. Thus an applied afterload stress can serve as an indicator that a heart is operating near either the upper or lower limits of preload [14]. The concept that afterload mismatch can exist even in the basal state explains why therapeutic afterload reduction in conditions such as severe left ventricular dysfunction or mitral regurgitation can significantly improve cardiac output, so long as preload is maintained.

In addition to the acute afterload response studies on the intact heart in unanesthetized large animal subjects, the longer term effects of a sustained increase in afterload have also been extensively studied in animal models. Ross et al. instrumented 12 dogs with ultrasound transducers placed across the left ventricle for measuring

the extent and velocity of wall shortening, and a micromanometer measuring left ventricular cavity pressure. Transaortic constriction was performed using an inflatable rubber cuff around the proximal aorta to maintain an average systolic blood pressure of 210 mmHg. Ventricular pressures and dimensions were recorded prior to constriction, immediately after constriction, at an early phase after constriction (average 9 days) and a later phase (average 2.5 weeks). Calculations of wall forces relied on a spherical model. Immediately after constriction there was a decrease in ventricular wall thickness, and a 55% increase in calculated peak wall stress above control. Percentage shortening fell by 24% acutely and mean circumferential shortening velocity (V_{CF}) decreased by 39% from control. In the acute phase (mean 9 days) the ventricles were seen to dilate with a 4% increase in end-systolic diameter and peak wall stress fell to 37% above control despite a constant peak systolic left ventricular pressure averaging 210 mmHg. Percentage shortening and mean V_{CF} remained below control levels at −12 and −20% respectively. By the later phase at mean 2.5 weeks, the left ventricular walls had significantly hypertrophied with a 15% increase in ventricular wall crosssectional area above control, with the increased wall thickness successfully reducing peak wall stress to 22% above control. End-diastolic diameter and percent shortening returned to normal [14]. The ventricle was considered to have successfully compensated at this time point by resuming its baseline fractional shortening in the face of a marked sustained elevation in afterload. This study reinforces the concept that the initial afterload mismatch, which causes an acute reduction in stroke volume, can be overcome by the development of physiological hypertrophy with thickened walls once again generating baseline stroke volumes. However, the limited duration in this early proof of concept study does not permit observation of the rapidly hypertrophied heart as it continues to maintain the higher degree of pressure generation against an increased afterload over time. The technique of transaortic banding has been applied to many species of experimental animal models, most commonly mice, enabling investigators to study the development to physiological hypertrophy and, in some settings, subsequent progression to heart failure, so elucidating the myocardial signaling pathways that govern the hypertrophic response [15].

Ventriculo-Arterial Coupling and Pressure-Volume Loops

The relationship between the ventricle and its afterload is key to the concept of ventriculo-arterial coupling, and can be illustrated by pressure-volume loops. The effective arterial elastance (E_a) describes the ability of the vessel to accommodate pulsatile flow. E_a can be calculated by dividing the end-systolic pressure by the stroke volume and is therefore the slope of the stress/strain or pressure/diameter graphs ($\Delta P/\Delta D$). Elastance is the reciprocal of compliance, compliance being the ease of distension. At lower levels of arterial pressure, the arterial wall is supported by compliant elastin fibers, whereas the stiffer collagen fibers predominate at higher pressures. Therefore the slope of the curve will be greater at higher levels of arterial pressure. Collagen in the human aorta is at least 500 times stiffer than elastin and more than double in aortic wall composition from age 20 to 70 years (Fig. 2.5).

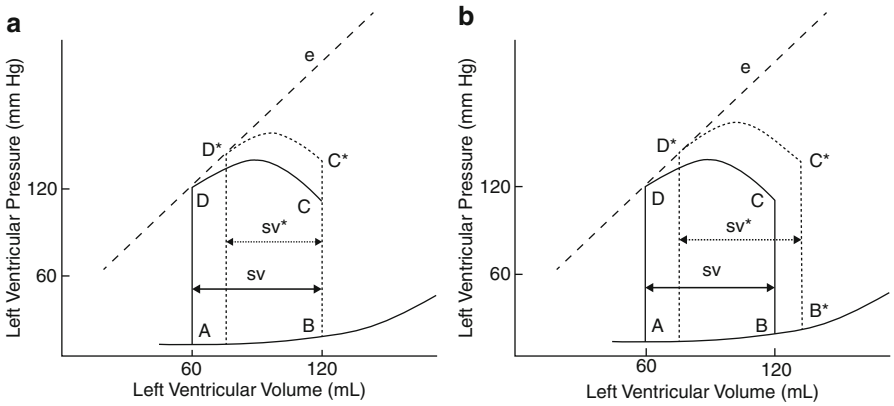

Fig. 2.5 Effects of acutely increasing afterload on the pressure-volume loop (From Loushin MK, Quill JL, Iaizzo PA. Mechanical Aspects of Cardiac Performance. In: Iaizzo PA, editor. Handbook of Cardiac Anatomy, Physiology, and Devices. 2nd ed. New York: Springer; 2009. p. 271–296)

During the left ventricular ejection phase of the cardiac cycle, as ventricular volume decreases, the potential for the ventricle to develop pressure also drops. The smallest volume reached is the end-systolic volume, at which point the whole stroke volume has been ejected. The aortic valve subsequently closes and the diastolic phase begins. The end-systolic volume at a certain degree of contractility and preload will therefore be determined by the afterload. A rise in aortic pressure, all else being equal, will correlate with a decreased stroke volume and a lower aortic pressure with an increased stroke volume. For example, in an individual with aortic stenosis, the pressure-volume loop may show a higher peak pressure, a lesser stroke volume, and an increased end-systolic volume, so shifting the curve into a taller and narrower configuration. Over time, compensatory hypertrophy will mitigate the high wall stress and improve the ventricle's ability to overcome the high afterload and increase the stroke volume, thus causing the loop to increase in width. With a sudden increase in afterload the stroke volume will be diminished, which causes the end-systolic volume to rise. Over the following few beats the increase in end-systolic volume predominates over the increased end-diastolic volume (which usually augments ventricular function), with the net change being a decrease in stroke volume and hence a decrease in the width of the pressure-volume loop. With a reduced afterload, the left ventricle ejects blood with greater ease, so augmenting the stroke volume and decreasing end-systolic volume. With less blood remaining in the ventricle after the ejection phase, the ventricle will fill to a lesser end-diastolic volume compared to prior to the afterload reduction. Despite this mild reduction in preload, stroke volume shows a net increase because the reduction in end-diastolic volume is less than the reduction in end-systolic volume.

The ratio of the effective arterial elastance to the E_{es} (which is the slope of the ventricular end-systolic pressure-volume line) represents a measure of pump efficiency in expelling blood into the vasculature. This value can be used as a reflection of the ventriculo-arterial coupling and helps conceptualize the relationship between the pump and the vasculature. As E_a increases initially, the arteries accommodate greater

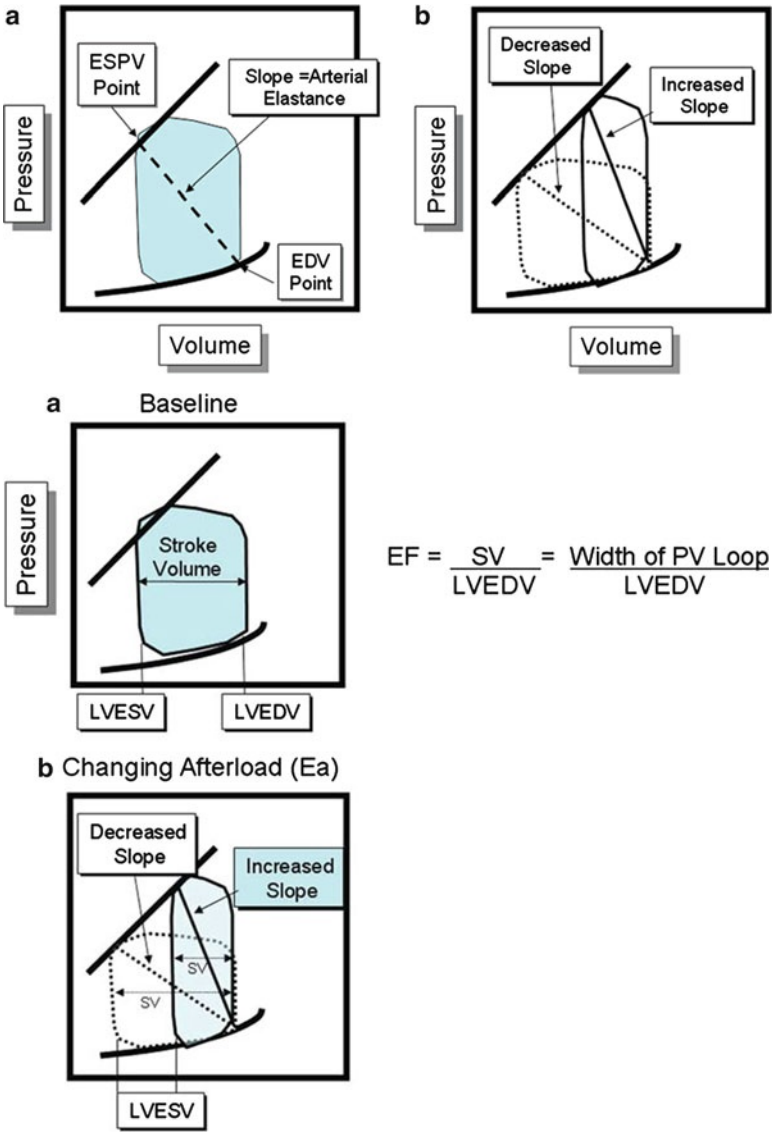

Fig. 2.6 The pressure-volume relationship and elastance (From Bashore TM. Clinical Hemodynamics in Valvular Heart Disease. In: Wang A, Bashore TM, editors. Valvular Heart Disease. New York: Humana-Springer; 2009. p. 93–122)

blood flow, permitting a greater stroke work. If E_a were to continue to increase, the stroke work would reach a maximal plateau value where arterial and ventricular properties are equal, meaning that $E_a = E_{es}$. The E_a also increases with improvements in ventricular efficiency, which is defined by external stroke work/MVO_2/beat. Ventricular efficiency is maximal at $E_a = E_{es}/2$, meaning that the most favorable ventriculo-arterial coupling occurs when the E_a/E_{es} ratio lies in the range 0.5–1.0 [16] (Fig. 2.6).

Afterload and Cardiac Efficiency

The heart requires significant energy generation to perform its functions. Cardiac metabolism is predominantly aerobic, and hence the work performed by the heart is typically gauged in terms of myocardial oxygen consumption (MVO_2). Myocytes are densely packed with mitochondria to generate sufficient ATP, predominantly from fatty acid breakdown, to fulfill the required cellular mechanics to sustain the cardiac cycle. The energy required for development and maintenance of systolic wall tension is a key factor in determining myocardial energy expenditure. One hallmark of the failing heart is its disordered and inefficient myocardial metabolism. The degree of afterload is also highly relevant in the ischemic heart, where reducing afterload and reducing heart rate are the major strategies in reducing myocardial oxygen consumption. A systolic pressure increase of only 20–30 mmHg can have a dramatic negative impact on function in a failing or ischemic left ventricle, both by inducing a lower stroke volume and by raising myocardial oxygen demands. Oxygen extraction in the capillary bed is near-maximal and hence the capacity to meet the oxygen demands of the myocardium may not be possible in the setting of a high afterload, especially if coronary blood flow can no longer be increased due to flow-limiting stenoses. The other determinants of myocardial oxygen demand are the heart rate, preload, and contractility. The MVO_2 in the resting heart is approximately 8 mL O_2/min per 100g [17]. The instantaneous cardiac oxygen consumption can be measured in a human heart by employing the Fick principle; however, this does require catheterization of the coronary sinus to directly measure the venous oxygen saturation and coronary blood flow. Therefore indirect assessments of the MVO_2 are necessary. Relative changes can be estimated by calculating the pressure-rate product. A simple method, described as early as 1912 using isolated cat and rabbit myocardium is multiplication of the heart rate with the systolic blood pressure [18]. This noninvasive hemodynamic determinant of oxygen consumption has been validated by other investigators using the isolated dog heart, with the aortic pressure being shown to be the dominant influence in determining myocardial oxygen requirement. A 175% increase in work with afterload elevation was matched with a 178% increase in oxygen consumption as calculated by the product of coronary flow and coronary arteriovenous oxygen difference [19]. These investigators also established the use of the time-tension index/beat in mmHg seconds, derived from the area under the systolic portion of the aortic pressure curve, as an alternate metric of oxygen consumption. They also point out, by the Law of LaPlace, that the generation of the same intraventricular time-tension index will require greater myocardial fiber tension in a large radius heart compared to a smaller one. This fact highlights the inherent mechanical inefficiency of the dilated failing heart. Also of note is a study using healthy humans that demonstrated a correlation of 0.88 between MVO_2 and heart rate alone and 0.90 using the rate-pressure product [20], although some authors have emphasized the limitations of these indirect indices of MVO_2 which do not capture all potentially important changes in myocardial contractility and ventricular dimensions, particularly in less healthy subjects [21].

The Law of LaPlace can also be used to explain why the pressure-overloaded left ventricle (such as that associated with aortic stenosis) will incur a higher myocardial

oxygen demand than the volume-overloaded ventricle (as in aortic regurgitation). LaPlace stated that wall tension is proportional to $PR/2$, where P is chamber pressure, and R is chamber radius. The pressure-overloaded ventricle shows a large increase in the pressure variable, which will equate to much higher wall tension, and hence MVO_2. Conversely, in the volume-overloaded ventricle the radius will increase, but not as dramatically as the pressure in the pressure-overload model. Hence the rise in wall stress in the volume overload setting will be less substantial, and the corresponding MVO_2 less dramatically elevated.

Afterload in Clinical Practice

Afterload in the Pulmonary Vasculature

Afterload is most frequently discussed in reference to the left ventricle, but can also be applied to the right ventricle and the pulmonary vasculature into which this chamber pumps. It should be noted that significant differences exist in the manners in which the right and left ventricle handle increases in their afterloads. Normally the resistance to flow in the pulmonary vascular system is much lower at about one-tenth of the resistance met by the left ventricle for the same stroke volume. The thicker walled left ventricle is able to generate much greater pressures and usually successfully generates unchanged stroke volumes in the face of afterload increases. The right ventricle operates much nearer to its full contractility capacity, because it has only a sixth of the muscle mass of the left ventricle and yet performs a quarter of the work. It succeeds in pumping the same cardiac output as the left ventricle due to the much lower resistance in the pulmonary vasculature than the systemic circulation. Operating within this closely matched ventriculo-arterial framework, the right ventricle is extremely sensitive to elevations in its afterload. Even a structurally normal right ventricle may decrease its stroke volume to small elevations in pulmonary vascular resistance. However, the right ventricle can also remodel and adapt to higher pulmonary pressures with time, with the maximal mean artery pressure normally accommodated without right ventricular failure being in the order of 40 mmHg. Severe right ventricular dilatation and dysfunction usually results from its attempts to compensate and maintain stroke volume as the pulmonary pressures rise beyond this [22].

- The pulmonary arterioles also serve as the site of major resistance to flow; however, the pulmonary arterioles receive a more pulsatile input of blood flow than their systemic counterparts. Within this much smaller vascular system, the roles of cushion, conduit, and resistance are not as clearly ascribed to certain generations of vessels as in the systemic circulation. Pulmonary hypertension is currently defined as a mean pulmonary artery pressure of greater than 25 mmHg with a pulmonary capillary wedge pressure less than 15 mmHg [23]. The various etiologies of pulmonary hypertension all tend to show common histopathology

features, namely initial fibrosis, medial thickening, and pulmonary arteriolar occlusion [24]. Right ventricular afterload reduction with pulmonary vasodilators is key to the management of pulmonary hypertension and right ventricular failure. Inhaled nitric oxide has a role during the invasive assessment of pulmonary vascular pressures to help determine the potential for pulmonary vasodilatation, and the use of continuous oxygen therapy can help reduce the degree of hypoxic vasoconstriction. Pulmonary hypertension therapeutics include calcium channel antagonists (nifedipine, amlodipine), prostacyclin analogs (epoprostenol, treprostinil, iloprost), endothelin receptor antagonists (bosentan, ambrisentan), and phosphdiesterase-5 inhibitors (sildenafil) [25].

Afterload and the Respiratory Cycle

The potential for mechanical ventilation to affect invasive assessments of preload (such as the right atrial and pulmonary capillary wedge pressures) and possibly reduce preload by decreasing the pressure gradient into the thorax was discussed in Chap. 1. Positive pulmonary pressures during mechanical ventilation also affect afterload. The degree of pulmonary vascular resistance, and hence RV afterload, is proportional to the degree of airway pressure elevation. With significant RV afterload elevations the right ventricle will dilate and induce intraventricular dependence, with shifting of the septum into the left ventricle, which reduces left ventricular filling and stroke volume. Conversely, the direct effect of positive airway pressure on the left ventricle is to increase stroke volume by increasing the intrathoracic aortic pressures relative to peripheral arterial pressure. Also worth mentioning in the consideration of valvular lesions and afterload is the effect of mitral regurgitation on the degree of cardiac afterload. Mitral regurgitation will decrease afterload because, during ventricular systole, a fraction of the left ventricular end-diastolic volume will take a retrograde route and flow back into the left atrium through the incompetent valve. Hence the left ventricle will be working against a reduced afterload, as some blood ejection is into the lower-pressure atrium rather than the usual anterograde flow into the higher-pressure aorta.

Total Peripheral Resistance

The term “total peripheral resistance” (TPR) encompasses the sum of all regional resistances in the systemic circulation. It is sometimes used to infer the total afterload faced by the heart, although as we have already seen the resistance to flow, largely imposed by the arterioles, is actually only one component of the complete cardiac afterload. TPR can be approximated from Ohm’s law. In the patient with Swan-Ganz calculations of cardiac output, values for systemic vascular resistance

(SVR) and pulmonary vascular resistance (PVR) are routinely derived in Wood units from:

SVR = 80 x (mean arterial pressure – mean right atrial pressure) / cardiac output

PVR = 80 x (mean pulmonary artery pressure – pulmonary capillary wedge pressure) / cardiac output

These equations give values in dyn s cm^{-5}. Other units for measuring vascular resistance are pascal seconds per cubic meter (Pa s/m^3), or for convenience when using pressure in mmHg and cardiac output in l/min resistance can be expressed in mmHg min/L. This equates to hybrid reference units (HRU), also known as Wood units, favored by pediatric cardiologists. Multiplying by a factor of 8 converts from Wood units to MPa.s/m^3, or by a factor of 80 to convert from Wood units to the international unit of dyn.s.cm^{-5}.

The resistances imposed by the arterial system are arranged in both serial and parallel orientations. In a circuit where resistances lie in series, the total resistance will be the sum of the individual resistive components. Conversely a parallel circuit will have a total resistance equaling the sum of the reciprocals of the individual resistive components, thus creating a much lower overall resistance than in a series circuit. Therefore, most organ arterial supplies are configured in a parallel arrangement, so limiting the pressure generation required by the ventricle to perfuse all organs. A rise in resistance within one organ bed will have minimal impact on the other arterial beds.

The majority of the resistance component of arterial input impedance lies in the arterioles. These vessels range from 10 to 150 μm in diameter and are under constant vasoactivity regulation from the sympathetic nervous system and local mediators, thus controlling the flow of blood into specific capillary beds. Local vasodilators include platelet-derived substances such as serotonin, and endothelium-derived mediators such as nitric oxide.

Therapeutic Afterload Reduction

The concept of therapeutic afterload reduction was initially clinically applied in the form of intra-aortic balloon counterpulsion to support patients with cardiogenic shock post myocardial infarction. This technique was demonstrated to unload the left ventricle, enhance left ventricular ejection fraction, and improve coronary artery perfusion. Pharmacological strategies for unloading the left ventricle, principally the use of a sodium nitroprusside infusion, have also become useful tools in acute cardiac care. Nitroglycerin, which combines more venodilation with arteriolar vasodilation in comparison to nitroprusside, may also be used for afterload reduction. Hydralazine and the ACE inhibitors are additional options. Vasodilating drugs have little direct effect on the large elastic arteries, but can markedly reduce the amplitude of reflected waves from the periphery. The decreased amplitude and velocity of the reflected wave results in a general decrease in systolic arterial pressure and increased proximal aortic flow during the deceleration phase. The resulting afterload reduction can help to optimize

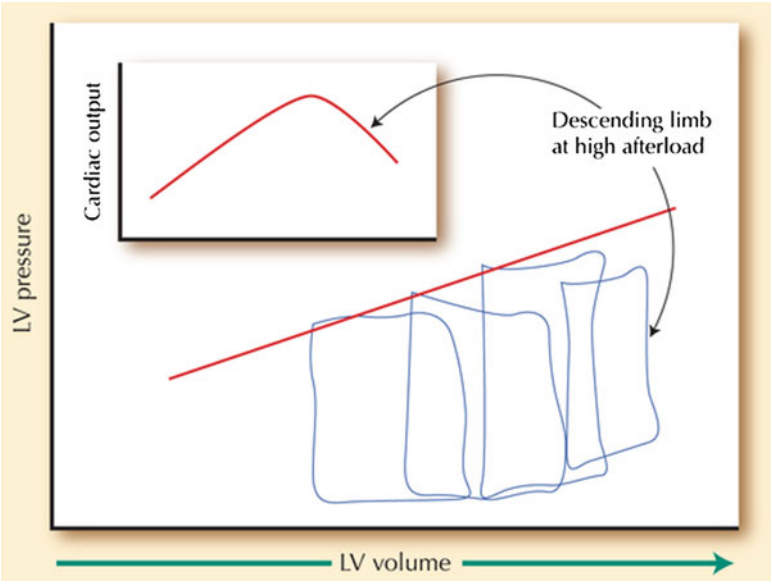

Fig. 2.7 Conditions for afterload mismatch in systolic heart failure (From Ross J, Jr. Afterload mismatch and preload reserve: a conceptual framework for the analysis of ventricular function. Prog Cardiovasc Dis. 1976; 18:255–264)

cardiac output and clinical status in patients with cardiogenic shock, severe mitral or aortic regurgitation, or even aortic stenosis with decompensated left ventricular dysfunction[26], by correcting the afterload mismatch. The afterload tends to be high in decompensated heart failure due to activation of the renin-angiotensin-aldosterone system, as well as a higher effective blood velocity due to slow forward flow. Although the sympathetic activation causing vasoconstriction in heart failure is compensatory to maintain arterial blood pressure despite low output, these adaptations can be counterproductive and impose further afterload on the failing ventricle. Pharmacological afterload reduction can therefore achieve marked improvements in cardiac output and symptoms (Fig. 2.7).

The use of afterload reduction in patients with aortic stenosis may initially seem counterintuitive as the cardiac output across a stenotic aortic valve has traditionally been considered to be fixed with a risk of hypotension without improvements in output if the blood pressure is lowered. However, this scenario underlines the complexity of afterload, because the aortic stenosis in not actually the sole factor determining the force against which the ventricle must pump. Resistances in series are additive, and so the resistive component of aortic input impedance can still be lowered by reducing the most distal resistances in the arterioles despite the proximal resistance across the valve remaining constant. The reduction in total peripheral resistance and hence mean arterial pressure with nitroprusside can therefore successfully reduce the afterload mismatch of the dysfunctional ventricle pumping against a high afterload despite the presence of severe and fixed aortic stenosis. Conversely, the administration of nitroprusside to a

relatively normal cardiovascular system, or to the heart with aortic stenosis but a preserved ejection fraction, would be expected to lower the cardiac output. This is due to some concurrent venodilation, which will reduce preload and actually induce an afterload mismatch. Another setting where pharmacological afterload reduction can precipitate a worsened clinical status is in the setting of a significant pulmonary shunt. Nitroprusside can inhibit the hypoxic vasoconstriction in a region of pulmonary vasculature, thus supplying blood flow to an area of the lung not receiving good oxygenation (for example due to lobar consolidation). This will exaggerate a perfusion-ventilation mismatch and potentially worsen the arterial oxygen saturation. The use of nitroprusside as a lone afterload reducer in the setting of ischemia should also be avoided. Nitroprusside has been shown to decrease myocardial perfusion in the setting of coronary stenoses, whereas nitroglycerin can enhance myocardial perfusion, largely through dilatation of coronary collateral vessels [27].

Bullet Point Summary

- Afterload consists of the forces against which the heart pumps to expel blood into the vasculature.
- Afterload can be defined in terms of wall stress, using the law of LaPlace.
- Alternatively, afterload can be conceptualized as arterial input impedance, drawing parallels from electrical circuits.
- An inverse relationship exists between stroke volume and afterload.
- The aorta and proximal large arteries have a higher ratio of elastic to collagen and are therefore highly compliant.
- These elastic arterial walls absorb the systolic pulsations in blood flow, converting stored energy into recoil that maintains the pressure and flow during diastole—the Windkessel effect.
- The arterioles are the site of the majority of arterial resistance, with arteriolar tone being highly dependent on the sympathetic nervous system and local mediators.
- Reflected waves from bifurcations and arterial discontinuities can increase afterload when they return to the proximal aorta during systole.
- With aging, or pathological processes such as hypertension, afterload rises due to increased magnitude of the incident systolic wave and also early return of the reflected wave.
- Afterload mismatch is a scenario in which the ventricular performance is not well coupled to the afterload it encounters, which increases myocardial oxygen consumption and decreases cardiac energy efficiency.
- Over time, an afterload mismatch can induce ventricular hypertrophy.
- Intra-aortic balloon counterpulsion, nitroprusside, and ACE inhibitors can decrease systemic afterload.
- Pulmonary vasodilators are the cornerstone of pulmonary hypertension management and decrease the afterload faced by the right ventricle.

Review Questions

1. The primary determinant of cardiac output is:

   a) Preload
   b) Myocardial contractility
   c) Heart rate
   d) Afterload
   Answer is a).

2. Which one of the following statements regarding the vasculature is *false*?

   a) With aging, medial degeneration of the large elastic arteries causes them to stiffen
   b) Vascular compliance is heart rate dependent
   c) The small peripheral vessels show a prominent "Windkessel effect"
   d) Retrogradely reflected pressure waves usually arise from arterial branch points such as the iliac bifurcation
   e) A reflected wave falling during diastolic is more advantageous to the cardiovascular system

   Answer is c). It is the proximal elastic arteries that show the "Windkessel effect." The smaller peripheral arteries and arterioles have the capacity to vasoconstrict substantially, but are not exposed to highly pulsatile blood flow and do not have the elastic properties to permit significant recoil if the pressure within the vessel falls. A reflected wave falling within diastole can help to augment coronary blood flow.

3. Which one of the following statements is true regarding the concept of "afterload mismatch"?

   a) Afterload mismatch can occur when the patient is vasodilated
   b) An increase in afterload is usually accompanied by a decrease in venous return, due to decreased availability of blood in the venous system
   c) Afterload mismatch may occur with sudden infusion of vasopressor in the setting of volume depletion
   d) Afterload mismatch can be induced in a normal left ventricle with high preload, when a sudden increase in both afterload and myocardial contractility occurs
   e) A chronic afterload mismatch does not result in structural myocardial changes

   Answer is c). Under normal physiologic circumstances, an increase in afterload is usually accompanied by increased venous return, due to movement of blood from the arterial to venous systems. A mismatch can be induced acutely in a normal heart if end-diastolic volume is not allowed to compensate for the increase in afterload. Alternatively, additional afterload applied to a ventricle already working at a maximal end-diastolic volume will cause a sharp drop in stroke volume, unless contractility is also enhanced.

4. Which one of the following statements is true regarding potential strategies to reduce afterload clinically?

   a) The goal of intra-aortic balloon counterpulsion is to lower systolic blood pressure and hence reduce afterload
   b) In the setting of some pulmonary conditions, nitroprusside can cause hypoxia
   c) Afterload reduction is strictly contraindicated in the setting of a fixed obstructive lesion such as aortic stenosis
   d) The sympathetic activation causing vasoconstriction in heart failure is compensatory to maintain blood pressure despite low cardiac output, and hence afterload reduction should be avoided
   e) Sildenafil is a selective pulmonary arterial vasodilator and has no effect on the systemic vasculature

   The answer is b). Nitroprusside can inhibit the hypoxic vasoconstriction in a region of pulmonary vasculature, thus supplying blood flow to an area of the lung not receiving good oxygenation (for example due to lobar consolidation). This will exaggerate a perfusion-ventilation mismatch and potentially worsen the arterial oxygen saturation. Intra-aortic balloon counterpulsion augments diastolic blood pressure, thus reducing left ventricular wall stress. Afterload reduction with an IABP or nitroprusside may be indicated in acutely ill patients with severe aortic stenosis and a reduced left ventricular ejection fraction. Vasodilation in the setting of decompensated systolic heart failure can correct an afterload mismatch and improve the cardiac output. Sildenafil does have some peripheral vasodilating affects, and hence dosage may be limited by systemic hypotension.

5. A 70-year-old with severe aortic stenosis (peak/mean pressures by echocardiography 68/42, aortic valve area by continuity equation 0.6 cm^2) presents with worsening dyspnea, lower extremity edema, oliguria, and a 15 lb weight gain. The blood pressure is 88/74. He is peripherally cool and mildly confused. The left ventricular ejection fraction on his most recent echo was 25%. Are the following statements true or false?

   a) Due to the severity of the aortic valve stenosis, they only option for reducing afterload is to valvuloplasty or valve replacement.
   b) There is an afterload mismatch.
   c) Pressure recovery may lead to overestimation of the valve gradient by Doppler measurements, and is more likely to occur with smaller ascending aorta diameter.
   d) The calculated SVR is likely to be elevated; a lower than expected SVR may suggest a septic component to the hypotension.

   a) False. The total resistance presented by the arterial system is a sum of the many components arranged in series through the vasculature. The significant resistive contribution provided by the arterioles is additive to the resistance imposed by the stenotic valve. Therefore, the afterload can be reduced by vasodilatation of the arterioles.

b) True. Although we do not have invasive hemodynamics provided for this patient, the cool peripheries, delayed mentation and oliguria strongly suggest a low cardiac output state. Therefore, the poor ventricular performance is not well matched to the high afterload imposed by the aortic stenosis plus peripheral vasoconstriction due to activation of the rennin-angiotensin system in cardiogenic shock. Better matching of the low stroke volume may be achieved through peripheral vasodilatation, if this can be tolerated by the low blood pressure. Aortic balloon counterpulsion, and/or low doses of intravenous nitroprusside may be successful in improving the cardiac output and stabilizing the decompensated patient ahead of definitive aortic stenosis management.
c) True. Pressure recovery is a phenomenon arising from the decrease in velocity and increase in pressure in the proximal aorta, beyond the stenotic aortic valve. This can lead to overestimation of the valve gradient by Doppler measurements, and is more likely to occur with smaller ascending aorta diameter.
d) True. As described above, the systemic vascular resistance would be expected to be at the higher end, or above, the normal range for SVR. A value in the range of 1,200–2,500 dyn s/cm^5 would be consistent with the scenario. If the calculated value lies much below this, consideration should be made of an additional distributive shock process, such as sepsis. Of note, a patient with cardiogenic shock and a poor cardiac output can sometimes be seen to have an encouraging rise in their mixed venous saturation, cardiac output and a fall in the SVR, with the actual etiology being early sepsis causing peripheral vasodilatation.

6. A 55-year-old female with hypertension, diabetes, and chronic kidney disease presents acutely dyspneic. Her blood pressure is 210/110, heart rate 92 bpm. Her examination is consistent with pulmonary edema. A diagnosis of hypertensive emergency is made. Are the following statements true or false?

a) The decrease in arterial compliance associated with hypertension and diabetes is most pronounced in the arterioles.
b) Effective arterial elastance is calculated by dividing the stroke volume by end-systolic pressure.
c) If the mean arterial pressure is known to be 143 mmHg and the cardiac output 4.0 L/min, the systemic vascular resistance will calculate in the region of 2,500 dyn s/cm5.
d) If this patient receives an arteriovenous fistula in preparation for future hemodialysis, the afterload would be expected to fall and the preload increase.

a) False. The arteriosclerosis associated with hypertension and diabetes is most prominent in the large elastic arteries. The enhanced incident wave increases afterload, as does the early return of reflected pressure waves.
b) False. Effective arterial elastance is calculated by dividing the end-systolic pressure by the stroke volume. It is visualized as the slope on the stress/strain graph.

c) True. MAP = ((2 × diastolic pressure + systolic pressure)/3 = 143. SVR = 80 × (MAP − RA pressure)/cardiac output = 80 × (143 − 15)/4 = 2,560.
d) True. Creation of a shunt from the arterial to venous system would be expected to decrease the afterload by directing blood flow away from the high resistance arterioles into the lower resistance venous system, and so enhancing venous return to the heart. The decreased afterload has been shown to slightly reduce myocardial oxygen demand, but also negatively impacts the coronary blood flow [27].

References

1. Fuster V, Walsh R, Harrington R. Hurst's the heart, vol. 1. 13th ed. New York: McGraw Hill; 2011.
2. MacGregor DC, Covell JW, Mahler F, Dilley RB, Ross J Jr.. Relations between afterload, stroke volume, and descending limb of Starling's curve. American Journal of Physiology. 1974 227;4:884-890.
3. Hales S. Statistical essays: containing haemastaticks. History of medicine series. Library of New York Academy of Medicine. Hafner, New York, 1733. Reproduced in 1964, no. 22.
4. Poiseuille JLM. Recherches experimentales sur le mouvement des liquids dans les tubes de tres petits diametres. Mem Savant Etrangers. 1846;9:433–544.
5. Nichols WW, Edwards DG. Arterial elastance and wave reflection augmentation of systolic blood pressure: deleterious effects and implications for therapy. J Cardiovasc Pharmacol Ther. 2001;6:5.
6. Mitchell GF, Parise H, Benjamin EJ, Larson MG, Keyes MJ, Vita JA, Vasan RS, Levy D. Changes in arterial stiffness and wave reflection with advancing age in healthy men and women: The Framingham Heart Study. Hypertension. 2004;43:1239–45.
7. Hashimoto J, Ito S. Some mechanical aspects of arterial aging: physiological overview based on pulse wave analysis. Ther Adv Cardiovasc Dis. 2009;3:367.
8. O'Rourke MF, Hashimoto J. Mechanical factors in arterial aging: a clinical perspective. J Am Coll Cardiol. 2007;50:1–13.
9. Little RC, Little WC. Cardiac preload, afterload, and heart failure. Arch Intern Med. 1982;142(4):819–22.
10. Westerhof N, Stergiopulos N, Noble MIM. Snapshots of hemodynamics: an aid for clinical research and graduate education. 2nd ed. New York: Springer; 2010.
11. Niederberger J, Schima H, Maurer G, Baumgartner H. Importance of pressure recovery for the assessment of aortic stenosis by doppler ultrasound. role of aortic size, aortic valve area, and direction of the stenotic jet in vitro. Circulation. 1996;94:1934–40.
12. Covell JW, Pouleur H, Ross Jr J. Left ventricular wall stress and aortic input impedance. Fed Proc. 1980;39(2):202–7.
13. Ross Jr J. Afterload mismatch and preload reserve: a conceptual framework for the analysis of ventricular function. Prog Cardiovasc Dis. 1976;18(4):255–64.
14. Ross J Jr, Franklin D, Sasayama S. (1976) Preload, afterload, and the role of afterload mismatch in the descending limb of cardiac function. Eur J Cardiol. 4 Suppl:77–86.
15. Rockman HA, Ross RS, Harris AN, Knowlton KU, Steinhelper ME, Field LJ, Ross J. Jr, and K R Chien Segregation of atrial-specific and inducible expression of an atrial natriuretic factor transgene in an *in vivo* murine model of cardiac hypertrophy. Proc Natl Acad Sci. 1991;88:8277–81.
16. Fuster V, Walsh R. Hurst's the heart, vol. 1. 13th ed. McGraw Hill: Harrington; 2011.

17. Iaizzo PA. Handbook of cardiac anatomy, physiology and devices. Springer 2009, 2nd edn.
18. Rhode E, Ogawa S. Uber den einfluss der mechanischen bedingungen auf die totigkeit und den sauerstaffverback des warmbluterheizens. Arch Exp Path u Pharmakol. 1912;68:401–34.
19. Sarnoff SJ, Braunwald E, Welch Jr GH. Case RB, Stainsby WN. Macruz R Hemodynamic determinants of oxygen consumption of the heart with specific reference to the tension time index Am J Physiol. 1958;192:148–56.
20. Kitamura K, Jorgensen CR, Gobel FL, Taylor HL, Wang Y. Hemodynamic correlates of myocardial oxygen consumption during upright exercise. J Appl Physiol. 1972;32:516–22.
21. Goldstein RE, Epstein SE The use of indirect indices of myocardial oxygen consumption in evaluating angina pectoris. Chest 63(3):302-305,1973
22. EK Daily, JS Schroeder. Techniques in bedside hemodynamic monitoring, 5th edn, St. Louis: Mosby. 1994.
23. Badesch DB, Champion HC, Sanchez MA, Hoeper MM, Loyd JE, Manes A, McGoon M, Naeije R, Olschewski H, Oudiz RJ, Torbicki A. Diagnosis and assessment of pulmonary arterial hypertension. J Am Coll Cardiol 2009; 54: Suppl., S55–S66.
24. Farber HW, Loscalzo J. Pulmonary arterial hypertension. N Engl J Med. 2004;351:1655–65.
25. Khot UN, Novaro GM, Popovi ZB, Mills RM, Thomas JD, Tuzcu EM, Hammer D, Nissen SE, Francis GS. Nitroprusside in critically ill patients with left ventricular dysfunction and aortic stenosis. N Engl J Med. 2003;348:1756–63.
26. Flaherty JT, Magee PA, Gardner TL, Potter A, MacAllister NP. Comparison of intravenous nitroglycerin and sodium nitroprusside for treatment of acute hypertension developing after coronary artery bypass surgery. Circulation. 1982;65:1072–7.
27. Bos WJ, Zietse R, Wesseling KH, Westerhof N. Effects of arteriovenous fistulas on cardiac oxygen supply and demand. Kidney Int. 1999;55(5):2049–53.

Suggested Reading

Fuster V, Walsh R, Harrington R. Hurst's the heart, vol. 1. 1st ed. New York: McGraw Hill; 2011 (Part 2, Chapter 5 and Part 3, Chapter 14.).

Nichols WW, Edwards DG. Arterial elastance and wave reflection augmentation of systolic blood pressure: deleterious effects and implications for therapy. J Cardiovasc Pharmacol Ther. 2001;6:5.

Ross Jr J. Afterload mismatch and preload reserve: a conceptual framework for the analysis of ventricular function. Prog Cardiovasc Dis. 1976;18(4):255–64.

Chapter 3
Contractility

Justin M. Dunn and Frederick Heupler Jr.

Introduction

Myocardial contractility—often referred to as inotropy—is the inherent capacity of the myocardium to contract *independent* of preload and afterload (discussed in Chaps. 1 and 2, respectively). Thus for a given preload and afterload, contractility is a manifestation of all other factors that influence the interactions between contractile proteins. The incorporation of all these factors makes a simple definition of "contractility" difficult, and it is more easily understood through discussions of *changes* in contractility. Clinically, a change in left ventricular contractility can be defined as a change in the work performed per beat at a constant end-diastolic volume and aortic pressure.

Contractility is best understood by assessing the rate of rise of left ventricular pressure, or dP/dt (Fig. 3.1). The contours of these left ventricular pressure curves provide a reasonable index of myocardial contractility. The slope of the ascending limb of each curve indicates the maximal rate of force development by the ventricle. The maximal rate of change in pressure over time, thus the maximum dP/dt, is shown by the tangents to the steepest portion of the ascending limb of each curve. This slope is maximal during the isovolumic phase of systole in the cardiac cycle, from closure of the mitral valve until opening of the aortic valve (Fig. 3.2).

Accurate clinical measurement of contractility is difficult. The ejection fraction (EF), defined as the ratio of stroke volume to end-diastolic volume, is widely used clinically as a noninvasive index of cardiac contractility [1]. It is measured noninvasively with echocardiography. Ejection fraction normally ranges from 55 to 80% at rest, with an EF of less than 55% suggesting depressed myocardial contractility. In the cardiac catheterization lab, the maximum rate of pressure development

J.M. Dunn, MD, MPH • F. Heupler Jr., MD (✉)
The Cleveland Clinic, Cleveland, OH, USA
e-mail: dunnj@ccf.org; Heupler@ccf.org

A.T. Askari et al. (eds.), *Cardiovascular Hemodynamics: An Introductory Guide*, Contemporary Cardiology, DOI 10.1007/978-1-60761-195-0_3,

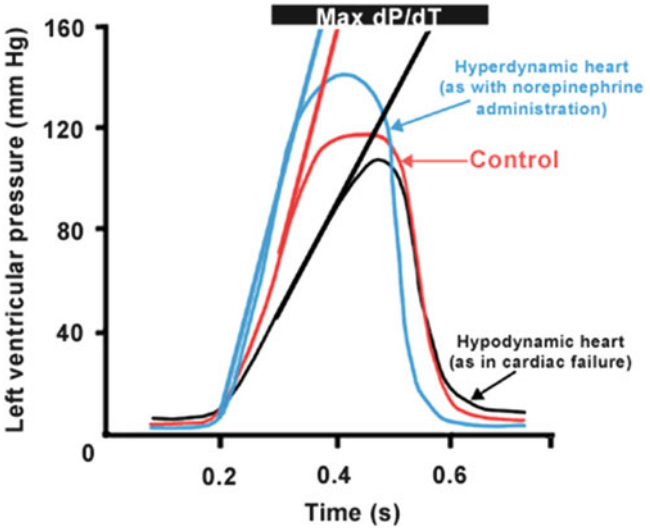

Fig. 3.1 Left ventricular pressure curves with tangents drawn to the steepest portions of the ascending limbs to indicate maximal dP/dt values. *Red*: Control. *Blue*: Hyperdynamic heart, as with norepinephrine administration. *Black*: Hypodynamic heart, as in cardiac failure. (Adapted from Berne and Levy: Physiology, 5th edition, St. Louis, Mosby, p. 313 Figure 16-9)

(dP/dt_{max}) can be measured during isovolumetric contraction by placing catheters directly in the ventricle. This measurement is often used as an index of contractility [2]. Decreases in left ventricular dP/dt_{max} below the normal values of 1,500–2,000 mmHg/s suggest depressed myocardial contractility. New methods of measuring myocardial strain and strain rate via MRI or tissue doppler echocardiography may improve the ability to measure contractility [3].

Physiology of Contraction

Contraction of cardiac muscle begins when a wave of excitation spreads via gap junctions along the myocardial sarcolemma and into the cells via T tubules. During phase 2 of the action potential, calcium permeability in the sarcolemma increases, and calcium enters the cell via calcium channels in the sarcolemma/T tubules (invaginations in the sarcolemma). This extracellular calcium triggers the release of a much larger store of calcium from the sarcoplasmic reticulum within the cell. This calcium then binds to troponin C forming the calcium–troponin complex, which subsequently interacts with tropomyosin to unblock active sites between the thin actin and thick myosin filaments and allows cross-bridge cycling and thus contraction.

To understand the concept of contractility, it is important to revisit the underlying mechanisms by which contractility changes, beginning at the cellular level. This discussion must begin with the fundamental role of calcium in cardiac contraction

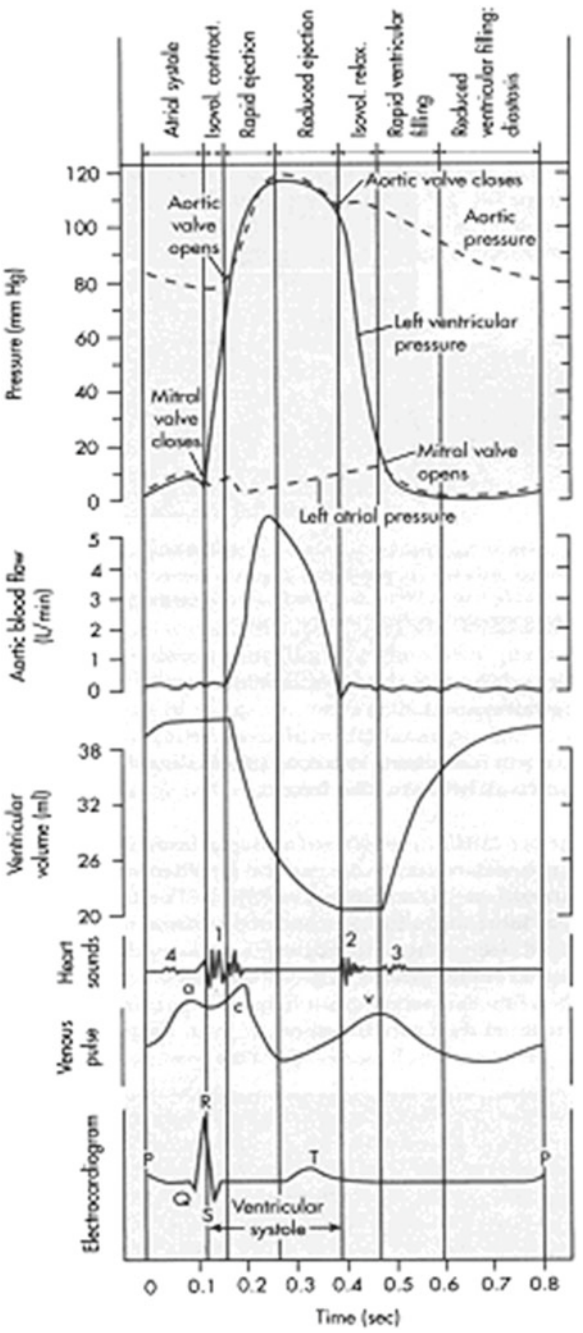

Fig. 3.2 Left atrial, aortic, and left ventricular pressure pulses correlated in time with aortic flow, ventricular volume, heart sounds, venous pulse, and the electrocardiogram for a complete cardiac cycle. (Adapted from Berne and Levy [21], p. 313, Figure 16-10)

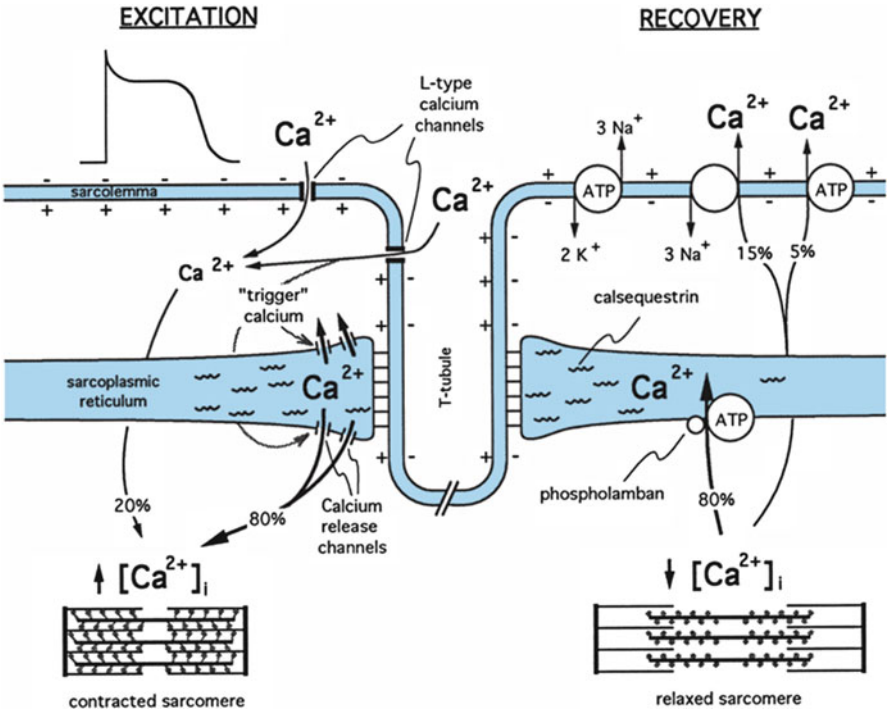

Fig. 3.3 Schematic diagram of the movements of calcium in excitation-contraction coupling in cardiac muscle. The influx of calcium (Ca^{2+}) from the interstitial fluid during excitation triggers the release of Ca^{2+} from the sarcoplasmic reticulum. The free cytosolic Ca^{2+} activates contraction of the myofilaments (systole). Relaxation (diastole) occurs as a result of uptake of Ca^{2+} by the sarcoplasmic reticulum, by extrusion of intracellular Ca^{2+} by Na^{+}–Ca^{2+} exchange, and to a limited degree by the Ca^{2+} pump. (Adapted from Berne and Levy, p. 365 [21])

and relaxation. With each spontaneous wave of excitation in the myocardium, sodium channels in the sarcolemma are opened by an action potential. Sodium moves into the cytosol depolarizing the membrane. Depolarization opens voltage-gated L-type calcium channels in the sarcolemma/T-tubules, allowing an influx of calcium from the extracellular space. Each calcium channel controls a number of calcium release channels which are composed of four ryanodine receptors in the membrane of the sarcoplasmic reticulum. The influx of calcium through the L-type calcium channels triggers a conformational change in the ryanodine receptors which allows calcium to flow from the sarcoplasmic reticulum into the cytosol via the calcium release channels. The amount of calcium released from the sarcoplasmic reticulum is approximately 10 times the amount entering from the extracellular space (Fig. 3.3).

During systole, calcium in the cytosol binds to troponin C, initiating myocardial contraction by relieving the baseline inhibition of the contractile proteins (thin actin filament and thick myosin filament) by troponin I. When cytosolic calcium levels are low, the troponin complex (troponin C/I/T) holds tropomyosin in a position on

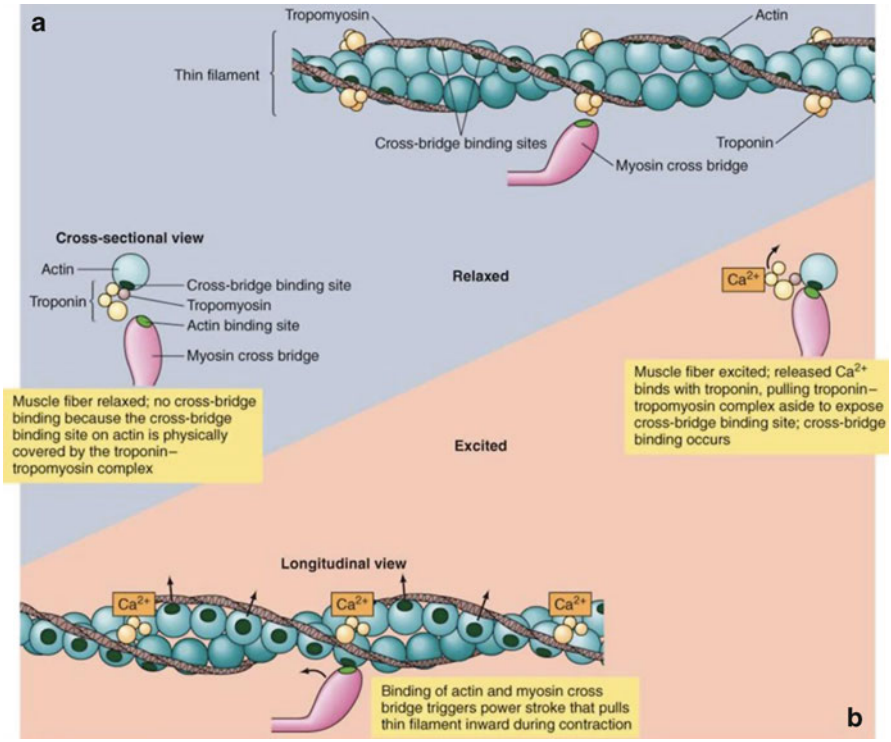

Fig. 3.4 Organization of the thin filament in both the relaxed and excited states. In the relaxed state the myosin binding site on actin is covered by the troponin-tropomyosin complex. In the presence of elevated calcium (Ca^{2+}), the troponin-tropomyosin complex is pulled away from the myosin binding site when Ca^{2+} binds to troponin, allowing the myosin cross-bridge to interact with actin. Hydrolysis of ATP causes a conformational change in the myosin molecule, which pulls the actin filament toward the center of the sarcomere. A new ATP binds to myosin causing release of the cross-bridge. If Ca^{2+} levels are still elevated the cycle repeats. If Ca^{2+} are low, relaxation results

the thin actin filament that prevents interaction between the cross-bridges on the thick myosin filament and the myosin binding sites on the thin actin filament. When calcium binds to troponin C, a conformational change occurs which weakens the bond between troponin I and actin. This conformational change moves the tropomyosin away from the myosin binding sites and allows the myosin cross-bridges to interact with actin (Fig. 3.4).

At the end of systole, the calcium influx from the extracellular space ceases and the sarcoplasmic reticulum is no longer stimulated to release calcium. The sarcoplasmic reticulum then begins to avidly take up calcium via an ATP-dependent process. A cAMP-dependent protein kinase A (cAMP-PKA) phosphorylates phospholamban, which in turn stimulates the sarcoendoplasmic reticulum calcium ATPase (SERCA) pump in the membrane of the sarcoplasmic reticulum to take up calcium and facilitate relaxation. Phosphorylation of troponin I by cAMP-PKA also

inhibits the calcium binding to troponin C, allowing tropomyosin to return to its resting inhibition of the myosin binding sites and allowing diastole.

Cardiac contraction and relaxation are both enhanced by catecholamines, a physiologic phenomenon which has important clinical implications. Catecholamines (primarily endogenous norepinephrine, but also endogenous epinephrine) acting at the ß receptor in the myocardial sarcolemma lead to the formation of cAMP from ATP and activation of PKA, which in turn increases the influx of extracellular calcium via increased opening of L-type calcium channels in the sarcolemma as discussed above. Catecholamines also enhance myocardial contractile force by increasing the rate of calcium release from the ryanodine receptor in response to calcium entry. The inotropic and lusitropic (relaxation) effects of catecholamine stimulation are mediated by the phosphorylation of phospholamban, accelerating calcium uptake into the sarcoplasmic reticulum by the SERCA receptors. Phosphorylation of phospholamban by cAMP-PKA removes its baseline inhibitory effect on SERCA receptors. While less physiologically significant, catecholamine stimulation of $\alpha 1$ receptors increases the formation of inositol 1,4,5-triphosphate (IP3) in the cytosol which also stimulates some calcium release from the sarcoplasmic reticulum.

The parasympathetic nervous system has a much smaller effect on contractility as the vagus nerve fibers, mediated via acetylcholine at muscarinic (M2) receptors, are primarily distributed to the atria with very few to the ventricles. This explains the primary effect of parasympathetic stimulation on heart rate rather than contractility. However, under normal circumstances there is a complex interplay between the sympathetic and parasympathetic nervous systems such that the sympathetic nerve fibers discharge continuously against tonic vagal inhibition.

There are two factors which affect inotropy that are worth mentioning despite the fact they are poorly understood: the Anrep effect and the Bowditch effect. The Anrep effect is the intrinsic ability of the heart to increase inotropy in response to abrupt increases in afterload [4]. This is seen in denervated hearts, suggesting it is an intrinsic mechanism. The other factor is the Bowditch or treppe effect, also called frequency-dependent activation. This is the ability of the heart to increase contractility slightly in the setting of an increase in heart rate [5]. This phenomenon is likely due to the inability of the Na/K-ATPase to keep up with the sodium influx at high heart rates, leading to an increase in intracellular calcium via the sodium-calcium exchanger.

Contractility in Cardiac Disease

Ischemia

Myocardial ischemia causes a decrease in contractility primarily by reducing ATP production in the mitochondria secondary to inadequate oxygen delivery [6]. This reduction in aerobic ATP formation results in dysfunctional contractile shortening and reduced sarcoplasmic reticulum calcium pump function. Under these conditions

there is an increase in glycolysis, glucose uptake, and glycogen breakdown resulting in an increase in pyruvate [7]. Pyruvate is not readily oxidized in the mitochondria and is converted to lactate in the cytosol, resulting in a fall in intracellular pH [8]. When the intracellular pH falls, the sarcoplasmic calcium pump requires even more ATP to function properly [9]. In addition, the calcium concentration required for a given amount of myocyte force generation increases as the pH falls [10]. This leads to more ATP use in order to pump calcium back into the sarcoplasmic reticulum, leaving even less ATP to be used for contraction.

Heart Failure

At low inotropic states, the force-generating capabilities of ventricular muscle strips from normal and failing human hearts are similar [11]. As the inotropic demand increases, however, the ability of the failing heart to maintain its contractility reserve (the ability to increase contractility with heart rate or sympathetic stimulation) is severely depressed [12].

One of the major mechanisms of poor contractile reserve in heart failure is blunted adrenergic effects on myocyte contractility compared to normal myocardium [13]. Myocardium from heart failure patients shows significant reduction in beta-adrenergic receptor density, isoproterenol-mediated adenylyl cyclase stimulation, and contractile response to beta-adrenergic agonists [14]. The poor pump performance of the failing heart produces a reflex-mediated, sustained increase in sympathetic activity to maintain blood pressure [15]. It is this sustained sympathetic activity and an increased concentration of norepinephrine at the beta-adrenergic receptors that induce significant changes in beta-adrenergic signaling and down-regulation of beta-adrenergic receptors [16]. In dilated cardiomyopathy, the ß1 receptor density is selectively reduced compared to the ß2 receptor which maintains its density but appears to be uncoupled from some downstream effector molecules. It is yet unclear whether adrenergic signaling abnormalities are adaptive or maladaptive in heart failure. By reducing LV contractility, desensitization may be detrimental; however, it may also be advantageous by reducing energy expenditure and protecting muscle from the effects of sustained adrenergic stimulation.

A second major mechanism contributing to altered contractility in the failing heart is abnormal calcium regulation within the myocyte. The sarcoplasmic reticulum is altered in heart failure such that the peak systolic cytosolic calcium level is decreased and the uptake of calcium into the sarcoplasmic reticulum is slowed. These abnormalities can explain features of systolic dysfunction including reduced force-generating capacity and slower rates of force decay [17] as well as diastolic dysfunction due to rate-dependent elevations in diastolic calcium levels [18]. There is some evidence to suggest that alterations in SERCA, L-type calcium channels, the ryanodine receptor, Na/K-ATPase, and the Na/Ca exchanger may all play some role in the initiation and progression of heart failure. Research is ongoing to further elucidate the mechanisms of heart failure in the hope that targeted therapies may be developed.

Medications and Contractility [19, 20]

Dobutamine (ß1 > ß2 > α)

Dobutamine is a synthetic sympathomimetic amine that approximates the hemodynamic profile of a pure ß1 agonist. The clinically available formulation is a racemic mixture of enantiomers. Both the (+) and (−) enantiomers stimulate ß1 receptors and, to a lesser degree, ß2 receptors. The (+) enantiomer, however, acts as an α1 antagonist while the (−) enantiomer acts as an α1 agonist. Thus the enantiomers essentially negate one another in their effect on the α1 receptor. The aggregate effect is that of an agonist at the ß1 receptor leading to increased heart rate, contractility, and diastolic relaxation. Dobutamine does have a modest agonist effect at peripheral ß2 receptors causing mild peripheral vasodilation. Due to the increase in stroke volume secondary to its effects on contractility, however, blood pressure often does not change and can even increase despite the peripheral vasodilatory effects. Dobutamine is often used for short-term management of low output heart failure. Usual dosage: 2.5 μg/kg/min initial dose, titrated to desired effect. Max dose is 20 μg/kg/min, though doses over 10 μg/kg/min are rarely needed. Onset is within 1–2 min, with a peak effect in 10 min. Drug effects cease very shortly after the drug infusion is discontinued. Tachycardia and ectopy are seen at higher doses, though these side effects are seen more frequently with dopamine.

Dopamine (D → ß → α)

Dopamine is an endogenous sympathomimetic amine that functions as a neurotransmitter. It is a biosynthetic precursor of norepinephrine and epinephrine, and unlike dobutamine it releases endogenous norepinephrine from stores in the nerve endings in the heart (this is overridden peripherally by prejunctional dopaminergic receptors which inhibit norepinephrine release). At low doses (<3 μg/kg/min) it has a peripheral vasodilatory effect by activating D1 receptors in the renal and mesenteric vascular beds. At intermediate doses (3–10 μg/kg/min) dopamine stimulates ß1 and ß2 receptors increasing heart rate, contractility, and peripheral vasodilation. At high doses (>10 μg/kg/min) dopamine begins to activate peripheral α1 receptors. This effect leads to a progressive increase in peripheral vasoconstriction with increasing doses. At these higher doses the actions of dopamine become more like norepinephrine. Higher doses can also cause pulmonary vasoconstriction, and PCWP may be an unreliable estimate of LVEDP in the setting of a high dose dopamine infusion. Dopamine is typically not recommended for patients with pulmonary edema because its venoconstrictor effects can increase venous return.

Onset of action is within 1–5 min and lasts for approximately 10 min. Tachycardia and ventricular arrhythmias are common at higher doses.

Norepinephrine (ß1 > α>ß2)

Norepinephrine (noradrenaline) is an endogenous neurotransmitter and is a potent ß1 receptor agonist in the heart, with positive inotropic and chronotropic effects. It is also a potent peripheral α1 receptor agonist (more than epinephrine) and causes a dose-dependent increase in systemic vascular resistance. Due to these potent alpha effects, the resultant vasoconstriction limits the inotropic benefit of norepinephrine. It does have a small effect on ß2 receptors. It is synthesized from dopamine and is precursor of epinephrine. Norepinephrine can be used in cardiogenic shock and is considered safer than epinephrine in ischemic disease, though it is still not a first-line choice.

Dosing: Typically start with 8–12 μg/min and titrate or wean to desired effect. Effects are seen within 1–2 min and duration is approximately 1–2 min.

Epinephrine (ß1 = ß2 > α)

Epinephrine (adrenaline) is an endogenous neurotransmitter synthesized from norepinephrine which is relatively nonselective at all receptors, but it primarily gives mixed ß1 and ß2 stimulation with some added α-mediated effects at higher doses. A low physiologic infusion rate (<0.01 μg/kg/min) increases contractility and speeds impulse generation via ß1 activation, but often decreases peripheral resistance and blood pressure via ß2 activation. Higher doses (>0.2 μg/kg/min) increase peripheral resistance when α-medicated constriction dominates over ß2-mediated vasodilation. The positive inotropy, positive chronotropy, and vasoconstriction act together to raise blood pressure.

Epinephrine should typically be avoided in patients with cardiogenic shock due to myocardial ischemia because of the dramatic increases in cardiac work and myocardial oxygen consumption. Usual dosing: for ACLS 1 mg IV (10 mL 1:10,000), for anaphylaxis 0.1 mg SQ/IM (0.1 mL 1:1,000) or 0.1 mg IV (1 mL 1:10,000) over 5–10 min. The effects are seen within seconds of administration and last for 1–2 min.

Isoproterenol (ß1 > ß2)

Isoproterenol (isoprenaline) is a synthetic epinephrine analog. It is a pure ß-agonist with almost no α effect. It has positive inotropic and chronotropic effects in the heart. In the peripheral vessels, ß2 stimulation leads to a decrease in peripheral resistance and often causes a drop in blood pressure. This drug causes a significant increase in myocardial work and oxygen consumption, so it is rarely used in patients with ischemic heart disease. Its use is typically limited to temporary treatment of bradyarrhythmias, refractory torsades de pointes, refractory bronchospasm, and in

cardiac transplant patients to increase heart rate. Dosing: Initially 0.5 μg/min, with most patients responding to 2–20 μg/min. Onset is seen within 30–60 s and lasts anywhere from 8 to 50 min.

Milrinone (PDE-3 Inhibitor)

Milrinone exerts its positive inotropic actions by inhibiting phosphodiesterase in cardiac myocytes. This inhibition reduces the breakdown of intracellular cAMP, ultimately leading to enhanced calcium entry into the cell and increased force of contraction. It also causes some peripheral vasodilation. Milrinone therefore has inotropic, vasodilatory, and minimal chronotropic effects. It is used for short-term management of low output heart failure, similar to dobutamine. Dosing: Initial loading dose of 50 μg/kg over 10 min followed by 0.25–0.75 μg/kg/min. The effect is usually seen within 5–15 min. Milrinone is primarily excreted unchanged by the kidney, so dose adjustments may be necessary in patients with significant renal dysfunction.

Digoxin

It is theorized that digoxin (digitalis) improves contractility via inhibition of the sarcolemmal Na^+K^+-ATPase pump, normally responsible for maintaining transmembrane Na^+ and K^+ gradients. Inhibiting this pump causes intracellular Na^+ to rise which then reduces Ca^{++} extrusion from the cell by the Na^+–Ca^{++} exchanger. This leads to more Ca^{++} being pumped into the sarcoplasmic reticulum with higher amounts of Ca^{++} being released into the myofilaments with each action potential. Increased Ca^{++} release from the sarcoplasmic reticulum enhances the force of contraction. The magnitude of the positive inotropic effect correlates with the degree of Na^+ K^+-ATPase inhibition.

Digoxin is a relatively weak inotropic agent and is used primarily for the treatment of chronic systolic dysfunction, especially if accompanied by an atrial arrhythmia.

Bullet Point Summary

- Contractility, or inotropy, is the inherent capacity of the myocardium to contract *independent* of preload and afterload.
- Contractility is best understood by assessing the rate of rise of left ventricular pressure, or dP/dt.

- In relation to a normal heart, a hypodynamic heart has an elevated end-diastolic pressure, a slowly rising ventricular pressure, and a prolonged ejection phase. A hyperdynamic heart has a reduced end-diastolic pressure, a fast-rising ventricular pressure, and a brief ejection phase.
- Contractility is primarily determined by the way calcium is handled in the cardiac myocyte.
- Ischemia causes reduced contractility primarily via a decrease in ATP production.
- The failing heart loses its contractile reserve via multiple mechanisms, including blunting of the response to adrenergic stimulus and abnormalities in the handling of calcium within the cardiac myocyte.
- Exogenous inotropic agents work to enhance cardiac contractility via several different mechanisms.

Review Questions

1. An influx of calcium into the cell triggers a conformational change in which receptors to allow calcium release from the sarcoplasmic reticulum?

   A. SERCA
   B. L-type
   C. Calcium release channels
   D. Na/Ca exchanger
   E. Ryanodine

   Answer: E. Depolarization of the myocyte membrane causes calcium inflow via voltage-gated L-type calcium channels. This calcium inflow then triggers a conformational change in ryanodine receptors in the sarcoplasmic reticulum membrane which allows calcium to flow out into the cytosol via the calcium release channels.

2. The ability of the heart to increase inotropy in response to abrupt increases in afterload is known as the:

   A. Bowditch effect
   B. Lusitropic effect
   C. ANREP effect
   D. Chronotropic effect
   E. Treppe effect

   Answer: C. The Anrep effect is the intrinsic ability of the heart to increase contractility in response to an acute increase in afterload. This is even seen in denervated hearts. The Bowditch or treppe effect is the ability of the heart to increase contractility in the setting of an increasing heart rate.

References

1. Berne RM, Levy MN. Cardiovascular Physiology. 8th ed. St. Louis: Mosby; 2001.
2. Mohrman DE, Heller LJ. Cardiovascular physiology. 6th ed. London: McGraw-Hill; 2006.
3. Abraham TP, Nishimura RA. Myocardial strain: can we finally measure contractility? J Am Coll Cardiol. 2001;37:371–4.
4. von Anrep G. On the part played by the suprarenals in the normal vascular reactions of the body. J Physiol. 1912;45:307.
5. Bowditch HP. Uber die Eigenthiimlichkeiten der Reizbarkeit, welche die Muskelfasern des Herzens zeigen. Ber Sachs Ges Wiss. 1871;23:652–89.
6. Leidtke AJ. Alterations of carbohydrate and lipid metabolism in the acutely ischemic heart. Prog Cardiovasc Dis. 1981;23:321–36.
7. Young LH, et al. Regulation of myocardial glucose uptake and transport during ischemia and energetic stress. Am J Cardiol. 1999;83:25H–30.
8. Stanley WC. Myocardial energy metabolism during ischemia and the mechanisms of metabolic therapies. J Cardiovasc Pharmacol Ther. 2004;9:S31–45.
9. Fabiato A, et al. Effects of pH on the myofilaments and the sarcoplasmic reticulum of skinned cells from cardiac and skeletal muscles. J Physiol. 1978;276:233–55.
10. Murphy E, et al. Amiloride delays the ischemia-induced rise in cytosolic free calcium. Circ Res. 1991;68:1250–8.
11. Hasenfuss G, et al. Calcium cycling in congestive heart failure. J Mol Cell Cardiol. 2002;34:951–69.
12. Houser SR, et al. Is depressed myocyte contractility centrally involved in heart failure? Circ Res. 2003;92:350–8.
13. Mann DL. Basic mechanisms of disease progression in the failing heart: the role of excessive adrenergic drive. Prog Cardiovasc Dis. 1998;41:1–8.
14. Bristow MR. Beta-adrenergic receptor blockade in chronic heart failure. Circulation. 2000;101:558.
15. Alpert NR, et al. The failing human heart. Cardiovasc Res. 2002;54:1–10.
16. Bristow MR. The adrenergic nervous system in heart failure. N Engl J Med. 1984;311:850–1.
17. Houser SR, et al. Functional properties of failing human ventricular myocytes. Trends Cardiovasc Med. 2000;10:101–7.
18. Beuckelmann DJ, et al. Altered diastolic [Ca2+]i handling in human ventricular myocytes from patients with terminal heart failure. Am Heart J. 1995;129:684–9.
19. Opie LH. Drugs for the heart. 7th ed. Philadelphia: Saunders Elsevier; 2009.
20. Marino PL. ICU book. 3rd ed. Philadelphia: Lippincott Williams & Wilkins; 2007.
21. Berne RM, Levy MN. Physiology. 4th ed. St. Louis: Mosby; 1998.

Suggested Reading

Darovic GO. Hemodynamic monitoring: invasive and noninvasive clinical application. 3rd ed. Philadelphia: WB Saunders; 2002.
Kern MJ. Hemodynamic rounds: interpretation of cardiac pathophysiology from waveform analysis. 2nd ed. New York: Wiley-Liss; 1999.
Ragosta M. Textbook of clinical hemodynamics. Philadelphia: Saunders; 2008.

Chapter 4
Cardiac Output

Marwa Sabe and Frederick Heupler Jr.

Definition and Determinants of Cardiac Output

Cardiac output is defined as the volume of blood ejected from the heart every minute. At rest the normal adult cardiac output is approximately 5–6 L/min [1] and the normal cardiac index is 2.6–3.2 L/min/m^2. Cardiac output is the product of stroke volume and heart rate [2]. The three major determinants of stroke volume, and thus cardiac output, are preload, afterload, and contractility. Preload and contractility are directly correlated to stroke volume while afterload is inversely correlated [2] (Fig. 4.1).

Preload contributes to cardiac output by its effects on stroke volume and heart rate (see Chap. 1). The effect of preload on stroke volume is described by the Frank-Starling mechanism [3]. This law states that the greater the amount of blood that enters the heart, the greater the stretch on the walls of the cardiac chambers, which increases the force of contraction of the heart, and thus stroke volume [3]. However, in isolated heart preparations, if the stretch on the myocardium exceeds a certain point, the opposite occurs, and stroke volume as well as cardiac output decrease. Preload also affects another parameter that contributes to cardiac output: heart rate. Although the common conception is that volume depletion leads to tachycardia due to a reduction in baroreceptor firing, an increase in the effective circulating volume may also lead to an increase in heart rate. With increased stretching on the heart muscle, the heart pumps at a faster rate due to stretch of the sinus node. The stretching of the right atrium also causes the Bainbridge reflex, a sympathetic nervous system-mediated reflex that increases heart rate in response to stretching of the right atrium [4].

Afterload is a force that opposes myocardial contraction (see Chap. 2). It is equal to the tension across the ventricular wall during systole. The Law of Laplace describes the relationship between the determinants of ventricular wall tension, or afterload by

M. Sabe • F. Heupler Jr., MD (✉)
The Cleveland Clinic, Cleveland, OH, USA
e-mail: sabem@ccf.org; heuplef@ccf.org

A.T. Askari et al. (eds.), *Cardiovascular Hemodynamics: An Introductory Guide*, Contemporary Cardiology, DOI 10.1007/978-1-60761-195-0_4,

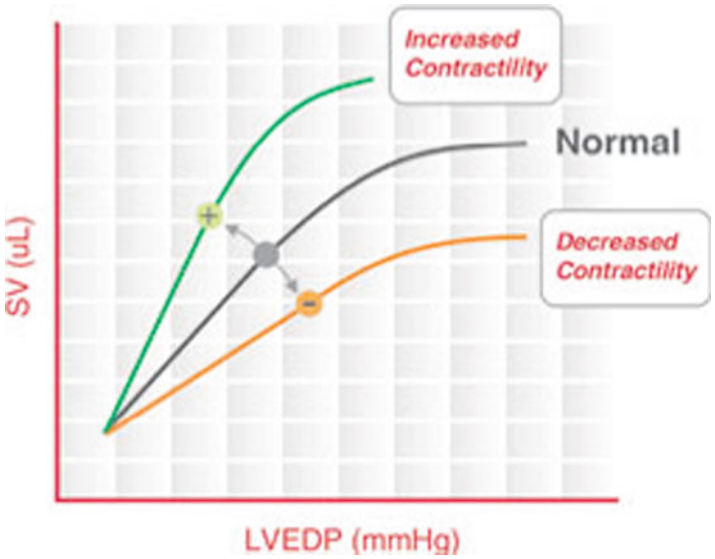

Fig. 4.1 Relationship between cardiac output, preload, and contractility. (*SV* stroke volume; *LVEDP* left ventricular end diastolic pressure, a measure of preload) (Adapted from http://scisense.com/education/cv-application.html)

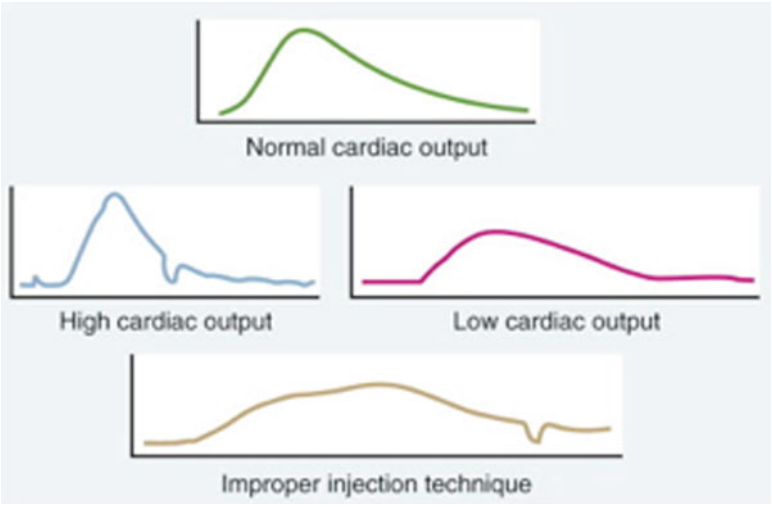

Fig. 4.2 Thermodilution cardiac output curves (Adapted from Braunwald et al. [3])

this equation: $T=(P_r)/h$, where T is tension, P is chamber pressure, r is the radius of the chamber, and h is the wall thickness. In other words, tension (afterload) is directly proportional to ventricular pressure and size (radius) and indirectly related to wall thickness. Ventricular dilation increases afterload, and left ventricular hypertraphy (LVH) is a compensatory mechanism that attempts to decrease afterload [9].

Please refer to Chap. 3 for an in-depth discussion of the relationship between contractility and cardiac output.

Methods of Measuring Cardiac Output

Human tissues require a constant supply of oxygen to maintain aerobic metabolism. This supply may be impaired by low cardiac output and/or inadequate oxygen-carrying capacity of the blood, as in anemia or hypoxemia. When this impairment is severe, the body tissues slowly revert to anaerobic metabolism, producing toxic metabolic breakdown products, such as lactic acid. Therefore, maintenance of cardiac output above the minimum threshold for aerobic metabolism is necessary for the health and survival of body tissues.

In critically ill patients, decreased cardiac output may be related to increased morbidity and mortality [5], therefore, it is essential to have reliable methods to measure cardiac output. There are several clinical parameters that help estimate the adequacy of cardiac output and tissue perfusion including proportional pulse pressure, mental status, urine output, and extremity temperature [6]. The proportional pulse pressure is the ratio of the difference between the systolic and diastolic blood pressures divided by the systolic blood pressure ((SBP-DBP)/SBP). A ratio of less than 25% suggests a cardiac index of less than 2.2 L/min/m^2 [7]. Mental status, specifically, patients falling asleep during their interviews, decreased urine output, and cool forearms and legs are all clinical signs of low cardiac output [6].

There are several methods of measuring cardiac output. These include invasive methods such as thermodilution and Fick methods, which require the use of a pulmonary artery catheter, and noninvasive methods such as transpulmonary thermodilution [12]. Noninvasive clinical measures may help determine whether a patient is in a low output state; however, invasive methods of measuring CO in the ICU are important for precise monitoring and specific therapeutic management.

With the use of a pulmonary artery catheter, CO may be measured directly by the thermodilution method (introduced in 1953 by Fegler) or indirectly by means of the Fick principle [1]. The thermodilution method of measuring CO involves injection of cold fluid into the Swan-Ganz catheter positioned in the pulmonary artery. This injectate flows through the catheter into the right ventricle where it mixes with blood, which is warmer than the injected fluid. This mixture of blood and indicator fluid then moves into the pulmonary artery, where the thermistor at the catheter tip senses temperature changes [8]. With each beat, the blood temperature rises as the cold fluid is washed out of the right side of the heart [1]. A time-temperature curve is electronically obtained, and the cardiac output is calculated using the Stewart-Hamilton Formula. The key components of this formula are cardiac output, amount of indicator, and the integral of the amount of indicator concentration over time. The cardiac output is inversely related to the area under the thermodilution curve as measured by the integral of the amount of indicator concentration over time [3, 8]. When cardiac output is low, it takes longer for the cold fluid to wash out of the right ventricle and thus for the temperature of the blood to return to baseline, producing

a low amplitude, prolonged curve with a large area underneath it. On the other hand, the blood temperature returns to baseline quicker when the injection fluid moves at a faster rate through the heart, as it does with higher cardiac output [3]. This produces a higher amplitude, shorter curve with a smaller area Fig 4.2. The advantage of this method is the use of computer calculations to give quick measurements as well as less need for blood draws. However, this method becomes less useful in patients with CO less than 2.5 L/min as it tends to overestimate the CO in these cases [3]. It also miscalculates CO in patients with tricuspid regurgitation because the indicator fluid is recycled, thus producing a curve that is similar to the low cardiac output curve and thus underestimates CO [9]. On the other hand, left-to-right shunts tend to overestimate the CO as a portion of the injectate crosses through the shunt and thus the temperature change that is detected downstream occurs quickly as would occur in a true high CO state [9].

Another thermal method of measuring CO is the CCO method, or the continuous cardiac output method. This method uses a warm indicator rather than a cold one in the standard thermal dilution [10]. A thermal filament on the right ventricular portion of the pulmonary artery catheter releases small amounts of heat, which is measured by the thermistor at the tip of the pulmonary artery catheter. The CO is automatically calculated and updated every 30–60 s, giving an average CO over 3–6 min. The major disadvantage of this method is that it does not respond quickly in unstable hemodynamic conditions, such as fluid resuscitation or hemorrhage [11].

The Fick principle is employed to provide an indirect measurement of cardiac output that is based on the oxygen saturation of blood samples obtained through a Swan-Ganz catheter. This method was developed by Eugene Fick in 1870, and is based on the principle that the rate of oxygen consumption is equal to the cardiac output multiplied by the rate of oxygen delivery (i.e., the difference between oxygen delivery in the arterial and venous system) [1]. In other words, the lower the cardiac output, the more the peripheral tissues extract oxygen from the red blood cells, and thus the greater the difference in arterial and venous oxygen content. This principle is expressed below:

$$\text{Cardiac Output (L / min)} = \text{VO}_2\text{(mL / min)} / (\text{SaO}_2 - \text{SvO}_2) \times 1.34 \times \text{Hgb} \times 10$$

(VO_2 = oxygen consumption, SaO_2 = arterial oxygen saturation, SvO_2 = mixed venous oxygen saturation)

Cardiac output is usually corrected for body size using this equation: cardiac index (CI) = CO/BSA where CI is the cardiac index and BSA is the body surface area. CI is commonly used in the ICU setting to monitor a patient's hemodynamic status and guide therapy. The normal CI is 2.6–4.3 L/min/m^2 [14], and it is normally lower in elderly persons. In healthy adults, the normal value for VO_2 is 200–300 mL/min, or 110–160 mL/min/m^2 when body size is adjusted for [9]. The Fick method is more accurate when VO_2 is measured using a calorimeter rather than estimated, as is the usual practice, especially in hyperdynamic states such as sepsis [12]. However, in general practice, even if the calculated CI is not exactly precise, monitoring

changes in CI is still valuable as it may indicate the utility of therapies being used. The disadvantages of the Fick method are similar to other invasive methods including risk of infection or pulmonary hemorrhage.

Another invasive method of measuring cardiac output is angiography [1]. Cardiac output may be determined angiographically with the calculation CO=SV×HR. The stroke volume is calculated by subtracting the end systolic volume from the end diastolic volume. This method is particularly useful in the setting of valve stenosis or regurgitation. However, the CO may be miscalculated in patients with enlarged ventricles [1].

A less invasive method of measuring CO is called the transpulmonary thermodilution technique, which is used by the PICCO monitor. There is no need for catheter placement into the heart using this method [12]. Instead, a central venous catheter is placed along with an arterial catheter with a thermistor at the tip. Indicator fluid is injected into the central line, and the arterial catheter thermistor senses the blood as it passes through the thorax, producing a similar thermodilution curve as the standard thermodilution method. The advantage of this method is that it is less invasive and less influenced by the respiratory cycle than the thermodilution technique, which employs a pulmonary artery catheter [13]. However, it may be inaccurate in patients with aortic stenosis, aortic aneurysm, and intracardiac shunts.

Other noninvasive or minimally invasive methods of measuring CO include esophageal Doppler analysis of aortic blood flow, the indirect Fick method which uses partial carbon dioxide rebreathing, thoracic electrical bioimpedance, and pulse contour analysis of the arterial pressure waveform [8]. Each of these methods has disadvantages that make them less practical in the clinical setting. Esophageal Doppler analysis requires sufficient training to obtain accurate measurements. The indirect Fick method, which is applicable to intubated patients, is less accurate in severe lung injury or when there is variability in tidal volume (as is seen with spontaneous breathing) [8]. Thoracic electrical bioimpedance is less accurate in patients with peripheral edema or pleural effusions, and pulse contour analysis requires that another method of measuring CO be used in order to calibrate the pulse contour device [8].

Clinical Relevance

Circulatory shock is a life-threatening cardiovascular condition in which blood circulation is severely impaired, resulting in inadequate oxygen supply to body tissues. From a hemodynamic standpoint, the three major types of circulatory shock are hypovolemic, cardiogenic, and vasogenic. The hemodynamic status of patients who are in circulatory shock is commonly determined by measurement of: (1) pressures in peripheral arterial, pulmonary arterial, and pulmonary capillary wedge (PCWP) positions; (2) Cardiac output; and (3) derived values, such as systemic vascular resistance (SVR) and peripheral vascular resistance (PVR) see (Table 4.1) for normal values of CO, SVR, and PVR. Cardiogenic and hypovolemic shock are low cardiac output states, whereas vasogenic (also known as distributive) shock is a high

Table 4.1 Hemodynamic parameters

Hemodynamic parameter	Formula	Normal range
CO	HR × SV	4–6 L/min
CI	CO/BSA	2.6–4.3 L/min/m^2
SVR	(MAP-CVP)/CO × 80	800–1,400 dyn s/cm^5
SVRI	(MAP-CVP)/CI × 80	1,500–2,300 dyn s/cm^5/m^2
PVR	(PAP-PCWP)/CO × 80	140–250 dyn s/cm^5
PVRI	(PAP-PCWP)/CI × 80	240–450 dyn s/cm^5/m^2

CO cardiac output; *CI cardiac* index; *BSA* body surface area; *SVR* systemic vascular resistance; *SVRI* SVR index; *PVR* peripheral vascular resistance; *PVRI* PVR index

output type of shock [9]. Cardiogenic and hypovolemic shock are both associated with high SVR, but may be differentiated by PCWP, which is elevated in the former and decreased in the latter. Vasogenic shock is a low SVR state due to vasodilation, and includes sepsis, thyrotoxicosis, anemia, anaphylaxis, and AV fistulas [8].

Cardiogenic shock is usually associated with a low CO, a high PCWP, and a low systemic arterial BP. In cases of impending cardiogenic shock the arterial BP may sometimes be "normal" due to severe vasoconstriction. Recall the basic physics principle that the pressure across a tube is equal to the product of flow and resistance. In other words $P = Q \times R$, and thus $Q = P/R$. Q represents cardiac output, R is resistance or systemic vascular resistance, and P represents the arterial-venous pressure gradient. In the systemic circulation, this pressure gradient is determined by subtracting the central venous pressure, CVP (equal to the right atrial pressure, RAP), from the mean arterial pressure, MAP (equal to 2/3 DBP+1/3 SBP). Thus, CO = (MAP–CVP)/SVR. This equation demonstrates that blood pressure in a low CO state may be preserved by peripheral vasoconstriction and thus an increase in the systemic vascular resistance. It is important to realize that the cardiac output may be inadequate in a patient with a normal or elevated blood pressure. Knowledge of these hemodynamic parameters may help guide therapy.

In cases of impending cardiogenic shock, vasodilator therapy (nitroprusside, nitroglycerin) is the preferred initial therapy, with the addition of diuretics if the wedge pressure remains elevated after adequate vasodilation [9]. Inodilators such as dobutamine or milrinone may also be used, and are especially useful in acute decompensated right heart failure. In low blood pressure cardiogenic shock, increasing blood pressure to a MAP of 60 is the first priority and this can be done using dopamine or norepinephrine. Dobutamine may be added to further enhance the cardiac output. In these cases, mechanical assist devices such as intra-aortic balloon pumps or ventricular assist devices may be useful in the acute period [9].

Summary

- Cardiac output is defined as stroke volume multiplied by heart rate, and the determinants of stroke volume are afterload, preload, and contractility.

- Cardiac output is most commonly measured with a Swan-Ganz catheter using either the thermodilution or the Fick method.
- The Fick principle states that cardiac output is inversely proportional to the arteriovenous oxygen difference and directly proportional to oxygen consumption.
- It is important to measure cardiac output in patients who are extremely hemodynamically unstable in order to guide therapy.
- Cardiogenic shock is a low cardiac output, high wedge pressure state that is often associated with hypotension. In cases of impending cardiogenic shock, blood pressure may be preserved.

Equations

$$CO = SV \times HR$$

$$CI = CO / BSA$$

$$\text{Fick Principle}: \quad CO = VO_2 / 1.34 \times 10 \times Hgb\ (SaO_2 - SvO_2)$$

$$CO = (MAP - CVP) / SVR$$

Review Questions

1. A 65-year-old male with a history of coronary artery disease status post CABG 5 years prior and known ischemic cardiomyopathy with an ejection fraction of 35% on his last echocardiogram, presents to the ER with palpitations and shortness of breath. His vital signs are blood pressure 120/95, heart rate 130 in sinus rhythm, and oxygen saturation 88% on room air. During his medical interview, he falls asleep between questions. On physical examination, his JVP is estimated to be 14 cm, he has an audible S3, bilateral crackles, and his extremities are cool to the touch. A Swan-Ganz catheter is placed. What is his most likely hemodynamic profile?

   a. CI = 3.5, PCWP = 24, SVR = 400
   b. CI = 1.8, PCWP = 30, SVR = 2500
   c. CI = 2.5, PCWP = 10, SVR = 1800
   d. CI = 2.0, PCWP 10, SVR = 800

   Answer: b; this patient is cold and wet on physical exam and is in severe, decompensated HF.

2. What therapeutic agent would you add at this point?

   a. Diuretics
   b. Vasodilators
   c. Intra-aortic balloon pump
   d. Beta-blocker

   Answer: b; in this patient with normal blood pressure, low cardiac output, and elevated filling pressures, a vasodilator such as nitroprusside ± nitroglycerine would be the appropriate next step in management. These agents would decrease afterload (nitroprusside) and thus increase cardiac output and decrease left sided filling pressures (nitroglycerine), or wedge pressure. If the wedge pressure is still elevated after treatment with vasodilators, the next step would be to add a diuretic.

3. A 40-year-old female is diagnosed with postpartum cardiomyopathy. A Swan-Ganz catheter is placed to calculate her cardiac output. Her SvO_2 is 40, Hgb is 11, and SaO_2 is 98. What is her cardiac in L/min output using the Fick equation?

   a. $CO = 250/1.34 \times 10 \times 11 \times (98–40)$
   b. $CO = 250/\ 1.34 \times 11 \times (98–40)$
   c. $CO = 250/1.34 \times 11 \times 40$
   d. $CO = (250 \times 1.34 \times 10)/(98–40)$

   Answer: a; The Fick cardiac output is calculated as follows:
   $CO = VO_2$ (assumed) / $1.34 \times 10 \times$ Hgb (SaO_2-SvO_2). The VO_2 is assumed to be 250 mL/min or 135 mL/min/m2 × BSA.

4. In which of the following situations would the thermodilution method overestimate the cardiac output?

   a. A 55-year-old woman with carcinoid syndrome associated with severe tricuspid regurgitation.
   b. A 48-year-old male who presents with an acute inferior myocardial infarction associated with right ventricular failure.
   c. A 40-year-old male who had an acute ST elevation myocardial infarction one week ago who now presents with acute cardiogenic shock due to ventricular septal rupture (VSR).
   d. A 66-year-old female who presents with a type A dissection associated with severe aortic insufficiency.
   Answer: c; Shunts tend to overestimate CO when the thermodilution technique is used as a portion of the injectate crosses through the VSR and thus the temperature change that is sensed downstream occurs at a rate similar to a high CO state. Severe TR (choice a) tends to underestimate the cardiac output when using their modulation.

5. In which of the following situations is the estimated oxygen consumption (VO_2) (rather than a direct measurement) most likely to be inaccurate?

   a. A 60-year-old female with right ventricular infarction.
   b. A 80-year-old male with sepsis due to Clostridium difficile colitis.

c. A 48-year-old male with acute ischemic mitral regurgitation.
d. A 90-year-old male with severe aortic stenosis.

Answer: b; The estimated VO_2 is inaccurate in hyperdynamic states such as sepsis.

References

1. Fuster R, O'Rourke R, Walsh R, Poole-Wilson P (2008) Hurst's The Heart, 12th edn. The McGraw-Hill Companies, Inc
2. Lilly L (2003) Pathophysiology of heart disease, 3rd edn. Lippincott Williams & Wilkins, Philadelphia. pp. 61, 213–214
3. Braunwald E, Libby P, Bonow R, Mann D, Zipes D (2008) Braunwald's heart disease, 18th edn. Saunders, Philadelphia, pp 452–5
4. Boron W, Boulpaep E (2009) Textbook of medical physiology. Saunders, Philadelphia
5. Dupont H, Squara P (1996) Cardiac output monitoring. Curr Opin Anaesthesiol 9:490–4
6. Nohria A, Lewis E, Stevenson LW (2002) Medical management of advanced heart failure. JAMA 287(5):628–40
7. Stevenson LW, Perloff JK (1989) The limited reliability of physical signs for estimating hemodynamics in chronic heart failure. JAMA 261:884–8
8. Hall J, Schmidt G, Wood L (2005) Principles of critical care. McGraw-Hill, New York
9. Marino P (2007) The ICU book, 3rd edn. Philadelphia: Lippincott Williams & Wilkins. p. 168–77, 263–68.
10. Miller R (2010) Miller's anesthesia, 7th edn. Churchill Livingstone, New York
11. Siegel LC, Hennessy MM, Pearl RG (1996) Delayed time response of the continuous cardiac output pulmonary artery catheter. Anesth Analg 83:1173–7
12. Mohammed I, Phillips C (2010) Determining cardiac output in the intensive care unit. Crit Care Clin 26:355–64
13. Sakka SG, Ruhl CC, Pfeiffer UJ et al (2000) Assessment of cardiac preload and extravascular lung water by single transpulmonary thermodilution. Intensive Care Med 26(2):180–7
14. Longo DL, Fauc; AS Kasper DL, Hauser SL, Jameson JL, Loscalto J, eds. (2012) Harrijan's Principles of internal medicine. 18th ed. New York: Mccraw–Hill

Suggested Reading

Braunwald E, Libby P, Bonow R, Mann D, Zipes D (2008) Braunwald's heart disease, 18th edn. Saunders, Philadelphia, pp 452–455
Hall J, Schmidt G, Wood L (2005) Principles of critical care. McGraw-Hill, New York
Marino P (2007) The ICU book, 3rd ed. Philadelphia: Lippincott Williams & Wilkins, p. 168–77, 263–68

Part II
Methods of Hemodynamic Evaluation

Chapter 5
Key Clinical Findings

Sachin S. Goel and William J. Stewart

From inability to let well alone;
from too much zeal for the new and contempt for what is old;
from putting knowledge before wisdom, science before art, and cleverness before common sense;
from treating patients as cases;
and from making the cure of the disease more grievous than the endurance of the same, Good Lord, deliver us.

Sir Robert Hutchison, MD, FRCP (1871–1960)

Case 1

A 65-year-old male with history of coronary artery disease, anterior wall myocardial infarction 10 years ago, ischemic cardiomyopathy with left ventricular ejection fraction of 30%, presents to the emergency room with worsening dyspnea on exertion and orthopnea for 1 week. On examination, his heart rate is 88 beats/min (bpm) and regular, blood pressure is 126/74 mmHg, respiratory rate is 18/min with oxygen saturation measuring 94% at room air. The jugular venous pressure (JVP) is elevated to 14 cm of water. Examination of the lungs is notable for bibasilar rales. Cardiovascular exam reveals a laterally displaced apical impulse. The S1 is normal, S2 is physiologically split, and there is a moderately loud S3. There is no audible murmur. Abdominal examination reveals mild hepatomegaly, with the edge 2 cm below the costal margin, with no evidence of ascites. The lower extremities demonstrate moderate pitting edema to the mid-calf bilaterally.

S.S. Goel • W.J. Stewart, M.D.(✉)
The Cleveland Clinic, Cleveland, OH, USA
e-mail: goels@ccf.org; stewarw@ccf.org

A.T. Askari et al. (eds.), *Cardiovascular Hemodynamics: An Introductory Guide*, Contemporary Cardiology, DOI 10.1007/978-1-60761-195-0_5,

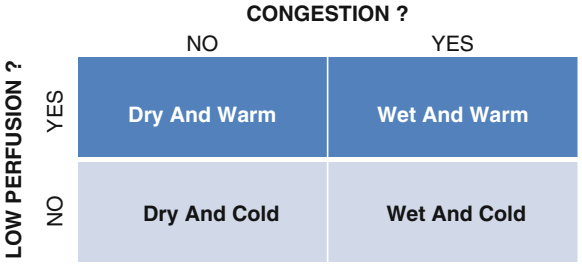

Fig. 5.1 Hemodynamic profiles in acute decompensated heart failure (ADHF). Evidence for CONGESTION (the "yes-no" delineation of the two columns) includes orthopnea, elevated jugular venous pressure (JVP), hepatojugular reflux, S3, rales, hepatomegaly, ascites, peripheral edema, and a loud P2. Evidence for LOW PERFUSION (the "yes-no" delineation of the two rows) includes narrow pulse pressure, cool and clammy extremities, altered mentation and oliguria

This patient is in acute decompensated heart failure (ADHF), which, even today, remains a clinical diagnosis performed at the bedside, based primarily on history and physical examination, rather than on laboratory data. The most important clues to this diagnosis are symptoms related to dyspnea and signs related to biventricular congestion and volume overload. Of the symptoms, orthopnea correlates best with elevated pulmonary capillary wedge pressure (PCWP), with a sensitivity approaching 90% [1]. Clinically evident edema usually indicates a volume excess of at least 3–4 L. Measuring blood pressure is of critical importance in patients with ADHF since hypotension is one of the strongest predictors of poor outcomes [2] and has important implications for therapy.

JVP is a cardinal aspect of the cardiovascular examination in the assessment of volume status in patients in general, and in those with ADHF in particular. However estimation of JVP is highly dependent on examiner's skill, experience, and patience. An abnormally elevated JVP is a pressure defined as >5 cm of water. If the patient is sitting at a 45° angle to the bed, there should be no visible pulsations above the angle of Louis. JVP reflects right atrial (RA) pressure. It is often used as a surrogate for left ventricular filling pressure, however right heart failure is often absent in patients with left sided heart failure. The most common cause of right ventricular failure is left ventricular failure. In a study consisting of 1,000 consecutive patients with advanced heart failure undergoing right heart catheterization, RA pressure was found to somewhat reliably predict PCWP ($r=0.64$) and the positive predictive value of RA pressure >10 mmHg for PCWP >22 mmHg was 88% [3]. Hepatojugular reflux (HJR) is jugular venous distension induced by firm pressure over the liver. An increase in JVP>3 cm by this maneuver is a positive HJR, which is a sign of right sided volume overload. The presence of jugular venous distension, at rest or inducible, is the bedside clinical sign that has the best combination of sensitivity (81%), specificity (80%) and predictive accuracy (81%) for prediction of elevation of PCWP (≥18 mmHg) [4].

The third heart sound (S3) occurs in early diastole due to abrupt cessation of rapid early diastolic left ventricular inflow as a consequence of increased LV

filling pressures and an abnormally stiff, non-compliant left ventricle [5]. It is a fairly specific marker for LV dysfunction and correlates with BNP levels [6]. However, it is not as sensitive as other bedside findings. In a comprehensive analysis evaluating all studies published between 1966 and 2005 which assessed the precision and diagnostic accuracy in diagnosing the cause of dyspnea, the S3 was found to increase the likelihood of ADHF more than any other part of the physical examination (likelihood ratio 11, 95% confidence interval 4.9–25.0) [7]. The S3 is associated with elevated LV filling pressures [8]. In a comprehensive study of the physiology of the S3 comparing findings from phonocardiography, tissue Doppler echocardiography, BNP and invasive LV hemodynamics, patients with an audible S3 were found to have a higher early mitral inflow velocity (*E*), a more rapid deceleration time (DT) of early mitral inflow, reduced mitral annular velocity (e') and therefore higher E/e' ratio. The E/e' ratio has been correlated with elevated LV filling pressures [9, 10].

Hepatomegaly results from increased central venous pressure and is often accompanied by right upper quadrant tenderness. Based on various components of the history and physical examination, patients with ADHF can be assigned to one of the quadrants of a 2×2 table, each of which represents a distinct hemodynamic profile defined by the presence or absence of congestion (wet or dry) and low or normal perfusion (cold or warm) (Fig. 5.1) [11]. This strategy is very useful in selecting initial therapy and identifying prognosis in patients with ADHF.

Case 2

A 54-year-old lady with known history of a heart murmur for over two decades presents with symptoms of worsening fatigue, dyspnea on exertion, and palpitations for the last 2 years. On examination, her pulse is irregular with a heart rate of 110 bpm and her blood pressure is 132/84 mmHg. The JVP is elevated to 12 cm of water. Cardiovascular exam reveals laterally displaced, brisk, enlarged, and hyperdynamic apical impulse. The S1 is normal and there is a loud 3/6 holosystolic murmur radiating to the axilla and to the left paravertebral region. In addition, a parasternal right ventricular heave is palpable and a loud P2 is audible. The pulmonary exam is notable for bibasilar rales. Abdominal examination is unremarkable and there is trace bilateral pedal edema.

This patient has chronic severe mitral regurgitation (MR), likely secondary to mitral valve prolapse (MVP). Although this patient's history and physical findings are classic, clinical findings in MR vary depending on acuity, severity, and the mechanism. For example, in acute severe MR, sometimes caused by acute papillary muscle rupture or endocarditis, the apical LV impulse is not displaced because the LV has not had a chance to dilate. In acute severe MR, the systolic murmur may be early in timing and decrescendo in configuration due to rapid systolic equalization of pressures between the left ventricle and the left atrium (LA). The LA pressure would have a large *V* wave during ventricular systole. MVP is sometimes associated

with: (1) one or more systolic clicks, produced by sudden tensing of the elongated chordae tendinae as the leaflets prolapse and (2) a holosystolic or late systolic murmur. In less than severe MR, it is useful to observe the onset of the murmur and the timing of systolic click in MVP, both of which move earlier in systole with maneuvers which reduce left ventricular end diastolic volume (such as standing and the Valsalva maneuver), while the murmur becomes louder. Conversely, the onset of the murmur and the timing of systolic click in MVP are delayed later in systole with maneuvers that increase left ventricular end diastolic volume (such as squatting) and the murmur becomes softer (Fig. 5.2) [12]. Severe MR is often associated with a holosystolic murmur that radiates posteriorly to the axilla and around to the left paravertebral region in the back, irrespective of which mitral leaflet is involved. As mitral regurgitation becomes chronic, left ventricular volume overload leads to left atrial enlargement and atrial fibrillation is common. With development of pulmonary hypertension, the P2 component of the second heart sound becomes louder. The S2 splitting may widen with more severe MR, due to a combination of early A2 as a result of decrease in left ventricular ejection time and delay in P2.

Case 3

A 64-year-old man with history coronary artery bypass grafting (CABG) 15 years ago presents with complaints of increasing dyspnea on exertion over the last 12 months. Recently he has also noted worsening leg edema and increasing abdominal girth. On examination, his heart rate is 90 bpm and regular, and his blood pressure is 108/74 mmHg. The JVP is elevated to 14 cm of water with a prominent, rapidly collapsing *y* descent and a positive Kussmaul sign. The apical impulse is not displaced. The S1 and S2 are normal and there is a high-pitched early diastolic sound, corresponding with the prominent *y* descent seen in jugular venous waveform, which is heard best at the LV apex. Abdominal examination reveals pulsatile hepatomegaly with evidence of ascites. Bilateral lower extremity edema is present.

This patient likely has pericardial constriction, based on his history and physical findings. Subsequent imaging and cardiac catheterization confirmed this diagnosis. Constriction is characterized by thickened, scarred and/or calcified pericardium that markedly limits diastolic filling of the heart. The jugular venous waveforms help clarify hemodynamics in constrictive pericarditis. JVP contour normally has two distinct positive waves (*a* and *v* wave) and two negative waves (*x* and *y* descent) (Fig. 5.3a). The *a* wave occurs with right atrial systole and follows the *P* wave on EKG and precedes the first heart sound (S1). The *x* descent normally occurs as RA pressure falls after the *a* wave and ventricular systole pulls the tricuspid valve and the RA downward. The *c* wave interrupts the *x* descent during early ventricular systole as the tricuspid valve is briefly pushed in to the right atrium as the ventricle begins contracting, thereby elevating RA pressure briefly. The *v* wave occurs with RA filling at the end of ventricular systole, just after the second heart sound (S2). The *y* descent follows the *v* wave and occurs with fall in RA pressure after the tri-

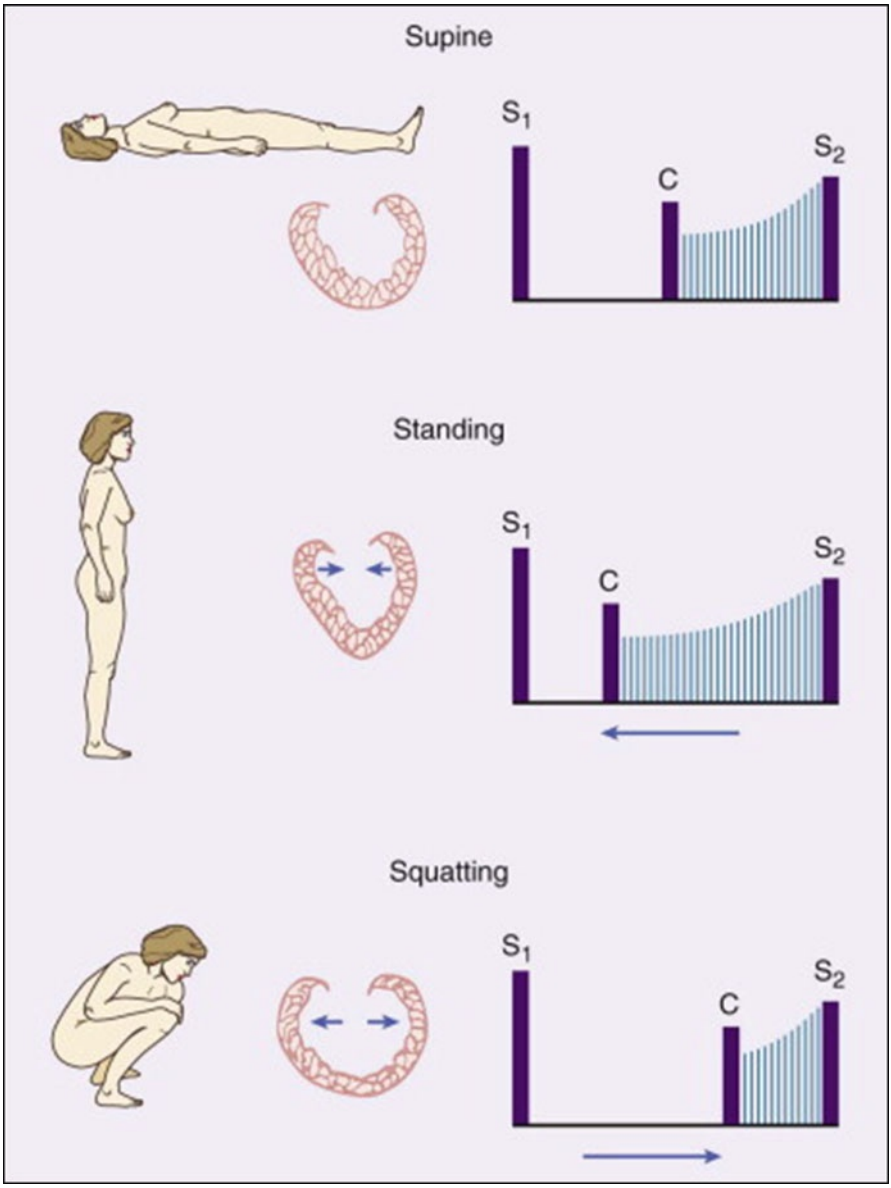

Fig. 5.2 Behavior of the nonejection click (C) and systolic murmur of mitral valve prolapse (MVP). The *top panel* shows the first heart sound (S1) the mid-systolic click (C) and the second heart sound (S2), with the late systolic murmur of moderate mitral regurgitation; while the patient is supine. With standing, (*middle panel*) venous return decreases, the heart becomes smaller, and the prolapse occurs earlier in systole. The click and murmur move closer to S1. With squatting, (*lower panel*) venous return increases, causing an increase in left ventricular chamber size. The click and murmur occur later in systole and move away from S1 (from Shaver JA, Leonard JJ, Leon DF. Examination of the heart. Part IV: Auscultation of the heart. Dallas: American Heart Association; 1990. p. 13)

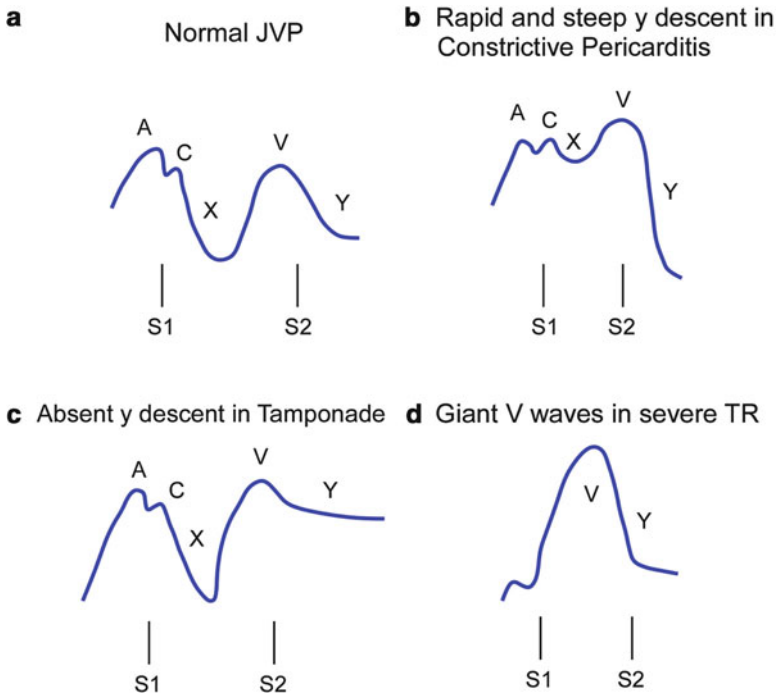

Fig. 5.3 Jugular venous waveform patterns—in normal patients, constrictive pericarditis, pericardial tamponade, and severe tricuspid regurgitation (TR). *JVP* jugular venous pressure; *S1* first heart sound, *S2* second heart sound. The *A*, *C*, and *V* positive waves, and the *X* and *Y* negative waves, are explained in the text

cuspid valve opens and fills the RV in diastole. Regarding the abnormal JVP waveform in constrictive pericarditis, the most prominent wave is the rapid *y* descent, as the ventricles fill rapidly during early diastole due to elevated atrial pressures. Once the pericardial constraining volume is reached, however, ventricular filling slows abruptly due to the development of high ventricular pressure, which is manifested as the characteristic dip and plateau in ventricular diastolic pressures. The JVP contour therefore has an M or W-shaped contour (Fig. 5.3b), with a prominent, rapidly collapsing *y* descent, along with a normal or reduced *x* descent. Another feature of constriction is the respirophasic changes in JVP. In normal individuals, JVP falls with inspiration as a reflection of the reduction in the intra-thoracic pressure; the increased venous return is accommodated by the compliant right ventricle. In constrictive pericarditis, the increased venous return is not accommodated well; the increased venous return meets the stiff and inelastic pericardium, resulting in a rise in JVP with inhalation, characteristically referred to as Kussmaul sign [13]. The classic (sometimes the only) auscultatory finding in constrictive pericarditis is a high-pitched early diastolic sound, referred to as pericardial knock, which occurs due to the abrupt cessation of blood during early diastolic ventricular filling. The pericardial knock corresponds in timing with the prominent *y* descent in JVP [14].

Case 4

A 66-year-old lady with history of metastatic breast carcinoma presents with worsening dyspnea on exertion for the last 3 days. On examination, her heart rate is 110 bpm, blood pressure is 88/56 mmHg and there is a paradoxical pulse of 20 mmHg. The JVP is markedly elevated to the angle of the jaw, with an absent *y* descent. The apical impulse is reduced and the heart sounds are muffled and distant. Pulmonary examination reveals clear breath sounds bilaterally.

The triad of hypotension, elevated JVP, and muffled heart sounds, also known as Beck's triad, should alert one to the possibility of cardiac tamponade. This was first described in 1935 by Claude Schaeffer Beck, who was Professor of Cardiovascular Surgery at Case Western Reserve University. Cardiac tamponade occurs when fluid of any kind accumulates in the pericardial space, to an extent where high intrapericardial pressure limits cardiac filling. This leads to markedly elevated venous pressures and reduced cardiac output, which can be rapidly fatal if not treated promptly. A relatively small amount of fluid that accumulates rapidly in the pericardial space can lead to tamponade. In case of a slowly accumulating pericardial effusion, a much larger volume of fluid may be necessary to cause tamponade as the pericardial pressure–volume relation shifts to the right, with greater compliance of the parietal pericardium [15, 16]. In either situation, once a critical amount of fluid has accumulated in the pericardial space, the intrapericardial pressure rises significantly even with relatively smaller rises in volume. The increased intrapericardial pressure may impair cardiac filling and reduce cardiac output. As a compensatory mechanism for maintaining cardiac output and blood pressure, tachycardia is nearly always present in tamponade. One exception to this rule is when the underlying cause for pericardial effusion and resultant tamponade is hypothyroidism. The JVP in pericardial tamponade is almost always elevated, and is sometimes associated with venous distension in the forehead and scalp. The jugular venous waveform is characterized by an absent *y* descent (Fig. 5.3c) due to restricted or diminished ventricular filling even in early diastole with the markedly elevated pericardial pressure. This pattern is in contrast to constrictive pericarditis where ventricular filling in early diastole is rapid and abbreviated prior to its cessation in mid-diastole due to the pericardial constraint. Pulsus paradoxus, described by Adolf Kussmaul in 1873, is a helpful sign of cardiac tamponade. Pulsus paradoxus is defined as an abnormally large (>10 mmHg) decline in systolic blood pressure during inhalation and is a consequence of exaggerated ventricular interdependence and exaggerated effects on left and right sided filling due to changes in intra-thoracic pressure (Fig. 5.4). Normally, the inspiratory decrease in intra-thoracic pressure causes an increase in systemic, venous return and a decrease in pulmonary venous return, with a small movement of the interventricular septum toward the left. The small decrease in left ventricular stroke volume and aortic peak systolic blood pressure results primarily due to inspiratory decrease in LV filling from the decrease in intra-thoracic pressure. With tamponade, in presence of pericardial fluid compressing all the walls of the heart, these respiratory changes in venous return are exaggerated. With inhalation, the

drop in left sided filling reduces left ventricular stroke volume and the systemic systolic blood pressure drops by a greater extent than in normal physiology, i.e., more than 10 mmHg. In patients with true tamponade, pulsus paradoxus can be masked by the presence of numerous conditions, including severe hypotension, pericardial adhesions, right ventricular hypertrophy, severe aortic regurgitation, a stiff left ventricle or other conditions which elevate LV filling pressure, and atrial septal defect [16].

Case 5

A 78-year-old male with history of hypertension, hyperlipidemia, and diabetes mellitus presents with worsening dyspnea on exertion over the last 2 years. On examination, he has a slow-rising, late-peaking, low-amplitude carotid contour by palpation. His heart rate is regular at 88 bpm and blood pressure 108/66 mmHg. The JVP is normal. The apical impulse is sustained and non-displaced. Cardiac auscultation reveals normal S1, a soft S2 without splitting, and a 3/6 late peaking systolic ejection murmur, best heard in the right second intercostal space and radiating to the carotids. Pulmonary examination reveals clear breath sounds bilaterally. Abdominal examination is unrevealing and he has no pedal edema.

Based on clinical findings, this patient likely has severe aortic stenosis (AS). Hemodynamically, AS is characterized by a pressure gradient between the left ventricle and aorta during systole (Fig. 5.5a), and the magnitude of this pressure gradient is an indication of the severity of AS. Several physical findings have been shown to correlate with severity of AS, including the characteristic carotid pulse contour, a reduced or absent S2, and the timing and intensity of murmur (Table 5.1) [17]. The quality of carotid pulse in severe AS has classically been described as “parvus et tardus,” i.e., weak and slow-rising and delayed. This can be best assessed best by simultaneously palpating the carotid pulse and auscultating the heart. In severe AS, the weak and delayed carotid pulse reflects severe obstruction, with a reduced early systolic rate of blood flow across the aortic valve into the arterial circulation. Delay between brachial and radial pulse (brachioradial delay) has also been described as a clinical indicator of severe AS [18]. With worsening AS, the aortic valve leaflets become increasingly calcified and immobile, leading to a soft or inaudible A2 component of the second heart sound. A normal intensity of A2 implies flexible and mobile aortic valve leaflets and can essentially be very helpful in ruling out severe senile AS. However, the A2 may still be normal in severe AS in young people whose stenosis reflects more congenital fusion of the cusps and less calcific restriction. The gradient between the left ventricle and aorta in AS is greatest in mid-systole and is relatively small early and late in systole. The murmur therefore has a diamond shape; it starts soft and builds to a peak in mid-systole and then becomes quiet in late systole immediately before S2 (Fig. 5.5a). It is referred to as a systolic ejection murmur, since it begins after S1 and ends before S2. The intensity of murmur correlates generally with severity of AS, but there are many exceptions to that correlation. It is best heard at the base of the heart in the second right

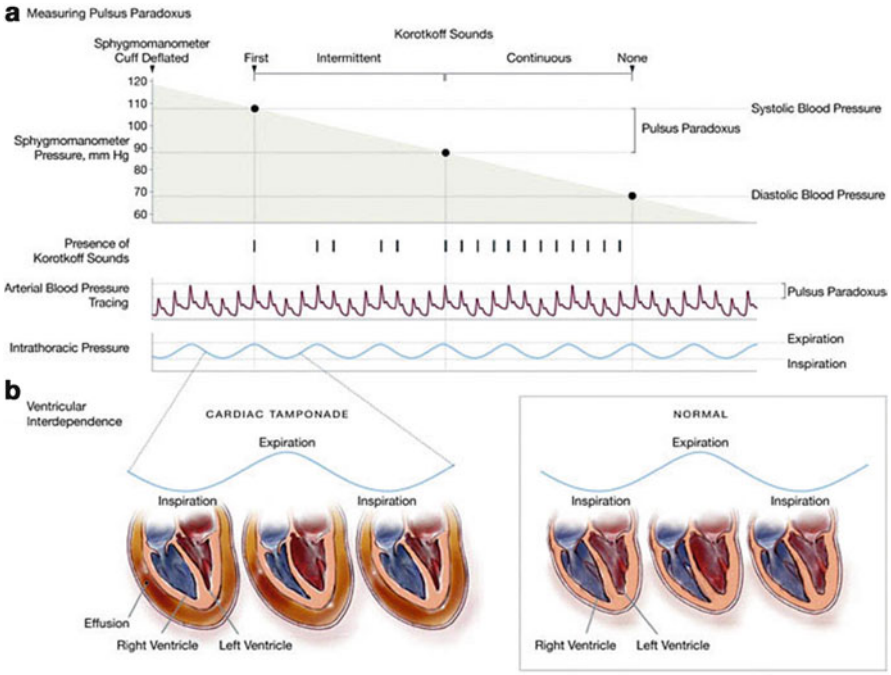

Fig. 5.4 Measurement and mechanism of pulsus paradoxus (**a**), The examiner inflates the sphygmomanometer cuff fully, listens for Korotkoff sounds as the cuff is slowly deflated, and then notes the pressure at which Korotkoff sounds are initially audible only during expiration. As the cuff is further deflated, the examiner notes the pressure at which Korotkoff sounds become audible during expiration and inspiration. The difference between these two pressures is the pulsus paradoxus, which can normally be from 0 to 10 mmHg. In cardiac tamponade, the pulsus paradoxus measures greater than 10 mmHg. Inspiratory diminution in the arterial blood pressure tracing represents the pulsus paradoxus. A similar phenomenon may be observed on a pulse oximeter waveform. (**b**) During inspiration in the normal heart, negative intrapleural pressures increase venous return to the right ventricle and decrease pulmonary venous return to the left ventricle by increasing the pulmonary reservoir for blood. As a result of increased right ventricular distention, the interventricular septum bows slightly to the left, and the filling, and stroke volume of the left ventricle are mildly reduced. In expiration, these changes are reversed, resulting in the septum bowing to the right and a mild reduction in right ventricular filling. In the presence of cardiac tamponade, the reciprocal changes seen in the normal heart are exaggerated when the pericardial sac is filled with fluid, thus limiting distensibility of the entire heart. This results in a more dramatic reduction in filling of the left ventricle during inspiration, exacerbating the normal inspiratory decrease in stroke volume and blood pressure (from Roy CL, et al. Does this patient with pericardial effusion have cardiac tamponade. JAMA. 2007;297:1810–8)

intercostal space and radiates to the carotids. The timing of the peak intensity of systolic ejection murmur also corresponds to the severity of AS. With mild AS, the maximum instantaneous gradient between the left ventricle and aorta occurs early in systole; hence the systolic murmur peaks in early systole. As the severity of AS worsens, the maximum instantaneous gradient between the left ventricle and the aorta occurs progressively later in systole, and correspondingly the murmur peaks late. No single physi-

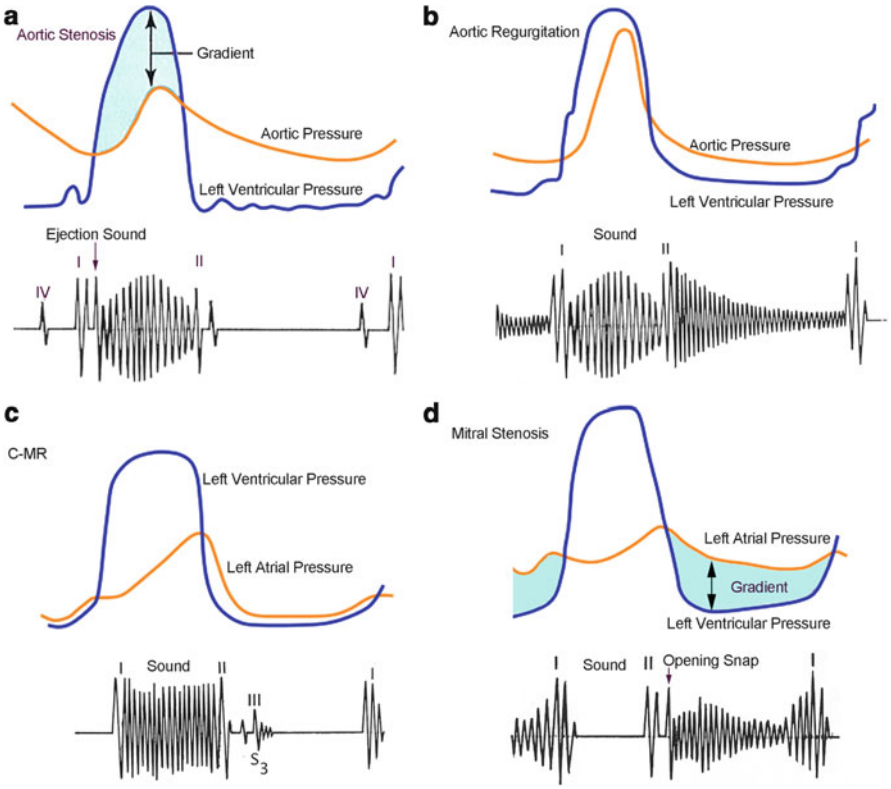

Fig. 5.5 Relationship of murmurs to LV, Aortic, and LA pressure waveforms and hemodynamics in various valve diseases. (**a**) Aortic stenosis (AS). The gradient between the left ventricle and aorta in AS is greatest in mid-systole and is relatively small early and late in systole. The murmur therefore has a diamond shape, i.e., starts soft and builds to a peak in mid-systole and then becomes quiet in late systole immediately before S2. In young AS patients, there may be an early ejection sound. In senile AS, A2 becomes diminished or absent. An S4 is common due to LV noncompliance. (**b**) Aortic regurgitation (AR). The early diastolic murmur (EDM) begins with S2, and has a decrescendo contour. The duration of the murmur continues for a variable time in diastole, depending on severity and acuity of AR. Notice that aortic diastolic pressure is low. (**c**) Mitral regurgitation. There is a pansystolic murmur with a flat profile due to the regurgitant flow into the left atrium. Note that the left atrial pressure rises during systole, a *v* wave. An early diastolic S3 or flow rumble may occur. (**d**) Mitral stenosis (MS). A loud S1 is heard since the mitral gradient is high and the leaflets are not very thickened or calcified. An important indicator of the severity of MS is the time interval between the S2 and opening snap (OS), which is the time it takes for LV pressure to fall from late systolic aortic pressure to early diastolic left atrial pressure. The mitral valve snaps open due to the increased gradient, causing an opening snap (OS). The diastolic murmur correlates with the gradient across the mitral valve, which is largest in early diastole, and increases again in late diastole in this patient in sinus rhythm

cal examination finding rules in or rules out severe AS, however, a combination of slow and delayed carotid impulse, reduced intensity of S2 and mid- to late-peaking systolic ejection murmur at the base radiating to the neck is fairly accurate in diagnosing severe AS clinically [19].

Table 5.1 Physical findings in severe aortic stenosis

Examination	Finding
Carotid pulse	Weak, slow-rising and delayed carotid pulse (Pulsus parvus et tardus)
Second heart sound (S2)	Soft or inaudible A2 component of S2
Murmur	Mid- to late-peaking in systole, radiating to the neck

Case 6

A 56-year-old asymptomatic male is referred for evaluation after his primary care physician heard a heart murmur. On examination, he has a rapidly collapsing pulse with a regular heart rhythm, heart rate of 90 bpm and blood pressure of 144/40 mmHg, and therefore a pulse pressure of 104 mmHg. Cardiac examination reveals a wide and hyperdynamic apical impulse that is displaced laterally and inferiorly. A high frequency, blowing decrescendo diastolic murmur is heard, best at the left sternal border in end expiration with the patient sitting up. There is also a short early systolic murmur of moderate intensity. In addition, a systolic and diastolic bruit is heard when the femoral artery is partially compressed, and popliteal systolic cuff pressure is >170 mmHg. Pulmonary and abdominal exam are unremarkable.

No other disease condition in cardiovascular medicine has more eponymous signs associated with it than chronic aortic regurgitation (AR) (Table 5.2). The principal hemodynamic abnormality in chronic AR responsible for these signs is the wide pulse pressure (Fig. 5.5b). The low diastolic arterial pressure results from the rapid run-off of blood from the aorta back into the left ventricle. There is an increase in left ventricular end diastolic volume and hence an increase in left ventricular stroke volume and the pulse pressure. The arterial pulse contour has a rapidly rising and collapsing pulse referred to as "water hammer" pulse, or Corrigan sign, first described by Sir Dominic Corrigan in 1832. The carotid upstroke is rapid resulting from the increased stroke volume. Few studies have systematically assessed the predictive value of these eponymous signs in Table 5.1, however Duroziez's sign, Corrigan pulse, and Hill's sign are perhaps most important useful signs in detecting severe chronic AR [20]. In a literature review, the presence of an diastolic decrescendo murmur as heard by a cardiologist was the most useful finding for detecting AR (positive likelihood ratio of 8.8) and its absence was most useful in ruling out AR [21]. The diastolic murmur of chronic AR is high pitched and blowing in character, and is best heard along the left sternal border at the left third or fourth intercostal space, with the patient sitting up and leaning forward, with held exhalation. The severity of chronic AR correlates somewhat with the duration of the murmur, while its intensity varies widely. With severe chronic AR, the murmur can be holodiastolic. However, in very severe AR, particularly sudden onset acute AR, the murmur may be early diastolic and short, due to rapid equilibration of LV and aortic pressure. Most patients with severe AR also have an early peaking systolic flow murmur which results from the increased stroke volume even in the absence of concomitant AS. Finally, an apical mid-late diastolic rumble, referred to as the Austin-Flint murmur is

Table 5.2 Eponymous signs of chronic aortic regurgitation

Sign	Description
Hill's sign	Exaggerated difference in lower and upper extremity blood pressure
Corrigan's sign	Rapidly collapsing arterial pulse
Duroziez's sign	Systolic and diastolic bruit heard on partial femoral artery compression
Quincke's sign	Exaggerated capillary pulsations of the nail beds
deMusset's sign	Head bobbing with each heart beat
Traube's sign	Pistol shot sound heard over the femoral artery
Mueller's sign	Pulsatile uvula
Becker's sign	Pulsatile retinal arteries
Rosenbach's sign	Pulsatile liver
Gerhard's sign	Pulsatile spleen
Mayne's sign	More than 15 mmHg drop in diastolic blood pressure with arm elevated compared to arm in standard position

audible in occasional patients with chronic severe AR, reflecting the impact of the AR jet on the anterior mitral valve leaflet; this should not be confused with the diastolic rumble of mitral stenosis.

Case 7

A 62-year-old male with 30 pack year history of smoking, hypertension, hyperlipidemia, and diabetes mellitus presents to the ER after experiencing worsening substernal chest discomfort radiating to the left arm for 8 h. On arrival, he appears diaphoretic with a heart rate of 104 bpm, blood pressure of 90/68 mmHg and he is tachypneic with a respiratory rate of 20/min and an oxygen saturation of 94% on room air. He is drowsy and somewhat disoriented. Stat 12 lead EKG reveals widespread 3 mm ST segment elevation in precordial leads V1 through V6 and reciprocal ST segment depression in inferior limb leads. Cardiovascular examination reveals elevated JVP at 12 cm and normal heart sounds with no murmurs, rubs, or gallops. Pulmonary examination reveals bibasilar rales. Abdominal examination is unrevealing and he has no lower extremity edema, but his extremities are cold and clammy. With a diagnosis of acute ST segment elevation myocardial infarction (STEMI) and cardiogenic shock, he is emergently taken to the cardiac catheterization laboratory. The proximal left anterior descending coronary artery (LAD) is found to be totally occluded, so it is opened and stented. Pulmonary artery catheterization shows a PCWP of 28 mmHg, with a cardiac index of 1.7 L/min/m^2, and an intra-aortic balloon pump (IABP) is placed. Emergent echocardiogram did not show any evidence of mechanical complications of MI.

Cardiogenic shock is characterized by end organ hypoperfusion due to cardiac dysfunction, and is hemodynamically defined by persistent hypotension (systolic

blood pressure <80–90 mmHg or mean arterial pressure 30 mmHg lower than baseline) with severe reduction in the cardiac index (<1.8 L/min/m^2 without support or <2.0–2.2 L/min/m^2 with support) and adequate or elevated filling pressures [22]. The most common cause of cardiogenic shock is acute myocardial infarction (MI) with left ventricular failure. In the setting of MI, it is very important to rule out mechanical complications such as acute severe MR secondary to papillary muscle dysfunction, ventricular free wall rupture, or ventricular septal defect; all of which can contribute to cardiogenic shock. Other causes of these alarming hemodynamics include acute severe LV or RV dysfunction of any etiology, valvular heart disease such as acute mitral or aortic regurgitation, pericardial tamponade, massive pulmonary embolism, acute aortic dissection, hypertrophic obstructive cardiomyopathy, and acute myocarditis. The hallmark of cardiogenic shock is hypoperfusion of the extremities and vital organs. Loss of cardiac output from any cause increases sympathetic activation, which increases arteriolar constriction and systemic vascular resistance, in an attempt to maintain blood pressure and tissue perfusion. Clinically, cardiogenic shock manifests with signs of reduced end organ perfusion such as altered mental status, oliguria, respiratory distress due to pulmonary congestion, and cool, clammy extremities. Such patients are typically in the bottom right on the hemodynamic profile chart presented in Fig. 5.1, i.e., wet and cold. However, not all patients in cardiogenic shock have vasoconstriction and elevated systemic vascular resistance. Almost a fifth of patients with cardiogenic shock studied in the SHOCK trial had hemodynamic findings of low systemic vascular resistance, similar to patients with sepsis. This probably results from inappropriate vasodilation, which may represent a systemic inflammatory response state (SIRS) similar to sepsis [22, 23]. Cardiogenic shock can be diagnosed based on clinical findings, but invasive hemodynamic monitoring helps confirm and quantify the degree of vasoconstriction or vasodilation, quantifying filling pressures and cardiac output, and ultimately guiding therapy.

Case 8

A 78-year-old woman is brought to the ER with fever, cough, shortness of breath, and altered mental status. She has had intermittent fever and cough with productive sputum for the last 3 days. On arrival to the ER, she is drowsy but arousable and confused. She is febrile with a temperature of 39 °F, heart rate of 120 bpm and regular, blood pressure of 80/50 mmHg, tachypneic with a respiratory rate of 22 bpm, and an oxygen saturation of 90% on room air. Cardiovascular examination reveals no jugular venous distension and rapidly collapsing jugular vein distension even when supine. She has normal heart sounds and no murmurs, rubs, or gallops. Pulmonary exam reveals bronchial breath sounds and rales in the right lower zone with egophony and dullness on percussion. Abdominal exam is unrevealing, and peripheral extremities are warm to touch

with capillary refill >3 s and mottling of skin. Chest X-ray confirms right lower lobe consolidation.

This patient is in septic shock. It is similar to the patient in Case 7, however the mechanism and pathophysiology are different. Also called distributive or vasodilatory shock, the hallmark of septic shock is profound vasodilation and inadequate tissue extraction of oxygen. Vasodilation is mediated by three mechanisms: activation of ATP-sensitive potassium channels in the vascular smooth muscle cell plasma membranes, activation of inducible nitric oxide synthetase, and deficiency of vasopressin [24]. This is followed by leukocyte migration and activation and release of pro-inflammatory markers such as tumor necrosis factor (TNF) and interleukins, which lead to tissue damage and organ dysfunction, which manifest as a SIRS [25]. SIRS is defined by the presence of one of the following:

- Temperature >38.5 °F or <35 °F
- Heart rate >90 bpm
- Respiratory rate >20/min or $PaCO_2 < 32$ mmHg
- WBC >12,000 cells/mm^3, <4,000 cells/mm^3, or >10% immature band forms

Sepsis is defined as SIRS in presence of an infection. Similarly, severe sepsis and septic shock are largely clinical diagnoses [25]. Severe sepsis is defined as the presence of sepsis and one of the following signs of organ dysfunction:

- Areas of mottled skin
- Capillary refilling requires 3 s or longer
- Urine output <0.5 mL/kg for at least 1 h, or the need for renal replacement therapy
- Elevated blood lactate levels >2 mmol/L
- New decrease in mental status
- Platelet count <100,000 platelets/mL
- Disseminated intravascular coagulation
- Acute lung injury or acute respiratory distress syndrome (ARDS)
- Cardiac dysfunction, as defined by echocardiography or direct measurement of the cardiac index

Septic shock is defined by the presence of severe sepsis and one of the following:

- Systemic mean blood pressure <60 mmHg (<80 mmHg if previous hypertension) after adequate fluid resuscitation or PCWP between 12 and 20 mmHg
- Need for dopamine >5 mcg/kg/min or norepinephrine or epinephrine <0.25 mcg/kg/min to maintain mean blood pressure above 60 mmHg (80 mmHg if previous hypertension)

Thus sepsis has a continuum of severity ranging from sepsis manifesting as SIRS to severe sepsis and septic shock. Despite optimal management, mortality from severe sepsis and septic shock can range from 40 to 50% or higher. The key for successful outcome is early identification of the severity of this continuum and of a potential infectious focus.

Case 9

A 54-year-old man with history of chronic alcohol abuse and liver cirrhosis presents with hematemesis. On examination, he is afebrile with a heart rate of 78 bpm and blood pressure of 130/80 mmHg when supine and 110 bpm and 102/60 mmHg when standing. He feels dizzy on standing. His tongue, axillae, and mucous membranes are moist. Cardiac, pulmonary, and abdominal exams are unrevealing.

This patient has hypovolemia likely secondary to blood loss, in this case, bleeding esophageal varices. Hypovolemia occurs when extracellular sodium and fluid are lost at a rate greater than intake. This may occur by way of gastrointestinal losses (hemorrhage, vomiting, diarrhea), renal losses (diuresis, salt wasting), loss from skin (burns), or third space sequestration (acute pancreatitis, acute intestinal obstruction, fracture). One of the most common causes of hypovolemia is excessive use of diuretic medications. History and physical examination are important in identifying the presence, etiology, and severity of hypovolemia, perhaps even more so than laboratory testing. For example, the initial hemoglobin correlates poorly with the degree of blood loss, even in patients whose hypovolemia is due to gastrointestinal hemorrhage. Similarly prerenal azotemia is a late finding in acute dehydration. Postural assessment of systolic blood pressure is the most rapid and reliable bedside tool, in the absence of autonomic neuropathy or overuse of antihypertensive drugs. A drop of more than 10 mmHg when the patient goes from supine to standing is indicative of at least a 10% deficit in intravascular volume. In a systematic review of physical findings in assessment of patients with blood loss and hypovolemia, severe postural dizziness, and an increase in pulse rate ≥30 bpm, were found to be the most sensitive and specific findings for large blood loss [26]. In the same study, the presence of dry axilla supported the diagnosis of hypovolemia in patients with vomiting, diarrhea or decreased oral intake. Moist mucous membranes and a normal furrowed appearance of the tongue were found to argue against it. It is important to remember that postural blood pressure and heart rate should be measured with the intervention of the patient standing still for 1 min. JVP is usually low in patients with hypovolemia, and it may be necessary to lay the patient down to see the venous pulsations above the clavicle. Normal skin has elasticity or turgor, i.e., it immediately returns to its normal position after being pinched and released. This is due to elastin content in the subcutaneous tissue, which is affected by moisture content and age. In younger individuals, poor skin turgor may represent hypovolemia.

Case 10

A 53-year-old lady with history of rheumatic heart disease with long-standing history of mitral stenosis, s/p balloon mitral valvotomy 15 years ago, and mitral valve replacement 8 years ago, presents with worsening fatigue, exercise intolerance,

abdominal distension, and lower extremity swelling. On examination, she has an irregularly irregular pulse with a heart rate of 80 bpm, blood pressure of 110/68 mmHg, and respiratory rate of 16/min. JVP is elevated to 14 cm of water with a prominent *V* wave and a sharp *Y* descent. Cardiac exam reveals a palpable right ventricular heave. On auscultation, the P2 is loud and a 3/6 holosystolic murmur is audible at the left lower sternal border. The murmur increases in intensity with inspiration. Abdominal examination reveals a pulsatile and enlarged liver with evidence for ascites. Moderate bilateral pedal edema is also present.

Tricuspid regurgitation (TR) is a valve lesion that occurs commonly, as a result of right ventricular dilatation from any cause, through the effects of secondary pulmonary hypertension. The most frequent cause is left sided heart failure due to mitral valve disease or left ventricular dysfunction. TR also occurs in the setting of cor pulmonale, from intrinsic lung disease, or from primary pulmonary hypertension. Pathophysiologically, long-standing pulmonary hypertension causes right ventricular pressure overload, which causes dilatation of the right ventricle and tricuspid annulus. In patients with chronic severe TR, the JVP waveform is characterized by the loss of *X* descent and a prominent systolic *V* wave (or *C*-*V* wave) caused by markedly increased right atrial pressure during ventricular systole, which is followed by a rapid *Y* descent (Fig. 5.3d). Auscultation usually reveals a loud P2 in presence of pulmonary hypertension. There may be a pansystolic murmur, loudest in about the 4th intercostal space in the left or right parasternal region. Classically, the systolic murmur intensity increases with inspiration (Carvallo sign) as the venous return on the right side of the heart increases; however, this finding is inconsistent. Many patients with significant TR do not have respirophasic variation, and some have an unimpressive murmur. In the absence of pulmonary hypertension, TR may also occur as a primary valve abnormality, due to trauma, or endocarditis classically in patients who have used intravenous drugs, but increasingly in patients with infected pacemaker leads. In severe TR, there is an increase in diastolic flow, so many patients have a diastolic rumble (sometimes quite loud) along the left sternal border and/or a right sided S3. With severe long-standing TR, the pressure gradient between the right atrium and right ventricle is minimized and the TR murmur may be short early systolic, barely audible, or absent. A pulsatile liver is often present in severe TR, and ascites and extremity edema are commonly present.

Case 11

A 52-year-old male with no risk factors for coronary artery disease, presents with symptoms of shortness of breath on exertion and 2 episodes of near syncope. He has family history of sudden death. On examination, his carotid pulse has a rapid upstroke, followed by a second peak. His heart rate is 60 bpm and blood pressure 120/80 mmHg. His jugular veins are not distended. The apical impulse is wide,

Table 5.3 Effect of maneuvers on hypertrophic cardiomyopathy (HCM) and aortic stenosis

Maneuver	Hemodynamic effect	AS murmur intensity	HCM murmur intensity
Valsalva	Decreased preload	Decreases	Increases
Squat to stand	Decreased preload	Decreases	Increases
Stand to squat	Increased preload	Increases	Decreases
Amyl nitrite inhalation	Decreased preload	No change	Increases

sustained, and laterally displaced. On cardiac auscultation, S1 is normal and S2 is paradoxically split. A harsh crescendo-decrescendo 3/6 systolic murmur, heard best at the left sternal border, increases in intensity with the Valsalva maneuver, breath holding with increased abdominal pressure. His lungs are clear on auscultation, and abdominal examination is unrevealing.

Based on physical findings, this patient has hypertrophic cardiomyopathy (HCM). HCM is a common genetic cardiovascular disease and is defined as significant myocardial hypertrophy in the absence of an identifiable cause. The most common sites of ventricular hypertrophy are, in decreasing order, the septum, apex, and mid-ventricle. It is further classified as obstructive or non-obstructive, depending on whether a dynamic left ventricular outflow tract (LVOT) gradient is present, either at rest or with provocative maneuvers. LVOT obstruction is the main pathophysiologic mechanism in HCM. The hypertrophied proximal interventricular septum combines with systolic anterior motion (SAM) of the mitral valve leaflets towards the septum, which causes LVOT obstruction and also mitral regurgitation. LVOT obstruction in HCM is dynamic, in contrast to valvular or membranous AS where obstruction to LV outflow is fixed. In dynamic LVOT obstruction, the degree of obstruction varies with cardiac contractility and loading conditions, whereas in case of fixed obstruction such as AS, the degree of obstruction doesn't vary as much with maneuvers. Purposeful alterations in cardiac hemodynamics can be very useful at the bedside in differentiating systolic murmurs of HCM and AS (Table 5.3). Almost all cardiac murmurs decrease in intensity with the Valsalva maneuver except the murmur of HCM. The Valsalva maneuver decreases preload which results in reduced filling of the left ventricle and hence an increase in LVOT obstruction, thus increasing the intensity of systolic murmur in HCM. Similarly, change in position from squatting to standing reduces venous return and preload, thus increasing murmur intensity in HCM. Inhalation of amyl nitrite results in vasodilation and decreased preload, which again worsens LVOT obstruction in HCM and the murmur intensity increases. The gradient also increases in the beat after a premature ventricular complex (PVC) and during other types of positive inotropic activity, such as intravenous or endogenous catecholamies. Presence of a loud murmur of at least grade 3/6 usually implies LVOT outflow gradient of greater than 30 mmHg. The carotid pulse in patients with HCM is characterized by an initial rapid upstroke as no LVOT obstruction exists in early systole. This is followed by a collapse in the pulse as LVOT

obstruction develops, followed by a second peak as left ventricular pressure increases to overcome the obstruction. This is referred to as bisferiens pulse, which contrasts markedly from the carotid contour in valvular AS, as mentioned above. The second heart sound in HCM is normal in intensity, and can be paradoxically split due to prolonged ejection time with severe LVOT obstruction.

Case 12

A 45-year-old female, who immigrated from India, presents with new onset palpitations and dyspnea on exertion. She recalls having a prolonged febrile illness during childhood, followed by a murmur. On examination she has an irregularly irregular pulse with a heart rate of 84 bpm at rest and a blood pressure of 110/70 mmHg. Her jugular veins are not distended. The apical impulse has a tapping quality and is undisplaced. A parasternal RV heave is felt along with a palpable P2. On auscultation, S1 is loud, P2 is loud, and an opening snap is heard just after the second heart sound. A low-pitched "rumbling" early diastolic murmur is heard at the apex with the bell of the stethoscope, with the patient in left lateral decubitus position, in held exhalation. Bibasilar rales are heard on lung auscultation. Abdominal and lower extremity exam is unrevealing.

This patient likely has significant mitral stenosis (MS) secondary to rheumatic heart disease. MS is characterized by a pressure gradient between the left atrium and left ventricle during diastole (Fig. 5.5d). The transmitral pressure gradient for any given valve area depends on the transvalvular flow rate. Increase in transmitral flow, most commonly due to exercise, leads to increased pressure gradient and elevated left atrial pressure, which in turn raises pulmonary venous and pulmonary capillary pressures, resulting in dyspnea. Atrial fibrillation or any pathologic state involving an increased heart rate, such as anemia, hyperthyroidism, or others, shortens diastole more than systole. Because the time available for flow across the mitral valve is shorter, the heart spends more percentage of the time in the early phase of diastolic mitral valve flow, when gradients are higher, contributing to marked elevation in left atrial pressure. Chronic pulmonary venous and capillary hypertension leads to pulmonary arterial hypertension and often right sided heart failure, though not yet in this patient. Atrial fibrillation with rapid ventricular response is often a precipitating or exacerbating factor of the onset of symptoms in patients with MS and may result in pulmonary edema. In fact, MS with rapid AF is a condition where pulmonary edema responds well to beta blocker therapy. Diastolic filling time increases with reduction in heart rate, which reduces the left atrial pressure (because the mitral flow spends more time in "mid to late diastole" when the gradient is lower) and hence the pulmonary venous and capillary pressures are lower.

The physical findings in MS are attributable to two aspects of the inflammatory rheumatic process that leads to fibrosis: (1) Thickening and fibrosis of the valve cusps, and (2) commissural fusion. The classic auscultatory signs in mild MS, before the leaflets are very thickened, calcified or markedly immobile, include a loud S1 and an audible opening snap (OS) after S2. The intensity of S1 and presence of the opening snap (OS) reflect the pandiastolic pressure gradient. An important indicator of the severity of MS is the time interval between the S2 and OS, which is the time it takes for LV pressure to fall from late systolic aortic pressure to early diastolic left atrial pressure. With more severe MS, the left atrial pressure is higher and mitral valve opening occurs closer to S2, causing the S2-OS interval to decrease (Fig. 5.5d). With marked calcification and immobility of the mitral valve leaflets, both S1 and the OS become softer. The murmur of MS is a low-pitched rumbling diastolic murmur at the apex, best heard with the bell of the stethoscope with the patient in left lateral decubitus position. Listening in held exhalation brings the heart closer to the stethoscope and stops the interference of respiratory sounds. The diastolic murmur of MS can be accentuated by brief period of exercise, even just walking or running in place, due to the increased heart rate and the increase in cardiac output. In severe MS, the murmur is usually longer. In patients in sinus rhythm, the rumble is loudest when the gradients are highest, in very early and late diastole (during the atrial kick). The pre-systolic (late diastolic) accentuation of the diastolic murmur is lost when atrial fibrillation occurs.

Self-Assessment Questions

1. A 40-year-old asymptomatic lady presents for evaluation of a murmur that was heard by her primary care physician. On examination, her vital signs are normal. Her jugular veins are not distended and carotid upstrokes are normal. There is a systolic click followed by a 2/6 mid-late systolic murmur at the apex. In order to confirm your suspicion of mitral valve prolapse (MVP), you ask the patient to perform squatting and standing maneuvers. What happens to the click and the murmur with squatting and standing maneuvers in a patient with MVP?

   A. The click and murmur move closer to S1 with squatting and away from S1 with standing.
   B. The click and murmur move closer to S1 with standing and away from S1 with squatting.
   C. There is no change in the click or the murmur with standing or squatting.
   D. The click and the murmur decrease in intensity with standing and increase in intensity with squatting.

2. Each of the following statements regarding the jugular venous pressure (JVP) waveform and cardiac hemodynamics is true EXCEPT

A. Constrictive pericarditis is characterized by a prominent and steep or rapidly collapsing *y* descent.
B. Cardiac Tamponade is characterized by an absent *y* descent.
C. A cannon *a* wave is present in severe tricuspid regurgitation.
D. The *X* descent is lost in severe tricuspid regurgitation.

3. A 52-year-old lady with history of rheumatic heart disease, with history of open mitral commissurotomy 20 years ago, presents with new onset dyspnea on exertion and worsening palpitations. On examination she has an irregularly irregular pulse with a heart rate of 118 bpm and a blood pressure of 100/60 mmHg. Her jugular veins are distended. The apical impulse has a tapping quality and is undisplaced. A parasternal RV heave is felt along with a palpable P2. On auscultation, a low-pitched rumbling mid-diastolic murmur is heard at the apex with the bell of the stethoscope, with the patient in left lateral decubitus position. Bibasilar rales are heard on lung auscultation. What is the next best step in the management of this patient?

A. Sodium nitroprusside for afterload reduction.
B. Intravenous nitroglycerin infusion for preload reduction.
C. Intravenous Morphine.
D. Intravenous beta blocker therapy for rate control.

4. All of the following increase the murmur intensity in patients with hypertrophic obstructive cardiomyopathy, except:

A. Squatting.
B. Standing.
C. Valsalva maneuver.
D. Inhalation of amyl nitrite.

5. Each of the following is a finding in severe aortic stenosis, except

A. Pulsus parvus et tardus.
B. Soft or inaudible A2.
C. Mid-late peaking systolic murmur.
D. Bisferiens pulse.

Answers to Self-Assessment Questions

1. B.
Standing leads to reduction in venous return and preload. The left ventricle therefore becomes smaller, and prolapse occurs earlier in systole, i.e., closer to S1. Concurrently the intensity of the murmur increases. Squatting leads to increase in preload, causing an increase in LV chamber size, therefore the click and murmur occur later in systole and move away from S1.

2. C.
Cannon *a* wave is present in tricuspid stenosis or complete heart block where the right atrium contracts against a closed tricuspid valve due to atrio-ventricular dissociation. All other statements are true.
3. D.
This patient has rheumatic mitral stenosis and is in heart failure secondary to atrial fibrillation with rapid ventricular response. Tachycardia shortens diastole more than systole, thus reducing the time available for flow across the mitral valve and contributing to marked elevation in left atrial pressure and pulmonary edema. Pure mitral stenosis is the only condition where acute heart failure is treated with beta blocker therapy for heart rate control.
4. A.
Decrease in preload, secondary to any maneuver (valsalva, standing, and inhalation of amyl nitrite) results in reduced filling of the left ventricle and hence LVOT obstruction increases, thus increasing the intensity of systolic murmur in HCM. Squatting on the other hand increases preload, increasing ventricular volume and reducing the LVOT gradient, hence making the murmur softer in intensity.
5. D.
In severe AS, the weak and delayed (parvus et tardus) carotid pulse reflects severe obstruction of blood flow across the aortic valve into the peripheral circulation. With worsening AS, the aortic valve leaflets become increasingly calcified and immobile, leading to a soft or inaudible A2 component of S2. With mild AS, the maximum instantaneous gradient between the left ventricle and aorta occurs early in systole; hence the systolic murmur peaks in early systole. As the severity of AS worsens, the maximum instantaneous gradient between the left ventricle and the aorta occurs progressively later in systole, and correspondingly the murmur peaks late. Bisferiens pulse is seen in patients with severe AR or HOCM.

References

1. Stevenson LW, Perloff JK. The limited reliability of physical signs for estimating hemodynamics in chronic heart failure. JAMA. 1989;261:884–8.
2. Gheorghiade M, Abraham WT, Albert NM, Greenberg BH, O'Connor CM, She L, et al. Systolic blood pressure at admission, clinical characteristics, and outcomes in patients hospitalized with acute heart failure. JAMA. 2006;296:2217–26.
3. Drazner MH, Hamilton MA, Fonarow G, Creaser J, Flavell C, Stevenson LW. Relationship between right and left-sided filling pressures in 1000 patients with advanced heart failure. J Heart Lung Transplant. 1999;18:1126–32.
4. Butman SM, Ewy GA, Standen JR, Kern KB, Hahn E. Bedside cardiovascular examination in patients with severe chronic heart failure: importance of rest or inducible jugular venous distension. J Am Coll Cardiol. 1993;22:968–74.
5. Braunwald E, Perloff JK. Physical examination of the heart and circulation. New York: Elsevier; 2005. p. 817–8.

6. Marcus GM, Gerber IL, McKeown BH, Vessey JC, Jordan MV, Huddleston M, et al. Association between phonocardiographic third and fourth heart sounds and objective measures of left ventricular function. JAMA. 2005;293:2238–44.
7. Wang CS, FitzGerald JM, Schulzer M, Mak E, Ayas NT. Does this dyspneic patient in the emergency department have congestive heart failure? JAMA. 2005;294:1944–56.
8. Marcus GM, Vessey J, Jordan MV, Huddleston M, McKeown B, Gerber IL, et al. Relationship between accurate auscultation of a clinically useful third heart sound and level of experience. Arch Intern Med. 2006;166:617–22.
9. Shah SJ, Marcus GM, Gerber IL, McKeown BH, Vessey JC, Jordan MV, et al. Physiology of the third heart sound: novel insights from tissue Doppler imaging. J Am Soc Echocardiogr. 2008;21:394–400.
10. Nagueh SF, Mikati I, Kopelen HA, Middleton KJ, Quinones MA, Zoghbi WA. Doppler estimation of left ventricular filling pressure in sinus tachycardia. A new application of tissue Doppler imaging. Circulation. 1998;98:1644–50.
11. Nohria A, Mielniczuk LM, Stevenson LW. Evaluation and monitoring of patients with acute heart failure syndromes. Am J Cardiol. 2005;96:32G–40.
12. Weis AJ, Salcedo EE, Stewart WJ, Lever HM, Klein AL, Thomas JD. Anatomic explanation of mobile systolic clicks: implications for the clinical and echocardiographic diagnosis of mitral valve prolapse. Am Heart J. 1995;129:314–20.
13. Little WC, Freeman GL. Pericardial disease. Circulation. 2006;113:1622–32.
14. Tyberg TI, Goodyer AV, Langou RA. Genesis of pericardial knock in constrictive pericarditis. Am J Cardiol. 1980;46:570–5.
15. Freeman GL, LeWinter MM. Pericardial adaptations during chronic cardiac dilation in dogs. Circ Res. 1984;54:294–300.
16. Spodick DH. Acute cardiac tamponade. N Engl J Med. 2003;349:684–90.
17. Munt B, Legget ME, Kraft CD, Miyake-Hull CY, Fujioka M, Otto CM. Physical examination in valvular aortic stenosis: correlation with stenosis severity and prediction of clinical outcome. Am Heart J. 1999;137:298–306.
18. Leach RM, McBrien DJ. Brachioradial delay: a new clinical indicator of the severity of aortic stenosis. Lancet. 1990;335:1199–201.
19. Etchells E, Glenns V, Shadowitz S, Bell C, Siu S. A bedside clinical prediction rule for detecting moderate or severe aortic stenosis. J Gen Intern Med. 1998;13:699–704.
20. Babu AN, Kymes SM, Carpenter Fryer SM. Eponyms and the diagnosis of aortic regurgitation: what says the evidence? Ann Intern Med. 2003;138:736–42.
21. Choudhry NK, Etchells EE. The rational clinical examination. Does this patient have aortic regurgitation? JAMA. 1999;281:2231–8.
22. Reynolds HR, Hochman JS. Cardiogenic shock: current concepts and improving outcomes. Circulation. 2008;117:686–97.
23. Kohsaka S, Menon V, Lowe AM, Lange M, Dzavik V, Sleeper LA, et al. Systemic inflammatory response syndrome after acute myocardial infarction complicated by cardiogenic shock. Arch Intern Med. 2005;165:1643–50.
24. Landry DW, Oliver JA. The pathogenesis of vasodilatory shock. N Engl J Med. 2001;345:588–95.
25. Annane D, Bellissant E, Cavaillon JM. Septic shock. Lancet. 2005;365:63–78.
26. McGee S, Abernethy III WB, Simel DL. The rational clinical examination. Is this patient hypovolemic? JAMA. 1999;281:1022–9.

Chapter 6
Echocardiography

Omeed Zardkoohi and Richard A. Grimm

Introduction

Echocardiography is a powerful, noninvasive imaging tool that can provide useful hemodynamic information to guide patient management. Intracardiac pressures, cardiac output, vascular resistance, shunt fractions, and valve lesions can be assessed by using a combination of two-dimensional imaging, color Doppler, Pulse and Continuous wave Doppler, and Tissue Doppler. While echocardiography can provide data complementary to catheter-derived measurements and in some situations has even supplanted invasive monitoring, its application requires meticulous technique, an understanding of basic physics principles, and an appreciation of its limitations.

Basic Physics of Echocardiography

Doppler Principle

The Doppler principle explains that the frequency of a wave increases as the source of the wave moves toward an observer, while the frequency of a wave decreases as the source moves away from an observer [1]. The change in the frequency of sound depends on the velocity of the moving object, the velocity of sound, and the angle at which the sound hits the object. Echocardiography extrapolates this principle of frequency shift to determine the velocity of blood flow in the heart. When a sound wave is transmitted from the transducer crystal at a given frequency, it is reflected by a red blood cell at a certain frequency back to the transducer (Fig. 6.1). If the red

O. Zardkoohi, M.D. • R.A. Grimm, D.O. (✉)
The Cleveland Clinic, Cleveland, OH, USA
e-mail: zardkoo@ccf.org; grimmr@ccf.org

A.T. Askari et al. (eds.), *Cardiovascular Hemodynamics: An Introductory Guide*, Contemporary Cardiology, DOI 10.1007/978-1-60761-195-0_6,

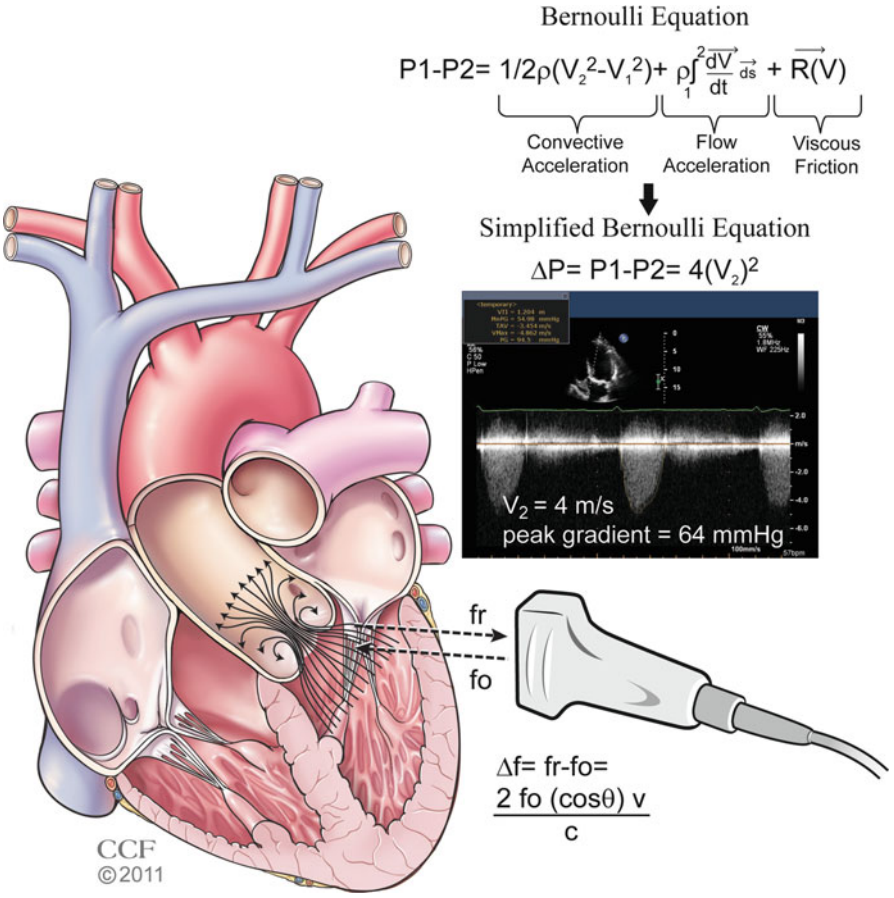

Fig. 6.1 The Doppler principle and Bernoulli equation. *Bottom right*: The echo transducer sends ultrasound waves at a given frequency (f_0) to the heart, and the sound waves are reflected back to the transducer at a different frequency (f_r). The difference between (f_0) and (f_r) is the *Doppler shift*. As shown in the equation, the Doppler shift is directly proportional to the transmitted frequency (f_0), the cosine of the angle of incidence θ (angle between the ultrasound wave and vector of the red blood cell), and the velocity of the red blood cells, however, is inversely proportional to the speed of ultrasound in the medium (c). Rearrangement of the equation allows one to determine the velocity of the red blood cells. *Top right*: The Bernoulli equation enables one to determine the pressure gradient across a stenosis, in this case, a stenotic aortic valve. Flow accelerates just before and at the level of the stenosis. The velocity proximal to the stenosis is V_1, and the velocity distal to the stenosis is V_2. Based on certain assumptions (see text), the Bernoulli equation can be simplified to $P1-P2=\Delta P=4(V_2)^2$. In this case, the peak gradient is 64 mmHg based on the peak velocity across the aortic valve (V_2) of 4 m/s. Reprinted with permission, Cleveland Clinic Center for Medical Art & Photography © 2011

blood cell is moving toward the sound waves, the frequency will increase, but if the red blood cell is moving away from the sound wave, the frequency will decrease. The Doppler shift is the change in frequency between the transmitted sound and the reflected sound, and is expressed in the following Doppler equation [2]:

$$\Delta f = f_r - f_0 = \frac{2f_0(\cos\theta)(v)}{c}$$

where f_0 = transmitted frequency; f_r = reflected frequency; θ = angle between the ultrasound beam and blood flow; v = velocity of red blood cells; c = speed of ultrasound in blood (1,540 m/s).

Algebraic rearrangement of the equation allows one to solve for velocity:

$$v = \frac{(c)(\Delta f)}{2(f_0)(\cos\theta)}$$

Note that the number "2" in the equation results from the fact that there are actually two Doppler shifts: one when the sound wave sent from the transducer strikes the red blood cell, and the other when the wave reflected from the red blood cell is sent back to the transducer. Doppler echocardiography is highly angle-dependent. *The angle should ideally be <20° which results in <10% underestimation of true flow velocity* [2]. When the ultrasound beam is ideally oriented parallel to the direction of blood flow, that is, when the angle θ is 0°, the equation is simplified since the cosine of 0° is 1. Using the simplified Bernoulli principle (see below), it follows that velocity can be used to estimate pressures.

Continuous Wave vs. Pulse Wave Doppler

Two forms of Doppler echocardiography are pulse wave (PW) Doppler and continuous wave (CW) Doppler. Pulse wave Doppler employs a single crystal that emits short bursts or pulses of ultrasound at a certain rate per second, known as the *pulse repetition frequency (PRF)*, which is dependent on the depth of interrogation. These pulses are sent to a particular sampling location or depth, and the same crystal listens or waits for the reflected frequency (Fig. 6.2a). Because the same crystal sends and receives the ultrasound wave, the maximum velocity that can be measured is limited by the time it takes to send and receive the wave. This is called the *Nyquist limit*, which is one-half the PRF. *The PRF and the Nyquist limit are solely determined by the depth of the sample volume and not by the transducer frequency*. The shallower the sample volume, the higher the PRF or number of pulses sent per second by the transducer. If the Doppler frequency shift is greater than the Nyquist limit, then the velocities above this limit are cut off the spectral Doppler profile and

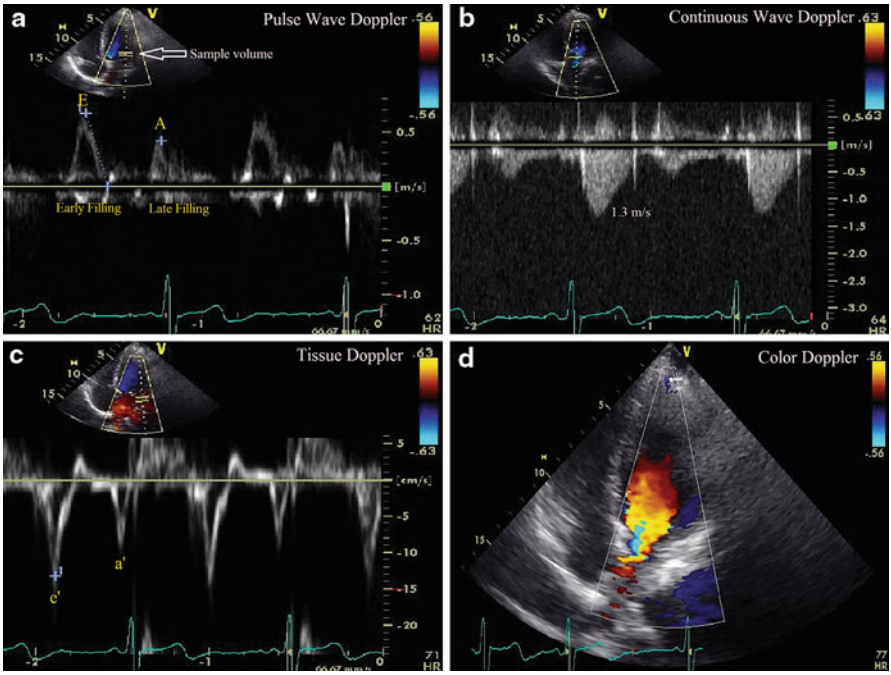

Fig. 6.2 Various forms of Doppler in echocardiography. (**a**) Pulse wave (PW) Doppler of the mitral inflow with the sample volume placed at the leaflet tips. In PW, the same transducer crystal sends and receives waves to determine the Doppler shift at a particular sample volume, marked by the *white arrow*. Because PW obtains information about a particular location, it is said to have "range resolution," however, it is prone to aliasing. Note that in diastole there is early filling (*E* wave) and Late Filling (*A* wave). Diastasis is known as the period between the *E* and the *A* wave. The *E* velocity is 68 cm/s. (**b**) Continuous wave (CW) Doppler across the aortic valve. In CW, one crystal sends sound waves continuously and another crystal receives the sound waves. Because the CW profile represents all the velocities along the path of interrogation (represented by the *dotted line*), the peak velocity cannot be localized based on the CW signal alone. This phenomenon is known as "range ambiguity." The *y* axis is velocity and the *x* axis is time, and therefore the area under the curve is the velocity time integral (VTI), or the aortic valve VTI, in units of distance (cm). In this example, the peak velocity is 1.3 m/s and the Aortic Valve VTI is 22 cm. (**c**) Tissue Doppler of the mitral annulus characterizes annular velocities, with the corresponding annular e' and a' waves. These waves correspond temporally with the *E* and *A* waves of the mitral inflow. Because $E = 68$ cm/s and $e' = 13$ cm/s, the ratio E/e' is roughly 5, suggesting normal PCWP pressures. (**d**) Color Doppler in which the color pixels represent the mean velocity vector at a particular location

wrap around to the opposite direction, a phenomenon known as aliasing [1]. Anyone who has watched a wagon wheel in a Western movie appreciates this phenomenon. As the wagon starts to move away, the wheel appears to be moving clockwise. But as the wagon wheel picks up speed and exceeds the "Nyquist limit" of the movie camera, the wheel appears to be moving counterclockwise, which is the equivalent of aliasing. An example of aliasing in echocardiography can be found in Fig. 6.4c,

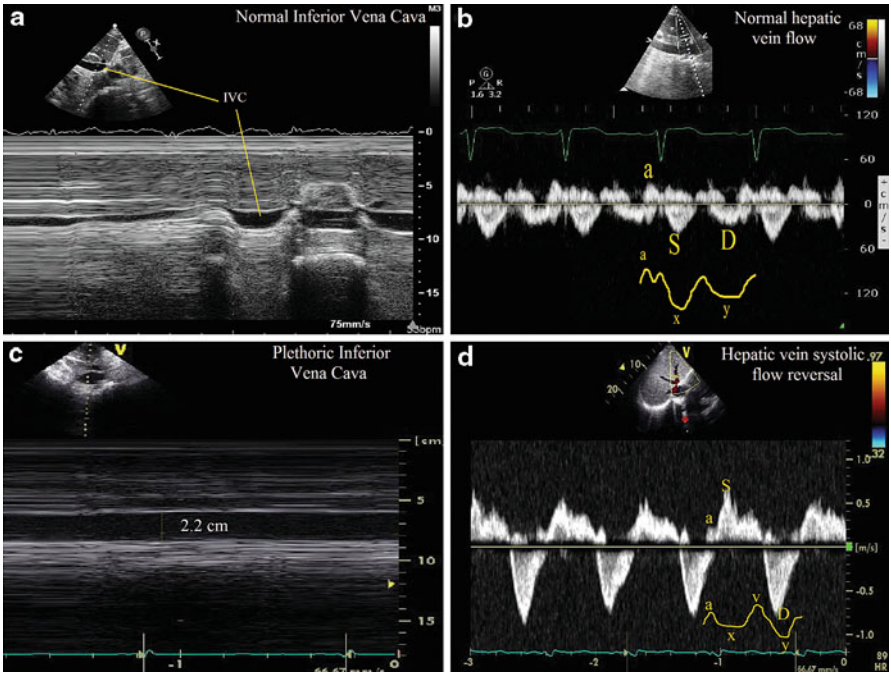

Fig. 6.3 Right sided pressures. (**a**) M-mode through the IVC from the subcostal view. Note that the IVC size is <2.1 cm and collapses greater than 50%, suggesting normal right atrial pressure (0–5 mmHg). (**b**) Pulse wave (PW) Doppler of the hepatic vein showing normal hepatic vein flow. Note that there are two antegrade waves (*S* and *D*), and one retrograde wave (*a* reversal). The representative portions on the JVP waveform are shown (*S* corresponds to the *x* descent, and *D* corresponds to the *y* descent). The onset of the *S* wave corresponds to the onset of the QRS (isovolumic contraction), although the peak occurs in mid to late systole. In this example, the velocity of the *S* wave is larger than the *D* wave, indicating normal right atrial pressures. (**c**) A plethoric IVC greater than 2.1 cm in width which does not collapse, suggesting a right atrial pressure between 10 and 20 mmHg. (**d**) Systolic flow reversal in the hepatic veins in severe tricuspid regurgitation. Notice that the *S* wave is above the baseline, indicating flow reversal. This corresponds to the blunted *x* descent and tall *v* wave in the JVP waveform

in which PW is used to determine the right ventricular outflow tract (RVOT) velocity. Note that during diastole, the pulmonary regurgitation jet velocity exceeds the Nyquist limit of 1 m/s and wraps around (aliases) to the negative portion of the spectral Doppler profile. Therefore, PW *is suited for measuring low velocity flow (<2 m/s) at specific locations in the heart*, such as the left ventricular outflow tract (LVOT), right ventricular outflow tract (RVOT), mitral inflow, tricuspid inflow, and hepatic vein inflow. PW has the property of "range specificity" in that it provides information at a specific location. Figure 6.2a shows PW of the mitral inflow with sample volume at the leaflet tips, demonstrating the three phases of diastole: early filling (*E* wave), diastasis, and late filling (*A* wave).

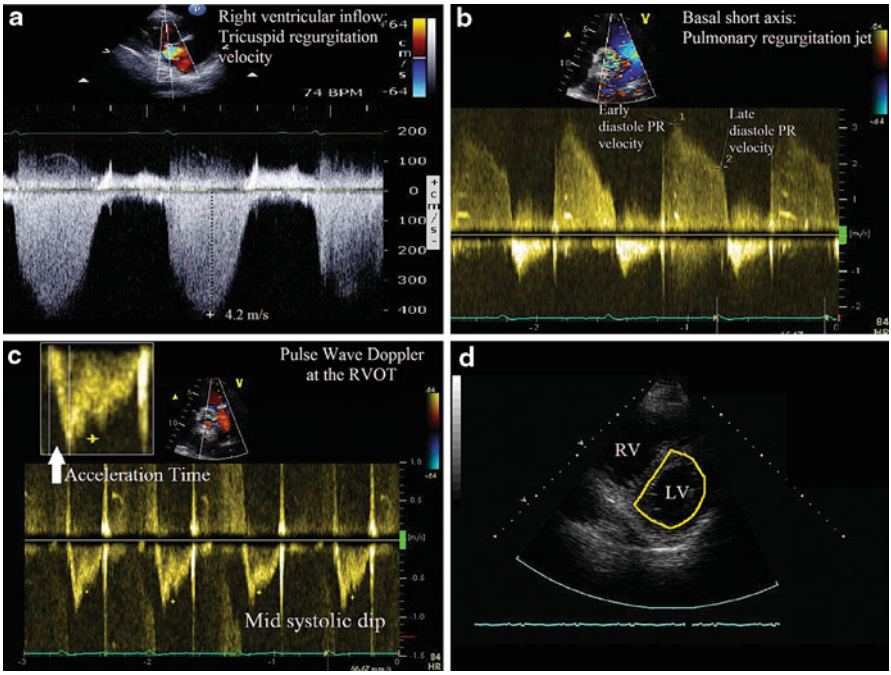

Fig. 6.4 Pulmonary pressures and signs of pulmonary hypertension. (**a**) The right ventricular systolic pressure can be estimated from the peak tricuspid regurgitation velocity obtained in the right ventricular inflow view (*see Question 1*). (**b**) The Continuous wave (CW) Doppler profile of the pulmonary regurgitation jet. The early peak velocity can be used to determine the mean pulmonary artery (PA) pressure by the following formula: Mean PA Pressure $= 4v_{\text{EarlyDPR}}{}^2$. In this case, early pulmonary regurgitation (PR) jet velocity is 3.9 m/s and the end-diastolic PR velocity is 1.9 m/s. Therefore, the mean PA pressure is roughly 39 mmHg. Also, the pulmonary artery end-diastolic pressure (PAEDP) can be determined from the end-diastolic velocity and estimated right atrial (RA) pressure: PAEDP $= \text{RA} + 4v_{\text{EDPR}}{}^2$ (*see Question 2*). Note that in pulmonary hypertension, there is absence of the typical end-diastolic dip in the pulmonary regurgitation CW profile that normally corresponds to atrial systole. (**c**) The sample volume is in the RVOT, just below the pulmonic valve. In pulmonary hypertension, there is a steep slope in early systole (acceleration phase becomes shorter, *upper left corner*) and there can be a mid-systolic dip in the RVOT profile (*yellow stars*), due to high afterload. A simplified formula to calculate the mean pulmonary artery pressure (MPAP) is MPAP $= 80 - 0.5$ (acceleration time (ms)). Acceleration time is roughly 90 ms, yielding a MPAP of 35 mmHg. (**d**) Note the D-shaped septum during systole, suggestive of RV pressure overload

Because continuous wave (CW) Doppler employs two crystals, one continuously emitting ultrasound waves and the other continuously receiving reflected waves, it does not fall under the Nyquist limitation (Fig. 6.2b). This allows for interrogation of higher velocities without aliasing. *In CW, all the velocities along the ultrasound beam are recorded, rather than the velocities at one particular location. The peak velocity cannot be localized based on the CW signal alone, a phenomenon known as* "range ambiguity." CW is used to assess gradients in aortic stenosis and mitral

stenosis, peak mitral regurgitation velocity, peak tricuspid regurgitation velocity, and intracardiac shunt velocity.

Finally, Tissue Doppler is a specialized form of PW that allows the interrogation of myocardial and annular velocities by focusing on lower velocities of higher amplitude with a high frame rate (Fig. 6.2c). Tissue Doppler Imaging is employed in the estimation of intracardiac pressures, quantification of wall motion in stress echo, detection of diastolic dysfunction, and intra ventricular dyssynchrony, among other applications.

Color Doppler

Color Doppler provides a visual representation of intracardiac flow by translating the velocity vector into color: red and yellow represent flow moving toward the transducer and blue hues represent flow moving away from the transducer (Fig. 6.2d). Note that in the color scale which appears to the right of Fig. 6.2d, the darker the color shade, the closer to zero the velocity becomes, with black representing 0 m/s. The color image is constructed by the summation of multiple scanning lines which translates Doppler shifts into mean velocity, and then the mean velocity into a color based on the color scale. To determine real-time, accurate blood velocities along the path of multiple scanning lines, the transducer must rapidly send multiple groups of pulses or "packets" with pulse wave Doppler. While having more pulses per "packet" increases the accuracy of velocity measurements, this occurs at the expense of temporal resolution because more time is needed to acquire the information from the pulses. Because color Doppler relies on PW, if the velocity of flow is greater than the Nyquist limit, color aliasing occurs, in which color may reverse from blue to yellow, for example.

Bernoulli Equation

The *Bernoulli equation* can be widely applied to echocardiographic hemodynamic assessment. It is used to calculate the gradient across a stenosis, a regurgitant valve, or a septal defect between two cardiac chambers, and it consists of three components: *convective acceleration, flow acceleration*, and *viscous friction* (Fig. 6.1) [3].

$$P1 - P2 = \underbrace{\frac{1}{2}\rho(V_2^2 - V_1^2)}_{\text{Convective acceleration}} + \underbrace{\rho\int_1^2 \frac{\overrightarrow{dV}}{dt}\overrightarrow{ds}}_{\text{Flow acceleration}} + \underbrace{R(\vec{V})}_{\text{Viscous friction}}$$

where $P1$ = pressure proximal to stenosis; $P2$ = pressure distal to the stenosis, ρ = mass density of blood (1.06×10^3 kg/m^3); V_1 = velocity at proximal location; V_2 = velocity at distal location; ds = acceleration distance; R = viscous resistance.

Convective acceleration is the increase in kinetic energy that corresponds to the pressure drop across the orifice, and is analogous to the conversion of potential energy to kinetic energy that occurs when an object falls by gravity [3]. The *flow acceleration* component describes the pressure drop required to accelerate the blood by overcoming the blood's inertial forces. Finally, the *viscous friction* component describes the frictional, viscous force that results from neighboring blood cells moving at different velocities.

There are some features of blood flow in the human heart that allow for simplification of the Bernoulli equation. First, the *viscous friction* term is negligible because the velocity profile of blood through a stenotic valve is relatively flat (little variation in blood velocity and therefore little friction), as well as because orifice diameters in the heart are relatively large, minimizing the effect of friction at the center of the orifice. In addition, previous studies have indicated that in most clinical situations the *flow acceleration* component is negligible [3]. In single, stenotic lesions, the proximal velocity term V_1 is typically small (<1 m/s) and can be ignored. Therefore, because in most clinical scenarios the *viscous friction*, *flow acceleration*, and V_1 components are negligible, the Bernoulli equation is simplified to $P1 - P2 = \Delta P = 4(V_2)^2$ (Fig. 6.1).

Intracardiac Pressures

The guide through echocardiographic assessment of various cardiac chamber pressures will follow the same sequence as during a diagnostic right heart catheterization, beginning with the right atrium. A summary of the equations discussed is presented at the end of the chapter (Fig. 6.10).

Right Atrium

Right atrial pressure is reflected in the size of the inferior vena cava (IVC), its response to changes in intrathoracic pressure, and the hepatic vein Doppler profile. Interrogation of the IVC by transthoracic echocardiography can be performed with the subcostal view (Fig. 6.3a, c). An *IVC diameter ≤2.1 cm that collapses >50% with sniffing (which causes an acute drop in intrathoracic pressure resulting in decreased venous return) suggests a normal RA pressure of 3 mmHg (range 0–5 mmHg)* [4]. *An IVC diameter >2.1 cm that collapses <50% with a sniff suggests a high RA pressure around 15 mmHg (range 10–20 mmHg)*. IVC profiles that do not fit into these two categories (i.e., IVC ≤ 2.1 cm but <50% collapse or IVC > 2.1 cm but >50% collapse) can be designated as an intermediate RA pressure of 8 mmHg. Other additional parameters such as hepatic vein profile can be used to further refine this estimated pressure. Young healthy adults may have dilated IVCs but normal RA pressure, and estimation of RA pressure using the IVC index may not be reliable in patients who are intubated [4]. An additional estimate of right

atrial pressure is derived from the ratio of the tricuspid inflow diastolic *E* wave velocity and the right ventricular annular *e′* velocity, which is the right sided correlate of estimating left atrial pressure by tissue Doppler. A ratio of $E/e' > 6$ is suggestive of high right atrial pressures. This method can be used in situations where IVC measurements are unobtainable or inaccurate [5].

Because the hepatic vein drains into the IVC, which then drains into the RA, the hepatic vein Doppler profile can provide complementary information regarding right atrial and ventricular hemodynamics. The hepatic vein profile consists of two main antegrade flow waves (systolic (*S*) and diastolic (*D*) waveforms) and a retrograde atrial wave (*a*) (Fig. 6.3b). The *S*, *D*, and *a* waves correspond to the *x*, *y*, and *a* waves of the jugular venous pressure waveform, respectively. Flow in the hepatic vein is sensitive to respiration, with increasing antegrade flow during inspiration and decreasing flow during expiration. With normal RA pressure, there is a predominance of the *s* wave in the antegrade waveform, whereas with elevated RA pressure, because the pressure gradient between the RA and the hepatic vein is lower, the *s* wave is blunted and the *d* wave predominates. *More quantitatively, a ratio of the s wave velocity divided by the sum of the s and d wave velocity [Vs/(Vs + Vd)] less than 55% is highly correlated with an elevated RA pressure* [6]. In addition, in severe tricuspid regurgitation, there may even be systolic wave reversal, which is the echocardiographic equivalent of the loss of the *x* descent in the jugular venous waveform (Fig. 6.3d). In pulmonary hypertension, there may prominent flow reversal during atrial systole (prominent *a* wave) due to high pulmonary pressures transmitting back to the atrium during diastole. Utilizing the ECG to accurately differentiate systolic flow reversal in the hepatic vein (which should occur coincident with isovolumic contraction) from a prominent (*a*) wave can be key to avoiding misinterpretation of quite different hemodynamic conditions.

Right Ventricle

In the absence of tricuspid stenosis, the right ventricular end-diastolic pressure should equal the RA pressure as estimated from the IVC measurement. If tricuspid regurgitation (TR) is present, the peak velocity (v_{TR}) measured at end-expiration can be used to estimate the pressure gradient between the right ventricle and right atrium during systole ($\Delta P = 4V_{TR}^2$) (Fig. 6.4a). This pressure gradient can be added to the RA pressure to estimate the right ventricular systolic pressure ($RVSP = RA + 4V_{TR}^2$). A TR velocity greater than 2.8–2.9 cm/s, in the setting of a normal RA pressure (0–5 mmHg), corresponds roughly to an RVSP of 36 mmHg, which indicates the presence of mild pulmonary hypertension [4].

In cases of severe TR, in which the tricuspid valve is essentially "wide-open" during systole and there is no longer a fixed orifice with a significant pressure drop across the orifice, the RVSP may be underestimated. This is due to the fact that the flow acceleration (inertance) component of the Bernoulli equation in is no longer negligible (a pressure drop must occur to overcome the inertance of the large

volume of blood), while the convective flow component is less important (large orifice). Therefore, the simplified Bernoulli equation, which includes only the convective component, typically underestimates the RVSP in this scenario [4, 7].

If there is no RVOT obstruction or pulmonary stenosis, then the RVSP should be equal to the pulmonary artery systolic pressure (PASP). In the presence of pulmonary stenosis, because the peak gradient across the pulmonary valve during systole represents the pressure drop from the RV to the pulmonary artery (PA), the PASP can be derived from subtracting the peak gradient across the pulmonary valve during systole (obtained by CW) from the RVSP obtained from the TR jet [8].

Pulmonary Artery

As stated above, the PASP is equal to the right ventricular systolic pressure in the absence of RVOT obstruction. The end-diastolic pressure gradient between the pulmonary artery and the right ventricle is extrapolated from the end-diastolic velocity of the pulmonary regurgitation jet ($\Delta P = 4V_{PRed}{}^2$) (Fig. 6.4b). Because this jet represents the difference between pulmonary artery end-diastolic pressure (PAEDP) and RVEDP (i.e., $\Delta P = 4V_{PRed}{}^2 = \text{PAEDP} - \text{RVEDP}$), and RVEDP equals RA pressure in the absence of tricuspid stenosis, it follows by algebraic manipulation that $\text{PAEDP} = \text{RA} + 4V_{EDPR}{}^2$ [9]. Also, the mean PA pressure can be estimated from the peak pulmonary regurgitation jet velocity (Mean PA Pressure $= 4V_{EarlyDPR}{}^2$) or the RVOT flow measured by PW Doppler using the formula $80 - 0.5 * (\text{pulmonic acceleration time(ms)})$ (Fig. 6.4c) [10]. These formulae can be useful when TR velocity signal is weak and unreliable. Estimation of pulmonary vascular resistance can be made by determining the ratio of the Peak TR velocity and the RVOT VTI (right ventricular outflow tract velocity time integral) in the following formula:

$\text{PVR(Woods units)} = 10 * (\text{peak TR velocity(m/s)}/\text{RVOT VTI(cm)}) + 0.16$ [11].

Echocardiographic signs of pulmonary hypertension include a D-shaped left ventricle, loss of the atrial systolic dip in the pulmonary regurgitation jet, and a mid-systolic decrease in the pulmonary outflow velocity (Fig. 6.4).

Pulmonary Capillary Wedge/Left Atrial Pressure

One method of estimating the left atrial (LA) pressure is to determine the peak mitral regurgitation velocity (V_{MR}), from which one can derive the pressure gradient between the left ventricle (LV) and LA (LV systolic pressure − LA pressure $= 4V_{MR}{}^2$) [12]. Because the LV systolic pressure equals the systolic blood pressure (SBP) in the absence of LVOT obstruction, the LA pressure $= \text{SBP} - 4V_{MR}{}^2$. A more common method of estimating the left atrial pressure is to determine the ratio of the mitral inflow *E* velocity to septal mitral annular velocity (*e′*), or *E*/*e′* [13]. *An E/e′ ratio of*

>15 is highly correlated with a pulmonary capillary wedge pressure (PCWP) >20, while an E/e′ ratio less than 8 corresponds to a normal PCWP [13]. This method is valid for patients with normal and abnormal systolic function. Tissue Doppler derived estimates of PCWP can be used in patients with atrial fibrillation as well. However, in patients with constriction the exaggerated *e′* velocity, which corresponds to the rapid *y* descent on JVP waveform, yields a low *E*/*e′* ratio in spite of the fact that the left atrial pressures are elevated. This is the so called *annulus paradoxus* [14].

Finally, in patients with aortic insufficiency, because the end-diastolic velocity of the aortic regurgitation jet ($4V_{AI}^2$) represents the pressure gradient between the aorta (diastolic blood pressure or DBP) and the LV end-diastolic blood pressure (LVEDP), one can estimate the LVEDP using the following formula: $\text{LVEDP} = \text{DBP} - 4V_{\text{EDAI}}^2$. Measurement error inherent with sphygmomanometric readings provides the primary limitation of this method. In the case of severe acute AI, where the end-diastolic velocity of the aortic insufficiency jet approaches zero, the LVEDP approaches the DBP.

Cardiac Output and System Vascular Resistance

The flow rate through a vessel is the product of the cross-sectional area of the vessel and the velocity of blood. However, because velocity varies over time throughout the cardiac cycle due to pulsatility, one cannot take an instantaneous velocity to measure overall flow rate. Rather, an integral of the velocities over time, called the VTI from the Doppler profile, is used to characterize integrated velocity in a given time period to determine flow (volume), rather than flow rate (volume/time) (Fig. 6.5a, b). VTI is essentially a measure of stroke distance. When the VTI (distance) is multiplied by the cross-sectional area (distance squared), the product is a volume (distance cubed). Therefore, stroke volume of the left ventricle can be estimated by multiplying the cross-sectional area of the LVOT ($\pi r^2 = \pi (D/2)^2 = \pi D^2/4 = D^2 * 0.785$, where r is radius and D is diameter) obtained in the parasternal long axis view and multiplying it by the VTI of the PW Doppler profile obtained in the apical long axis view (Fig. 6.5a). The PW cursor is typically placed about 0.5–1 cm below the valve to obtain a laminar flow curve. It is important to measure the PW Doppler profile at the same location as the measured cross-sectional area to maintain accuracy. This stroke volume can be multiplied by the heart rate to give an estimated cardiac output (in the absence of significant aortic regurgitation). If there is no regurgitation or intracardiac shunts, then the stroke volume through the tricuspid, pulmonary, mitral, and aortic valves should be equivalent, and therefore, the principle of multiplying the cross-sectional area of these valves by the VTI of flow across the valves can be applied throughout the heart. Practically speaking however, stroke volume is typically measured in the LVOT.

If a left to right shunt is present (i.e., ASD or VSD), then it is clinically relevant to estimate the severity of the shunt by determining the ratio of pulmonary blood flow (Q_p) to systemic blood flow (Q_s). Figure 6.6 shows an example of a secundum ASD with left to right flow. Systemic stroke volume is measured by multiplying the LVOT

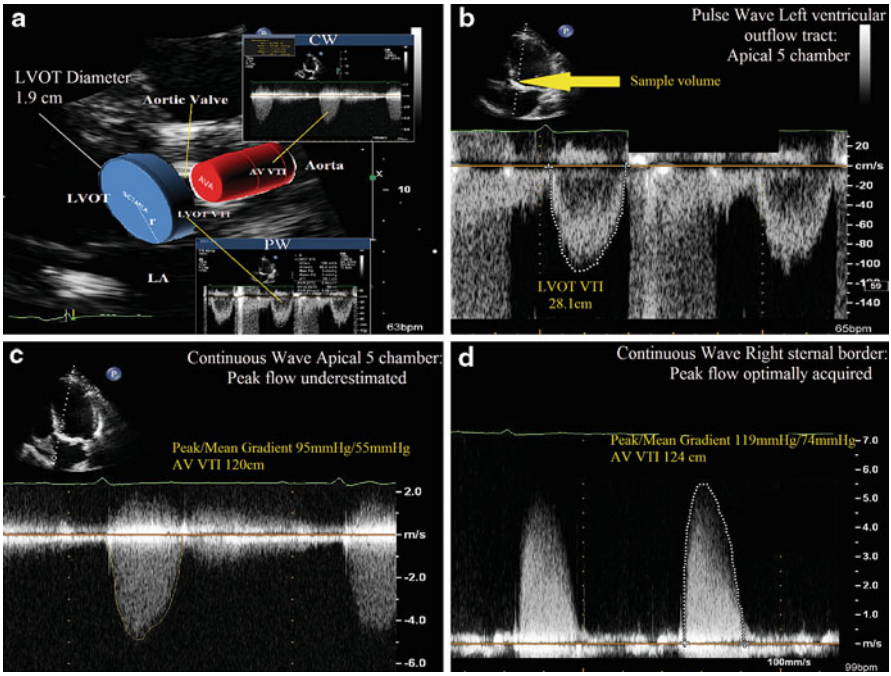

Fig. 6.5 Stroke volume and aortic valve area (AVA) calculation using the continuity equation. (**a**) Based on the continuity equation, the flow through the left ventricular outflow tract (LVOT), or the volume of the *blue cylinder*, must equal the flow through the aortic valve, or the volume of the *red cylinder*. The stroke volume (represented by the *blue cylinder*) is estimated by multiplying the LVOT area by the LVOT VTI. The LVOT area is obtained using the equation Area = πr^2 = (Diameter)^2*0.785, with the diameter measured in the parasternal long axis view. Because the LVOT diameter in this case is 1.9 cm, the LVOT area is 2.84 cm^2. From the apical 5 chamber or apical long axis view, the LVOT VTI is obtained, which in this case is 28.1 cm (*bottom right* and (**b**)). Therefore, the stroke volume = 28.1 cm*2.84 cm^2 = 79.8 cm^3. The product of the stroke volume and the heart rate (SV*HR) can give an estimate of cardiac output. The volume of the *red cylinder* is the product of the AVA and the AV VTI (**c**, **d**). Because the volume of the *blue cylinder* (LVOT Area*LVOT VTI) must equal the volume of the *red cylinder* (AVA*AV VTI) to satisfy the continuity equation, it follows that $\text{AVA} = [\text{LVOT VTI} * (\text{LVOT diameter})^2 * 0.785] / [\text{AV VTI}] = \text{Stroke volume} / \text{AV VTI}$ (*see Question 3*). (**b**) Pulse wave Doppler Sample volume is placed just below the aortic valve in the 5 chamber view, and the LVOT VTI is traced. (**c**) Continuous wave Doppler measures the highest velocity along its path to estimate the peak and mean gradient across the aortic valve. The peak and mean gradients are 95/55 mmHg from the 5 chamber view, which is an underestimation of peak flow in this particular patient. Multiple views are necessary to obtain the highest, most representative jet velocity, as seen in (**d**) Right sternal border view obtains peak and mean gradients of 119/74 mmHg, higher than the peak gradient of 95 mmHg from the apical 5 chamber view

area (D^2*0.785) by the LVOT VTI from the parasternal long axis views and the apical long axis views, respectively,. The pulmonary stroke volume is measured by multiplying the RVOT Area by the RVOT VTI, measured in the basal short axis view across the pulmonary valve. The ratio of Q_p/Q_s, which equals [(RVOT VTI)(RVOT D^2*0.785)]/[(LVOT VTI)(LVOT D^2*0.785)], gives an estimate of the shunt fraction (Fig. 6.6). The

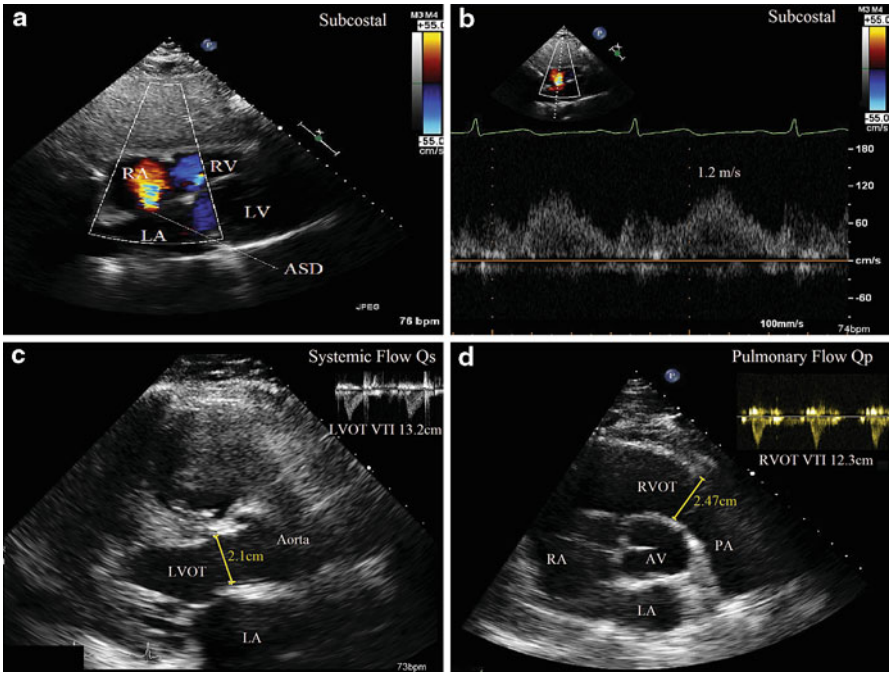

Fig. 6.6 Shunt calculation in a patient with a secundum atrial septal defect (ASD). (**a**) Color flow Doppler demonstrates left to right flow across the ASD in this subcostal view. (**b**) Pulse wave Doppler at the level of the ASD confirms that there is left to right continuous flow. During peak systole, based on the velocity of 1.2 m/s, the pressure gradient between the right atrium (RA) and the left atrium (LA) is $4v^2 = 4(1.2)^2 = 5.8$ mmHg. The RA pressure was estimated at 10 mmHg, so the LA pressure during systole is estimated at 15.8 mmHg ($LA = RA + 4v^2$). (**c**) Measurement of systemic flow (Q_s) based on the LVOT area and LVOT VTI (pulse wave Doppler from the apical 5 chamber view, *right upper corner*). (**d**) Measurement of pulmonary flow (Q_p) based on the RVOT area and the RVOT VTI (pulse wave Doppler from the basal short axis view, *right upper corner*). The Q_p/Q_s or shunt fraction is 1.3:1 (*see Question 4 for calculation of* Q_p, Q_s, *and shunt fraction*)

term 0.785 cancels, and the ratio simplifies to (RVOT VTI)(RVOT D^2)/(LVOT VTI)(LVOT D^2). A ratio greater than 1.5 is considered a significant left to right shunt.

Just as pulmonary vascular resistance correlates with the TR velocity/RVOT VTI, systemic vascular resistance (SVR) correlates relatively well with *MR velocity/LVOT VTI*. A ratio of *MR velocity/LVOT VTI* > *0.27* has a relatively high sensitivity and specificity for *SVR* > *14 Woods units* [15].

Valve Disease

It is important to recognize that an integrated approach using multiple echocardiographic methods of analysis and clinical context to determine severity of valve lesions is crucial, rather than relying on one specific measurement.

Aortic Stenosis

Echocardiography is currently the standard method to evaluate aortic valve stenosis. Application of the continuity equation is central to the calculation of aortic valve area (AVA). Based on the conservation of mass, the flow in the left ventricular outflow tract (LVOT) should be equal to the flow through the aortic valve orifice. First, one must determine the flow in the LVOT, or the stroke volume, by multiplying the cross-sectional area of the LVOT by the LVOT VTI determined by PW Doppler in the apical long axis or 5 chamber view (Fig. 6.5a, b). The PW sample volume should be located in the LVOT beneath the valve, and a crisp laminar Doppler signal with no contamination from the pre-stenotic flow acceleration should be sought. This is typically 0.5–1.0 cm from the aortic valve. The LVOT diameter should be measured from the septum to the anterior mitral leaflet in mid-systole, roughly 0.5–1.0 cm from the aortic valve in the parasternal long axis view to approximate the location where the PW was measured in the other echocardiographic view [16]. This flow should equal the product of the cross-sectional area of the aortic valve (AVA) and the AV VTI as determined by CW Doppler, typically the highest VTI obtained from a given view (suprasternal, apical, right parasternal) (Fig. 6.5c, d). The volume of blood in the cylinder in the LVOT (blue cylinder) must equal the volume of blood in the cylinder at the aortic valve (red cylinder) to not violate the law of mass conservation. The AV VTI obtained by CW Doppler is highly dependent on technique and the ability to obtain a good signal that is parallel to flow. Occasionally the right parasternal approach is used to obtain the highest gradient (Fig. 6.5d).

Based on the continuity equation:

$$\text{LVOT Cylinder Volume or Stroke Volume} = \text{AV Cylinder Volume}$$

$$\text{LVOT VTI} * \text{LVOT area} = \text{AV VTI} * \text{AVA}$$

$$\text{LVOT VTI} * (\text{LVOT diameter})^2 * 0.785 = \text{AV VTI} * \text{AVA}$$

Rearrangement yields:

$$\text{AVA} = [\text{LVOT VTI} * (\text{LVOT diameter})^2 * 0.785] / [\text{AV VTI}]$$ [17] (Fig. 6.5)

This equation gives a reliable estimate of the AVA; less than 1.0 cm^2 is considered severe aortic stenosis [16, 18]. Because the LVOT diameter is squared and measurements can vary, this is the greatest source of error in the formula.

The AVA is just one method among many to assess severity of aortic stenosis. Other methods include identifying the peak and mean gradient across the aortic valve, peak velocity across the aortic valve, and dimensionless index [17]. The peak velocity across the aortic valve is obtained from the CW Doppler profile, from which the peak gradient is calculated (from the peak velocity using $\Delta P = 4V^2$), and the mean gradient is calculated by averaging the instantaneous gradients during the ejection period [17]. A mean gradient gradient >40 mmHg is considered severe. Echocardiographic assessment of peak gradient provides the instantaneous gradient between the LV and the aorta, which is different from cardiac catheterization in which often a peak to peak gradient is reported, a less physiologic value. Importantly,

Table 6.1 Aortic stenosis severity [16]

Parameter	Aortic sclerosis	Mild	Moderate	Severe
Aortic jet velocity (m/s)	≤2.5	2.6–2.9	3.0–4.0	>4.0
Mean gradient (mmHg)		<20	20–40	>40
AVA (cm^2)		>1.5	1.0–1.5	<1.0
AVA indexed to BSA (cm^2/m^2)		>0.85	0.60–0.85	<0.60
AV/LVOT velocity ratio		>0.50	0.25–0.50	<0.25

AVA Aortic valve area; *LVOT* left ventricular outflow tract; *BSA* body surface area

the mean gradient on cardiac catheterization correlates well with the Doppler derived mean gradient.

Table 6.1 shows a summary of the parameters for aortic stenosis severity.

Although the peak velocity and estimated AVA are usually concordant (i.e., either velocity >4 m/s and AVA < 1.0 cm^2 or velocity <4 m/s and AVA > 1.0 cm^2), there may be scenarios in which the jet velocity and AVA may be discordant. In the case of velocity >4 m/s and AVA > 1.0 cm^2, possibilities include a high stroke volume, concomitant moderate to severe aortic regurgitation, and a large body size. In the case of velocity <4 m/s and AVA < 1.0 cm^2, possibilities include low stroke volume, severe concomitant mitral regurgitation, and small body size [16]. In either situation, the peak velocity is the better predictor of clinical outcome and it is suggested that it be used to determine valve stenosis severity [16].

In patients who have left ventricular dysfunction (LVEF < 40%) with concomitant aortic stenosis, the calculated AVA may be severe (<1.0 cm^2), but the mean gradient may not be severe (<30–40 mmHg). It is important to then determine if the aortic stenosis is truly severe and causing left ventricular dysfunction, which would imply improved left ventricular function with valve replacement, or if the aortic stenosis is only moderate in the presence of LV dysfunction from another cause (i.e., coronary disease, non-valvular cardiomyopathy, etc.), in which the perceived small AVA is related to the inability of the left ventricle to generate the necessary valve opening forces (pseudostenosis). In the latter scenario, valve replacement would not be expected to improve left ventricular dysfunction. Low-dose dobutamine stress protocols (described in detail elsewhere [16]) can distinguish the two clinical scenarios. Recall from the continuity equation that the AVA is proportional to the *LVOT VTI/AV VTI*. If the patient truly has severe aortic stenosis, with the administration of dobutamine, the LVOT VTI and AV VTI should increase proportionally due to increased flow across a fixed, stenotic orifice, so the AVA should remain relatively unchanged. However, if the aortic stenosis only appears severe because of concomitant left ventricular dysfunction, dobutamine infusion will increase the LVOT VTI without a concomitant increase in AV VTI because of improved valve opening, thereby resulting in an increased calculated AVA. It follows that if the AVA increases above 1.0 cm^2 with dobutamine infusion, it is not likely to be severe aortic stenosis. Severe AS is suggested by a peak jet velocity >4.0 m/s provided that the valve area does not increase to >1.0 cm^2 [16]. In addition, the presence of contractile reserve (increase in EF or SV ≥ 20%) during dobutamine

stress predicts a lower mortality rate (<10%) with AVR than if contractile reserve is absent (>30%) [19].

The velocity ratio, also known as the dimensionless index, which is flow independent, is the ratio of the LVOT peak velocity and the AV peak velocity (can also use VTI ratio). A velocity index <0.25 is considered severe. This is used to compare aortic stenosis severity over time in patients who may have different loading conditions.

Accurate estimation of aortic stenosis severity depends on meticulous technique to obtain both an accurate LVOT diameter assessment, as well as the highest velocity jet which may require multiple echocardiographic views. In general, inaccuracies in measuring gradients by echocardiography typically err on the side of underestimation. However, there are two situations in which echocardiography may overestimate severity of stenosis. First, as stated earlier, the peak gradient estimated by the simplified Bernoulli equation ignores the velocity in the LVOT (V_1) as it is usually very small (<1 m/s). Scenarios in which the proximal velocity is >1.5 m/s or the peak velocity is <3 m/s, the flow velocity and gradient may be overestimated since the V_1 is ignored. Therefore, a more accurate estimate of peak gradient across the valve is the $\Delta P = 4(V_2^2 - V_1^2)$ [16]. Another scenario in which the stenosis severity may be overestimated is the pressure recovery phenomenon. This occurs when some of the potential energy which was converted to kinetic energy at the level of the aortic stenosis is converted back to potential energy as flow decelerates (i.e., increasing pressure distal to the valve in the aorta). This pressure recovery is typically negligible, except in the case of small aortas with gradual widening after the stenosis (typically less than 3 cm in diameter). With larger aortas, much of the kinetic energy is converted to heat due to turbulence and viscous friction, so pressure recovery is not an issue [16]. Pressure recovery can be quantitatively calculated as $\Delta P = 4V^2 * 2(\text{AVA} / \text{aorta area}) * (1 - \text{AVA} / \text{aorta area})$. As can be seen by the equation, if the AVA is small, and the aorta area is large, the AVA/Aorta Area ratio is small and pressure recovery is minimal [16].

One collateral method to confirm the pressure gradient across the LVOT or aortic valve is to assess the peak mitral regurgitation velocity. As described previously, LV systolic pressure − LA pressure = $4V_{MR}{}^2$. If the LA pressure is estimated to be between 10 and 20 mmHg, then the LV systolic pressure can be estimated by 10–20 mmHg + $4V_{MR}{}^2$. If the SBP is known, then the difference between the estimated LV systolic pressure and SBP approximates the peak pressure gradient across the LVOT or aortic valve.

Mitral Stenosis

The most common cause of mitral stenosis (MS) is commissural fusion as a result of rheumatic fever. Several echocardiographically derived measurements can be used to assess mitral stenosis, including pressure gradient, pressure half-time, continuity equation, proximal isovelocity surface area (PISA) method, and planimetry. Although planimetry may well provide the most accurate measurement of the mitral

valve area (MVA) provided that the images are acquired at leaflet tip level and are a true on-axis view, this section will focus on the pressure gradient, pressure half-time, and continuity equation to assess the valve area. PISA method and planimetry are discussed in detail in another reference [16]. Peak and mean pressure gradients across the mitral valve in diastole are measured by CW from the apical 4 chamber view (Fig. 6.7). It is essential to interrogate the mitral valve during a regular rhythm and normal heart rate (60–80 bpm). If the patient is in atrial fibrillation, then several cardiac cycles (6–8) should be averaged. Mean gradient is preferred to the peak gradient, since the peak gradient may be influenced by mitral regurgitation, atrial

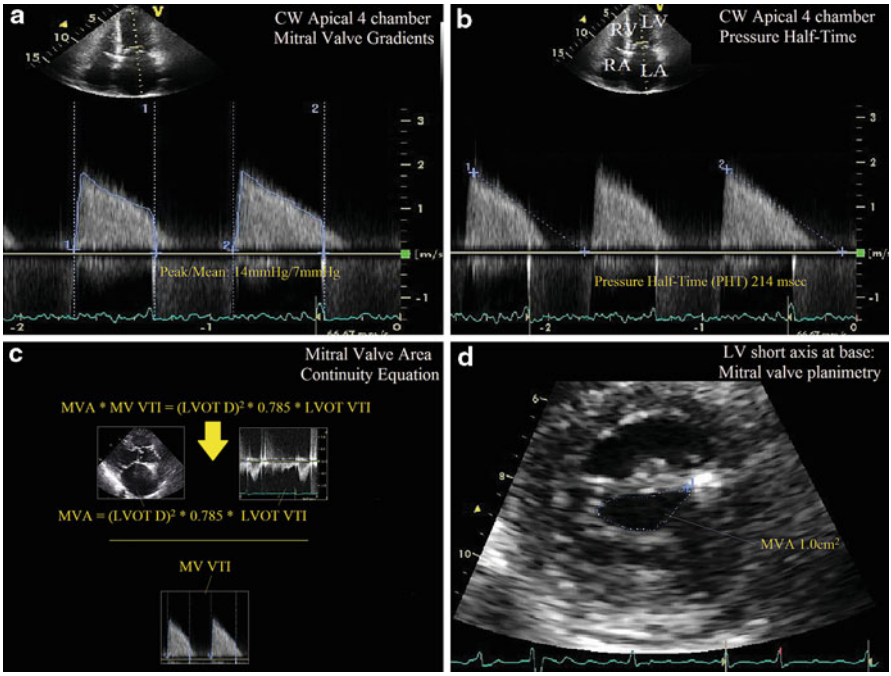

Fig. 6.7 Assessment of mitral stenosis. (**a**) Continuous wave Doppler across the mitral valve yields the peak and mean gradient (14/7 mmHg). Given the irregular heart rhythm, 6–8 beats are measured and averaged to obtain the peak and mean gradient. (**b**) The pressure half-time (PHT) is the time for the pressure gradient to decrease by 50%, and is equal to 0.29*Deceleration time. Again, multiple beats are averaged (6–8) to obtain the PHT of 214 ms. The mitral valve area (MVA) is estimated by the following empiric equation: MVA = 220/PHT, giving a MVA of 220/214, or 1.0 cm^2, by the PHT method. (**c**) Calculation of MVA using the continuity equation. The flow across the mitral valve must equal the flow across the aortic valve, and therefore, $\text{MVA} * \text{MV VTI} = \text{LVOT area} * \text{LVOT VTI}$. In this case, the LVOT diameter is 1.9 cm, the LVOT VTI is 20 cm, and the MV VTI is 56.4 cm. Therefore, the calculated MV Area is 1.0 cm^2. Note that the MV VTI is measured using CW and the LVOT VTI is measured using PW in this situation. (**d**) Planimetry is another method of estimating the MVA. Note the commissural fusion and "fish-mouth" appearance of the mitral opening, characteristic of rheumatic mitral valve disease. In this example, planimetry yields a MVA of 1.0 cm^2, concordant with the PHT and continuity methods

compliance, and left ventricular diastology. One cause of a very high peak gradient out of proportion to the mean gradient, for example, is severe mitral regurgitation. While pressure gradients are important parameters in the assessment of mitral stenosis severity, they are highly influenced by heart rate, cardiac output, and mitral regurgitation [16]. Mean pressure gradients supportive of mild, moderate, and severe MS are <5 mmHg, 5–10 mmHg, and >10 mmHg, respectively [20].

Pressure half-time (PHT) is the time (in ms) it takes for the peak pressure gradient across the mitral valve in diastole to decrease by 50%. Based on the relationship between pressure and velocity, it is also the time in ms it takes for the peak velocity to decrease by 29%. This measurement is obtained by tracing the slope of the *E* wave during early diastole (Fig. 6.7b). It has been found that there is an inverse relationship between PHT and MVA by the following equation: MVA (cm^2) = 220/PHT [21]. In addition, the MVA (cm^2) = 759/Deceleration Time (ms). See Table 6.2 for measurements and valve stenosis severity.

Pressure half-time may be low even in severe MS if atrial compliance is low. In severe aortic insufficiency, due to the increase in the LVEDP during diastole as a result of regurgitation, the pressure between the LV and LA will equilibrate sooner, so the PHT will be reduced and the MVA estimate using the PHT will be inaccurate.

The continuity equation estimates the MVA if there is no aortic insufficiency or mitral regurgitation. The flow through the mitral valve should equal the flow through the LVOT by conservation of mass. The formula for flow through the LVOT (i.e., stroke volume), as described previously, is $\text{LVOT VTI} * (\text{LVOT diameter})^2 * 0.785$. Again, this can be thought of as a cylinder, in which the base of the cylinder is the area of the LVOT and the height is the LVOT VTI. The flow through the mitral valve equals the product of the cross-sectional area of the mitral orifice (base of the cylinder) multiplied by the MV VTI (height of the cylinder). The MV VTI is determined by the computer package from the tracing of the CW mitral inflow from the 4 chamber view (Fig. 6.7c).

LVOT Cylinder Volume or Flow MV Cylinder Volume or Flow

$$\text{LVOT VTI} * \text{LVOT area} = \text{MV VTI} * \text{MVA}$$

$$\text{LVOT VTI} * (\text{LVOT diameter})^2 * 0.785 = \text{MV VTI} * \text{MVA}$$

$$\text{MVA} = [\text{LVOT VTI} * (\text{LVOT diameter})^2 * 0.785] / (\text{MV VTI})$$

Because MS elevates LA pressures, pulmonary hypertension may result. In general, the more severe the MS is, the more severe the pulmonary hypertension becomes. Pulmonary artery (PA) pressures can be assessed using the estimated RVSP, assuming there is no RVOT obstruction or pulmonic stenosis. A resting PASP > 50 mmHg or exercise-induced pulmonary hypertension (PASP > 60 mmHg) in the absence of other causes implies hemodynamically significant mitral stenosis [22].

Table 6.2 Mitral stenosis severity [22]

Parameter	Mild	Moderate	Severe
MVA (cm^2)	>1.5	1.0–1.5	<1.0
Mean gradient (mmHg)	<5	10–15	>10
PASP (mmHg)	<30	30–50	>50

MVA Mitral valve area; *PASP* pulmonary artery systolic pressure

Mitral Regurgitation

Echocardiographic assessment of mitral regurgitation severity relies on a "weighted average" of the information obtained from multiple modalities (Table 6.3). Color Doppler is the most readily apparent and visualized method of assessing mitral regurgitation. The jet area in the atrium on color Doppler is highly dependent on PRF and color scale. Typically, a large jet area spanning more than 40% of the atrium is considered severe MR. However, there are many caveats to using jet area. The appearance of the color is highly technique-dependent, and can be affected by hemodynamic changes and atrial size. In addition, a very eccentric jet may "hug" the wall and appear to be smaller than a more central jet, giving the false impression that the eccentric MR is not severe. In addition, in the case of acute, severe mitral regurgitation, the jet duration may be very short given the acute rise in LA pressure, and technical factors such as insufficient color resolution may lead to underestimation [23]. Given its many limitations, jet area should not be the sole method used for quantification of mitral regurgitation.

Table 6.3 Mitral regurgitation severity [16]

Parameters	Mild	Moderate	Severe	Advantages	Limitations
Vena contracta width (cm)	<0.3	0.3–0.69	≥0.7	Simple to measure, not affected by jet eccentricity; good at identifying mild and severe regurgitation	Requires optimization of color, temporal, and lateral resolution; not applicable with multiple jets; small measurement errors result in large % error
Regurgitant volume (mL/beat)	<30	30–59	≥60	Quantitates volume load; useful in non-holosystolic jets such as prolapse	Subject to measurement error, tedious calculation; cannot use stroke volume method if AI is present
Regurgitant fraction (%)	<30	40–49	≥50	Quantitative; useful in non-holosystolic jets such as prolapse	Subject to measurement error; tedious calculation
EROA (cm^2)	<0.20	0.20–0.39	≥0.40	Quantitative; simplified version $r^2/2$ is easy to perform	Radius measurement, which is subject to error, is squared; involves multiple calculations and less accurate in eccentric jets; cannot assess multiple jets; assumes consistent area throughout cycle

EROA Effective regurgitant orifice area; *AI* aortic insufficiency; *r* radius

Another method of MR assessment is the flow convergence or PISA method, which is an extension of the continuity principle and has been shown to correlate well with angiographically determined severity [24]. As flow converges toward a regurgitant orifice, the flow organizes into several concentric hemispheres, each with a specific velocity (Fig. 6.8a). As blood approaches the regurgitant orifice, the radius of the hemisphere decreases, while the velocity of blood at the surface of the hemisphere increases. Since the surface area (cm^2) of the hemisphere can be derived from the radius (surface area of hemisphere $= 2\pi r^2$), and the velocity of the blood cells (cm/s) at the surface of the hemisphere (aliasing velocity, V_a) can be obtained from the color scale, the product of these two values (in units of cm^3/s) gives the flow rate proximal to the orifice (Fig. 6.8a). The flow rate distal to the orifice, which must equal the flow rate proximal to the orifice, can be calculated from the effective regurgitant orifice area (EROA) multiplied by the peak mitral regurgitant velocity, obtained from the CW Doppler in the 4 chamber view (Fig. 6.8c). To determine the velocity of the hemisphere of the proximal flow convergence, the color baseline or Nyquist limit are shifted downward toward the direction of flow (Fig. 6.8a). As shown in the figure, this maneuver increases the radius of the hemisphere, allowing easy visualization of color transition from blue to yellow, which is the location where the velocity is equal to the aliasing velocity. By having a larger radius and a lower aliasing velocity, propagation of error in radius measurement is reduced.

It follows that:

$$\text{Flow rate proximal to orifice} = \text{Flow rate distal to the orifice}$$

$$\text{Hemisphere surface area} * V_a = \text{EROA} * \text{peak mitral velocity}$$

$$2\pi r^2 * V_a = \text{EROA} * V_{MR}$$

$$\text{EROA} = (6.28r^2 * V_a) / V_{MR}$$

This, of course, assumes that the hemisphere radius is measured at the time that the peak MR velocity occurs, so attempts must be made and standardizing the timing of measurement (i.e., mid-systole). As seen in Table 6.2, ERO > 0.4 is severe MR, and <0.2 is mild MR. The PISA method is not very accurate in situations of very eccentric MR jets (may overestimate severity) and noncircular orifices. A geometric correction factor for eccentric jets that create a wedge of a hemisphere instead of a full hemisphere has been described [25]. The angle created by the wedge (α) is divided by 180° and multiplied by the EROA to obtain the geometrically corrected EROA. Therefore, $\text{Geometrically corrected EROA} = (\alpha / 180) * (6.28r^2 * V_a) / V_{MR}$. Furthermore, flow velocity calculated by the PISA method represents an instantaneous flow rate. For instance, in mitral valve prolapse, the instantaneous EROA may be large but if the regurgitation only occurs in mid to late systole, the total regurgitant volume may not be very large. So perhaps a more accurate measurement of MR severity in this situation would be regurgitant volume.

To determine the regurgitant volume (RV), the EROA is multiplied by the MV VTI.

$$\text{RV} = \text{EROA} * \text{MV VTI}$$

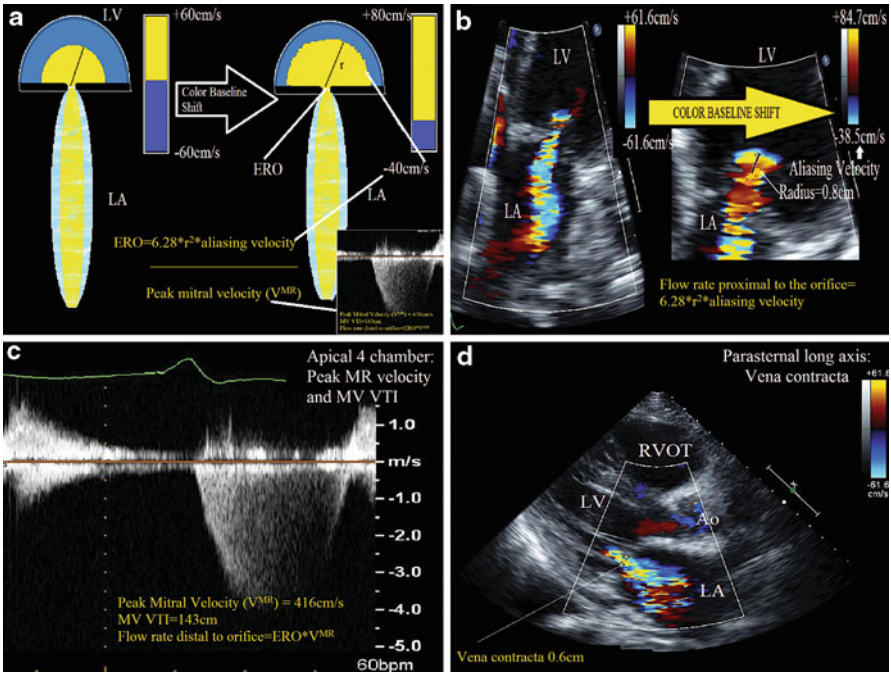

Fig. 6.8 PISA (proximal isovelocity surface area) method for mitral regurgitation and vena contracta. (**a**) Artistic rendition of the PISA concept. As flow converges during systole toward the regurgitant orifice, it accelerates and forms concentric hemispheres of increasing velocity and decreasing radius. For example, the velocity at the edge of the *yellow hemisphere* is higher than the velocity at the edge of the *blue hemisphere*. First the image should be optimized and zoomed. Next, the color baseline is shifted downward toward the direction of flow, from −65 to −40 cm/s, creating the *larger yellow hemisphere* with a lower velocity on the right. The velocity at the boundary between the *yellow* and *blue hemisphere* is the aliasing velocity (V_a = −40 cm/s). The flow proximal to the orifice equals the product of the hemisphere surface area ($2\pi r^2$) and the aliasing velocity (V_a). This proximal flow should equal the flow distal to the orifice, which is the product of the regurgitant orifice area (EROA) and peak MR velocity (V_{MR}). Therefore, EROA = $(2\pi r^2 * V_a)/V_{MR}$. (**b**) Similar to *panel A*, after creating a zoomed-in image, the color baseline is shifted toward the direction of flow, and a larger hemisphere with a known radius (0.8 cm) and aliasing velocity (V_a = 38.5 cm/s) is created. Based on the above equation, the proximal flow rate is 154.7 cm^3/s. (**c**) Continuous wave Doppler across the mitral valve to obtain the peak mitral regurgitant velocity (V_{MR}) = 416 cm/s and MV VTI. The distal flow rate is V_{MR}*EROA. The EROA, which is equal to $(2\pi r^2 * V_a)/V_{MR}$, is 0.37 cm^2, consistent with moderately-severe MR. Regurgitant volume can be calculated with the information in this figure (*see Question 5*). Using the simplified PISA formula, $r^2/2$, estimated EROA is 0.32 cm^2, likely slightly underestimated because the aliasing velocity is 38.5 cm/s, not the 40 cm/s assumed in the simplified formula. (**d**) The vena contracta, the narrowest jet width at the orifice, measured in the parasternal long axis view, is 0.6 cm, consistent with moderately-severe MR

EROA calculation using the PISA may be cumbersome, which can discourage its routine use. A simplified formula can be used if certain assumptions are made [26]. First, one assumes a pressure gradient between the LV and LA of 100 mmHg, which yields a mitral velocity (V_{MR}) of 5 m/s or 500 cm/s (from the Bernoulli equation, LV

systolic pressure − LA pressure = $4V_{MR}^{2}$). If aliasing velocity (V_a) is set to 40 cm/s, then plugging these into the equation:

$$\text{EROA} = (6.28r^2 * V_a) / V_{MR}$$

$$\text{EROA} = (6.28r^2 * 40\text{cm/s}) / 500\text{cm/s}$$

$$\text{EROA} \approx r^2 / 2$$

The vena contracta is the narrowest color flow at or upstream of the valve orifice [16]. For mitral regurgitation, it is typically assessed in the parasternal long axis view, and is considered to be independent of flow and pressure for a fixed orifice, even for eccentric jets (Fig. 6.8d). A vena contracta width of <0.3 cm is considered mild MR, and >0.7 cm is considered severe [16]. This parameter, when measurable, should always be considered a key component to the integrated approach to determining mitral regurgitation severity.

Other signs of severe MR are a triangular shape in the CW profile of the mitral regurgitant (early peaking) rather than a smooth parabolic profile, which implies rapid equilibration of LV and LA pressure from severe MR [16]. In addition, in the mitral inflow PW profile, severe MR is typically associated with a tall *E* wave >120 cm/s. Stage 1 diastolic dysfunction pattern on mitral inflow virtually excludes severe MR. In severe MR, the elevated LA pressures during systole decreases the gradient between the LA and the pulmonary veins, so the pulmonary vein *s* wave may be blunted or even reversed.

Aortic Insufficiency

In the parasternal long axis view, the percentage of the LVOT width that the regurgitant jet occupies has been correlated with aortic insufficiency (AI) severity [16]. If the jet width is in diastole occupies more than 65% of the LVOT diameter, then it is considered severe. However, just as with jet area in MR, jet width in AI is not valid for eccentric jets in which severity may be underestimated (Fig. 6.9a) [27]. The vena contracta is the narrowest neck of the jet at the level of the valve. The width of the vena contracta correlates with regurgitant orifice area and is unaffected by jet eccentricity [28]. To accurately measure the vena contracta width, a zoomed-in parasternal long axis view should be obtained that shows the flow convergence zone, the vena contracta, as well as the regurgitant jet in the LVOT. A vena contracta width ≥6 mm suggests severe AI (Table 6.4). The utility of this method is limited if there are multiple jets [16]. The PISA method has been applied for the calculation of the aortic regurgitant EROA. This measurement is should be made in the apical 5 chamber or apical long axis view in early diastole, but is technically more difficult to obtain than the PISA for MR. The same principle applies as with MR, in that the flow rate proximal to the orifice (aorta) which is the product of the hemisphere area and the aliasing velocity ($2\pi r^2 * V_a$) equals the flow rate distal to the orifice in the LVOT (EROA*peak aortic regurgitant velocity). However, the color baseline is shifted up rather than down, as this is toward the direction of flow. EROA ≥0.3 cm^2 correlates with severe AI (Table 6.4). The simplified PISA method used for MR ($r^2/2$) does not apply to AI.

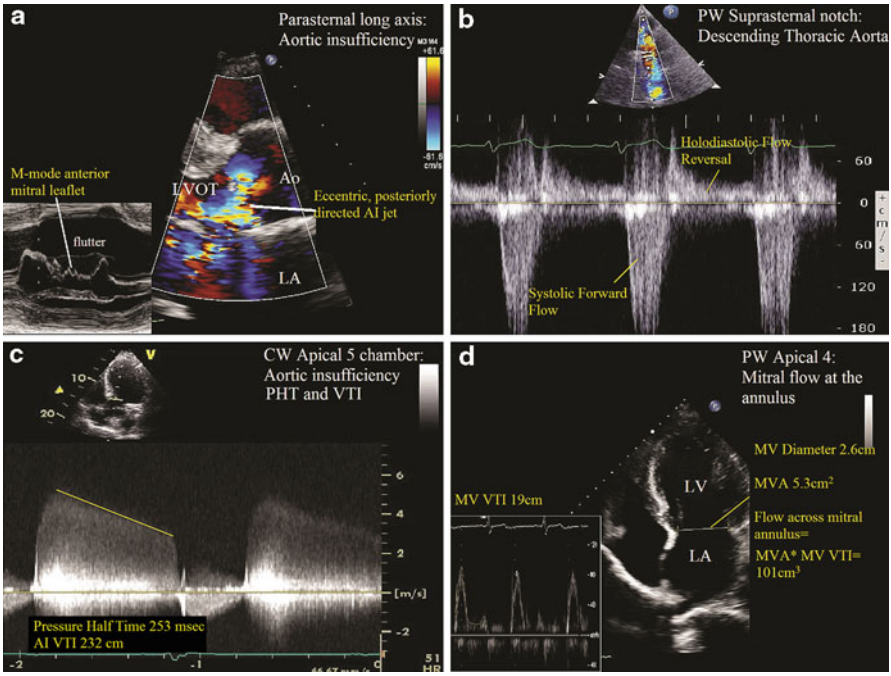

Fig. 6.9 Severe aortic insufficiency (AI). (**a**) Parasternal long axis view Color Doppler demonstrates a very a severe, eccentric, and posterior directed jet. Note that the M-Mode across the mitral leaflet shows fluttering of the anterior leaflet due to the aortic insufficiency jet (*lower left corner inset*). Given the eccentricity, one cannot use the LVOT jet area to assess severity. (**b**) Pulse wave Doppler with sample volume in the upper descending thoracic aorta, demonstrating holodiastolic flow reversal, a sign of severe AI. (**c**) Continuous wave Doppler across the aortic valve in the apical 5 chamber view. The PHT is 253 ms, consistent with severe AI. The aortic insufficiency VTI is 232 cm based on the CW profile. (**d**) Application of the continuity equation allows for calculation of the regurgitant AI volume. Flow across the mitral valve plus the regurgitant volume should equal the flow across the aortic valve (Stroke volume). The MVA is determined by measuring the mitral valve diameter, and this area (5.3 cm^2) is multiplied by the MV VTI at the annulus (19 cm) to yield a flow of 101 cm^3. Flow across the aortic valve is determined by the product of the LVOT VTI and LVOT area, which yields a volume of 169 cm^3, calculation not shown. Therefore, the aortic insufficiency regurgitant volume is 169 $cm^3 - 101$ $cm^3 = 68$ cm^3, consistent with severe AI. The regurgitant orifice area (EROA) of the aortic valve is calculated by dividing the regurgitant volume (68 cm^3) by the AI VTI (232 cm), which equals 0.3 cm^2, also consistent with severe AI

Pulse wave Doppler in the upper descending thoracic aorta from the suprasternal view can both qualitatively and quantitatively assess aortic regurgitation severity [27]. Holodiastolic flow reversal in the proximal descending aorta is specific for at least moderately-severe aortic insufficiency, and is considered to be the echocardiographic equivalent of the *Duroziez's sign* [16] (Fig. 6.9b). This is a much more specific finding if there is flow reversal is present when sampling in the abdominal aorta. The ratio of the reverse flow (diastolic VTI*cross-sectional area of the aorta in diastole) to the forward flow (systolic VTI*cross-sectional area of the aorta in systole) is proportional to the regurgitant fraction [29].

Table 6.4 Severity of aortic insufficiency [16]

Parameter	Mild	Moderate	Severe	Advantages	Limitations
Flow reversal	No early diastolic flow reversal in the DA		Holodiastolic flow reversal in the DA	Simple; very specific for severe AI if present in the abdominal aorta	Depends on compliance of aorta; brief reversal is common
LV size	Normal LV size (if chronic)		Enlarged LV (if chronic)	LV enlargement specific for chronic severe AI	Nonspecific
Jet width in LVOT	<25%	26–65%	>65%	Simple to perform	Not accurate for eccentric jets
Vena contracta (cm)	<0.3	0.3–0.6	>0.6 cm	Simple and quantitative	Not valid for multiple jets; small errors can be significant
RV (mL/beat)	<30	30–60	≥60	Quantitative volume load	Prone to multiple measurements and calculation error
RF (%)	<30	30–49	≥50	Quantitative volume load	Prone to multiple measurements and calculation error
EROA (cm^2)	<0.10	0.10–0.29	≥0.30	Quantitative assessment of AI severity	Not accurate for multiple or eccentric jets; difficult to perform with severe aortic calcification
Pressure half-time (ms)	>500	200–500	<200	Simple to perform	Affected by diastolic pressure changes in the LV and aorta

EROA Effective regurgitant orifice area; *RV* regurgitant volume; *RF* regurgitant fraction; *DA* descending aorta; *LV* left ventricle

PHT of the aortic regurgitation jet reflects the rate of equalization between the aortic and LV pressures (Fig. 6.9c). Therefore, this PHT is not only influenced by the severity of aortic insufficiency but also by LV pressure, LV compliance, and afterload conditions. Hence, it may be the least reliable method for assessing regurgitation severity [16]. A PHT <200 ms is supportive of severe aortic insufficiency, and a pressure half-time greater than 400 ms is unlikely to represent more than moderate AR. However, even in severe AI, if the LV has dilated as a chronic adaptation to the increased preload and afterload, then the pressure half-time could be normal since the LV and aorta pressures would not rapidly equilibrate. If vasodilators are given or LV pressures increase for a given degree of AI, the PHT would decrease.

The continuity equation can also be applied to aortic insufficiency if there is no more than mild mitral insufficiency. Think of the flow across the aortic valve as gross income, the regurgitant volume as the tax, and the flow across the mitral valve as the net income. The difference between the flow across the aortic valve ("gross" systolic stroke volume) and the flow across the mitral valve ("net" forward stroke volume) is equal to the "tax" or regurgitant volume per beat. The "gross" stroke volume can be obtained either from the LVOT VTI method or from the difference between the LV volumes in systole and diastole. To calculate "net" forward flow across the mitral valve, it is important to use PW and place the sample volume at the annulus of the mitral valve to measure and accurate flow across the mitral valve during diastole (Fig. 6.9d).

$$\text{Regurgitant volume(RV)} = \text{Stroke volume across aortic valve} - \text{Flow across mitral valve annulus}$$

$$\text{RV} = (\text{LVOT VTI} * \text{LVOT area}) - (\text{MV VTI(diastole)} * \text{MV annulus area})$$

$$\text{RV} = [\text{LVOT VTI} * (\text{LVOT diameter})^2 * 0.785] - [\text{MV VTI} * (\text{MV diameter})^2 * 0.785]$$

Once the regurgitant stroke volume is obtained, it can be divided by the regurgitant jet VTI obtained from CW in diastole to calculate the EROA [16]. If the EROA is in the severe range but the RV is not, it may be because in acute AI, the rapid increase in the LVEDP shortens the time for regurgitation, so the regurgitant volume may not be as large as expected from the EROA (Fig. 6.10).

Questions

1. What is the estimated right ventricular systolic pressure (RVSP) in the patient in Fig. 6.4a if the inferior vena cava (IVC) measures 2.5 cm and there is no collapse with sniff?
   A. 60 mmHg
   B. 70 mmHg
   C. 30 mmHg
   D. 85 mmHg

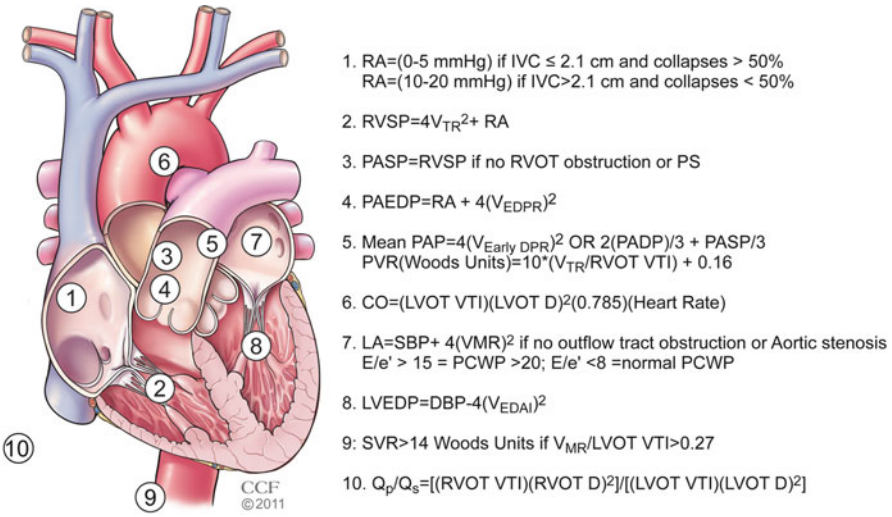

Fig. 6.10 Summary of intracardiac pressure calculations. *RA* Right atrial pressure; *IVC* inferior vena cava; *RVSP* right ventricular systolic pressure; V_{TR} peak tricuspid regurgitation velocity; *PASP* pulmonary artery systolic pressure; *RVOT* right ventricular outflow tract; *PS* pulmonic stenosis; *PAEDP* pulmonary artery end-diastolic pressure; V_{EDPR} end-diastolic pulmonary regurgitation velocity; *PAP* pulmonary artery pressure; $V_{EarlyDPR}$ early diastolic pulmonary regurgitation velocity; *PVR* pulmonary vascular resistance; *VTI* velocity time integral; *LVOT* left ventricular outflow tract; *D* diameter; *LA* left atrial pressure; *SBP* systolic blood pressure; V_{MR} peak mitral regurgitation velocity; *PCWP* pulmonary capillary wedge pressure; *LVEDP* left ventricular end-diastolic pressure; *DBP* diastolic blood pressure; V_{EDAI} end-diastolic aortic insufficiency velocity; *SVR* systemic vascular resistance; Q_p pulmonary flow; Q_s systemic Flow. Reprinted with permission, Cleveland Clinic Center for Medical Art & Photography © 2011

2. What is the estimated end-diastolic pulmonary artery pressure in Fig. 6.4b?
   A. 14.4 mmHg
   B. 14.4 mmHg + RA pressure
   C. 38.5 mmHg
   D. 38.5 mmHg + RA pressure
3. Based on the continuity equation, what is the estimated aortic valve area (AVA) in Fig. 6.5? Is this severe AS or moderate AS?
   A. 1.2 cm^2, moderate AS
   B. 1.2 cm^2, severe AS
   C. 0.6 cm^2, severe AS
   D. 0.6 cm^2, moderate AS
4. The patient in Fig. 6.6 has a known secundum atrial septal defect, and as shown in panel (a), there is left to right flow across the atrial septal defect. The echocar-

diogram was performed to estimate the shunt fraction. Based on the information provided in Fig. 6.6, what is the estimated Q_p/Q_s ratio?
A. 1:1
B. 1.3:1
C. 0.5:1
D. 2:1

5. In Fig. 6.8, the regurgitant orifice area is 0.37 cm^2. Based on the information in panel (c), what is the estimated regurgitant volume per beat?
A. 143 mL/beat
B. 416 mL/beat
C. 53 mL/beat
D. 100 cc/beat

Answers

1. The peak TR velocity is 420 cm/s, or 4.2 m/s. Based on the simplified Bernoulli equation, the difference between the RV and RA pressure is $4V_{TR}{}^2$, or $4*(4.2)^2 = 70.56$ mmHg, roughly 70 mmHg. The RA pressure is estimated at 15 mmHg based on the dilated IVC that does not collapse greater than 50% with the sniff. Therefore, because the RVSP is equal to RA pressure plus the $4V_{TR}{}^2$, R VSP = 70 mmHg + 15 mmHg = 85 mmHg, compatible with severe pulmonary hypertension.
2. In Fig. 6.4b, the spectral Doppler shows the CW across the RVOT and pulmonic valve. From the pulmonary regurgitation jet, the late diastolic pulmonary regurgitation velocity represents the pressure difference between the pulmonary artery and the right ventricle at end diastole (Note the timing just at the onset of the QRS). Therefore, the $4v_{PRed}{}^2 = RVEDP - PAEDP$. It follows that $PAEDP = RVEDP + 4v_{PRed}{}^2$. Because the RVEDP is equal to RA pressure, $PAEDP = RA + 4v_{PRed}{}^2$. Here the end-diastolic velocity is 1.9 m/s. Therefore, PAE $DP = RA + 4(1.9)^2 = 14.4$ mmHg + RA pressure.
3. Based on the continuity equation, $AVA = [LVOT\ VTI * (LVOT\ diameter)^2 * 0.785] / [AV\ VTI]$. The LVOT VTI from Fig. 6.5b is 28.1 cm, and the LVOT diameter from Fig. 6.5a is 1.9 cm. The highest AV VTI was obtained from the right sternal border view, which is 124 cm. Note that this corresponded to a peak and mean gradient of 119/74 mmHg, severe aortic stenosis (AS) by gradients. Using the continuity equation, $AVA = [28.1 * (1.9)^2 * 0.785] / [124] = 0.6 cm^2$, also compatible with severe AS.
4. The ratio of pulmonary blood flow to systemic blood flow is the Q_p/Q_s, or shunt fraction. The systemic blood flow (Q_s) is estimated by multiplying the LVOT area, (LVOT $D)^2$*0.785, by the LVOT VTI. As shown in Fig. 6.6c, the LVOT diameter is 2.1 cm and the LVOT VTI is 13.2 cm. Therefore, the systemic flow

is $(2.1)^2 * 0.785 * 13.2 = 45.7 \text{cm}^3$. The pulmonary blood flow (Q_p) is estimated by multiplying the RVOT area, (RVOT D)^2*0.785, by the RVOT VTI. As shown in Fig. 6.6d, the RVOT diameter is 2.47 cm and the RVOT VTI is 12.3 cm. Therefore, the pulmonary blood flow is $(2.47)^2 * 0.785 * 12.3 = 58.9 \text{cm}^3$. The Q_p/Q_s ratio is 45.7/58.9 = 1.3:1. Note that because the 0.785 constant is present in both the numerator and denominator, the Q_p/Q_s calculation can be simplified to $[(\text{RVOT D})^2 * (\text{RVOT VTI})] / [(\text{LVOT D})^2 * (\text{LVOT VTI})]$.

5. The regurgitant volume is equal to the product of the regurgitant orifice area (EROA, cm^2) and the MV VTI (cm). In this case, the product of the EROA (0.37 cm^2) and the MV VTI (143 cm) gives a regurgitant volume of 53 mL/beat, which is consistent with moderately-severe MR.

References

1. Anavekar NS, Oh JK. Doppler echocardiography: a contemporary review. J Cardiol. 2009;54(3):347–58.
2. Quinones MA, Otto CM, Stoddard M, Waggoner A, Zoghbi WA. Doppler Quantification Task Force of the Nomenclature and Standards Committee of the American Society of Echocardiography. Recommendations for quantification of Doppler echocardiography: a report from the Doppler Quantification Task Force of the Nomenclature and Standards Committee of the American Society of Echocardiography. J Am Soc Echocardiogr. 2002;15(2):167–84.
3. Hatle L, Angelsen B. Doppler ultrasound in cardiology: physical principles and clinical applications. 2nd ed. Philadelphia: Lea & Febiger; 1985. p. 331.
4. Rudski LG, Lai WW, Afilalo J, et al. Guidelines for the echocardiographic assessment of the right heart in adults: a report from the American Society of Echocardiography endorsed by the European Association of Echocardiography, a registered branch of the European Society of Cardiology, and the Canadian Society of Echocardiography. J Am Soc Echocardiogr. 2010;23(7):685–713; quiz 786–8.
5. Nageh MF, Kopelen HA, Zoghbi WA, Quinones MA, Nagueh SF. Estimation of mean right atrial pressure using tissue Doppler imaging. Am J Cardiol. 1999;84(12):1448–51, A8.
6. Nagueh SF, Kopelen HA, Zoghbi WA. Relation of mean right atrial pressure to echocardiographic and Doppler parameters of right atrial and right ventricular function. Circulation. 1996;93(6):1160–9.
7. Firstenberg MS, Vandervoort PM, Greenberg NL, et al. Noninvasive estimation of transmitral pressure drop across the normal mitral valve in humans: importance of convective and inertial forces during left ventricular filling. J Am Coll Cardiol. 2000;36(6):1942–9.
8. Lima CO, Sahn DJ, Valdes-Cruz LM, et al. Noninvasive prediction of transvalvular pressure gradient in patients with pulmonary stenosis by quantitative two-dimensional echocardiographic Doppler studies. Circulation. 1983;67(4):866–71.
9. Masuyama T, Kodama K, Kitabatake A, Sato H, Nanto S, Inoue M. Continuous-wave Doppler echocardiographic detection of pulmonary regurgitation and its application to noninvasive estimation of pulmonary artery pressure. Circulation. 1986;74(3):484–92.
10. Beard II JT, Newman JH, Loyd JE, Byrd III BF. Doppler estimation of changes in pulmonary artery pressure during hypoxic breathing. J Am Soc Echocardiogr. 1991;4(2):121–30.
11. Scapellato F, Temporelli PL, Eleuteri E, Corra U, Imparato A, Giannuzzi P. Accurate noninvasive estimation of pulmonary vascular resistance by Doppler echocardiography in patients with chronic failure heart failure. J Am Coll Cardiol. 2001;37(7):1813–9.

12. Gorcsan III J, Snow FR, Paulsen W, Nixon JV. Noninvasive estimation of left atrial pressure in patients with congestive heart failure and mitral regurgitation by Doppler echocardiography. Am Heart J. 1991;121(3 pt 1):858–63.
13. Ommen SR, Nishimura RA, Appleton CP, et al. Clinical utility of Doppler echocardiography and tissue Doppler imaging in the estimation of left ventricular filling pressures: a comparative simultaneous Doppler-catheterization study. Circulation. 2000;102(15):1788–94.
14. Ha JW, Oh JK, Ling LH, Nishimura RA, Seward JB, Tajik AJ. Annulus paradoxus: transmitral flow velocity to mitral annular velocity ratio is inversely proportional to pulmonary capillary wedge pressure in patients with constrictive pericarditis. Circulation. 2001;104(9):976–8.
15. Abbas AE, Fortuin FD, Patel B, Moreno CA, Schiller NB, Lester SJ. Noninvasive measurement of systemic vascular resistance using Doppler echocardiography. J Am Soc Echocardiogr. 2004;17(8):834–8.
16. American College of Cardiology/American Heart Association Task Force on Practice Guidelines, Society of Cardiovascular Anesthesiologists, Society for Cardiovascular Angiography and Interventions, et al. ACC/AHA 2006 guidelines for the management of patients with valvular heart disease: a report of the American College of Cardiology/American Heart Association Task Force on Practice Guidelines (writing committee to revise the 1998 Guidelines for the Management of Patients With Valvular Heart Disease): developed in collaboration with the Society of Cardiovascular Anesthesiologists: endorsed by the Society for Cardiovascular Angiography and Interventions and the Society of Thoracic Surgeons. Circulation. 2006;114(5):e84–231.
17. Baumgartner H, Hung J, Bermejo J, et al. Echocardiographic assessment of valve stenosis: EAE/ASE recommendations for clinical practice. J Am Soc Echocardiogr. 2009;22(1):1–23; quiz 101–2.
18. Oh JK, Taliercio CP, Holmes Jr DR, et al. Prediction of the severity of aortic stenosis by Doppler aortic valve area determination: prospective Doppler-catheterization correlation in 100 patients. J Am Coll Cardiol. 1988;11(6):1227–34.
19. Monin JL, Quere JP, Monchi M, et al. Low-gradient aortic stenosis: operative risk stratification and predictors for long-term outcome: a multicenter study using dobutamine stress hemodynamics. Circulation. 2003;108(3):319–24.
20. Rahimtoola SH, Durairaj A, Mehra A, Nuno I. Current evaluation and management of patients with mitral stenosis. Circulation. 2002;106(10):1183–8.
21. Thomas JD, Weyman AE. Doppler mitral pressure half-time: a clinical tool in search of theoretical justification. J Am Coll Cardiol. 1987;10(4):923–9.
22. Bonow RO, Carabello BA, Chatterjee K, et al. 2008 focused update incorporated into the ACC/AHA 2006 guidelines for the management of patients with valvular heart disease: a report of the American College of Cardiology/American Heart Association Task Force on Practice Guidelines (Writing Committee to revise the 1998 guidelines for the management of patients with valvular heart disease). Endorsed by the Society of Cardiovascular Anesthesiologists, Society for Cardiovascular Angiography and Interventions, and Society of Thoracic Surgeons. J Am Coll Cardiol. 2008;52(13):e1–142.
23. Smith MD, Cassidy JM, Gurley JC, Smith AC, Booth DC. Echo Doppler evaluation of patients with acute mitral regurgitation: superiority of transesophageal echocardiography with color flow imaging. Am Heart J. 1995;129(5):967–74.
24. Bargiggia GS, Tronconi L, Sahn DJ, et al. A new method for quantitation of mitral regurgitation based on color flow Doppler imaging of flow convergence proximal to regurgitant orifice. Circulation. 1991;84(4):1481–9.
25. Pu M, Vandervoort PM, Griffin BP, et al. Quantification of mitral regurgitation by the proximal convergence method using transesophageal echocardiography. Clinical validation of a geometric correction for proximal flow constraint. Circulation. 1995;92(8):2169–77.
26. Pu M, Prior DL, Fan X, et al. Calculation of mitral regurgitant orifice area with use of a simplified proximal convergence method: initial clinical application. J Am Soc Echocardiogr. 2001;14(3):180–5.

27. Zoghbi WA, Enriquez-Sarano M, Foster E, et al. Recommendations for evaluation of the severity of native valvular regurgitation with two-dimensional and Doppler echocardiography. J Am Soc Echocardiogr. 2003;16(7):777–802.
28. Tribouilloy CM, Enriquez-Sarano M, Bailey KR, Seward JB, Tajik AJ. Assessment of severity of aortic regurgitation using the width of the vena contracta: a clinical color Doppler imaging study. Circulation. 2000;102(5):558–64.
29. Touche T, Prasquier R, Nitenberg A, de Zuttere D, Gourgon R. Assessment and follow-up of patients with aortic regurgitation by an updated Doppler echocardiographic measurement of the regurgitant fraction in the aortic arch. Circulation. 1985;72(4):819–24.

Suggested Readings

Hatle L, Angelsen B. Doppler ultrasound in cardiology: physical principles and clinical applications. 2nd ed. Philadelphia: Lea & Febiger; 1985. p. 331.

Quinones MA, Otto CM, Stoddard M, Waggoner A, Zoghbi WA. Doppler Quantification Task Force of the Nomenclature and Standards Committee of the American Society of Echocardiography. Recommendations for quantification of Doppler echocardiography: a report from the Doppler Quantification Task Force of the Nomenclature and Standards Committee of the American Society of Echocardiography. J Am Soc Echocardiogr. 2002;15(2):167–84.

Baumgartner H, Hung J, Bermejo J, et al. Echocardiographic assessment of valve stenosis: EAE/ASE recommendations for clinical practice. J Am Soc Echocardiogr. 2009;22(1):1–23; quiz 101–2.

Zoghbi WA, Enriquez-Sarano M, Foster E, et al. Recommendations for evaluation of the severity of native valvular regurgitation with two-dimensional and Doppler echocardiography. J Am Soc Echocardiogr. 2003;16(7):777–802.

Chapter 7
CT and MR Cardiovascular Hemodynamics

Andrew O. Zurick III and Milind Desai

Introduction

Noninvasive cardiac imaging has experienced dynamic improvements over the past several decades. Multiple, complementary technologies, including magnetic resonance imaging (MRI), computed tomography (CT), echocardiography, nuclear scintigraphy, fluoroscopy and angiography, are now capable of directly or indirectly providing information on cardiac and great vessel anatomy, volumes and function, perfusion, valvular function, and presence or absence of myocardial fibrosis or scar. Further, several of these technologies now are capable of providing a noninvasive hemodynamic assessment, which has otherwise primarily in the past been the domain and strength of echocardiography and invasive catheterization. Both CT and MRI have been proven to be accurate and reproducible, with each now capable of providing noninvasive hemodynamic information which is capable of enhancing clinical decision-making and impacting patient care. However, the use of this information must be based on a thorough knowledge of the strengths and weaknesses of the various noninvasive methods of hemodynamic assessment. Understanding the applications and limitations of these modalities will permit their effective and efficient usage in the future (Table 7.1).

A.O. Zurick III, MD
St. Thomas Heart, Nashville, TN, USA

M. Desai, MD (✉)
The Cleveland Clinic, Cleveland, OH, USA
e-mail: desaim2@ccf.org

S. Anwaruddin et al. (eds.), *Cardiovascular Hemodynamics: An Introductory Guide*, Contemporary Cardiology, DOI 10.1007/978-1-60761-195-0_7,

Table 7.1 CT and MRI advantages and disadvantages

	Advantages	Disadvantages
Computed tomography	Rapid image acquisition	Radiation exposure
	Excellent spatial resolution (<1 mm)	Potential need for iodinated contrast dye
	3D data-set acquisition for ability for post-processing/reconstruction	Limited temporal resolution (Best temporal resolution with current generation scanners on order of 75 ms)
	Typically well tolerated by patients	Limited hemodynamic assessment options currently
	Not contra-indicated in patients with ferromagnetic/metallic implants	
Magnetic resonance imaging	Tissue characterization	Increased image acquisition time
		Potential for patient claustrophobia
	Excellent spatial resolution (1–2 mm)	Possibility, although rare, for NSF following gadolinium contrast administration
	Temporal resolution better than CT (typically 25–50 ms)	Inability to image patients with absolute contra-indications including those with ferromagnetic implants (i.e., pacemakers, ICDs, intra-cerebral vascular coils, etc.)
	Unlimited imaging plane orientation and ability to acquire 3D data-sets	
	No need for contrast (i.e., can be performed on patients with decreased GFR)	
	Increased ability to assess cardiovascular hemodynamics noninvasively via volumetric and phase-contrast analysis	

General Overview of MR and CT Physics and Techniques

Physics Overview

MRI is based on the resonance, or increased amplitude of oscillation of a system exposed to a periodic force, of atomic nuclei. Following the application of radio waves, MRI involves measuring the signals that are emitted from atomic nuclei. Hydrogen is the most simple and abundant element in the human body, consisting of a single proton and electron, and therefore, it represents an ideal substrate for clinical MRI. There exists a unique relationship between electricity and magnetism, namely moving electrical charges are capable of generating a magnetic field and a time-varying magnetic field can create electric fields that can promote the flow of electrical charges. Atomic nuclei of several atoms behave as small magnets with angular momentum, and when placed within a magnetic field, they have a tendency to align with the direction of a field applied and precess, or rotate about their own axis, as would a top.

Most current clinical MRI involves superconducting magnets, where a magnetic field is generated perpendicular to an electrical current flowing along a cylindrical coiled wire. The creation of MR images involves the excitation of protons, within a magnetic field, using pulses of radiofrequency energy, which can be specifically

applied to body parts of interest through the concurrent application of magnetic field gradients. Following excitation of a tissue, a signal is created within a "receive" coil, which subsequently undergoes analog-to-digital conversion (ADC), which is then processed by the MRI computer as raw data into "k-space." The "Fourier transform" of the raw data ultimately generates 2 or 3D MR images that can be viewed for interpretation. MR imaging of the heart must contend with both cardiac and respiratory motion, conflicting requirements for both high temporal and spatial resolution, and do all of this both accurately and reproducibly in the clinical setting.

As with CMR, the small dimensions of the coronary arteries and rapid motion of cardiac structures pose significant challenges to effective imaging with cardiac computed tomography (CT). Current generation multi-row detector CT (MDCT) scanners involve a rotating X-ray source, which emit photons, which pass through a patient, as they are moved through the machine gantry. Due to continued improvements in gantry rotation times, and the development of dual-source CT, temporal resolution has improved. Slice collimation, or thickness, has also continued to improve, resulting in greater spatial resolution. Increased X-ray tube strength has also resulted in decreased image noise and recent generation scanners have continued to improve simultaneous slice acquisition, now up to as many as 320 slices per rotation, which allows one to cover a larger volume per rotation, decrease overall data acquisition time, and reduce duration of required breath hold. Through the simultaneous registration of the ECG, it is possible to synchronize image reconstruction with the relative cardiac phase. Ongoing developments in tube-current modulation, prospective ECG-gated scanning, and improved table pitch (speed with which the patient table is advanced through the scanner) continue to lower radiation exposure (effective dose).

MRI Techniques

Phase-Contrast Imaging

Phase-contrast imaging (PCI) is an MRI technique for quantifying velocity and blood flow in the heart and great vessels. By measuring the phase shift, or change in precessional frequency, of protons in blood as they move through a magnetic field with a bipolar gradient, velocity, direction, and volume of blood flow can be determined. The amount of relative phase difference is proportional to the velocity of the moving spin, and these phase shifts are measured in degrees within a range of ±180°. Similar to aliasing velocity in Doppler echocardiography, the encoding velocity (VENC) chosen for this technique should optimally be chosen to correspond to a phase shift of 180°. If the phase shift exceeds 180°, then the spins will be interpreted as having a different orientation, which would therefore result in abnormal velocity interpretation. Ultimately, phase contrast MR imaging produces velocity-encoded images where signal intensity is proportional to the velocity of blood moving through or within the slice plane. Unlike echocardiography, which is constrained by acoustic windows, PCI, utilizing a single imaging plane that is most commonly perpendicular to the direction of blood flow, generates a velocity encoded image of multiple phases

of the heart cycle either with or without breath-holding. Quantification of blood flow is subsequently determined by various software applications that require the user to manually outline the vessel of interest for each cardiac phase, which then produces time-velocity and time-flow curves (Fig. 7.1). Many studies have now demonstrated the reliability of PCI with CMR; however it must be noted that the accuracy of the technique can be significantly affected by the presence of eddy currents [1].

Myocardial Tagging

Myocardial tagging is a series of techniques that impose a saturation grid or series of saturation lines across the myocardium [1]. Deformation of these lines due to myocardial contraction and relaxation are then monitored and can be used to assess myocardial function by tracking the motion of the myocardium during the various phases of the cardiac cycle [2] (Fig. 7.2). When combined with cine imaging, myocardial tagging can provide complementary information regarding myocardial contraction, performance, and can be used to measure myocardial strain in three dimensions. In clinical practice, myocardial tag lines are typically evaluated subjectively to differentiate normal and hypokinetic myocardial segments. While predominantly used as a supplementary technique to cine imaging to evaluate cardiac wall motion, the research applications of myocardial tagging are continuing to evolve, particularly with recent advances in image acquisition speed and improved signal-to-noise ratios.

Volumetric and Functional Assessment

Through continued improvement in hardware and software, MRI has evolved into the "gold standard" for ventricular volumetric and function assessment owing to its excellent accuracy and reproducibility. With manual or automated contours of multi-phase, ECG-gated epi- and endocardial contours, ventricular volumes, function, and mass can be determined (Fig. 7.3). In addition, while Doppler echocardiography has typically been considered the reference standard for assessment of diastolic dysfunction, recent studies have also demonstrated the utility and reproducibility of CMR techniques for flow and phase contrast data analysis to extract velocity-related diastolic parameters [3]. The degree of myocardial fibrosis is related to the degree of left ventricular stiffness. Malaty et al. evaluated 50 patients with dilated cardiomyopathy (DCM) with Doppler echocardiography and breath-hold segmented inversion recovery sequence imaging following intravenous gadolinium administration to determine amount of left ventricular scar burden. Hyperenhancement (HE) was present in 31 patients with a mean scar burden of $4 \pm 7.6\%$, and patients with DCM without HE had significantly higher septal E/E' ratio than patients with scar ($p = 0.05$) suggesting that factors other than scar burden likely contribute to LV stiffness to a greater extent than replacement fibrosis in this patient population [4]. However, other groups have also shown that cardiac fibrosis correlates with impaired LV diastolic function and functional capacity, elevated NT-pro

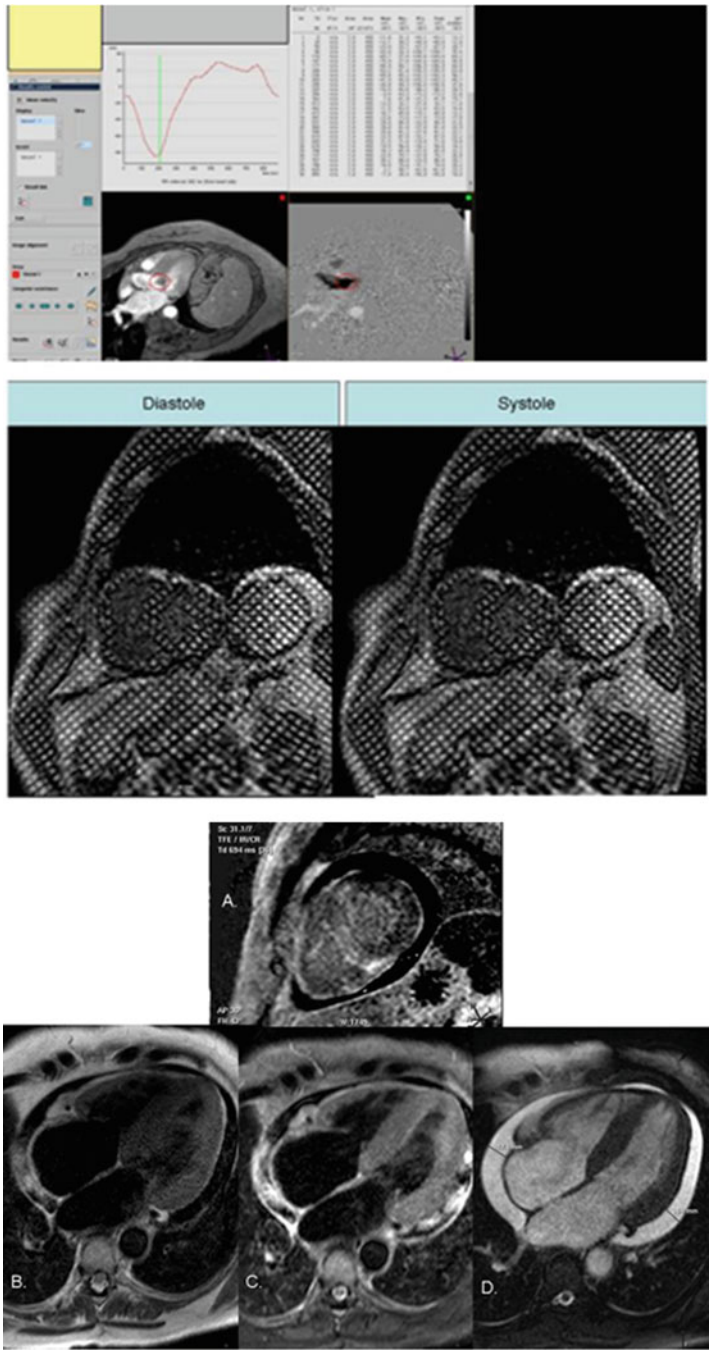

Fig. 7.1 Hypertrophic cardiomyopathy with severe systolic anterior motion of the mitral valve (SAM). Representative phase-contrast image (*top*) demonstrating manual contouring of the left ventricular outflow tract. Contours are propagated to images from multiple cardiac phases. Image at *bottom left* represents single cardiac-phase magnitude axial gradient echo image at end-systole. Peak left ventricular outflow tract velocity can be measured and converted to pressure gradient through utilization of modified Bernoulli equation. (*Bottom*) Myocardial tagged image (short axis orientation) with saturation lines depicted across the myocardium in both systole (*right*) and diastole (*left*)

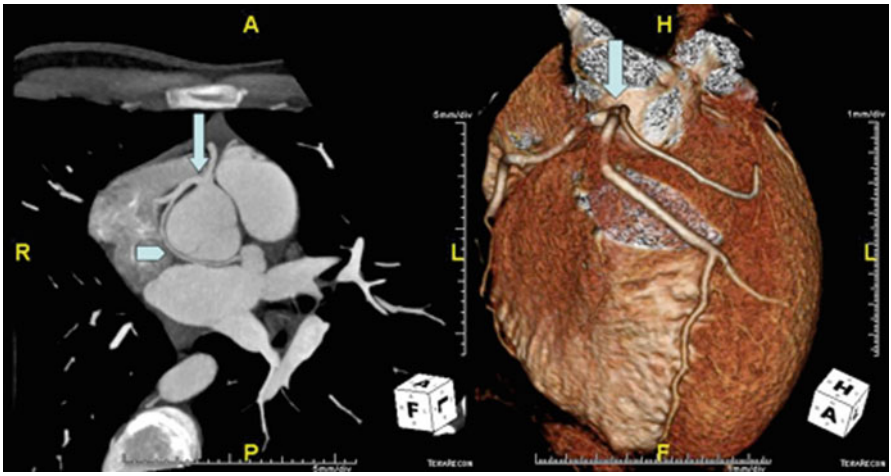

Fig. 7.2 Anomalous origin of the coronary arteries. Image at left demonstrates a maximum intensity projection (MIP) image of a common origin of both the left and right coronary arteries from a single, common ostium with the circumflex coronary artery passing retro-aortic (*arrow-head*). Image at left is a 3D volume-rendered image depicting same (*arrow*)

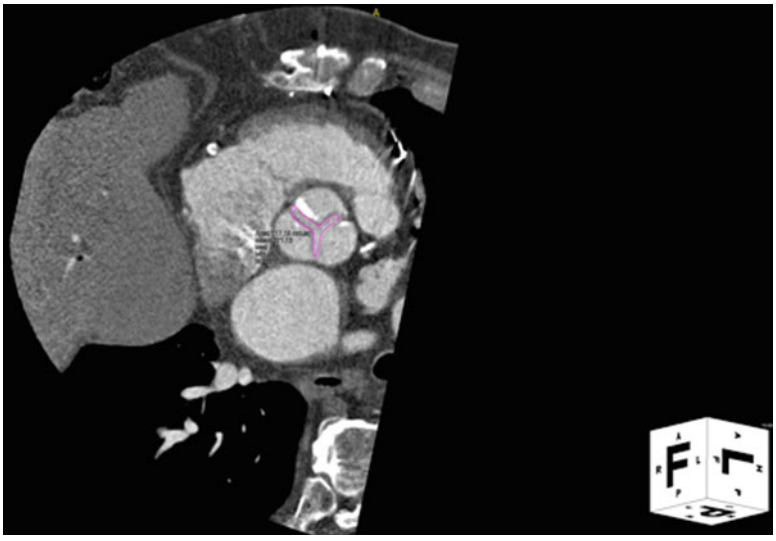

Fig. 7.3 Aortic stenosis. Cardiac CT 3D reconstructed multi-planar image of the aortic valve in short axis at end-systole with planimetry of aortic valve area

BNP, and adverse cardiac remodeling in patients with non-ischemic DCM [5]. Other groups have utilized CMR phase contrast velocity mapping (i.e., tissue phase mapping) to evaluate regional wall motion patterns and longitudinally and circumferentially directed movements of the left ventricle [6]. The complex pattern of

ventricular twisting and longitudinal motion in the normal human heart can be better understood through applications such as these, ultimately helping to provide a better understanding of the complex mechanics of the normal heart.

Delayed Enhancement Imaging

The intensity of voxels in an MR image is a direct result of the amount of signal that can be measured by a receiver coil. MR intravenous contrast agents are useful for depicting anatomy and physiology, evaluating vascular supply to both normal and pathologic tissues, and assessing myocardial viability. Most MR contrast agents work by shortened T1 relaxation times, which results in increased signal intensity. The most commonly used MR contrast agents are chelates of gadolinium (Gd3+), a heavy metal ion.

Inversion recovery imaging is capable of selectively suppressing signal from certain tissues based on their T1 recovery times, and is useful for assessing myocardial infarction and viability. Following gadolinium administration, infracted myocardium demonstrates a delayed pattern of gadolinium washout, and through the use of inversion recovery techniques, uninfarcted myocardium is "nulled" so that infracted myocardium appears bright by comparison.

Tissue Characterization (T1- and T2-Weighted Imaging)

One of the unique features of cardiac MRI is the ability to characterize normal and pathologic tissues through the use of various pulse sequences. In addition to fat suppression and gadolinium contrast enhancement, T1- and T2-weighted imaging are the most widely utilized techniques. Tissues that tend to appear brighter on T1-weighted images include lipid, hemorrhagic products, proteinaceous fluid, and gadolinium. T2-weighted images of the heart help to characterize tissues with longer T2-times, and are typically performed with concurrent blood nulling.

CT Techniques

ECG-Triggering

Through the simultaneous registration of the ECG, it is possible to synchronize image reconstruction with the relative cardiac phase. Due to cardiac and respiratory movements, motion artifacts can significantly affect cardiovascular CT images. Appropriate collimation size and image acquisition speed are important to obtain images free from artifacts. Currently, the collimation size for coronary artery calcium screening and angiography is 0.6–3 mm and acquisition speed ranges from 50 to 250 ms. Currently, two ECG-trigger techniques are utilized in cardiac CT imaging, retrospective and prospective triggering. Prospective triggering can be performed with R wave triggering, end-systolic triggering, and both end-systolic and

end-diastolic combined triggering. Alternatively, retrospective triggering is widely used and synchronized to an ECG signal that is recorded simultaneously with images. Changes in heart rate or rhythm can induce mis-registration artifact in both prospective and retrospective triggered images.

Contrast Media

The primary purpose of contrast media injection is to increase contrast between the structure of interest and surrounding tissues by increasing the CT Hounsfield units. Care must be taken regarding circulation time for contrast media, the time interval that it takes blood to move from the point of venous access, the structure/region of interest, with several factors having influence, including cardiac output, injection rate, and venous anatomy. Circulation time can be measured using a small contrast bolus injection with serial scanning of single image slice to obtain peak enhancement time through the time density curve. Alternatively, automatic bolus triggering utilizes a monitoring scan obtained 10–12 s following the start of contrast injection and when the Hounsfield units (HU) reaches a prespecified threshold (typically 120 HU), imaging is initiated.

Clinical Applications

Shunts

Cardiac MRI has become a valuable tool in the evaluation of both cardiac anatomy and quantification of physiologic function. CMR can detect, provide morphologic information, and quantify both intra- and extra-cardiac shunts. Shunt volume can be calculated through the use of volumetric cine MR imaging or PCI. Provided that there is absence of concurrent valvular regurgitation, total forward flow through the proximal ascending aorta and main pulmonary artery can be utilized to determine shunt fraction (Shunt fraction % (Q_p/Q_s) = total PCI pulmonary artery volume flow (mL)/total PCI ascending aortic volume flow (mL)). Alternatively, shunt severity can be calculated by comparing the ratio of right ventricular to left ventricular stroke volumes (Q_p/Q_s), again provided that there is not significant simultaneous valvular regurgitation. In addition, MR angiography can provide excellent 3D anatomic examination of vessels including the presence of anomalous pulmonary veins.

Cardiac CT is a useful adjunctive imaging modality in the assessment of intra- and extra-cardiac shunts. It is typically reserved for patients with contraindications for CMR or when there are issues associated with severe claustrophobia. Excellent spatial resolution provides the ability to visualize inter-atrial and inter-ventricular septal defects (VSDs) [7]. Further, due to the large field of view, as with CMR, detailed imaging of not only the heart, but mediastinum, lungs, and pulmonary arterial assessment and other

associated intra-thoracic anomalies is obtained [8]. Previous studies have shown that cine CT, through evaluation of indicator dilution curves, provides a precise, noninvasive technique for measuring shunt lesions in congenital and acquired heart diseases [9].

Atrial Septal Defect

Atrial septal defect (ASD) is the most common shunt lesion detected de novo in adulthood [10]. Sinus venosus, septum secondum and primum defects can clearly be identified with MR imaging in the transverse plane or along the short axis. Further, spin-echo MR imaging has been found to have a greater than 90% sensitivity and specificity for identification of atrial septal defects [11]. PCI enables more precise evaluation of both size and shape of atrial septal defects and permits more accurate quantification of the degree of shunting present [12, 13]. In addition, cardiac CT has been also shown to detect and characterize ASDs with high sensitivity (66–100%) and specificity (86–100%) [14] (Fig. 7.4).

Ventricular Septal Defect

VSD is the second most common congenital defect of the heart, accounting for nearly 20% of all cardiac malformations [10]. VSD can be further categorized into four groups based on location and margin: outlet, membranous, trabecular, and inlet [15]. Membranous is the most common. MR imaging possesses greater than 90% sensitivity for the detection of VSD [16].

Atrioventricular Septal Defect

Atrioventricular septal defects presents as a common atrioventricular valve with abnormal arrangement of the valvular leaflets, and variable defects in the primum atrial septum and ventricular inlet septum [17]. In the most severe form of atrioventricular septal defect, there exists bidirectional shunting, where all four chambers of the heart communicate. CMR is a particularly valuable tool in the evaluation of atrioventricular septal defects to delineate anatomical features which are important for surgical planning, cardiac chamber dimension, and presence and size of ventricular component of defects.

Patent Ductus Arteriosus

Before birth, the ductus arteriosus allows blood to bypass the baby's lungs by connecting the pulmonary arteries with the aorta. Patent ductus arteriosus (PDA) is a congenital disorder within the great vessels wherein a neonate's ductus arteriosus fails to close after birth. PDA accounts for 10–12% of all congenital heart disease [10].

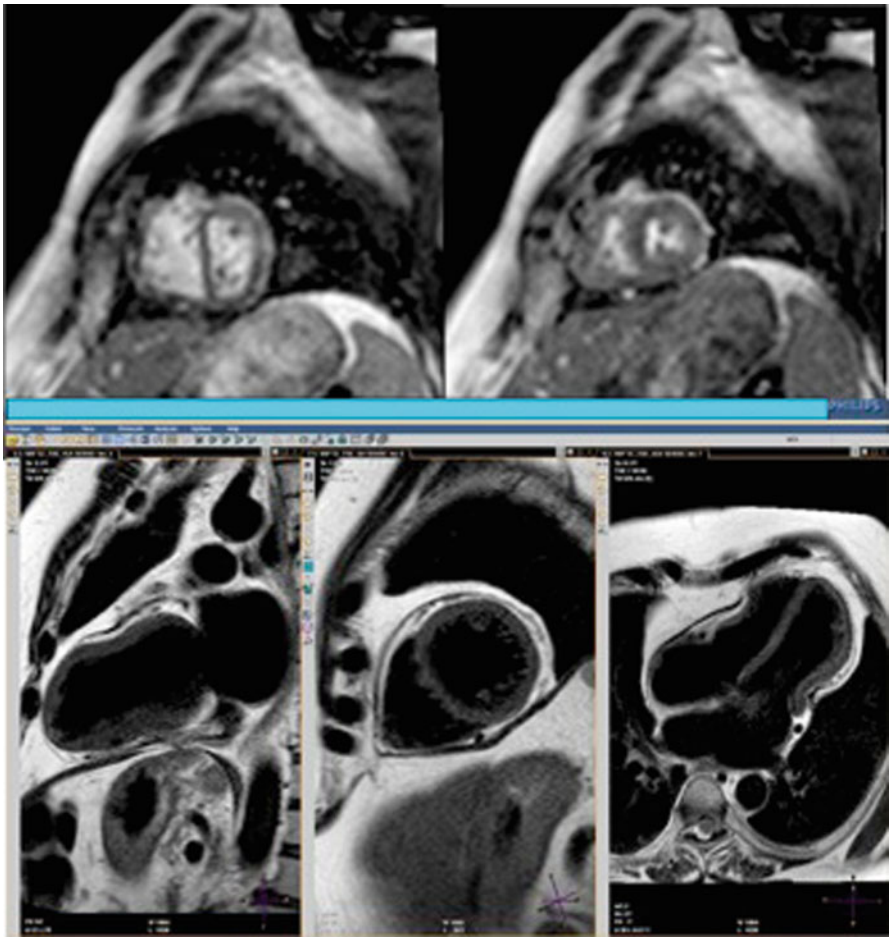

Fig. 7.4 Constrictive pericarditis cardiac MRI. Images at *top* demonstrate real-time free-breathing gradient echo short axis image of the left ventricle demonstrating ventricular interdependence in patient with constrictive pericarditis. Images at *bottom* are spin-echo "dark-blood" images in multiple orientations demonstrating pericardial thickening

CMR is capable of clearly demonstrating the persistent communication between the aorta and pulmonary artery; however due to the often small size of these defects (<3 mm), echocardiography remains the primary diagnostic tool for their identification and evaluation (Fig. 7.5).

Partial Anomalous Pulmonary Venous Return

Partial anomalous pulmonary venous return (PAPVR) involves one or more pulmonary veins returning aberrantly to the superior or inferior vena cava, right atrium, or

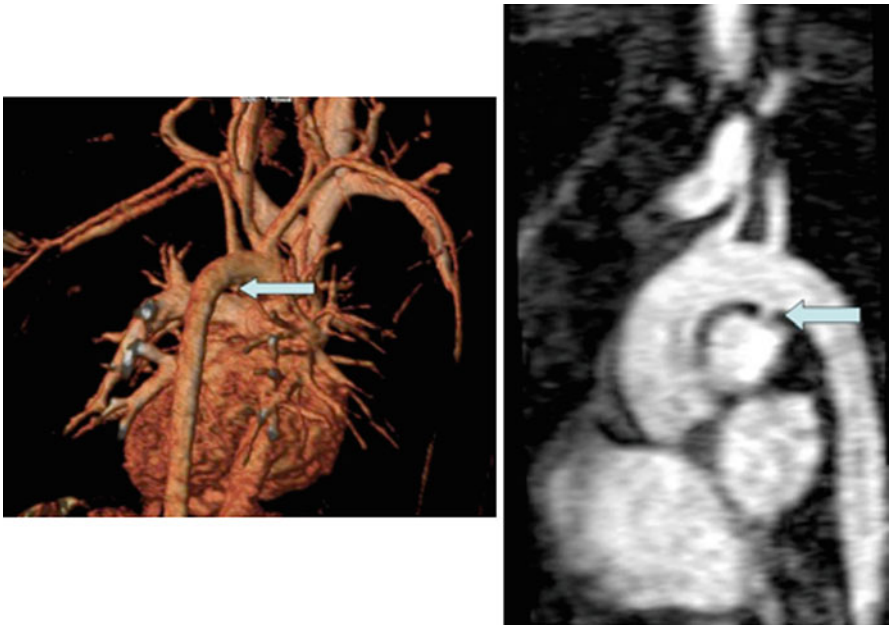

Fig. 7.5 Patent ductus arteriosus. Image at right is 3D, volume rendered MR image of PDA (*arrow*). Image at *left* is MR angiography sagittal image demonstrating PDA in an alternate orientation (*arrow*)

coronary sinus. PAPVR is present in 10–15% of patients with secundum-type atrial septal defects and 100% of patients with sinus venosus-type defects [17]. Children with PAPVR are typically asymptomatic, whereas adults with the condition will typically present with dyspnea and palpitations. CMR is a particularly attractive imaging modality for identifying PAPVR as it provides a large field of view, and can be performed without ionizing radiation or contrast material. CMR has been reported to have greater sensitivity (95%) for identification of PAPVR compared with echocardiography and angiography [18] (Fig. 7.6).

Diastology

CMR is now playing an increasing role in understanding the physiology of diastolic function. CMR is capable of evaluating myocardium in both active and passive phases, providing insight into relaxation and compliance characteristics. Further, CMR through PCI can assess inflow and myocardial velocities. Previous studies comparing CMR to TTE in the assessment of diastolic function have shown that velocities of mitral valve flow (E and A wave) measured by CMR correlated well with TTE ($r=0.81$; $p<0.001$), but also demonstrated systematic underestimation by CMR compared to TTE [19, 20]. Myocardial tagging with CMR can provide

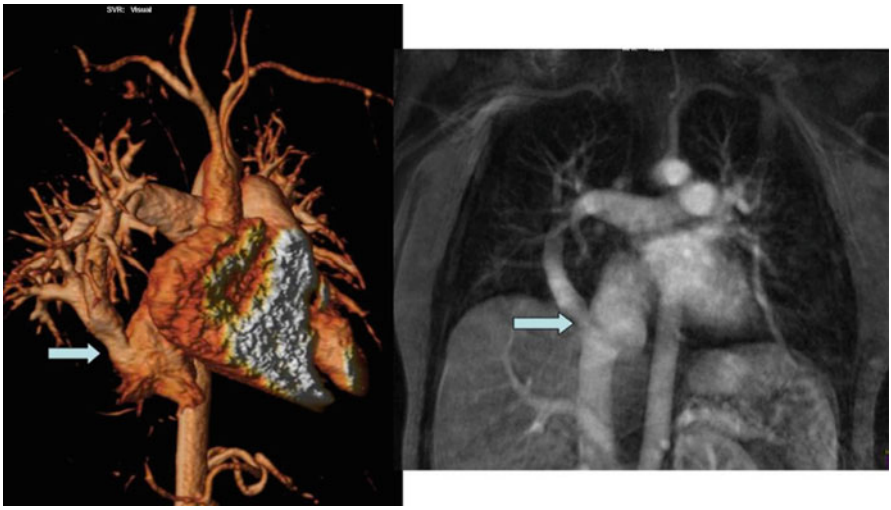

Fig. 7.6 Scimitar syndrome patient (partial anomalous pulmonary venous drainage). Image at *left* demonstrates 3D volume-rendered MR image of anomalous pulmonary venous return with right inferior pulmonary vein draining via antrum on inferior vena cava. Image at right is coronal MR maximum intensity projection (MIP) depicting same

complementary information regarding myocardial contraction performance, and can be used to measure myocardial strain in three dimensions.

While not typically thought of as a reliable source for assessment of diastolic function, recent studies have demonstrated that CT is capable of providing information regarding cardiac diastolic function. Boogers et al. evaluated 70 patients who had undergone CT and 2D echocardiography with TDI. Good correlations were observed between cardiac CT and 2D echocardiography for assessment of E ($r=0.73$; $p<0.01$), *E/A* ($r=0.87$; $p<0.01$), E_a ($r=0.82$; $p<0.01$), and E/E_a ($r=0.81$; $p<0.01$). In addition, a good diagnostic accuracy (79%) was found for detection of diastolic dysfunction using cardiac CT [21]. Other groups have evaluated the arterial enhancement of the aortic-root lumen on contrast-enhanced CT, and plotted its change over time to determine the time-enhancement curve. Nakahara et al. evaluated 30 patients with suspected coronary artery disease who underwent MDCT and echocardiography. On univariate analysis, the slope of the time-enhancement curve was found to correlate with the e' ($r=0.686$; $P=0.000$) and E/e' ($r=-0.482$; $P=0.007$) ([22]).

Valvular Heart Disease

From the time of its initial development, PCI has been successfully utilized for the study of valvular heart disease. Regurgitant valvular lesions involve a state of volume overload. Through a combination of PCI and ventricular volumetric assessment, it is

possible to determine both regurgitant volume and fraction across mitral and tricuspid valves. Further, PCI has been demonstrated to help in the stratification of aortic regurgitant (AR) severity. Holodiastolic reversal in the mid-descending thoracic aorta using PCI has been shown to indicate severe AR and can be used with quantified regurgitant values obtained from PCI to further stratify AR severity [23].

One measure of severity of a valvular stenosis involves the peak transvalvular pressure gradient that is generated across the area of narrowing. For stenotic valvular lesions, PCI can be positioned through-plane or in-plane to estimate the maximum trans-valvular velocity (V_{max}). As is seen with spectral Doppler echocardiography, if the imaging slice does not pass through the area of maximum velocity, then the pressure gradient, estimated using the modified Bernoulli equation (pressure gradient (mmHg) = $4 \times V_{max2}$), will be underestimated. Aliasing will have a similar appearance as in Doppler echocardiography, and if this is seen at the time of image acquisition, this sequence must be repeated using a height encoding velocity (V_{enc}). Additionally, PCI can also evaluate volume flow rates by measuring the mean velocity of blood across its lumen (V_{mean}) and multiplying by the cross-sectional area of the vessel lumen (volume flow (mL/s) = V_{mean} (cm/s) × area (cm^2)).

Computed tomography can provide some limited valvular heart disease assessment; however given its relatively low temporal resolution, particularly compared to echocardiography, at this time it remains a supplement imaging modality in the assessment of valvular heart disease.

Aortic valve stenosis continues to be one of the most common valvular disorders in older adults with a prevalence of 8% at age 85 [24]. Open surgical aortic valve replacement is the only treatment that has been demonstrated to improve symptoms, survival, and functional status [25]. However, certain patient subsets are deemed exceedingly high-risk for surgical repair, which has lead to the development of transcatheter aortic valve replacement. CT now plays a vital role in assessing patients prior to percutaneous aortic valve implantation. 3D reconstructed multi-planar images allow assessment of the aortic valve in multiple phases of the cardiac cycle, and permit direct valve area planimetry (Fig. 7.7). Further, ECG-gated imaging of the thoracic aortic permits accurate assessment of aortic anatomy and morphology. Contrasted imaging of the abdominal aorta and peripheral arteries is also very important for determining whether the peripheral arteries are large enough to accommodate the large diameter of the delivery catheters (currently 18 F for the Medtronic CoreValve ReValving System (Medtronic, Minneapolis, MN) and 22 and 24 F for the Edwards SAPIEN transcatheter heart valve (Edwards Lifesciences, Irvine, CA)). The results of the recently published PARTNER trial have shown that at 1 year, the rate of death from any cause was 30.7% with TAVI, compared to 50.7% with standard therapy. However, at 30 days, TAVI as compared to standard therapy was associated with a high incidence of major strokes (5 vs. 1.1%, $p = 0.06$) and major vascular complications (16.2 vs. 1.1%, $p < 0.001$) [26].

CT is also capable of assessing ventricular volumes on multi-phase gated images to help in the determination of ventricular dilatation with regurgitation valvular lesions. Further, in patients with mechanical valves, CT provides a rapid, low-radiation exposure technique to image the valve in multiple phases of the cardiac cycle to determine opening and closure angles.

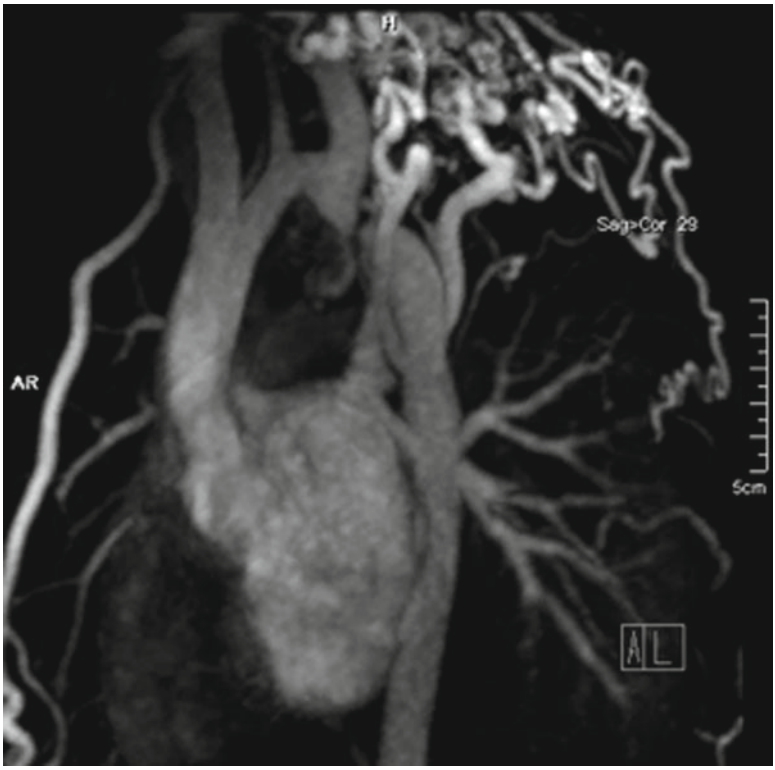

Fig. 7.7 3D volume rendered MR angiography image of aortic coarctation (*arrow*) with significant collateral vessels

Cardiomyopathies

CMR provides excellent qualitative as well as quantitative assessment of ventricular function. When compared with Doppler echocardiography, phase-contrast measurements correspond well, and show fair correspondence when compared with invasive techniques utilizing the Fick principle, indicator-ink method, or thermodilution [27, 28]. Volumetric and functional assessment of the ventricles typically involves retrospectively gated stead-state free precession imaging of the chambers either in short or long axis orientations. Utilizing post-processing software, contours of the epi- and endocardium are typically drawn manually for each imaging slice. Post-processing software generates quantitative data regarding cardiac function (ejection fraction, cardiac output), mass, and volumes. Alternatively, determination of cardiac output can be performed with phase-contrast imaging. By comparing cardiac output of the left ventricle in the ascending aorta with the cardiac output of the

right ventricle in the main pulmonary artery, there is an internal control of these measurements, with gross differences typically indicating either unknown intra- or extra-cardiac shunt or more commonly, error in the initial prescription of the phase-contrast technique with either incorrectly selected imaging plane or encoding velocity.

CMR is now evolving as an important imaging modality in the assessment of patients with hypertrophic cardiomyopathy [29]. Cine imaging provides anatomic and morphologic assessment, allowing for measurement of myocardial wall thickness, papillary muscle anatomy, and left ventricular outflow tract obstruction. Phase-contrast imaging has proven useful in the assessment of gradients in patients with hypertrophic obstructive cardiomyopathy [30]. In patients with left ventricular outflow tract obstruction, PCI (both in plane and through plane) is useful to determine the peak velocity in a manner similar to Doppler echocardiography [29]. Post-gadolinium contrast delayed enhancement imaging also permits assessment of myocardium for scar. CMR also has proven useful in the evaluation of myocardial sarcoidosis [31], amyloidosis [32–34], and hemochromatosis [34, 35].

Through the simultaneous registration of the ECG, it is possible to synchronize image reconstruction with the relative cardiac phase with cardiac CT imaging. In patients with suspected or documented heart disease, precise, accurate quantification of cardiac function is vital for diagnosis, risk stratification, treatment, and prognosis. The same data that is acquired for coronary arterial evaluation, as part of coronary CT angiography, can also be used for evaluation of cardiac function. Previous studies have demonstrated that multi-phase, gated cardiac CT demonstrates good correlation when compared with 2D surface echocardiography [36, 37].

Pericardial Disease

CMR is an excellent modality for assessing pericardial disease. CMR can accurately demonstrate pericardial thickness, effusion, pericardial cysts and through various pulse sequences, also demonstrate pericardial edema and/or inflammation. Real-time gradient-echo CMR in a single imaging slice can evaluate ventricular function with simultaneous respiration visualization and assess for ventricular interdependence that might suggest tamponade or constrictive physiology (Fig. 7.8). One area where CMR has significant limitations is in the assessment of pericardial calcification. Pericardial calcium causes significant susceptibility artifact on bright-blood cine MRI sequences.

Cardiac CT provides the ability, whether gated or non-gated, with iodinate contrast or without, to visualize the pericardium and assess and quantify pericardial thickening, calcification, or effusion. Multi-phase, retrospectively ECG-gated cardiac CT imaging with iodinated contrast also allows for a functional assessment of inter-ventricular septal motion and ventricular interdependence, although with a somewhat lesser temporal resolution (Fig. 7.9).

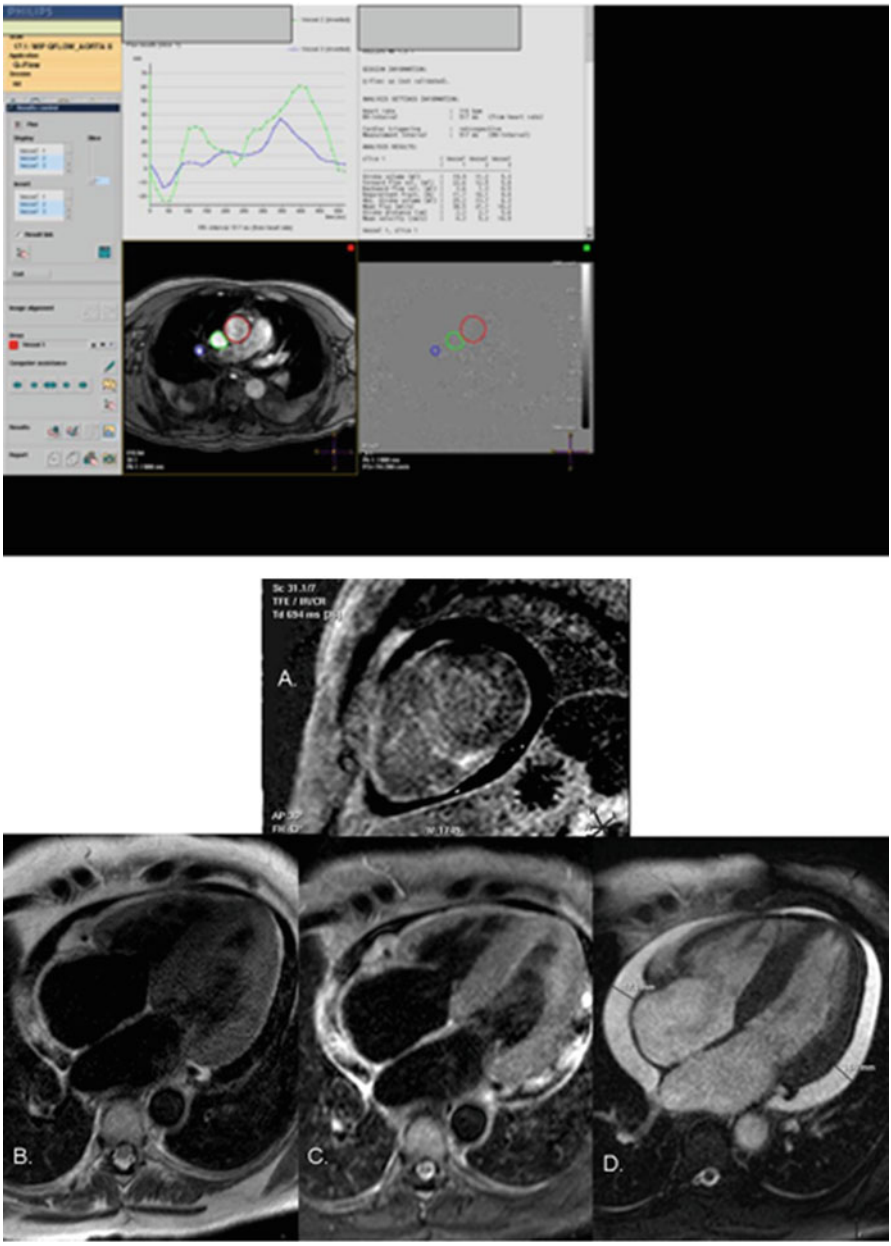

Fig. 7.8 Cardiac amyloidosis. Image at *top* are from representative phase-contrast image demonstrating manual contouring of the ascending aorta, superior vena cava, and right upper pulmonary vein. Flow curves in *upper left panel* demonstrate systolic blunting consistent with diastolic dysfunction. Images at *bottom* demonstrate tissue characterization of myocardium in cardiac amyloidosis through multiple, different cardiac MRI pulse sequences

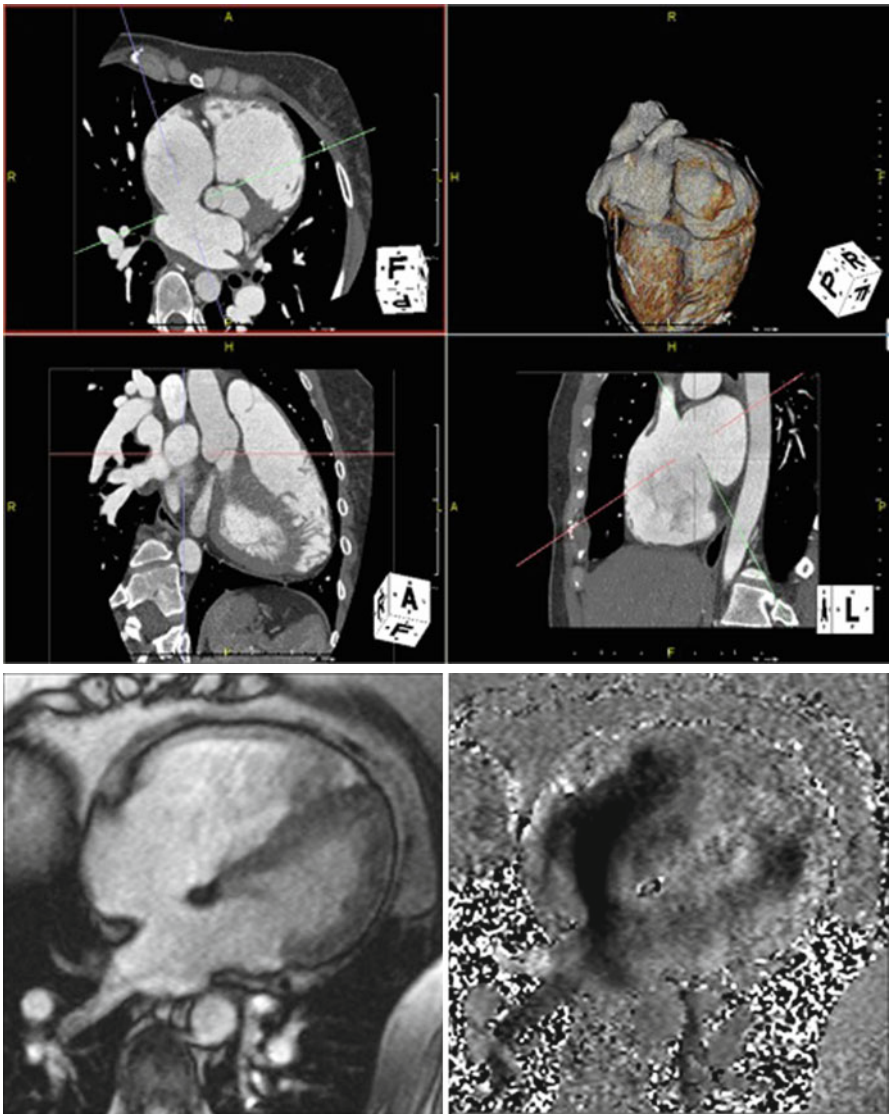

Fig. 7.9 ECG-gated cardiac computed tomography with iodinated contrast axial image demonstrating atrial septal defect (ASD), ostium secundum type (*top*). Cardiac MRI (*bottom*) steady-state free precession 4-chamber image demonstrating ASD, ostium secundum type (*right*), and phase-contrast image demonstrating left to right shunt across ASD (*left*)

Vascular Hemodynamics

Vascular anatomy and pathology can be imaged using CMR with or without gadolinium-based contrast. Black-blood imaging provides excellent vascular anatomic detail with nulling of the blood pool. Alternatively, cine bright-blood CMR imaging

provides additional information about vascular wall pathology and flow dynamics. First pass gadolinium-enhanced magnetic resonance angiography (MRA) can now be performed on nearly any MR scanner and produces high-spatial resolution images with broad anatomic coverage. Artifacts with MRA may occasionally result in mis-diagnosis of pseudostenosis in a vessel due to metal artifacts, susceptibility artifact from concentrated gadolinium, and volume averaging.

Phase-contrast imaging has also proven useful in the assessment of gradients across aortic coarctation [5]. With aortic coarctation, collateral flow can be assessed by measuring blood flow within 2 cm of the coarctation and above the diaphragm. In patients with significant coarctation, the flow within the coarctation increases toward the diaphragm due to retrograde perfusion of the dilated intercostals arteries, which are providing collateral circulation [38]. Additionally, measurements within the coarctation can help determine peak velocity and therefore pressure gradient within the stenosis. Pressure gradients greater than 20 mmHg measured during cardiac catheterization have been previously considered an indication for intervention [39].

Alternatively, CT angiography can also provide excellent spatial resolution when imaging arterial phase vascular images. Typically vascular imaging with CT angiography does not necessitate ECG-gating, unless there is specific concern regarding the aortic root, which will typically be affected by cardiac motion artifact on non-ECG-gated images.

Coronary Angiography

Through the simultaneous administration of intravenous iodinated contrast material, oral and intravenous beta blockers to lower the heart rate, and sublingual nitroglycerin for coronary vasodilation, imaging of the coronary arteries has become increasingly feasible. Studies have now shown that detection of hemodynamically significant coronary artery stenoses with coronary CT have sensitivities between 83 and 99% and specificities ranging from 93 to 98% [40]. Further, due to very high negative predictive values (95–100%), modern CT scanners can be used to reliably rule out the presence of significant coronary artery stenoses.

While the strength of coronary CT is its excellent spatial resolution and anatomic definition, its most commonly cited weakness is its inability to provide hemodynamic data. Studies with coronary CT are now beginning to assess coronary flow. Chow et al. calculated changes in corrected coronary opacification (CCO) and compared this with severity of coronary stenosis and thrombolysis in myocardial infarction (TIMI) flow in patients undergoing both coronary CT angiography and invasive coronary angiography. Abnormal coronary arterial flow was identified in 104 coronary arteries with a sensitivity, specificity, positive predictive value and negative predictive value of 83.3% (95% confidence interval (CI): 57.7–95.6%), 91.2% (95% CI: 75.2–97.7%), 83.3% (95% CI: 57.7–95.6%), and 91.2% (95% CI: 75.2–97.7%), respectively [41]. In addition, Yamashita et al. evaluated 64-slice multi-detector

computed tomography in 87 high-risk patients following ST-elevation myocardial infarction (STEMI) to differentiate TIMI flow grade 3 from TIMI flow grade 2. The MDCT findings were compared to TIMI flow grades with invasive coronary angiography performed 20 ± 5 min later. A CT number ratio was calculated by dividing the CT number of the contrast-enhanced coronary lumen at the most distal infarct related artery (IRA), by that at the proximal site to the culprit lesion in patients with repurfusion on MDCT. The sensitivity, specificity, and accuracy of a diagnosis of TIMI flow grade 3 on the basis of CT number ratio ≥0.54 determined by receiver-operator characteristic curve analysis were 92, 97, and 97% respectively [42]. Additionally, several groups have now started to look at the potential role of stress and rest myocardial perfusion imaging with CT [43–45].

Coronary artery disease remains the leading cause of morbidity and mortality in the industrialized world. While conventional coronary angiography remains the "gold standard" for evaluation of coronary arterial disease, it does possess limitations, namely its invasive nature, cost, and need for radiation and iodinated contrast exposure. Due to these limitations, alternative noninvasive imaging modalities have evolved for the evaluation of coronary artery disease that can avoid some of these undesirable attributes. While CT coronary angiography provides excellent spatial and temporal resolution, its use still requires patient breath-holding, exposure to radiation, and use of iodinated contrast agents. MR imaging of the coronary arteries does not require radiation exposure, can be performed either with or without administration of contrast material, and is capable of being accomplished with or without patient breath-hold. Similar to other noninvasive modalities, MR imaging of the coronary arteries is limited by both cardiac and respiratory motion. In addition, the small size and tortuosity of the coronary vessels, coupled with rapid spatial displacement and increased distance from the body or surface coils, present challenges for accurate imaging.

Initial studies with coronary MRA demonstrated that this technique was capable of accurate diagnosis of left main coronary artery and three-vessel disease [46]. With the continued development and improvement in MRI software and hardware, improvements in spatial resolution and image quality have been possible. Additional studies have now reported that contrast-enhanced MRA (CE-MRA) at 3.0 T is able to depict significant coronary artery stenoses with high sensitivity (94.6%), and negative predictive values of 98.5 and 97.7% on a per-segment and per-vessel basis respectively [47]. Additional studies have compared the visual and quantitative analysis high-spatial resolution CMR perfusion at 3.0 T against invasively determined fractional flow reserve (FFR) [48]. At an FFR threshold <0.75 to define hemodynamically significant lesions, visual CMR analysis reported sensitivity and specificity of 0.82 and 0.94 ($p < 0.0001$) respectively.

Further developments in coronary artery imaging have come through the use of ECG and respiratory triggered, segmented, 3D data acquisition. During free-breathing, monitoring of diaphragmatic motion is performed by a unique navigator echo, and the decision to accept or reject image data are made based on the position of the diaphragm [49]. In addition, stress-induced myocardial ischemia can now be assessed noninvasively with the use of blood oxygen level-dependent (BOLD) CMR [50]. Perfusion CMR imaging has been compared with quantitative coronary angiograpy

(QCA) and fractional flow reserve (FFR). Futamatsu et al. evaluated 37 patients with perfusion CMR imaging, quantitative coronary angiography, and FFR. Myocardial perfusion reserve (MPR) using a cutoff of 2.06 was found to have sensitivity and specificity for identification of hemodynamically significant CAD (defined as FFR ≤0.75) of 92.9 and 56.7% respectively. Sensitivity and specificity of anatomically significant CAD (>50% diameter stenosis) were 87.2 and 49.2% respectively [51].

Future Directions

The future of cardiac imaging is dynamic. With ever increasing advances in both hardware and software, cardiac MRI and CT will continue to evolve and improve. Increasing magnetic field strength, coupled with multi-phased array coils promise to improve CMR spatial resolution. Continued improvements in gantry rotation times, table pitch, X-ray tube strength, and improved simultaneous slice acquisition are all promising areas of improvement in cardiac CT technology at present. With these continued advancements, cardiac CT and MRI will continue to play an ever increasing role in the noninvasive hemodynamic evaluation of our patients.

Questions

1. A 47-year-old female has developed increasing shortness of breath over the preceding 6 months. Transthoracic echocardiogram has demonstrated severe ventricular hypertrophy. Subsequent cardiac MRI is performed to assess LVOT gradients and papillary muscle morphology.

   Among the following, CMR can best evaluate diastolic dysfunction via:

   A. Phase-sensitive inversion recovery imaging (PSIR) post-gadolinium contrast.
   B. Phase-contrast imaging.
   C. Non-breath-hold T2-weighted axial images of the myocardium.
   D. Magnetic resonance angiography.

   Answer B: Phase-contrast imaging (PCI) is capable of assessing both inflow and myocardial velocities, and plotting flow curves relative to the various phases of the cardiac cycle. This modality can provide insight into both myocardial relaxation and compliance characteristics. PCI has been shown to correlate well with TTE in the assessment of diastolic function, however tend to underestimate velocities of mitral valve flow (*E* and *A* waves) compared to TTE.

2. A 69-year-old African American male previously underwent coronary artery bypass graft surgery and mitral valve repair 10 years ago. Over the past 9 months, he has developed increasing shortness of breath, lower extremity edema, and abdominal fullness. Transthoracic echocardiogram demonstrates septal bounce

and tubular shaped left ventricle with atrial tethering. Subsequent cardiac MRI is performed to evaluate for constrictive pericaritis.

Among the following, which method is most useful for evaluating for ventricular interdependence?

A. Real-time gradient echo CMR.
B. Breath-hold, 4-chamber steady-state free precession cine imaging.
C. Short-axis, breath-hold delayed-hyperenhancement imaging post-gadolinium contrast.
D. Short-tau inversion recovery imaging (STIR).

Answer A: Real-time gradient echo CMR typically provides a single image slice, the short axis left ventricle is most often chosen. Through simultaneous evaluation of both ventricular function with respiration, it is possible to assess for ventricular interdependence. Breath-hold, 4-chamber steady-state free precession cine imaging is a good method for assessing ventricular function. Short-axis, breath-hold delayed-hyperenhancement imaging post-gadolinium contrast has been shown to be an effective method for evaluating for active pericardial inflammation; however this in and of itself does not necessarily reflect evidence of constriction. Short-tau inversion recovery imaging (STIR) is an effective method for evaluating for myocardial and/or pericardial inflammation.

3. With cardiac CT, it is possible to synchronize image reconstruction with the relative cardiac phases via:

A. Iterative reconstruction.
B. ECG-triggering.
C. Filtered back-projection.
D. Myocardial tagging.

Answer B: ECG-triggering, through the simultaneous registration of the ECG at the time of image acquisition, can allow for image reconstruction that is synchronized to the relative cardiac phase. ECG-triggering can be performed both prospectively and retrospectively. Iterative reconstruction is a method or group of algorithms used in 2D and 3D image sets. Filtered back-projection is also a reconstruction technique used for CT that applies a filter to the raw data collected during CT and attenuation information is simultaneously collected that are then utilized in image creation. Myocardial tagging is a cardiac MRI technique that applies saturation grid lines to the myocardium, and their subsequent deformation can be used to assess myocardial contraction and relaxation.

4. Shunt volume and shunt fraction (Q_p/Q_s) using MRI can be calculated through use of:

A. Volumetric cine MRI.
B. Phase-contrast imaging (PCI).

C. Neither.
D. Both A and B.

Answer D: Both volumetric cine MRI and PCI can be used to calculate shunt volume and shunt fraction (Q_p/Q_s) provided that there is no significant concurrent valvular regurgitation. Specifically, total forward flow through the proximal ascending aorta and main pulmonary artery can be used to determine shunt fraction (Shunt fraction % (Q_p/Q_s) = total PCI pulmonary artery volume flow (mL)/total PCI ascending aortic volume flow (mL)) Alternatively, by using the ratios of the right ventricular to left ventricular stroke volumes, acquired by use of volumetric cine MRI, the shunt fraction can be calculated—provided there is again no significant simultaneous valvular regurgitation.

5. A 17-year-old girl is found to have bicuspid aortic valve by echocardiography. What imaging modality, among those listed below, would be best suited to assess for a common associated cardiovascular anomaly with this condition?

A. CT.
B. Chest X-ray.
C. PET.
D. MRI.

Answer D: Patients with bicuspid aortic valve often have other congenital aortic and cardiac abnormalities [52]. The most common association is with coarctation of the aorta, which in autopsy series has been reported to be found in 6% of cases. Alternatively, 30–40% of patients with coarctation are subsequently found to have a bicuspid aortic valve. MRI not only is an excellent modality for assessing the aortic valve morphology and function, but also provides excellent spatial resolution and a large field of view (see Fig. 7.7) to evaluate noncardiac thoracic anatomy. While CT also is a versatile modality with excellent spatial resolution and broad field-of-view, the radiation exposure in this young patient is less than desirable. Chest X-ray is an indirect method of assessing for additional complications associated with coarctation such as notching noted along the ribs. PET has no significant role in imaging coarctation.

References

1. Finn JP, Nael K, Deshpande V, Ratib O, Laub G. Cardiac MR imaging: state of the technology. Radiology. 2006;241:338–54.
2. Hillenbrand HB, Lima JA, Bluemke DA, Beache GM, McVeigh ER. Assessment of myocardial systolic function by tagged magnetic resonance imaging. J Cardiovasc Magn Reson. 2000;2:57–66.
3. Bollache E, Redheuil A, Clément-Guinaudeau S, Defrance C, Perdrix L, Ladouceur M, Lefort M, De Cesare A, Herment A, Diebold B, Mousseaux E, Kachenoura N. Automated left ven-

tricular diastolic function evaluation from phase –contrast magnetic resonance and comparison with Doppler echocardiography. J Cardiovasc Magn Reson. 2010;12:63.
4. Malaty AN, Shah DJ, Abdelkarim AR, Nagueh SF. Relation of replacement fibrosis to left ventricular diastolic function in patients with dilated cardiomyopathy. J Am Soc Echocardiogr. 2011;24:333–8.
5. Karaahmet T, Tigen K, Dundar C, et al. The effect of cardiac fibrosis on left ventricular remodeling, diastolic function, and N-terminal pro-B-type naturetic peptide levels in patients with non-ischemic dilated cardiomyopathy. Echocardiography. 2010;27:954–60.
6. Codreanu I, Robson MD, Golding SJ, et al. Longitudinally and circumferentially directed movements of the left ventricle studied by cardiovascular magnetic resonance phase contrast velocity mapping. J Cardiovasc Magn Reson. 2010;12:48.
7. MacMillan RM, Rees MR, Eldredge WJ, Maranhao V, Clark DL. Quantitation of Shunting at the atrial level using rapid acquisition computed tomography with comparison with cardiac catherization. J Am Coll Cardiol. 1986;7:946–8.
8. Rajiah P, Kanne JP. Computed tomography of septal defects. J Cardiovasc Comput Tomogr. 2010;4:231–45.
9. Garrett JS, Jaschke W, Botvinick EH, Higgins CB, Lipton MJ. Quantitation of intracardiac shunts by cine CT. J Comput Assist Tomogr. 1988;12:82–7.
10. Diethelm L, Dery R, Lipton MJ, Higgins CB. Atrial-level shunts: sensitivity and specificity of MR in diagnosis. Radiology. 1987;162:181–6.
11. Holmvang G, Palacios IF, Vlahakes GJ, et al. Imaging and sizing of atrial septal defects by magnetic resonance. Circulation. 1995;92:3473–80.
12. Hundley WG, Li HF, Lange RA, et al. Assessment of left-to-right intracardiac shunting by velocity-encoded, phase-difference magnetic resonance imaging: a comparison with oximetric and indicator dilution techniques. Circulation. 1995;91:2955–60.
13. Anderson RH, Lenox CC, Zuberbuhler JR. The morphology of ventricular septal defects. Perspect Pediatr Pathol. 1984;8:235–68.
14. Williamson EE, Kirsch J, Araoz PA, Edmister WB, Borgeson DD, Glockner JF, Breen JF. ECG- gated cardiac CT angiography using 64-MDCT for detection of patent foramen ovale. AJR Am J Roentgenol. 2008;190:929–33.
15. Didier D, Higgins CB. Identification and localization of ventricular septal defect by gated magnetic resonance imaging. Am J Cardiol. 1986;57:1363–8.
16. Higgins CB. Radiography of congenital heart disease. In: Higgins CB, editor. Essentials of cardiac radiology and imaging. Philadelphia: Lippincott; 1992. p. 49–90.
17. Ferrari VA, Scott CH, Holland GA, Axel L, Sutton MS. Ultrafast three-dimensional contrast-enhanced magnetic resonance angiography and imaging in the diagnosis of partial anomalous pulmonary venous drainage. J Am Coll Cardiol. 2001;37:1120–8.
18. Rathi VK, Doyle M, Yamrozik J, Williams RB, Caruppannan K, Truman C, Vido D, Biederman RW. Routine evaluation of left ventricular diastolic function by cardiovascular magnetic resonance: a practical approach. J Cardiovasc Magn Reson. 2008;8:36.
19. Rathi VK, Biederman RW. Expanding role of cardiovascular magnetic resonance in left and right ventricular diastolic function. Heart Fail Clin. 2009;5:421–35.
20. Boogers MJ, van Werkhoven JM, Schuijf JD, Delgado V, El-Naggar HM, Boersma E, Nucifora G, van der Geest RJ, Paelinck BP, Kroft LJ, Reiber JH, de Roos A, Bax JJ, Lamb HJ. Feasibility of diastolic function assessment with cardiac CT feasibility study in comparison with tissue Doppler imaging. JACC Cardiovasc Imaging. 2011;3:246–56.
21. Nakahara T, Jinzaki M, Fukuda N, Takahashi Y, Ishihara T, Takada A, Suzuki K, Manita M, Imanari T, Kanesawa N, Kuribayashi N, Kuribayashi M. Estimation of the left ventricular diastolic function with cardiac MDCT: correlation of the slope of the time-enhancement-curve with the mitral annulus diastolic velocity. Eur J Radiol. 2011;81(2):234–8 [Epub ahead of print].
22. Bolen MA, Popovic ZB, Rajiah P, Gabriel RS, Zurick AO, Lieber ML, Flamm SD. Cardiac MR assessment of aortic regurgitation: holodiastolic flow reversal in the descending aorta helps stratify severity. Radiology. 2011;260(1):98–104 [Epub ahead of print].

23. Ambler G, Omar RZ, Royston P, Kinsman R, Keogh BE, Taylor KM. Generic, simple risk stratification model for heart valve surgery. Circulation. 2005;112:224–31.
24. Bonow RO, Carabello BA, Kanu C, de Leon AC Jr, Faxon DP, Freed MD et al. American College of Cardiology/American Heart Association Task Force on Practice Guidelines. ACC/AHA guidelines for the management of patients with valvular heart disease: a report of the American College of Cardiology/American Heart Association Task Force on Practice Guidelines. Circulation.2006;114:e84–231
25. Leon MB, Smith CR, Mack M, Miller DC, Moses JW, Svensson LG, Tuzcu EM, et al. Transcatheter aortic-valve implantation for aortic stenosis in patients who cannot undergo surgery. N Engl J Med. 2010;363:1597–607.
26. Kondo C, Caputo GR, Semelka R, Foster E, Shimakawa A, Higgins CB. Right and left ventricular stroke volume measurements with velocity encoded cine MR imaging: in vitro and in vivo validation. Am J Roentgenol. 1991;157:9–16.
27. Hoeper MM, Tongers J, Leppert A, Baus S, Maier R, Lotz J. Evaluation of right ventricular performance with a right ventricular ejection fraction thermodilution catheter and magnetic resonance imaging in patients with pulmonary hypertension. Chest. 2001;120:502–7.
28. Kwon D, Desai M. Cardiac magnetic resonance in hypertrophic cardiomyopathy: current state of the art. Expert Rev Cardiovasc Ther. 2010;8:103–11.
29. Proctor RD, Shambrook JS, McParland P, Peebles CR, Brown IW, Harden SP. Imaging hypertrophic heart diseases with cardiovascular MR. Clin Radiol. 2011;66:176–86.
30. Cheong BY, Muthupillai R, Nemeth M, Lambert B, Dees D, Huber S, Castriotta R, Flamm SD. The utility of delayed-enhancement magnetic resonance imaging for identifying nonischemic myocardial fibrosis in asymptomatic patients with biopsy-proven systemic sarcoidosis. Sarcoidosis Vasc Diffuse Lung Dis. 2009;26:39–46.
31. Syed IS, Glockner JF, Feng D, Araoz PA, Martinez MW, Edwards WD, Gertz MA, Dispenzieri A, Oh JK, Bellavia D, Tajik AJ, Grogan M. Role of cardiac magnetic resonance imaging in the detection of cardiac amyloidosis. JACC Cardiovasc Imaging. 2010;3:155–64.
32. Austin BA, Tang WH, Rodriguez ER, Tan C, Flamm SD, Taylor DO, Starling RC, Desai MY. Delayed hyper-enhancement magnetic resonance imaging provides incremental diagnostic and prognostic utility in suspected cardiac amyloidosis. JACC Cardiovasc Imaging. 2009;2:1369–77.
33. Desai MY, Lima JA, Bluemke DA. Cardiovascular magnetic resonance imaging: current applications and future directions. Methods Enzymol. 2004;386:122–48.
34. Cheong B, Huber S, Muthupillai R, Flamm SD. Evaluation of myocardial iron overload by T2* cardiovascular magnetic resonance imaging. Tex Heart Inst J. 2005;32:448–9.
35. Vural M, Ucar O, Selvi NA, Pasaoglu L, Gurbuz MO, Cicekcioglu H, Aydogdu S, Koparal S. Assessment of global left ventricular systolic function with multidetector CT and 2D echocardiography: a comparison between reconstructions of 1-mm and 2-mm slice thickness at multidetector CT. Diagn Interv Radiol. 2010;16:236–40.
36. Ko SM, Kim YJ, Park JH, Choi NM. Assessment of left ventricular ejection fraction and regional wall motion with 64-slice multidetector CT: a comparison with two-dimensional transthoracic echocardiography. Br J Radiol. 2010;83:28–34.
37. Lotz J, Meier C, Leppert A, Galanski M. Cardiovascular flow measurement with phase-contrast MR imaging: basic facts and implementation. Radiographics. 2002;22:651–71.
38. Campbell M. Natural history of coarctation of the aorta. Br Heart J. 1970;32:633–40.
39. Achenbach S. Computed Tomography Coronary Angiography. J Am Coll Cardiol. 2006;48:1919–28.
40. Chow BJ, Kass M, Gagne O, Chen L, Yam Y, Dick A, Wells GA. Can differences in corrected coronary opacification measured with computed tomography predict resting coronary artery flow. J Am Coll Cardiol. 2011;57:1280–8.
41. Yamashita M, Lee S, Hamasaki S, Nishimoto T, Kajiya T, Toyonaga K, Arima R, Toda H, Ohba I, Otsuji Y, Tei C. Noninvasive evaluation of coronary reperfusion by CT angiography in patients with STEMI. JACC Cardiovasc Imaging. 2011;4:141–9.
42. Ho KT, Chua KC, Klotz E, Panknin C. Stress and rest myocardial perfusion imaging by evaluation of complete time-attenuation curves with dual-source CT. JACC Cardiovasc Imaging. 2010;3:811–20.

43. Blankstein R, Jerosch-Herold M. Stress myocardial perfusion imaging by computed tomography: a dynamic road is ahead. JACC Cardiovasc Imaging. 2010;3:821–3.
44. Tamarappoo BK, Dey D, Nakazato R, Shmilovich H, Smith T, Cheng VY, Thomson LE, Hayes SW, Friedman JD, Germano G, Slomka PJ, Berman DS. Comparison of the extent and severity of myocardial perfusion defects by CT angiography and SPECT myocardial perfusion imaging. JACC Cardiovasc Imaging. 2010;3:1010–9.
45. Kim WY, Danias PG, Stuber M, Flamm SD, Plein S, Nagel E, et al. Coronary magnetic resonance angiography for the detection of coronary stenoses. N Engl J Med. 2001;345:1863–9.
46. Chen Z, Duan Q, Xue X, Chen L, Ye W, Jin L, Sun B. Noninvasive detection of coronary artery stenoses with contrast-enhanced whole-heart coronary magnetic resonance angiography at 3.0 T. Cardiology. 2010;117:284–90.
47. Lockie T, Ishida M, Perera D, Chiribiri A, De Silva K, Kozerke S, Marber M. Nagel, Rezavi R, Redwood S, Plein S. High-resolution magnetic resonance myocardial perfusion imaging at 3.0-Tesla to detect hemodynamically significant coronary artery stenoses as determined by fractional flow reserve. J Am Coll Cardiol. 2011;57:70–5.
48. Weber OM, Martin AJ, Higgins CB. Whole-heart steady-state free precession coronary artery magnetic resonance angiography. Magn Reson Med. 2003;50:1223–8.
49. Mymin D, Sharma GP. Total and effective coronary blood flow in coronary and noncoronary heart disease. J Clin Invest. 1974;52:363–73.
50. Weber OM, Martin AJ, Higgins CB. Whole-heart steady-state free precession coronary artery magnetic resonance angiography. Magn Reson Med. 2003;50:1223–8.
51. Steffens JC, Bourne MW, Sakuma H, O'Sullivan M, Higgins CB. Quantification of collateral blood flow in coarctation of the aorta by velocity encoded cine magnetic resonance imaging. Circulation. 1994;90:937–43.
52. Therrien J, Webb GD. Congenital heart disease in adults. In: Braunwald E, editor. Heart disease: a textbook of cardiovascular medicine. 6th ed. Philadelphia, Pa: Saunders; 2001. p. 1592–621.

Chapter 8
Cardiac Catheterization: Right and Left Heart Catheterization

Praneet Kumar and Michael D. Faulx

Introduction

Catheterization remains the gold standard for cardiovascular hemodynamic assessment because it provides direct, "real time" hemodynamic information. Catheterization plays a major role in the diagnosis and management of conditions such as valvular heart disease, complex congenital heart disease, acutely decompensated heart failure, shock, and pulmonary hypertension.

Cardiac catheterization is widely available and in most centers these procedures are performed quite safely. However one must always respect the fact that invasive procedures are inherently risky. In most cases invasive hemodynamic assessment should be pursued only after noninvasive modalities have failed to furnish the anticipated results.

Invasive Hemodynamic Assessment: Fundamental Concepts

The goal of invasive hemodynamic assessment is to accurately reflect real cardiovascular physiology. The accuracy of the data depends on the means through which they are obtained. A basic understanding of how hemodynamic information is acquired in the laboratory is therefore essential in order to accurately interpret the data that is obtained.

P. Kumar, MD (✉) • M.D. Faulx, MD
The Cleveland Clinic, Cleveland, OH, USA
e-mail: kumarp@ccf.org; faulxm@ccf.org

A.T. Askari et al. (eds.), *Cardiovascular Hemodynamics: An Introductory Guide*, Contemporary Cardiology, DOI 10.1007/978-1-60761-195-0_8,

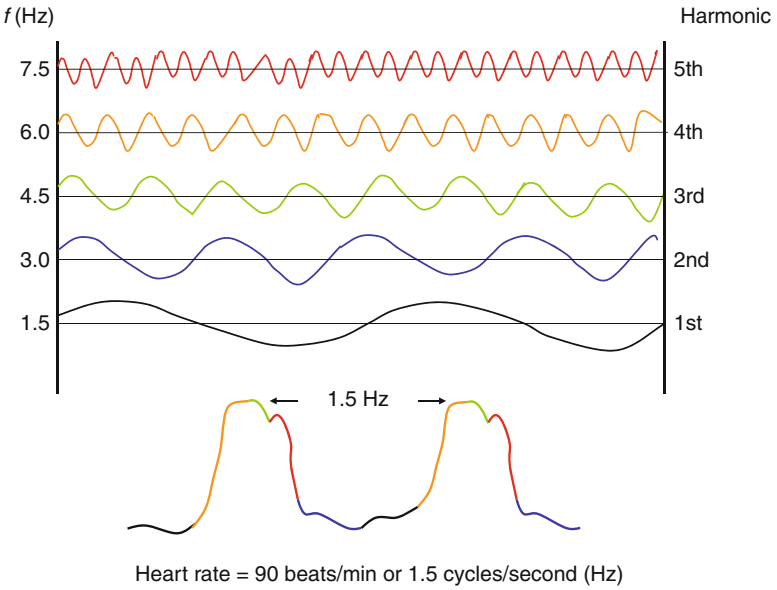

Fig. 8.1 Harmonics in cardiac hemodynamic assessment. The aortic pressure waves shown at the bottom of the image are composed of simpler sinusoidal harmonic waves. Each harmonic is a multiple of the fundamental frequency, in this case 1.5 Hz. The data contained within each harmonic contributes in some way to the reconstructed wave form, depicted in this illustration by color. Exclusion of one or more harmonics by a monitoring system can produce a distorted, inaccurate pressure tracing

Pressure Measurements

Complex pressure waves generated by the heart and great vessels are periodic, meaning that each cycle repeats itself at a fundamental frequency determined by the heart rate (expressed as cycles/s or Hertz, Hz). The French physicist Jean Baptiste Fourier (1786–1830) demonstrated that complex periodic waves can be expressed as the sum of any number of simpler sinusoidal waves, each with its own frequency and amplitude. These are referred to as *harmonics* and the frequency of each harmonic is an integral multiple of the fundamental frequency (Fig. 8.1). Fourier's theorem is important to us because the physical properties of a monitoring system must be configured to accurately reproduce pressures across a broad range of harmonic frequencies.

The challenge of constructing a practical hemodynamic monitoring system was tackled by the American physician Carl J. Wiggers (1883–1963). Wiggers employed a fluid-filled catheter system in contact with a rubber diaphragm coupled to a recording device and this design, after several refinements, is still used in monitoring devices today.

The fidelity of pressure measurements obtained by fluid-filled catheters is heavily dependent on the characteristics of the transducer membrane [5]. Flexible membranes are *sensitive* because they can accurately reflect most received amplitudes

but they do not respond well to higher frequency harmonics. Conversely rigid membranes respond to a wide range of harmonic frequencies (have better *frequency response*) but tend to be less sensitive. Recording systems used in modern clinical practice tend to have stiffer membranes in order to capture the range of harmonics expected in human physiology, sacrificing sensitivity to some degree.

Another major hindrance to accurate pressure measurement is the fact that transducer membranes resonate in response to stimulation, generating their own pressure waves at a fundamental frequency called the *natural frequency*. When the harmonic frequency of a recorded wave approaches the natural frequency of the monitoring system, the amplitudes reflected to the monitor at or near that frequency will be greatly exaggerated. The ability of a catheter system to attenuate the pressure waves produced by the transducer membrane is referred to as *damping*. An ideally damped system is one in which the ratio of input amplitude to output amplitude is maintained close to 1:1 across a broad range of frequencies. Natural frequency (and also frequency response) increases with membrane stiffness and catheter diameter and decreases with catheter length, catheter stiffness, and fluid viscosity. Damping responds in the opposite manner to these factors. Thus, catheters with high fidelity, tip-mounted transducers (Millar Instruments, Houston, TX) have excellent frequency response and are well suited for capturing high frequency pressure changes over short time intervals (i.e., measurement of left ventricular dP/dt). Longer, stiffer, fluid-filled catheters coupled to a transducer at the hub are well damped and reasonably sensitive across most of the harmonic frequencies encountered in human studies.

The basic equipment required for pressure measurement in the catheterization lab includes a fluid-filled hollow catheter, multi-port manifold, transducer membrane in contact with an electrical strain gauge, signal amplifier, and a monitor. The catheter tip is placed in the cardiac chamber of interest and connected to the transducer via a dedicated port on the manifold. Pressures at the catheter tip are transmitted through the fluid medium (saline, blood, or contrast) to the transducer membrane, which stretches and vibrates in response to the pressure it sees. The membrane is coupled to a tiny strain gauge contained within a housing unit that has been equilibrated to atmospheric pressure (referred to as *zeroing*). Movement of the piston across the wires of the strain gauge produces an electrical current that is subsequently amplified, reconfigured, and displayed on the monitor.

Hemodynamic waveforms obtained from fluid-filled catheters are subject to a variety of artifacts. Common encountered artifacts are demonstrated and extensively reviewed in Fig. 8.2a–e.

Blood Flow Measurements

Accurate measurement of cardiac output is vital not only as an index of myocardial performance but also as a component in the quantification of valvular stenoses, vascular resistances, and shunts. In clinical practice cardiac output is assessed by two methods: Fick and thermodilution.

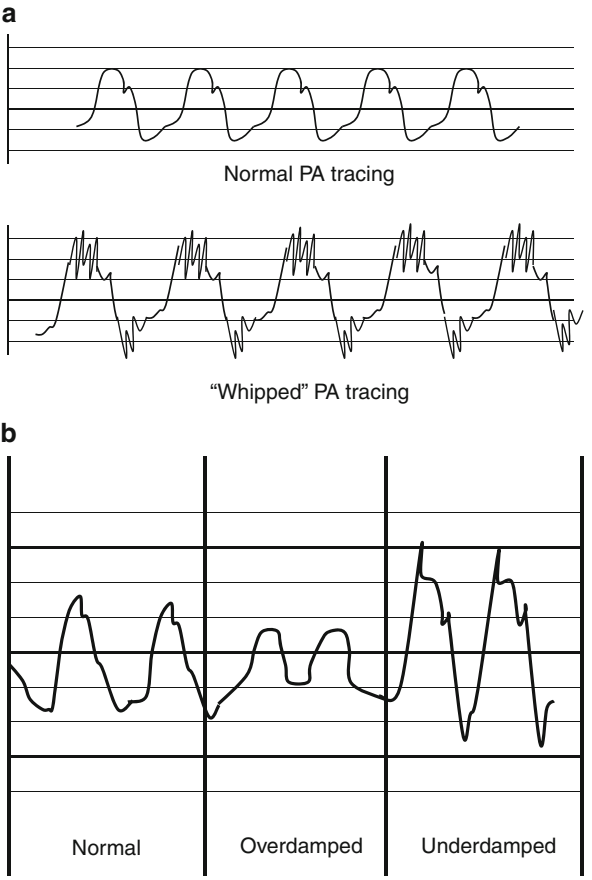

Fig. 8.2 (**a**) Catheter whip in a pulmonary artery (PA) pressure tracing. Whip occurs when the catheter tip vibrates in response to ventricular contraction or valvular motion. Whip causes high frequency distortion of the waveforms, particularly at the high and low pressure points of the complex. Since the extremes of the waveform are usually equally affected, the mean pressure data obtained from a "whipped" tracing is generally accurate. Whip can be attenuated by catheter repositioning, the use of a high frequency filter or increased damping. (**b**) Damping-related artifacts. Overdamping results in a flat, low amplitude waveform that lacks contour detail. Overdamping can be caused by catheter kinking, air bubbles, or blood in the transducer circuit and the use of long, small caliber catheters. It can be overcome by removing kinked tubing, meticulous flushing of the catheter and manifold, and use of shorter, large caliber catheters. Underdamping produces exaggerated waveforms with overestimated amplitudes. It occurs when the natural frequency of the catheter system approximates a harmonic frequency in the pressure wave. This can be offset by lowering the natural frequency of the catheter system (use a longer, smaller caliber catheter) or the patient (treat tachycardia). (**c**) Positional artifact. This is characterized by flattening of the pressure tracing with a gradual rise in pressure. It most often occurs when the catheter tip is pressed against the wall of a vessel or chamber. Gentle withdrawal and redirection of the catheter typically solves the problem. (**d**) Transducer malposition. In this example the true mean right atrial pressure is 10 mmHg. When the transducer is zeroed at a level 5 cm below the sternal angle the catheter recording is accurate. When the transducer is zeroed at a level above the chest the pressure is underestimated. When the transducer is zeroed at a level well below the right atrium the pressure is overestimated. (**e**) Respiratory variation of right atrial pressure. The thin walled right-sided

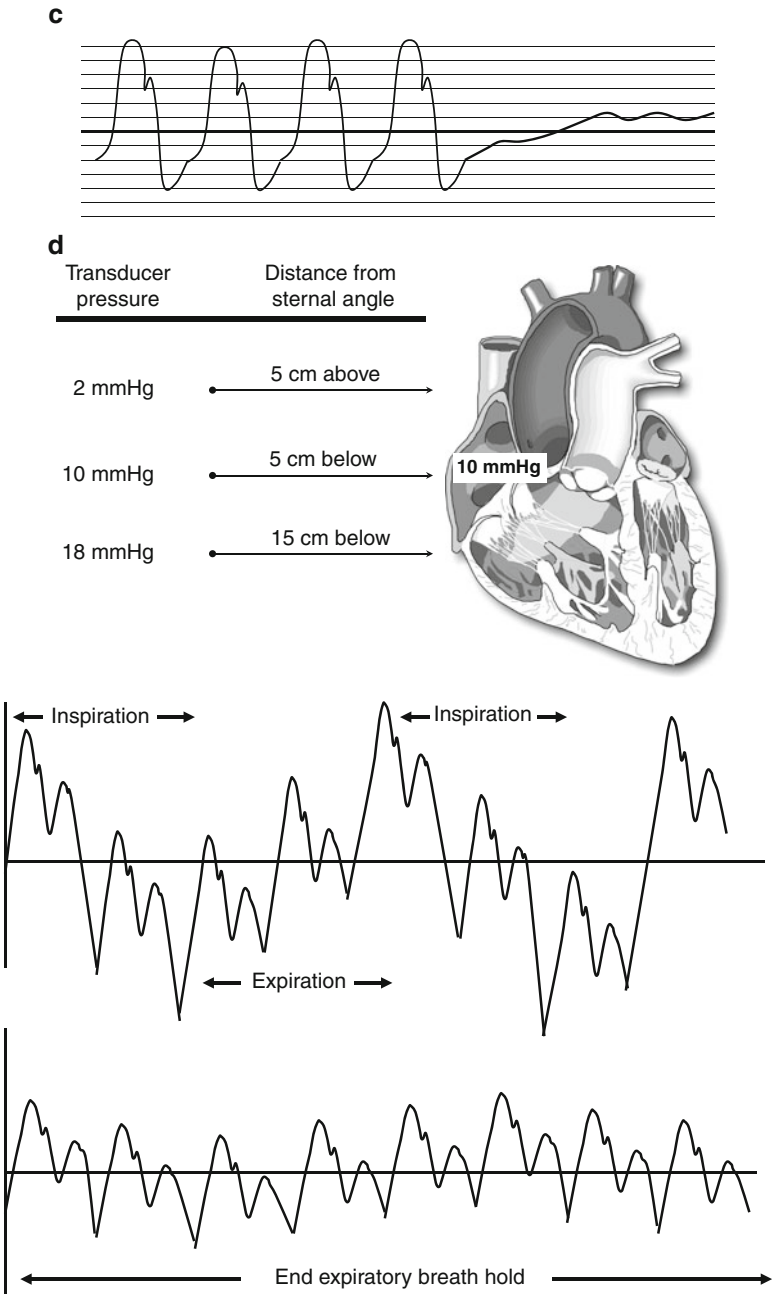

Fig. 8.2 (continued) chambers are subject to respiratory variation, particularly in subjects with underlying obstructive lung disease. Pressure measurements taken during a few seconds of breath holding at the end of normal expiration (when intrathoracic pressure is theoretically zero) are much less variable

Oxygen Extraction and Utilization: The Fick Method

The German physiologist Adolph Fick (1829–1901) theorized that the utilization of any substance by an organ can be expressed as the product of the blood flow to the organ and the difference between the arterial and venous concentrations of the substance. When this principle is applied to the lungs, oxygen uptake (VO_2) would be equal to pulmonary blood flow *x* the difference between pulmonary arterial ($A[O_2]$) and venous ($V[O_2]$) oxygen content. Assuming that there is no pulmonary-systemic shunt and that flow through the pulmonary and systemic circuits are equal, the Fick equation can provide a measure of cardiac output (CO):

Fick equation

$$CO(L/min) = \frac{VO_2(mL/min)}{A[O_2]\text{-}V[O_2](mL/L)}$$

Oxygen consumption for an individual patient can be directly measured by devices that employ a closed rebreathing circuit with a CO_2 detector. However this approach is expensive and technically cumbersome and many laboratories assume a resting VO_2 of 1.25 mL/min/m^2. The reader should be aware that assumed VO_2 values are based on studies of basal metabolic activity in predominantly young subjects. Measured VO_2 can significantly vary from baseline in subjects with underlying cardiopulmonary disease, so the use of assumed oxygen consumption values can introduce significant error in the calculation of cardiac output.

Hemoglobin binds approximately 1.36 mL of elemental oxygen per gram and oxygen bound to the hemoglobin molecule accounts for over 98% of the total oxygen content of human blood. Oxygen dissolved in plasma accounts for the rest and is represented by the product of oxygen solubility in plasma (0.003 mL/dL/mmHg) and the partial pressure of oxygen in plasma, PaO_2. The oxygen content of blood is represented by the following equation:

$$Cb[O_2] = \{[\text{hemoglobin}] \times 1.36 \times SaO_2 \times 10\} + 0.003 \times PaO_2 \times 10.$$

SaO_2 is the percent oxyhemoglobin as detected by oximetry. For the sake of simplicity the content of dissolved O_2 is often omitted from this calculation, but the reader should be aware that under certain circumstances (i.e., high FiO_2 with positive pressure ventilation) the amount of dissolved oxygen in blood can become clinically relevant.

The Fick method is generally the most accurate method of cardiac output measurement but error can be introduced at several levels. The Fick method relies on several key assumptions such as the absence of an intracardiac shunt and the notion that oxygen consumption and cardiac output are constant during measurement. In critically ill patients with pulmonary disease, oxygen consumption can be overestimated since the delivery of oxygen from the lungs to the blood is not uniform. The Fick equation also requires several measurements, each with its own degree of measurement error. The use of an assumed value for oxygen consumption, as mentioned previously, is common and a major potential source of error.

Indicator Dilution over Time: The Thermodilution Technique

Thermodilution measures the rate of change of blood temperature over time. By injecting a fixed volume (10 mL) of chilled or room air temperature injectate (5% dextrose or 0.9% saline) into the right atrial port of the catheter and continuously measuring temperature with a thermistor located at the catheter tip, we can estimate the rate of flow from the right atrium to the catheter tip. Thermodilution calculations are mathematically complex as they account for factors such as the expected degree of catheter warming during injection and the specific heat and gravities of blood and the injectate. Numerical cardiac outputs are provided by computerized analysis of temperature versus time curves and the final cardiac output is typically reported as an average of several injections.

Thermodilution correlates reasonably well with other measures of cardiac output, but there are several contributors to measurement error. Pulmonary artery temperature can vary with respiration so injection during the same portion of the respiratory cycle (i.e., end expiration) each time reduces the potential for error. Shorter injection periods (<3 s) are preferable to longer ones for similar reasons and the injection periods should be as uniform as possible. Smaller injectate volumes with warmer injectate temperatures (i.e., 5 mL injected at room temperature) produce more measurement error that colder, larger volume injections because the signal-to-noise ratio is lower. Thermodilution is not reliable in the presence of significant tricuspid regurgitation or in low output states because the injectate tends to cycle between the right atrium and right ventricle, resulting in a flattened temperature-time curve.

Catheterization Risk

Proper informed consent should be obtained from the patient or a designated medical decision maker prior to cardiac catheterization. The major risks related to right and left cardiac catheterization appear in Table 8.1. Decompensated heart failure, shock, acute coronary syndromes, left ventricular dysfunction, morbid obesity, depressed mental status, and advanced kidney disease are all associated with increased procedural risk. The risk for stroke increases significantly with cannulation of the left ventricle. Although debilitating strokes are rare the incidence of small, clinically silent strokes assessed by MRI was found to be 22% in one series of patients with severe aortic stenosis who underwent left ventricular cannulation [2]. For this reason routine left ventricular catheterization should be avoided in favor of a selective approach, reserving left ventricular cannulation for patients with nondiagnostic or conflicting noninvasive test results.

The most common catheterization complications are related to problems with the vascular access site or subsequent hemostasis. When feasible ultrasound or radiographic guidance should be employed to localize landmarks and guide cannulation of large arteries and veins. Morbid obesity is a common contributor to access-related

Table 8.1 Complications associated with diagnostic left- and right-heart catheterization (adapted from Noto et al. [7])

Complication (% risk)	Contributing factors	Prevention
Death (0.11%)	High acuity of illness	Reassess necessity of the procedure
	Emergency procedure	Have ACLS equipment on stand by
Myocardial Infarction (0.05%)	Acute coronary syndromes	Appropriate medical therapy for ACS
	Profound hypertension	Medical management of hypertension
	Profound tachycardia	Medical management of tachycardia
Stroke (0.07%)	Cannulation of left ventricle	Avoid crossing aortic valve unless absolutely necessary
	Atrial fibrillation	Over-the-wire catheter exchanges
	Ascending aortic atheroma	
Vascular access complications (0.43%)	Anticoagulation	Correction of coagulopathy
	Morbid obesity	Imaging-guided vascular cannulation
Major hematomas Retroperitoneal bleeds Arteriovenous fistulas	Agitation	Appropriate conscious sedation
Major arrhythmias (0.38%)	Electrolyte disturbances	Correct metabolic derangements
Ventricular fibrillation		Supplement oxygen
	Hypoxemia	Cautious injection of right coronary
Ventricular tachycardia Complete heart block	Right coronary conus branch injection	Use pig tail catheter in left ventricle
	Catheter-induced endocardial trauma	
	Underlying bundle branch blocks	
Other embolic events (rare)	Preexisting deep vein thrombosis	Exclude thromboses prior to study
Pulmonary embolism/ infarction	Prolonged immobility	Limit duration of PA catheterization Perform over-the-wire catheter exchanges
Distal atheroembolism	Aortic atheromatous disease	
Contrast nephropathy (variable)	Preexisting kidney disease	Adequate hydration
	Dehydration	Use of *N*-acetylcysteine
	Large contrast volume	Minimize use of contrast
Serious allergic reactions Contrast agents (0.37%)	Preexisting allergies	Pretreatment with corticosteroids and antihistamines
Local anesthetic (rare)		Use of amide anesthetics
Respiratory arrest (variable)	Underlying pulmonary disease	Limit the use of sedatives
		Optimize heart failure and lung disease prior to the study
		Frequent airway assessment
	Decompensated heart failure	Anesthesiology consultation
	Morbid obesity	
Other vascular complications	Balloon inflation in small arteriole	Never inflate the balloon in the distal pulmonary arterial tree
Pulmonary artery perforation (rare)	Catheter trauma	Cautious catheter withdrawal
Coronary artery dissection (rare)		

ACLS advanced cardiac life support; *ACS* acute coronary syndrome; *PA* pulmonary artery

complications, particularly when femoral access is attempted. In extremely obese patients arterial access may be more safely obtained from the radial or brachial approach, and venous access may be more safely obtained with ultrasound-guided cannulation of the internal jugular vein.

Right Heart Catheterization Technique

Right heart catheterization is generally performed using a 7- or 8-French vascular sheath placed in the common femoral vein or right internal jugular vein using modified Seldinger technique. A balloon tipped pulmonary artery catheter is inserted through the sheath and the balloon is inflated once the tip of the catheter has cleared the sheath. The catheter tip, guided by flow and the manipulation of the operator, traverses the heart from the great veins to the pulmonary artery and the pulmonary artery wedge position [3]. The catheter is then connected to the pressure transducer via a multi-port manifold. Blood can also be withdrawn from the catheter for oximetry and chemistry sampling. There is a proximal lumen at the level of the right atrium to allow for thermodilution assessment of cardiac output. Rarely, situations arise where direct measurement of left atrial pressure is desirable, such as in the evaluation of severe native or prosthetic mitral stenosis. Left atrial cannulation can be performed from the right atrium by fluoroscopy-guided needle puncture of the interatrial septum at the level of the fossa ovalis and the use of a Brockenbrough catheter.

Left Heart Catheterization Technique

Left heart catheterization is performed by placing a 4-, 5-, or 6-French sheath into a large artery using modified Seldinger technique [6]. Access is typically obtained in the right or left common femoral artery but radial and brachial approaches are also used. Once vascular access is obtained the arterial catheters are advanced retrogradely through the aorta preceded by a J-tipped flexible guidewire. The catheters are controlled by the operator, and there are numerous specialized catheters available for use. Endhole catheters are useful for pressure measurements and contrast injection during coronary angiography. They are not ideal for opacification of the aorta or left ventricle because they promote contrast streaming and ventricular ectopy. Multi-hole pigtail catheters record pressure and are better for the opacification of large structures because they uniformly distribute a larger volume of pressured contrast within a chamber. Aortography and ventriculography should be performed using a pig tail catheter. Some pig tail catheters have proximal and distal transducer ports to allow for simultaneous pressure measurements across a given structure such as the aortic valve.

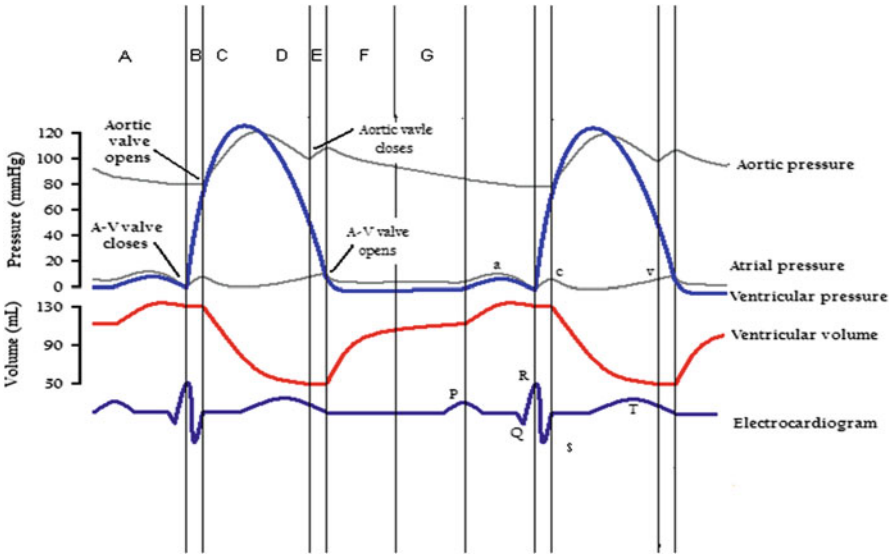

Fig. 8.3 Wiggers' diagram with schematic representation of the major electrical and mechanical events during the cardiac cycle: *A* atrial contraction; *B* isovolumic contraction; *C* rapid ejection; *D* reduced ejection; *E* isovolumic relaxation; *F* rapid ventricular filling; *G* reduced ventricular filling

Data Derived from Right and Left Heart Catheterization

Pressure Measurements

When intracardiac pressure measurements are gated to the surface electrocardiogram one can accurately assess the systolic and diastolic performance of the heart (Fig. 8.3). Pressure measurements are obtained by advancing the catheter to the chamber of interest and recording wave forms over several cardiac cycles. Right sided pressures can vary greatly with respiration in some patients (see Fig. 8.2e), making interpretation difficult. In this case one can ask the patient to perform several seconds of an end-expiratory breath hold to maintain thoracic pressure at its theoretical "zero point" for a few cardiac cycles. Normal cardiovascular waveforms and their descriptions follow.

Right Atrial Pressure

The normal right atrial pressure wave includes the "a" wave, produced by atrial contraction and the corresponding "x" descent during atrial relaxation. Early in the "x" descent there may be a small positive reflection called the "c" wave which represents closure of the tricuspid valve. The second major wave in the right atrial tracing is the "v" wave, produced by the combination of vena cava flow into the

atrium and the upward displacement of the closed tricuspid valve during right ventricular contraction. Once the tricuspid valve opens the right atrial pressure drops in early diastole, producing the "y" descent. Normal mean right atrial pressure is between 1 and 10 mmHg (Fig. 8.4a).

Right Ventricular Pressure

The normal right ventricular wave is characterized by a rapid pressure rise during systole followed by a rapid fall during isovolumic relaxation. Diastolic pressure gradually increases until late diastole when the right atrium contracts and right

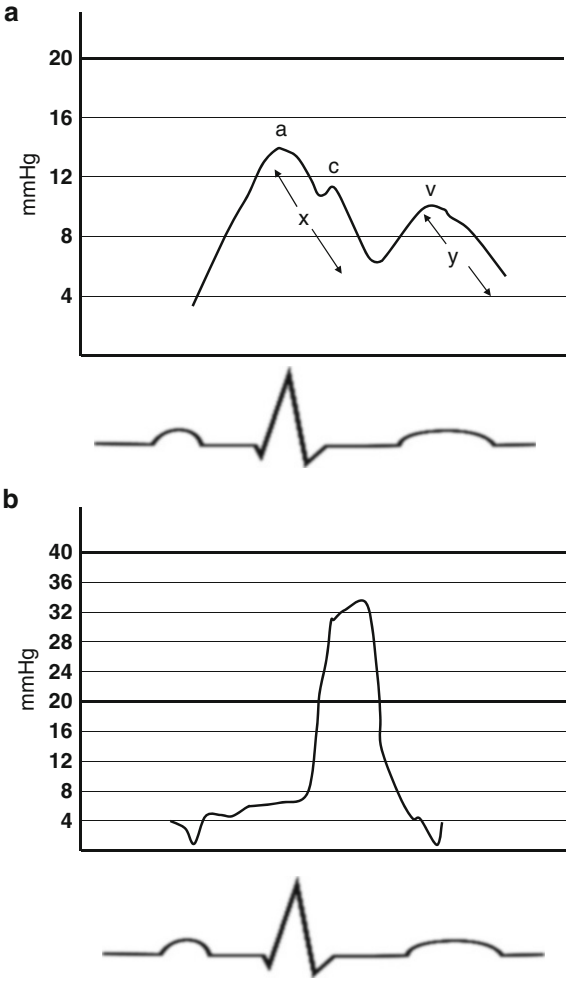

Fig. 8.4 (**a**–**f**) Normal cardiac pressure tracings. Descriptions of each tracing are found within the chapter text (From Wikimedia Commons. Original creator Destiny Qx, revised by Daniel Chang MD)

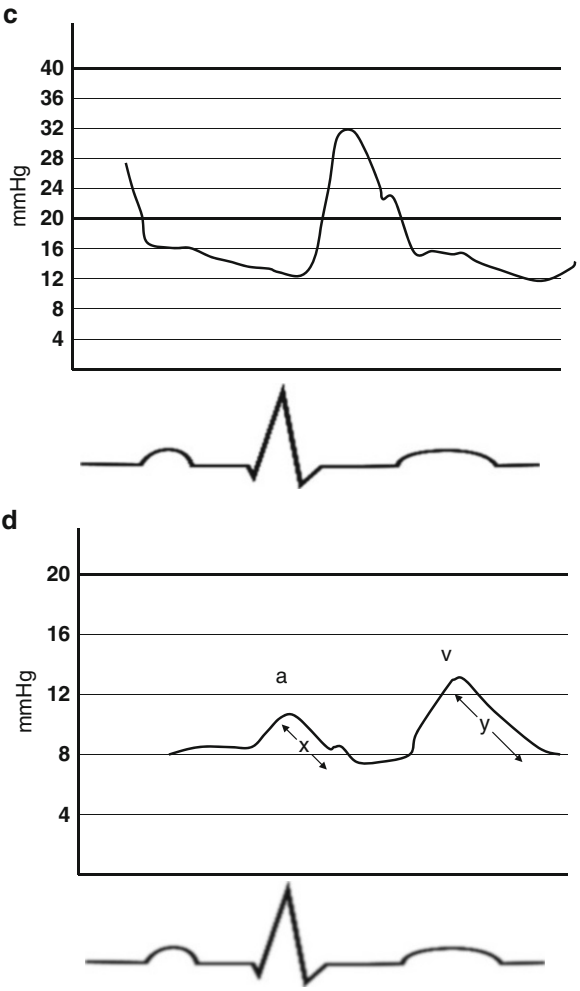

Fig. 8.4 (continued)

ventricular end diastolic pressure rises to the level of the atrial "a" wave. Normal right ventricular systolic and diastolic pressure is 15–30 and 1–10 mmHg, respectively (Fig. 8.4b).

Pulmonary Artery Pressure

The normal pulmonary artery pressure tracing is a typical arterial waveform with a rapid systolic upstroke. There is a dicrotic notch produced by closure of the pulmonic valve and the diastolic pressure gradually decreases as blood flows from the main pulmonary artery to the lungs. Normal pulmonary artery systolic and diastolic

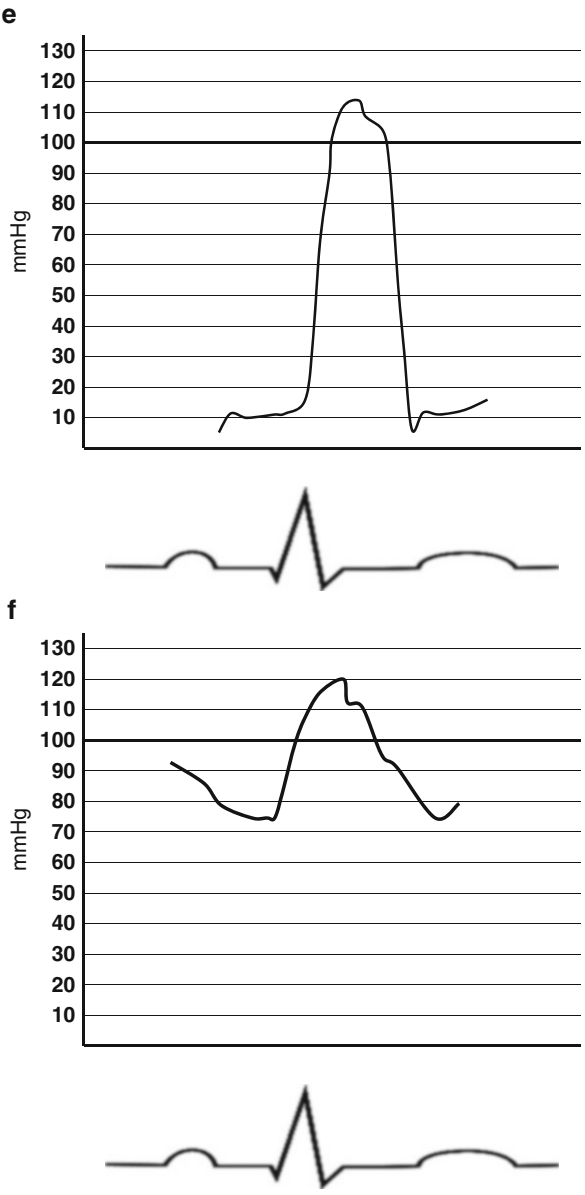

Fig. 8.4 (continued)

pressure is 15–30 and 5–10 mmHg, respectively. In intensive care settings it is common practice to follow the PA end diastolic pressure as an indirect measure of left atrial pressure. However this assumption is only true if the pulmonary vascular resistance is close to normal (Fig. 8.4c).

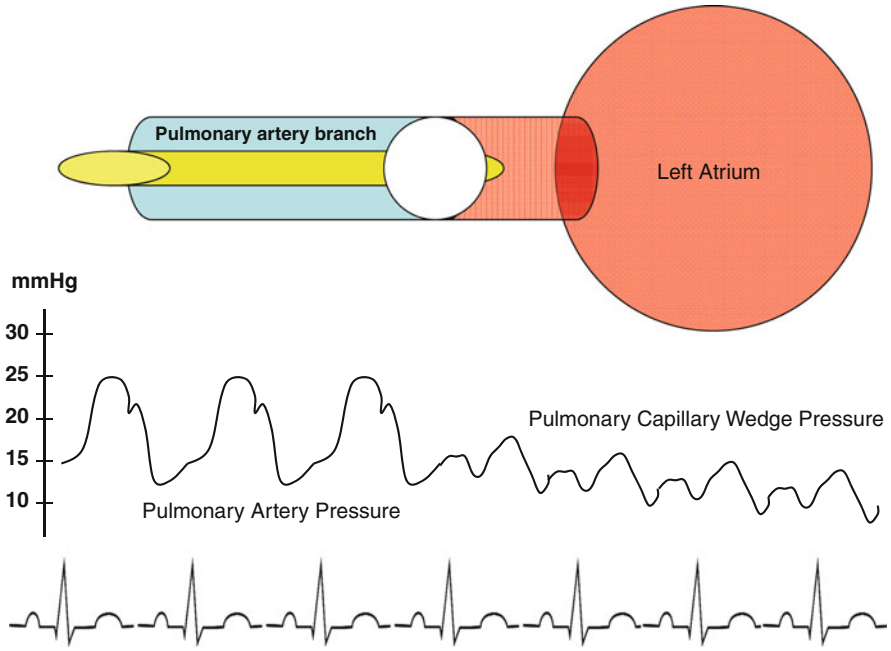

Fig. 8.5 Diagram of the pulmonary capillary wedge technique. With the balloon inflated the catheter traverses the pulmonary artery until it becomes wedged into a distal branch. The catheter tip then "sees" only left atrial pressure that is reflected back to it through the pulmonary capillary bed. The result is a clear change in the pressure tracing from an arterial waveform to a central venous waveform

Pulmonary Capillary Wedge Pressure, PCWP

The PCWP is commonly used as a surrogate for left atrial pressure. This pressure is obtained by cautiously advancing the catheter tip through the pulmonary artery with the balloon inflated until the balloon will no longer advance and appears fixed or "wedged" in the pulmonary bed by fluoroscopy. Inflating the balloon with the catheter tip in the distal pulmonary arterial tree increases the risk for pulmonary artery rupture. The PCWP reflects left atrial pressure because when the balloon is properly wedged there is no longer flow from the proximal PA to the catheter tip. The catheter tip only "sees" the left atrial pressure waves that are reflected back to it through the pulmonary artery capillary bed (Fig. 8.5).

The normal PCWP is analogous to left atrial pressure, with "a" and "v" waves that correspond to left atrial contraction and left ventricular contraction, respectively and their corresponding "x" and "y" descents (Fig. 8.4d). It is important to know that left atrial activity precedes the reflected wedge pressure by a few milliseconds. This causes the PCWP "v" wave to appear later than the left atrial "v" wave. When the PCWP and left ventricular pressures are superimposed during assessment for mitral stenosis, the result may be overestimation of the transmitral

pressure gradient. Normal mean PCWP pressure is between 5 and 12 mmHg and in the absence of mitral stenosis it approximates left ventricular end diastolic pressure.

Left Ventricular Pressure

Left ventricular pressure has a rapid upstroke during early systole followed by a rapid descent. Diastolic pressure is low in early diastole and rises slowly until the left atrium contracts. The left ventricular end diastolic pressure (LVEDP) represents the true preload for the left ventricle and it is typically measured just prior to the abrupt rise in systolic pressure. Normal LVEDP is 5–12 mmHg (Fig. 8.4e).

Aortic Pressure and Waveform

Aortic pressure is measured with the catheter tip in the proximal aorta. Central aortic pressures are usually 10–20 mmHg lower than femoral artery pressures due to the greater size and elasticity of the normal aorta. In a normal, high fidelity system, the aortic waveform is characterized by a dicrotic notch which occurs at the closure of aortic valve (Fig. 8.4f).

Cardiac Output

The Fick method requires sampling of blood from both sides of the pulmonary vascular bed, namely the pulmonary artery and pulmonary veins or left atrium. Pulmonary artery blood is obtained via aspiration from the distal port of the right heart catheter. Direct sampling from the left atrium requires transseptal puncture which is impractical for routine diagnostic testing. For this reason an arterial blood sample (i.e., from the femoral artery sheath) is typically used as a substitute. The thermodilution technique has been previously described.

Normal cardiac output is between 5.0 and 7.5 L/min but varies broadly with patient size and gender (men generally have higher cardiac outputs than women). The human heart can augment its cardiac output over fivefold in certain disease states (i.e., severe anemia, thyrotoxicosis). The cardiac index (cardiac output divided by body surface area, BSA) is a better measure of myocardial performance than cardiac output. The normal range for cardiac index is 2.5–4.0 L/min/m^2. A cardiac index <1.0 L/min/m^2 is not compatible with life.

Vascular Resistance

In a fluid-filled system resistance (R) is proportional to the pressure difference across the system (ΔP) and inversely proportional to flow (Q); $R = \Delta P/Q$.

By measuring mean aortic pressure (AoP) and mean right atrial pressure (RAP) we can calculate systemic vascular resistance (SVR) in the following manner:

Systemic vascular resistance

$$\text{SVR} = \frac{(\text{mean AoP} - \text{mean RAP})}{\text{Cardiac output}}$$

Similarly, by measuring mean pulmonary artery pressure (PAP) and left atrial pressure (LAP), either directly or with its surrogate (wedge pressure) we can calculate pulmonary vascular resistance (PVR):

Pulmonary vascular resistance

$$\text{PVR} = \frac{(\text{mean PAP} - \text{mean LAP or PCWP})}{\text{Cardiac output}}$$

Vascular resistances can be expressed in Wood units (mmHg/L/min) or dynes×s/cm^{-5}. A dyne is the amount of force required to accelerate a 1 g mass by 1 cm/s^2. 1 Wood unit = 80 dyn×s/cm^{-5}. Normal systemic vascular resistance is between 8 and 20 Wood units. Normal pulmonary vascular resistance is between 0.25 and 1.6 Wood units.

Shunt Assessment

Shunt flow from the systemic circulation to the pulmonary circulation can be localized and quantified during right heart catheterization by performing an oximetry saturation run. As the catheter is passed through the great veins to the pulmonary artery small (2 mL) aliquots of blood are obtained for oximetry from the proximal and distal superior vena cava (SVC), proximal and distal inferior vena cava (IVC), right atrium (low, mid and high), right ventricle (proximal, mid and apex), pulmonary artery (main, left and right), left ventricle, and aorta distal to the ductus arteriosus [4].

A left-to-right shunt is detected by an oximetry "step-up", where oxygenated left circulation blood mixes with deoxygenated right circulation blood. A "step-up" of ≥7% is considered significant at the level of the great veins and right atrium. A step-up of ≥5% is considered significant at levels distal to the right atrium. Right-to-left shunts are difficult to locate and quantify and oximetry to detect a "step-down" is generally not performed.

The degree of left-to-right shunting can be quantified by calculating the ratio of pulmonary blood flow (Q_p; oxygen consumption divided by the difference in arteriovenous oxygen content across the lungs) to systemic blood flow (Q_s; oxygen consumption divided by the difference in arteriovenous oxygen content across the systemic circulation). Systemic mixed venous saturation (MVO_2) is defined as:

Mixed venous saturation

$$\text{MVO}_2 = \frac{[(3)\text{SVC saturation} + \text{IVC saturation}]}{4}$$

If we assume constant oxygen consumption, hemoglobin concentration, and atmospheric pressure then many of the terms in this complex calculation cancel out, leaving only the oximetry saturations:

Shunt fraction

$$Q_p / Q_s = \frac{(\text{Arterial sat}) - (\text{MVO}_2\ \text{sat})}{(\text{Arterial sat}) - (\text{pulmonary artery sat})}$$

The pulmonary venous saturation cannot be obtained without transseptal puncture or retrograde catheterization through the mitral and aortic valves. In the absence of a significant right-to-left shunt at the level of the left atrium, ventricle, or proximal aorta we would expect systemic arterial saturation and pulmonary venous saturation to be the same, thus pulmonary venous saturation is often replaced by systemic arterial saturation in this equation.

Small shunts are defined by $Q_p/Q_s < 1.5$ and are often asymptomatic. Large shunts are defined by $Q_p/Q_s > 2.0$ and often require closure. Frequently the location of the shunt is known or suspected from an alternative study such as an echocardiogram, CT scan, or MRI and catheterization is used to quantify the shunt fraction. In this case it is not necessary to sample from multiple levels in the same chamber or vessel.

Assessment of Valvular Stenosis

The invasive assessment of valvular stenosis requires measurement of the cardiac output and measurement of the pressure gradient across the valve in question. Ideally pressure measurements should be made simultaneously with two catheters, each coupled to its own transducer and neither crossing the affected valve. The catheters should be placed in the chambers or vessels on either side of the valve and the pressure tracings should be superimposed to accurately calculate the mean pressure gradient (area under the curve, AUC) (Fig. 8.6).

Assessment of mitral stenosis is performed by measuring simultaneous left ventricular and left atrial pressures. If transseptal puncture is not desired the pulmonary capillary wedge pressure may be used as a surrogate for the left atrium; however this may overestimate the magnitude of the gradient since the wedge pressure lags behind true left atrial pressure by a few milliseconds. Assessment of aortic stenosis involves simultaneous measurements in the left ventricle and ascending aorta. Two arterial sheaths can be placed but this increases the risk for access site complications. Dual lumen pigtail catheters have proximal (ascending aorta) and distal (left ventricle) ports that require two transducers but one arterial access site. Another method is the "pullback method," where the catheter is withdrawn from the left ventricle into the ascending aorta during continuous recording. This allows for a peak-to-peak measurement of the systolic pressure difference that is not simultaneous

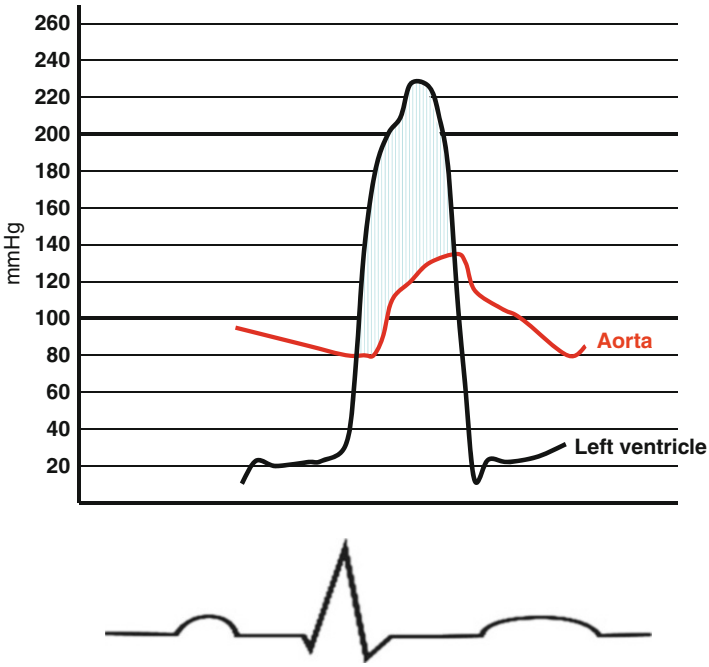

Fig. 8.6 Estimating the transaortic pressure gradient. The pressure waves produced by simultaneous catheterization of the left ventricle and proximal ascending aorta are superimposed. The shaded area under the curve (AUC) is calculated, providing the mean transvalvular gradient. The measured gradient is used to calculate aortic valve area with the Gorlin formula

and provides a crude approximation of the integrated or mean pressure difference. When aortic stenosis is severe the catheter itself promotes stenosis, resulting in a higher gradient and potential overestimation of stenosis severity.

The Gorlin formula is typically used to calculate valve areas in the catheterization lab:

Gorlin formula

$$\text{Valve area } (\text{cm}^2) = \frac{\text{CO}/[\text{HR}][\text{EP}]}{44.3 \times (K) \times \sqrt{\Delta \text{P}}}$$

where CO is cardiac output (L/min), HR is heart rate (bpm), EP is the ejection period (systolic or diastolic as calculated from the ECG, in seconds/beat), 44.3 is a constant that accounts for energy loss due to acceleration and gravity (cm/s/s), K is a unit-less correction factor (1.0 for the aortic valve and 0.85 for the mitral valve), and $\sqrt{\Delta P}$ is the square root of the mean pressure gradient across the valve. An abbreviated version of the Gorlin formula, called the Hakki formula, provides a reasonable estimate of valve area as well.

Table 8.2 Criteria for estimating the degree of mitral valvular regurgitation from angiography

Severity	Grade	Criterion
Mild	1+	Incomplete opacification of left atrium
Moderate	2+	Complete opacification of left atrium but with less relative intensity than the left ventricle
Moderately severe	3+	Complete opacification of left atrium with intensity equal to the left ventricle after 4 beats
Severe	4+	Complete opacification of left atrium with intensity equal to the left ventricle within 3 beats

The same principle can be applied to the assessment of aortic regurgitation by assessing the degree of left ventricular opacification relative to the ascending aorta

Hakki formula

$$\text{Valve area } (\text{cm}^2) = \frac{\text{CO}}{\sqrt{\Delta P}}$$

The normal aortic valve orifice area is 3.0–4.0 cm^2. The normal mitral valve orifice area is 4.0–6.0 cm^2.

Assessment of Valvular Regurgitation

The invasive assessment of valvular regurgitation is largely subjective. The severity of aortic and mitral regurgitation can be estimated by applying qualitative criteria to the appearance of aortography and ventriculography, respectively (Table 8.2). The severity of tricuspid and mitral regurgitation can be estimated from the relative magnitude of the "v" waves in the right atrial and PCWP tracings, respectively. However atrial compliance and ventricular function also influence the amplitude of "v" waves, making this approach fairly nonspecific.

Review Questions

Question 1.

Figure shows a pulmonary capillary wedge tracing from a spontaneously breathing patient. Which of the following represents the best estimate of the mean wedge pressure?

a. 5 mmHg
b. 10 mmHg
c. 15 mmHg

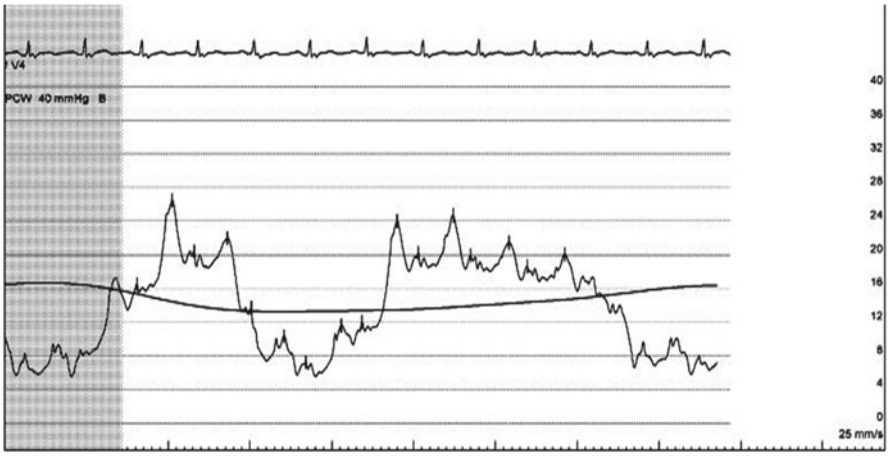

Fig. 8.7

d. 20 mmHg
e. 25 mmHg

The answer is c.

The wedge pressure tracing varies with the intrathoracic pressure swings produced by respiration. At functional residual capacity (FRC) the diaphragm is not moving and the elastic recoil forces of the lungs and chest wall are balanced; this is the theoretic "zero pressure point" of the chest. FRC occurs at the end of passive expiration. Therefore in a spontaneously breathing patient the mean wedge pressure should be measured at the top of the curve, just prior to the drop in pressure produced by spontaneous inspiration. In patients receiving positive pressure ventilation the wedge should be measured at the bottom of the curve, just prior to the rise in pressure produced by mechanical inspiration.

In this example the mean wedge pressure (produced by the monitoring system) is represented by the solid line across the tracing. A respirometer tracing (not shown) can be a useful adjunct to invasive hemodynamic measurement, particularly in cases of pericardial constriction.

Question 2

Which component(s) are missing from the right atrial pressure tracing shown in Figs. 8.7 and 8.8?

a. *a* wave
b. *a* wave and *x* descent
c. v wave
d. *v* wave and *y* descent
e. *c* wave

The answer is b.

This patient is in atrial fibrillation and has lost atrial contraction and relaxation, the physiologic events that produce the *a* wave and *x* descent, respectively. The *c*

Fig. 8.8

wave represents tricuspid valve closure and remains in the presence of atrial fibrillation. The *v* wave and *y* descent are unaffected by atrial fibrillation.

In tricuspid stenosis the *a* waves can be quite large. You can also see large *a* waves during complete heart block when the atrium contracts against a closed tricuspid valve. In tricuspid regurgitation the *v* waves can be large.

Question 3

A 65-year-old man with hypertension and diabetes presents with worsening exertional dyspnea that began 1 week after he experienced a prolonged episode of "severe indigestion," heralded by epigastric discomfort, nausea, and diaphoresis. His physical exam reveals a systolic murmur along the left sternal border with a palpable thrill. His ECG demonstrates sinus rhythm with anterolateral Q waves. Laboratory assessment is remarkable for mildly elevated serum troponin with normal CK-MB. A limited echocardiogram performed in the emergency department suggests moderate LV systolic dysfunction with anterior and anteroseptal akinesis. No significant valvular disease is seen.

Coronary angiography reveals total occlusion of the mid LAD with well-defined collaterals. There is mild disease in the other vessels. Right heart catheterization is performed, revealing the following:

Chamber	Pressure (mmHg)	Saturation (%)
SVC	–	59
IVC	–	63
RA	12	60
RV	58/12	79
PA	52/22	78
PCWP	20	–
Aorta	90/54	96

The Q_p/Q_s is…

a. 1.0
b. 1.5
c. 2.0
d. 2.5
e. 3.0

The answer is c.

$$Q_p / Q_s = [SaO_2 - MvO_2] / [PvO_{2-}PaO_2] \quad \text{and} \quad MvO_2 = (3 \times SVC + IVC) / 4$$

Thus for this example $MvO_2 = [(3 \times 59) + 63]/4 = 60$.
$Q_p/Q_s = [96–60]/[96–78] = 2.0$.

This patient presented with an anterior myocardial infarction complicated by ventricular septal rupture. This diagnosis was suggested by his history and physical examination and confirmed by a full oximetry run. His shunt fraction and symptoms favors repair of this defect.

Question 4

A 79-year-old woman presents with progressive dyspnea and angina. Her echocardiogram suggests severe aortic stenosis with normal left ventricular systolic function. Her preoperative left and right heart catheterization demonstrates minimal angiographic coronary artery disease. Her mean transaortic gradient measures 49 mmHg. Her right heart data are shown:

Chamber	Pressure (mmHg)
RA (mean)	8
RV	42/8
PA	46/22
PCWP	20
CO/CI Fick	5.0/2.8

Her aortic valve area is approximately…

a. 1.5 cm^2
b. 1.0 cm^2
c. 0.7 cm^2
d. 0.4 cm^2
e. The valve area cannot be calculated from the data provided

Using the Hakki equation:

$$\text{Valve area } (cm^2) = \frac{CO}{\sqrt{\Delta P}} = 5.0 / \sqrt{49} = 0.71 cm^2 = 0.71 cm^2$$

The Hakki equation is less precise than the Gorlin equation but it nonetheless provides a reasonable estimate of valve area.

Question 5

A 65-year-old woman with scleroderma and hypertension presents with several months of increasing shortness of breath. Her echocardiogram reveals normal left ventricular size and systolic function with mild right ventricular enlargement and mild systolic dysfunction. She has moderately severe tricuspid regurgitation and her estimated right ventricular systolic pressure is 70 mmHg. She is referred for invasive hemodynamic assessment.

Left heart catheterization reveals angiographically normal coronary arteries. Her transaortic pressure gradient is not significantly elevated and her left ventricular end diastolic pressure is 10 mmHg.

Right heart catheterization data are shown:

Right atrium: 13 (mean)

Right ventricle: 66/13

Pulmonary artery: 68/26 (mean = 40)

PCWP: 11 (mean)

Cardiac output/Index by thermodilution method: 4.5/2.4

Calculate this patient's pulmonary vascular resistance.

Transpulmonic gradient (TPG) = mean PA − mean PCWP

= 40 − 11 = 29 mmHg

Pulmonary vascular resistance = TPG/CO

= 29/4.5 = 6.4 Woods units

This patient has pulmonary arterial hypertension, characterized by her normal wedge pressure and increased transpulmonic pressure gradient. Her clinical history suggests pulmonary hypertension secondary to a connective tissue disorder (WHO group 1.3).

References

1. Wiggers CJ. Determinants of cardiac performance. Circulation. 1951;4(4):485–95.
2. Harmon M, Gomes S, Oppenhein C, et al. Cerebral microembolism during cardiac catheterization and risk of acute brain injury: a prospective diffusion-weighted magnetic resonance imaging study. Stroke. 2007;37(8):2035–8.
3. Todorovic M, Jensen EW, Th gerson C. Evaluation of dynamic performance in liquid filled catheter systems for measuring invasive blood pressure. Int J Clin Monit Comput. 1996; 13(3):173–8.
4. Bashore TM, Bates ER, Berger PB, et al. American College of Cardiology/Society for Cardiac Angiography and Interventions Clinical Expert Consensus Document on cardiac catheterization laboratory standards. A report of the American College of Cardiology Task Force on Clinical Expert Consensus Documents. J Am Coll Cardiol. 2001;37:2170–214.
5. Antman EM, Marsh JD, Green LH, Grossman W. Blood oxygen measurements in the assessment of intracardiac left to right shunts: a critical appraisal of methodology. Am J Cardiol. 1980;46:265–71.
6. Swan HJ, Ganz W, Forrester J, Marcus H, Diamond G, Chonette D. Catheterization of the heart in man with use of a flow-directed balloon-tipped catheter. N Engl J Med. 1970;283:447–51.
7. Noto Jr TJ, et al. Cardiac catheterization 1990: a report of the Registry of the Society for Cardiac Angiography and Interventions (SCA&I). Cathet Cardiovasc Diagn. 1991;24:75–83.

Part III
Specific Disease States

Chapter 9
Tamponade

Olcay Aksoy and Leonardo Rodriguez

Case Presentation

The patient is a 47-year-old female with history of systemic lupus erythematosus (SLE) who presents with exertional dyspnea. She reports development of peripheral edema in the past month and has had onset of exertional dyspnea in the past few days.

Salient physical examination findings include a heart rate of 92, blood pressure of 136/72, elevated JVP at 16 mmHg, and grade I/VI early systolic murmur at left lower sternal border. The lung fields are clear. There is 2+ pitting lower extremity edema. Pulsus paradoxus is measured to be 8 mmHg.

A chest X-ray shows an enlarged cardiac silhouette. An EKG shows electrical alternans (Fig. 9.1). An urgent echocardiogram shows increased respirophasic variation across mitral and tricuspid valves (Fig. 9.2a, b).

The patient is then admitted to the hospital for further evaluation and management. Over the course of the admission, the patient becomes gradually confused. Laboratory evaluation reveals evidence of mild renal dysfunction and a mild transaminitis noted in her hepatic profile. She now has a heart rate of 108 and her blood pressure is 92/56. She is transferred to the Intensive Care Unit and a pulmonary artery catheter is placed with right atrial tracings showing blunted *y* descent (Fig. 9.3a). She subsequently receives a pericardiocentesis with improvement in hemodynamics (post-pericardiocentesis tracings shown in Fig. 9.3b). The patient improves clinically and subsequently is discharged on an intensified treatment regimen for SLE with follow-up echocardiogram scheduled.

O. Aksoy, M.D. • L. Rodriguez, M.D. (✉)
The Cleveland Clinic, Cleveland, OH, USA
e-mail: aksoyo@ccf.org; rodrigl@ccf.org

A.T. Askari et al. (eds.), *Cardiovascular Hemodynamics: An Introductory Guide*, Contemporary Cardiology, DOI 10.1007/978-1-60761-195-0_9,

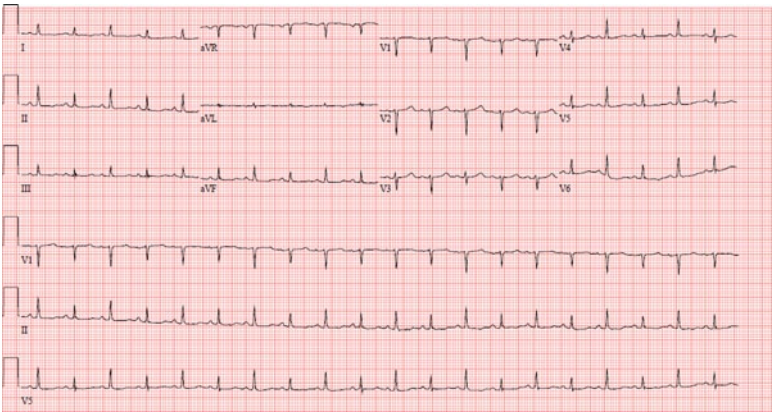

Fig. 9.1 EKG demonstrating electrical alternans

Introduction

Anatomy

The myocardium is encased in a relatively rigid and noncompliant structure called the pericardium. The pericardium is formed by two layers. The outer sac, called the fibrous pericardium, is composed of fibrous tissue and encases the inner layer of pericardium and the heart. The inner sac has two layers—called the parietal and visceral pericardium. The parietal pericardium is attached to the internal surface of the fibrous pericardium and is contiguous with the visceral pericardium as it gets reflected on the cardiac surfaces. In between the visceral and the parietal pericardium lies the pericardial space. This space normally contains up to 50 mL of serous fluid to maintain a low friction environment for the myocardium as it contracts and relaxes within the pericardium throughout the cardiac cycle. The pericardium effectively restrains the cardiac chambers to a confined space and due to this pericardial constraint, any change in the volume of one chamber of the heart is reciprocated by changes in other chambers in the opposite direction [1]. It is this complex interaction of pericardial space with the intracardiac chambers that leads to the hemodynamic consequences of pericardial effusions.

Several diseases and complications of invasive procedures may lead to pathologic accumulation of fluid in the pericardial space, which may impact cardiac output. When the accumulation of pericardial fluid interferes with diastolic filling of the heart, hemodynamic consequences associated with varied clinical presentations including tamponade ensue.

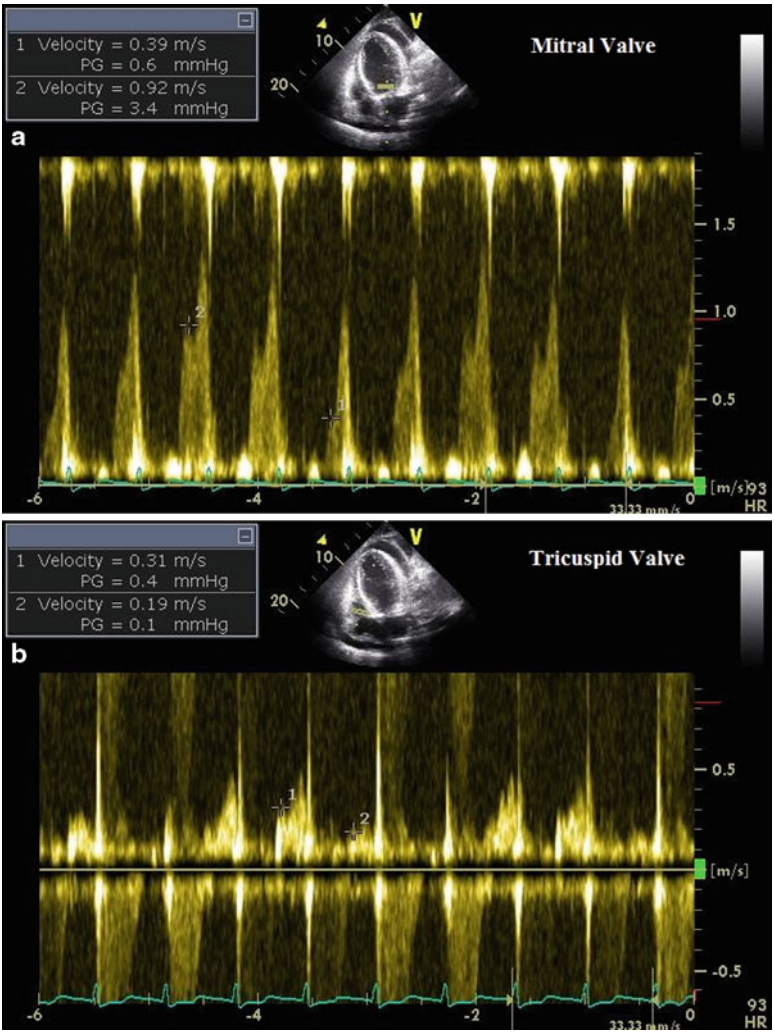

Fig. 9.2 Echocardiogram with Doppler evaluation demonstrating respiratory flow variation across mitral (**a**) and tricuspid valves (**b**)

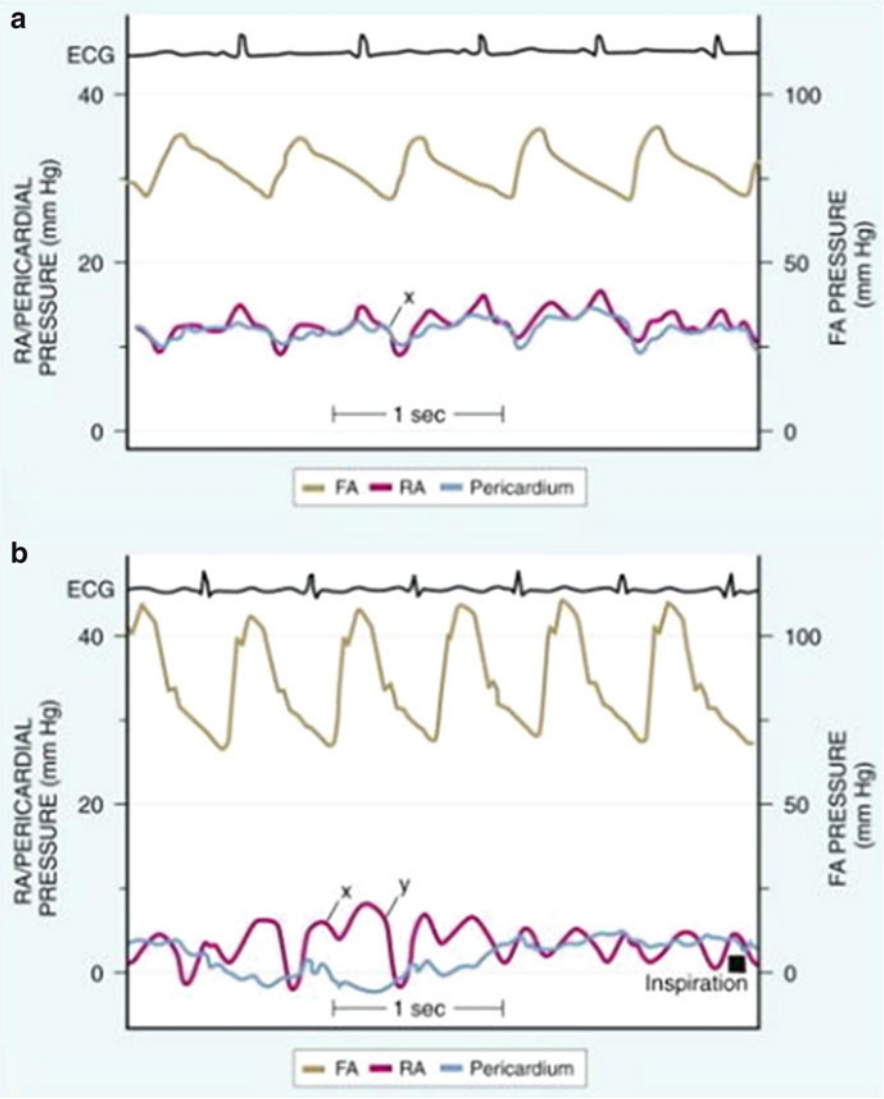

Fig. 9.3 Pre-pericardiocentesis—(**a**) and Post-pericardiocentesis—(**b**) (Reprinted from modification by LeWinter MM. Pericardial diseases: In: Braunwald's heart disease: a textbook of cardiovascular disease. Philadelphia: Saunders Elsevier; 2008. p. 1836 from original by "Lorell BH, Grossman W. Profiles in constrictive pericarditis, restrictive cardiomyopathy and cardiac tamponade. In: Baum DS, Grossman W, editors. Grossman's cardiac catheterization, angiography, and intervention. Philadelphia: Lippincott Williams & Wilkins; 2000. p. 840")

Pathophysiology of Tamponade

Progression of a pericardial effusion to tamponade depends on several factors. These include the rate of fluid accumulation, tensile properties of the pericardium, intracardiac pressures, and tensile properties of the myocardium. Ultimately, it is the intrapericardial pressure and its interaction with intracardiac pressures (transmural pressure) that determines the presence of tamponade.

$$\text{Transmural pressure} = \text{intracardiac pressure} - \text{intrapericardial pressure}$$

When the intrapericardial pressure equalizes or exceeds that of the intracardiac chambers, the transmural pressure is then <0 and impaired filling occurs. In patients with pericardial effusions, negative transmural pressure is more often due to increased pericardial pressure but decreased intracardiac pressures also contribute to the development of tamponade.

Determinants of intrapericardial pressure include the volume of pericardial fluid and the compliance of the pericardium. The relationship between size of the effusion and the associated increase in pressure is not linear and is modified by the compliance of the pericardium itself. As such, a larger but chronic effusion might be better tolerated than a smaller but rapidly accumulating one due to the higher compliance of the pericardium that develops in the chronic setting (Fig. 9.4). Therefore, size of the effusion should not be used as a sole criterion for the presence of tamponade.

Progression of a pericardial effusion to tamponade also depends on the intravascular volume status of the patient as well as the compliance of the myocardium. Patients who are intravascularly depleted are more likely to present with compromised hemodynamics due to diminished filling pressures in the cardiac chambers. On the contrary, those with ventricular hypertrophy or restrictive heart disease may not present with tamponade physiology for a given intrapericardial pressure as this pressure is not readily transmitted to the intracardiac chambers due to the diminished compliance of the myocardium.

Stages of Pericardial Tamponade

Pericardial tamponade was previously thought of as an "all or none" clinical disorder [2]. However, it is now recognized that patients might present at different stages along the spectrum of tamponade physiology (Table 9.1). The first stage (pretamponade) occurs when the pressure in the pericardium is less than right and left ventricular end diastolic pressures (transmural pressure still >0). In this stage, the effusion does not have a clinically significant hemodynamic impact; however there may be subtle changes in echocardiographic respiratory flow variation across mitral and tricuspid valves and minimally increased pulsus paradoxus pressure (<10 mmHg). In the second stage, the pericardial pressure equals the right ventricular diastolic pressure leading to collapse of the right ventricle during early

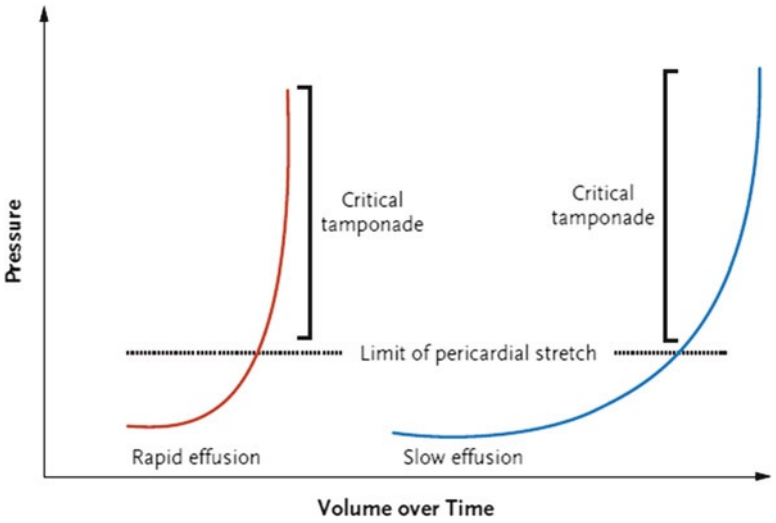

Fig. 9.4 Intrapericardial pressure that is critical in determining the transmural pressure is affected by the time course of fluid accumulation. Rapidly developing effusions reach the limits of the pericardial stretch sooner, whereas slowly developing effusions are better tolerated due to time allowed for the pericardium to adapt to the changes imposed by the effusion (adapted from Spodick DH. Acute cardiac tamponade. N Engl J Med. 2003;349(7):684–90)

Table 9.1 Three stages of tamponade

1. Pretamponade: No clinical evidence of tamponade as transmural pressure >0, however exaggerated tricuspid and mitral inflow patterns noted
2. Early tamponade: Right sided chambers are affected as the pericardial pressure increases. Clinical presentation might become apparent
3. Tamponade: Both right and left sided chambers are affected as there is equalization of pressures with pericardium. Clinical tamponade is evident

diastole. In this case, while there is no collapse in the left ventricle, clinical and hemodynamic evidence for tamponade is present with decrease in right ventricular stroke volume. Hypotension, compensatory tachycardia, and elevated pulsus paradoxus might be present. Finally, the most severe stage presents when left ventricular filling is also affected by the increased pericardial pressure. In this case, there is equilibration of pericardial, right ventricular and left ventricular diastolic pressures leading to severely impaired filling of the ventricles and low stroke volume (Fig. 9.5) [3]. Patients in the final stage of tamponade require expeditious diagnosis with direct intervention to drain the pericardial fluid and reestablish hemodynamic stability.

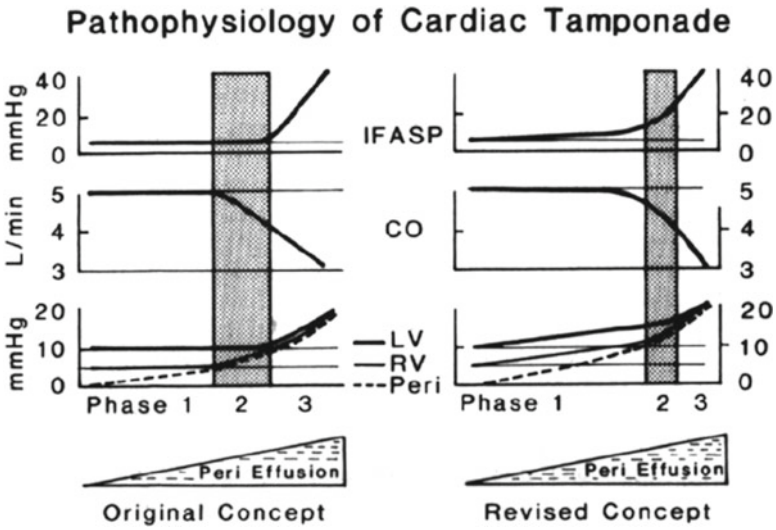

Fig. 9.5 Stages of pericardial tamponade showing pressures in right atrium, right ventricle, pulmonary capillary wedge pressure, and intrapericardium (*Peri* pericardium; *RV* right ventricle; *LV* left ventricle; *CO* cardiac output; *IFASP* inspiratory decrease in arterial systolic pressure). Initial concept and its revision with further data is shown below detailing changes in the pressures across stages of tamponade (adapted from Reddy et al. [3])

Low-Pressure Tamponade

This condition has been described as a form of tamponade in which relatively low intrapericardial pressure causes cardiac chamber compression in patients with low right sided pressures. Reported to be present in 20% of patients with tamponade physiology, this condition might be associated with hypovolemia, vasodilator, and diuretic use [4]. Overall, findings from pulmonary artery catheterization are similar with equalization of diastolic pressures albeit at lower pericardial and diastolic pressures. Given the low pressures, patients might not present with typical findings in physical examination (elevated JVD, tachycardia); however they benefit from pericardiocentesis with improved cardiac indices and arterial pressures [4]. When evaluating a patient with a pericardial effusion and hypotension, this clinical entity should be kept in mind.

Diagnosis

Physical Exam Findings

While physical exam might vary in patients with tamponade, there are certain classic findings as defined by Dr. Claude Beck in 1935: Low blood pressure, jugular venous distension, and muffled heart sounds. While all three might not be present

even in the most advanced cases of tamponade, hypotension and tachycardia with narrow pulse pressure should alert the clinician to its presence.

Pulsus Paradoxus

Originally described by Kussmaul in 1873, pulsus paradoxus is defined by a ≥10–12 mmHg or a >9% decline in arterial systemic pressure with inspiration [5]. While the etiology of this drop is debatable, the most widely accepted explanation has to do with intrathoracic pressure changes with inspiration and the fact that the total volume within the pericardium is fixed. Intrapericardial pressure normally ranges from −5 to +5 cm of water and fluctuates significantly with respiratory cycle. The drop in the intrathoracic pressure with inspiration is transmitted to the pericardium and the right atrium which results in increased venous return to the right side of the heart. The opposite occurs in the left heart where there is diminished filling of the left ventricle in early inspiration and slightly reduced systemic stroke volume. The reverse is true in expiration: As the intrathoracic pressure increases, the right sided filling diminishes resulting in improved filling of the left ventricle leading to a higher systemic stroke volume. In a normal individual, these respiratory changes result in a 3–4 mm change in systolic pressure as measured peripherally. When there is a hemodynamically significant tamponade however, there is interventricular dependence of LV and RV, which leads to exaggeration of the above described pressure changes with respiration. This is due to the fixed space that the myocardium is constrained with as the increased filling of the RV compromises the filling of the LV, which subsequently leads to the diminished systemic stroke volume with the next contraction. As the underfilled LV cannot generate the normal stroke volume, the blood pressure drops >10 mmHg, which is recognized as pulsus paradoxus on physical exam.

While checking for the presence of pulsus paradoxus allows for quick assessment of patient at the bedside, several coexisting conditions might diminish the accuracy of this test. In patients who have lung disease and shock, pulsus paradoxus might already be present without tamponade. Also, this finding might be absent despite a hemodynamically significant tamponade in the presence of coexisting LV dysfunction with elevated LVEDP, severe aortic insufficiency, pulmonary hypertension, and right ventricular hypertrophy [6, 7].

Echocardiographic Findings

Although tamponade is a clinical diagnosis, echocardiographic evaluation of the patient is a very useful adjunct as it provides direct visualization of the pericardium, the cardiac chambers, and early signs of tamponade physiology. Several echocardiographic parameters may be used to evaluate for evidence of tamponade including M-mode, Doppler interrogation, and 2D visualization. While 2D and M-mode provide visual confirmation of the effusion and the collapse of chambers, Doppler

Table 9.2 Evidence of tamponade on echocardiogram

Presence of an effusion. Size, while predictive, is not a reliable determinant of clinical tamponade
Early diastolic collapse of right ventricle
Late diastolic right atrial inversion
Dilated inferior vena cava (>2.5 cm) with failure to collapse of the vessel with inspiration >50%
Respiratory inflow variations across the tricuspid valve (>40%) and the mitral valve (>25%)

Table 9.3 Typical order of findings in tamponade

Tricuspid inflow variation with respiration increased
Mitral inflow variation with respiration increased
Right atrial exaggerated late diastolic collapse (sensitive, nonspecific finding on echocardiogram)
Right ventricular outflow tract collapse (specific finding on echocardiogram)
Right ventricular free wall collapse
Left ventricular free wall collapse

evaluation can be useful in determining the above mentioned flow variations in tamponade (Table 9.2).

Exaggerated diastolic right atrial free wall collapse and diastolic right ventricular outflow tract collapse are early signs of elevated intrapericardial pressure. Brief inversion of the atrial wall can be seen during atrial contraction and does not represent tamponade physiology. More prolonged atrial wall inversion (>1/3 of cardiac cycle) is more indicative of increased intrapericardial pressures. Right ventricular outflow tract is the most easily compressible component of the right ventricle and may also be affected early from elevated intrapericardial pressure. As the intrapericardial pressure increases, the right ventricular free wall may also collapse in diastole signaling to the progression of disease. Collapse of these above right sided chambers is indirect evidence that the intrapericardial pressure have exceeded the intracardiac pressures leading to the inversion of the free walls [1]. As tamponade progresses, further collapse of the left ventricle can also be seen due to similar mechanisms (Table 9.3). Both 2D and M-mode techniques may be used to identify these anatomic manifestations of tamponade.

Doppler evaluation is very helpful in assessing the hemodynamic impact of the pericardial effusion. Outflow across aortic and pulmonary valve (Velocity Time Integral) and inflow across mitral and tricuspid valves (peak velocity) can be measured. In a normal patient, these parameters of flow demonstrate minimal respiratory variation with the pulmonic and aortic valve velocity time integral varying <10% and the mitral and tricuspid valve peak inflow velocities varying <15% and <25%, respectively. In patients with tamponade, however, respiratory variation across the mitral valve is usually >25% and that across the tricuspid valve >40% (Fig. 9.6). This exaggerated variation in flow across valves provides indirect evidence for ventricular interdependence and suggests a hemodynamically significant effusion.

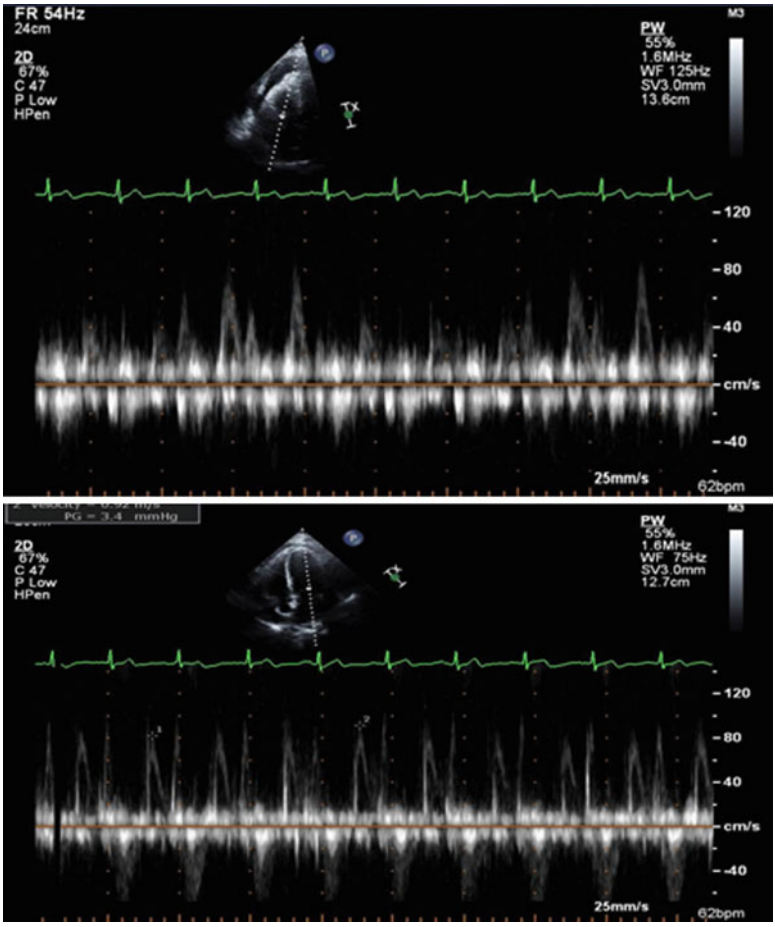

Fig. 9.6 *Top panel* showing tricuspid and *bottom panel* showing mitral valve inflow pattern

Also helpful, although often ignored, is the Doppler flow pattern of the hepatic vein. The hepatic vein flow pattern reflects the venous pressure. The normal hepatic vein flow has three major waves: positive systolic and diastolic flows (towards the atrium) and a negative flow corresponding to the atrial contraction (away from the atrium). The systolic flow wave corresponds to the *x* descent and the diastolic flow wave to the *y* descent. In patients with tamponade physiology, blood enters the right atrium only or mostly during ventricular systole. This is reflected in the hepatic vein flow as a predominant systolic wave with decreased or even absent diastolic flow wave (i.e., corresponding to blunted *y* descent on the RA tracing). After pericardiocentesis, the diastolic flow is reestablished (Fig. 9.7).

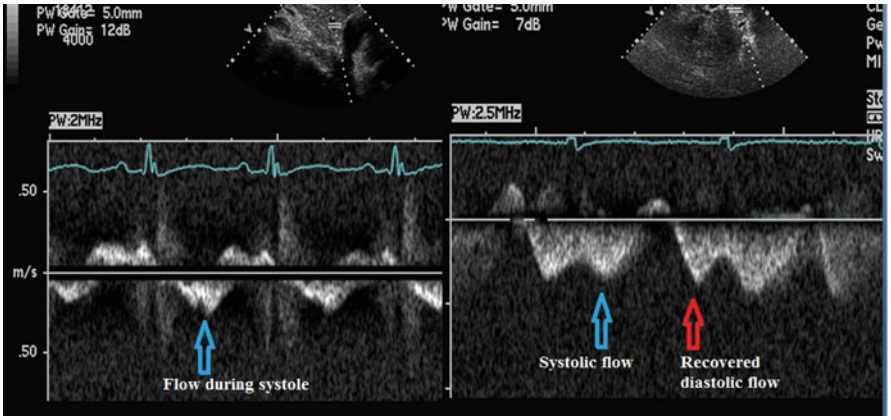

Fig. 9.7 Hepatic vein tracing showing flow to the atrium predominantly during systole and blunted return in diastole. After pericardiocentesis, flow to atrium during diastole is recovered

Pulmonary Artery Catheter Findings

While not routinely used for diagnosis, insertion of a pulmonary artery catheter may provide insight into the pathophysiology of tamponade as it helps determine the exact diagnosis and may demonstrate success of the pericardiocentesis.

The cardinal finding on PA catheterization during tamponade is diastolic equalization of pressures of the right atrium, RV diastolic pressure, pulmonary arterial diastolic pressure, and pulmonary capillary wedge pressure. A difference <5 mmHg suffices to establish this equivalency. This pressure is felt to be the passive pressure in the intracardiac chambers and equal to the intrapericardial pressure in severe tamponade (Fig. 9.8).

As mentioned above the other abnormal finding is blunted *y* descent following the *v* wave in the right atrial tracing. In tamponade, the *a* wave, *x* descent, and *v* wave remain unaffected as the contraction of the atrium, its relaxation, rapid filling remain unchanged. The *y* descent, which represents the rapid emptying of the atrium into the right ventricle, is blunted. This is due to the impaired RV relaxation in early diastole due to the effusion-related elevation in RV diastolic pressure. Thus, the rapid emptying of atrium to ventricle, i.e., the *y* descent is blunted (Fig. 9.9). This finding is readily reversed when pericardiocentesis is performed and the intrapericardial pressure is reduced. As the right ventricle is able to relax more efficiently, there is improved flow from the atrium to the ventricle hence a normalized *y* descent.

Distinction from Constriction

Intrathoracic pressures and changes during inspiration are readily transmitted to the pericardium and the intracardiac chambers in the case of a pericardial effusion with a relatively normal pericardium. In patients who have constrictive pericardium,

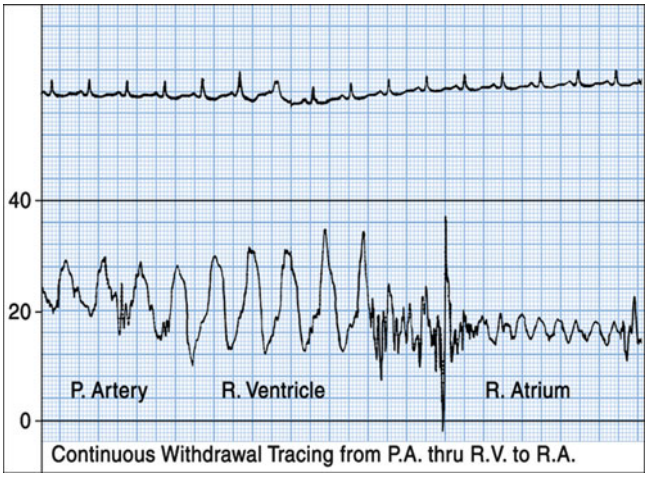

Fig. 9.8 Diastolic equalization of right atrial (mean), right ventricular end diastolic, pulmonary arterial diastolic pressures demonstrated as the PA catheter is pulled back from the pulmonary artery

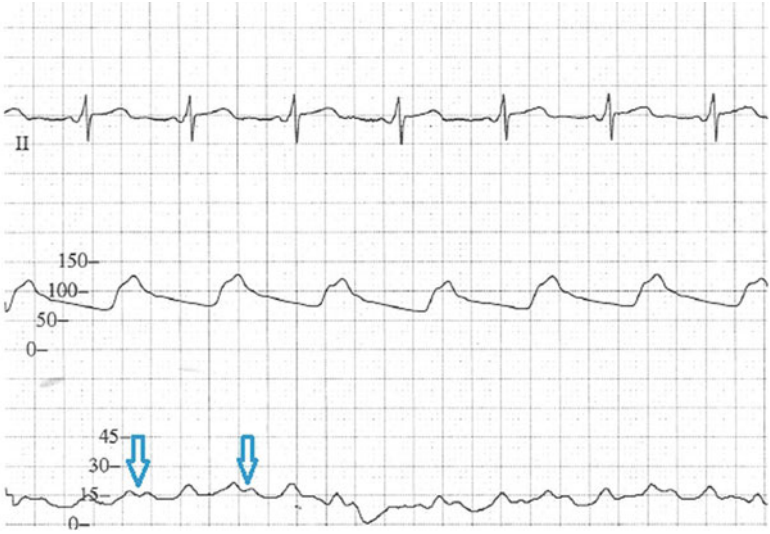

Fig. 9.9 Right atrial pressure waveform with blunted *y* descent

these pressures are not transmitted, which as a result leads to differences in physical exam and invasive hemodynamic findings. Constriction is notable for lack of decreased right sided pressure with inspiration leading to the Kussmaul's sign, a finding not seen in tamponade. Furthermore, in patients with constriction, there is rapid ventricular filling in early diastole, which is recognized as a prominent *y*

descent with a “dip and plateau” appearance (square-root sign) on pulmonary artery catheterization. Such is not the case for tamponade where ventricular filling in early diastole is in fact impaired leading to a blunted *y* descent.

Computed Tomography and Magnetic Resonance Imaging

Advanced imaging such as CT and MRI may be useful to evaluate chronic pericardial effusions but should not be used in the setting of tamponade.

Pericardial effusion might be incidentally diagnosed with these imaging modalities. When this occurs, clinical assessment of the patient should be performed. In the event that there is a question of tamponade, hemodynamic assessment with a focused physical exam and echocardiography should not be delayed. MRI, in fact, can provide further hemodynamic information in these patients; however when tamponade is suspected, testing and treatment should not be delayed for performing this test.

Pericardial Tamponade in the Postsurgical Patient

While most effusions seen in clinical practice are circumferential, loculated effusions may be seen in postoperative settings and posttrauma. Chronic effusions though initially circumferential might organize into loculated effusions as well. In this setting, the aforementioned discussions about hemodynamics might not hold true. There may be focal compression of a cardiac chamber that might only be visible by 2D echocardiography. Doppler findings are also less helpful in postsurgical effusions; it is not uncommon to see exaggerated respiratory flow variation even in patients with small effusions. This may be due to increased respiratory effort secondary to pleural effusions or abnormal respiratory dynamics. When a case of focal tamponade is suspected, the clinical status of the patient and location of the effusion should be carefully assessed for further management.

Management

Patients who present with clinical tamponade should be treated emergently. While preparing the patient for removal of the pericardial fluid, intravenous administration of fluids to maintain adequate perfusion pressure is necessary. The administration of fluids improves the intracardiac filling and might stabilize the patient’s hemodynamics by increasing the transmural pressure. Either a pericardiocentesis or a pericardial window might be necessary to resolve the compression of the cardiac chambers. Typically anterior, lateral, and apical effusions might be drained by a percutaneous approach; however surgical drainage is preferred for postoperative

patients, loculated, and posterior effusions. The risks and benefits of both approaches in conjunction with the clinical scenario should be taken into account.

Pearls of Assessment

- Pericardial tamponade is a clinical diagnosis.
- Tamponade occurs when transmural pressure is <0.
- When tamponade is in question, all measures for accurate diagnosis and stabilization of the patients should be undertaken.
- Echocardiography is the primary modality to establish the presence of an effusion and support the clinical diagnosis of tamponade.
  - Right atrial and/or ventricular wall inversion.
  - Increased respiratory variation in mitral and tricuspid flows.
  - IVC plethora—dilated IVC with blunted diastolic hepatic vein flow is the most sensitive early echocardiographic finding in tamponade. This may be absent in patients with low-pressure tamponade.
- Pulmonary artery catheterization might be useful to confirm the clinical suspicion in select cases.

Board Style Questions

1. A 72-year-old man presents with exertional dyspnea and work up including an echocardiogram shows a large pericardial effusion. Which of the following is more specific sign of tamponade?

   A. Systolic flow reversal in hepatic veins
   B. Early diastolic collapse of right atrium
   C. Diastolic collapse of right ventricle
   D. Hypotension in a patient with pericardial effusion
   E. Presence of a large pericardial effusion

2. A 67-year-old female with morbid obesity and rheumatoid arthritis presents with hypotension of unclear etiology. An echocardiogram is performed; however parasternal and apical windows are difficult to interpret due to body habitus, but there is a moderate circumferential pericardial effusion. Best Doppler hemodynamics are only obtained in the subcostal views. What's expected in the hepatic vein flow pattern in the setting of tamponade?

   A. Diminished forward flow during systole
   B. Diminished forward flow during diastole
   C. Flow reversal during systole
   D. Hepatic vein flow pattern is not expected to change with tamponade

E. Exaggerated forward flow during diastole

3. Which of the following is not a part of Beck's triad?

   A. Muffled heart sounds
   B. Hypotension
   C. Elevated JVD
   D. Kussmaul's sign

4. A 39-year-old female with a history of tuberculosis as a child presents with pitting peripheral edema and increased fatigue. Echocardiographic evaluation shows pericardial thickening with a moderate effusion. Her heart rate is 102 and blood pressure is 94/64. Which of the following can be helpful in distinguishing tamponade from constriction?

   A. Presence of a pericardial effusion
   B. Absence of Kussmaul's sign
   C. Pericardial thickening seen on CT
   D. Exaggerated flow across tricuspid valve during inspiration
   E. None of the above

5. What's the initial treatment strategy in a hypotensive and tachycardic patient with a pericardial effusion if tamponade is suspected?

   A. Pericardiocentesis
   B. IV fluid infusion
   C. Inotrope infusion
   D. Consultation with cardiothoracic surgery for a pericardial window
   E. Beta blocker administration

Answers to Board Style Questions

1. Correct Answer is C. Systolic flow reversal in hepatic veins is seen in severe tricuspid regurgitation. While options other than C can be seen in tamponade, they are not specific to tamponade.
2. Correct Answer is B. Diastolic forward flow is expected to be reduced in the hepatic veins due to elevated right ventricular pressures. Other options do not apply in tamponade.
3. Correct Answer is D. Beck's triad consists of muffled heart sounds, hypotension, and elevated neck veins.
4. Correct Answer is B. Other options can be seen with both conditions; however Kussmaul's sign is specific to constriction and is not seen with tamponade.
5. Correct Answer is B. An unstable patient in tamponade needs to be fluid repleted emergently in attempt to overcome the pericardial pressure. Further treatment modalities might include pericardiocentesis or a surgical window placement. Beta blockers are contraindicated in compensatory tachycardia.

References

1. Armstrong WF, Ryan T, Feigenbaum H. Feigenbaum's echocardiography. 7th ed. Philadelphia: Wolters Kluwer Health/Lippincott Williams & Wilkins; 2010. xv, 785 p.
2. Kern MJ, Lim MJ. Hemodynamic rounds: interpretation of cardiac pathophysiology from pressure waveform analysis. 3rd ed. Hoboken: Wiley-Blackwell; 2009. xxii, 473 p.
3. Reddy PS, Curtiss EI, Uretsky BF. Spectrum of hemodynamic changes in cardiac tamponade. Am J Cardiol. 1990;66(20):1487–91.
4. Sagrista-Sauleda J, et al. Low-pressure cardiac tamponade: clinical and hemodynamic profile. Circulation. 2006;114(9):945–52.
5. Curtiss EI, et al. Pulsus paradoxus: definition and relation to the severity of cardiac tamponade. Am Heart J. 1988;115(2):391–8.
6. Sharkey SW. A guide to interpretation of hemodynamic data in the coronary care unit. Philadelphia: Lippincott-Raven; 1997. 214 p.
7. Stouffer GA, Ebrary Inc. Cardiovascular hemodynamics for the clinician. Malden: Blackwell Futura; 2008.

Chapter 10
Pericardial Constriction and Restrictive Cardiomyopathy

Parag Patel and Allan Klein

Introduction

Despite being different disease processes, pericardial constriction and restrictive cardiomyopathy are often discussed together due to their similar clinical and hemodynamic features. Physiologically, both processes lead to impaired diastolic filling via different mechanisms; a rigid, adherent pericardium is noted in constriction while abnormal myocardium is the culprit in restriction. Pericardial constriction (or constrictive pericarditis [CP]) usually is a chronic process, and variant forms do exist (effusive-constrictive, subacute, transient, occult) which share many of the clinical findings, but have subtle clinical nuances that distinguish each type. Restrictive cardiomyopathy is associated with a normal pericardium, but is often associated with infiltrative diseases such as amyloidosis, hemochromatosis, and sarcoidosis. Given the spectrum of disease and the various clinical manifestations of pericardial constriction and cardiac restriction, initial history and physical findings along with hemodynamic considerations and newer non-invasive imaging criteria now lead the way in making the diagnosis. However, using all available data in distinguishing between the two processes becomes important, as the treatment for each is very different.

Pathophysiology

Pericardial Constriction

The pericardium is an avascular, fibrous sac that consists of two layers, the visceral and parietal pericardium. The space between them houses serous pericardial fluid

P. Patel
Cleveland Clinic, Heart and Vascular Institute, Cleveland, OH 44195, USA

A. Klein (✉)
The Cleveland Clinic, Cleveland, OH, USA
e-mail: kleina@ccf.org

A.T. Askari et al. (eds.), *Cardiovascular Hemodynamics: An Introductory Guide*, Contemporary Cardiology, DOI 10.1007/978-1-60761-195-0_10,

(typically <50 mL) which serves as a lubricant during cardiac motion between the adjoining layers to prevent irritation. The pericardium itself is made up of stiff collagen fibers that are relatively elastic at low volumes but when stretched become rapidly inelastic. When a scarred or calcified, noncompliant pericardium becomes adherent to various areas on the surface of the heart (constriction)—the cardiac chambers are unable to relax completely during diastole due to extrinsic limits placed on it by the pericardium. As a result, in the ventricles, mid and late diastolic filling occurs earlier in diastole as the constraining force on the ventricle prevents further expansion and filling of the cavity leading to elevation in end diastolic pressures and decrease in cardiac output. Once identified, pericardial stripping (pericardiectomy) is the treatment of choice as medical therapy is often unable to effect symptomatic relief.

As negative intrathoracic pressure is developed (−6 to 0 mmHg) during inspiration, it is transmitted to the heart via the pericardium and pericardial right atrium (RA) space. This negative pressure results in increased systemic venous return to the as well as augmenting passive filling of the right ventricle (RV). As the RV fills, the free walls are able to expand in the presence of a normal pericardium and allow for the capacitance of the RV. In CP, this process is impeded as the rigid encasement of the ventricles prevents transmission of the negative intrathoracic pressure to the heart. As the stiff outer shell limits capacitance, the RV free walls are unable to expand and accommodate the increased systemic venous inflow during inspiration. This leads to bowing of the septum toward the left ventricle (LV) to accommodate the volume of the RV inflow. The pulmonary venous circulation, which sits outside of the pericardium, behaves similarly to changes in intrathoracic pressure as the systemic venous system, thus leading to changes in LV filling during the respiratory cycle. On inspiration, the pulmonary venous pressure decreases; however, the negative intrathoracic pressure is not transmitted to the LV, leading to decreased flow gradient into the LV and thus limiting LV filling. During expiration, positive intrathoracic pressure reduces systemic venous return leading to decreased RV end diastolic pressure. Passive filling of the LV now overcomes RV pressure and the interventricular septum shifts rightward into the RV. This phenomenon is known as *ventricular interdependence*; it occurs to a lesser extent in normal physiology but is exaggerated in CP.

Restrictive Cardiomyopathy

The term “restrictive cardiomyopathy” defines a group of diseases that affect the myocardium and/or endocardium resulting in impaired ventricular relaxation with restricted filling affecting one or both of the ventricles. Increased LV thickness and near normal systolic function are noted in most cases, with a decline in ejection fraction during the latter stages of the disease. The pericardium and pericardial compliance are normal in pure restrictive cardiomyopathies; however, depending on the cause (e.g., radiation), aspects of both restriction and constriction can exist.

Restrictive cardiomyopathies can be divided into primary and secondary forms; the secondary forms can be further subdivided into infiltrative storage disorder categories. Histologically, the infiltrative disorders are associated with deposits in the interstitial space between myocytes, while storage disorders focus primarily on accumulation within the cardiac myocytes. Pathophysiologically, the increased stiffness of the LV leads to rapid changes in LV pressure with incremental volume increases. This leads to the characteristic hemodynamic "dip and plateau" filling pattern, due to rapid early diastolic filling (dip) and cessation or diastasis of flow in mid- and late-diastole (plateau).

Evaluation

History/Clinical Presentation

Distinguishing between constriction and restriction is often difficult due to similar presenting symptoms and physical findings. There are subtle findings in the history and physical that can help discern which process is responsible for the patient's symptoms. The history should be aimed at trying to elucidate any etiologic causes for either constriction or restriction. For example, an antecedent history of cardiac trauma, cardiac surgery, or pericarditis would favor constriction, while a prior history of infiltrative or glycogen storage diseases (amyloid, sarcoid, Fabry's disease) suggests restriction. Of note, a history of radiation (mantle radiation) can lead to symptoms via a myriad of physiologic processes including constriction, restriction, pulmonary fibrosis as well as valvular disease. Patients will present with a varying degree of symptoms depending on how advanced the disease process is. Dyspnea on exertion or at rest, edema (lower extremity, ascites, and effusions), pulmonary congestion, and eventually symptoms of low cardiac output are noted in both processes. Late stages of both are heralded by severe heart failure. Table 10.1 lists the different etiologies of CP and restriction.

Physical Exam

Most patients with CP and restriction will have elevated jugular venous pressure (JVP). Kussmaul's sign (increase in JVP with inspiration due to the inability of the RA to accommodate increased venous return) can be seen in both conditions; however, it is more common in CP. A steep *Y*-descent of the JVP (Friedreich's sign) along with peripheral edema, ascites, hepatic congestion, and pleural effusions can also be seen in both conditions as markers of right-sided heart failure. Physical exam findings suggestive of CP are the presence of a pericardial knock (diastolic gallop usually heard before S3 consistent with abrupt cessation of ventricular filling); friction rub (if active pericarditis); and apical retraction (inability

Table 10.1 Causes of constrictive pericarditis and restrictive cardiomyopathy

Constrictive pericarditis	Restrictive cardiomyopathy
Idiopathic	Primary
Viral	Endomyocardial fibrosis
Post-surgical	Loeffler cardiomyopathy
Post-radiation therapy	Idiopathic restrictive cardiomyopathy
Connective tissue disorder	Secondary
Post-MI (Dressler's syndrome)	Infiltrative
Postinfectious	Amyloidosis
Uremia	Sarcoidosis
Sarcoidosis	Radiation therapy
	Storage disease
	Hemochromatosis
	Glycogen storage diseases

to transmit a palpable ventricular impulse due to a calcified pericardium). Wheras, an audible S3 or S4 and prominent PMI are more likely to indicate restriction. Pulsus paradoxus is usually absent but is seen occasionally in CP cases involving pericardial effusion, such as effusive-CP.

Chest Radiography and Electrocardiography

Pericardial calcification is often seen on chest X-ray and is indicative of CP; however, it is not seen in all cases. Mild cardiomegaly due to atrial (rather than ventricular) enlargement is seen in cases of restrictive cardiomyopathy. Electrocardiography (ECG) findings, such as atrial fibrillation and repolarization abnormalities, are often seen in both conditions, while LV hypertrophy, low voltage QRS, and conduction abnormalities can signify the presence of restriction.

Echocardiography (TTE)

The multimodality aspects of echocardiography make it an essential tool in establishing a diagnosis of CP or restrictive cardiomyopathy. The ability to obtain both anatomic and hemodynamic information is useful in the context of the other diagnostic information to help make the diagnosis.

2D and M-Mode

Echocardiography can be used to image the pericardium. However, echocardiography is not the most sensitive test for identifying pericardial thickening as not all

cases of constriction will show a thickened or calcified pericardium since the thin visceral layer may become scarred and lead to constrictive physiology. 2D echocardiography is also useful in assessing atrial and ventricular cavity sizes as well as in characterizing the myocardium. Depending on the etiology, different morphological characteristics can be present, such as thickened myocardium with speckling or a granular pattern as found in amyloidosis. In restrictive cardiomyopathy, increased bi-atrial enlargement (less so in CP) can be seen on echocardiography along with a tendency for inter-atrial septal bulging due to increased pressure in the left atrium (LA) as compared to the RA. The characteristic findings of CP on echocardiography are abnormal septal motion ("septal bounce"), myocardial tethering, as well as IVC and hepatic vein plethora. The septal bounce is a result of respirophasic changes in diastolic flow into the LV and RV and underfilling of the LV as filling rapidly stops due to the rigid pericardium. M-mode can also be used to further investigate for constriction. Although M-mode is not diagnostic for CP, absence of certain key findings, such as abnormal septal motion, early pulmonic valve opening (due to rapid RV diastolic pressure increase), and an inspiratory increase in systemic venous return, may help to rule out the diagnosis. Figure 10.1 illustrates the M-mode findings in CP as well as some of the other hemodynamic findings discussed later in this section.

Doppler Echocardiography and Tissue Doppler Imaging

Information obtained from Doppler echocardiography has been vital in making the diagnosis of CP. The addition of tissue Doppler imaging (TDI) information (mitral annular velocities) has helped to improve the overall sensitivity of echocardiography in the diagnosis of CP while also distinguishing cases of CP from restriction. Doppler has been beneficial by allowing for a non-invasive hemodynamic assessment. Specifically it looks at ventricular filling (mitral and tricuspid inflow velocities), pulmonary and hepatic venous flow, and especially the respirophasic changes brought about by CP and restriction in these parameters. The respiratory variation of diastolic inflow velocities across both the mitral and tricuspid valve (*E* velocity) is different in CP and restriction and can provide compelling evidence for either diagnosis while ruling out other processes. In CP, the mitral *E* velocity can decrease between 25 and 40% with inspiration (due to intrathoracic-intracardiac disassociation) and the tricuspid inflow velocity is notably exaggerated; these changes reverse with expiration (see Fig. 10.1). In restriction, the mitral *E* velocities vary with respiration but to a much lesser degree (usually less than 10%). These findings can be affected by preload conditions in the LA; an increase in left atrial pressure will diminish the variation with respiration, while volume depleted states will exaggerate it. Pulmonary and hepatic venous flows represent left and right-sided filling and are also another important measurement in distinguishing constrictive and restrictive physiology. Pulmonary vein systolic flow (*S* wave) is diminished and diastolic flow (*D* wave) is increased irrespective of respiration in restriction. In CP, however, there is an increase in both systolic and diastolic flow during expiration (as compared to blunted

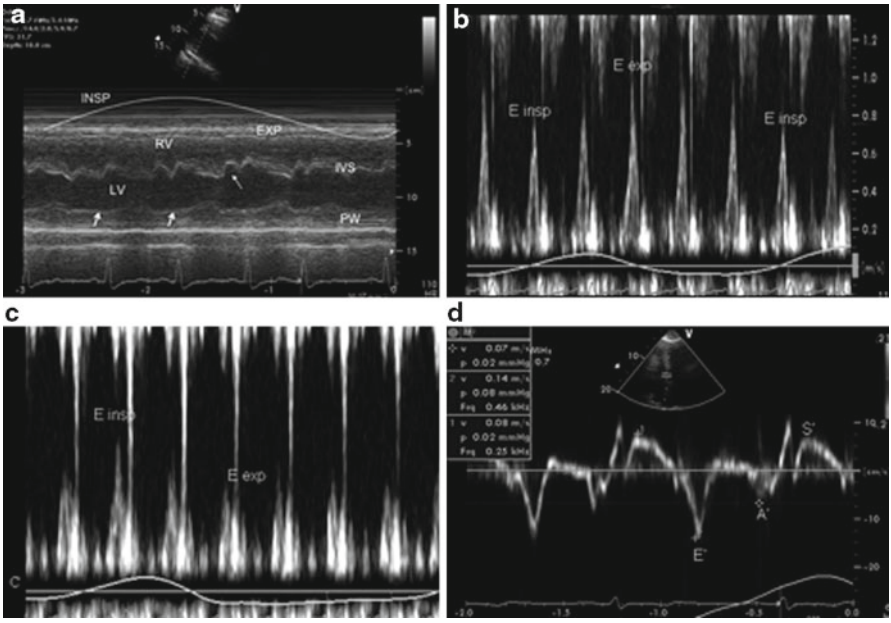

Fig. 10.1 Key M-mode and Doppler findings in constrictive pericarditis. (**a**) M-mode recording in the parasternal long-axis view showing a respiratory shift of the interventricular septum toward the left ventricle with inspiration and toward the right ventricle with expiration as a result of exaggerated ventricular interdependence. *Arrow* denotes the early diastolic septal bounce, typically seen in constrictive pericarditis. There is flattening of the posterior left ventricular wall during diastole (*white arrows*). (**b**) Pulsed wave Doppler echocardiography of the mitral valve with simultaneous respirometry. Constrictive pericarditis is characterized by dissociation of intrathoracic and intracardiac pressures, resulting in an increase in diastolic driving pressure into the left ventricle with expiration, and a decrease with inspiration. This leads to marked (>25%) respiratory changes of early mitral inflow velocity (*E*). (**c**) Tricuspid inflow velocity, showing the opposite changes. Tricuspid valve early diastolic velocity *E* increases with inspiration and decreases with expiration. (**d**) The early diastolic septal mitral annular velocity *E′* (in this case 14 cm/s) is usually increased in patients with constriction because diastolic filling occurs predominantly by longitudinal relaxation. However, adherence of the pericardium to the basolateral wall may occasionally inhibit normal or decreased motion of the lateral mitral annulus. *A′* indicates late diastolic mitral annular velocity; *E′* early diastolic mitral annular velocity; *EXP* expiration; *INSP* inspiration; *IVS* interventricular septum; *LV* left ventricle; *PW* posterior wall; *RV* right ventricle; *S′* systolic mitral annular velocity. (From Verhaert D, Gabriel RS, Johnston D, et al. The role of multimodality imaging in the management of pericardial disease. Circ Cardiovasc Imaging. 2010;3:333–43)

S and *D* during inspiration) which is a distinguishing feature. Hepatic vein flows, designated by *S* and *D* waves, as well as AR wave (atrial systole) and VR wave (ventricular systole), can also be used to further identify patients suspected of having CP or restriction. Normal patients will have a more prominent *S* wave as compared to the *D* wave—however, little to no respiratory variation is noted. In those with CP, there is a significant increase in the diastolic flow (*D* wave) during inspiration and marked blunting during expiration with diastolic flow reversal (notable

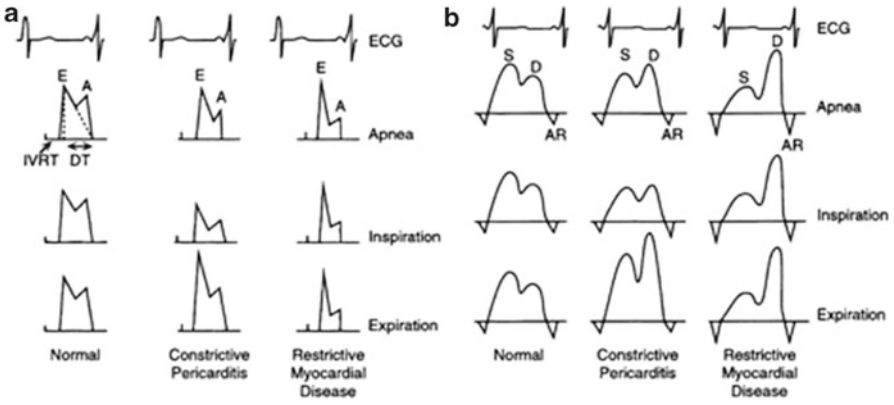

Fig. 10.2 Left ventricular inflow velocities (**a**) and pulmonary venous flow (**b**) during different phases of respiration

by an increase in AR and VR). Restriction patients have an increased diastolic flow (*D* wave) as compared to *S* wave and no respiratory variation is noted. Figures 10.2 and 10.3 demonstrate the changes seen in CP and restriction at different points in the respiratory cycle in the MV and TV inflow, as well as hepatic and pulmonary vein flows.

TDI and mitral annular velocities have become an integral part of the diastology assessment as well as in the diagnosis of CP and restriction. The mitral annular velocity (E') is measured at the septum and lateral annulus—both of which give information regarding the motion of the annulus with respect to the axis of measurement (i.e., cursor line). These measurements give information about myocardial relaxation and longitudinal motion of the heart, both of which are affected in CP and restriction. In cases with abnormal relaxation (restriction), tissue Doppler velocities are predictably reduced ($E' < 8$ cm/s). In pure CP (no myocardial involvement), the mitral annulus velocity can be normal or mildly elevated ($E' > 12$ cm/s). This is due to limited lateral expansion of the heart during filling due to pericardial encasement resulting in a compensatory increase in longitudinal movement to accommodate filling. Figures 10.1 and 10.4 both show mitral annular tissue Doppler velocities in CP and restriction. Also, in patients without pericardial disease, there is a concordant relation between E/E' (mitral inflow velocity over mitral annular velocity) and LV filling pressure. The term "annulus paradoxus" has been used to describe the inverse relationship between E/E' and LV filling pressures on the left side of the heart (both LV end diastolic pressure and PCWP) as a diagnostic criteria for CP. The term "annulus reversus" has also been used to describe another tissue Doppler property of CP that relates to the medial and lateral annular velocity (E'). In patients without pericardial disease, the lateral annular velocity is noted to be higher than the medial annular velocity. In CP, this relationship reverses, and medial annular velocity is greater than the lateral velocity, hence the term "annulus reversus."

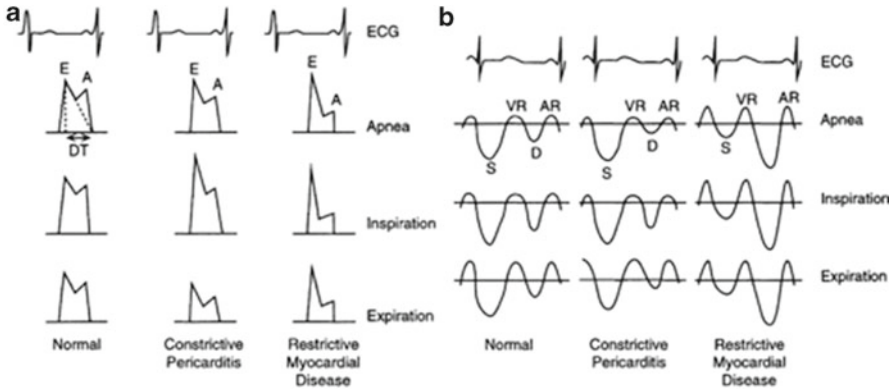

Fig. 10.3 Right ventricular inflow velocities (**a**) and hepatic venous flow (**b**) during different phases of respiration

Transesophageal Echocardiography

Given some of the limitations of TTE, transesophageal echocardiography (TEE) is can be used in situations where TTE is non-diagnostic or image quality is affected due to habitus or positioning. TEE can be used to image the pericardium to assess thickness and areas of adherence, as well as to obtain higher fidelity Doppler signals through the MV/TV (*E* velocity) and pulmonary vein flows. Often TEE evaluation is useful as an adjunctive modality since it is better able to image the posterior aspect of the heart and improve the accuracy of the overall assessment

Computed Tomography and Magnetic Resonance Imaging

Computed tomography (CT) and magnetic resonance imaging (MRI) offer higher resolution imaging and additional information as compared to echocardiography in the evaluation of CP and restrictive cardiomyopathy. CT can assess pericardial thickening (>4 mm) and calcification better than TTE or TEE; though the absence of either does not rule out CP. It also offers information regarding IVC volume status, as well as ventricular and septal contours associated with constriction. In patients with a prior history of cardiothoracic surgery, CT is useful in assessing the location of important vascular structures prior to surgery as well as assessing for any lung injury/entrapment (in cases of radiation exposure).

Gated MRI provides better visualization and resolution of the pericardium than either CT or echocardiography. CT still offers a better assessment of pericardial calcification, but MRI is superior when evaluating for pericardial inflammation,

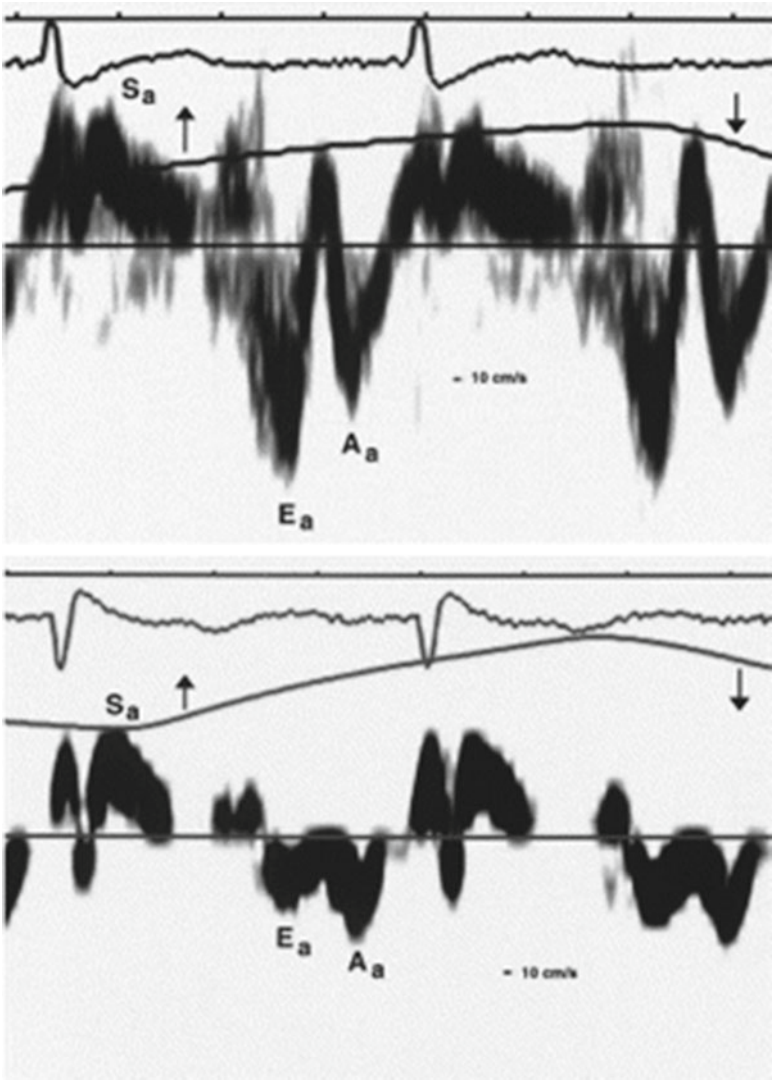

Fig. 10.4 Mitral annular velocities in constrictive pericarditis and restrictive cardiomyopathy. Representative tracings of the tissue Doppler echocardiographic velocities in the longitudinal axis in a patient with constrictive pericarditis (*top*) and a patient with restrictive cardiomyopathy (*bottom*) with respiratory monitoring with inspiration (*up-arrow*) and expiration (*down-arrow*). Note the peak systolic velocities are similar in both patients (10 cm/s), but a marked difference in early diastolic longitudinal axis velocities E_a was noted for the patient with constrictive pericarditis (15 cm/s) compared with the patient who had restrictive cardiomyopathy (5 cm/s). (From Rajagopalan N, Garcia MJ, Rodriguez L, et al. Comparison of new Doppler echocardiographic methods to differentiate constrictive pericardial heart disease and restrictive cardiomyopathy. Am J Cardiol. 2001;87(1):86–94)

small pericardial effusions, and myocardial tethering as well as resolving hemodynamic correlates such as IVC plethora and abnormal septal motion.

Catheterization/Hemodynamic Assessment

Right and left heart catheterization has been used in the past as the gold standard in distinguishing between restriction and CP. Improvements in non-invasive imaging have helped in increasing the early diagnosis of CP and restriction. Although there are many similar hemodynamic characteristics in CP and restriction, certain unique findings, if present, can help to clarify the diagnosis.

Hemodynamic findings often seen in patients with CP are increased RA pressure (due to adherent pericardium around RA preventing expansion), Kussmaul's sign (usually present), as well as prominent *x* and *y*-descents of RA pressure tracings (due to rapid atrial emptying and underfilled RV). The presence of an increased RV end-diastolic pressure (usually greater than or equal to one third of the RV systolic-pressure) is due to constraint of the RV leading to higher filling pressure. Constriction is generally not known to cause pulmonary hypertension, thus the RV systolic pressure is not affected. The "dip-and-plateau" (square-root) sign is seen in the RV and LV pressure tracings as a result of rapid early diastolic flow (dip) and diastasis once pressure equalization occurs (plateau) during mid and late diastole. Another key feature is found in the diastolic (plateau) pressures of the LV and RV, which equalize due to the rigid non-elastic pericardium, as shown in Fig. 10.5. This finding is relatively common in patients who undergo catheterization and have constriction—however, in some patients it is only seen on inspiration (due to increased systemic venous return). Lastly, RV and LV systolic pressures exhibit an inverse relation as a result of ventricular interdependence. With inspiration, the LV systolic pressure falls and the RV systolic pressure rises and vice versa with expiration. Patients with restrictive cardiomyopathy will have ventricular concordance. The difference in hemodynamic findings is illustrated in Fig. 10.6. To further quantify this hemodynamic difference—a systolic area index can be calculated with the use of commercially available software to calculate the area under each (LV and RV) hemodynamic curve with respiration. A ratio RV:LV area during inspiration divided by the ratio during expiration results in the systolic area index. An index of greater than 1.1 has been shown to have 97% sensitivity in predicting patients with CP. The salient features as described in this section of CP and restriction are shown in Table 10.2.

Respirometer/Dual Transducer

When performing a constriction study in the catheterization laboratory—a few key steps need to be taken to ensure that the most information is derived from the study. Given the importance of the pressure measurements and their relation to respirophasic changes—it is important to ensure that the transducer is level with the RA. This approximation can be difficult depending on the habitus of the patient—however, it

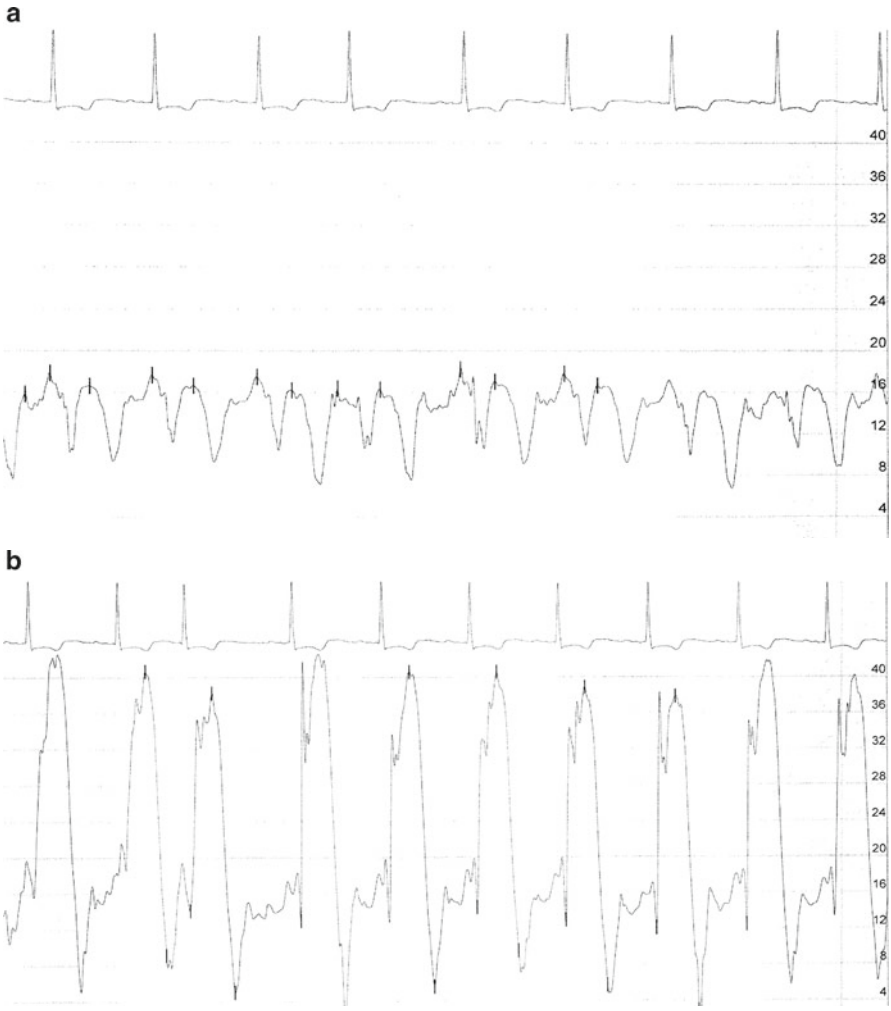

Fig. 10.5 (**a**, **b**) Combination figure showing dip/plateau and M/W sign in RA. (**a**) RA tracing with typical M (or W) pattern. (**b**) RV tracing with dip and plateau feature. Equalization of pressure also noted in both panels as average pressure is ~15 mmHg in both chambers

is an important step in ensuring the fidelity of the hemodynamic measurements. Another necessary part of the procedure is a dual-transducer setup so that simultaneous pressures can be obtained and super-imposed upon one another. Sequential measurements can be affected by respiratory patterns as well as rhythm changes (atrial fibrillation, or extra atrial/ventricular beats)—hence it is paramount that both the LV and RV pressures (as well as pulmonary capillary wedge pressure [PCWP] and LV pressures) are measured simultaneously. Lastly, a respirometer is required to help delineate inspiration and expiration when assessing for respirophasic changes and ventricular discordance.

Table 10.2 Key findings in constrictive pericarditis and restrictive cardiomyopathy

Evaluation	Constrictive pericarditis	Restrictive cardiomyopathy
Physical exam	Kussmaul's sign	Kussmaul's sign (rare)
	Pericardial knock	S4 (early) and S3 (late presentation)
	Regurgitant murmurs present	Prominent apical impulse
Echocardiography	Pericardial thickening	Large atria
	Pericardial effusion (may be present)	Small LV cavity
	Diastolic bounce	Thickened wall thickness (usually present)
		Speckling of myocardium (amyloid)
Doppler		
Tricuspid inflow	Inspiratory increase in TV *E* wave, peak velocity	Minimal respiratory variation in *E* wave
	Expiratory decrease in *E* wave and peak velocity	No change in peak velocity with respiration
		E/*A* ratio ≥2
Mitral inflow	Decrease in *E* wave with inspiration	No respiratory variation in *E* wave
	Increase in *E* wave with expiration	*E*/*A* ratio ≥2
Tissue Doppler	High filling velocity (≥8 cm/s)	Low filling velocity (<8 cm/s)
Cardiac catheterization	Dip and plateau	Dip and plateau
	Inspiratory increase in RV systolic pressure	Pulmonary hypertension (RVSP > 50 mmHg)
	Inspiratory decrease in LV systolic pressure	LVEDP may be equal to or greater than RVEDP
	Opposite change with expiration	
	Diastolic equalization of pressure (RVEDP/LVEDP)	

Modified from Kushwaha SS, Fallon JT, Fuster V. Restrictive cardiomyopathy. N Engl J Med. 1997;336(4):267–76

Fig. 10.6 (**a**, **b**) Ventricular discordance with respirophasic variation of RV and LV pressures and ventricular concordance. LV and RV high-fidelity manometer pressure tracings from two patients during expiration and inspiration. Note that both patients have early rapid filling and elevation and end-equalization of the left ventricular (LV) and right ventricular (RV) pressures at end expiration. (**a**) A patient with surgically documented constrictive pericarditis. During inspiration, there is an increase in the area of the RV pressure curve (*orange shaded area*) compared with expiration. The area of the LV pressure curve (*yellow shaded area*) decreases during inspiration as compared with expiration. (**b**) A patient with restrictive myocardial disease documented by endomyocardial biopsy. During inspiration, there is a decrease in the area of the RV pressure curve (*orange shaded area*) as compared with expiration. The area of the LV pressure curve (*yellow shaded area*) is unchanged during inspiration as compared with expiration. (**c**) An RV and LV hemodynamic tracing showing ventricular discordance in a constriction patient. (From Talreja DR, Nishimura RA, Oh JK, Holmes DR. Constrictive pericarditis in the modern era: novel criteria for the diagnosis in the cardiac catheterization laboratory. J Am Coll Cardiol. 2008;51(3):315–9)

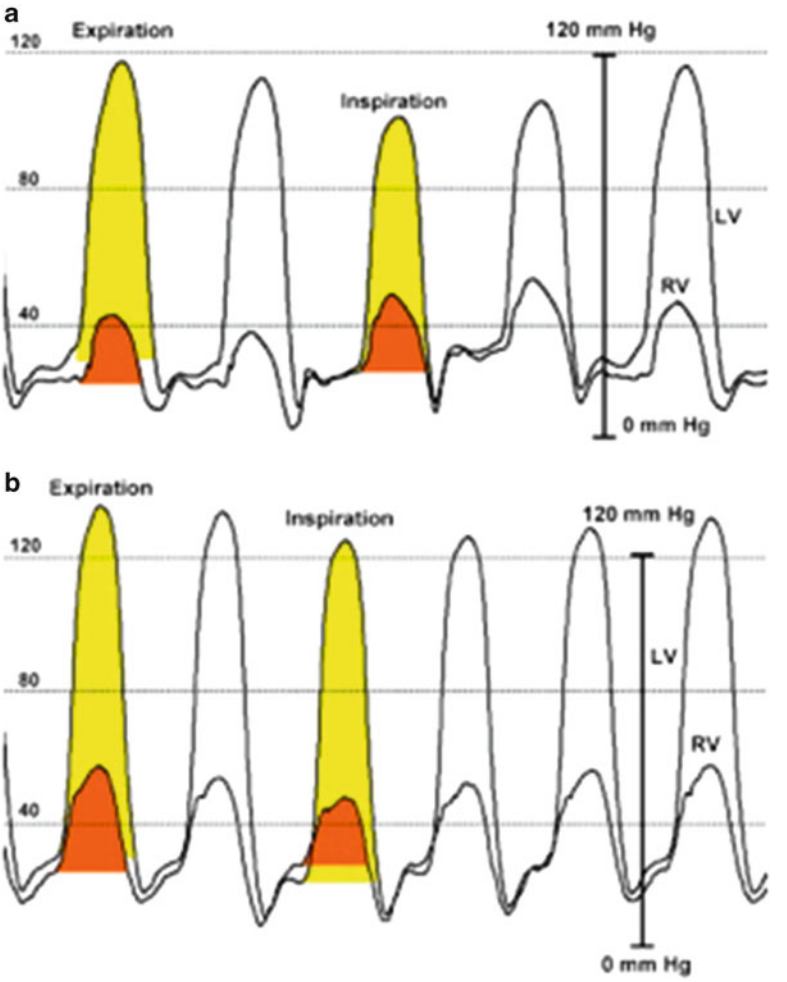
a
120
Expiration
120 mm Hg
Inspiration
80
LV
RV
40
0 mm Hg
b
Expiration
Inspiration
120 mm Hg
120
LV
80
RV
40
0 mm Hg

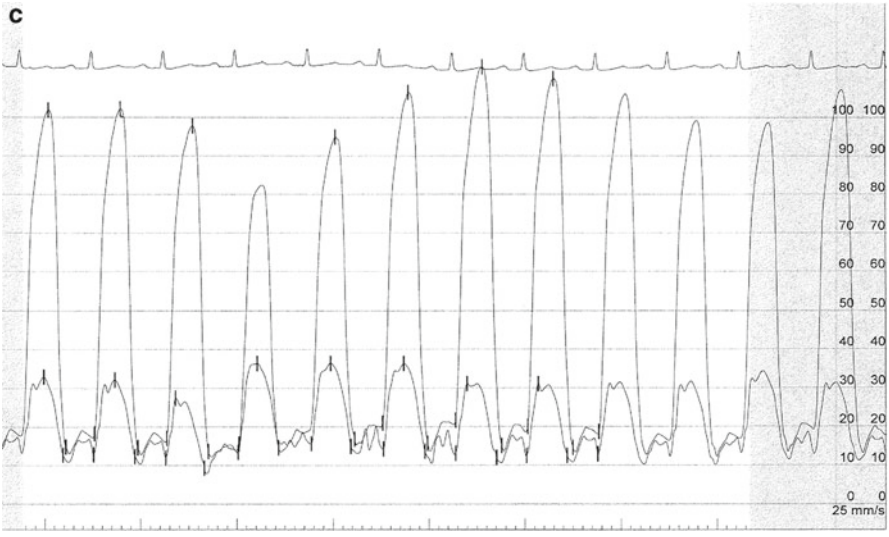
c
100 100
90 90
80 80
70 70
60 60
50 50
40 40
30 30
20 20
10 10
0 0
25 mm/s

Preload/RA Pressure

The loading conditions of the RA are important when performing a constriction study. Often patients are on maintenance diuretics for symptom relief; this can affect loading conditions in the RA, especially if the RA pressure is less than 15 mmHg, thus masking some of the hemodynamic features of CP. If during initial assessment the RA pressure is found to be less than 15 mmHg, a 1-L warmed saline infusion can be initiated to help increase the RA pressure and draw out some of the more subtle findings that may not be initially apparent. When the filling pressures are low, the chambers are not distended enough to come in contact with the rigid pericardium and be constrained. However, a low RA pressure is not the only situation that can affect diagnostic workup for constriction. A markedly elevated RA pressure can also mask some of the subtle hemodynamic findings and often these patients require diuresis to elucidate a pattern of constriction on their workup.

Rhythm and Trans-Venous Pacing

The importance of sinus rhythm in hemodynamic assessment cannot be understated. Beat-to-beat variability will reduce the overall efficacy of the study and often a long strip of measurements needs to be taken to show the general trends associated with respiration. Patients who are in atrial fibrillation or atrial flutter may benefit from temporary placement of a transvenous pacemaker to regularize the rhythm as well as the hemodynamic tracings. Given the preponderance of atrial fibrillation in this group of patients, this is an important part of the optimal assessment to make the catheterization as high yield as possible.

Transjugular Right Ventricular Biopsy

Although biopsy is not currently considered as a routine part of the workup in CP and restriction, if all other testing is inconclusive and a strong suspicion for primary or secondary restrictive cardiomyopathy exists—it may be considered to help establish a diagnosis.

Clinical Examples

Calcific Constrictive Pericarditis

A 56-year old male with a history of increasing dyspnea on exertion and progressive heart failure symptoms (lower extremity edema and orthopnea) was referred for evaluation. His medical history is significant for non-Hodgkin's lymphoma which was treated

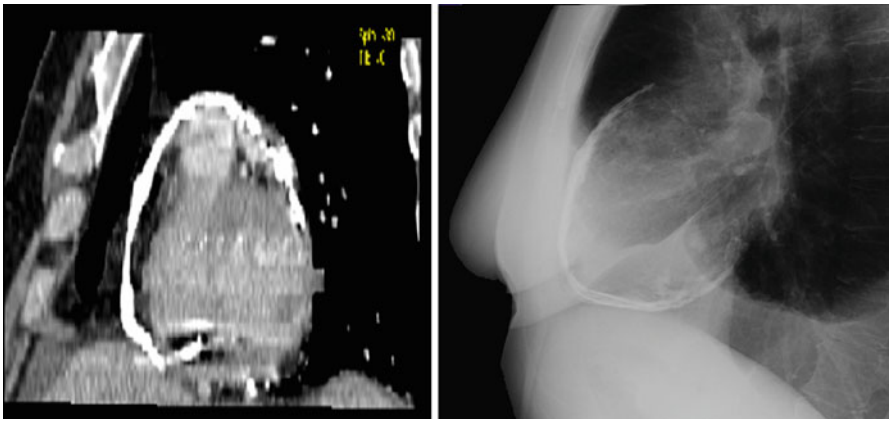

Fig. 10.7 Calcific pericarditis findings on cardiac CT and CXR

with chemotherapy alone (no radiation) and achieved remission approximately 10 years ago. On physical exam, he has pitting LE edema, elevated JVP, and a pericardial knock. Chest radiography (CXR) showed no pulmonary edema or effusion but was significant for scattered calcification of the pericardium (see Fig. 10.7). Echocardiogram showed preserved LV and RV function, moderate pericardial thickening with associated focal calcification, diastolic septal bounce, and IVC plethora. Mitral valve and hepatic vein flows are noted to have respiratory variation and increased tissue Doppler velocities are noted. Imaging of the chest via MRI showed tethering of the pericardium to the RA and heavy calcification in the pericardium. Cardiac catheterization showed normal coronaries and hemodynamic finding of diastolic equalization of pressures in both the LV and RV. The patient was referred for pericardiectomy and had marked improvement in his symptoms. Although radiation is usually considered the offending agent in the development of CP—the development of heart failure symptoms and calcification on echocardiogram prompted a workup leading to surgery.

Restriction (Amyloid)

A 76-year-old male initially presented with new onset atrial fibrillation and dyspnea at rest. Echocardiogram performed showed a depressed ejection fraction (35%), marked biatrial enlargement with severe (stage IV) diastolic dysfunction, moderate pulmonary hypertension, and a granular pattern of the myocardium. The patient was treated with beta-blockers and diuretics presumptively, while serum and urine electrophoresis (negative) and bone marrow biopsy were pending. The biopsy was significant for plasma cell population and congo red staining consistent with amyloidosis. Given the diagnosis of systemic amyloidosis and severe diastolic dysfunction, the patient was presumed to have cardiac amyloid and

started on treatment for amyloidosis with prednisone and IV melphalan. Due to the chronic nature of the condition and the late presentation as well as lack of efficacious treatment options—the patient did not respond to therapy and continued to deteriorate over the next few months. Cardiac amyloidosis usually presents later in life with an insidious onset and often is diagnosed as a result of key echocardiographic features. In this case further testing including CT, MRI, or catheterization was not required to make the diagnosis.

Effusive-Constrictive Pericarditis

A 61-year-old male presents with a history of intermittent chest pain that was associated with fever. The patient was subsequently diagnosed with viral myocarditis and treated conservatively with anti-inflammatory medications. He was doing well until 5 years ago when he noted a gradual decrease in his exercise tolerance and mild lower extremity swelling. An echocardiogram was performed and was normal. A repeat episode of chest pain occurred 2 months later. The patient was hospitalized and referred for stress testing which was also normal. He improved somewhat with anti-inflammatory medications and was discharged home. After improving mildly, the patient began to notice a dramatic decline in his exercise tolerance and unremitting heart failure symptoms. He was seen and noted to have elevation of his JVP as well as pericardial friction rub. ECG was consistent with acute pericarditis and echocardiography showed a moderate-sized pericardial effusion and normal ventricular function. Erythrocyte sedimentation rate (ESR) and high-sensitivity C-reactive protein (hs-CRP) are laboratory markers for pericarditis and both were elevated as well. After pericardiocentesis—patient did not have significant improvement in symptoms. The patient was treated with sustained, higher dose anti-inflammatory medications and was able to achieve remission of his pericarditis. Effusive-CP usually is a combination of both pericardial effusion and mild constriction associated with ongoing pericarditis. The removal of the pericardial effusion often does not improve symptoms as there is a component of pericardial constriction from the visceral layer of the pericardium. Often, longer courses of anti-inflammatory medications including prednisone are required to achieve remission and abate the process of inflammation and scarring.

Pearls of Assessment

When assessing a patient who may have CP or restriction, a focused history and physical with emphasis on symptoms as well as clues or signs that suggest either diagnosis is essential. Basic chest X-ray and ECG are also useful in the initial workup to assess for cardiomegaly and pericardial calcification as well as voltage pattern for possible restrictive cardiomyopathy. Non-invasive imaging is the mainstay of the workup and transthoracic or TEE with respirometer to assess for pericardial thickness, as well as changes in

filling velocity and pressures is usually the next step. Depending on the echocardiographic results and suspicion for a pericardial or myocardial process, further non-invasive imaging including either a cardiac CT or MRI can be useful to obtain more information than can be provided by echocardiography (pericardial inflammation, myocardial assessment, etc.). If the diagnosis is still elusive, cardiac catheterization with a focus on the hemodynamic findings of "dip-and-plateau" on RV and LV pressure tracings as well as ventricular discordance and respiratory variation point to a specific diagnosis of CP. Treatment of symptoms with diuretics is usually a temporizing measure and often patients require surgical pericardiectomy for symptomatic relief.

Review Questions

1. Which of the following is not a cause of pericardial constriction?

   A. Infection (bacterial or viral)
   B. Prior cardiac surgery
   C. Mantle radiation for lymphoma
   D. Obesity
   E. None of the above

   D. Obesity is not an established cause of constrictive pericarditis. It has been known to cause hemodynamic findings consistent with constriction (termed "pseudoconstriction").

2. Which of the following features are seen in constriction?

   A. Elevated right-sided diastolic pressures
   B. Square-root (dip-plateau) pattern in LV/RV pressure waveforms
   C. M (or W) pattern on right atrial waveform
   D. Steep or rapid *y*-descent
   E. All of the above

   E. All of the findings listed above are typically seen in constrictive pericarditis.

3. True or False: respiratory variation of intracardiac pressures is a hallmark of restrictive cardiomyopathy?
   False: respiratory variation is not prominent in restrictive cardiomyopathy since intrathoracic pressure is able to be transmitted to the cardiac chambers. Whereas in constriction, respirophasic changes are seen in both the left- and right-sided hemodynamics.

4. Which of the following echocardiographic findings is not consistent with restrictive physiology?

   A. Large atria
   B. Blunted *S*/*D* ratio in pulmonary and hepatic vein flows

C. Low velocity early filling (<8 cm/s) on TDI
D. Decreased mitral inflow velocity (*E* wave) with inspiration
E. A and C

D. Decreased mitral inflow (*E* wave) is found in constrictive pericarditis—whereas in restrictive cardiomyopathy, mitral inflow is not changed with respiration. The other findings are all seen in restrictive cardiomyopathy.

5. Which of the following is not part of the optimal assessment of constriction by cardiac catheterization?

A. Using a temporary pacemaker to regularize rhythm
B. Saline bolus to increase RA pressure >15 mmHg
C. Dual-transducer system with simultaneous RV/LV measurement
D. RV biopsy to assess for restrictive cardiomyopathy
E. B and C

D. RV biopsy is not considered to be part of the normal workup for constrictive pericarditis. It can be utilized in difficult cases after performing a full diagnostic workup to help distinguish between constrictive pericarditis and restrictive cardiomyopathy.

Suggested Reading

1. LeWinter M. Pericardial diseases. In: Libby P, Bonow RO, Mann DL, Zipes DP, editors. Braunwald's heart disease: a textbook of cardiovascular medicine. 8th ed. Philadelphia, PA: Saunders; 2008. p. 1829–52.
2. Jurrens TL, Ammash NM, Oh JK. Pericardial diseases: constriction and pericardial effusion. In: Klein AL, Garcia MJ, editors. Diastology: clinical approach to diastolic heart failure. 1st ed. Philadelphia, PA: Saunders; 2008. p. 301–12.
3. Klein AL, Asher CR. Diseases of the pericardium, restrictive cardiomyopathy, and diastolic dysfunction. In: Topol EJ et al., editors. Textbook of cardiovascular medicine. 3rd ed. Philadelphia, PA: Lippincott, Williams & Wilkins; 2006. p. 420–59.
4. Troughton RW, Asher CR, Klein AL. Pericarditis. Lancet. 2004;363:717–27.
5. Schewefer M, Aschenbach R, Heidemann J, et al. Constrictive pericarditis, still a diagnostic challenge: comprehensive review of clinical management. Eur J Cardiothorac Surg. 2009;36:502–10.
6. Choi JH, Choi JO, Ryu DR, et al. Mitral and tricuspid velocities in constrictive pericarditis and restrictive cardiomyopathy: correlation with pericardial thickness on computed tomography. JACC Cardiovasc Imaging. 2011;4(6):567–75.
7. Zurick AO, Bolen MA, Kwon DH, et al. Pericardial delayed hyperenhancement with CMR imaging in patients with constrictive pericarditis undergoing surgical pericardiectomy: a case series with histopathological correlation. JACC Cardiovasc Imaging. 2011;4(11):1180–91.
8. Klein AL, Dahiya A. Annular velocities in constrictive pericarditis: annulus and beyond. JACC Cardiovasc Imaging. 2011;4(6):576–9.

Chapter 11
Valvular Heart Disease

Amar Krishnaswamy and Brian P. Griffin

Introduction

The diagnosis and management of valvular heart disease is challenging and requires a knowledge of the relevant historical clues, appreciation of salient physical exam findings, and the ability to critically interpret imaging and invasive hemodynamic data. This chapter will focus on diagnosis of the valve disorders most frequently encountered in the care of patients on the cardiac ward.

Aortic Stenosis

Case Presentation

The patient is a 78-year-old man with a history of hypertension, hyperlipidemia, and percutaneous coronary intervention with drug-eluting stent to the mid-left anterior descending artery 4 years prior. He noted the development of exertional dyspnea over the past 6–12 months, as well as mild chest discomfort over the past 3 months that resolved with rest. Initially attributed to "old age," he finally decided to seek medical attention due to progression of his symptoms.

Salient physical examination findings included mild hypertension (BP 145/90 mmHg) and a normal heart rate (70 bpm). The PMI was not displaced and an S4 gallop was appreciated. A 2/6 systolic crescendo/decrescendo murmur was heard at the upper sternal border peaking late in systole and radiating to the carotids bilaterally. The carotid artery upstrokes were mildly delayed and weak.

A. Krishnaswamy • B.P. Griffin, M.D. (✉)
Department of Cardiovascular Medicine, Cleveland Clinic,
Cleveland, OH, USA
e-mail: krishna2@ccf.org; griffib@ccf.org

A.T. Askari et al. (eds.), *Cardiovascular Hemodynamics: An Introductory Guide*,
Contemporary Cardiology, DOI 10.1007/978-1-60761-195-0_11,

Given the symptoms and physical exam findings, transthoracic echocardiography (TTE) was performed. The TTE revealed normal left ventricular function with moderate concentric hypertrophy, a moderately thickened and calcified aortic valve, and severe aortic stenosis with peak and mean gradients of 85 mmHg and 50 mmHg, respectively. With a diagnosis of severe, symptomatic aortic stenosis, the patient was referred for coronary angiography in anticipation of open-heart surgery. Angiography revealed only mild coronary artery disease (CAD) and a patent stent in the mid LAD, and the patient went to have uneventful valve replacement with an aortic bioprosthesis.

Epidemiology and Pathophysiology

Aortic stenosis (AS) is present in almost 5% of individuals over the age of 75 years [1]. AS may develop due to a congenital valve disorder (unicuspid or bicuspid valve), as the result of rheumatic valvular heart disease, as a complication of chest radiation, or most commonly due to degenerative ("senile") thickening and calcification. Over time, AS causes increased pressure on the left ventricle (LV) and leads to a chronically increased afterload state. In order to compensate, the ventricle hypertrophies. Due to increased LV mass and worsening diastolic filling mechanics, diastolic dysfunction ensues. With worsening and long-standing stenosis, LV systolic function eventually falls. Furthermore, impaired LV diastolic and/or systolic function may lead to pulmonary hypertension due to left-sided heart disease. Since senile AS shares many risk factors with CAD, the clinical presentation may reflect progressive coronary stenosis in these patients in addition to increased myocardial oxygen demand due to the valvular stenosis.

Patients with aortic stenosis may live for years with a "known murmur" that is clinically silent, especially in cases of bicuspid or rheumatic valve disease. It is estimated that valve area decreases by approximately 0.12 cm^2/year in patients with senile disease, providing a long period of asymptomatic disease [2]. On the other hand, the development of symptoms portends a grave prognosis: without treatment, angina, syncope, and heart failure are associated with a 50% mortality at 5 years, 3 years, and 2 years, respectively [3].

Physical Examination

The physical examination of patients with AS provides a number of characteristic findings. A systolic murmur is best heard in the aortic position (right upper sternal border) and radiates to the carotid arteries. As stenosis worsens, the peak of the murmur moves closer to the second heart sound (S2) since LV ejection across the valve requires a longer ejection time. With very severe disease, the S2 may be almost inaudible due to the proximity of the murmur's peak to the closing of the valve. With severe AS, a murmur mimicking mitral regurgitation may also be heard at the

apex, but does not radiate to the axilla; this is known as Gallivardin's phenomenon. Palpation of the pulse (preferably at the carotid arteries) in patients with severe AS reveals the characteristic slow ascent (*parvus*) and delayed (*tardus*) peak. Additionally, palpation of the pulses at the upper extremity may reveal a "brachioradial" delay in patients with severe AS that often presents prior to LV failure or clinical symptoms. Of note, the finding is subtle, with a measured delay of 53.5 ms [4]. An S4 gallop may be heard in the setting of left ventricular hypertrophy (LVH) and a stiffened ventricle.

An important differentiation to be made is between the murmur of AS and that of hypertrophic cardiomyopathy (HCM). In patients with AS, a reduction in preload (i.e., with the Valsalva maneuver or moving from squatting to standing) will reduce flow across the stenotic valve and therefore lessen the murmur. Conversely, a reduction in preload causes decreased filling of the LV cavity resulting in a smaller LVOT (left ventricular outflow tract) diameter and worsening SAM (systolic anterior motion) of the mitral valve, and therefore augments the murmur in patients with HCM.

Echocardiography

TTE is the cornerstone of AS assessment and provides information on left ventricular function, aortic valve morphology, degree of stenosis, and an assessment of pulmonary pressures. Rarely, transesophageal echocardiography (TEE) may be necessary for diagnosis if TTE images are limited, or for precise planimetry of the valve area (discussed below). In the early stages of AS, LV systolic function is preserved, with varying degrees of compensatory LVH. Over time, with LV stiffening, diastolic filling becomes more dependent upon atrial systole and diastolic dysfunction ensues. Eventually, the chronically after-loaded LV dilates and left ventricular systolic function declines.

The degree of valvular stenosis can be assessed both qualitatively and quantitatively. The presence of congenital disorders (i.e., unicuspid, bicuspid, etc.) is assessed in the parasternal long-axis (the valve does not coapt in the center-line or may have a "doming" appearance) and short-axis views (the number of cusps can be identified along with the presence of a "raphe"), as well as the degree of thickening and calcification. The short-axis view is also useful for performing planimetry of the aortic orifice.

Hemodynamic assessment of AS by TTE requires an assessment of the following: jet velocity, peak and mean gradients, and the dimensionless index (DI) (Table 11.1) [5]. Peak jet velocity gives a rough estimate of stenosis severity; velocity >4 m/s is considered severe. The peak gradient is calculated using the peak velocity via the Bernoulli equation ($\Delta P = 4v^2$). The mean gradient is calculated using the velocity time integral (VTI), which sums the velocities over an entire cardiac cycle and is provided by tracing the continuous wave Doppler aortic outflow envelope. The dimensionless index a ratio of the velocity (or VTI) in the LVOT to that in the aorta; a ratio <0.25 implies an aortic valve area (AVA) that is

Table 11.1 Echocardiographic evaluation of aortic stenosis severity

	Mild	Moderate	Severe
Peak jet velocity (m/s)	<3.0	3.0–4.0	>4.0
Mean gradient (mmHg)	<25	25–40	>40
Valve area (cm^2)	>1.5	1.0–1.5	<1.0
Dimensionless index	*	*	<0.25

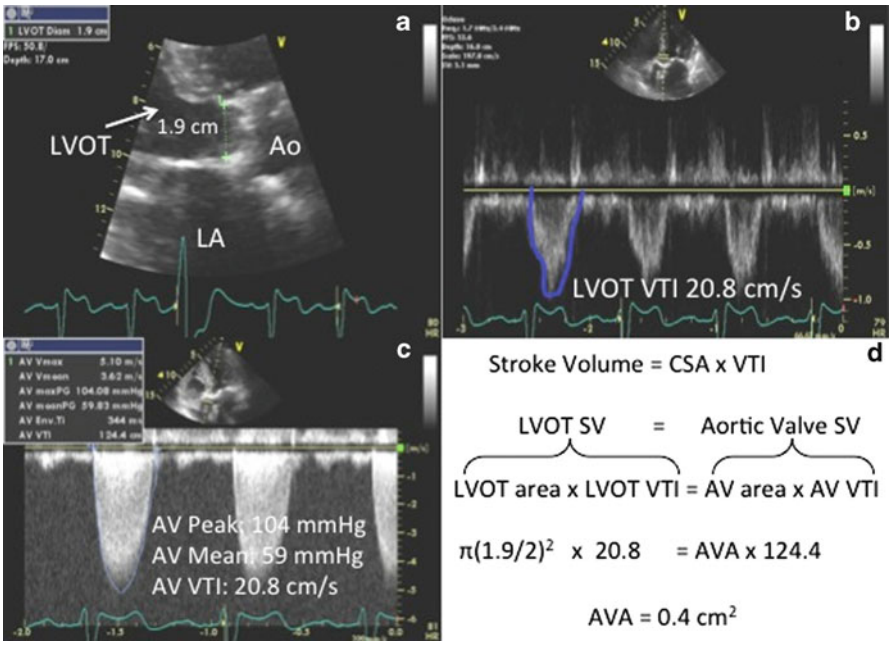

Fig. 11.1 Calculation of aortic valve area (AVA) using the continuity equation. Measurement of the left ventricular outflow tract (LVOT) diameter (**a**), velocity time integral (VTI) in the LVOT (**b**), and aortic valve (AV) VTI (**c**) is necessary to calculate the AVA (**d**)

<25% of the LVOT area. The DI is helpful in patients for whom LVOT diameter is difficult to measure.

Calculation of AVA may be performed by planimetry as above, or by using the continuity equation. The continuity equation makes the assumption that flow and volume are constant. Since Flow = Cross sectional area (CSA) × Velocity, the relationship can also be described as: Stroke volume = CSA × VTI, and since volume is constant the equation can be rearranged as: $A_{AV}V_{AV} = A_{LVOT}V_{LVOT.}$ Calculation of the AVA is demonstrated in Fig. 11.1. Common mistakes in calculation of the AVA include incorrect measurement of the LVOT diameter (underestimation of the LVOT leads to an underestimation of the AVA) or LVOT/AV outflow gradients.

Table 11.2 Possible outcomes of dobutamine stress echocardiography (DSE) in low-flow, low-gradient aortic stenosis

Dobutamine response	Diagnosis
Increase in CO and gradient	Contractile reserve present True AS
Increase in CO and AVA with constant/decreased gradient	Contractile reserve present Pseudo-AS
No response to DBA	No contractile reserve Indeterminate re: AS

CO Cardiac output; *AVA* aortic valve area; *AS* aortic stenosis; *DBA* dobutamine

Low-Flow, Low-Gradient Aortic Stenosis

Patients with chronic pressure overload from AS, CAD, or intrinsic myocardial dysfunction may present with depressed LV function and aortic stenosis with a low gradient. Low-flow/low-gradient (LF/LG) AS is defined as an LVEF <35%, mean gradient <30 mmHg, and AVA <1.0 cm^2. Evaluation of the true degree of AS in these patients presents a common clinical quandary, as patients may have truly severe AS or "functional" AS caused by poor leaflet excursion in the setting of a low cardiac output (pseudo-AS).

Dobutamine stress echocardiography (DSE) is a common diagnostic tool in this setting. With infusion of increasing doses of dobutamine (DBA; 5–20 μg), the stroke volume, peak velocity, mean gradient, and AVA are measured/calculated. An increase in SV >20% implies contractile reserve. Increases in peak velocity and/or mean gradient imply true AS; the increased flow across the valve is limited by intrinsic valve disease and results in higher gradients and does not simply cause increased leaflet excursion. An increase in AVA >0.3 cm^2 implies pseudo AS; increase in LVOT velocity is greater than the increase in AV velocity due to increased leaflet excursion, providing a higher calculated AVA. The potential outcomes of DSE and the clinical diagnosis are summarized in Table 11.2 [6].

For patients with pseudo-AS, treatment is directed toward the medical management of heart failure. Studies on AVR in patients with LF/LG true AS have shown that perioperative mortality is only mildly increased (5%) in patients with contractile reserve on DSE. On the other hand, patients with LF/LG true AS but without contractile reserve face a significant perioperative mortality (32%) [7]. However, survival thereafter is reasonable and improvement in ejection fraction is similar in both groups [8].

Cardiac Catheterization

Outside of the evaluation for CAD, cardiac catheterization in patients with AS is reserved for situations when the degree of symptoms and severity of AS are

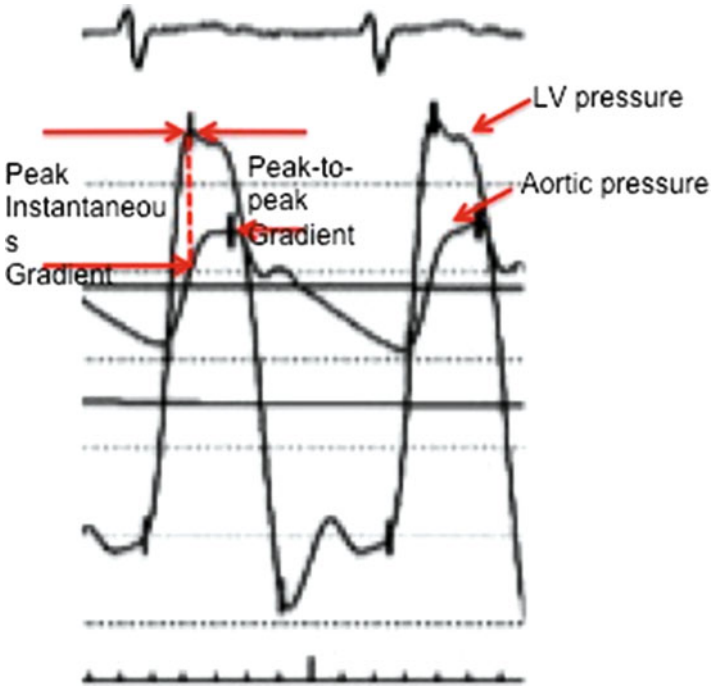

Fig. 11.2 Simultaneous LV and aortic pressure tracing. Peak-to-peak gradient is measured as the difference between peak LV and aortic pressures during cath; peak gradient by echocardiography is an instantaneous peak. Mean gradient is calculated as the average pressure difference between LV and aorta pressures (area between the curves)

contradictory based on noninvasive testing [5]. Catheterization may be used to measure intracardiac pressures, cardiac output, valve gradient, and calculate the AVA.

Historically, measurements of the valve gradient were taken by placing a catheter in the aortic root and another in the LV via transseptal puncture, but this is rarely performed now. Valve gradient may be measured with a dual-lumen pigtail catheter that simultaneously measures pressures in the LV and aorta, or by placing a catheter in the LV and then quickly pulling it back to the aortic root ("pullback gradient"). It should be noted that this "peak-to-peak" gradient is generally lower than the peak gradient obtained by Doppler echocardiography, which is sampled as the peak instantaneous velocity (Fig. 11.2). The peak-to-peak gradient correlates well to the mean gradient.

The valve area is usually calculated using the *Gorlin equation*:

$$\mathrm{AVA} = \mathrm{CO} \mid (\mathrm{HR} \cdot \mathrm{SEP} \cdot 44.3 \cdot \sqrt{\text{mean gradient}})$$

[CO : cardiac output; HR : heart rate; SEP : systolic ejection period]

Since the Gorlin method is dependent on flow across the aortic valve, patients with LF/LG AS will have a significantly underestimated AVA. In these cases, DBA infusion during catheterization may reveal pseudo-AS similar to that described during DSE above (increased cardiac output with increased AVA and stable or decreased gradient).

A simplification of the Gorlin equation is the *Hakki equation*, based upon the assumption that the (HR × SEP × 44.3) approximates one under normal conditions [9]:

$$\text{AVA} = \text{CO} \mid \sqrt{\text{mean gradient}}$$

For patients with a heart rate >100 bpm, the AVA obtained using the Hakki method should be divided by 1.35 for increased accuracy.

Aortic Regurgitation

Case Presentation

A 42-year-old man presented with progressive dyspnea over a 6-month period. He was quite active previously, running 3 miles every other day, but now required a break after just 2 miles due to dyspnea. He also noticed some dyspnea with walking the three flights of stairs to his apartment, which was new over the prior 1–2 months. He had not experienced orthopnea, but has had a few episodes of paroxysmal nocturnal dyspnea over the prior 3 months. He denied chest discomfort or lower extremity edema.

On physical examination, cardiac auscultation was significant for a long, decrescendo, holodiastolic murmur heard best at the left sternal border as the patient leaned forward. Palpation of the brachial pulse revealed a brisk and forceful upstroke and wide pulse pressure. Gentle pressure applied at the tip of the fingernails revealed a "to-and-fro" filling of the nailbeds.

TTE performed revealed a bicuspid aortic valve with fusion of the right and left coronary leaflets and with minimal calcification. There was mild anterior leaflet prolapse resulting in severe, posteriorly directed aortic regurgitation. The aortic root and ascending aorta were normal in size without evidence of dilation. LV systolic function and chamber size were normal.

Given a diagnosis of severe, symptomatic aortic regurgitation, the patient underwent pre-operative coronary angiography that revealed minimal atherosclerosis. He then underwent successful aortic valve repair.

Epidemiology and Pathophysiology

Aortic regurgitation (AR) is present in up to 12% of men and may complicate rheumatic valve disease, radiation valvular disease, or bicuspid aortic valve. Infective endocarditis may cause AR due to valve degeneration, leaflet perforation, or paravalvular leakage. Anorectic drugs, such as fenfluramine and phentermine ("fenphen"), may cause AR through a serotonin-mediated pathway that results in degenerative changes in valve morphology. Additionally, aortic pathology such as ascending dissection or aortic root dilation can cause malcoaptation of the valve and resultant AR. A rare cause of AR is the supracristal VSD, which can result in AR due to prolapse of the non-coronary leaflet.

Of the causes listed above, aortic dissection and endocarditis often cause acute severe AR. This is usually poorly tolerated from a hemodynamic perspective, primarily due to a degree of LV compliance that does not accommodate the massive increase in volume and leads to acute volume overload and diminished cardiac output. As a result, acute AR is usually a surgical emergency.

The degree of regurgitation is dependent on the diastolic pressure gradient between the aorta and LV, duration of diastole, size of the regurgitant orifice, and LV compliance. In chronic AR, compensatory LV cavity dilation, increase in LV compliance, and LV wall hypertrophy ensue to accommodate the increased filling and afterload. Maintenance of an adequate heart rate (i.e., judicious use of negative chronotropic agents) is also important to minimize diastolic regurgitation time. Together, these changes allow the LVEDP to stay relatively normal and stroke volume to increase. Patients may therefore remain asymptomatic for long periods of time and develop symptoms or LV dysfunction at an average of 4.3% per year [5].

It should also be noted that since diastolic pressure in the aorta is reduced in patients with AR, coronary perfusion pressure is also reduced. Patients may therefore develop symptoms of coronary insufficiency, even in the absence of flow-limiting coronary stenoses, due to decreased coronary flow and increased LV oxygen demand.

Physical Examination

In acute AR, the hallmark diastolic murmur of AR may not be appreciated as easily, since the aortic diastolic and LV diastolic pressures equalize rapidly, and patients are often quite tachycardic due to hemodynamic instability. This also highlights the importance of the judicious use of agents that decrease chronotropy (i.e., beta blockers, non-dihydropyridine calcium-channel blockers, etc.), as slower heart rates allow a longer period of regurgitation.

With chronic AR, however, the long-standing increase in LV volume and concomitant hypertrophy allow the ventricle to accommodate a long period of diastolic backflow through the regurgitant lesion, providing the classic auscultory diastolic murmur. The murmur is best heard at the aortic position (left sternal border) and may be more

Table 11.3 Physical findings in the peripheral examination of severe aortic regurgitation

Physical sign	Description
Corrigan's pulse ("Water Hammer pulse")	Rapid rise and fall of the arterial pulse
Duroziez's sign	"To-and-fro" murmur heard at the femoral artery elicited with femoral artery compression
Quincke's sign	Capillary pulsations at the nail bed elicited by gentle compression of the distal nail
de Musset's sign	Bobbing of the head
Mueller's sign	Pulsation of the uvula
Hill's sign	Lower extremity BP>upper extremity BP
Rosenbach's sign	Pulsatile liver
Gerhard's sign	Pulsatile spleen

Adapted from Babu et al. Ann Intern Med. 2003, with permission

easily appreciated with the patient leaning forward. Typically, AR due to aortic dilation is heard at the right sternal border, and that due to valvular disease is heard at the left sternal border. A murmur resembling mitral stenosis may also be heard at the apex. It is thought that this *Austin Flint* murmur is the result of premature closure of the anterior mitral leaflet due to pressure from the regurgitation jet of AR.

Measurement of the blood pressure often reveals a widened pulse pressure (SBP−DBP). This is due to the fact that both the SBP is increased in the setting of higher stroke volume, and DBP is decreased due to regurgitation of blood into the LV.

The peripheral examination in AR provides a number of eponymous findings that have variable degrees of sensitivity and specificity for diagnosis (Table 11.3) [10]. Most of these findings are the result of an increase in stroke volume accompanied by a sudden drop in aortic pressure due to the valvular regurgitation (i.e., wide pulse pressure). Although the majority of these clinical findings lack significant clinical relevance, two signs, Durozier's sign and Hill's sign, have demonstrated clinical correlation with the severity of AR.

Echocardiography

When suggested by history and physical examination, echocardiography provides the definitive diagnosis of AR and provides an assessment of valve morphology, LV size and function, aortic root structure, and of course regurgitation severity.

An assessment of valve anatomy is important to define the etiology of AR. Congenital bicuspid valve disease is responsible for most cases of valvular AR in the developed world, though rheumatic disease remains the most common cause worldwide. In patients with a bicuspid valve, an assessment of the degree of leaflet degeneration and calcification is important to determine whether valve repair may be feasible, or whether valve replacement will be necessary. Similarly, assessment for endocarditis is important for antibiotic management and planning the treatment strategy (i.e., large vegetation, presence of abscess, leaflet perforation, etc.).

Table 11.4 Echocardiographic characteristics of severe aortic regurgitation (AR)

Vena contracta	>0.6 cm
Jet width/LVOT height	>60%
PISA	ERO >0.3 cm^2
Pressure half-time	<250 ms
Descending aorta pulsed-wave Doppler	Pandiastolic reversal of flow with velocity >20 cm/s

LVOT Left ventricular outflow tract; *ERO* effective regurgitant orifice

LV size and systolic function are important to the treatment algorithm. In patients with severe, asymptomatic AR, surgery is not indicated unless there is evidence of LV dilation (end-diastolic dimension >7.5 cm or end-systolic dimension >5.5 cm) or systolic dysfunction (LVEF < 50%). It is therefore recommended that patients with chronic AR have close echocardiographic surveillance in the absence of symptoms (every 1 year with mild/moderate AR and every 6 months with severe AR) [5].

Evaluation of ascending aorta and root structure is important for diagnosis and also may dictate the course of management. For instance, in patients with bicuspid AV dilation of the aorta beyond 5 cm is considered an indication for surgery, and concomitant AV surgery may therefore be performed even in the absence of symptomatic AR. Aortic dissection involving the ascending aorta is a surgical emergency and should be managed accordingly as appropriate.

An accurate assessment of AR severity is nuanced and requires a critical appraisal of numerous parameters taken together. Considerations include: regurgitant jet width/LVOT height, vena contracta (VC), calculation of the proximal isovelocity surface area (PISA), subjective appearance of AR jet density and pressure half-time (PHT) of the AR jet on continuous-wave (CW) Doppler, and evidence of diastolic flow reversal in the descending aorta using pulsed-wave (PW) Doppler (Table 11.4).

The regurgitant jet width is measured in the LVOT in the parasternal long-axis view and compared to the height of the LVOT; a ratio of >60% indicates severe AR. The VC is usually measured in the same view (though the apical 5-chamber view may be used) and is the width of the jet at its narrowest point at the AV; a width of >0.6 cm signifies severe AR. By definition, the VC is smaller than the regurgitant jet width.

The PISA method is used most commonly in the assessment of mitral regurgitation (discussed in detail later in this chapter), but can be applied in AR as well to calculate the effective regurgitant orifice (ERO). An ERO >0.3 cm^2 is considered severe.

The basis for measuring PHT (the time required to reduce the gradient across the valve by ½) is as follows: with worsening AR, the aortic diastolic pressure and LVEDP equilibrate more quickly, resulting in a shorter PHT. A PHT <250 ms signifies severe AR and PHT >400 ms mild AR. While this method is used clinically, it should be noted that changes in loading conditions (i.e., alterations in SVR, LV compliance) may have effects on the PHT that are contrary to the regurgitant fraction measured. Furthermore, patients with chronic AR may have modified their LV compliance enough that the LV accommodates a long period of diastolic filling (i.e., long PHT). Therefore, the PHT should be used only as a piece of the diagnostic puzzle [11]. Evaluation of the AR jet density on CW is a subjective measure, and pitfalls include a lack of coaxial alignment of the Doppler signal with the regurgitant

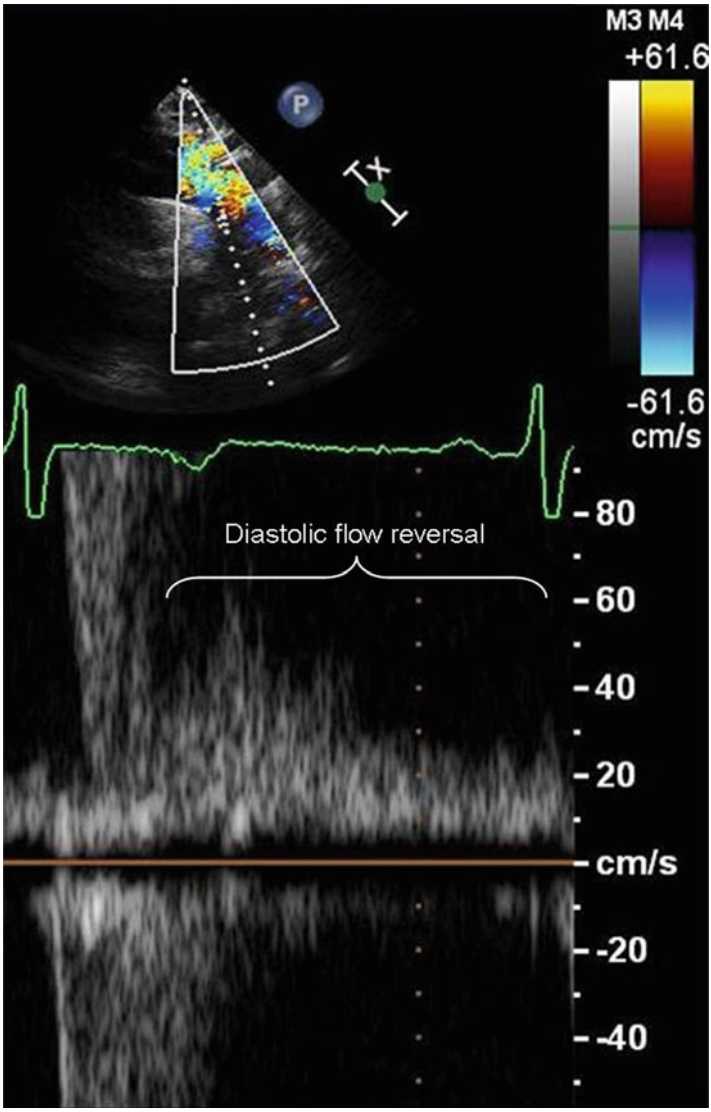

Fig. 11.3 Pulsed-wave Doppler demonstrating pan-diastolic flow reversal in the descending thoracic aorta in a patient with severe aortic regurgitation

flow. Nevertheless, a dense jet with a short PHT may increase the suspicion of severe AR. It should also be noted that due to the large stroke volume ejected by the LV in chronic severe AR, there may be a small outflow gradient measured though this does not reflect true AS.

The presence of some regurgitant flow in the descending aorta in early diastole is common and is due to closure of the AV. Persistent holodiastolic flow reversal with a velocity >20 cm/s, however, is a marker of severe AR (Fig. 11.3). The presence of diastolic MR

(appreciated on the CW or PW Doppler in the apical 4-chamber view) may be seen in patients with severely elevated LV pressures, such as in acute severe AR.

Cardiac Catheterization

Invasive catheterization holds a diminishing role in the diagnosis of AR. Similar to patients with AS, it is recommended only when the clinical scenario is not substantiated by non-invasive testing. Catheterization can be used to measure the LVEDP, examine the aortic pressure tracing, and quantify the degree of AR.

The aortic pressure tracing reveals elevated SBP (due to increased stroke volume) and a rapid systolic upstroke due to heightened LV contractility. The pulse pressure is widened (as discussed above) and diastolic aortic pressure approximates LVEDP near the end of diastole. In patients with chronic AR, increased LV compliance results in an LVEDP that is near-normal or only mildly elevated. In acute AR, there is a steep, marked rise in LVEDP. The SBP is reduced due to a decline in stroke volume.

The degree of AR is measured using ascending aortography by placing a pigtail catheter in the aortic root, 2 cm above the AV. A left-anterior-oblique (LAO) projection is selected to properly visualize the ascending aorta and branching arch vessels. Use of a power injector is mandatory, and generally 40 cc of dye is necessary to properly opacify the aorta. The AR is evaluated over 2 cardiac cycles and quantified as follows: incomplete LV opacification (1+); moderate LV opacification < aortic root opacification (2+); LV opacification = aortic root opacification within 2 cycles (3+); immediate LV opacification > aortic root opacification (4+).

Mitral Stenosis

Case Presentation

A 48-year-old woman presented to an emergency department with complaints of progressive dyspnea over the past 3 weeks associated with orthopnea and mild lower-extremity edema. She had not noticed any chest discomfort or palpitations. She had been having less urine output over the past week, despite a relatively stable diet. She reported a history of rheumatic fever as a teenager, but had not been followed by a physician for a number of years. She was therefore unaware of any other medical problems.

On exam, she was in mild distress manifest as tachypnea and labored breathing. She was tachycardic with an irregular heart rate of 120 bpm and a BP 100/65 mmHg. The cardiovascular exam was significant for an opening snap (OS) heard at the left-lower sternal border just after the S2, with a short

interval between the S2 and OS, followed by a mid-diastolic murmur at the apex heard best in the left lateral position. The JVP was elevated to the angle of the jaw while sitting upright. Examination of the periphery revealed 2+ lower extremity edema bilaterally to the shins and cool extremities.

An ECG revealed atrial fibrillation (AFib) with a ventricular rate of 125 bpm and no evidence of ischemic changes. Given the examination findings, urgent bedside echocardiography was performed and revealed a low-normal LV ejection fraction (50%) and mild aortic valve thickening and calcification. Most significant was a doming appearance of the anterior mitral leaflet, restricted motion of the posterior mitral leaflet, and fusion of the leaflets at both commissures. The peak and mean gradients across the mitral valve were 34 mmHg and 20 mmHg, respectively.

With a clinical diagnosis of suspected cardiogenic shock due to decompensated heart failure and severe mitral stenosis complicated by rapid AFib, the patient was moved urgently to the cardiac intensive care unit. Pulmonary artery catheterization (Swan–Ganz) confirmed the diagnosis with a cardiac index of 1.5, pulmonary artery catheter in the wedge position (PCWP) of 35 mmHg, and mixed venous oxygen saturation of 40%. Urgent cardioversion was performed and was successful in restoring a normal sinus rhythm of 70 bpm. With restoration of the rhythm, the patient's urine output increased immediately, and treatment of her volume overload was continued. Repeat TTE revealed a decrease in the mean mitral gradient to 12 mmHg. After successful management of her acute episode, the patient went on to have successful percutaneous mitral balloon valvotomy which decreased her mean mitral gradient to 4 mmHg.

Epidemiology and Pathophysiology

Mitral stenosis (MS) was the first valvular lesion to be diagnosed echocardiographically and treated surgically. Rheumatic heart disease is the leading cause of MS worldwide (prevalence of 6 per 1,000 children, compared with 0.5 per 1,000 in the United States) [12]. In developed countries, other etiologies such as severe mitral annular calcification (MAC) due to end-stage renal disease (ESRD), endocarditis, inflammatory disorders (i.e., lupus and rheumatoid arthritis), radiation therapy, and LA myxoma causing MV obstruction are more often considered. MS is a slowly progressive disease that eventually leads to AFib, pulmonary hypertension, and decreased cardiac output. Once symptoms develop, patients face a dismal prognosis, with a 10-year mortality of 70% [13].

In rheumatic fever, inflammation results in nodule formation at the leaflet edge, followed by leaflet thickening, commissural fusion, and chordal thickening and shortening. Smoldering inflammation coupled with turbulent flow across the valve leads to progressive valvular dysfunction [14]. Patients with end-stage kidney disease have disordered calcium metabolism and resultant MAC. As calcification of the annulus progresses to involve the leaflets, obstruction to flow across the valve

may occur due to the smaller mitral orifice. And restricted leaflet motion [15]. In contrast to rheumatic MS, in which the smallest valve area is at the leaflet tips, obstruction in non-rheumatic MS is predominantly at the annular level.

Physical Examination

The classic findings of MS include the opening snap and mid-diastolic murmur. The source of the OS is mobility of the anterior mitral leaflet, and is usually heard best at the LLSB; it is generally not appreciated at the apex. The OS may be differentiated from physiologic splitting of the S2 during exhalation (when the presence of two sounds indicates the OS of MS). A short interval between the S2 and OS indicates severe MS, as a high LA pressure causes quick opening of the mitral valve in diastole.

The murmur of MS is best heard in the left lateral decubitus position with the stethoscope placed at the ventricular PMI. As with other valve lesions, a louder murmur signifies a large degree of flow (and hence a higher gradient) across the valve. Similarly, in patients with AFib a diastolic murmur leading up to the S1 during a long R-R interval implies severe MS with a persistent gradient even at the end of diastole.

Echocardiography

A subjective assessment of the mitral valve apparatus involves an appraisal of leaflet mobility (typically "doming" of the anterior leaflet and restriction of the posterior leaflet) and thickness, as well as the degree of thickening, calcification, and/or fusion of the commissures and subvalvular apparatus. The systematic scoring system provided by Wilkins et al. takes these factors into consideration and is also useful in assessing the feasibility of percutaneous balloon mitral valvotomy (Table 11.5) [16].

The objective evaluation of MS includes a measurement of valve area, valve gradient, and pulmonary artery pressure (PAP) (Table 11.6) [17]. The mitral valve area (MVA) can be assessed using planimetry in the parasternal short-axis projection, though a common pitfall of this method is measuring proximal to the true orifice and thereby overestimating the MVA. Valve area is also estimated using the PHT method, which as with AR is a measure of the time it takes for the gradient across the valve to fall by one-half (Fig. 11.4). Notably, the PHT method is unreliable in patients with severe AR or significant LV diastolic dysfunction since the pressure gradient between the LA and LV equalizes rapidly, providing an abnormally short PHT (thereby overestimating MVA).

The valve gradient in MS is best assessed by tracing the mitral inflow Doppler signal obtained in the apical-4 chamber view (Fig. 11.5). The main consideration is

Table 11.5 Echocardiographic scoring system for mitral valve stenosis

Grade	*Mobility*	*Subvalvar thickening*	*Thickening*	*Calcification*
1	Highly mobile valve with only leaflet tips restricted	Minimal thickening just below the mitral leaflets	Leaflets near normal in thickness (4–5 mm)	A single area of increased echo brightness
2	Leaflet mid and base portions have normal mobility	Thickening of chordal structures extending up to one third of the chordal length	Mid-leaflets normal, considerable thickening of margins (5–8 mm)	Scattered areas of brightness confined to leaflet margins
3	Valve continues to move forward in diastole, mainly from the base	Thickening extending to the distal third of the chords	Thickening extending through the entire leaflet (5–8 mm)	Brightness extending into the mid-portion of the leaflets
4	No or minimal forward movement of the leaflets in diastole	Extensive thickening and shortening of all chordal structures extending down to the papillary muscles	Considerable thickening of all leaflet tissue (> 8–10 mm)	Extensive brightness throughout much of the leaflet tissue

A score ≤8 is generally associated with favorable outcome from percutaneous mitral balloon valvotomy. Reproduced with permission from Wilkens et al. Br Heart J. 1988;60(4):299–308

Table 11.6 Echocardiographic evaluation of mitral stenosis severity

	Mild	Moderate	Severe
Mean gradient (mmHg)	<5	5–10	>10 or >15 with stress
Valve area (cm^2)	>1.5	1.0–1.5	<1.0
Pulmonary artery systolic pressure (mmHg)	<30	30–50	>50 or >60 with stress

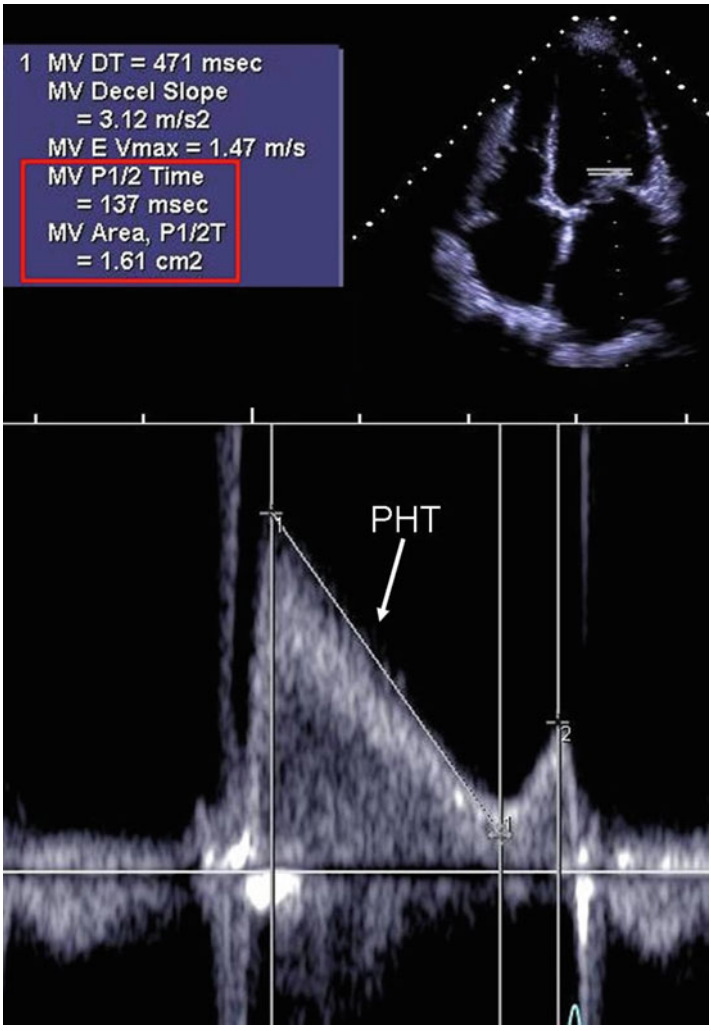

Fig. 11.4 Pulsed-wave Doppler of mitral inflow demonstrating calculation of the mitral valve area (MVA) using the pressure half-time (PHT) method. MVA = 220/PHT

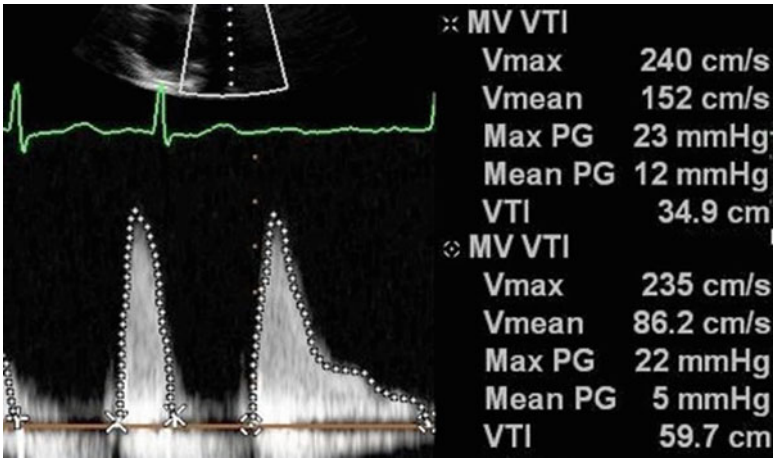

Fig. 11.5 Patient with moderate mitral stenosis and atrial fibrillation (AFib). The mean gradient across the mitral valve is significantly increased in the setting of decreased diastolic filling time (i.e., increased heart rate) (beat 1: 12 mmHg vs. beat 2: 5 mmHg)

the mean gradient, which is automatically calculated by summing the gradient over the cardiac cycle. As shown in the figure, a shorter R-R interval results in a marked increase in mitral gradient and highlights the need for appropriate heart rate control in patients with MS, particularly those with concomitant AFib.

An estimation of pulmonary pressures using the right ventricular systolic pressure (RVSP) is an important part of the evaluation of MS. An RVSP >50 mmHg at rest, or >60 mmHg on exercise, TTE is consistent with significant pulmonary hypertension and provides an indication for intervention of MS.

Cardiac Catheterization

As with other valve disorders, catheterization is recommended in the diagnosis of MS when there is discrepancy between the clinical scenario and non-invasive methods [5]. Right heart catheterization (RHC) is often indispensable in the critical care unit to guide management of volume status in patients presenting with pulmonary congestion, depressed cardiac output, and severe mitral stenosis.

The mitral valve gradient is measured by taking simultaneous pressure tracings via an LV catheter and either a pulmonary artery catheter in the wedge position (PCWP) or a direct left atrial catheter (Fig. 11.6). Use of the PCWP is unreliable in patients with pulmonary veno-occlusive disease. It is also important to remember that the "true" wedge pressure is the measured PCWP minus the mean mitral gradient.

As discussed above, the mean gradient is exquisitely sensitive to heart rate, since a faster heart rate leaves less time for diastolic emptying of the atrium and results in

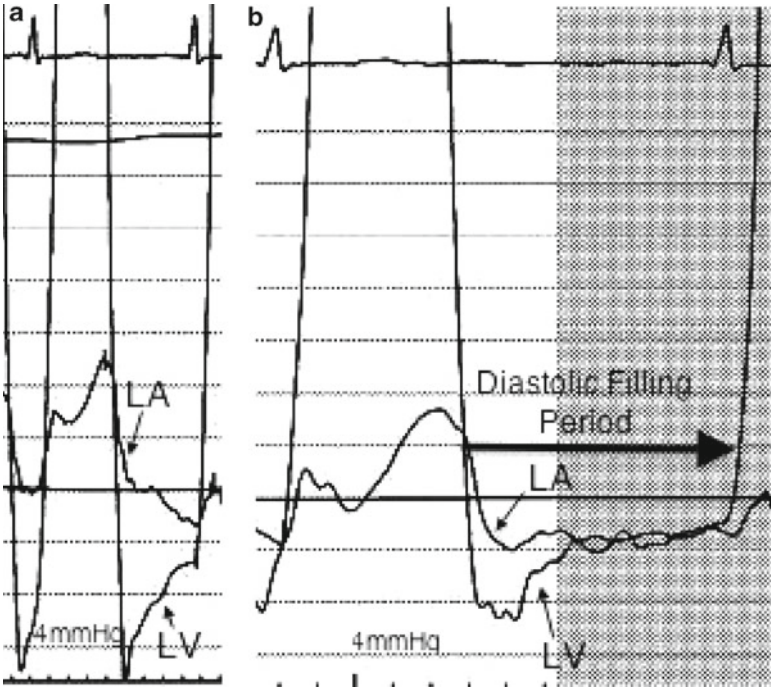

Fig. 11.6 Simultaneous measurement of left atrial (LA) and left ventricular (LV) pressures in a patient with mitral stenosis before (**a**) and after (**b**) percutaneous mitral balloon valvuloplasty. Prior to PMBV, a substantial gradient is present until the end of diastole. In this patient, the pre-procedural resting gradient was 10 mmHg and post-procedural gradient was 4 mmHg. Paper speed is faster in (**a**)

a higher gradient. In patients with AFib, it is therefore recommended to average the gradient over 10 cardiac cycles.

The valve area is estimated using the Gorlin formula as follows:

$$\text{MVA} = (\text{SV} \mid \text{DFP}) \mid (37.7 \cdot \sqrt{\text{mean gradient}})$$

$$[\text{SV} : \text{stroke volume}; \text{DFP} : \text{diastolic filling period}]$$

Of note, calculation of the SV using the thermodilution method is not accurate in patients with low cardiac output or significant tricuspid regurgitation. As in patients with AS, the valve area can also be calculated using the Hakki equation:

$$\text{MVA} = \text{CO} \mid \sqrt{\text{mean gradient}}$$

In patients with a HR <75 bpm, the value above is divided by 1.35 to provide greater accuracy.

Mitral Regurgitation

Case Presentation

The patient is an 87-year-old man with prior history of diabetes, hypertension, hyperlipidemia, chronic kidney disease (Stage IV, GFR 25 mL/min/1.73 m^2). He had undergone two prior coronary bypass graft operations, with recent angiography showing patent grafts to the left anterior descending, circumflex, and right coronary arteries. He noted worsening exertional dyspnea over the past 12 months, with recently increasing orthopnea and lower extremity edema. He had initially experienced relief with an increasing dose of diuretics and hydralazine, but his symptoms again worsened.

Physical examination revealed AFib with a controlled heart rate of 80 bpm and BP 110/75 mmHg. The PMI was laterally displaced to the mid axillary line and there was a 3/6 systolic murmur heard best at the apex and radiating to the axilla as well as the spine posteriorly. The JVP was elevated at 12 cm H_2O. TTE revealed severely depressed LV function (EF 25%) with moderate LV cavity dilation and moderate LA enlargement. There was severe, posteriorly directed mitral regurgitation due to MV annular dilation, apical displacement of the mitral leaflets, and restriction of the posterior mitral valve.

Given the patient's age, co-morbidities, and two prior open-heart surgeries, he was deemed an inoperable risk for surgical mitral valve repair. He therefore underwent percutaneous mitral valve repair using the MitraClip device (approximating the Alfieri stitch method of surgical repair), which provided a substantial reduction in his degree of MR and improvement in his clinical symptoms.

Epidemiology and Pathophysiology

Mitral regurgitation (MR) affects more than two million people in the United States [18]. Classification of MR is broadly defined by two groups: primary and secondary MR. Primary MR, which is a disorder of the valve itself, is most commonly due to myxomatous (degenerative) disease or mitral valve prolapse (MVP; Barlow's Disease) in the developed world, and rheumatic disease in developing countries. Secondary MR is the result of a disordered left ventricular geometry and is usually referred to as "functional" or "ischemic" MR. In secondary MR, annular dilation, apical tethering of the MV leaflets, and/or excessive leaflet motion due to chordal avulsion or papillary muscle rupture lead to the regurgitant lesion.

Acute MR is most often caused by myocardial infarction that leads to papillary muscle rupture or chordal avulsion, supranormal contraction of the non-infarcted papillary muscle, or regional LV dysfunction. Similar to acute AR, it is a severe volume overload state that results in pulmonary edema and depressed cardiac output. Management requires urgent pharmacologic and mechanical afterload reduction

and timely surgical referral. Chronic MR, over time, results in a volume overloaded state for the LV and leads to LV dilation and dysfunction, LA enlargement, atrial fibrillation, and pulmonary hypertension.

Physical Examination

A salient physical finding in patients with MR includes the classic high-pitched, holosystolic murmur heard at the apex with radiation to the axilla. If the MR is due to MV prolapse, the murmur may not start until mid-systole, after prolapse of the affected leaflet(s). In patients with severe, posteriorly directed MR (i.e., functional MR or patients with anterior leaflet prolapse), the murmur may also be appreciated by auscultation at the thoracic spine. With posterior prolapse, the regurgitant jet is directed anteriorly and may be best heard at the upper sternal border (similar to AS). The severity of the murmur does not correlate well with the severity of the MR, as other factors including LV cavity dilation and depressed cardiac output can diminish the murmur in the setting of severely decompensated disease. Similar to the murmur in AS, the sound is augmented by increasing afterload (i.e., handgrip) and diminished by reducing venous return (i.e., Valsalva maneuver).

The S1 sound is often diminished due to poor coaptation of the MV leaflets, and the S2 sound may be widely split due to a premature closure of the aortic valve (A2 component) in the setting of poor forward output. In patients with MV prolapse, a mid-systolic click may be appreciated at the time of maximum leaflet prolapse. With heart failure and a dilated LV, an S3 gallop may be also heard. The peripheral exam in severe MR often reveals a prominent upstroke and reflects the increased left ventricular ejection volume, similar to severe AR. In contrast to the pulse in AR, however, the pulse pressure with severe MR is normal.

Echocardiography

Echocardiography is used to quantify MR, evaluate the presence of valve pathology and define the specific nature of the lesion, and evaluate LV size and systolic function. Quantification of MR is based on a number of parameters including color Doppler, continuous and pulsed wave Doppler, and pulmonary venous flow pattern (Table 11.7) [19]. Color Doppler imaging can provide an overall impression of the degree of regurgitation based upon the visual estimation of the regurgitant jet in the LA. Slightly more quantitative methods include measurement of the vena contracta (thinnest portion of the regurgitant jet at the regurgitant orifice) and measurement of the regurgitant jet area (RJA) relative to the LA area.

The PISA method, as discussed previously in the evaluation of AR, provides the most precise echocardiographic estimation of MR. Briefly, the technique is based upon the idea that as blood converges toward a regurgitant orifice, velocity increases

Table 11.7 Echocardiographic determinants of mitral regurgitation severity

	Mild	Moderate	Severe
Color flow mapping			
RJA/LAA (%)	<20	20–40	>40
VC (cm)	<0.40	0.40–0.69	>0.70
ERO (cm^2)	<0.20	0.20–0.40	>0.40
RV (mL/beat)	<30	30–60	>60
Pulsed wave Doppler			
Mitral E-wave velocity			>1.2 m/s
PV flow pattern			Systolic blunting or reversal

RJA Regurgitant jet area; *LAA* left atrial area; *VC* vena contracta; *ERO* effective regurgitant orifice; *RV* regurgitant volume; *PV* pulmonary vein
Reproduced with permission from Krishnaswamy et al. Coron Artery Dis. 2011

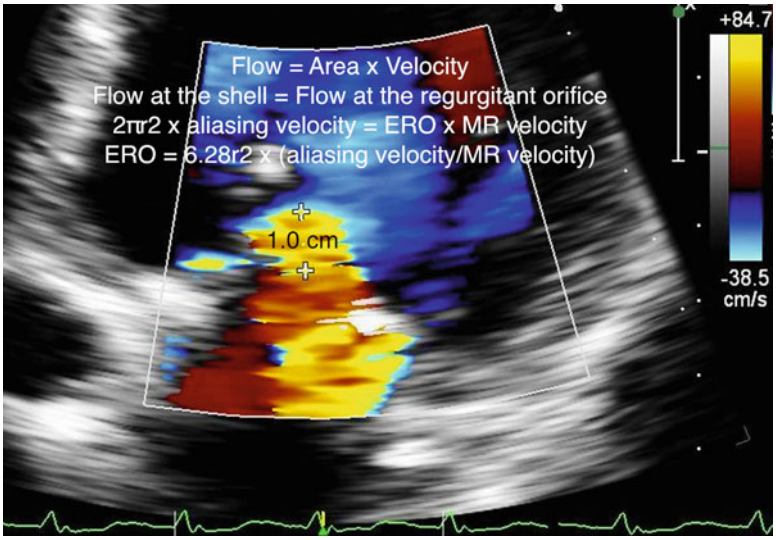

Fig. 11.7 Demonstration of the mitral regurgitation (MR) jet and calculation of the proximal isovelocity surface area (PISA). In this patient with an aliasing velocity set at 38.5 cm/s and a MR velocity of 500 cm/s (not shown), the simplified effective regurgitant orifice (ERO) calculation can be used ($r^2/2$), providing an ERO of 0.5 cm^2, which is consistent with severe MR. Adapted with permission from Krishnaswamy et al. Coron Artery Dis. 2011

and forms a series of hemispheric shells with the same velocity (hence isovelocity). The velocity at a given shell can be set on the machine as the "aliasing velocity," and calculation of the area bounded by the shell (by measuring the radius) provides the flow at the surface of the shell. Since flow is constant (i.e., conservation of flow principle), the ERO can be calculated as in Fig. 11.7 using the color flow Doppler envelope and the continuous wave (CW) Doppler tracing to measure MR velocity. If the MR velocity is assumed to be 5 m/s, and the aliasing velocity set at 40 cm/s,

the PISA formula can be simplified as follows: $ERO = r^2/2$. The regurgitant volume can also be calculated using the following: $R_{vol} = ERO \times MR_{VTI}$ (MR_{VTI} is obtained by tracing the MR envelope on CW Doppler).

Pulsed-wave (PW) Doppler is used to interrogate the mitral inflow and stage diastolic function. In the setting of MR, assessment of the peak inflow velocity is useful in quantification. Severe regurgitation results in a higher LA–LV gradient, and therefore a higher E-wave velocity during mitral inflow. Use of PW Doppler is also important to evaluate the pulmonary vein flow, specifically for the presence of systolic blunting or reversal in the pulmonary veins that signifies elevated LA pressure (assumedly due to severe MR).

Cardiac Catheterization

Invasive hemodynamic assessment in patients with MR is rarely necessary, but may be performed when non-invasive testing is not definitive. In acute MR, the PCWP tracing (or direct LA measurement) demonstrates a large "v" wave due to the large volume of regurgitant blood into a low-compliance LA, and the amplitude of the "v" wave and the LV systolic pressure may be nearly equivalent (Fig. 11.8). It is important

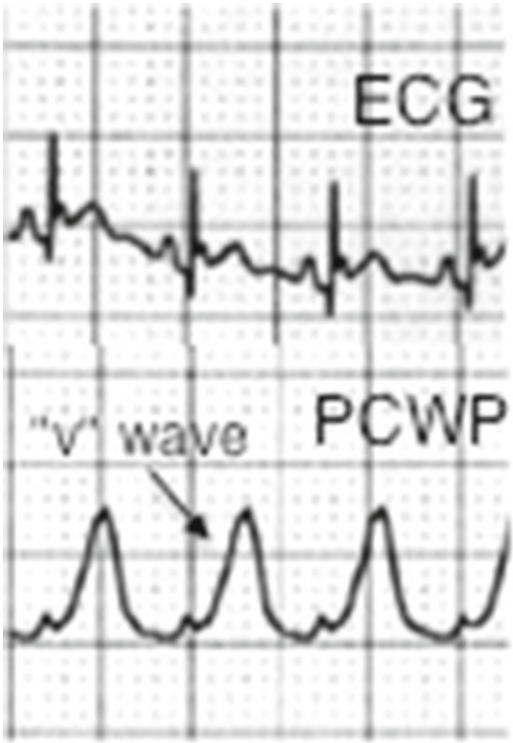

Fig. 11.8 Pulmonary artery catheter pressure tracing in the wedge position (PCWP) in a patient with acute severe mitral regurgitation due to papillary muscle rupture complicating acute myocardial infarction demonstrates a large v-wave

to keep this in mind during percutaneous balloon mitral valvotomy as an indicator of complications. The volume overload of the regurgitant lesion on the LV results in elevated LV pressures as well.

In patients with chronic MR, compliance of the LA increases over time (as does the LV in chronic AR). The "v" wave is therefore smaller than that seen with acute MR. The use of vasodilators in chronic MR produces a similar result. The LV responds to the chronic volume overload of MR as it does in chronic AR and compliance increases, resulting in a less drastic increase in LV pressures than in acute MR.

Ventriculography can also be used to assess the severity of MR. Grading of the regurgitation employs a similar scale as in AR: 1+ = brief LA opacification without LA enlargement; 2+ = moderate LA opacification less than LV opacification and without LA enlargement; 3+ = equal LA and LV opacification that clears over many cycles and with LA enlargement; 4+ = immediate LA>LV opacification with pulmonary vein filling and LA enlargement. Caution should be exercised in performing ventriculography in patients with MR, in light of the contrast load that it requires in patients who may already be volume overloaded.

Review Questions

Q1. A 74-year-old man presented with exertional dyspnea and orthopnea. Echocardiography revealed a moderately thickened and calcified trileaflet aortic valve with severely restricted motion and an LVEF 20%. Results of interrogation of the AV was performed at rest and with infusion of dobutamine (DBA) as follows:

Rest		DBA	
LVEF	20%	LVEF	25%
LVOT diameter	2.4 cm	LVOT diameter	2.4 cm
LVOT VTI	15.9 cm/s	LVOT VTI	20.2 cm/s
Calculated AVA	0.6 cm^2	Calculated AVA	0.9 cm^2

What is the appropriate next step?

A. Refer for aortic valve replacement
B. Refer for invasive hemodynamic study
C. Medical management of LV dysfunction
D. Refer for balloon aortic valvuloplasty

A1. C. This case demonstrates the diagnosis of "pseudo-AS," for which management of the underlying LV systolic dysfunction is appropriate. In patients with low-flow, low-gradient AS, provocative testing with DBA infusion may be helpful to distinguish true- and pseudo-AS. In this patient, the stroke volume (LVOT area × LVOT VTI) is 71 mL, and at stress is 91 mL. This increase of >20% implies the presence of contractile reserve. The increase in calculated AVA of 0.3 cm^2 with stress provides evidence of improved AV leaflet excursion with higher SV; i.e., the "stenosis" is not fixed due to an intrinsic leaflet issue. Surgical intervention or

valvuloplasty is not helpful in this setting. An invasive study is not necessary as the diagnosis is clear by echocardiography alone.

Q2. A 45-year-old woman with a history of rheumatic fever presents with worsening exertional dyspnea. Physical examination reveals a regular rate and rhythm. Cardiac auscultation reveals an opening snap and diastolic murmur heard at the apex. There is no lower-extremity edema and the JVP is appreciated at 5 cm above the sternum. Transthoracic echocardiography (TTE) reveals a normal LVEF, doming of the anterior MV leaflet with restriction of the posterior MV leaflet, and a mean gradient across the MV of 7 mmHg. The estimated RVSP is 40 mmHg. What is the next step in management?

A. Evaluate non-cardiac causes of dyspnea
B. Perform exercise echocardiography to evaluate the MV
C. Refer for invasive cardiac catheterization to evaluate the MV
D. Return for follow-up echocardiogram in 6 months

A2. B. This patient with a history of rheumatic fever presents with exertional dyspnea and a typical echocardiographic appearance of rheumatic mitral valve disease. The mean valve gradient is moderate at best, with a suggestion of borderline pulmonary hypertension (RVSP 40 mmHg). Given the patient's exertional symptoms, however, exercise echocardiography would be the next appropriate step in order to evaluate the MV gradient and pulmonary pressures with exertion. In this patient, TTE during stress revealed a mean MV gradient of 16 mmHg and RVSP of 65 mmHg. She subsequently underwent percutaneous balloon mitral valvuloplasty and was symptom-free with significant exertion afterward. Cardiac catheterization is considered to be less accurate in the evaluation of MS than echocardiography and is therefore not yet indicated in this patient.

Q3. A 42-year-old man with bicuspid aortic valve seeks to establish a new cardiologist after many years of loss to follow-up. He doesn't take any medications. He feels well and exercises on a treadmill for 45 min four times per week. He has no exertional or positional dyspnea. On exam, his HR is 70 bpm and BP 115/50 mmHg. He has a holodiastolic murmur heard best at the left sternal border, and peripheral exam reveals bounding pulses with rapid collapse. TTE reveals normal LVEF 60% with LVIDd 7.2 cm and LVIDs 5.7 cm, a bicuspid aortic valve, and quantification of the degree of AR provides a vena contract of 0.7 cm, PHT 200 ms, and holodiastolic flow reversal in the descending aorta. What is the best next step?

A. Routine clinical follow-up with TTE in 6 months
B. Initiation of an ACE-inhibitor
C. Referral for aortic valve surgery
D. Exercise stress testing

A3. C. This patient with asymptomatic severe AR demonstrates LV cavity dilation (LVIDd>7.5 cm or LVIDs>5.5 cm), which is a criteria for aortic valve repair or

replacement in patients with asymptomatic but severe AR (ACC/AHA Class IIa). For patients with severe AR and normal LV cavity size but without symptoms, follow-up echocardiography is indicated every 6 months (ACC/AHA Class I). Vasodilators are reasonable for symptomatic relief in patients with severe AR (Class IIa), but should not supersede definitive treatment in the setting of LV cavity dilation. Exercise stress testing may be helpful to distinguish whether or not the "asymptomatic" patient is truly asymptomatic (ACC/AHA Class IIa), but the patient described here has LV cavity dilation and therefore symptoms are not necessary to make the recommendation for surgery.

Q4. A 67-year-old man with hypertension and hyperlipidemia presents with an inferior STEMI and undergoes primary percutaneous coronary intervention to a proximally occluded right coronary artery. The procedure is uneventful and he is transferred to the cardiac ICU in stable condition. Fourteen hours later, he develops sudden hypotension and dyspnea. There are no new ECG changes. Which of the following would be expected of diagnostic testing:

A. Large "v"-wave on a PCWP tracing
B. LA>LV opacification within 1 cycle on a ventriculogram
C. Pulmonary vein flow-reversal during systole on TTE
D. All of the above

A4. D. The patient above provides a classic presentation of mechanical complication after acute MI, in this case with severe MR due to papillary muscle rupture. Choices A–C all provide diagnostic evidence for severe MR. Appropriate management consists of emergent afterload reduction (using intra-aortic balloon counterpulsation and/or vasodilators if tolerated) and surgical referral for mitral valve surgery.

Q5. A 40-year-old man presents with worsening exertional dyspnea over the past 1 week, along with fevers to 102°. He admits to regular intravenous drug use and claims to have had a "murmur" since childhood. His bedside echocardiogram suggests severe AR. What other diagnostic findings would be expected?

A. Holodiastolic murmur at the left sternal border
B. Bradycardia
C. AR Pressure half-time (PHT) <250 ms
D. Systolic murmur resembling MR heard at the apex

A5. C. In acute AR, the rapid rise in LV pressure due to a non-compliant chamber results in rapid equilibration of aortic and LV pressures and results in a short PHT. The hallmark diastolic murmur of AR may not be appreciated as easily in the acute setting for the same reason. Patients with acute AR are often quite tachycardic due to the poorly tolerated hemodynamic consequences of the lesion. The *Austin Flint* murmur of AR resembles the murmur of MS and is thought to be due to premature closure of the anterior MV leaflet by the regurgitant AR jet.

References

1. Nkomo VT, Gardin JM, Skelton TN, Gottdiener JS, Scott CG, Enriquez-Sarano M. Burden of valvular heart diseases: a population-based study. Lancet. 2006;368:1005–11.
2. Otto CM, Burwash IG, Legget ME, et al. Prospective study of asymptomatic valvular aortic stenosis. Clinical, echocardiographic, and exercise predictors of outcome. Circulation. 1997;95:2262–70.
3. Carabello BA. Clinical practice. Aortic stenosis. N Engl J Med. 2002;346:677–82.
4. Leach RM, McBrien DJ. Brachioradial delay: a new clinical indicator of the severity of aortic stenosis. Lancet. 1990;335:1199–201.
5. Bonow RO, Carabello BA, Chatterjee K, et al. 2008 Focused update incorporated into the ACC/AHA 2006 guidelines for the management of patients with valvular heart disease: a report of the American College of Cardiology/American Heart Association Task Force on Practice Guidelines (Writing Committee to revise the 1998 guidelines for the management of patients with valvular heart disease). Endorsed by the Society of Cardiovascular Anesthesiologists, Society for Cardiovascular Angiography and Interventions, and Society of Thoracic Surgeons. J Am Coll Cardiol. 2008;52:e1–142.
6. deFilippi CR, Willett DL, Brickner ME, et al. Usefulness of dobutamine echocardiography in distinguishing severe from nonsevere valvular aortic stenosis in patients with depressed left ventricular function and low transvalvular gradients. Am J Cardiol. 1995;75:191–4.
7. Monin JL, Quere JP, Monchi M, et al. Low-gradient aortic stenosis: operative risk stratification and predictors for long-term outcome: a multicenter study using dobutamine stress hemodynamics. Circulation. 2003;108:319–24.
8. Quere JP, Monin JL, Levy F, et al. Influence of preoperative left ventricular contractile reserve on postoperative ejection fraction in low-gradient aortic stenosis. Circulation. 2006;113:1738–44.
9. Hakki AH, Iskandrian AS, Bemis CE, et al. A simplified valve formula for the calculation of stenotic cardiac valve areas. Circulation. 1981;63:1050–5.
10. Babu AN, Kymes SM, Carpenter Fryer SM. Eponyms and the diagnosis of aortic regurgitation: what says the evidence? Ann Intern Med. 2003;138:736–42.
11. Griffin BP, Flachskampf FA, Reimold SC, Lee RT, Thomas JD. Relationship of aortic regurgitant velocity slope and pressure half-time to severity of aortic regurgitation under changing haemodynamic conditions. Eur Heart J. 1994;15:681–5.
12. Padmavati S. Rheumatic fever and rheumatic heart disease in India at the turn of the century. Indian Heart J. 2001;53:35–7.
13. Selzer A, Cohn KE. Natural history of mitral stenosis: a review. Circulation. 1972;45:878–90.
14. Bonow RO, Braunwald E. Valvular heart disease (chapter 57). In: Braunwald E, editor. Braunwald's heart disease. 7th ed. Philadelphia, PA: Elsevier Saunders; 2005.
15. Muddassir SM, Pressman GS. Mitral annular calcification as a cause of mitral valve gradients. Int J Cardiol. 2007;123:58–62.
16. Wilkins GT, Weyman AE, Abascal VM, Block PC, Palacios IF. Percutaneous balloon dilatation of the mitral valve: an analysis of echocardiographic variables related to outcome and the mechanism of dilatation. Br Heart J. 1988;60:299–308.
17. Baumgartner H, Hung J, Bermejo J, et al. Echocardiographic assessment of valve stenosis: EAE/ASE recommendations for clinical practice. Eur J Echocardiogr. 2009;10:1–25.
18. Enriquez-Sarano M, Akins CW, Vahanian A. Mitral regurgitation. Lancet. 2009;373:1382–94.
19. Zoghbi WA, Enriquez-Sarano M, Foster E, et al. Recommendations for evaluation of the severity of native valvular regurgitation with two-dimensional and Doppler echocardiography. J Am Soc Echocardiogr. 2003;16:777–802.

Chapter 12
Pulmonary Hypertension

George M. Cater and Richard A. Krasuski

Introduction

The pulmonary circulation is normally a low pressure, low-resistance, highly compliant system. Pulmonary hypertension (PH) is a pathologic state characterized by distinct changes in the pulmonary vasculature coupled with elevations in the mean pulmonary arterial pressure (mPAP) and, in the case of pulmonary arterial hypertension (PAH), increased pulmonary vascular resistance (PVR). Attention to PH has risen in recent years due to difficulty in defining the disease, assigning appropriate strategies for management, and poor outcomes in certain forms. The prevalence of PH is high, particularly due to the pervasiveness of secondary causes. Left sided heart disease, such as left ventricular dysfunction, hypertensive heart disease, aortic and mitral valve dysfunction, and cardiomyopathy, can elevate left atrial and subsequently pulmonary arterial pressures. Thus pulmonary venous hypertension must be distinguished from PAH, which is less common with an estimated prevalence of 15 cases per million [1]. Other forms of PH, such as chronic thromboembolic PH (CTEPH), PH due to lung diseases, and PH due to multifactorial mechanisms such as systemic and metabolic disorders are also recognized in the current classification system (Table 12.1).

In PAH, the pulmonary capillary wedge pressure (PCWP), a surrogate of the left atrial pressure and in the absence of mitral stenosis, the left ventricular end-diastolic pressure (LVEDP) as well, is normal (≤15 mmHg), yet the mPAP is elevated (>25 mmHg). Some definitions also require that the PVR be >3 Wood units (240 dyn/s/cm^5). Previous definitions also have made reference to mPAP elevation during exercise (to >30 mmHg), but exercise-induced PH in patients with normal resting pressures remains a very poorly characterized phenomenon, and the most recent guidelines have removed this from the definition [2, 3].

G.M. Cater, M.S.E. • R.A. Krasuski, M.D. (✉)
The Cleveland Clinic, Cleveland, OH, USA
e-mail: caterg@ccf.org; krasusr@ccf.org

A.T. Askari et al. (eds.), *Cardiovascular Hemodynamics: An Introductory Guide*, Contemporary Cardiology, DOI 10.1007/978-1-60761-195-0_12,

Table 12.1 Pulmonary hypertension Dana point classification system set by the World Health Organization (2008)

Group 1: Pulmonary Arterial Hypertension (PAH)
1.1 Idiopathic PAH
1.2 Heritable (BMPR2, ALK1, endoglin, unknown)
1.3 Drug- and toxin-induced
1.4 Associated with autoimmune PAH: connective tissue diseases, HIV infection, portal hypertension, congenital heart disease, schistosomiasis, chronic hemolytic anemia
1.5 Persistent pulmonary hypertension of the newborn
Group 1': Pulmonary veno-occlusive disease and/or pulmonary capillary hemangiomatosis
Group 2: Pulmonary hypertension due to left heart disease
2.1 Systolic dysfunction
2.2 Diastolic dysfunction
2.3 Valvular disease
Group 3: Pulmonary hypertension due to lung diseases and/or hypoxemia
3.1 Chronic obstructive pulmonary disease
3.2 Interstitial lung disease
3.3 Other pulmonary diseases with mixed restrictive and obstructive pattern
3.4 Sleep disordered breathing
3.5 Alveolar hypoventilation disorders
3.6 Chronic exposure to high altitude
3.7 Developmental abnormalities
Group 4: Chronic thromboembolic pulmonary hypertension (CTEPH)
Group 5: Pulmonary hypertension with unclear and/or multifactorial mechanisms
5.1 Hematological disorders: myeloproliferative disorders, splenectomy
5.2 Systemic disorders: sarcoidosis, pulmonary Langerhans cell histiocytosis, lymphangioleiomyomatosis, neurofibromatosis, vasculitis
5.3 Metabolic disorders: glycogen storage disease, Gaucher disease, thyroid disorders
5.4 Others: tumoral obstruction, fibrosing mediastinitis, chronic renal failure on dialysis

Epidemiology of Pulmonary Hypertension

Idiopathic PAH

PAH may be due to intrinsic cardiac, pulmonary, heritable, or systemic disease; however in about 40% of PAH cases a cause cannot be found and is therefore referred to as idiopathic PAH (IPAH) [1]. IPAH (previously referred to as primary pulmonary hypertension, PPH) is nearly twice as likely in adult women, and has a mean age at diagnosis of 37 years. A familial version of IPAH accounts for ~6% of PAH and is inherited in autosomal dominant fashion, but with low penetrance. Bone morphogenic protein receptor 2 (BMPR2) gene mutations, originally mapped in patients with familial PAH, have also been identified in 26% of patients with nonfamilial IPAH [4]. This has stimulated investigation into the receptor for this gene, transforming growth factor-beta (TGF-B), for its role in the pathogenesis and possible treatment of this disorder. Historically, IPAH had a devastating prognosis, with estimated 1, 2, and 3-year survivals of 77, 69, and 35% respectively when left untreated [5].

Patients with unclassified disease, but diagnosed with PAH, have a 1-year survival rate of 88% [1]. Depending on the etiology, long-term prognosis is highly variable. Current pharmacologic therapies, such as endothelin antagonists, prostanoids, and phophodiesterase-5 inhibitors, modify the disease course and improve outcomes in patients with PAH. The impact of medical therapy is profound, and thus the push for prompt diagnosis and appropriate treatment is paramount. IPAH patients treated with epoprostenol appear to have a 43% reduction in mortality, with 5-year survival ranging from 47 to 55% [6, 7]. In addition to improving quality of life in these patients, newer selective oral therapies may also improve survival [8]. Additionally anticoagulation with warfarin may favorably impact survival [9]. Prognostic factors will be further discussed in the section on clinical evaluation.

PAH in Systemic Disease

The prevalence of PAH in systemic diseases is difficult to assess due to limited hemodynamic data in most patients, reliance on echocardiography for estimation of pulmonary pressures, and nonstandardized definitions of PAH among studies. Nonetheless, PAH is frequently present in scleroderma (8–26%), systemic lupus erythematosus (0.5–14%), advanced liver disease (portopulmonary hypertension, 1–6%), HIV (0.5%), thromboembolic disease (CTEPH develops in 3–5% at 1 year following the initial event), and schistosomiasis (25%) [10]. Correlations with PAH have also been found in patients having undergone splenectomy: 11.5% of IPAH patients in one series had prior splenectomy and patients with a pulmonary embolism and prior splenectomy were 13 times more likely to develop CTEPH [11]. Hematologic diseases such as myeloproliferative and chronic hemolytic anemia have highly variable rates of PH depending on the cohort studied. Sickle cell anemia appears to have the strongest association, with a PH prevalence between 20 and 40% [12]. Both hypo- and hyperthyroidism are associated with mild PH (~40% of cases), which typically resolves following appropriate treatment of the underlying disorder [13]. Prognosis for patients with PAH and systemic disease is not well defined, and studies not infrequently classify and treat them as IPAH.

PAH in Congenital Disease

PAH is common in congenital heart disease patients, most frequently associated with left to right shunting lesions (particularly post-tricuspid shunts), and often resolving rapidly following defect repair when recognized early. In adults with previously treated congenital disease, PAH is present in only ~4%. Adult congenital patients who present with PAH commonly have a history of septal defects (atrial septal defects (ASD) or ventricular septal defects (VSD)) with long-standing unrepaired left-to-right shunts. Approximately 12% of patients with closed ASD and 34% of patients with unrepaired ASD present with PAH [14].

Eisenmenger syndrome, the most severe congenital heart disease complication, occurs in 25–50% of congenital patients who develop PAH (~5% of all shunt patients) and has a poor prognosis [15].

PAH in Hypoxic Lung Disease

Hypoxic vasoconstriction appears to be the primary mechanism for PH in chronic obstructive pulmonary disease (COPD), obstructive sleep apnea, and interstitial lung disease. Arterial oxygen tensions of <60 mmHg and carbon dioxide partial pressure of >40 mmHg are considered thresholds for development of PH in COPD. Acidosis associated with hypoventilation works synergistically with hypoxia to induce pulmonary vascular vasoconstriction. Prevalence of PH in COPD is estimated to be ~5%, with between 5 and 14% of these patients developing severe PH (mean PAP >35 mmHg) [16]. Some studies recognize PAP as a prognostic factor in COPD patients undergoing long-term oxygen therapy, with poor pulmonary hemodynamics (mean PAP >25 mmHg) resulting in a doubling of mortality at 5 years [17]. The prevalence of PH in obstructive sleep apnea is 15–20%, but the PH is usually very mild and corrects with treatment. Anorexigens, such as the diet pill Fen-phen (fenfluramine and phentermine), are widely known to induce severe isolated PH in addition to causing valvular disease. Methamphetamine and cocaine use are also associated with the development of PAH; roughly 30% of IPAH patients report prior stimulant use [18].

The 2008 revised Dana Point classification system set by the World Health Organization defines PH into five categories in a treatment-based approach (Table 12.1). While convenient for determining appropriate therapeutic interventions, it does not focus on prevalence of disease or assist in the focused evaluation of individual etiologies. Because the clinical presentation of PH often overlaps with other underlying disease processes, specific guidelines for further diagnostic workup are not uniformly agreed upon. Usually the decision to perform the gold standard testing with RHC is based on the need to confirm the presence of PH, to differentiate whether it is PAH or pulmonary venous in etiology, and to assess pulmonary vasoreactivity. Initial RHC also provides important prognostic data [19]. Repeat RHC is also extremely valuable for monitoring therapeutic response and facilitating subsequent medicinal changes. The decision to proceed to RHC should always be balanced by the risks of an invasive procedure and the time and costs that are involved.

Clinical Presentation

The suspicion for pulmonary hypertension requires an astute clinician, especially in idiopathic PAH where there is generally no identifiable initial insult. Patients are commonly asymptomatic until the disease is fairly advanced; and without early diagnosis

and treatment, death can occur within a matter of months to years. Symptoms are often nonspecific and may be falsely attributed to deconditioning. PAH patients are typically young and otherwise healthy, and their complaints may be discounted by both themselves and their physicians. Placing the patient in the context of other ongoing diseases and exposures is also important in identifying patients at risk for PAH.

Dyspnea is the most common presenting symptom (60% of patients with IPAH), with nearly all patients developing this symptom during the course of the disease. Fatigue, syncope, palpitations, and chest pain are also common presenting symptoms, increasing in severity and frequency over time. Advanced disease presents with signs of right heart failure including peripheral edema, fatigue, and volume overload.

The auscultatory physical exam findings in early PH are subtle, most commonly including an increased intensity of P2 in 93% of patients. During disease progression nearly all patients will develop the low-frequency holosystolic murmur of tricuspid insufficiency, best heard over left lower sternal border. A right sided S4 may also be heard, along with a right parasternal heave. The waveforms of the jugular venous pulse demonstrate a prominent *a* wave; and in florid right ventricular (RV) failure, distention of the neck veins with prominent *a* and *v* waves. Late in the disease, significant edema, ascities, and hepatomegally are present along with a right sided S3.

Guidelines focus on World Health Organization (WHO) function class for clinical assessment of PH severity over New York Heart Association (NYHA) function class [3]. WHO class I patients have no physical limitations. Class II patients are comfortable at rest, and have slight limitations in activity, though ordinary physical activity causes symptoms. Class III patients have marked limitations in physical activity, and less than ordinary activity causes symptoms. Class IV patients are unable to carry out physical activity without symptoms, may be symptomatic at rest, often present with signs of right heart failure, and have the worst prognosis.

Evaluation of Pulmonary Hypertension

Noninvasive Evaluation

The initial evaluation of patients with a clinical course suspicious for PH typically involves multiple diagnostic modalities. Early in the disease process the electrocardiogram is typically normal; but by the time symptoms arise there is some amount of RV hypertrophy present, and subsequently RA enlargement and right axis deviation develop. The chest radiograph is often normal in PAH; however with moderate pulmonary hypertension (PAP 40–45 mmHg), some enlargement of the pulmonary arteries is noted, and with progression to advanced disease, RA and RV enlargement are present. A measured 6 min walk distance is easily performed and is very useful for prognosis, with a distance <332 m associated with worse outcomes [20]. Formal exercise testing with measurement of oxygen consumption is also an independent predictor for survival and closely correlates with 6 min walk distance.

Transthoracic echocardiography is an excellent screening tool for PH. Its utility is limited, however, by patient body habitus impacting the quality of the images and (quality of the images) and operator experience. Tricuspid regurgitation (TR) is nearly always evident in PH and allows for calculation of the RV systolic pressure. Studies comparing echo-Doppler to RHC pressures have found as much as a 45% false positive rate when a TR jet velocity >2.8 m/s is used to define PH [21]. Echocardiography also allows identification of valvular disease, left ventricular dysfunction, and shunt lesions through color Doppler and agitated saline. Certain clues, such as prominent left atrial enlargement and more than grade I diastolic dysfunction suggest a pulmonary venous etiology for the PH.

Cardiac magnetic resonance (CMR) can provide high resolution structural information; and with phase-contrast studies, hemodynamic data as well. However, because of the limited availability and the high cost involved, this modality should not be used for screening.

Computed tomography is particularly helpful to identify CTEPH. Ventilation/perfusion lung scintigraphy remains the gold standard for assessment of the latter, with the sensitivity and specificity to differentiate CTEPH from IPH approaching 100%. Pulmonary function testing can elucidate underlying airway or parenchymal disease such as COPD, and overnight pulse oximetry can identify sleep apnea as well as undiagnosed cardiac shunting. Blood tests such as brain natriuretic peptide (BNP) and N-terminal pro-brain natriuretic peptide (NT-proBNP) are also useful. Baseline BNP >150 pg/mL identifies patients with lower survival rates and decreasing BNP with therapy is associated with improved survival [22].

Hemodynamic Evaluation

The cornerstone for the diagnosis of PH remains the right heart cardiac catheterization (RHC). Measurement of RA pressure, PAP, cardiac output/index (CO/CI), PVR, and assessment of vasoreactivity are key elements for establishing diagnosis, collecting prognostic indicators and assisting in the selection of therapy. RHC is recommended in all patients with PAH to confirm the diagnosis, evaluate severity, and assess the need for PAH-specific drugs (Class IC) [3]. Repeat RHC is recommended to evaluate efficacy of PAH therapy when deterioration occurs or prior to escalation of therapy (Class IIaC).

In normal adults the resting mPAP should not exceed 20 mmHg. During exercise the mPAP typically remains <30 mmHg, though this depends on the level of exertion and the type and posture during exercise. PAP also increases with age and even slight levels of exertion in patients >50 years old may increase mPAP to >45 mmHg.

The 2009 guidelines define PAH as an mPAP of >25 mmHg with a PCWP or left ventricular end-diastolic pressure (LVEDP) ≤15 mmHg and a PVR greater than 3 Wood units [3]. The definition no longer includes an exercise-induced component,

given the variability in measurements noted above. PH assessment is also best performed in euvolemic states of low or normal CO. Measurement of CO is critical, because high output states such as anemia, pregnancy, sepsis, thyrotoxicosis, and intracardiac shunts may elevate PAP. In such cases the pulmonary vascular resistance remains normal. CO is best measured utilizing the Fick principle, because the frequent presence of significant tricuspid regurgitation can adversely impact thermodilution measurements. If thermodilution is used, results should be consistently collected in triplicate to assure accuracy.

If not automatically calculated by the cath lab software, the mPAP can be estimated by adding the diastolic pressure to 1/3 the pulse pressure (systolic–diastolic pressure). Stratification by severity by mPAP remains a major determinant of prognosis. Mild PH (mPAP 25–35 mmHg) and moderate PH (mPAP 35–45 mmHg) are more common in PH due to secondary causes, whereas severe PH (mPAP >45 mmHg) is typically found in CTEPH and PAH. Pulmonary vascular resistance in the normal individual is roughly 70–100 dyn/s/cm^5 (0.7–1.1 Wood units) and is calculated by using Ohm's Law. PVR = (mPAP−mPCWP)/CO. This equation gives a result in Wood units, which may be converted into dynes/cm/s^5 by multiplying by 80.

In a normal individual the transpulmonary gradient (mPAP−mPCWP) is typically between 5 and 9 mmHg. The transpulmonary gradient is generally not elevated in patients with left heart disease or states of high CO; however, when grossly elevated it has been considered pathognomonic for PAH. The assessment of appropriate PCWP can be technically challenging, but remains the most crucial measurement collected during RHC. The PCWP is used as a surrogate for the LA pressure (and in the absence of mitral stenosis, the LVEDP), and is useful to exclude PH due to left heart disease. It is recommended that a balloon flotation catheter be wedged in several different segments of the pulmonary vasculature, and that these measurements be taken in the lower lobes of the pulmonary vasculature (West zone 3). Zone 3 is the only location in the pulmonary circulation where one can be certain that the PA pressure is both greater than the pulmonary venous and pulmonary alveolar pressures, and thus the contributions of these pressures to the arterial measurements are minimized. Measurement of PCWP should be performed at end-expiration, again to minimize the impact of alveolar pressure gradients.

An elegant way to document whether PAH is present is continuous recording of the PCWP and then the PAP after balloon deflation +/− careful withdrawal of the catheter (Fig. 12.1a,b). A significant step up in the pressure waveform should be noted, resuming the PAP waveform almost immediately after deflation.

If the PCWP waveform has large *v*-waves, this suggests increased left atrial stiffness or possibly significant mitral regurgitation. In severe pulmonary hypertension, accurate measurement of PCWP may be difficult due to hybrid tracings resulting from incomplete seal of the balloon against the arterial wall. Though pulmonary arterial rupture has been a reported concern when attempting to wedge the catheter in PH patients, we have never encountered this problem. It can be fatal, however, should it occur. The overall risk of morbidity (~1.1%) and mortality (~0.05%) from RHC in PH in experienced centers is quite low [23]. If wedge pressure measurement is uncertain, direct measurement of the LVEDP (through left heart cath by

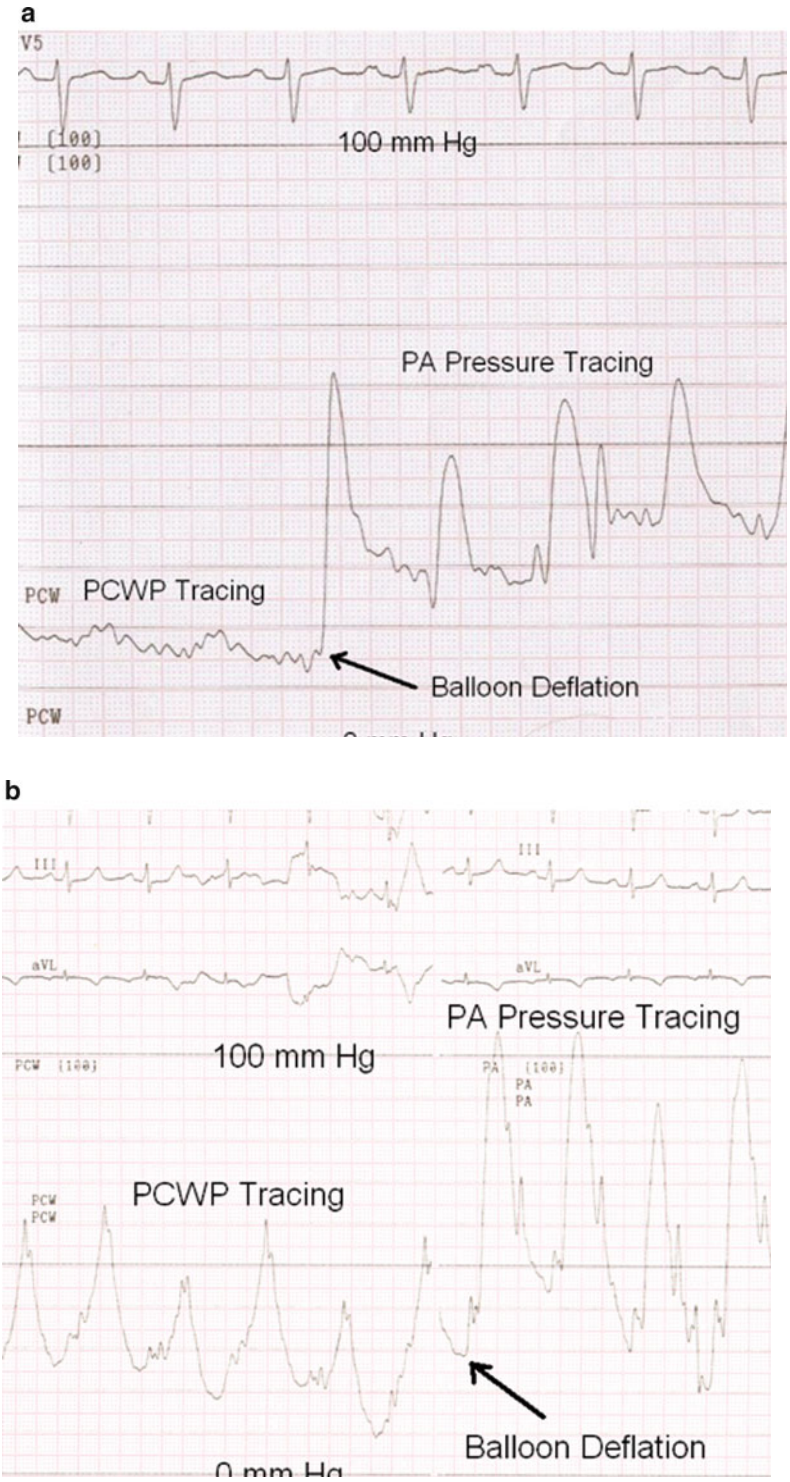
a
V5
100 mm Hg
PA Pressure Tracing
PCW
PCWP Tracing
Balloon Deflation
PCW
b
III
aVL
PA Pressure Tracing
100 mm Hg
PCW
PCWP Tracing
Balloon Deflation
0 mm Hg

retrograde crossing of the aortic valve) should be performed. This is particularly important if left heart disease is likely to be the etiology of PH.

The RA pressure waveform (and consequently the central venous waveform) of PH may have several distinctive features. A prominent *a* wave is common when the RV diastolic pressure is elevated and the normal x-descent (reflecting relaxation during systole) may be attenuated. In some cases a "peak-dome pattern" or prominent *cv* wave may be evident with a rapid y descent. Additionally, the expected decrease in RA pressure with inhalation may not occur in patients with severe PH and significant tricuspid regurgitation; on occasion RA pressure may even increase with inhalation creating confusion that pericardial disease (effusive/constrictive physiology) may be present. Pulsus alternans in the RV and pulmonary arterial tracing can occasionally be seen in severe PH and suggests considerable RV dysfunction. It is characterized by alternating strong and weak beats, resulting from the altered Frank–Starling relationship and dyssynchrony of noncompliant right ventricle.

Acute vasoreactivity testing (AVT) is another important component of the hemodynamic assessment and helps to determine prognosis and guide therapeutic strategies. Pressure measurements including the mPAP and PCWP are made at baseline and after administration of a short-acting pulmonary vasodilating agent such as intravenous prostacyclin, intravenous adenosine, or inhaled nitric oxide. Although AVT has traditionally been utilized to identify patients with idiopathic PAH who may be candidates for calcium channel blocker therapy [24, 25], recent studies have suggested that AVT response may also provide independent prognostic information that extends to other WHO Group I PH patients (PAH) and even those with non-Group I pulmonary hypertension [26, 27].

A positive response to the vasodilator challenge has been defined as a reduction in the baseline mPAP by ≥10 mmHg to a mPAP of ≤40 mmHg, with preserved or increased CO. Response to AVT suggests that the pulmonary vasculature has satisfactory amounts of vasodilatory reserve, likely an earlier stage of disease; and suggests an excellent prognosis, with possibly as high a survival as 95% at 5 years. The proportion of patients with a positive study ranges from 12 to 40%, depending on age and other comorbid conditions. It is important to note that the currently utilized definition of responsiveness was derived from a cohort of patients with IPH, with the goal of identifying patients who did well treated solely with calcium channel blockade [24]. In this cohort only ~5% of patients did well with calcium channel blocker therapy long-term; and with the proliferation of newer and more potent

Fig. 12.1 (**a**) Deflation of the wedged pulmonary capillary balloon catheter results in a rapid increase in the pressure recordings identifying the pulmonary artery pressure. In this case the mPAP is >25 mmHg and PCWP is <15 mmHg consistent with a diagnosis of PAH. (**b**) Identification of pulmonary venous hypertension using continuous right heart pressure monitoring during acute balloon inflation and deflation. The PA pressure is elevated but the mPCWP is well in excess of 15 mmHg with large *v*-waves, reflecting the impact of severe mitral regurgitation in this case

modern therapies, such a strategy is hard to justify. As such, the modern use of AVT helps to identify (by lack of response) a high-risk cohort that may only benefit from the most aggressive of therapies.

Inhaled nitric oxide (iNO) is most commonly utilized in AVT because of its specificity in targeting the pulmonary vasculature and the avoidance of decreased coronary blood flow (as can be seen during prostacyclin and adenosine administration). Also beneficial is the extremely short half-life of iNO, allowing rapid offset of effect in the event of clinical instability. The maximal effect of iNO is obtained after 5–10 min inhalation at 40 ppm [28]. In the presence of masked left ventricular diastolic dysfunction (due to low filling pressures) or significant mitral regurgitation, vasodilator testing may increase LVEDP/PCWP and result in acute pulmonary edema. A substantial increase in the *v*-wave of the PCWP tracing suggests that this may be occurring. It is also important to be aware of pulmonary venoocclusive disease. In this circumstance AVT can lead to life-threatening consequences.

In cases where left ventricular diastolic dysfunction is suspected but filling pressures are low (likely related to dehydration from fasting status), volume challenge may be necessary for accurate pressure determination. Although not standardized, typically increments of 250 mL of normal saline are bolus injected under careful hemodynamic observation. An increase in mean PCWP to >15 mmHg is suggestive of pulmonary venous hypertension, and warrants very different management than PAH.

A full oxygen saturation run should be performed in all patients undergoing initial RHC for PH in order to exclude congenital or structural causes of PH. Saturations should be measured in the innominate vein, superior vena cava (SVC), inferior vena cava (IVC), right atrium, right ventricle, and pulmonary artery. At the minimum the high SVC (to prevent sampling error in the event that isolated right upper anomalous pulmonary venous return is present) and PA saturations should be measured. If the latter is more than 5% higher than the SVC saturation, then a full collection of saturations is mandatory. If a full saturation run is performed, it is important to recognize that the RA saturation receives three different components (SVC, IVC, and coronary sinus). The mixed venous saturation is thus estimated by adding three times the SVC saturation to the IVC saturation and dividing by 4. Treatment decisions of which shunts benefit from repair is beyond the scope of the chapter, but patients with significant shunt lesions should generally be referred to cardiologists with experience in managing adults with congenital heart disease.

Hemodynamic data maintains a critical prognostic role in PAH, with increased RA pressure (≥12 mmHg), decreased CI (<2 L/m^2), and lack of AVT response all associated with increased risk of death [29]. PA pressure appears less predictive, however, likely related to the expected disease course. As the disease progresses RV function declines, leading to a reduction in CO. Despite progressive increase in PVR, the mPAP plateaus and may even decrease, as the output generally declines more rapidly than the PVR (uncoupling of the right ventricle). This lessens the prognostic capability of PAP and makes serial monitoring of the RA pressure and CI much more helpful for prognostic purposes.

Case Examples

Case 1

M.H. is a 53-year-old gentleman with scleroderma diagnosed 10 years ago as well as well-controlled essential hypertension, who presented with complaints of worsening exertional dyspnea. A pulmonologist evaluated him 5 years ago and diagnosed him with mild interstitial lung disease. He was stable until ~3 months prior to referral, but his fatigue and dyspnea had since progressed to WHO function Class III. There was no prior cardiac history.

His examination showed a JVP of 12 cm, a mildly prominent P2, a I/VI murmur of tricuspid regurgitation and 1+ peripheral edema. An echocardiogram revealed a dilated IVC, right heart enlargement, and mild RV systolic dysfunction with an estimated RV systolic pressure of 60 mmHg. There was stage 1 LV diastolic dysfunction and LA size was normal. He was taken to the cardiac catheterization laboratory where pressures included mean RA 12 mmHg, RV 66/12 mmHg, PA 71/41 with mean 51 mmHg, mean PCWP 41 mmHg. CI was 2.3 L/min/m^2 and calculated PVR 1.9 Wood Units. He was treated with diuretics by his physician but then developed hypotension and mild acute renal failure.

After seeing the patient in consultation, we felt that the hemodynamics (suggesting pulmonary venous hypertension) did not match the clinical story (suggesting PAH). We then reviewed the hemodynamic tracings (Fig. 12.2) which brought the measured PCWP into question (little respiratory variation and a "fusion" appearance). It had been measured only in one position and the tracing suggested incomplete balloon occlusion of the PA. With some disenchantment the patient agreed to return to the cath lab, where data revealed: RA mean 8 mmHg; RV 60/8 mmHg; PAP 60/33 with mean 40 mmHg; PCWP 12 mmHg; CI 2.2 L/min/m^2; and PVR 6.4 Wood units (Fig. 12.3). LVEDP was also measured (11 mmHg). With 40 ppm iNO: PAP dropped to 54/30 with mean 36 mmHg and PCWP remained at 12 mmHg. CI was 2.3 L/min/m^2 and calculated PVR 5.4 Wood units. He was started on an endothelin blocker, as part of a study protocol, and on follow-up he experienced an ~50 m increase in 6 min walk and improvement to WHO function class II.

This patient presents the dilemma of an RHC where data has not been properly collected. In cases like this it is important to review the actual waveforms and assess if measurements were appropriately performed. In this case the initial RHC evaluated a hybrid PCWP waveform that grossly overestimated the PCWP. With repeat RHC and confirmation with measurement of the LVEDP, the appropriate diagnosis of PAH was made and the proper therapy was initiated. Other techniques to ensure appropriate PCWP measurement include repeat measurements in both lung fields in different segments, assurance of appropriate respiratory variation in the tracing, collection of a wedge saturation (which should be ≥95%) and a small (~2 to 3 cm^3), gentle injection of contrast dye which should not be washed out until the balloon is deflated. Figure 12.4 shows an example of such an injec-

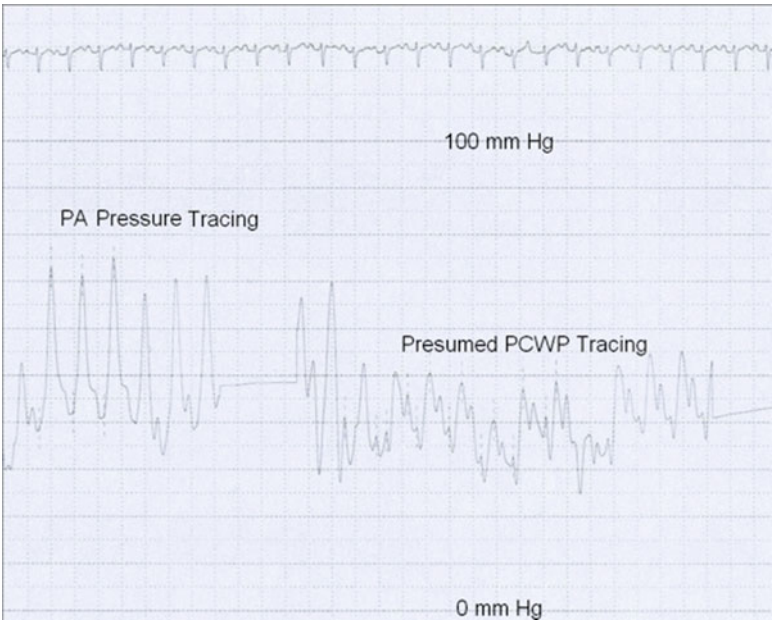

Fig. 12.2 Initial right heart catheterization in a patient with scleroderma that suggests the presence of pulmonary venous hypertension. There is limited respiratory variation in the PCWP tracing and the tracing appears to be a hybrid (fusion of PAP and PCWP waveforms) suggesting incomplete balloon occlusion of the pulmonary artery. These tracings were not consistent with the expected findings. In such cases multiple measurements should be obtained in different locations and the LVEDP should then be measured for confirmation. This patient required repeat hemodynamic assessment to obtain the proper measurements

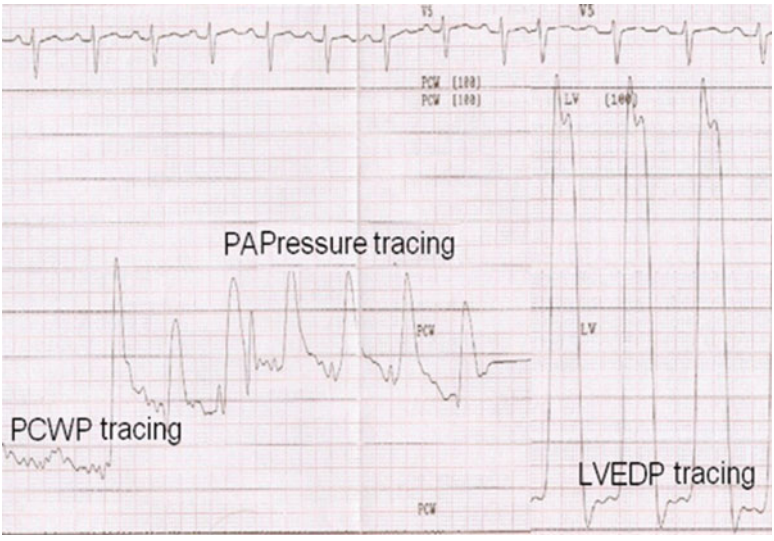

Fig. 12.3 Repeat right heart catheterization which indicates the presence of PAH (the expected finding given the clinical history). The LVEDP confirms that the PCWP is low in this case

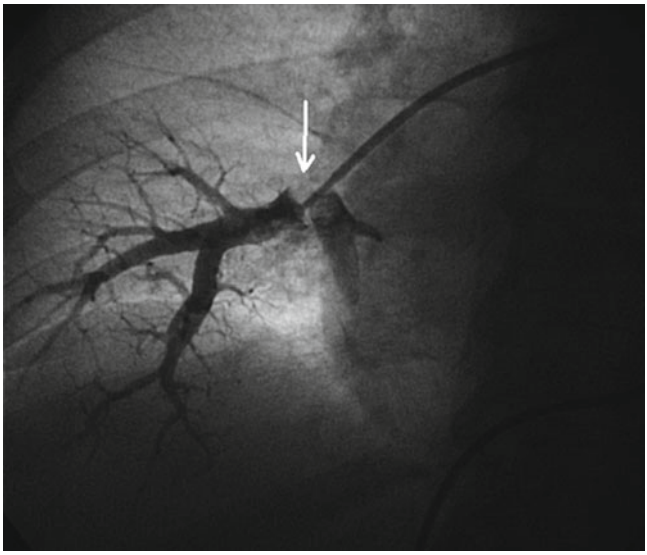

Fig. 12.4 Gentle contrast injection into the right pulmonary artery under balloon inflation (pulmonary wedge angiogram). The tip of the balloon is highlighted by the (*arrow*). Dye is seen filling a branch pulmonary artery proximal to the balloon and suggests incomplete occlusion. In such a case, a hybrid tracing would be present and would lead to an inappropriately high PCWP recording

tion where contrast dye is seen proximal to the balloon. This suggests incomplete occlusion and can explain the presence of a hybrid tracing (which can lead to an inappropriately high PCWP measurement).

Case 2

J.T. is a 66-year-old woman with multiple medical problems including advanced renal disease, dilated cardiomyopathy (LVEF ~20%), and resultant severe mitral and tricuspid regurgitation. She was admitted to the coronary care unit for further management of worsening congestive heart failure and hemodynamic instability. On examination she was severely volume overloaded and in respiratory distress with JVD above the angle of the jaw at 45° and a large *cv* wave. There was a prominent P2 present and a III/VI holosystolic murmur heart best over apex, a laterally displaced point of maximal impulse and a palpable RV heave. Lungs showed bibasilar rales and there was 2+ pitting peripheral edema.

Echo showed 4 chamber dilatation with severe mitral and tricuspid regurgitation. Estimated RV systolic pressure was 80 mmHg. RHC at the bedside revealed RA pressure 24 mmHg, RV 96/22 mmHg, PA 96/40 with mean 62 mmHg, mean PCWP 34 mmHg, CI 1.8 L/min/m^2, and PVR 10 Wood units. She was seen in consultation

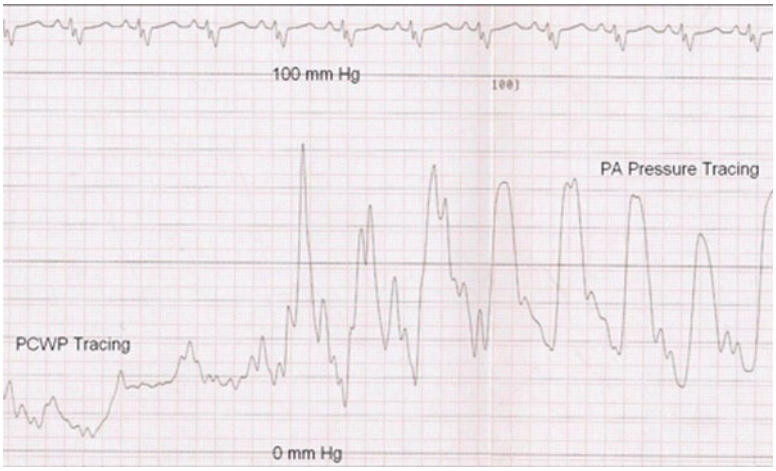

Fig. 12.5 Collected right heart catheterization waveforms in patient with heart failure and severe mitral regurgitation leading to pulmonary hypertension after aggressive diuresis. These suggest the presence of PAH and initially supported a potential role for selective pulmonary vasodilator therapy in this patient

for possible initiation of pulmonary selective therapies, and we instead recommended continued aggressive dieresis and afterload reduction with hydralazine and nitrates (baseline creatinine was 2.5 mg/dL) with the plan for repeat hemodynamic assessment when stable.

RHC in the cath lab 10 days later showed RA pressure 15 mmHg, RV 73/15 mmHg, PA 73/28 with mean 44 mmHg, PCWP 16 mmHg, CI 1.5 L/min/m^2, and PVR 12.2 Wood units (Fig. 12.5). During inhalation of 40 ppm of nitric oxide, the PA pressure remained essentially unchanged (73/30 with mean 46 mmHg) but the pulmonary capillary wedge increased to a mean of 30 with *v*-waves to 65 mmHg (Fig. 12.6). The team was instructed that the patient was not a candidate for selective pulmonary vasodilator therapy and surgical consultation for consideration of mitral and tricuspid valve repair was recommended.

This patient had long-standing RV dysfunction that likely arose from pulmonary venous hypertension consequent to high left sided filling pressures from left ventricular dysfunction and mitral regurgitation. The PH in this case is therefore the offshoot of long-standing left heart disease and is likely compensatory to "protect" the left ventricle. AVT provides some insight into what would happen with pulmonary-selective therapy and the results suggest that the patient would be poorly tolerant of this therapeutic approach. In such cases this type of therapy could worsen her clinical course and precipitate decompensation and even death. Thorough assessment of hemodynamics in this case led to better understanding of the physiology and avoided a potential pharmacologic misadventure.

Fig. 12.6 Collected right heart catheterization waveforms during inhalation of 40 ppm of inhaled nitric oxide. Note the dramatic increase in mPCWP to ~30 mmHg and prominent *v*-waves to >65 mmHg. The PA pressure remained essentially unchanged (73/30 with mean 46 mmHg) compared to baseline (Fig. 12.5). In this case acute vasodilator testing unmasked the left heart pathology leading to pulmonary venous hypertension in this patient

Case 3

R.B. is a concerned 36-year-old gentleman who presented with progressive exertional dyspnea and fatigue that had significantly limited his ability to work in construction over the last few years. A recent echo suggested right sided enlargement and borderline elevated RV systolic pressure. A bubble study was performed that suggested the presence of a "PFO." His right heart catheterization revealed: mean RA pressure 10 mmHg, RV 40/9 mmHg, PA 40/18 with mean 25 mmHg, PCWP mean 12 mmHg, cardiac index 4.0 L/min/m^2, and PVR 1.3 Wood Units. O_2 saturation measurements: SVC 75%, IVC 76%, RA 89%, RV 88%, PA 88%, and Ao 98%.

This case highlights the diagnostic capability of a properly performed shunt run. In this case there is a clear increase in saturation at the RA level. A contrast injection was subsequently performed that showed an anomalous right upper pulmonary vein draining into the border of the SVC and RA and the presence of a right to left shunt in the superior septum. This was most consistent with a sinus venosus ASD and concomitant partial anomalous pulmonary venous return. It is important to recognize that partial anomalous pulmonary venous return can also be present in isolation. In such cases the echo bubble study may be negative. Performing a shunt run or at least SVC and PA saturations during RHC ensures that such a shunt will not be missed. The anomalous vein can be entered quite easily, and a gentle contrast injection can delineate its entry point into the heart (Fig. 12.7). A blood gas drawn in the vein should demonstrate a saturation (≥95%).

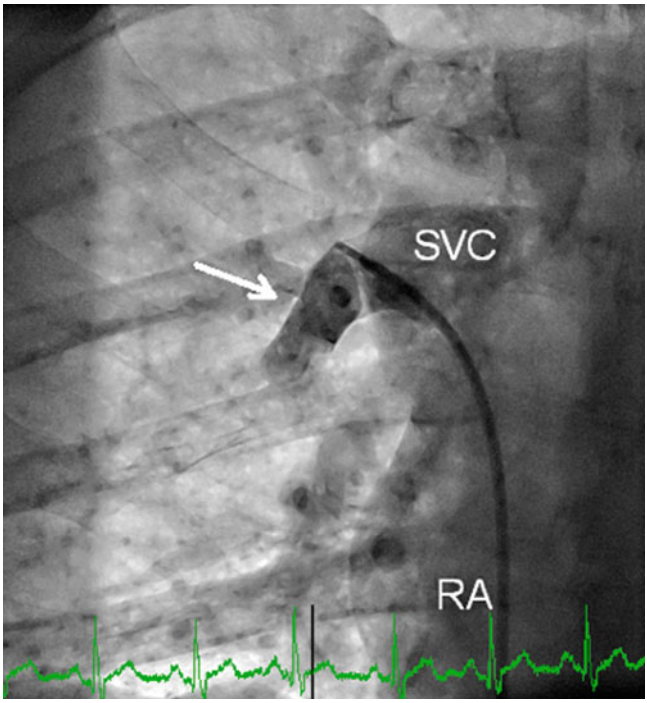

Fig. 12.7 Limited pulmonary vein angiogram (AP projection) of an anomalous right upper pulmonary vein performed via right femoral vein access (hand injection via end-hole catheter). The *white arrow* highlights the distal segment of the pulmonary vein which drains into the SVC at the RA junction. Samples drawn from this vein showed oxygen saturations >95%. A high CO at catheterization in the presence of right heart enlargement and a negative bubble study should prompt careful assessment for possible anomalous pulmonary venous return

A major clue to the presence of an underlying shunt is revealed in the cardiac index. Most patients with pulmonary hypertension will have at least slightly reduced CO (if not grossly decreased). If the CO/CI is normal or high in a patient with echocardiographic evidence of right sided enlargement (as it was in this case), a shunt is probable and should be carefully sought out. A patent foramen ovale (PFO) does not usually result in left to right shunting and would certainly not be expected to result in right heart enlargement. The patient in this case was referred to cardiac surgery and underwent successful repair. Repeat echocardiography has demonstrated normalization of his right sided pressures and chamber sizes after repair.

Pearls of Assessment of Pulmonary Hypertension

- Clinical suspicion for PH should remain high, especially in young patients with vague complains such as dyspnea. Family and social history can provide important clues to a possible diagnosis.

- PAH is a diagnosis of exclusion, and patients must undergo a complete workup before a diagnosis of PAH is entertained. Secondary causes resulting in pulmonary venous hypertension are a far more common cause of PH.
- The use of echocardiography is not adequate for evaluating mild to moderate PH. Only in severe PH does Doppler echocardiography provide reliable data for estimating RVESP. Echocardiography is essential for exclusion of left heart disease.
- The diagnosis of PAH can only be confirmed with RHC. Guidelines define PAH as mPAP >25 mmHg, PCWP ≤15 mmHg, and PVR >3 Wood units with a normal or reduced CO/CI.
- Appropriate patients undergoing RHC should be further evaluated with vasodilator testing. This aids in selecting therapy and helps determine prognosis.
- For patients in whom PCWP is not believed to be reliable, LVEDP should be directly measured.
- Beware of hybrid tracings and confirm that an accurate PCWP measurement has been recorded.
- Prognostic information and therapeutic decision-making are dependent on hemodynamics. Thus appropriate techniques and proper and immediate interpretation are vital to performing RHC in patients with PH.
- Communication with referring and treating physicians is essential to streamline appropriate patient therapy in this very serious clinical disorder.

Questions

1a. A 46-year-old African American woman complains of cough, lower extremity edema, and dyspnea on exertion over the last 3 months. Medical history is significant for sarcoidosis diagnosed at 35 years of age and she has a 30 pack year history of smoking. Vitals are: BP 135/78, P 87, RR 20, and SpO_2 88% on room air. She has a prominent P2, but no other murmurs, rubs, or gallops. Arterial blood gas is notable for hypoxemia; SaO_2 90% PO_2 49 mmHg and PCO_2 35 mmHg. Chest X-ray demonstrates bilateral infiltrates, perihilar lymphadenopathy, and pulmonary vascular dilatation. EKG shows sinus rhythm with right axis deviation.

What is the next step in the management of this patient?

A. Pulmonary function testing
B. Transthoracic echocardiogram
C. CT angiography of chest
D. Right heart catheterization
E. 6 min walk test

Answer C is correct Although clinical suspicion for pulmonary hypertension remains high, other more acute causes of hypoxemia must be ruled out. Pulmonary embolism should be ruled out with high resolution CT angiography. Subsequent

evaluations with echo, PFTs, and thorough laboratory workup are warranted afterwards with RHC if other workup is suggestive of PAH.

1b. CT scan shows the expected findings of sarcoidosis and no pulmonary embolism. Evaluation with Doppler echo reveals RV systolic pressure of 70 mmHg with enlargement of right sided heart structures and normal left heart function. She desaturates to 83% on 6 min walk test and is only able to complete 300 m. Right heart catheterization is scheduled.
Which of the following hemodynamics is most consistent with PAH?

A. mPAP 54 mmHg, PCWP 10 mmHg, CO 5.1 L/min, PVR 8.6 Wood units
B. mPAP 40 mmHg, PCWP 26 mmHg, CO 5.2 L/min, PVR 2.7 Wood units
C. mPAP 52 mmHg, PCWP 14 mmHg, CO 13.4 L/min, PVR 2.8 Wood units
D. mPAP 18 mmHg, PCWP 12 mmHg, CO 5.5 L/min, PVR 1.1 Wood units
E. mPAP 28 mmHg, PCWP 15 mmHg, CO 4.9 L/min, PVR 4.7 Wood units

Answer A is correct and most consistent with the current guidelines for a hemodynamic diagnosis of PAH. Peripheral vascular resistance is calculated by mPAP-PCWP/CO (54–10)/5.1 = 8.6 Wood units. Answer B is more indicative of left sided heart failure, leading to right sided pressure elevation. The transpulmonary gradient is grossly elevated in answer C, but the CO is also grossly elevated, suggesting the presence of a condition such as hyperthyroidism or an intracardiac shunt. This patient should have a full saturation run performed to investigate the latter possibility more thoroughly. Answer D is consistent with completely normal hemodynamics. Answer E would have been correct if the PVR had not been calculated incorrectly. The actual PVR is (28–15)/4.9 = 2.7 Wood units, which does not meet the formal criteria for PAH.

1c. Acute vasoreactivity testing with inhaled nitric oxide at 40 ppm is performed. After 5 min which of the following hemodynamics is most consistent with a positive response (baseline mPAP 54 mmHg and PCWP 10 mmHg)?

A. mPAP 42 mmHg and PCWP 10 mmHg on iNO
B. mPAP 38 mmHg and PCWP 10 mmHg on iNO
C. mPAP 52 mmHg and PCWP 18 mmHg on iNO
D. mPAP 68 mmHg and PCWP 8 mmHg on iNO

Answer B is correct as the drop in mPAP is >10 mmHg and reaches <40 mmHg during AVT. Answer A shows a substantial drop in mPAP, but not to <40 mmHg. Answer C shows a slight drop in mPAP but also an increase in PCWP. Providing that the PCWP was properly recorded, this suggests the possibility of unmasked left ventricular diastolic dysfunction. Initiation of selective pulmonary vasodilator therapy would not be recommended in this patient. Answer E is illogical as the mPAP is not expected to rise, or the PWCP to fall, during AVT.

2. A 45-year-old man undergoes RHC for suspected mild PAH. He weighs 80 kg, is 1.75 m tall, and his body surface area is 1.97 m^2. His hemoglobin is 12.5 g/dL. A shunt run is performed.
   Which of the following would be most suspicious for PAH secondary to a congenital heart lesion?

   A. SVC Saturation 75%, IVC Saturation 77%, PA saturation 74%
   B. SVC Saturation 78%, IVC Saturation 84%, PA saturation 68%
   C. SVC Saturation 70%, IVC Saturation 74%, PA saturation 72%
   D. SVC Saturation 69%, IVC Saturation 72%, PA saturation 71%
   E. SVC Saturation 74%, IVC Saturation 77%, PA saturation 90%

Answer E: is correct The mixed venous saturation is estimated by (3×SVC+IVC)/4. If the pulmonary artery saturation is at least 7% greater than the mixed venous saturation, a shunt is highly likely. In answer E, the estimated mixed venous saturation is (74×+77)/4=75% with a PA saturation of 90%. The pulmonary venous saturation (if not collected) is estimated at ~97%. The calculated Q_p/Q_s=(aortic sat−mixed venous sat)/(pulmonary vein sat−pulmonary artery sat)=(97–75)/(97–90)=3.1:1, suggesting a large left to right shunt. None of the other choices show a step-up in saturation. The PA saturation in B must be incorrect as a step-down in saturation in the right heart is not possible. This saturation should be repeated ensuring to tap out any residual air bubbles from the syringe (which can lead to aberrant readings) before analysis.

3. A 44-year-old man has familial PAH and has been stable on a regimen of 20 mg amlodipine daily for the past 3 years, which he takes as prescribed. He presents for his yearly follow-up and reports increasing dyspnea and fatigue over the last 3 months. He is comfortable at rest and able to perform some activities of daily living, but has fatigue with repetitive actions such as brushing teeth while standing up. A 6 min walk shows desaturation to 83% after 50 m. One year ago he desaturated to 92% after 100 m. He does not report any new medications and liver function tests are consistent with prior studies.
   What functional class should he be classified as and what is the next step in the care of this patient?

   A. Function Class II: Begin prostanoid or endothelin-receptor antagonist therapy
   B. Function Class II: Repeat a full hemodynamic assessment before altering medications
   C. Function Class III: Begin prostanoid or endothelin-receptor antagonist therapy
   D. Function Class III: Repeat a full hemodynamic assessment before altering medications
   E. Function Class VI: Begin prostanoid or endothelin-receptor antagonist therapy
   F. Function Class VI: Repeat a full hemodynamic assessment before altering medications

Answer D is correct. This patient presents with worsening symptoms that are consistent with WHO function class III, as he is stable at rest, but less than ordinary activity causes him symptoms. He is on a reasonable dose of an effective calcium channel blocker, but with his progression in symptoms, it is likely that additional medical therapy is necessary. Ideally he should first undergo repeat RHC to reassess his CO and filling pressures before a change is made, as he is a candidate for oral, inhaled, or intravenous therapies and hemodynamic data can help to properly select the most advantageous therapy.

References

1. Humbert M, Sitbon O, Chaouat A, et al. Pulmonary arterial hypertension in France: results from a national registry. Am J Respir Crit Care Med. 2006;173(9):1023–30.
2. Kovacs G, Berghold A, Scheidl S, Olschewski H. Pulmonary arterial pressure during rest and exercise in healthy subjects: a systematic review. Eur Respir J. 2009;34(4):888–94.
3. McLaughlin VV, Archer SL, Badesch DB, et al.; ACCF/AHA 2009 expert consensus document on pulmonary hypertension a report of the American College of Cardiology Foundation Task Force on Expert Consensus Documents and the American Heart Association developed in collaboration with the American College of Chest Physicians; American Thoracic Society, Inc.; and the Pulmonary Hypertension Association. J Am Coll Cardiol 2009;53(17):1573–619.
4. Sztrymf B, Coulet F, Girerd B, et al. Clinical outcomes of pulmonary arterial hypertension in carriers of BMPR2 mutation. Am J Respir Crit Care Med. 2008;177(12):1377–83.
5. Hopkins WE, Ochoa LL, Richardson GW, Trulock EP. Comparison of the hemodynamics and survival of adults with severe primary pulmonary hypertension or Eisenmenger syndrome. J Heart Lung Transplant. 1996;15(1 Pt 1):100–5.
6. McLaughlin VV, Shillington A, Rich S. Survival in primary pulmonary hypertension: the impact of epoprostenol therapy. Circulation. 2002;106(12):1477–82.
7. Sitbon O, Humbert M, Nunes H, et al. Long-term intravenous epoprostenol infusion in primary pulmonary hypertension: prognostic factors and survival. J Am Coll Cardiol. 2002;40(4):780–8.
8. Galiè N, Manes A, Negro L, et al. A meta-analysis of randomized controlled trials in pulmonary arterial hypertension. Eur Heart J. 2009;30(4):394–403.
9. Rich S, Kaufmann E, Levy PS. The effect of high doses of calcium-channel blockers on survival in primary pulmonary hypertension. N Engl J Med. 1992;327(2):76–81.
10. Badesch DB, Champion HC, Sanchez MAG, et al. Diagnosis and assessment of pulmonary arterial hypertension. J Am Coll Cardiol. 2009;54(1 Suppl):S55–66.
11. Bonderman D, Skoro-Sajer N, Jakowitsch J, et al. Predictors of outcome in chronic thromboembolic pulmonary hypertension. Circulation. 2007;115(16):2153–8.
12. Gladwin MT, Sachdev V, Jison ML, et al. Pulmonary hypertension as a risk factor for death in patients with sickle cell disease. N Engl J Med. 2004;350(9):886–95.
13. Marvisi M, Zambrelli P, Brianti M, et al. Pulmonary hypertension is frequent in hyperthyroidism and normalizes after therapy. Eur J Intern Med. 2006;17(4):267–71.
14. Duffels MGJ, Engelfriet PM, Berger RMF, et al. Pulmonary arterial hypertension in congenital heart disease: an epidemiologic perspective from a Dutch registry. Int J Cardiol. 2007;120(2):198–204.
15. Galie N, Manes A, Palazzini M, et al. Management of pulmonary arterial hypertension associated with congenital systemic-to-pulmonary shunts and Eisenmenger's syndrome. Drugs. 2008;68(8):1049–66.
16. Minai OA, Chaouat A, Adnot S. Pulmonary hypertension in COPD: epidemiology, significance, and management: pulmonary vascular disease: the global perspective. Chest. 2010;137(6 Suppl):39S–51.

17. Chaouat A, Naeije R, Weitzenblum E. Pulmonary hypertension in COPD. Eur Respir J. 2008;32(5):1371–85.
18. Chin KM, Channick RN, Rubin LJ. Is methamphetamine use associated with idiopathic pulmonary arterial hypertension? Chest. 2006;130(6):1657–63.
19. Groves BM, Turkevich D, Donnellan K, et al. Current approach to treatment of primary pulmonary hypertension. Chest. 1988;93(3 Suppl):175S–8.
20. Miyamoto S, Nagaya N, Satoh T, et al. Clinical correlates and prognostic significance of six-minute walk test in patients with primary pulmonary hypertension. Comparison with cardiopulmonary exercise testing. Am J Respir Crit Care Med. 2000;161(2 Pt 1):487–92.
21. McQuillan BM, Picard MH, Leavitt M, Weyman AE. Clinical correlates and reference intervals for pulmonary artery systolic pressure among echocardiographically normal subjects. Circulation. 2001;104(23):2797–802.
22. Nagaya N, Nishikimi T, Uematsu M, et al. Plasma brain natriuretic peptide as a prognostic indicator in patients with primary pulmonary hypertension. Circulation. 2000;102(8):865–70.
23. Hoeper MM, Lee SH, Voswinckel R, et al. Complications of right heart catheterization procedures in patients with pulmonary hypertension in experienced centers. J Am Coll Cardiol. 2006;48(12):2546–52.
24. Sitbon O, Humbert M, Jaïs X, et al. Long-term response to calcium channel blockers in idiopathic pulmonary arterial hypertension. Circulation. 2005;111(23):3105–11.
25. Morales-Blanhir J, Santos S, de Jover L, et al. Clinical value of vasodilator test with inhaled nitric oxide for predicting long-term response to oral vasodilators in pulmonary hypertension. Respir Med. 2004;98(3):225–34.
26. Krasuski RA, Devendra GP, Hart SA, et al. Response to inhaled nitric oxide predicts survival in patients with pulmonary hypertension. J Card Fail. 2011;17(4):265–71.
27. Skoro-Sajer N, Hack N, Sadushi-Koliçi R, et al. Pulmonary vascular reactivity and prognosis in patients with chronic thromboembolic pulmonary hypertension: a pilot study. Circulation. 2009;119(2):298–305.
28. Krasuski RA, Warner JJ, Wang A, et al. Inhaled nitric oxide selectively dilates pulmonary vasculature in adult patients with pulmonary hypertension, irrespective of etiology. J Am Coll Cardiol. 2000;36(7):2204–11.
29. D'Alonzo GE, Barst RJ, Ayres SM, et al. Survival in patients with primary pulmonary hypertension. Results from a national prospective registry. Ann Intern Med. 1991;115(5):343–9.

Chapter 13
Acute Decompensated Heart Failure

Andrew D.M. Grant, Michael A. Hanna, and Mazen A. Hanna

Epidemiology of Acute Decompensated Heart Failure

Heart failure is estimated to affect 2% of the adult population. There are over one million hospitalizations for acute decompensated heart failure in the United States per year and, among the Medicare population, it is the leading discharge diagnosis [1, 2]. About 25% of these patients present as de novo heart failure and 75% present as an exacerbation of chronic heart failure. When not due to an arryhthmia or primary valvular disease, heart failure may arise in those with either decreased (~50%) or preserved (~50%) systolic function of the left ventricle [3]. The inpatient mortality ranges from 3 to 25% depending on associated comorbidites and clinical characteristics [4]. The readmission rate at 30 days is a staggering 20–25%.

Hemodynamics of Decompensated Heart Failure

The hemodynamic perturbations in the syndrome of decompensated heart failure are characterized by elevated intracardiac filling pressures, normal or reduced cardiac output, and abnormalities in the systemic and pulmonary vascular resistance. Although there are syndromes in which the cardiac output is abnormally elevated, these will not be discussed in this chapter.

A.D.M. Grant
UTMB Department of Microbiology and Immunology, Galveston, TX, USA
e-mail: Granta2@ccf.org

M.A. Hanna
Chief of Medicine Huron Hospital, Chief of Cardiology Hillcrest Hospital, Medical Director of Heart Failure Center, 6770 Mayfield Road, #333 Mayfield Hts, OH 44124, USA

M.A. Hanna (✉)
The Cleveland Clinic, Cleveland, OH, USA
e-mail: hannam@ccf.org

A.T. Askari et al. (eds.), *Cardiovascular Hemodynamics: An Introductory Guide*, Contemporary Cardiology, DOI 10.1007/978-1-60761-195-0_13,

Intracardiac Filling Pressures

When volume overload (increased preload) and/or increased afterload occur, there is an elevation of the left ventricular end-diastolic pressure from the patient's baseline (which may already be elevated). This leads to elevation in left atrial pressure and thus pulmonary capillary wedge pressure (PCWP). The elevation in the PCWP leads to passive *pulmonary hypertension* (pulmonary venous hypertension), which in addition to volume overload leads to elevation of the right atrial pressure (RAP). The degree of resultant pulmonary hypertension depends on the degree and chronicity of the elevation of the PCWP and the degree of superimposed pulmonary vasoconstriction and vascular remodeling (see section "Vascular Resistance").

In patients with decompenstated heart failure, the PCWP is usually >22 mmHg and the right atrial pressure >10 mmHg, and such a patient is typically classified as "wet." In the average decompensated heart failure patient, a RAP >10 mmHg correlates to a PCWP >22 mmHg about 80% of the time [5–8]. In these "concordant" cases, the PCWP is usually about 2–2.5 times the RAP. About 20% of the time there is "discordance" in this relationship; one example is in patients with disproportionate RV failure in which the RAP is significantly raised with a normal or only mildly raised PCWP. The other example is when RAP is normal with a significantly elevated PCWP as one may see in acute left-sided heart failure without volume overload or due to a very noncompliant LV with high resting filling pressure despite euvolemia. These are important hemodynamic concepts to understand as they may affect management.

Cardiac Output

The cardiac output is a product of stroke volume and heart rate. The stroke volume is determined by the preload (filling pressure), myocardial contractility, and afterload (mainly the systemic vascular resistance). In patients with decompensated heart failure, a decrease in cardiac output is more likely due to inadequate stroke volume, but occasionally can be due to an inappropriately low heart rate. It is important to note that despite conventional belief, in the majority of cases of acute decompensated heart failure, the cardiac output remains normal. Low cardiac output, as measured by Fick or Thermodilution (we more often use the Fick method at our institution), occurs in a minority of patients who have advanced heart failure or excessively low filling pressures due to overdiuresis. Arbitrarily, a cardiac index (Cardiac output/Body surface area) of <2.2 is considered low, and such a patient is typically classified as "cold" vs. a patient with a cardiac index >2.2 who is classified as "warm." A patient with a low cardiac index may be compensated and have no signs or symptoms of low perfusion at rest, thus it is important to consider the overall clinical picture in addition to the calculated cardiac index when deciding prognosis and treatment options.

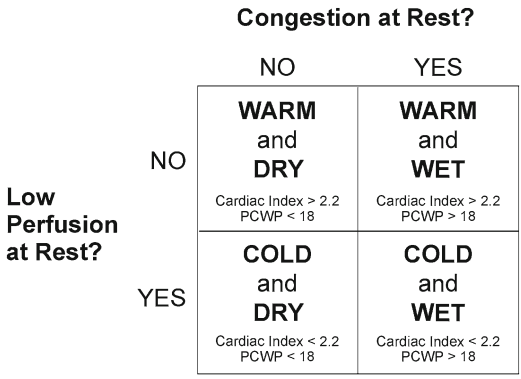

Fig. 13.1 Hemodynamic profiles in patients with left-sided heart failure

When evaluating a patient with decompensated heart failure, it is useful to categorize the patient according to the estimation or measurement of left-sided filling pressures and cardiac output. The classification scheme shown in Fig. 13.1 is a simple and efficient way to clinically categorize patients and help guide appropriate treatment strategies.

Vascular Resistance

The systemic vascular resistance (SVR) is measured as the difference between the mean arterial pressure and the right atrial pressure divided by the cardiac output. Classically, in decompensated heart failure, systemic vascular resistance is high as a result of an increased level of vasoconstricting neurohormones such as norepinephrine, angiotension II, and endothelin. However, in the contemporary era in which treatment with ACE inhibitors and beta blockers is common, the SVR can be normal and in fact sometimes even low. Patients with right-sided heart failure and renal insufficiency are more likely to have normal or low SVR. Knowing the blood pressure and/or the SVR is important with respect to determining treatment options.

The pulmonary vascular resistance (PVR) is measured as the difference between mean pulmonary artery pressure and the PCWP (left atrial pressure surrogate) divided by the cardiac output. It is important to note that in some patients, in addition to the resultant passive pulmonary hypertension due to elevated left atrial pressure, there is an additional component of pulmonary vasoconstriction, raising the pulmonary vascular resistance and thus further raising the pulmonary artery pressure (pulmonary arterial hypertension). Long-standing elevation of the pulmonary capillary wedge pressure can also lead to pulmonary vascular remodeling. This component of pulmonary vascular resistance cannot be reversed acutely by lowering the PCWP or with the use of pulmonary vasodilators. Patients with an elevated PVR that cannot be reversed have a worse prognosis.

Table 13.1 Signs and symptoms of elevated intracardiac filling pressures

	↑ RA pressure	↑ PCWP
Symptoms	Leg swelling	Dyspnea at rest or on exertion
	Abdominal bloating	Orthopnea
	Early satiety	PND
	Nausea, anorexia	Positional cough
	RUQ pain	Rales[c]
Signs	Lower extremity edema[a]	S_3 gallop
	Ascites	CXR with pulmonary congestion
	Enlarged/tender liver	
	Elevated JVP[b]	

[a]Nonspecific and can be due to venous insufficiency, DVT, calcium channel blockers, etc.
[b]Most specific and sensitive sign of elevated RA pressure and may often be the only sign
[c]Rare in chronic heart failure

Hemodynamic Evaluation of Decompensated Heart Failure

There are many ways to evaluate hemodynamics in heart failure. The initial and most practical strategy is starting with the clinical bedside evaluation. Further important hemodynamic information can be gleaned from echocardiography. The most invasive and accurate way to assess hemodynamics is with right heart catheterization using a pulmonary artery catheter, which is reserved for special situations.

Clinical Assessment

The history and physical examination together with a chest X-ray and basic labs provides the majority of the hemodynamic information needed to treat patients with acute decompensated heart failure. The shortcomings of the history and physical examination are important to acknowledge however, and some of these will be highlighted as we discuss each of the clinical cases at the end of the chapter.

Clinical Estimation of Filling Pressures

Using the history and physical examination, experienced clinicians can estimate, with reasonable accuracy, the intracardiac filling pressures [9, 10]. Some of the important signs and symptoms of elevated filling pressures are outlined in Table 13.1. Symptoms of elevated right atrial pressure, depending on the degree and chronicity, include abdominal bloating and discomfort, early satiety, and RUQ pain that can mimic an abdominal etiology. Signs of elevated right atrial pressure include lower extremity edema, hepatomegaly, and in advanced right heart failure, ascites. However, the most reliable sign of elevated right atrial

Table 13.2 Signs and symptoms of low cardiac output

Symptoms	Fatigue
	Decreased memory/mentation
	Lightheadedness
Signs	Cool extremities
	Sleepy/obtunded
	Narrow pulse pressure
	Oliguria

pressure is elevation of the jugular venous pressure, and depending on the skill of the examiner, the right atrial pressure can be reliably assessed at the bedside in most heart failure patients. Indeed, patients with elevation of right atrial pressure may have no edema or ascites and the only sign may be elevated jugular venous pressure. It is in these patients that congestion is often missed and the patient is incorrectly assumed to be euvolemic.

Elevation in left atrial pressure/PCWP pressure leads to symptoms of exertional/resting dyspnea, dry cough worse in the recumbent position, orthopnea, and paroxysmal nocturnal dyspnea. In fact, orthopnea and particularly paroxysmal nocturnal dyspnea are the most specific symptoms of elevated PCWP. The physical exam finding that is most specific for an elevated PCWP (in the absence of mitral stenosis) is an S3 gallop; however it is not a sensitive finding as most patients with an elevated PCWP do not have an S3 gallop. One of the best clues that a heart failure patient has an elevated PCWP is elevation in the jugular venous pressure. This is because elevated right atrial pressure is predictive of an elevated PCWP in most chronic heart failure patients (see section "Intracardiac Filling Pressures").

Clinical Estimation of Cardiac Output

Estimating cardiac output is more difficult at the bedside but there are several clues to low cardiac output (see Table 13.2). General fatigue, impaired mentation, cool extremities, low urine output, and increased lactate level are useful clues. An objective measure is to calculate the "proportional pulse pressure" which is the systolic blood pressure minus the diastolic blood pressure divided by the systolic blood pressure. A proportional pulse pressure <25% suggests a cardiac index of <2.2 [11].

Echocardiography

The echocardiogram is a very important tool in the assessment of heart failure. In patients presenting with a new diagnosis, it is essential in establishing the mechanism of heart failure (see Chap. 6). Performing a baseline echocardio-

gram is given a class I (should be performed) recommendation and described as "the single most useful diagnostic test" in patients with a new diagnosis of heart failure according to the ACC/AHA guidelines [12]. For patients with an acute exacerbation of chronic heart failure, it is not always necessary to obtain an echocardiogram. This is particularly true when there is an obvious precipitant for the change in clinical status. When the patient is critically ill or the symptomatic decline is precipitous, however, it is important to help exclude new structural abnormalities. This is given a IIa (reasonable to perform) recommendation by the ACC/AHA guidelines [12], and has been shown to provide reliable estimates of invasive hemodynamics in this setting [13].

Echo Assessment of Filling Pressures

The measured size of the inferior vena cava (IVC) and its changes with respiration is traditionally used to estimate right atrial pressure [14]. Using this method, there is an assumption that there is continuity between central veins and the right atrium, the same assumption used in interpreting the jugular venous pressure as a reflection of right atrial pressure. Patients with an IVC measuring ≤2.2 cm in diameter that collapses by 50% or more with a sniff are designated as having a low RA pressure (assigned a value of 3 mmHg for the purposes of calculations). Patients with a distended IVC that does not collapse with sniff are designated as having a high RA pressure (15 mmHg). Patients with intermediate findings are assigned an RA pressure of 8 mmHg [14]. An example of this technique is given in Case 3 below.

Echocardiographic estimation of left ventricular end-diastolic pressures is a large area of active investigation. The ratio of early diastolic inflow velocity across the mitral valve (E) to the early peak velocity of the mitral valve annulus (E′) has been shown to have a reasonably good correlation with LVEDP [15]. This technique is used in a semiquantitative fashion. An E:E′ ratio of <8 suggests a normal LVEDP. An E:E′ ratio of >15 suggests an LVEDP of greater than 15 [15]. The precision of this technique may be reduced among patients with advanced heart failure admitted to the ICU [16]. Ongoing research is underway to find more consistent and precise echocardiographic predictors of LVEDP.

Echo Estimation of Pulmonary Pressures

The most well-accepted means of estimating pulmonary pressures with echocardiography is to calculate the pressure gradient across the tricuspid valve using the peak velocity of the tricuspid regurgitation jet [14]. Using a simplified Bernoulli equation, the pressure gradient between the right ventricle and the right atrium can

be estimated as $P = 4v^2$. This is also discussed in detail elsewhere in this book and an example will be reviewed in Case 3.

Echo Assessment of Cardiac Output

Stroke volume (and therefore cardiac output) can be estimated by echocardiography, although it requires several important assumptions be made [17]. The technique for making this estimation is as follows:

The Doppler profile of flow through the LV outflow tract is a graph of velocity vs. time. Taking the integral of this curve gives a unit of distance. When this distance is multiplied by the surface area of the left ventricular outflow tract (LVOT), the resulting number (a volume) is the stroke volume. The LVOT area can be estimated by using 2D echo measurements of its diameter in long axis and then assuming that it is a circle. Although this method is not frequently employed, it should yield a reasonably accurate estimate of stroke volume and therefore of cardiac output (when multiplied by heart rate).

Right Heart Catheterization

Right heart catheterization remains the gold standard for measuring many of the hemodynamic parameters important in the management of heart failure. As noninvasive methodology has improved however, there are now fewer situations in which this information is necessary [12]. Additionally, a large randomized study showed no benefit to the routine use of a pulmonary artery catheter to manage patients with acute decompensated heart failure in terms of the endpoint of mortality and days outside of hospital at 6 months [18].

Right heart catheterization should be considered in a patient who is refractory to initial therapy, whose volume status and cardiac filling pressures are unclear, who has clinically significant hypotension (typically SBP <80 mmHg) or worsening renal function during therapy, or who is being considered for cardiac transplant and needs assessment of the degree and reversibility of pulmonary hypertension and pulmonary vascular resistance [19]. This latter issue will be discussed further in Case 3.

In each of Cases 1–3, pressures in the right atrium (RA) and pulmonary artery (PA) as well as the PCWP as derived from right heart catheterization are displayed. The RA pressure and PCWP are commonly used clinically as descriptors of right and left ventricular "preload" respectively (see Chap. 1). The PA pressure is reported as systolic PA pressure/diastolic PA pressure (mean PA pressure). The cardiac index, as estimated using the Fick principle (see Chap. 4), is also shown. The cardiac index is calculated by dividing the cardiac output by the patient's body surface area. This factor in the size of the patient which is clearly important as normal cardiac output varies with size.

General Principles of Management

The majority of patients who present with decompensated heart failure are congested and have elevated filling pressures. The central goal of therapy is to decongest the patient and optimize filling pressures to normal or near normal levels. This is most effectively achieved with the use of an intravenous loop diuretic. In instances of diuretic resistance, combining a loop diuretic with a thiazide, amiloride, and/or spironolactone can be highly effective. If this approach is not successful, as can be the case in advanced renal dysfunction, ultrafiltration should be considered [20].

To further optimize hemodynamics, vasodilators which reduce filling pressures can be used in conjunction with diuretics. Vasodilators, in addition to lowering filling pressures, improve cardiac output by reducing afterload, decreasing functional mitral regurgitation (and thereby increasing forward cardiac output), and reducing wall stress [21–23]. The patients who benefit the most from vasodilators are those with elevated blood pressure and minimal circulatory congestion. It is important to note, however, that a patient with "normal" blood pressure may still have an elevated systemic vascular resistance and benefit from vasodilator therapy. Both "wet and warm" and "wet and cold" patients may be treated with vasodilators.

Intravenous vasodilators used in heart failure are nitroprusside, nitroglycerin, and nesiritide. The vasodilator of choice at our own institution is nitroprusside, which should be administered in an ICU setting with hemodynamic monitoring using a right heart catheter and, in most instances, a blood pressure cuff (as opposed to an arterial line). This is well tolerated and the incidence of cyanide or thiocyanate toxicity is extremely rare to nonexistent [24, 25]. A mean arterial pressure of approximately 65 mmHg is targeted but this depends on the patient and may need to be higher if renovascular or coronary artery disease is present or suspected, or if the patient is chronically hypertensive with an altered renal autoregulatory threshold. Excessive or overexuberant vasodilation with decrease in blood pressure beyond the renal autoregulatory threshold often leads to decreased renal perfusion, worsening renal function, and should be avoided. Once patients have clinically and hemodynamically improved on intravenous vasodilators, they may be transitioned to an oral vasodilator regimen of either ACE inhibitors, the combination of hydralazine and isosorbide dinitrate, or a combination of all three agents [26].

Intotropic therapy (milrinone or dobutamine) should be reserved for low output states associated with hypotension and end-organ hypoperfusion [27]. The typical patient has advanced systolic dysfunction with a low proportional pulse pressure, cool extremities, and worsening renal function despite adequate filling pressure (need to rule out hypovolemia) and is unresponsive to or intolerant of intravenous vasodilators. These patients constitute no more than 5% of the total population of acutely decompensated heart failure. Inotropes can also be used as palliative therapy for end-stage heart failure or as a bridge to transplantation.

It is important to note that inotropes increase myocardial oxygen consumption by increasing heart rate and myocardial contractility and can precipitate atrial and ventricular arrhythmias as well as myocardial ischemia. In contrast to Dobutamine, Milrinone has a long half-life (2.5 h), is renally excreted, and the dose should be adjusted for renal function. Also, given that Milrinone is a more powerful vasodilator, hypotension is more common with this agent and therefore should be used with caution or even avoided when the systolic blood pressure is <90 mmHg. In the setting of background beta blocker therapy, Dobutamine will be ineffective unless used in high doses and Milrinone is favored [28, 29]. In rare circumstances, vasopressors are used (Dopamine, Norepinephrine, Vasopressin), when the patient is vasodilated with a low SVR and profound hypotension.

In patients who are managed on a telemetry floor without invasive monitoring, the goal of therapy is to normalize intravascular volume as reflected by relief of edema and normalization of the jugular venous pressure (<8 cmH_2O). When this is achieved, most patients will no longer have orthopnea or dyspnea. Signs of overdiuresis consist of orthostatic decrease in blood pressure and worsening renal function. A common clinical error is incorrectly assuming euvolemia has been achieved when edema has resolved yet unrecognized elevation of the jugular venous pressure persists. By the same token, one may have normalized the jugular venous pressure and achieved intravascular euvolemia but may still have residual edema due to low albumin, venous insufficiency, or drug side effect and wrongly assumed to be volume overloaded.

In patients managed with hemodynamic monitoring with a right heart catheter, vasodilator therapy (both intravenous and oral) and diuretics are "tailored" to certain hemodynamic goals. Typically a PCWP of ≤16 mmHg, an RA pressure of ≤8 mmHg, and an SVR of about 1,000–1,200 dyn is targeted. A common misconception that patients with dilated dysfunctional ventricles require higher filling pressures to maintain cardiac output based on the Starling curve has been dispelled by data showing that most of these patients can maintain and even improve cardiac output with normal or near normal PCWP [30]. As far as RA pressure goals, patients with primarily RV failure may require a higher RA pressure than 8 mmHg to maintain cardiac output and renal perfusion. It has been shown that patients with very elevated RA pressure can have worsening renal function on the basis of renal venous congestion. By lowering RA pressure with diuretics and vasodilators, the kidney is "decongested" or decompressed and renal function can improve [31–33] (see Fig. 13.2).

The goal of cardiac index is usually >2.2 but one has to acknowledge that using the Fick equation the oxygen consumption is estimated and not measured and that up to a 20% variation in cardiac output can be seen [34]. Thus, targeting a specific number per se is simplistic and the entire clinical picture needs to be considered (e.g., a patient with a cardiac index of 1.8 who with normal PCWP who feels well may not need further intervention). Although cardiac output frequently improves, the cardiac output is not the primary target of therapy, rather the reduction of the

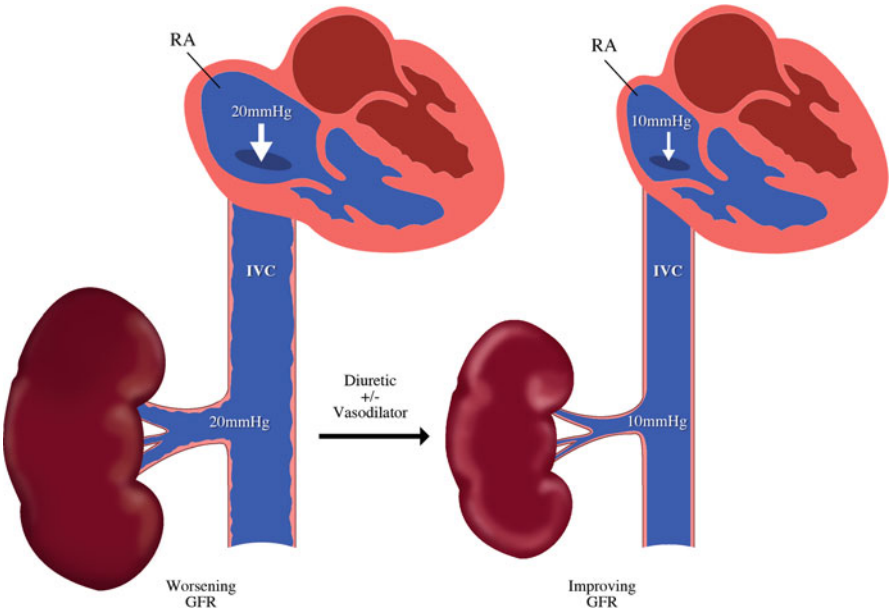

Fig. 13.2 Renal venous congestion: increased right atrial pressure leading to elevated pressure in the IVC and thus the renal vein (especially when coupled with low mean arterial pressure) can lead to worsening renal function by "congesting the kidney." Decreasing right atrial pressure and thus the renal venous pressure can lead to improved renal function

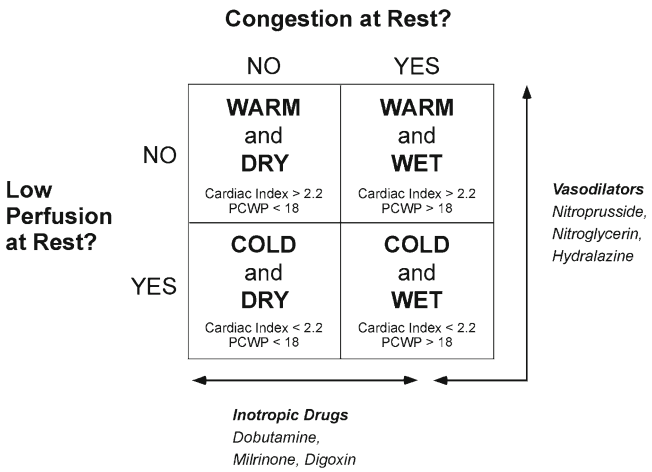

Fig. 13.3 Treatment paradigm in patients with left-sided heart failure

filling pressures [35]. The general principles of management for the different presentations of heart failure are shown in Fig. 13.3.

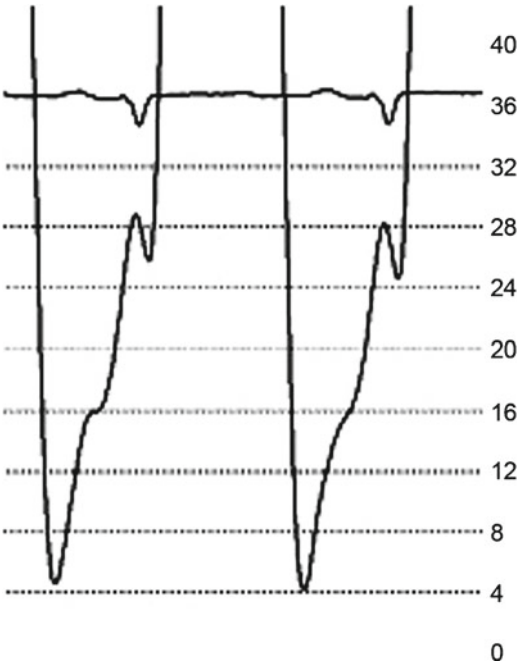

Fig. 13.4 Case 1: left ventricular pressure tracing

Clinical Presentations of Acute Heart Failure

Case 1

A 46-year-old male with a history of diabetes and hypertension presents with sudden onset of retrosternal chest pain. He is brought by emergency medical services to the hospital where he is found to have an elevated jugular venous pressure, bilateral rales, and edematous and well-perfused extremities. His electrocardiogram reveals ST segment elevation in the inferior leads (ECG leads II, III, and aVF). He is transferred to the cardiac catheterization laboratory but becomes dyspneic and hypoxic lying flat on the table. On examination, his HR is 90 bpm and BP measures 130/90 mmHg. His oxygen saturation is 93% on a high flow oxygen mask.

A left heart catheterization is performed. The right coronary artery is found to be completely occluded, and the patient undergoes successful angioplasty and stenting to the vessel with good results. A pulmonary artery catheter is placed yielding the following hemodynamics:

RA	PA	PCWP	Cardiac index
12	38/25 (30)	24	3.2

A sample from his left heart catheterization is shown in Fig. 13.4. The LVEDP is elevated and correlates closely with the PCWP obtained with right heart catheterization.

An echocardiogram is performed which demonstrates severe akinesis of the inferior wall from base to apex. The overall left ventricular systolic function is described as mildly decreased. Right ventricular function is reported as normal.

Case 1: Hemodynamic Assessment

This is an example of so-called "warm and wet" heart failure (based clinically on his JVP, lower extremity edema and warm extremities, and hemodynamically on an elevated PCWP with a cardiac index in the normal range). Occlusion of the right coronary artery led to systolic and diastolic dysfunction of the left ventricle. This resulted in elevation of the left-sided filling pressures with pulmonary edema.

The orthopnea and hypoxia suggested an acute rise in PCWP. The relationship between PCWP and clinical signs of pulmonary congestion has been well characterized in patients with acute myocardial infarction. The onset of pulmonary congestion generally occurs at a PCWP between 18 and 20, and acute pulmonary edema generally correlates with a PCWP of greater than 30 [36]. These data have been challenged however [37], and were collected prior to the use of reperfusion techniques such as fibrinolysis and primary percutaneous coronary intervention.

In this case, the importance of echocardiography was to confirm that the main problem was a left ventricular wall motion abnormality and not acute mitral regurgitation, which can be a mechanical complication of inferior myocardial infarction. Suspicion was low for this patient as such cases generally present with cardiogenic shock, but a high index of suspicion is important. Another known complication of inferior myocardial infarction can be right ventricular infarction. This occurs in some patients when there is proximal occlusion of the right coronary artery, but would generally be manifested by an elevated JVP and hypotension without pulmonary congestion. The right heart catheterization provided accurate measurement of cardiac output which has important prognostic implications [38].

In this case, the underlying cause of left ventricular dysfunction is acute coronary occlusion. This is best treated by promptly opening the culprit vessel (here with emergent PCI) in efforts to improve contractility by restoring flow to the compromised ischemic myocardium. Diuretic therapy was also provided to facilitate reduction of volume overload and clearance of pulmonary edema. This is generally considered to be a mainstay of the treatment of decompensated heart failure with increased RA pressure and PCWP. The patient was treated with intravenous furosemide with excellent response. After several days, he no longer required supplemental oxygen and clinical and radiographic evidence of pulmonary congestion had improved.

Case 2

A 19-year-old G_1P_1 female presents to the emergency department with profound fatigue and right upper quadrant discomfort. Two weeks prior, she gave birth to a healthy son via an uncomplicated vaginal delivery. Since the delivery, she has noticed gradual progression of tiredness to the point where she is no longer able to

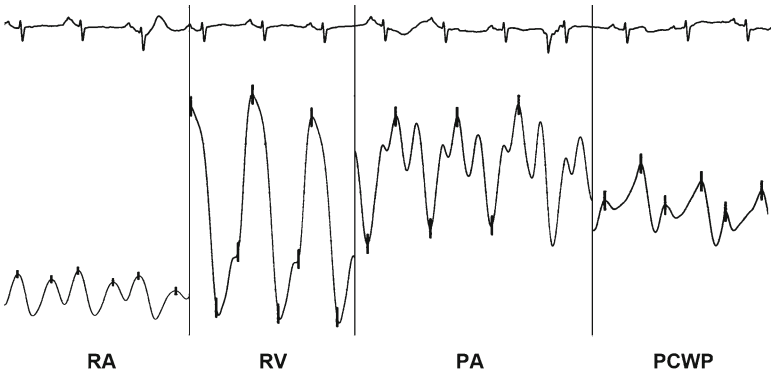

Fig. 13.5 Case 2 sample hemodynamic tracings: Pressures were recorded with the catheter positioned in the right atrium (RA), right ventricle (RV) and pulmonary artery (PA) as well as with pulmonary capillary 'wedging' (PCWP). The following pressures were noted: RA – mean pressure of 10 mmHg (normal – 0-8 mmHg); RV – pressure of 46/10 mmHg (normal – 15-30/0-8 mmHg); PA – pressure of 46/30 mmHg (Normal – 15-30/4-12 mmHg); and PCWP – mean pressure of 32 mmHg (normal – 1-10 mmHg)

carry out basic activities of daily living and is short of breath at rest. There is no orthopnea or leg swelling, but occasional paroxysmal nocturnal dyspnea. She complains of a dull aching discomfort in the right upper quadrant of her abdomen.

On examination, she is tachycardic with a HR of 120 bpm and BP of 106/88 mmHg. Her extremities are warm. The JVP is elevated to 8 cm above the sternal angle at 60°. The chest is clear to auscultation. In addition to loud first and second heart sounds, a prominent S3 is heard. There is right upper quadrant abdominal tenderness with no rebound tenderness or guarding. A chest X-ray is performed and shows an enlarged cardiac silhouette. An ECG shows sinus tachycardia with low voltages and a nonspecific ST abnormality. Labs are notable for elevated liver enzymes.

Echocardiography shows severe left ventricular dysfunction with an LVEF of 10%, moderate mitral regurgitation, and moderate right ventricular dysfunction. She is given a presumptive diagnosis of a peripartum cardiomyopathy. She is admitted to a heart failure intensive care unit and a pulmonary artery catheterization is performed. Samples from the tracings are seen in Fig. 13.5. Note the somewhat exaggerated waveforms on the section of the tracing labeled pulmonary artery, a commonly encountered artifact.

Her reported hemodynamics are as follows:

RA	PA	PCWP	Cardiac index
10	46/30 (35)	32	2.0

Case 2: Hemodynamic Assessment

This is a case of a patient with so-called "cold and wet" heart failure. The cardiac index is reduced and both the RA pressure and the PCWP are increased. When accompanied by findings of impaired end-organ function, this state would be termed

cardiogenic shock (see Chap. 14). For this patient, there is no clinical evidence of a low perfusion state, such as hypotension, decreased level of consciousness, cool extremities, or renal failure.

The right upper quadrant pain and elevated liver enzymes reflect passive congestion of the liver. The physical examination disclosed an elevated JVP which corresponds to the elevated RA pressure. Note that there were no rales on chest examination and only minimal pulmonary edema on chest X-ray. These findings may have led the clinician to suspect that PCWP was not elevated. Unfortunately, such findings of elevated PCWP are frequently not present among chronic heart failure patients when the time-course of the illness is gradual. In such cases, pulmonary lymphatic drainage is enhanced and sufficient to prevent the accumulation of interstitial edema in the lungs. The finding of an S3 should definitely steer the clinician in the right direction, however. The low cardiac output was not recognized at the bedside due to the lack of cool extremities, altered mentation, and low urine output underscoring the insensitivity of these findings [9, 39]. However, if one calculates the proportional pulse pressure in this patient (106–88/106) a value of 17% is obtained suggesting a low cardiac index of <2.2 (see section "Clinical Estimation of Cardiac Output" above) [11].

The presence of a significant resting sinus tachycardia is ominous however. It suggests that the patient is compensating for a reduced stroke volume by increasing heart rate to maintain cardiac output.

The echocardiogram was crucial in confirming that severe biventricular dysfunction was the cause of the heart failure syndrome. The right heart catheterization was performed because of a concern that the patient was potentially unstable and needed invasive monitoring. In this case, the right heart catheterization also shows mild elevation in pulmonary artery pressure. The calculated pulmonary vascular resistance (see Chap. 12 for more details) is normal at 1.0 Wood unit:

$$\text{PVR} = \frac{(\text{Mean PA pressure} - \text{PCWP})}{\text{Cardiac output}}$$

$$\text{PVR} = \frac{35 - 32}{3*} = 1$$

*cardiac index of 2.0 corresponded to cardiac output of 3 L/min because of body surface area of 1.5 m^2.

This suggests that the patient's pulmonary hypertension is passive and there is no element of pulmonary vasoconstriction or pulmonary vascular remodeling.

The patient was treated with diuretic therapy, ACE inhibitors, and digoxin, and observed carefully in an ICU setting. Beta blockers should not be initiated in such a patient until they become euvolemic and hemodynamically stable. She was discharged from the hospital 7 days later. Over the next 6 months, the patient was followed closely as an outpatient and had dramatic improvement in symptoms and complete resolution of her LV dysfunction. She was advised to avoid pregnancy in the future due to the high risk of recurrent heart failure.

Case 3

A 58-year-old male is referred to a specialized heart failure clinic for evaluation. He has been followed for several years for a non-ischemic dilated cardiomyopathy with severe limitation of his exercise tolerance. His physician sends him for evaluation for the possible need for heart transplantation due to end-stage heart failure. When questioned, he reports that over the past 3 weeks he has had worsened symptoms of weight gain and leg swelling. These symptoms began after he had started taking a nonsteroidal anti-inflammatory drug for arthritis. On examination, his HR is 90 bpm and his BP measures 98/70 mmHg. He is grossly edematous with pitting edema of both legs as well as scrotal edema. His JVP is elevated with prominent *v* waves. Auscultation of the chest reveals quiet breath sounds with no rales or wheeze. On examination of the precordium there is a loud pulmonic component of the second heart sound and an S3 gallop.

Echocardiography shows severe left ventricular dysfunction with an LVEF of 10% and moderate mitral regurgitation. Severe right ventricular dysfunction is also noted. The estimated RVSP by echocardiography is 88 mmHg (see Fig. 13.6).

The patient is admitted to hospital and a right heart catheterization is performed with the following results:

RA	PA	PCWP	Cardiac index
19	88/44 (59)	39	1.5

Case 3: Hemodynamic Assessment

This is another case of so-called "cold and wet" heart failure with reduced cardiac output and elevated right- and left-sided filling pressures. Note again that the patient was not hypoxic and auscultation of the chest did not reveal rales despite a very high PCWP. In contrast to the previous case, the pulmonary hypertension is severe with pulmonary artery pressures approaching the systemic pressures. The loud pulmonic component of S2 is consistent with these high pressures, although it is not a sensitive finding.

The calculated pulmonary vascular resistance is very high (see calculations below) suggesting that there is a pulmonary arterial component to the pulmonary hypertension that would not be immediately reversed if the PCWP was lowered.

$$\text{PVR} = \frac{(\text{Mean PA pressure} - \text{PCWP})}{\text{Cardiac output}}$$

$$\text{PVR} = \frac{59 - 39}{2.5} = 8\,\text{Wood units}$$

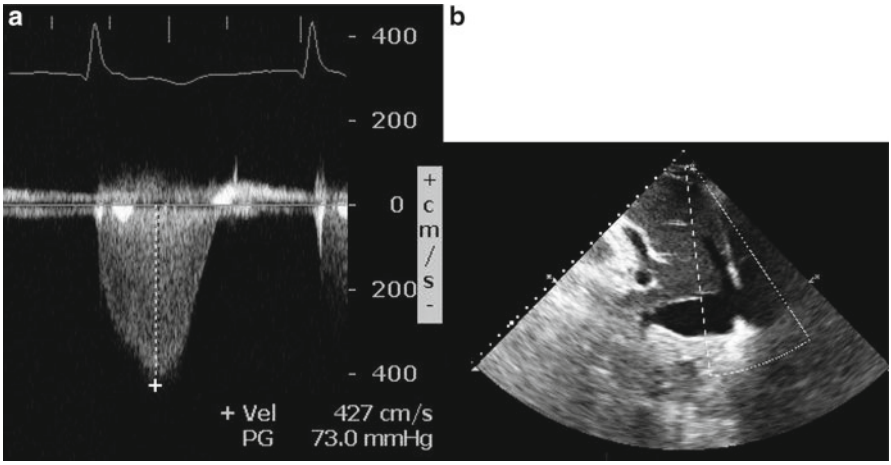

Fig. 13.6 Case 3: estimation of pulmonary artery systolic pressure by echocardiography. Peak velocity of the tricuspid regurgitation jet is 4.27 m/s (**a**)—this suggests a gradient from the RV to the RA of ~73 mmHg. RV to RA gradient = $4v^2 = 4 \cdot (4.27)^2 = 72.9$mmHg. The IVC is dilated (**b**) with a diameter of 2.8 cm and less than 50% variation with respiration—these findings suggest an RA pressure of 15 mmHg. Estimated peak pulmonary artery pressure is 88 mmHg (assuming no pulmonary valve stenosis) (73 + 15 = 88)

Note how closely the PA pressure was estimated by the transthoracic echocardiogram. Studying the parasternal short-axis images from the echocardiogram also gives us some idea of the relative left- and right-sided intracardiac pressures (Fig. 13.7). The flattened configuration of the interventricular septum during both systole and diastole suggests that the pressure in the right ventricle (and hence the pulmonary artery) is very high during both systole and diastole.

The patient was treated with inotropic therapy using milrinone, as well as a continuous infusion of furosemide. He was felt to have advanced heart failure but his high pulmonary vascular resistance precluded heart transplantation because of the risk that the transplanted heart would develop acute right ventricular failure. He underwent placement of a left ventricular assist device which functions as an additional mechanical pump that reroutes blood from the left ventricle into the aorta. With this intervention, he had a dramatic improvement in symptoms and exercise tolerance as well as a marked reduction in PCWP.

Pearls of Assessment

- The history and physical examination provide the majority of the hemodynamic information required to manage acute decompensated heart failure.
- No single symptom or sign is perfectly sensitive or specific for the diagnosis of acute decompensated heart failure.

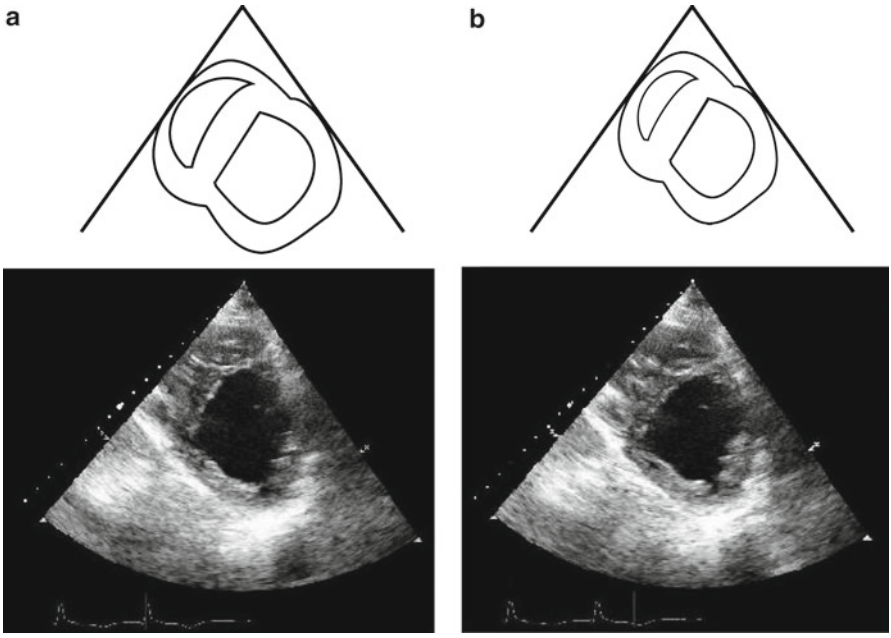

Fig. 13.7 Case 3: Parasternal short-axis echo images showing pronounced flattening of the interventricular septum during diastole (**a**) which is still present during systole (**b**). This produces a "D-shaped appearance" of the left ventricle as emphasized in the cartoon above. Severe left ventricular dysfunction is suggested by the minimal change in area of the left ventricular cavity

- The most reliable sign of elevated right atrial pressure is elevation of the jugular venous pressure.
- Paroxysmal nocturnal dyspnea is a specific symptom for elevated PCWP.
- Transthoracic echocardiography is an important means of establishing the mechanism of newly diagnosed heart failure, and of excluding new structural problems as the trigger for heart failure exacerbation.
- Echocardiography is not needed in routine heart failure exacerbations when a cause for decompensation is clear.
- Need for right heart catheterization is being obviated by noninvasive means of estimating hemodynamic parameters in most situations.
- Right heart catheterization in acute decompensated heart failure is indicated when volume status and cardiac filling pressures are unclear, clinically significant hypotension or worsening renal function during therapy occurs, and for the evaluation of pulmonary vascular resistance.

Review Questions

1. A patient with known chronic systolic heart failure is admitted with acute decompensated heart failure. The patient has orthopnea and paroxysmal nocturnal dypsnea. On exam, the jugular venous pressure (JVP) is elevated and estimated to be 10 cm above the sternal angle while the patient is seated upright. Auscultation reveals an S3 gallop. Which of the following suggests an elevated pulmonary capillary wedge pressure (PCWP)?

   A. Orthopnea
   B. S3 gallop
   C. Elevated JVP
   D. All of the above

Answer D

Orthopnea and paroxysmal nocturnal dyspnea are the most specific symptoms for an elevated PCWP. Although an S3 gallop is not sensitive, it is the most specific sign of an elevated PCWP. Elevated jugular venous pressure, although directly estimates right atrial pressure, is a surrogate for elevated PCWP in the vast majority of cases.

2. A patient admitted with decompensated heart failure undergoes right heart catheterization. The right atrial pressure is 5 mmHg, the pulmonary capillary wedge pressure is 10 mmHg, the cardiac output is 4.0 L/min with cardiac index 1.9 L/min/m^2.

This is an example of:

   A. Warm and wet heart failure
   B. Warm and dry heart failure
   C. Cold and wet heart failure
   D. Cold and dry heart failure

Answer D

The cardiac output of 4 L/min is close to normal. However, this patient has a large body surface area and his calculated cardiac index is low. The PCWP and RA pressure are both in the normal range.

3. A 72-year-old male presents to the emergency department with a 2-week history of progressive shortness of breath with orthopnea and paroxysmal nocturnal dyspnea. On exam, he has peripheral edema and an elevated JVP at 12 cm above the sternal angle while seated upright. A prominent third heart sound is heard. The patient has inspiratory rales to the mid lung zones bilaterally. A chest X-ray confirms the presence of pulmonary congestion with vascular redistribution, Kerley B lines, and small bilateral pleural effusions.

The most appropriate next study to assess this patient's etiology of heart failure and hemodynamics is:

   A. 2D echocardiogram with Doppler
   B. Right heart catheterization

C. Computed tomography with IV contrast
D. Magnetic resonance imaging

Answer A

Echocardiography is a noninvasive, readily available and relatively inexpensive tool for evaluation of left ventricular function, valvular disease, and hemodynamics. It is recommended as a first-line investigation for patients with a new diagnosis of heart failure.

4. The following are all appropriate indications for use of a pulmonary arterial catheter in heart failure except:

A. Distinction of pulmonary edema related to heart failure from other causes of hypoxia in a critically ill patient in the intensive care unit
B. Assessment of a patient in shock when intracardiac filling pressures cannot be adequately estimated by noninvasive means
C. Monitoring of response to beta blocker therapy on routine annual follow-up
D. Measurement of pulmonary pressures and calculation of pulmonary vascular resistance prior to planned heart transplantation

Answer C

For reasons discussed in the section on hemodynamic assessment, the use of pulmonary artery catheters in heart failure should be limited to certain scenarios such as those outlined in answers A, B, and D.

5. A patient admitted with decompensated heart failure undergoes right heart catheterization. The right atrial pressure is 10 mmHg, the pulmonary arterial pressures are 59/32 mmHg with a mean of 40 mmHg. The pulmonary capillary wedge pressure is 34 mmHg and the cardiac output is 4.0 L/min.

The pulmonary pressure in this case could be described as:

A. Normal—no evidence of pulmonary hypertension
B. Elevated on the basis of pulmonary venous hypertension
C. Elevated on the basis of pulmonary arterial hypertension
D. Representing a mixture of pulmonary venous and pulmonary arterial hypertension

Answer B

A pulmonary pressure in this range is clearly abnormal. Determining the extent to which these pressures are elevated due to elevated left-sided pressures alone hinges on the calculation of the pulmonary vascular resistance. The pulmonary vascular resistance calculates out to be 1.5 Wood units, which is within the normal range. This suggests that if the LVEDP could be brought down to normal (with diuresis for example), the pulmonary pressures would become normal. This is the definition of pulmonary venous hypertension.

References

1. Lloyd-Jones D, Adams R, Carnethon M, De Simone G, Ferguson TB, Flegal K, et al. Heart disease and stroke statistics–2009 update: a report from the American Heart Association Statistics Committee and Stroke Statistics Subcommittee. Circulation. 2009;119(3):480–6.
2. Kupari M, Lindroos M, Iivanainen AM, et al. Congestive heart failure in old age: prevalence, mechanisms and 4–year prognosis in the Helsinki Ageing Study. J Intern Med. 1997;241:387–94.
3. Owan TE, Hodge DO, Herges RM, et al. Trends in prevalence and outcome of heart failure with preserved ejection fraction. N Engl J Med. 2006;355:251–9.
4. Fonarow GC, Adams KF, Abraham WT, et al. Risk stratification for in-hospital mortality in acutely decompensated heart failure. JAMA. 2005;293:572–80.
5. Drazner MH, Hamilton MA, Fonarow GC, et al. Relationship between right and left-sided filling pressures in 1000 patients with advanced heart failure. J Heart Lung Transplant. 1999;18:1126–32.
6. Drazner MH, Prasad A, Ayers C, et al. The relationship of right- and left-sided filling pressures in patients with heart failure and preserved ejection fraction. Circ Heart Fail. 2010;3(2):202–6.
7. Campbell P, Drazner MH, Kato M, et al. Mismatch if right- and left-sided filling pressures in chronic heart failure. J Card Fail. 2011;17(7):561–8.
8. Drazner MH, Brown RN, Kaiser PA, et al. Relationship of right- and left-sided filling pressures in patients with advanced heart failure: a 14-year multi-institutional analysis. J Heart Lung Transplant. 2012;31(1):67–72.
9. Drazner MH, Hellkamp AS, Leier CV, et al. Value of clinician assessment of hemodynamics in advanced heart failure: the ESCAPE trial. Circ Heart Fail. 2008;1:170–7.
10. From AM, Lam CS, Pitta SR, et al. Bedside assessment of cardiac hemodynamics: the impact of noninvasive testing and examiner experience. Am J Med. 2011;124(11):1051–7.
11. Stevenson LW, Perloff JK. The limited reliability of physical signs for estimating hemodynamics in chronic heart failure. JAMA. 1989;261:884–8.
12. Hunt SA, Abraham WT, Chin MH, Feldman AM, Francis GS, Ganiats TG, et al. 2009 Focused Update Incorporated Into the ACC/AHA 2005 Guidelines for the Diagnosis and Management of Heart Failure in Adults: A Report of the American College of Cardiology Foundation/American Heart Association Task Force on Practice Guidelines Developed in Collaboration with the International Society for Heart and Lung Transplantation. J Am Coll Cardiol. 2009;53(15):e1–90.
13. Nagueh SF, Bhatt R, Vivo RP, Krim SR, Sarvari SI, Russell K, Edvardsen T, Smiseth OA, Estep JD. Echocardiographic evaluation of hemodynamics in patients with decompensated systolic heart failure. Circ Cardiovasc Imaging. 2011;4(3):220–7.
14. Rudski LG, Wyman WL, Afilalo J, Hua L, Handschumacher MD, Chandrasekaran K, Solomon SD, Louie EK, Schiller NB. Guidelines for the echocardiographic assessment of the right heart in adults: a report from the American Society of Echocardiography. J Am Soc Echocardiogr. 2010;23:685–713.
15. Ommen SR, Nishimura RA, Appleton CP, Miller FA, Oh JK, Redfield MM, Tajik AJ. Clinical utility of Doppler echocardiography and tissue Doppler imaging in the estimation of left ventricular filling pressures: a comparative simultaneous Doppler-catheterization study. Circulation. 2000;102:1788–94.
16. Mullens W, Borowski AG, Curtin RJ, Thomas JD, Tang WH. Tissue Doppler Imaging in the estimation of intracardiac filling pressures in decompensated patients with advanced systolic heart failure. Circulation. 2009;119:62–70.
17. Armstron WF, Ryan T, editors. Feigenbaum's echocardiography. 7th edn. Philadelphia: Lippincott Williams & Wilkins; 2009.
18. Binanay C, Califf RM, Hasselblad V, O'Connor CM, Shah MR, Sopko G, et al. Evaluation study of congestive heart failure and pulmonary artery catheterization effectiveness: the ESCAPE trial. JAMA. 2005;294(13):1625–33.

19. Lindenfeld J, Albert NM, Bochmen JP, et al. HFSA 2010 Comprehensive Heart Failure Practice Guideline. J Card Fail. 2010;16:e1–194.
20. Liang KV, Hiniker AR, Williams AW, et al. Use of a novel ultrafiltration device as a treatment strategy for diuretic resistant, refractory heart failure: initial clinical experience in a single center. J Cardiol Fail. 1996;12(9):707–14.
21. Stevenson L, Belili D, Grover-McKay M, et al. Effects of afterload reduction (diuretics and vasodilators) on left ventricular volume and mitral regurgitation in severe congestive heart failure secondary to ischemic or idiopathic dilated cardiomyopathy. Am J Cardiol. 1987;60:654–8.
22. Rosario LB, Stevenson LW, Soloman SD, et al. The mechanism of decrease in dynamic mitral regurgitation during heart failure treatment: importance of reduction in the regurgitant orifice size. J Am Coll Cardiol. 1998;32:1819–24.
23. Palardy M, Stevenson LW, Tasissa G, et al. Reduction in mitral regurgitation during therapy guided by measured filling pressures in the ESCAPE trial. Circ Heart Fail. 2009;2:181–8.
24. Mullens W, Abrahams Z, Francis GS, et al. Sodium nitroprusside for advanced low-output heart failure. J Am Coll Cardiol. 2008;52(3):200–7.
25. Opasich C, Cioffi G, Gualco A. Nitroprusside in decompensated heart failure: what should a clinician really know? Curr Heart Fail Rep. 2009;6(3):182–90.
26. Mullens W, Abrahams Z, Francis GS, et al. Usefulness of isosorbide dinitrate and hydralazine as add-on therapy in patients discharged for advanced decompensated heart failure. Am J Cardiol. 2009;103:113–9.
27. Cuffe MS, Calif RM, Adams Jr KF, et al. Short-term intravenous milrinone for acute exacerbation of chronic heart failure: a randomized controlled trial. JAMA. 2002;287:1541–7.
28. Jennings DL, Thompson ML. Use of combination therapy with a beta-blocker and milrinone in patients with advanced heart failure. Ann Pharmacother. 2009;43(11):172–1876.
29. Tsvetkova T, Feguson D, Abraham WT, et al. Comparative hemodynamic effects of milrinone and dobutamine in heart failure patients treated chronically with carvedilol. J Card Fail. 1998;4 Suppl 1:36.
30. Stevenson LW, Tillisch JH. Maintenance of cardiac output with normal filling pressures in patients with dilated heart failure. Circulation. 1986;74:1303–8.
31. Mullens W, Abrahams Z, Francis GS, et al. Importance of venous congestion for worsening of renal function in advanced decompensated heart failure. J Am Coll Cardiol. 2009;53:589–96.
32. Winton FR. The influence of venous pressure on the isolated mammalian kidney. J Physiol. 1931;72(1):49–61.
33. Firth JD, Raine AE, Ledingham JG. Raised venous pressure: a direct cause of renal sodium retention in oedema? Lancet. 1988;1(8593):1033–5.
34. Kendrick AH, West J, Papouchado M, et al. Direct Fick cardiac output: are assumed values of oxygen consumption acceptable? Eur Heart J. 1988;9:337–42.
35. Steimle AE, Stevenson LW, Chelimsky-Fallick C, et al. Sustained hemodynamic efficacy of therapy tailored to reduce filling pressures in survivors with advanced heart failure. Circulation. 1997;96:1165–72.
36. McHugh TJ, Forrester JS, Adler L, Zion D, Swan HJC. Pulmonary vascular congestion in acute myocardial infarction: Hemodynamic and radiologic correlations. Ann Intern Med. 1972;76:29–33.
37. Bergstra A, Svilaas T, van Veldhuisen DJ, van den Heuvel AF, van der Horst IC, Zijlstra F. Haemodynamic patterns in ST-elevation myocardial infarction: incidence and correlates of elevated filling pressures. Neth Heart J. 2007;15(3):95–9.
38. Forrester JS, Diamond G, Chatterjee K, Swan HJC. Medical therapy of acute myocardial infarction by application of hemodynamic subsets. N Engl J Med. 1976;295:1361.
39. Menon V, White H, LeJemtel T, Webb JG, Sleeper LA, Hochman JS. The clinical profile of patients with suspected cardiogenic shock due to predominant left ventricular failure: a report from the SHOCK trial registry. J Am Coll Cardiol. 2000;36:1071–6.

Chapter 14
Intracardiac Shunts

Alper Ozkan, Olcay Aksoy, and E. Murat Tuzcu

Introduction and Epidemiology of the Disease State

In the normal circulation, deoxygenated blood comes into the right heart and passes through the pulmonary circulation to become oxygenated. Then oxygenated blood goes through the left heart to the systemic circulation. An abnormal communication between two heart chambers resulting in an intracardiac (IC) shunt may take place from systemic to pulmonary circulation (left to right) or from pulmonary to systemic circulation (right to left) or may be bidirectional.

While congenital heart diseases are the most common causes of intracardiac shunts, acquired pathologies may also result in IC shunts. Left to right (L→R) shunt in post myocardial infarction VSD and right to left (R→L) shunt in platypnea orthodeoxia syndrome (POS) are two examples of acquired IC shunts.

Detection, localization, and quantification of intracardiac shunts are clinically important in the management of IC shunts and can be performed using noninvasive and invasive techniques. Noninvasive techniques include echocardiography, cardiovascular magnetic resonance (CMR), and radionuclide tests. Invasive techniques apply catheter insertion and selective blood sampling for oxygen saturation to diagnose and quantify IC shunts.

Noninvasive Assessment of Intracardiac Shunts

Transthoracic echocardiography (TTE) is a safe, reproducible, and a relatively inexpensive method that is widely used in the assessment of intracardiac shunts. Transesophageal echocardiography (TEE) is an excellent tool for defining the anatomy of IC shunts; however, its incremental value in shunt assessment is limited. Magnetic resonance

A. Ozkan, M.D • O. Aksoy • E.M. Tuzcu, M.D (✉)
Heart and Vascular Inst. Cleveland Clinic, Cleveland, OH, USA
e-mail: ozkana@ccf.org; aksoyo@ccf.org; tuzcue@ccf.org

A.T. Askari et al. (eds.), *Cardiovascular Hemodynamics: An Introductory Guide*, Contemporary Cardiology, DOI 10.1007/978-1-60761-195-0_14,

imaging (MRI) allows precise measurement of cardiac volumes and flows yielding accurate IC shunt calculations.

Echocardiographic Assesment of Intracardiac Shunts

Echocardiography has been the primary diagnostic tool and plays an essential role in providing morphologic assessment and hemodynamic evaluation in congenital heart disease. TTE permits comprehensive anatomic information regarding the location and the size of the defect. TEE may be needed as a complimentary imaging tool particularly in lesions located posteriorly and in patients who will undergo percutaneous or surgical intervention. Color flow Doppler plays critical role in detection and localization of IC shunts as well as in determinating direction of shunting. Pulmonary blood flow (Q_p) to systemic blood flow (Q_s) ratio can be easily calculated using Doppler and 2D echocardiography. Contrast echocardiography is another application which enables the demonstration of right to left shunts or bidirectional shunts.

Comprehensive evaluation of a patient with IC shunt is not limited to detection and quantification of the shunt flow. It also involves the evaluation of the associated abnormalities and secondary findings. For example, in a patient with ASD, evaluation of right atrial and right ventricular size and septal motion and for other associated anomalies such as anomalous pulmonary venos return is as important as quantification of the defect.

The hemodynamic significance of intracardiac shunts can be evaluated based on volumetric flow calculations using cross sectional area (CSA) and velocity time integral (VTI) across the outflow tracts of both ventricles. Pulmonary flow (Q_p) equals systemic flow (Q_s) in the absence of shunt. Formulas are used to calculate volumetric flow with two important assumptions. The first assumption is blood flow has a uniform pattern and constant velocity. The second assumption is that the shape of the outflow tract is circular. Flow formula is as follows:

$$Q = \mathrm{CSA} \times \mathrm{VTI}$$

(Q = flow, CSA = Cross sectional area, VTI = Velocity time integral)
CSA is calculated based on circular shape assumption:

$$\mathrm{CSA} = \pi \times \mathrm{r}^2$$

(π = pi constant which is 3.14, r = radius of the outflow tract)
For the pulmonary flow,

$$Q_p = \mathrm{CSARVOT} \times \mathrm{VTIRVOT}$$
$$Q_p = \pi \times (\mathrm{RVOTD}/2)^2 \times \mathrm{VTI\ RVOT}$$
$$Q_p = \pi \times (\mathrm{RVOT_D})^2 / 4 \times \mathrm{VTI_{RVOT}} (\pi / 4 = 0.785)$$
$$Q_p = 0.785 \times \mathrm{RVOTd}^2 \times \mathrm{VTI_{RVOT}}$$

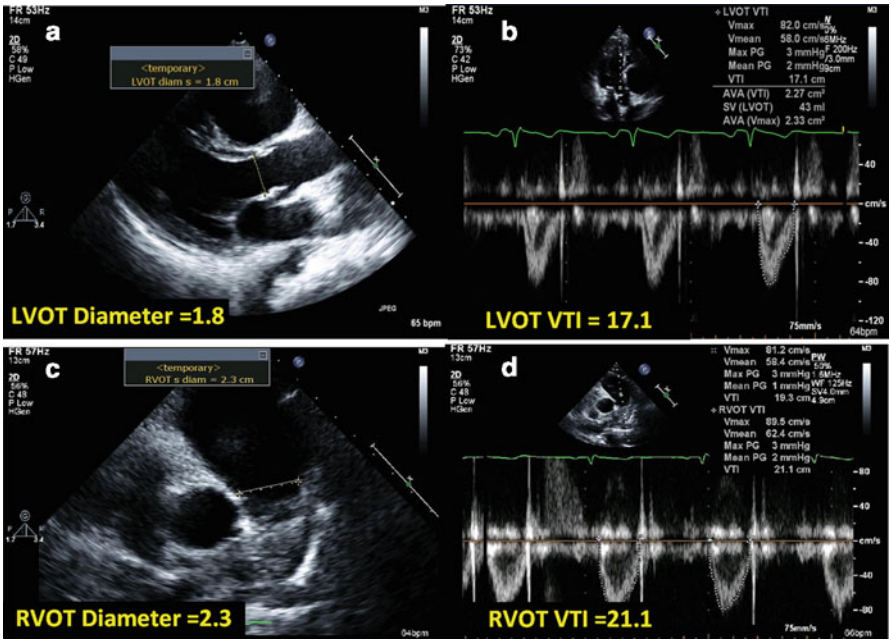

Fig. 14.1 Quantification of IC shunts using transthoracic echocardiography. Systemic stroke volume or flow (Q_s) can be calculated by using CSA of LVOT which is derived by LVOT diameter at the end of systole (**a**) and LVOT VTI (**b**) pulmonary stroke volume or flow (Q_p) can be measured using CSA of RVOT which is derived by RVOT diameter at the end of systole (**c**) and RVOT VTI (**d**)

$$\frac{Q_p}{Q_s} = \frac{\text{CSA of RVOT} \times \text{VTIRVOT}}{\text{CSA of LVOT} \times \text{VTILVOT}} \qquad \frac{Q_p}{Q_s} = \frac{3.14 \times (2.3/2)^2 \times 21.1}{3.14 \times (1.8/2)^2 \times 17.1} \qquad \frac{Q_p}{Q_s} = \frac{87.6}{43.5} = 2$$

CSA cross sectional area; *LVOT* left ventricle outflow tract; *VTI* velocity time integral; and *RVOT* right ventricle outflow tract

For the systemic flow, the formula would be simplified as follow:

$$Q_s = 0.785 \times \text{LVOTd}^2 \times \text{VTI}_{\text{LVOT}}$$

After simplification the formula of Qp/Qs is:

$$\frac{Q_p}{Q_s} = \frac{\text{RVOTd}^2 \times \text{VTIRVOT}}{\text{LVOTd}^2 \times \text{VTILVOT}}$$

See the example in Fig. 14.1. (Q_p = Pulmonary flow; Q_s = Systemic flow; RVOTd^2 = Right ventricle outflow tract diameter; LVOTd^2 = Left ventricle outflow tract diameter).

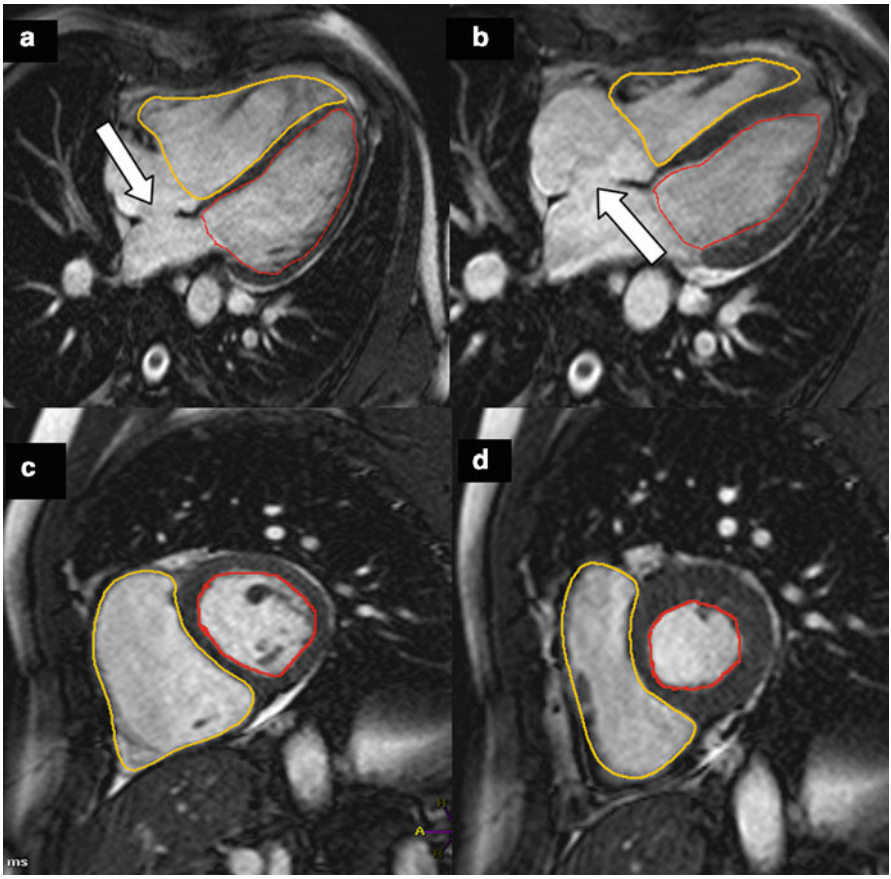

Fig. 14.2 Volumetric method for the quantification of IC shunt. Diastolic (**a**) and systolic (**b**) four chamber cine MR images of both ventricles demonstrate moderately dilated RV with normal systolic function. Diastolic (**c**) and systolic (**d**) short axis cine MR images of both ventricles. The ratio of the RV to LV stroke volumes gives shunt ratio (Q_p/Q_s). LV EDV = 194 cm^3; LV ESV = 102 cm^3; LV SV = 92 cm^3; LV EF = 48%, RV EDV = 289 cm^3; RV ESV = 124 cm^3; RV SV = 165 cm^3; and RV EF = 57%. Shunt ratio can be therefore calculated for this ASD case (*white arrows* show the defect); $Q_p/Q_s = 165/92 = 1.8$ (*ASD* atrial septal defect; *EDV* end diastolic volumes; *ESV* end systolic volumes; *LV* left ventricle; and *RV* right ventricle)

Potential Source of Errors and Pitfalls

Precise measurements of LVOT and RVOT diameters require appropriate site selection. LVOT diameter should be measured at the level of the aortic annulus during systole in parasternal long axis view of the LV, whereas RVOT is measured at the level of pulmonary valve annulus in parasternal short axis view (see Fig. 14.1). It is important to note that CSA is calculated as if it is a perfect circle. CSA of outflow tracts can change throughout cardiac cycle which may cause error. Positioning of sample volume of pulsed wave Doppler signals should be obtained at the levels where RVOT and LVOT diameters were measured.

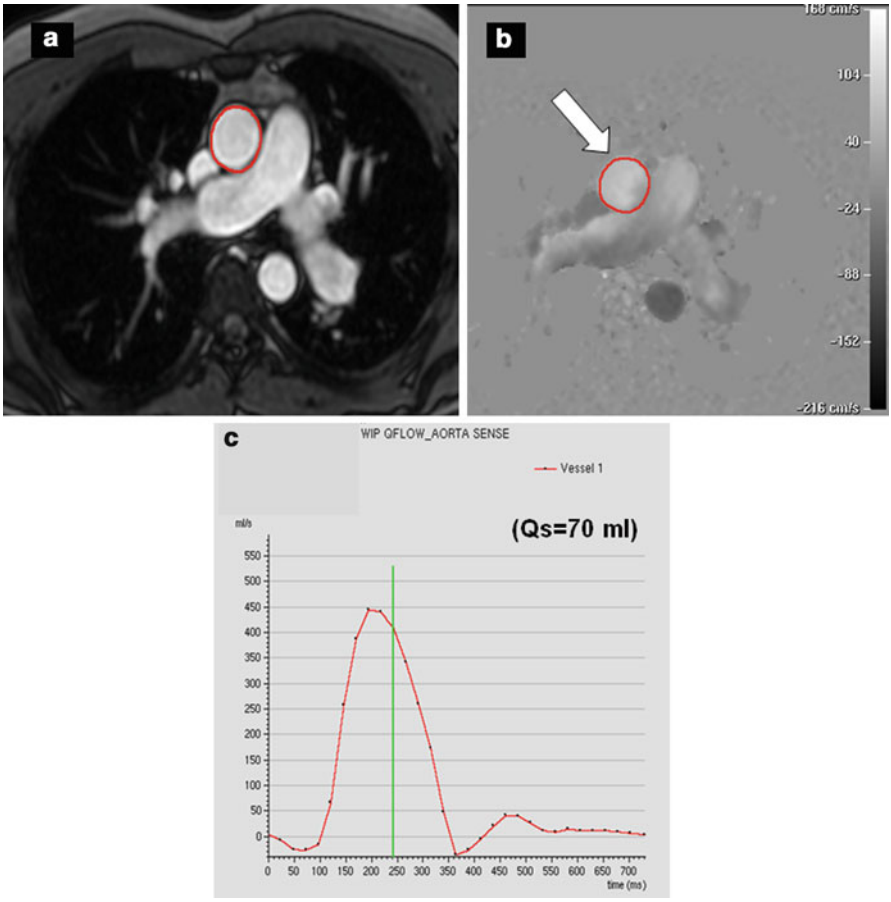

Fig. 14.3 (**a**–**c**) Velocity encoded (phase contrast) cine MR imaging for the quantitation of systemic flow (Q_s) (**a**) Magnitude image of the ascending aorta for the measurement of cross sectional area of the vessel. The plane is positioned at the level of the bifurcation of the main pulmonary artery, (**b**) phase contrast image perpendicular to the ascending aorta (*white arrow*) (**c**) Through-plane velocity mapping creates flow vs. time curves. The area under the curve represents stroke volume of the ascending aorta (Q_s) which was measured 70 mL/beat for this case. ($Q_s = 70$ mL). (**d**–**f**) Phase contrast cine MR imaging for the quantitation of pulmonary flow(Q_p) (**a**) Magnitude image of the main pulmonary artery, (**b**) Phase contrast image perpendicular to the main pulmonary artery (*white arrow*) (**c**) Through-plane velocity mapping demonstrates flow vs. time curves across the main pulmonary artery. The area under the curve represents stroke volume of the pulmonary artery (Q_p) which was calculated 162 mL/beat for this case. The shunt ratio was therefore calculated $Q_p/Q_s = 162/70 = 2.2$, which indicates significant left to right shunting

Optimal Doppler signals must be acquired for accurate velocities and VTI. Respiratory variations can affect position of PW sample location or Doppler velocities.

Many other pitfalls such as arrhythmia, heart rate variability, and presence of valvular heart disease in particular aortic and mitral regurgitation may also complicate

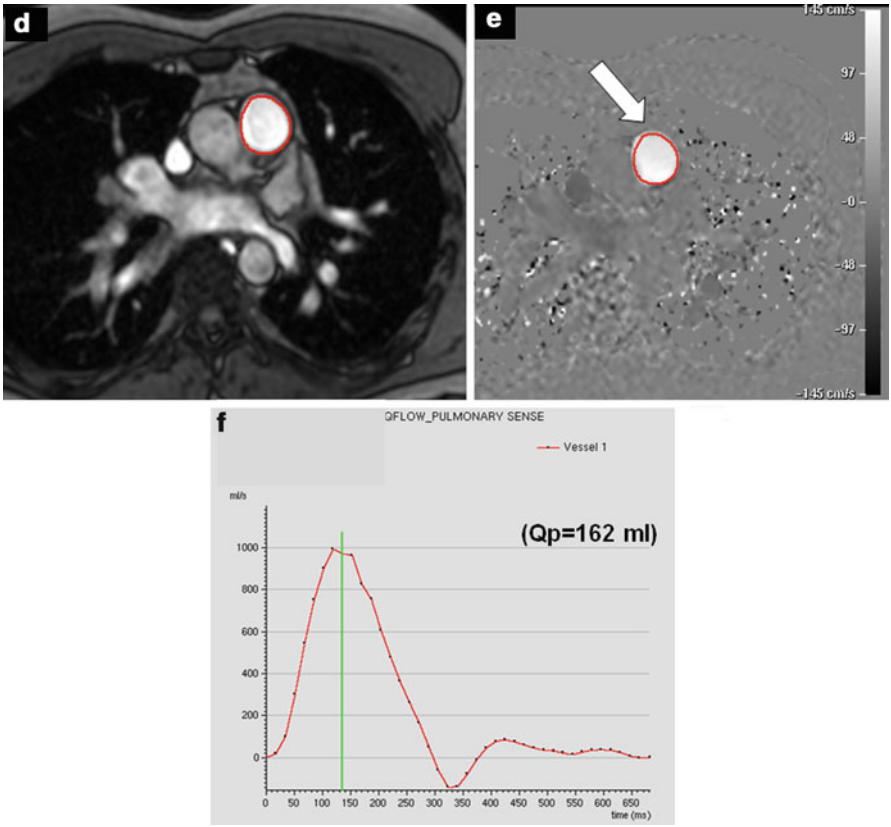

Fig. 14.3 (continued)

shunt assessment. A small error in the diameter measurement is magnified in the calculation of cross sectional area translating into large errors in flow calculations.

Assessment of Intracardiac Shunt with Cardiovascular Magnetic Resonance

Although echocardiography is initial diagnostic tool for the assessment of congenital heart disease (CHD), cardiovascular magnetic resonance (CMR) has become an important technique for the noninvasive evaluation of the size and morphologic features of the congenital cardiac defects. MRI provides not only the exact visual-

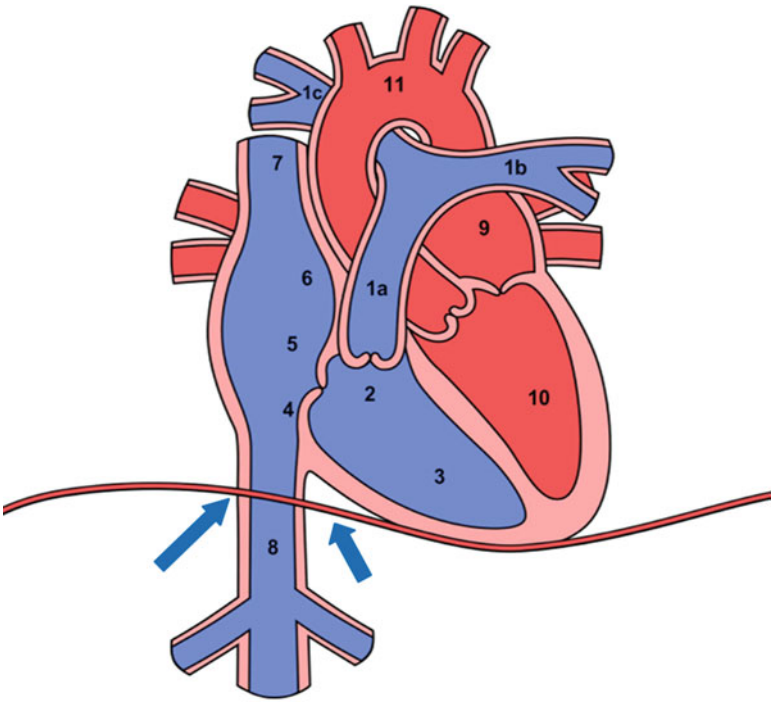

Fig. 14.4 Exact localization for the blood sampling in oxymetric run study. *1a* Main pulmonary artery, *1b* left pulmonary artery, *1c* right pulmonary artery, *2* right ventricular outflow tract, *3* right ventricle, *4* low right atrium, *5* mid right atrium, *6* high right atrium, *7* superior vena cava, *8* inferior vena cava (sample should be obtained just below the diaphragm (*blue arrows*); hepatic vein must be taken into account while obtaining inferior vena cava blood), *9* pulmonary vein, *10* left ventricle, *11* aorta or femoral artery

ization of cardiac anatomy but also allows accurate and reproducible quantification of IC shunts. Studies demonstrated MRI measurements of IC shunts correlate very well with those obtained by invasive methods in children [1–3] as well as in adults [4] using different MRI applications [5, 6]. Volumetric and phase contrast cine MRI are commonly used protocols for the assessment of IC shunt. Ventricular stroke volume can be easily calculated for each ventricle with short axis and/or four chamber views (Fig. 14.2). In the absence of significant valvular regurgitation or ventricular septal defect (VSD), the ratio of the RV to LV stroke volumes yields the Q_p/Q_s ratio. Velocity encoded (VENC) cine MR is another application for the measurement of IC shunt [5]. Each voxel has its own velocity across the vessel in the grey scale images. Flow can be estimated using cross sectional area of the vessel and integrated into the velocity of the blood at the same level. Magnitude images provide an accurate measurement for the cross sectional areas of the vessel and phase cine MR images offer reliable quantification for mean flow velocity [2] (Fig. 14.3a, b).

MRI has many advantages when compared to other noninvasive imaging modalities. Unlike echocardiography, MR allows visualization of vascular

structures in addition to cardiac chambers. It is possible to make reliable and reproducible measurements of blood flow velocities and assess stenotic and regurgitant valvular lesions by CMR. These can be accomplished with much less subjectivity compared with echocardiography. In contrast to radionuclide technique or cardiac computed tomography (CT), MR does not have any ionizing radiation. In addition to accurate quantification of IC shunts, MRI is a promising technique for the guidance of transcatheter closure of congenital heart defects [7]. After closure of such defects, MRI can clearly show anatomic location of the device and can quantify its effectiveness [8–10]. However MRI requires more patient compliance and a comprehensive MR exam takes time and is relatively expensive. Many stents, devices, and vascular filters are MR compatible. Whereas implantable cardiac devices have previously been considered as absolute contraindications, the FDA recently granted pre-market approval for an "MRI safe" pacemaker system (FDA press release February 8, 2011).

Other Noninvasive Imaging Modalities

Radionuclide techniques can also be used for the assessment of IC shunt. Radionuclide scintigraphy can be considered as an alternative noninvasive method for the quantification of IC shunt and evaluation of LV function in patients with post MI VSR [11].

Cardiac CT can provide comprehensive anatomic information in the assessment of congenital cardiac defects. Although cine CT makes some hemodynamic measurements possible such as cardiac output, quantification of IC shunts with CT has not been well established.

Invasive Quantification of Intracardiac Shunts

IC shunts have been calculated using various invasive methods. Indocyanin dilution and/or dye curve technique have been used in the past. Contrast angiography provides qualitative evaluation and localization of the shunts but is not suitable for precise shunt quantification. The widely used invasive technique is the oxymetric study, which is based on blood sampling from different locations in the circulation.

Oxygen Saturation Run

Knowledge of basic principles of Fick's method is fundamental to understand how IC shunts are calculated in catheterization laboratory.

Blood Sampling

Blood samples should be obtained after a "steady state" of heart rate, respiratory rate and blood pressure is reached. A large hole catheter should be used for easy blood draw. It should be kept in mind that very rapid aspiration or a faulty connection may allow entry of the micro bubbles into the syringe, resulting in erroneously increased O_2 saturation and overestimation of Q_p [12]. Sites for Blood sampling must be carefully chosen depending on the underlying pathology (Fig. 14.4) Blood sampling procedure should be completed within 5–10 min (or at the same time that oxygen consumption is calculated) in order to minimize the variability in oxygen consumption. After each sample is obtained, the catheter must be cleared with a saline flush. Obtaining blood samples from distal to proximal during catheter "pull-back" from pulmonary artery (PA) is more practical. If possible, the patient should not be receiving supplemental oxygen greater than 30% as the increased dissolved O_2 in the right heart might cause increased pulmonary flow resulting in overestimation of the shunt ratio.

Variability of oxygen measurements and oxygen content should be taken into account during the sampling process, particularly in the right-sided heart chambers. In a study with 980 patients [13] without shunting, differences of O_2 saturation were found between SVC and RA, RA and PA, SVC and PA $3.9 \pm 2.4\%$, $2.3 \pm 1.7\%$, and $4.0 \pm 2.5\%$, respectively. In another study, [14] 102 adults without left to right shunt were assessed in order to find the limits of normality of O_2 content differences. The outcomes were from right atrium to mixed venous, right ventricle to right atrium, and pulmonary artery to right ventricle, 0.5 mL/dL, 0.6 mL/dL, and 0.9 mL/dL, respectively.

Mixed Venous Oxygen Saturation

In the normal circulation, deoxygenated blood is mixed in the pulmonary artery (PA). However, in the setting of left to right shunt, site of mixed venous blood would vary according to the location of the lesion. Unfortunately, there is no practical way to measure mixed venous oxygen (MVO_2) because the various sources of MVO_2 (Superior vena cava, inferior vena cava, coronary sinus) have different amounts of blood with varying saturations. As a general rule, blood samples should be obtained proximal and distal to the lesion and blood from the chamber(s) proximal to the shunt site is used for MVO_2 measurement. For instance, in the case of patent ductus arteriosus (PDA), arterial blood mixes with venous blood at the pulmonary artery at the level of the aorta. Thus, venous samples should be taken from RV, which is the proximal chamber to the shunt site. In patients with a ventricular septal defect, RAO_2 saturation can represent MVO_2 site. In the case of an atrial septal defect, the location where the arterial shunt mixes with venous blood is not constant. Different formulae are used for the calculation of MVO_2. The most commonly used formula in the estimation of MVO_2 is $((3SVC + 1IVC)/4)$ [15]. Other formulae may also be considered for an estimation of MVO_2 as follows:

$$\mathrm{MVO_2} = \frac{((1 \times \mathrm{SVC_{Sat}}) + (2 \times \mathrm{IVC_{Sat}}))}{3} \quad \mathrm{MVO_2} = \frac{((2 \times \mathrm{SVC_{Sat}}) + (3 \times \mathrm{IVC_{Sat}}))}{5}$$

where $\mathrm{MVO_2}$ = Mixed venous oxygen saturation, $\mathrm{SVC_{Sat}}$ = Superior vena cava saturation, and $\mathrm{IVC_{Sat}}$ = Inferior vena cava saturation [14, 16].

Calculation of Shunt Size "Pulmonary to Systemic Flow Ratio (Q_p/Q_s)"

In the absence of a shunt, pulmonary blood flow (Q_p) is equal to the systemic blood flow(Q_s). Q_p/Q_s ratio is calculated based on Fick's principle as follows:

$$\text{Cardiac output} = \frac{\text{Oxygen consumption}}{(\text{Arterial } \mathrm{O_2} - \text{Venous } \mathrm{O_2}) \times \text{Hemoglobinconcentration} \times 1.36 \times 10}$$

Since the pulmonary circulation occurs between pulmonary veins and pulmonary artery, the formula is adapted as follows:

$$Q_p = \frac{\text{Oxygen consumption}}{(\mathrm{PVO_2} - \mathrm{PAO_2}) \times \text{Hemoglobin concentration} \times 1.36 \times 10}$$

where Q_p = Pulmonary blood flow, $\mathrm{PVO_2}$ = Pulmonary vein oxygen saturation, and $\mathrm{PAO_2}$ = Pulmonary artery oxygen saturation)

Systemic circulation takes place between the aorta and the point where the venous blood is assumed to be fully mixed. Therefore the formula corresponds to:

$$Q_s = \frac{\text{Oxygen consumption}}{(\mathrm{AoO_2} - \mathrm{MVO_2}) \times \text{Hemloglobinconcentration} \times 1.36 \times 10}$$

where Q_s = Systemic blood flow, $\mathrm{AoO_2}$ = Aortic or systemic arterial oxygen saturation, and $\mathrm{MVO_2}$ = Mixed venous oxygen saturation)

These formulae can be simplified to calculate Q_p/Q_s as follows:

$$\frac{Q_p}{Q_s} = \frac{(\mathrm{AoO_2} - \mathrm{MVO_2})}{(\mathrm{PVO_2} - \mathrm{PAO_2})}$$

For right to left or bidirectional shunts:

Effective pulmonary blood flow must be calculated. The net difference of systemic flow to shunt flow should be considered as effective pulmonary flow.

Clinical Utility of the Shunt Ratio in Practice

Shunt ratio (Q_p/Q_s) can help clinicians to better understand hemodynamic importance of the IC shunt and is clinically very important in decision making about the requirement of possible intervention. If the ratio is less than 1.5, it generally indicates a "small lesion," a ratio of 1.5–2.0 indicates "likely to require intervention," a ratio of 2 or more is usually considered to be "severe." Nevertheless, each case should be evaluated individually with its clinical presentation and shunt ratio should be determined within the clinical context of the disease state. If there is inconsistency between invasive and noninvasive measurements; symptoms attributable to shunt defect, possible associated congenital abnormalities, as well as measurement pitfalls should be carefully reviewed. Secondary findings such as quantification of chamber enlargement or ventricular function can also help in making decision.

Board Style Questions

Q1—A 30-year old woman presented with dyspnea on exertion. Echocardiographic examination revealed enlargement of right-sided heart chambers with an increased pulmonary flow. Left to right shunt was detected by color flow Doppler assessment in the inter-atrial septum. Which one of the following echocardiographic measurements is *not* necessary for the quantification of atrial shunt in this patient?

A) Diameter of LVOT
B) Diameter of RVOT
C) Diameter of defect
D) RVOT VTI
E) LVOT VTI

Q2—In which of the following congenital heart diseases, volumetric MRI measurement is *not* an appropriate method for the quantification of the intracardiac shunt?

A) Muscular type VSD
B) Secundum type ASD
C) Patent ductus arterious
D) Partial anomalous pulmonary venous return
E) Aorticopulmonary window

Q3—Which one of the following formulae can be used to estimate mixed venous blood (MVO_2) saturation during cardiac catheterization?

A)

$$MVO_2 = \frac{(3\times SVC_{sat} + 1\times IVC_{sat})}{4}$$

B)

$$MVO_2 = \frac{(SVC_{sat} + IVC_{sat})}{2}$$

C)

$$MVO_2 = \frac{(2 \times SVC_{sat} + 3 \times IVC_{sat})}{5}$$

D)

$$MVO_2 = SVC_{sat}$$

E) All of above

Q4—A 16-year old patient underwent cardiac catheterization for further investigation with the suspicion of congenital heart disease. Her hemoglobin level is 13 g/dL and calculated O_2 consumption is 190 mL/min. According to the saturation run study results, shown below, which is the correct diagnosis?

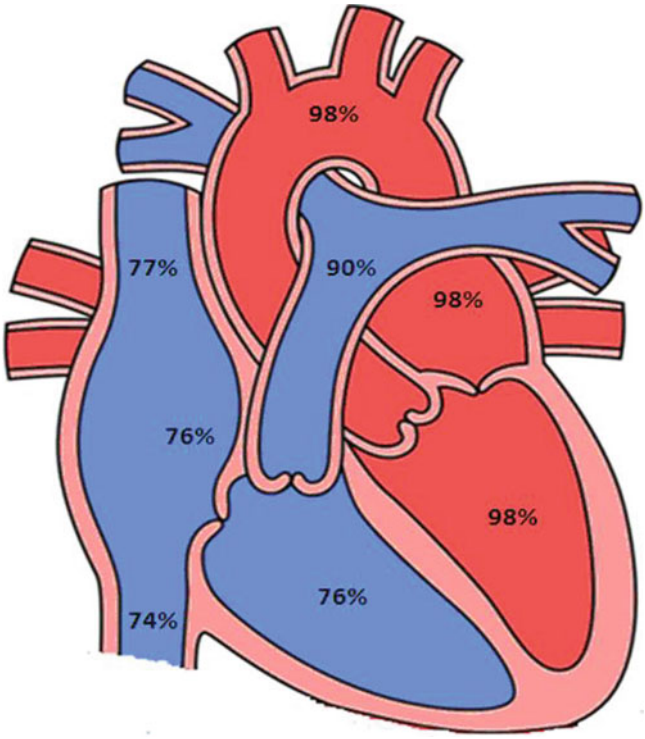

A) Muscular type VSD–$Q_p/Q_s = 1.5$
B) Ostium primum type ASD–$Q_p/Q_s = 2.8$
C) Ostium secundum type ASD–$Q_p/Q_s = 2.8$
D) Patent ductus arteriosus–$Q_p/Q_s = 2.8$
E) Patent ductus arteriosus–$Q_p/Q_s = 1.5$

Q5—A 36-year old man who was diagnosed secundum type ASD with left to right shunting. Calculated Q_p/Q_s ratio was reported as 2.1 with right atrial and ventricular enlargement. There was no associated significant valvular abnormality and he was still on normal sinus rhythm (68 beats/s).He was complaining of palpitations and exertional dyspnea and referred to you for further investigation and treatment. The following oxygen saturations were measured in catheterization room while patient was breathing 21% oxygen room air O_2 cont; IVCsat: 69%, SVCsat: 73%, PAsat: 80% Femoral artery sat: 98%.

What would you do for the next step in the evaluation of this patient?

A) Invasive Q_p/Q_s ratio cannot be calculated with these data; hemoglobin and cardiac output should have been reported.
B) Echocardiographic shunt ratio indicates significant left to right shunting with an enlargement of right-sided heart chamber, which is enough for the decision on closure of this ASD.
C) Room oxygen level is not enough; oxymetric study should be repeated while patient is breathing 80% oxygen.
D) Invasive Q_p/Q_s indicates significant left to right shunt so the defect should be closed as soon as possible.
E) Invasive Q_p/Q_s indicates nonsignificant left to right shunt, therefore patient should be treated medically and must be closely monitored.

Answers of the Questions

A1—The correct answer is C.
Echocardiography is the primary tool for the assessment of congenital heart disease. Although echocardiography can provide sizing of the defect, it is not required in the quantification of shunt ratio. The defect size, however, cannot give an idea about the shunt ratio. Small lesion can be associated with small shunt ratio whereas big lesions can be complicated by Eisenmenger physiology with right to left or bidirectional shunting.
A2—The correct answer is A.

Gradient echo cine MR can provide comprehensive volumetric assessment for both ventricles. The shunt volume can be easily calculated as net difference between LV and RV stroke volumes. In the setting of VSD, however, IC shunt occurs at the ventricular level and quantification of Q_p/Q_s is impossible using this method. On the other hand, if there is severe valvular regurgitation, due to substantial back flow into the atria, stroke volumes can be underestimated.

A3—The correct answer is E.

Although the most common formula is (3×SVC+IVC)/4, in the estimation of saturation MVO_2 blood**,** other formula can be considered.

A4—The correct answer is D.

The diagnosis is PDA with L□R shunt. O_2 step up can be clearly seen in main pulmonary artery. Although we can easily calculate Q_p/Q_s using simplified formula which is;

$$\frac{Q_p}{Q_s} = \frac{(AoO_2 - MVO_2)}{(PVO_2 - PAO_2)}$$

$$\frac{Q_p}{Q_s} = \frac{(98-76)}{(98-90)} = \frac{(22)}{(8)} = 2.75$$

Step by step approach for the assessment of intracardiac shunt quantification?

Step 1: Compute oxygen content for main locations

$$\text{Arterial oxygen content} = 0.98 \times 1.36 \times 13 \times 10 = 173$$

$$\text{Pulmonary vein oxygen content} = 0.98 \times 1.36 \times 13 \times 10 = 173$$

$$\text{Pulmonary artery oxygen content} = 0.90 \times 1.36 \times 13 \times 10 = 160$$

$$\text{Mixed venous oxygen content} = 0.76 \times 1.36 \times 13 \times 10 = 134$$

(Due to this is a PDA case, RVsat can represent MVO_2)

Step 2: Compute systemic flow (Q_s)

$$\frac{190}{173-134} = 4.87$$

Step 3: Compute pulmonary flow (Q_p)

$$\frac{190}{173-160} = 14.6$$

Step 4: Compute Q_p/Q_s

$$\frac{14.6}{4.87} = 3$$

A5—The correct answer is B.

Invasive oxymetric measurement of the Q_p/Q_s ratio is 1.5 which is inconsistent with echocardiographic shunt ratio. This is not uncommon situation in daily practice. Although Q_p/Q_s ratio is clinically very important in decision-making, if there is strong clinical suspicion or laboratory evidence of a significant shunt (this patient is symptomatic and TTE revealed right sided heart chambers enlargement), then defect should be closed. On the other hand, it should be kept in mind that atrial shunts can easily be affected by ventricular filling patterns such as compliance or stiffness and might be underestimated in the setting of severe tricuspid regurgitation or atrial fibrillation.

Hemoglobin and oxygen content are not exactly necessary for an estimation of Q_p/Q_s ratio. Because same parameters are used in the denominator and nominator of the equations, simplified method can be used practically.

References

1. Brenner LD, Caputo GR, Mostbeck G, et al. Quantification of left to right atrial shunts with velocity-encoded cine nuclear magnetic resonance imaging. J Am Coll Cardiol. 1992;20:1246–50.
2. Korperich H, Gieseke J, Barth P, et al. Flow volume and shunt quantification in pediatric congenital heart disease by real-time magnetic resonance velocity mapping: a validation study. Circulation. 2004;109:1987–93.
3. Beerbaum P, Korperich H, Barth P, Esdorn H, Gieseke J, Meyer H. Noninvasive quantification of left-to-right shunt in pediatric patients: phase-contrast cine magnetic resonance imaging compared with invasive oximetry. Circulation. 2001;103:2476–82.
4. Debl K, Djavidani B, Buchner S, et al. Quantification of left-to-right shunting in adult congenital heart disease: phase-contrast cine MRI compared with invasive oximetry. Br J Radiol. 2009;82:386–91.
5. Hundley WG, Li HF, Lange RA, et al. Assessment of left-to-right intracardiac shunting by velocity-encoded, phase-difference magnetic resonance imaging. A comparison with oximetric and indicator dilution techniques. Circulation. 1995;91:2955–60.
6. Beerbaum P, Korperich H, Gieseke J, Barth P, Peuster M, Meyer H. Rapid left-to-right shunt quantification in children by phase-contrast magnetic resonance imaging combined with sensitivity encoding (SENSE). Circulation. 2003;108:1355–61.
7. Ratnayaka K, Raman VK, Faranesh AZ, et al. Antegrade percutaneous closure of membranous ventricular septal defect using X-ray fused with magnetic resonance imaging. JACC Cardiovasc Interv. 2009;2:224–30.
8. Lapierre C, Raboisson MJ, Miro J, Dahdah N, Guerin R. Evaluation of a large atrial septal occluder with cardiac MR imaging. Radiographics 2003;23 Spec No:S51-8.
9. Weber M, Dill T, Deetjen A, et al. Left ventricular adaptation after atrial septal defect closure assessed by increased concentrations of N-terminal pro-brain natriuretic peptide and cardiac magnetic resonance imaging in adult patients. Heart. 2006;92:671–5.
10. Schoen SP, Kittner T, Bohl S, et al. Transcatheter closure of atrial septal defects improves right ventricular volume, mass, function, pulmonary pressure, and functional class: a magnetic resonance imaging study. Heart. 2006;92:821–6.
11. Wynne J, Fishbein MC, Holman BL, Alpert JS. Radionuclide scintigraphy in the evaluation of ventricular septal defect complicating acute myocardial infarction. Cathet Cardiovasc Diagn. 1978;4:189–97.

12. Matta BF, Lam AM. The rate of blood withdrawal affects the accuracy of jugular venous bulb. Oxygen saturation measurements. Anesthesiology. 1997;86:806–8.
13. Hillis LD, Firth BG, Winniford MD. Variability of right-sided cardiac oxygen saturations in adults with and without left-to-right intracardiac shunting. Am J Cardiol. 1986;58:129–32.
14. Pirwitz MJ, Willard JE, Landau C, Hillis LD, Lange RA. A critical reappraisal of the oximetric assessment of intracardiac left-to-right shunting in adults. Am Heart J. 1997;133:413–7.
15. Flamm MD, Cohn KE, Hancock EW. Measurement of systemic cardiac output at rest and exercise in patients with atrial septal defect. Am J Cardiol. 1969;23:258–65.
16. French WJ, Chang P, Forsythe S, Criley JM. Estimation of mixed venous oxygen saturation. Catheter Cardiovascular Diagnosis. 1983;9:25–31.

Chapter 15
Shock

Michael P. Brunner and Venugopal Menon

Epidemiology of Shock

Shock is a pathophysiologic state characterized by inadequate tissue oxygen delivery, which may lead to cellular death and vital organ dysfunction. Common clinical manifestations of shock include hypotension, diminished urine output, metabolic acidosis, and confusion. Shock is a major cause of morbidity and mortality.

Coronary artery disease is the leading cause of adult mortality in the United States and accounts for one-third of all deaths in patients older than age 35 [1]. Cardiogenic shock is estimated to complicate 3–8% of cases of acute myocardial infarction [2–4]. The mortality associated with cardiogenic shock in patients with acute myocardial infarction had historically approached 80% [2]. Despite medical advancements, the contemporary mortality associated with myocardial infarction complicated by cardiogenic shock remains 40–70% [4–6].

Septicemia is the 11th leading cause of death in the United States and accounts for over 34,000 deaths/year [7]. Mortality associated with severe sepsis and septic shock has been estimated at 10–38% and the economic impact at 16.7 billion dollars annually [8]. These figures are likely underestimated as severe sepsis and septic shock often occur concomitantly with other leading causes of mortality including chronic lower respiratory tract infection, influenza, pneumonia, and malignancy.

Hypovolemic shock related to traumatic injury, acute gastrointestinal bleeding, severe burns, plasma extravasation, fluid losses, and other etiologies is also associated with substantial morbidity and mortality.

M.P. Brunner, M.D. • V. Menon, M.D. (✉)
The Cleveland Clinic, Cleveland, OH, USA
e-mail: brunnem@ccf.org; menonv@ccf.org

S. Anwaruddin et al. (eds.), *Cardiovascular Hemodynamics: An Introductory Guide*, Contemporary Cardiology, DOI 10.1007/978-1-60761-195-0_15,

Clinical Presentation of Shock: Case Based

A fundamental understanding of the pathophysiology associated with various shock etiologies is essential to making appropriate clinical assessment and guiding appropriate therapy. Although classification schemes vary, the causes of shock can generally be divided into three categories: cardiogenic, distributive, and hypovolemic (see Table 15.1). The following cases are examples from each category of shock and provide a framework for further discussion of the clinical presentation of each.

Case 1: Cardiogenic Shock

A 40-year-old male smoker with hypertension, hyperlipidemia, and family history of myocardial infarction presents with crushing substernal chest pain and shortness of breath. An electrocardiogram reveals ST-segment elevation across the anterior precordial leads. He is tachycardic and hypotensive. A third heart sound (S3) is appreciated; there are no murmurs or rubs. He has inspiratory rales in the lung bases and jugular venous pulsations are elevated. His extremities are cool, mottled, and cyanotic.

The above case describes a patient with cardiogenic shock caused by acute myocardial infarction. Cardiogenic shock is a clinical condition in which inadequate tissue perfusion is the consequence of cardiac dysfunction. It is characterized by a reduction in cardiac output despite adequate filling pressures. Causes of cardiogenic shock include myopathic, mechanical, valvular, pericardial, extracardiac, and arrhythmic processes (see Table 15.1). Criteria typically used to define cardiogenic shock include systolic blood pressure less than 90 mmHg for at least 30 min or need for vasopressor or intra-aortic balloon support to maintain systolic blood pressure greater than 90 mmHg, pulmonary capillary wedge pressure greater than 15 mmHg, and cardiac index less than 2.2 L/min/kg/m^2 [9].

Hypotension, tachycardia, confusion, diminished urine output (less than 30 mL/h), and cool, mottled, and cyanotic extremities typically characterize the clinical presentation of cardiogenic shock. Tachycardia occurs in an effort to maintain cardiac output when the stroke volume has been reduced. Confusion and diminished urine output are the result of poor tissue perfusion. Cool, mottled, and cyanotic extremities are manifestation of the peripheral vasoconstriction that typically occurs in patients with cardiogenic shock.

Peripheral pulses are often diminished in cardiogenic shock due to decreased pulse pressure (pulsus parvus). In a failing left ventricle the strength of every other beat may alternate, a phenomenon known as pulses alternans. Delayed pulses (pulsus tardus) may be seen in cardiogenic shock related to severe aortic stenosis.

Cardiogenic shock related to obstructive extracardiac processes such as tension pneumothorax or pulmonary embolism may be accompanied by decreased breath sounds, tympany, deviated airway, dyspnea, tachypnea, and/or unilateral peripheral edema.

Table 15.1 Causes of shock

Cardiogenic	**Distributive**
Causes That May Complicate Acute Myocardial Infarction Italicized	Systemic Inflammatory Response Syndrome
(Myopathic)	Sepsis
Acute Myocardial Infarction	Pancreatitis
Left Ventricular Failure	Myocardial Infarction
Right Ventricular Failure	Anaphylaxis
Acute Myocarditis	Bacterial Toxins
Idiopathic Cardiomyopathy	Acidosis
Restritive/Constrictive Cardiomyopathy	Adrenal Crisis
Takotsubo Cardiomyopathy	Myxedema Coma
Acute Heart Transplant Rejection	Iatrogenic
Iatrogenic (Negative Inotropic or Vasodilatory Medications)	Neurogenic Insult
Post-cardiac Arrest	Post-resuscitation syndrome
Toxic/Metabolic	Post-cardiopulmonary bypass
(Mechanical)	End-stage Heart Failure
Ventricular Septal Rupture	**Hypovolemic**
Ventricular Free Wall Rupture	(Hemorrhagic)
Hypertrophic Obstructive Cardiomyopathy	Trauma
Dynamic Left Ventricular Outflow Tract Obstruction	Gastrointestinal Bleeding
Ruptured Aortic Aneurysm	Ruptured Hematoma
Acute Aortic Dissection	Hemorrhagic Pancreatitis
Atrial Myxoma	Fractures
Traumatic	Aortic or Ventricular Free Wall Aneurysm Rupture
(Valvular)	(Plasma Extravasation Related)
Papillary Muscle/Chordal Rupture	Systemic Inflammatory Response
Acute Mitral Regurgitation	Sepsis
Prosthetic Valve Obstruction	Major Surgery
Aortic Insufficiency	Pancreatitis
Critical Aortic Stenosis	(Fluid Loss Related)
Severe Mitral Stenosis	Dehydration
(Pericardial)	Severe Burns
Tamponade	Emesis
(Extracardiac)	Diarrhea
Pulmonary Embolism	Diaphoresis
Tension Pneumothorax	Insensible Losses
(Arrhythmic)	Inadequate Fluid Intake
Tachycardia	
Bradycardia	

Cardiogenic shock related to left ventricular failure may be associated with pulmonary congestion; associated findings include inspiratory rales and/or radiographic pulmonary vessel cephalization, Kerley B lines, and parenchymal edema. A third heart sound (S3) may be present and the apical impulse is displaced laterally when there is underlying left ventricular dilatation.

Of note, a significant proportion of patients in the SHOCK (SHould we emergently revascularize Occluded Coronaries in cardiogenic shocK?) trial had no pulmonary congestion [10]. Neither auscultation nor chest radiograph detected pulmonary edema in 28% patients.

Right ventricular infarction complicates up to half of all transmural inferior-posterior myocardial infarctions [11]. Patients with hemodynamically significant right ventricular infarction classically present with hypotension, clear lung fields, and jugular venous distention. Right ventricular failure may be associated with a holosystolic tricuspid regurgitation murmur at the left lower sternal border, jugular venous distension, liver engorgement, pulsatile liver, and peripheral edema. Patients with patent foramen ovale and acute right ventricular infarction may present with profound hypoxia. Decreased compliance in the infarcted right ventricle can result in right to left shunting.

Mechanical complications of acute myocardial infarction may occur in patients presenting with cardiogenic shock and will be evident on physical exam. Acute mitral regurgitation, tricuspid regurgitation, and ventricular septal rupture are associated with holosystolic murmurs. Prominent jugular *v*-waves suggest severe tricuspid regurgitation. Jugular cannon *a*-waves suggest complete heart block. Ventricular rupture may result in tamponade. Classic findings of tamponade include distant, muffled heart sounds, jugular venous distension, and decreased systolic blood pressure. Ventricular interdependace, manifest by an inspiratory drop in blood pressure (pulses paradoxus), greater than 10 mmHg may also be observed.

In cardiogenic shock a compensatory increase in systemic vascular resistance (SVR) typically occurs through peripheral vasoconstriction in an effort to maintain tissue perfusion. However, this classic paradigm has been challenged. Data from the SHOCK trial demonstrated that many patients with cardiogenic shock instead have low systemic resistance, similar to patients with septic shock [12] (see Fig. 15.1). It has been postulated that a systemic inflammatory response-like syndrome with a low SVR may be encountered in up to one-fifth of patients with acute myocardial infarction complicated by cardiogenic shock [13].

The clinical presentation can be utilized to risk stratify patients with acute myocardial infarction complicated by cardiogenic shock. Killip described a case series of 250 patients presenting to an academic university intensive care unit with myocardial infarction [14]. He divided the patients into four classes according to clinical presentation. Class I had no clinical signs of heart failure, class II presented with basilar rales and/or S3 gallop and/or elevated jugular venous pressure, class III had frank pulmonary edema, and class IV cardiogenic shock. Reported mortality was 6%, 17%, 38%, and 67% for each class, respectively.

Current mortality with reperfusion therapy is dramatically lower than that observed in the original observation. However findings of Killip >1 in the setting of an acute myocardial infarction continue to identify a high-risk patient subset.

Therapeutic measures for patients with cardiogenic shock often need to be implemented before invasive hemodynamic data are available. The clinical presentation may guide decision-making in choosing the most effective therapy. For example, patients with findings consistent with myocardial infarction require urgent

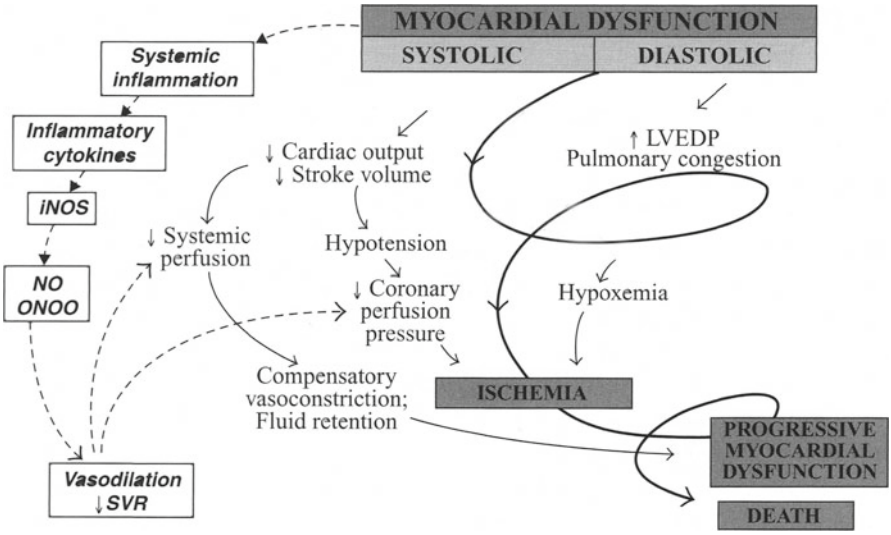

Fig. 15.1 Expansion of the pathophysiologic paradigm of cardiogenic shock to include the potential contribution of inflammatory mediators. *LVEDP* left ventricular end diastolic pressure; *NO* nitric oxide; *iNOS* inducible nitric oxide synthase; *ONOO*$^-$ peroxynitrite; *SVR* systemic vascular resistance (reprinted with permission from Hochman JS, Ohman EM. Pathophysiology. In: Cardiogenic shock. Wiley-Blackwell; 2009)

revascularization. Patients with findings consistent with left ventricular failure may require inotropes, vasoactive agents, and/or an intra-aortic balloon pump. Patients with findings consistent with right ventricular infarction may require rapid fluid resuscitation.

Case 2: Distributive Shock

An 80-year-old female with recurrent urinary tract infection presents with fever, tachycardia, hypotension, decreased urine output, and confusion. She is diaphoretic and has foul smelling urine. Her neck veins are flat and the lung fields are clear. The extremities are warm and hyperemic. Capillary refill is brisk. Her hypotension does not improve despite aggressive fluid resuscitation.

The above case describes a patient with distributive shock related to severe sepsis. Inappropriate vasodilation, decreased SVR, hypotension, and poor tissue oxygenation characterize distributive shock. Etiologies of distributive shock include systemic inflammatory response syndrome, severe sepsis, bacterial toxins (e.g., Staphylococcal toxic shock), anaphylaxis, adrenal insufficiency, myxedema coma, neurogenic insult, myocardial infarction, post-resuscitation syndrome, and post-cardiopulmonary bypass (see Table 15.1).

Septic shock is the most common presentation of distributive shock. Septic shock is defined by sepsis-induced hypotension that persists despite adequate fluid resuscitation (20–30 mL/kg starch or 40–60 mL/kg saline or PCWP 12–20 mmHg) [15].

Clinical presentations of distributive shock vary by etiology but are generally characterized by tachycardia, hypotension, decreased urine output (less than 30 mL/h), confusion, and warm, well-perfused extremities. Compensatory tachycardia occurs to cause an increase in cardiac output and maintain tissue perfusion. Decreased urine output and confusion are manifestations of poor tissue perfusion. Warm, hyperemic extremities with rapid capillary refill are the result of inappropriate vasodilatation and decreased SVR. The cardiac output is typically elevated in distributive shock and may manifest as bounding pulses. The lungs are typically clear and there is not any associated jugular venous distension or peripheral edema.

Patients with severe sepsis and shock may have fever or hypothermia, diaphoresis, and rigors. Findings associated with an infectious process (e.g., pneumonia) may be present. Tachypnea is common and occurs in an effort to compensate for severe metabolic acidosis caused by elevated lactate. Hoarse voice, stridor, wheezing, pruritus, skin flushing, hives, and abdominal pain may accompany anaphylactic shock. Hypothermia, hypoventilation, and somnolence are associated with myxedema coma. Profound orthostatic hypotension and skin hyperpigmentation may be presenting signs of adrenal insufficiency. Although most patients with distributive shock present with tachycardia, patients with neurogenic shock may have bradycardia due to sympathetic denervation.

Case 3: Hypovolemic Shock

A 25-year-old male presents shortly after a gunshot wound to the abdomen. He has experienced profound bleeding. He is tachycardic, hypotensive, and confused. Neck veins are flat and lung fields are clear. Mucus membranes and skin are dry. Extremities are cool and clammy. He has large drop in blood pressure and is more tachycardic when changing position from supine to standing.

The above case describes a patient with hypovolemic shock related to traumatic hemorrhage. Hypovolemic shock is characterized by inadequate intravascular volume. Etiologies are generally related to hemorrhage, plasma extravasation, or fluid losses (see Table 15.1). Hemorrhagic etiologies include trauma, gastrointestinal bleeding, ruptured hematoma, hemorrhagic pancreatitis, fractures, and aortic or ventricular free wall aneurysm rupture. Etiologies related to plasma extravasation include systemic inflammatory response, severe sepsis, major surgery, and pancreatitis. Fluid loss may be due to severe burns, emesis, diarrhea, diaphoresis, other insensible losses, and inadequate oral intake.

Hypotension, tachycardia, confusion, diminished urine output (less than 30 mL/h), and cool, mottled, and cyanotic extremities typically characterize the clinical presentation of hypovolemic shock. Cardiac output generally falls as a result of decreased ventricular preload. Compensatory tachycardia and an increase in SVR

mediated by peripheral vasoconstriction occur in an effort to improve tissue perfusion. Increased sympathetic activity may cause narrow pulse pressure and diaphoresis. Peripheral vasoconstriction results in cool, mottled, and cyanotic extremities.

The clinical history will generally suggest the etiology when patients present with cardiogenic or hypovolemic shock. However, clinical findings may appear similar in each. A key difference is that intracardiac filling pressures are adequate or elevated (pulmonary capillary wedge pressure greater than 15 mmHg) in cardiogenic shock, whereas hypovolemic shock is defined by inadequate intravascular volume. In hypovolemic shock the lung fields are generally clear and there is no evidence of jugular venous distension or peripheral edema.

The physical diagnosis of hypovolemia has been systematically reviewed in adults [16]. The most helpful physical findings include severe postural dizziness (preventing measurement of upright vital signs) or a postural pulse increment of 30 beats/min or more. Supine hypotension and tachycardia were frequently absent, even after up to 1,150 mL of blood loss. In patients with vomiting, diarrhea, or decreased oral intake, the presence of a dry axilla supports the diagnosis of hypovolemia, and moist mucous membranes and a tongue without furrows argue against it. In adults, the capillary refill time and poor skin turgor have no proven diagnostic value.

Diagnostic Evaluation of Shock

The etiology of shock can often be determined or narrowed to a few possibilities using the data acquired from the medical history, physical examination, basic laboratory evaluation, and radiographic findings. However, additional diagnostic test may be needed in the optimal assessment and management of shock. Intra-arterial pressure monitoring, echocardiography, pulmonary artery catheterization, and cardiac catheterization are frequently utilized diagnostic modalities.

Brachial cuff measurements are often inaccurate in states of shock. Intra-arterial pressure monitoring provides continuous assessment of the blood pressure and heart rate and allows for safe and effective titration of vasoactive medications. In addition, valuable hemodynamic data is obtained through assessment of the arterial waveform. Further, the pulse pressure (systolic − diastolic blood pressure) may be helpful in differentiating various shock states (further hemodynamic discussion below).

The 2004 American College of Cardiology/American Heart Association (ACC/AHA) executive summary guidelines for the management of patients with ST-segment elevation myocardial infarction state that intra-arterial pressure monitoring should be performed (class I indication) for severe hypotension (systemic arterial pressure less than 80 mmHg), during the administration of vasopressor and/or inotropic agents, and for cardiogenic shock [17]. Potential complications of intra-arterial pressure monitoring include pain, infection, hematoma, arterial insufficiency, and arterial embolus.

Echocardiography is an invaluable tool in the assessment of shock. In cardiogenic shock, echocardiography may help determine the etiology and guide management.

Echocardiography can be utilized to assess left and right ventricular function, and can detect tamponade, restrictive/constrictive physiology, severe valvular regurgitation or stenosis, ventricular septal rupture, and proximal aortic dissection. Echocardiographic findings of a clot in transit and right ventricular dysfunction may also suggest the presence of a hemodynamically significant pulmonary embolism when suspected.

Echocardiographic assessment with agitated saline is a sensitive diagnostic modality for detecting intracardiac and pulmonary vascular shunting. In addition, hemodynamic data can be assessed noninvasively utilizing echocardiography. The central venous pressure, pulmonary artery pressure, and left ventricular end diastolic pressure can be estimated using conventional methods.

The pulmonary artery catheter can be valuable in determining the etiology of shock and may help in guiding management. Data obtained from the pulmonary artery catheter includes central venous pressure, right atrial pressure, right ventricular pressure, pulmonary artery pressure, and pulmonary artery occlusion pressure (i.e., pulmonary capillary wedge pressure). Mixed venous oxygen saturation measurement and calculation of the cardiac output and systemic venous resistance are facilitated using a pulmonary artery catheter. Further, important diagnostic information is obtained through careful analysis of the right atrial, right ventricular, pulmonary arterial, and pulmonary capillary wedge waveforms.

The hemodynamic data gathered using a pulmonary artery catheter can be utilized to titrate vasopressors, assess the hemodynamic effects of changes in mechanical ventilation (e.g., positive end expiratory pressure), and guide fluid resuscitation. In addition, the data may help differentiate between cardiogenic and non-cardiogenic pulmonary edema when a trial of diuretic and/or vasodilator therapy has failed.

Pulmonary artery catheterization may aid in determining if pericardial tamponade is present when clinical assessment is inconclusive and echocardiography is not available. Findings of tamponade include diastolic equalization of pressures and blunted y descents (see Chap. 9). Other utilities of pulmonary artery catheterization include assessment of valvular heart disease severity and reversibility of pulmonary vasoconstriction in patients being considered for heart transplant. Oximetric investigation of cardiac shunts that may occur as a complication of myocardial infarction can also be performed using a pulmonary artery catheter.

Despite the potential advantages, pulmonary artery catheterization has not been shown to improve important patient outcomes and its use is controversial and is not favored in some centers. Whether the lack of benefit on important outcomes is a result of the severity of illness in the patients for whom the use of this tool is contemplated or a result of incorrect interpretation of the data gleaned is a debated topic. It is important to note that the Evaluation Study of Congestive Heart Failure and Pulmonary Artery Catheterization Effectiveness (ESCAPE) trial showed no significant difference in endpoints of mortality and days out of hospital at 6 months in the management of congestive heart failure refractory to standard medical therapy [18]. However, this trial demonstrated that the use of the pulmonary artery catheter for this group of patients was safe.

In ESCAPE, addition of a pulmonary artery catheter to careful clinical assessment was associated with higher frequency of adverse events but did not affect overall

mortality and hospitalization. Adverse events included implantable cardioverter-defibrillator firing, cardiogenic shock, ischemia/angina, pulmonary artery catheter infection, myocardial infarction, stroke or ischemic attack, cardiac arrest, and infection. The only individual event that was statistically different (p value<0.05) between the groups was pulmonary artery catheter infection (p value$=0.03$). The number of patients with at least one adverse event was more common in the pulmonary artery catheter group (p value$=0.04$).

The external validity of the ESCAPE findings has been debated [19]. The ESCAPE sites enrolled 439 patients to receive pulmonary artery catheterization without randomization in a prospective registry. On average, registry patients had lower blood pressure, worse renal function, less neurohormonal antagonist therapy, and higher use of intravenous inotropes compared with trial patients. The registry patients had longer length of stay and higher 6-month mortality. Many of the registry patients were not randomized to the trial because of investigator opinion that a pulmonary artery catheterization was necessary for management. Therefore, data interpreted from the patient population in the ESCAPE trial may not be applicable to the critically ill heart failure patients that are often considered for pulmonary artery catheterization.

Routine pulmonary artery catheterization in intensive care units is also controversial. A 2005 meta-analysis of 13 randomized trials including over 5,000 critically ill patients showed that the use of pulmonary artery catheters was associated with neither benefit nor increased mortality in the intensive care unit [20]. The meta-analysis included patients who were critically ill from a wide variety of causes.

There have not been any randomized studies aimed at directly evaluating the utility of pulmonary artery catheters in patients presenting with cardiogenic shock. There were 2,968 patients with cardiogenic shock enrolled in the GUSTO-1 (Global Utilization of Streptokinase and Tissue Plasminogen Activator for Occluded Coronary Arteries) trial. Mortality among patients ($n=995$) managed with PA catheters (45.2%) was less than among patients ($n=1{,}406$) not managed with PA catheters (63.4%) [21].

A potential limitation of pulmonary artery catheter hemodynamic monitoring is that most physicians may not know how to correctly interpret findings from the device [22]. A 31 question multiple-choice exam was administered to 496 medical doctors at 13 different institutions to assess their knowledge and understanding of the use of the pulmonary artery catheter and interpretation of data derived from it. The examination was given unannounced at general scheduled meetings in the departments of medicine, anesthesiology, and surgery (e.g., grand rounds). The mean score was 67% and 47% could not read a pulmonary capillary wedge pressure from a clear tracing.

The ACC/AHA executive summary guidelines for the management of patients with ST-segment elevation myocardial infarction provide guidance for appropriate pulmonary catheter use in hemodynamic assessment [17]. It is a class I indication to use pulmonary artery catheter monitoring in the assessment of hypotension unresponsive to fluid administration or when fluid administration may be contraindicated and for suspected mechanical complications of ST-segment elevation myocardial infarction if an echocardiogram has not been performed.

The guidelines also state that pulmonary artery catheters "can be" useful (class IIa indication) for hypotension in a patient without pulmonary congestion who has not responded to an initial trial of fluid administration, cardiogenic shock, severe or progressive heart failure or pulmonary edema that does not respond rapidly to therapy, persistent signs of hypoperfusion without hypotension or pulmonary congestion, and during the administration of vasopressor and/or inotropic agents.

Potential complications of pulmonary artery catheter use include infection, right bundle branch block, ventricular tachycardia, pulmonary artery rupture, and pulmonary infarction. Over time, pulmonary artery catheters tend to soften and migrate distally, leading to spontaneous wedging even when the balloon tip is not inflated.

Hemodynamic Assessment of Shock

A fundamental understanding of the hemodynamics of various shock states is critically important. As above, the etiology of shock may not be evident despite the data acquired from the medical history, physical examination, basic laboratory evaluation, and radiographic findings. Hemodynamic data can help diagnosis the correct etiology of shock and guide appropriate management. Hemodynamic assessment of shock requires invasive monitoring, namely intra-arterial pressure monitoring and pulmonary artery catheterization.

Systemic tissue perfusion (blood pressure) is determined by the cardiac output and SVR. Similar to Ohm's law, whereas electrical current through a circuit is directly proportional to the potential difference across the circuit, and inversely proportional to the resistance; cardiac output (CO) is directly proportional to the blood pressure difference across the systemic circulation (mean arterial pressure [MAP] – mean right atrial pressure [mean RAP]), and inversely proportional to the SVR. $\mathrm{CO} = (\mathrm{MAP} - \text{mean RAP}) / \mathrm{SVR}$.

The cardiac output can be measured with a pulmonary artery catheter by utilizing either the Fick method or thermodilution techniques (see Chap. 4). Different categories of shock can be discriminated using the calculated cardiac output. Whereas cardiac output is low in cardiogenic shock and hypovolemic shock, it is generally elevated in distributive shock (see Table 15.2). However, cardiac output can also be reduced in distributive shock due to myopathic processes such as severe acidosis or when preload is decreased because of inadequate intravascular volume.

The SVR can be calculated if the blood pressure, right atrial pressure, and cardiac output are known. The drop in arterial pressure across the systemic circulation divided by cardiac output is equal to SVR. $\mathrm{SVR} = [\mathrm{MAP} - \text{mean RAP}] / \mathrm{CO}$. The units for SVR are $\mathrm{mmHg/mL/m^2}$ (Woods units) and are typically multiplied by 80 to convert to dyn $\mathrm{s/cm^5}$ (dyn). Pulmonary vascular resistance can be calculated by substituting the drop in pressure across the systemic circulation with that of the pulmonary circulation (mean pulmonary artery pressure – mean pulmonary capillary wedge pressure).

Table 15.2 Hemodynamic patterns classically associated with different categories of shock

	RA (mmHg)	RV (mmHg)	PA (mmHg)	PCWP (mmHg)	CI (L/min/kg/m²)	PP (mmHg)	HR (bpm)	SVR (dynes)	SVO2 (%)
Normal Values	<6	<25/0–12	<25/0–12	<6–12	>2.5	40–50	60–100	800–1600	70
Cardiogenic	↑	↑	↑	↑ (>15)[1]	↓ (<2.2)	↑↓	↑	↑[2]	↓
Distributive	↑↓	↑↓	↑↓	↑↓	↑[3]	↑	↑[4]	↓	↑↓[5]
Hypovolemic	↓	↓	↓	↓	↓	↓	↑	↑	↓

RA Right atrium; *RV* right ventricle; *PA* pulmonary artery; *PCWP* pulmonary capillary wedge pressure; *CI* cardiac index; *PP* pulse pressure; *HR* heart rate; *SVR* systemic vascular resistance; SVO_2 mixed venous oxygen saturation

[1]In the SHOCK trial 28% of patients had no auscultatory or radiographic evidence of pulmonary edema suggestive of elevated PCWP

[2]A systemic inflammatory response-like syndrome with a low SVR may be encountered in up to one-fifth of patients with acute myocardial infarction complicated by cardiogenic shock

[3]Cardiac output can be reduced in distributive shock due to myopathic processes such as severe acidosis or when preload is decreased because of inadequate intravascular volume

[4]Patients with neurogenic shock may have bradycardia due to sympathetic denervation

[5]SVO_2 is generally increased in sepsis due to poor oxygen utilization

SVR is reduced in distributive shock but is generally elevated in cardiogenic and hypovolemic shock. However, as discussed above, SVR can be reduced in acute myocardial infarction complicated by shock [6].

The mixed venous oxygen concentration may help differentiate shock etiologies. The mixed venous oxygen concentration is utilized in the Fick method to calculate cardiac output (see Chap. 4) and is low in cardiogenic shock. In distributive shock related to sepsis, mixed venous oxygen concentration is generally elevated. In sepsis, the mitochondrial respiratory chain does not utilize oxygen appropriately. As a result, there is more oxygen than expected in the blood that is returned to the heart.

Elevated pulmonary capillary wedge pressure (greater than 15 mmHg) has classically been used to distinguish cardiogenic from non-cardiogenic causes of shock. However, in the SHOCK trial 28% of patients had no auscultatory or radiographic evidence of pulmonary edema to suggest elevated PCWP [10]. Severe sepsis can cause myocardial depression and may elevate left-sided pressures as well. Cardiogenic shock related to right ventricular infarction may be associated with marked hypotension, low cardiac output, and shock despite a normal pulmonary capillary wedge pressure.

The intra-arterial pressure waveform can help differentiate various shock etiologies. Pulse pressure equals the difference between systolic and diastolic blood pressure and is normally 40–50 mmHg (see Fig. 15.2). The pulse pressure is a reflection of the stroke volume and the strength of each ventricular contraction.

In patients with cardiogenic shock related to left ventricular failure, the pulse pressure is reduced (see Fig. 15.3). Narrow pulse pressure (pulse pressure <25% of the systolic blood pressure) has a sensitivity and specificity of 91 and 83% for a cardiac index of <2.2 [23]. Other causes of narrow pulse pressure include profound intravascular volume loss, tamponade, and aortic stenosis. Widened pulse pressure is a physiologic response to exercise and can be seen pathologically with atherosclerosis, aortic insufficiency, complete heart block, aortic dissection, arteriovenous fistula, fever, anemia, thyrotoxicosis, pregnancy, and elevated intracranial pressure (see Fig. 15.4).

The pulse width is also a reflection of stroke volume. Patients in shock with normal or hypercontractile ventricles often have aortic waveforms with narrow pulse widths but normal pulse pressures. Both non-cardiac (e.g., anaphylaxis and severe sepsis) and cardiac (e.g., tamponade, acute mitral regurgitation, post-myocardial infarction ventricular septal defect, and aortic dissection) etiologies of shock may be associated with narrow pulse width. A narrow pulse has a spike appearance and the dicrotic notch appears low (see Fig. 15.5).

Pulsus alternans occurs when there is alternating rise and fall in systolic pressure from beat to beat despite a regular rhythm (see Fig. 15.6). Pulsus alternans implies severe myocardial dysfunction and is most often seen in left ventricular failure. It may also occur in association with severe aortic stenosis and severe coronary artery disease. Pulsus alternans is thought to be due to alternation of myocardial contractility on a beat-to-beat basis because of abnormal intracellular calcium cycling [24].

Pulmonary artery catheter intravascular waveform tracings can also help differentiate various etiologies of shock. Large *v*-waves on the pulmonary capillary wedge pressure tracing suggest shock from acute, severe mitral regurgitation. Likewise, large *v*-waves may be seen on the RAP tracing with severe TR. Cannon *a*-waves

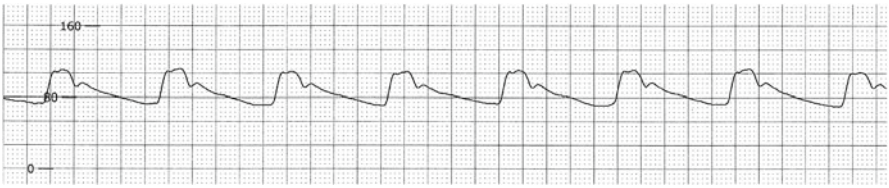

Fig. 15.2 Normal aortic waveform

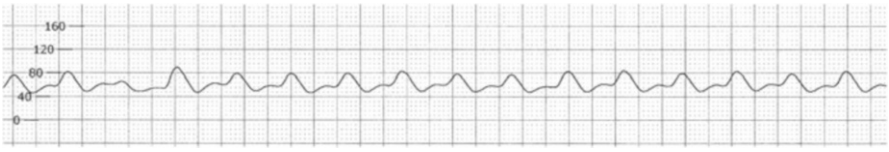

Fig. 15.3 Example of narrow pulse pressure in a patient with cardiogenic shock

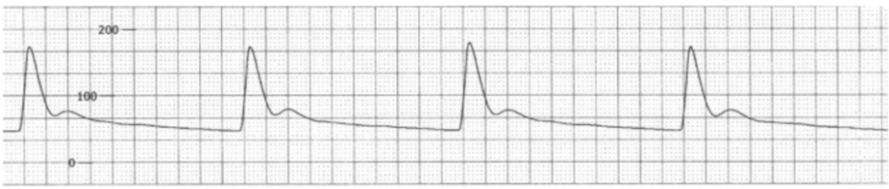

Fig. 15.4 Example of wide pulse pressure in a patient with complete heart block

Fig. 15.5 Example of narrow pulse width in a patient with acute aortic dissection

suggest complete heart block. Elevated and equalized diastolic pressures with loss of y descents suggest tamponade. Markedly elevated right atrial and right ventricular diastolic pressures and a normal pulmonary capillary wedge pressure suggest cardiogenic shock related to right ventricular infarction. An increase in right-sided pressures with inspiration (Kussmaul's sign) may be observed in right ventricular infarction due to decreased ventricular compliance.

Data obtained from the pulmonary artery catheter may reveal complications of acute myocardial infarction that occur in association with cardiogenic shock. For example, an oxygen step-up upon advancing from the right atria to the right

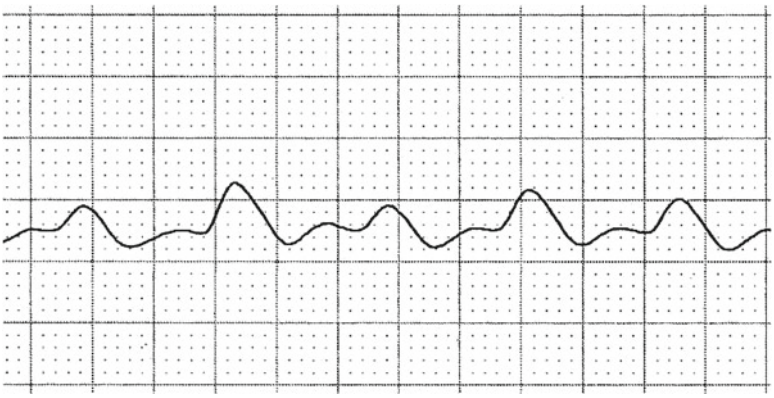

Fig. 15.6 Example of pulses alternans in a patient with advanced left ventricular failure

ventricle suggests left to right shunting related to ventricular septal rupture. As above, pulmonary artery catheter waveform analysis may suggest acute, severe valvular regurgitation, tamponade, and right ventricular infarction.

Arterial hypoxia may complicate shock. Evaluation of hypoxia begins with calculation of the alveolar-arterial (A-a) oxygen gradient. A normal A-a gradient equals 4 + (age/4) or 2.5 + (0.21 × age). Alveolar oxygen is calculated using the alveolar air equation: partial pressure alveolar oxygen (P_AO_2) = oxygen concentration (F_iO_2) × (barometric pressure at sea level (760 mmHg) − partial pressure water vapor (43 mmHg)) − (partial pressure carbon dioxide (P_ACO_2)/respiratory exchange ratio (0.8)). $P_AO_2 = (F_iO_2 \cdot (760 - 43)) - (P_ACO_2/0.8)$ $= (0.21 \cdot (760 - 43)) - (40/0.8) = 150 - 50 = 100\,\text{mmHg}$. Arterial partial pressure of oxygen is measured using conventional blood gas analysis.

If the A-a gradient is normal and P_aCO_2 is increased, hypoventilation is the suggested cause of hypoxia. With an elevated A-a gradient, proceed to check the mixed venous oxygen saturation. A low mixed venous oxygen saturation suggests hypermetabolism, anemia, or decreased cardiac output. If mixed venous oxygen is normal, administer 100% oxygen. If hypoxia corrects, ventilation/perfusion mismatch is suggested. Ventilation/perfusion mismatch is caused by airway (e.g., asthma and chronic obstructive pulmonary disease), alveolar (e.g., pneumonia and congestive heart failure), and vascular (e.g., pulmonary embolism) phenomenon. Shunting is suggested if hypoxia does not correct with oxygen and may be physiologic or vascular. Physiologic shunting occurs with alveolar collapse (e.g., atelectasis) or decreased alveolar filling (e.g., pneumonia and congestive heart failure). Vascular shunting occurs with right to left intracardiac shunts (e.g., atrial or ventricular septal defect) and intrapulmonary shunts (e.g., arteriovenous malformation and hepatopulmonary syndrome).

Hemodynamic data can also be utilized to risk stratify patients with acute myocardial infarction complicated by cardiogenic shock. In the SHOCK trial, cardiac power (cardiac power = MAP × CO/451) was the strongest independent correlate of in-hospital mortality in patients with cardiogenic shock [25].

Pearls of Assessment

There can be considerable overlap in the clinical presentation of the various categories of shock syndromes. Although classically associated with vasoconstriction and cold extremities, patients with cardiogenic shock can present with peripheral vasodilation and warm extremities. Indeed, in the SHOCK trial, the average SVR was not elevated and the range of values was wide, suggesting that compensatory vasoconstriction is not universal [6].

Patients with distributive shock typically have increased cardiac output. However, in sepsis, depressed myocardial function may occur due to metabolic acidosis and other factors. Acidemia is detrimental to LV contractility and may result from decreased clearance of lactate by liver, kidneys, and skeletal muscle, as well as, anaerobic metabolism. Inadequate intravascular volume may complicate distributive shock and result in decreased cardiac preload and cardiac output as well.

Review Questions

1. Which of the following types of shock is typically associated with a high mixed venous oxygenation saturation?

   a. Septic
   b. Cardiogenic
   c. Hypovolemic
   d. Anaphylactic

   Answer—a. In severe sepsis the mitochondrial respiratory chain does not utilize oxygen effectively. As a result there is more oxygen than expected in the blood that is returned to the heart.

2. Which of the following hemodynamic profiles is most consistent with cardiogenic shock?

   a. Systolic blood pressure 120 mmHg, pulmonary capillary wedge pressure 10 mmHg, cardiac index 3.5 L/min/m2, systemic vascular resistance (SVR) 1,000 dyn, mixed venous oxygen 75%.
   b. Systolic blood pressure 80 mmHg, pulmonary capillary wedge pressure 5 mmHg, cardiac index 1.3 L/min/m2, SVR 1,800 dyn, mixed venous oxygen 60%.
   c. Systolic blood pressure 80 mmHg, pulmonary capillary wedge pressure 10 mmHg, cardiac index 3.5 L/min/m2, SVR 600 dyn, mixed venous oxygen 85%.
   d. Systolic blood pressure 80 mmHg, pulmonary capillary wedge pressure 20 mmHg, cardiac index 1.3 L/min/m^2, SVR 1,800 dyn, mixed venous oxygen 60%.

   Answer—d. Hemodynamic criteria typically associated with cardiogenic shock include systolic blood pressure less than 90 mmHg for at least 30 min or need for vasopressor or intra-aortic balloon support to maintain systolic

blood pressure greater than 90 mmHg, pulmonary capillary wedge pressure greater than 15 mmHg, and cardiac index less than 2.2 L/min/kg/m^2 [9].

3. An 85-year-old male presents with hypotension, oliguria, and confusion. An electrocardiogram reveals inferior ST-segment elevations. A pulmonary artery catheter is inserted and the hemodynamic parameters are consistent with cardiogenic shock. His lung fields are clear and jugular venous pulse is elevated. A transthoracic echocardiogram reveals normal left ventricular function. What is the cause of this patient's clinical presentation?

   a. Right ventricular infarct
   b. Ventricular septal rupture
   c. Acute mitral regurgitation
   d. Tamponade

   Answer—a. The classic findings of right ventricular infarction are hypotension, jugular venous distension, and clear lung fields.

4. An 85-year-old female presents 1 week after developing severe chest pain. She has dyspnea with minimal activity. She is hypotensive and has pulmonary rales. An electrocardiogram reveals anterior *q*-waves. Troponin is elevated but CK-MB is within normal limits. Other laboratory analysis reveals renal and liver injury. Pulmonary artery catheter hemodynamic findings are consistent with cardiogenic shock. An oxygen saturation run reveals an increased oxygen gradient upon advancing from the right atria to the right ventricle. Which complication of acute myocardial infarction is the cause of this patient's shock?

   a. Ventricular free wall rupture
   b. Ventricular septal rupture
   c. Acute mitral regurgitation
   d. Tamponade

   Answer—d. Ventricular septal rupture may complicate myocardial infarction. An oxygen step-up upon advancing from the right atria to the right ventricle is typical.

References

1. Lloyd-Jones D, Adams RJ, Brown TM, et al. Executive summary: heart disease and stroke statistics—2010 update: a report from the American Heart Association. Circulation. 2010;121:948–54.
2. Goldberg RJ, Gore JM, Alpert JS, et al. Cardiogenic shock after acute myocardial infarction. Incidence and mortality from a community-wide perspective, 1975 to 1988. N Engl J Med. 1991;325:1117–22.
3. Goldberg RJ, Spencer FA, Gore JM, Lessard D, Yarzebski J. Thirty-year trends (1975 to 2005) in the magnitude of, management of, and hospital death rates associated with cardiogenic shock in patients with acute myocardial infarction: a population-based perspective. Circulation. 2009;119:1211–9.
4. Holmes Jr DR, Berger PB, Hochman JS, et al. Cardiogenic shock in patients with acute ischemic syndromes with and without ST-segment elevation. Circulation. 1999;100:2067–73.

5. Babaev A, Frederick PD, Pasta DJ, Every N, Sichrovsky T, Hochman JS. Trends in management and outcomes of patients with acute myocardial infarction complicated by cardiogenic shock. JAMA. 2005;294:448–54.
6. Hochman JS, Buller CE, Sleeper LA, et al. Cardiogenic shock complicating acute myocardial infarction—etiologies, management and outcome: a report from the SHOCK Trial Registry. SHould we emergently revascularize Occluded Coronaries for cardiogenic shocK? J Am Coll Cardiol. 2000;36:1063–70.
7. Kochanek KD, Jiaquan X, Murphy SL, Minino AM, Kung HC. Deaths: preliminary data for 2009: Centers for Disease Control and Prevention National Vital Statistics Reports; 2011.
8. Angus DC, Linde-Zwirble WT, Lidicker J, Clermont G, Carcillo J, Pinsky MR. Epidemiology of severe sepsis in the United States: analysis of incidence, outcome, and associated costs of care. Crit Care Med. 2001;29:1303–10.
9. Crawford MH. Current diagnosis & treatment cardiology. 3rd ed. New York: McGraw-Hill; 2009.
10. Menon V, White H, LeJemtel T, Webb JG, Sleeper LA, Hochman JS. The clinical profile of patients with suspected cardiogenic shock due to predominant left ventricular failure: a report from the SHOCK Trial Registry. SHould we emergently revascularize Occluded Coronaries in cardiogenic shocK? J Am Coll Cardiol. 2000;36:1071–6.
11. Kinch JW, Ryan TJ. Right ventricular infarction. N Engl J Med. 1994;330:1211–7.
12. Hochman JS. Cardiogenic shock complicating acute myocardial infarction: expanding the paradigm. Circulation. 2003;107:2998–3002.
13. Kohsaka S, Menon V, Lowe AM, et al. Systemic inflammatory response syndrome after acute myocardial infarction complicated by cardiogenic shock. Arch Intern Med. 2005;165:1643–50.
14. Killip III T, Kimball JT. Treatment of myocardial infarction in a coronary care unit. A two year experience with 250 patients. Am J Cardiol. 1967;20:457–64.
15. Dellinger RP, Levy MM, Carlet JM, et al. Surviving Sepsis Campaign: international guidelines for management of severe sepsis and septic shock: 2008. Crit Care Med. 2008;36:296–327.
16. McGee S, Abernethy III WB, Simel DL. The rational clinical examination. Is this patient hypovolemic? JAMA. 1999;281:1022–9.
17. Antman EM, Anbe DT, Armstrong PW, et al. ACC/AHA guidelines for the management of patients with ST-elevation myocardial infarction—executive summary: a report of the American College of Cardiology/American Heart Association Task Force on Practice Guidelines (Writing Committee to Revise the 1999 Guidelines for the Management of Patients With Acute Myocardial Infarction). Can J Cardiol. 2004;20:977–1025.
18. Binanay C, Califf RM, Hasselblad V, et al. Evaluation study of congestive heart failure and pulmonary artery catheterization effectiveness: the ESCAPE trial. JAMA. 2005;294:1625–33.
19. Allen LA, Rogers JG, Warnica JW, et al. High mortality without ESCAPE: the registry of heart failure patients receiving pulmonary artery catheters without randomization. J Card Fail. 2008;14:661–9.
20. Shah MR, Hasselblad V, Stevenson LW, et al. Impact of the pulmonary artery catheter in critically ill patients: meta-analysis of randomized clinical trials. JAMA. 2005;294:1664–70.
21. Hasdai D, Holmes Jr DR, Califf RM, et al. Cardiogenic shock complicating acute myocardial infarction: predictors of death. GUSTO Investigators. Global Utilization of Streptokinase and Tissue-Plasminogen Activator for Occluded Coronary Arteries. Am Heart J. 1999; 138:21–31.
22. Iberti TJ, Fischer EP, Leibowitz AB, Panacek EA, Silverstein JH, Albertson TE. A multicenter study of physicians' knowledge of the pulmonary artery catheter. Pulmonary Artery Catheter Study Group. JAMA. 1990;264:2928–32.
23. Stevenson LW, Perloff JK. The limited reliability of physical signs for estimating hemodynamics in chronic heart failure. JAMA. 1989;261:884–8.
24. Lab MJ, Lee JA. Changes in intracellular calcium during mechanical alternans in isolated ferret ventricular muscle. Circ Res. 1990;66:585–95.
25. Fincke R, Hochman JS, Lowe AM, et al. Cardiac power is the strongest hemodynamic correlate of mortality in cardiogenic shock: a report from the SHOCK trial registry. J Am Coll Cardiol. 2004;44:340–8.

Chapter 16
Intracoronary Hemodynamic Assessment: Coronary Flow Reserve (CFR) and Fractional Flow Reserve (FFR)

James E. Harvey and Stephen G. Ellis

Selective coronary angiography has been the gold standard for evaluating the presence and extent of epicardial coronary artery disease. Despite advances in fluoroscopic imaging and catheterization techniques, the evaluation of the intermediate coronary stenosis (luminal diameter narrowing between 40 and 70%) remains a challenge for invasive cardiologists secondary to multiple issues. Angiography provides only a 2D projection of the arterial lu along the length of the vessel. Vessel characteristics (e.g., significant angulation and tortuosity) as well as limitations related to image acquisition (e.g., vessel overlap, inability to obtain a true perpendicular projection of the lesion, and the visualization of a focal short stenosis) impair the accuracy of lesion severity assessment through the traditional technique of obtaining coronary angiograms in multiple fluoroscopic views. Studies comparing coronary angiography and postmortem histopathological analysis have demonstrated the discrepancy between angiographic and actual anatomic findings [1–3]. Significant intra- and inter-observer variability is also a factor when determining the percent narrowing of a stenosis by angiography [4]. The application of quantitative coronary angiography (QCA) may minimize this discrepancy but it does not eradicate the limitations of coronary angiography. Intravascular visualization techniques such as intravascular ultrasound (IVUS) or optical coherence tomography (OCT), augment anatomical analysis but do not necessarily provide information on the functional significance of a lesion. Thus, cardiologists have focuses on physiologic assessment of a lesion to aid in management decisions. Noninvasive testing (i.e., stress testing) to determine objective evidence of ischemia is frequently conducted prior to performing coronary angiography and subsequent percutaneous coronary intervention (PCI). However, these studies not always feasible nor are the

J.E. Harvey (✉) • S.G. Ellis
The Cleveland Clinic, Cleveland, OH, USA
e-mail: HarveyJ@ccf.org; elliss@ccf.org

A.T. Askari et al. (eds.), *Cardiovascular Hemodynamics: An Introductory Guide*, Contemporary Cardiology, DOI 10.1007/978-1-60761-195-0_16,

results always reliable; therefore a physiologic method of evaluating an intermediate coronary lesion while in the catheterization suite is desirable.

Sensor-tipped 0.014 in. diameter guidewires have been manufactured to accurately and safely measure flow velocities or pressure within a coronary artery. By employing this technology, two methods (coronary flow reserve (CFR) and fractional flow reserve (FFR)) have been developed to evaluate the physiologic or functional significance of coronary lesions in the cardiac catheterization suite.

Case Vignette #1

A 58-year-old woman with history of diabetes mellitus (DM) and family history of premature CAD presents with a 7-month history of exertional chest discomfort. Exercise nuclear stress test revealed reversible perfusion defects in the apical anterior and anteroseptal wall and in the mid inferior wall. Coronary angiography revealed "normal coronary arteries" and intravenous infusion of ergonovine did not precipitate coronary vasospasm. Coronary flow reserve (CFR) of the left anterior descending artery was 1.2, consistent with severe microvascular dysfunction.

Coronary Flow Reserve

CFR is defined as the ratio of mean blood velocity at maximal hyperemia to mean blood velocity at rest for a given coronary artery [5]. Developed in the 1970s, it is based on the principle that the volume of blood flow in a healthy coronary artery will increase with hyperemia to a greater extent than that of an artery with a physiologically significant stenosis (Figs. 16.1 and 16.2). Since blood flow as volume per time cannot be directly measured in the cardiac catheterization suite, blood velocity is measured as a surrogate because it is proportional to blood volume flow for a constant lumen area. CFR is assessed by placing a Doppler-tipped guide wire into a coronary artery distal to the epicardial stenosis in question. One then measures the flow velocities at rest and at maximal hyperemia. Hyperemia is pharmacologically induced typically by intravenous infusion of adenosine. The Doppler-derived CFR, which is inversely proportional to lesion severity [6], has been validated with good correlation to nuclear stress testing. A CFR value of ≤2.0 indicates a physiologically significant stenosis (Fig. 16.3) [7–10].

Unfortunately, CFR is affected by both the severity of epicardial stenosis and the extent of microvascular resistance. Microvascular resistance is influenced by common conditions such as diabetes mellitus, age, and ventricular hypertrophy. Each of these can significantly affect the CFR value regardless of the severity of epicardial stenosis [11–14]. In an effort to overcome this inherent limitation, the concept of relative CFR was developed. Relative CFR is determined by dividing the CFR of the diseased vessel by the CFR of another undiseased coronary vessel and accounts for the contribution of microvascular resistance to the CFR value. This improved the correlation to the detection of ischemia by stress myocardial perfusion imaging [15]. Use of this method requires the increased time and risk of evaluating an additional vessel. Due to these inherent limitations of CFR and relative CFR, these modalities are now rarely used to evaluate the severity of an epicardial arterial stenosis. Instead, FFR has become the method of choice for determining the physiologic significance of an epicardial arterial stenosis.

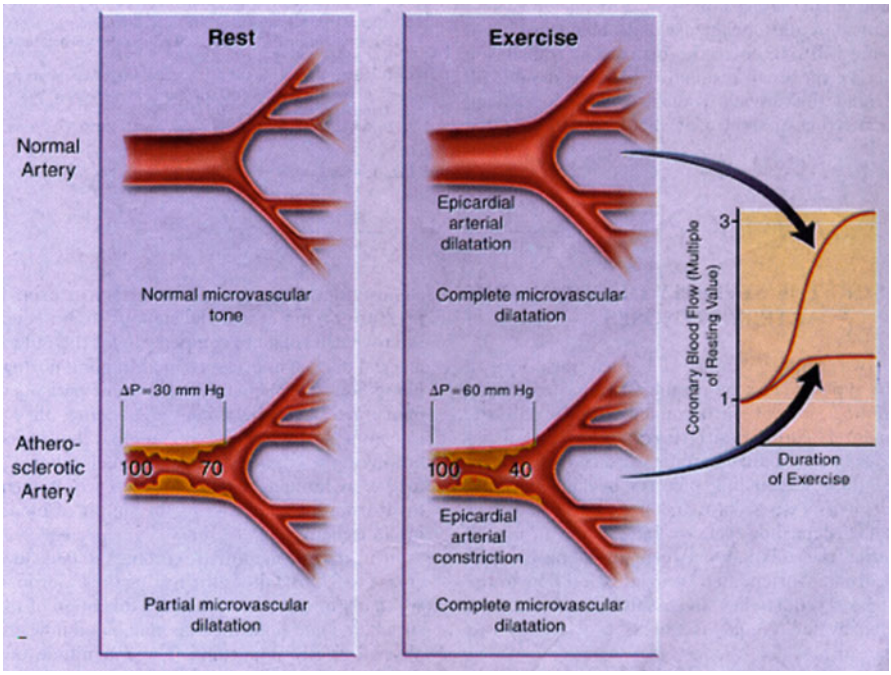

Fig. 16.1 Depiction of coronary blood flow at rest and at maximal hyperemia. A normal coronary artery will have a larger increase in blood flow than a diseased artery with a hemodynamically significant stenosis. By measuring the blood velocity or pressure proximal and distal to the stenosis, one can calculate the relative increase in blood flow or decrease in pressure caused by inducing maximal hyperemia

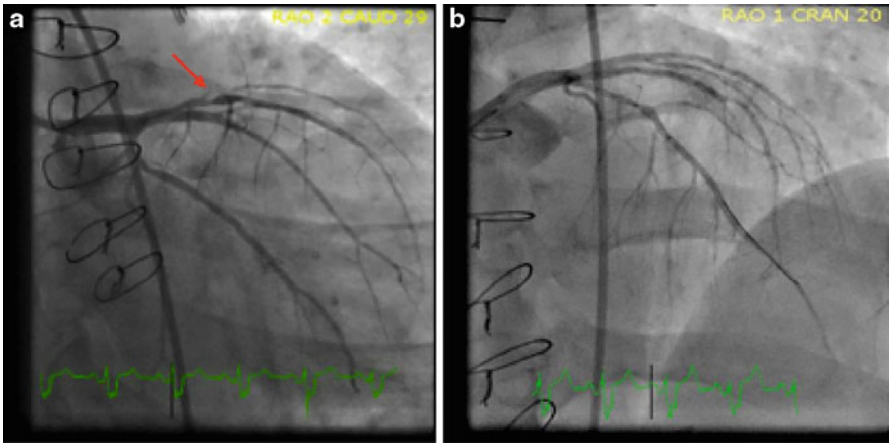

Fig. 16.2 (**a**) Coronary angiogram depicting an intermediate stenosis of the LAD (*red arrow*). (**b**) Coronary angiogram with pressure sensor-tipped 0.014 in. wire. In this case, FFR was performed on the LAD with a result of 0.70, however, a Doppler flow-sensor tipped 0.014 in. wire has the same appearance. PCI was successfully performed on the lesion

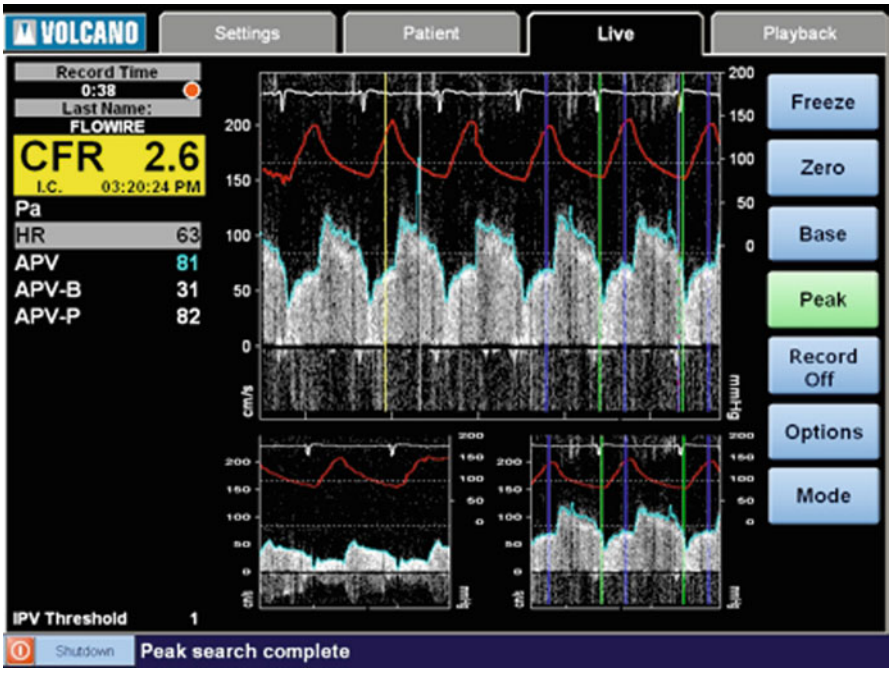

Fig. 16.3 A typical CFR display screen. Intracoronary Doppler blood flow velocity waveforms before intracoronary adenosine are shown on the small graph on the lower left portion of the display screen. Intracoronary Doppler blood flow velocity waveforms after intracoronary adenosine are shown on the small graph on lower right portion of the display screen and on the large graph in the center of the display. CFR is the ratio of the average peak velocities before and after adenosine; here it is reported as 2.6 on the top left portion of the display. This is suggestive of normal microvascular function

Cardiac Syndrome X

Despite its limitations in the interrogation of epicardial stenoses, CFR is the modality of choice for evaluation of coronary artery microvascular dysfunction. Cardiac syndrome X, or angina with an abnormal cardiac stress test and angiographically normal coronary arteries, is an increasingly recognized disorder with significant prognostic implications [16]. Diminished coronary flow velocity reserve in response to intracoronary adenosine, defined as a CFR ≤2.0, is suggestive of microvascular dysfunction and seen in up to 47% of patients with angina and no significant epicardial stenoses [17]. The patient described in *Clinical Vignette 1* has findings consistent with cardiac syndrome X. Patients with this condition have a rate of adverse cardiac events (myocardial infarction, congestive heart failure, stroke, and sudden cardiac death) of 2.5% per year [16].

Case Vignette 2

A 62 year old man with past medical history of hypertension, hyperlipidemia, and cigarette smoking presents with one month of worsening exertional chest discomfort that radiates down his left arm. Left heart catheterization reveals a focal 70% stenosis in proximal left circumflex artery (LCx) and a long 60% stenosis in the mid

right coronary artery (RCA). A pressure sensor-tipped 0.014 in. coronary wire was advanced down the LCx and FFR was performed with a value of 0.83. The pressure sensor-tipped 0.014 in. coronary wire was withdrawn and then advanced down to the distal RCA. FFR was 0.72. Percutaneous coronary intervention (PCI) was performed on the mid RCA lesion. No PCI was performed on the LCx, but rather aggressive medical management was employed.

Fractional Flow Reserve

Fractional flow reserve (FFR) is a newer method to invasively assess the hemodynamic significance of an intermediate coronary stenosis while in the catheterization suite. It is defined as the ratio of the mean distal coronary artery pressure to the mean aortic pressure while at maximal hyperemia [18–20]. It is performed by advancing a 0.014 in. pressure-sensor tipped coronary wire across an epicardial stenosis and simultaneously recording the pressure distal to the stenosis (via the coronary wire) and proximal to the stenosis (via the guide catheter) while at maximal hyperemia. (Fig. 16.2) Maximal hyperemia is typically achieved via intravenous or intracoronary infusion of adenosine because of its safety profile and low cost, however, papaverine or dobutamine can also be used [21–23].

As opposed to CFR, FFR measurement is independent of baseline blood pressure, heart rate, prior infarction, or contribution of collateral circulation [20, 24]. A normal FFR value is 1, while a value of <0.75–0.80 is associated with provocable ischemia; this has been shown to correlate well with ischemia demonstrated on noninvasive stress testing (Fig. 16.4) [19, 20, 25, 26]. Mortality and adverse cardiovascular event (MACE) rates have been shown to be very low in patients with an FFR >0.75–0.80 [27, 28] and multiple studies have demonstrated that PCI can be safely deferred in such patients [19, 27, 29].

Multivessel CAD

FFR is "lesion specific" and can be used to assess intermediate lesions in patients with single-vessel or multi-vessel CAD [30]. This is particularly useful in clinical scenarios in which patients present with symptomatic CAD and are found to have multi-vessel disease with multiple intermediate stenoses. In this subset of patients, noninvasive stress testing can demonstrate "balanced ischemia" and thus interpretations of culprit lesions are often inaccurate. Because of this, it has become commonplace to perform multi-vessel PCI for complete revascularization in this group, although this approach is not proven to be associated with improved outcomes. It was hypothesized that the utilization of FFR could aid in the better identification of culprit lesions and thus more appropriate management. To assess the utility of FFR in this group of patients, 1,005

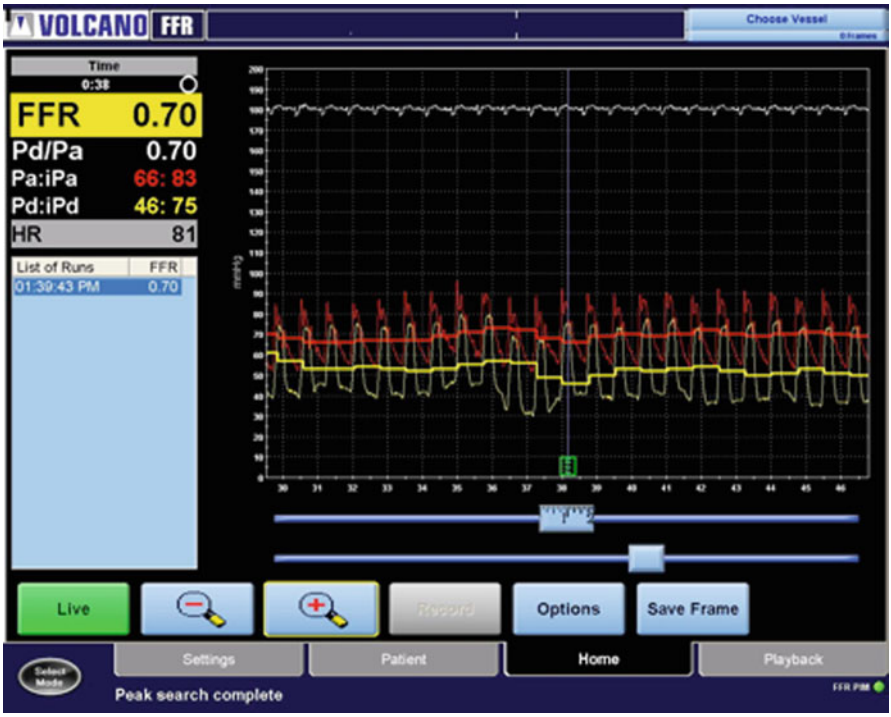

Fig. 16.4 A typical FFR measurement display screen. The aortic pressure is measured through the guiding catheter (*red line*). The pressure distal to the coronary lesion is measured by the 0.014 in. pressure sensor-tipped wire (*yellow line*). In this example, the ratio of the distal coronary pressure to proximal coronary pressure is 0.70 and consistent with a hemodynamically significant stenosis

patients with multivessel coronary artery disease were randomized to PCI with drug eluting stents of all stenoses ≥50% vs. FFR guided PCI of stenoses with a value ≤0.80. At 1 year, the rate of death, nonfatal myocardial infarction, and repeat revascularization was significantly lower in the FFR guided group than in the angiography guided group (13.2% vs. 18.3%) and the FFR group received a significantly fewer number of stents [31]. Eighty percent of patients in both groups were angina free at 1 year; however, the FFR guided strategy was significantly less expensive than the angiography guided group ($14,315 vs. $16,700) [31].

Assessment of Multiple Stenoses Within a Single Vessel

It is common for patients with CAD to have multiple sequential stenoses within a single coronary artery. One study described performing a "slow pull back" of the pressure-sensor tipped coronary wire in the coronary artery of patients with multiple intermediate stenoses in a single coronary vessel during continuous

adenosine infusion. It found that using this method, FFR can be performed and accurately assess the physiologic significance of each lesion in the artery and thus objectively select the most appropriate stenosis or percutaneous coronary intervention [32].

Diffuse CAD or Long Coronary Lesions

Another subset of patients in which FFR can be helpful to guide the decision for PCI is in patients with diffuse disease or long coronary lesions. Similar to the assessment of multiple lesions in a single vessel, the pressure-sensor tipped wire can be slowly withdrawn from a vessel during maximal hyperemia and concomitant fluoroscopy can be used to precisely indicate where hemodynamically significant lesions exist. A gradual loss of pressure is consistent with diffuse disease and may suggest that PCI is technically less favorable and that possibly coronary artery bypass grafting (CABG) or medical management should be considered. However, an abrupt decrease in pressure is consistent with a focal hemodynamically significant stenosis and suggests that PCI may be more favorable [32, 33].

Left Main Coronary Disease and Bifurcation Lesions

Angiographic assessment of a left main coronary artery stenosis poses a great challenge for operators. As previously mentioned, factors such as vessel overlap and unfavorable vessel orientation in relation to achievable camera angles often result in a suboptimal angiographic assessment of the vessel and significant intraobserver variability [34]. In this subset of patients, the use of FFR to further assess the vessel has been shown to be beneficial. One study demonstrated that patients with an intermediate left main stenosis and an FFR >0.75 had superb 3-year outcomes suggesting that PCI can safely be deferred in this subgroup [35].

Similar to left main coronary artery lesions, the evaluation of bifurcation lesions poses a significant challenge to the angiographer. By performing a separate FFR of each branch of the bifurcation, the hemodynamic significance of the lesions can be reliably determined and can assist the operator in deciding the most appropriate course of action for the patient [36].

Coronary Bypass Grafts

There is a paucity of data regarding the utility of FFR in assessing the physiologic significance of intermediate stenoses in a saphenous vein graft (SVG). A small study looked at ten veterans who had a stress myocardial perfusion imaging study (MPI)

and were referred for PCI of an SVG stenosis. The sensitivity, specificity, and accuracy of FFR <0.75 for the detection of ischemia on stress MPI were 50%, 75%, and 70%, respectively. The authors concluded that the use of FFR to assess the physiologic significance of SVG lesions was feasible and provided acceptable sensitivity and specificity in comparison to stress MPI.

Acute Myocardial Infarction and Post Myocardial Infarction

While FFR does provide valuable information regarding intermediate coronary lesions in patients with stable and unstable angina, it should not be used in the acute phase of a myocardial infarction (MI). Animal studies have shown that even after reperfusion of an epicardial coronary occlusion, significant perivascular edema and capillary leukocyte plugging occurs causing microvascular dysfunction and incomplete restoration of myocardial perfusion [37]. This has been shown to result in up to a 5% overestimation of FFR in humans [38]. Six days after an MI, however, FFR has been shown to be accurate and can be used to identify hemodynamically significant coronary lesions that supply areas with significant remaining ischemic but viable myocardium [39]. Myocardial perfusion SPECT imaging and FFR were performed in 57 patients who had sustained a myocardial infarction at least 6 days prior. Patients with demonstrable ischemia on SPECT imaging had a significantly lower FFR value than those who had evidence of scar without ischemia. When using a cutoff FFR value of 0.75, this demonstrated a sensitivity and specificity of 82% and 87%, respectively. However, when only truly positive and truly negative stress tests were considered, the sensitivity and specificity rose to 87% and 100%, respectively. When sensitivity and specificity were plotted against FFR, the value of FFR for which sensitivity and specificity were equal (88%) was 0.78, however, this value did not show a statistically significant difference in accuracy when compared to a cutoff value of 0.75.

FFR Post PCI

FFR has been shown to have significant prognostic value after PCI has been performed [40–42]. An FFR ≥0.90 is considered a successful result for balloon angioplasty and an FFR ≥0.94 is successful post stent deployment. FFR values lower than these predict adverse outcomes.

Another area where FFR can be helpful is in the evaluation of jailed side branches after stenting. One study looking at the feasibility of FFR for the assessment of jailed side branches showed that only 20% of lesions with QCA >75% had an FFR <0.75 and no lesion with QCA <75% had an FFR <0.75 [43]. This data suggests that most jailed side branches do not have hemodynamically significant stenoses and that PCI of the daughter vessel can likely be safely deferred. This information is particularly useful given the higher rate of restenosis and stent thrombosis associated with dual stenting of bifurcation lesions [44].

Limitations of FFR

While several randomized controlled trials have demonstrated the clinical benefit of FFR guided coronary revascularization, certain limitations do exist. As mentioned above, FFR is not always accurate in AMI and will often show an elevated value due to microvascular dysfunction. Other causes of microvasculor dysfunction, such as syndrome & mentioned above, can also conformed results in addition, animal studies have suggested that up to 16% of subjects undergoing FFR with adenosine or papaverine do not achieve maximal hyperemia [45]. This suggests that the physiologic significance of some lesions may be underestimated when using standard current vasodilator doses and that higher doses may be needed in order to achieve maximal hyperemia.

Conclusions

CFR and relative CFR can be used to invasively measure flow velocity in a coronary artery and thus evaluate the hemodynamic significance of epicardial stenoses or microvascular dysfunction. Due to the limitations of CFR and increased time requirements and risk of relative CFR, these methods are now rarely used to assess epicardial lesions. However, CFR is still the test of choice to evaluate for microvascular dysfunction.

FFR has emerged as the current method of choice to evaluate the physiologic significance of an intermediate epicardial stenosis. Designated as "lesion specific", it compares the ratio of distal to proximal pressure across an epicardial stenosis. This technique adds important functional information that augments the anatomic information provided by angiography and intravascular imaging modalities (i.e., IVUS and OCT). It has been validated to improve clinical outcomes when used to guide PCI in patients with single and multivessel CAD and also has been shown to provide useful information when examining a variety of coronary lesions. Furthermore, the use of FFR to guide PCI has been shown to significantly reduce the cost of treatment when compared to PCI guided by angiography alone.

Questions

Questions 1–2

A 62-year-old patient undergoing left heart catheterization for chest pain has a 65% stenosis in a large first diagonal branch. While performing an FFR measurement, the aortic pressure is 102/77 mmHg and the distal diagonal branch mean pressure is 60 mmHg.

1. What is the FFR of the diagonal branch?

   A. 0.779
   B. 0.588

C. 0.703
D. Can not be determined with the information provided

2. Is PCI of the diagonal branch indicated?

A. Yes. The FFR was >0.75
B. No. The FFR was <0.75
C. Yes. The FFR was <0.75
D. It depends on the severity of the stenosis in the artery

Questions 3–4

A 63 year old hypertensive patient presents with 12 months of intermittent exertional chest pain. An exercise nuclear stress test performed at an outside hospital reported a reversible perfusion defect involving the anteroseptal and lateral walls, however, left heart catheterization revealed angiographically normal coronary arteries. You perform CFR of the LAD which gives a result of 1.6.

3. What is the diagnosis does this patient have?

A. Non-cardiac chest pain.
B. Cardiac chest pain due to missed coronary stenosis.
C. False-positive nuclear stress test.
D. Cardiac syndrome X.

4. What is the risk of this patient having an adverse cardiovascular event in the next year?

A. 0.2.5%
B. 1%
C. 10%
D. 15%

5. You perform a left heart catheterization on a 59-year old man with worsening exertional angina. Coronary angiography of the RCA reveals a mid 60% stenosis followed by a distal 60% stenosis; the left main trunk, LAD, and LCx have mild disease. You perform FFR of the RCA with slow pullback of the pressure sensor-tipped 0.014 in. coronary wire. You obtain the following results:

FFR of the right posterior descending artery:	0.55
FFR of the RCA between the mid and distal lesions:	0.70
FFR of the proximal RCA	1.00

What is the most appropriate management decision at this time?

A. Perform PCI on both the mid and distal RCA lesions
B. Perform PCI on the mid RCA lesion
C. Perform PCI on the distal RCA lesion
D. None of the above

Answers

1. The Answer is *C*. In order to calculate the FFR you first need to calculate the mean pressure (MP) in the aorta. This can be calculated by the following equation: MP = Diastolic pressure + (Systolic pressure – diastolic pressure)/3. Plugging the numbers into the equation, the MP = 85.3 mmHg. FFR = MP_{distal}/MP_{aorta} = 60/85.3 = 0.703.
2. The Answer is *C*. PCI is indicated based on the DEFER (FFR <0.75) and FAME (FFR <0.80) studies.
3. The Answer is ***D*.** Cardiac syndrome X, or angina with an abnormal cardiac stress test and angiographically normal coronary arteries. A CFR ≤2 is suggestive of microvascular disease, the underlying pathophysiology of this syndrome.
4. The Answer is ***A*.** This patient has a 2.5% chance of having a myocardial infarction, stroke, sudden cardiac death, or developing congestive heart failure over the next year.
5. The Answer is ***B*.** Performing a slow pullback across multiple serial stenoses in a single vessel during FFR allows the operator to determine the hemodynamic significance of each individual stenosis. In this example, the hemodynamic contribution of the distal RCA stenosis was 0.85 (1–(0.70–0.55)) = (1–0.15) = 0.85. The hemodynamic significance of the mid RCA stenosis was 0.70. Thus, the most appropriate management decision is to perform PCI on the mid RCA lesion only.

References

1. Grondin CM, Dyrda I, Pasternac A, Campeau L, Bourassa MG, Lesperance J. Discrepancies between cineangiographic and postmortem findings in patients with coronary artery disease and recent myocardial revascularization. Circulation. 1974;49:703–8.
2. Hutchins GM, Bulkley BH, Ridolfi RL, Griffith LS, Lohr FT, Piasio MA. Correlation of coronary arteriograms and left ventriculograms with postmortem studies. Circulation. 1977;56:32–7.
3. Arnett EN, Isner JM, Redwood DR, et al. Coronary artery narrowing in coronary heart disease: comparison of cineangiographic and necropsy findings. Ann Intern Med. 1979;91:350–6.
4. Fisher LD, Judkins MP, Lesperance J, et al. Reproducibility of coronary arteriographic reading in the coronary artery surgery study (CASS). Cathet Cardiovasc Diagn. 1982;8:565–75.
5. Gould KL, Lipscomb K, Hamilton GW. Physiologic basis for assessing critical coronary stenosis. Instantaneous flow response and regional distribution during coronary hyperemia as measures of coronary flow reserve. Am J Cardiol. 1974;33:87–94.

6. Gould KL, Kirkeeide RL, Buchi M. Coronary flow reserve as a physiologic measure of stenosis severity. J Am Coll Cardiol. 1990;15:459–74.
7. Doucette JW, Corl PD, Payne HM, et al. Validation of a Doppler guide wire for intravascular measurement of coronary artery flow velocity. Circulation. 1992;85:1899–911.
8. Labovitz AJ, Anthonis DM, Cravens TL, Kern MJ. Validation of volumetric flow measurements by means of a Doppler-tipped coronary angioplasty guide wire. Am Heart J. 1993;126:1456–61.
9. Miller DD, Donohue TJ, Younis LT, et al. Correlation of pharmacological 99mTc-sestamibi myocardial perfusion imaging with poststenotic coronary flow reserve in patients with angiographically intermediate coronary artery stenoses. Circulation. 1994;89:2150–60.
10. Heller LI, Cates C, Popma J, et al. Intracoronary Doppler assessment of moderate coronary artery disease: comparison with 201Tl imaging and coronary angiography. FACTS Study Group. Circulation. 1997;96:484–90.
11. Akasaka T, Yoshida K, Hozumi T, et al. Retinopathy identifies marked restriction of coronary flow reserve in patients with diabetes mellitus. J Am Coll Cardiol. 1997;30:935–41.
12. Lorenzoni R, Gistri R, Cecchi F, et al. Coronary vasodilator reserve is impaired in patients with hypertrophic cardiomyopathy and left ventricular dysfunction. Am Heart J. 1998;136:972–81.
13. Czernin J, Muller P, Chan S, et al. Influence of age and hemodynamics on myocardial blood flow and flow reserve. Circulation. 1993;88:62–9.
14. Schafer S, Kelm M, Mingers S, Strauer BE. Left ventricular remodeling impairs coronary flow reserve in hypertensive patients. J Hypertens. 2002;20:1431–7.
15. Voudris V, Avramides D, Koutelou M, et al. Relative coronary flow velocity reserve improves correlation with stress myocardial perfusion imaging in assessment of coronary artery stenoses. Chest. 2003;124:1266–74.
16. Bugiardini R, Bairey Merz CN. Angina with “normal” coronary arteries: a changing philosophy. JAMA. 2005;293:477–84.
17. Reis SE, Holubkov R, Conrad Smith AJ, et al. Coronary microvascular dysfunction is highly prevalent in women with chest pain in the absence of coronary artery disease: results from the NHLBI WISE study. Am Heart J. 2001;141:735–41.
18. Pijls NH, van Son JA, Kirkeeide RL, De Bruyne B, Gould KL. Experimental basis of determining maximum coronary, myocardial, and collateral blood flow by pressure measurements for assessing functional stenosis severity before and after percutaneous transluminal coronary angioplasty. Circulation. 1993;87:1354–67.
19. Pijls NH, De Bruyne B, Peels K, et al. Measurement of fractional flow reserve to assess the functional severity of coronary-artery stenoses. N Engl J Med. 1996;334:1703–8.
20. Kern MJ, de Bruyne B, Pijls NH. From research to clinical practice: current role of intracoronary physiologically based decision making in the cardiac catheterization laboratory. J Am Coll Cardiol. 1997;30:613–20.
21. Di Segni E, Higano ST, Rihal CS, Holmes Jr DR, Lennon R, Lerman A. Incremental doses of intracoronary adenosine for the assessment of coronary velocity reserve for clinical decision making. Catheter Cardiovasc Interv. 2001;54:34–40.
22. Wilson RF, White CW. Intracoronary papaverine: an ideal coronary vasodilator for studies of the coronary circulation in conscious humans. Circulation. 1986;73:444–51.
23. Bartunek J, Wijns W, Heyndrickx GR, de Bruyne B. Effects of dobutamine on coronary stenosis physiology and morphology: comparison with intracoronary adenosine. Circulation. 1999;100:243–9.
24. de Bruyne B, Bartunek J, Sys SU, Pijls NH, Heyndrickx GR, Wijns W. Simultaneous coronary pressure and flow velocity measurements in humans. Feasibility, reproducibility, and hemodynamic dependence of coronary flow velocity reserve, hyperemic flow versus pressure slope index, and fractional flow reserve. Circulation. 1996;94:1842–9.
25. Caymaz O, Fak AS, Tezcan H, et al. Correlation of myocardial fractional flow reserve with thallium-201 SPECT imaging in intermediate-severity coronary artery lesions. J Invasive Cardiol. 2000;12:345–50.

26. Leesar MA, Abdul-Baki T, Akkus NI, Sharma A, Kannan T, Bolli R. Use of fractional flow reserve versus stress perfusion scintigraphy after unstable angina. Effect on duration of hospitalization, cost, procedural characteristics, and clinical outcome. J Am Coll Cardiol. 2003;41:1115–21.
27. Bech GJ, De Bruyne B, Bonnier HJ, et al. Long-term follow-up after deferral of percutaneous transluminal coronary angioplasty of intermediate stenosis on the basis of coronary pressure measurement. J Am Coll Cardiol. 1998;31:841–7.
28. Bech GJ, De Bruyne B, Pijls NH, et al. Fractional flow reserve to determine the appropriateness of angioplasty in moderate coronary stenosis: a randomized trial. Circulation. 2001;103:2928–34.
29. Kern MJ, Donohue TJ, Aguirre FV, et al. Clinical outcome of deferring angioplasty in patients with normal translesional pressure-flow velocity measurements. J Am Coll Cardiol. 1995;25:178–87.
30. Chamuleau SA, Meuwissen M, Koch KT, et al. Usefulness of fractional flow reserve for risk stratification of patients with multivessel coronary artery disease and an intermediate stenosis. Am J Cardiol. 2002;89:377–80.
31. Tonino PA, De Bruyne B, Pijls NH, et al. Fractional flow reserve versus angiography for guiding percutaneous coronary intervention. N Engl J Med. 2009;360:213–24.
32. Pijls NH, De Bruyne B, Bech GJ, et al. Coronary pressure measurement to assess the hemodynamic significance of serial stenoses within one coronary artery: validation in humans. Circulation. 2000;102:2371–7.
33. De Bruyne B, Pijls NH, Heyndrickx GR, Hodeige D, Kirkeeide R, Gould KL. Pressure-derived fractional flow reserve to assess serial epicardial stenoses: theoretical basis and animal validation. Circulation. 2000;101:1840–7.
34. Mintz GS, Kent KM, Pichard AD, Satler LF, Popma JJ, Leon MB. Contribution of inadequate arterial remodeling to the development of focal coronary artery stenoses. An intravascular ultrasound study. Circulation. 1997;95:1791–8.
35. Bech GJ, Droste H, Pijls NH, et al. Value of fractional flow reserve in making decisions about bypass surgery for equivocal left main coronary artery disease. Heart. 2001;86:547–52.
36. Ziaee A, Parham WA, Herrmann SC, Stewart RE, Lim MJ, Kern MJ. Lack of relation between imaging and physiology in ostial coronary artery narrowings. Am J Cardiol 2004;93:1404–7, A9.
37. Engler RL, Schmid-Schonbein GW, Pavelec RS. Leukocyte capillary plugging in myocardial ischemia and reperfusion in the dog. Am J Pathol. 1983;111:98–111.
38. Claeys MJ, Bosmans JM, Hendrix J, Vrints CJ. Reliability of fractional flow reserve measurements in patients with associated microvascular dysfunction: importance of flow on translesional pressure gradient. Catheter Cardiovasc Interv. 2001;54:427–34.
39. De Bruyne B, Pijls NH, Bartunek J, et al. Fractional flow reserve in patients with prior myocardial infarction. Circulation. 2001;104:157–62.
40. Hanekamp CE, Koolen JJ, Pijls NH, Michels HR, Bonnier HJ. Comparison of quantitative coronary angiography, intravascular ultrasound, and coronary pressure measurement to assess optimum stent deployment. Circulation. 1999;99:1015–21.
41. Pijls NH, Klauss V, Siebert U, et al. Coronary pressure measurement after stenting predicts adverse events at follow-up: a multicenter registry. Circulation. 2002;105:2950–4.
42. Rieber J, Schiele TM, Erdin P, et al. Fractional flow reserve predicts major adverse cardiac events after coronary stent implantation. Z Kardiol. 2002;91 Suppl 3:132–6.
43. Koo BK, Kang HJ, Youn TJ, et al. Physiologic assessment of jailed side branch lesions using fractional flow reserve. J Am Coll Cardiol. 2005;46:633–7.
44. Colombo A, Moses JW, Morice MC, et al. Randomized study to evaluate sirolimus-eluting stents implanted at coronary bifurcation lesions. Circulation. 2004;109:1244–9.
45. Jeremias A, Filardo SD, Whitbourn RJ, et al. Effects of intravenous and intracoronary adenosine 5'-triphosphate as compared with adenosine on coronary flow and pressure dynamics. Circulation. 2000;101:318–23.

ERRATUM

Cardiovascular Hemodynamics

Saif Anwaruddin, Joseph M. Martin, John C. Stephens, and Arman T. Askari

Editors

S. Anwaruddin et al. (eds.) *Cardiovascular Hemodynamics: An Introductory Guide*, Contemporary Cardiology, DOI 10.1007/978-1-60761-195-0, pp. iv.

DOI 10.1007/978-1-60761-195-0_17

The publisher regrets that in the print and online versions of this book the affiliation of Dr. Arman T. Askari on the copyright page is incorrect. The correct affiliation appears below.

Arman T. Askari
Adjunct Staff
Heart and Vascular Institute
Cleveland Clinic
Clinical Associate Professor of Medicine
Cleveland Clinic Lerner College of Medicine
Cleveland, OH, USA

Index

A.T. Askari et al. (eds.), *Cardiovascular Hemodynamics: An Introductory Guide*, Contemporary Cardiology, DOI 10.1007/978-1-60761-195-0,